28th International Geological Congress

Tectonic, Depositional, and Paleoecological History of Early Mesozoic Rift Basins, Eastern North America

Field Trip Guidebook T351

Leaders:
Paul E. Olsen and Pamela J. W. Gore

Gulf, North Carolina, USA to
Parrsboro, Nova Scotia, Canada
July 20-30, 1989

INTERNATIONAL GEOLOGICAL CONGRESS FIELD TRIP T-351

TECTONIC, DEPOSITIONAL, AND PALEOECOLOGICAL HISTORY OF EARLY MESOZOIC RIFT BASINS, EASTERN NORTH AMERICA

JULY 20, 1989-JULY 30, 1989

GULF, NORTH CAROLINA, USA to PARRSBORO, NOVA SCOTIA, CANADA

GUIDEBOOK EDITORS

Paul E. Olsen[1]
Roy W. Schlische[1]
Pamela J.W. Gore[2]

WITH CONTRIBUTIONS BY

Bruce Cornet[3]
Patricia Gallagher[4]
William Hoffman[4]
Amy R. McCune[5]
Nicholas G. McDonald[6]
Joseph P. Smoot[7]
Richard P. Tollo[8]
Donald U. Wise[9]
William K. Witte[1]

FIELD TRIP LEADERS

Paul E. Olsen
Pamela J.W. Gore

ASSOCIATE LEADERS

Roy W. Schlische
Joseph P. Smoot
Richard P. Tollo

[1]Department of Geological Sciences and Lamont-Doherty Geological Observatory of Columbia University, Palisades, NY 10964
[2]Department of Geology, Emory University, Atlanta, GA 30322
[3]Lamont-Doherty Geological Observatory of Columbia University, Palisades, NY 10964
[4]North Carolina Department of Natural Resources and Community Development, Geologic Survey Section, Raleigh, NC 27607
[5]Department of Ecology and Systematics, Cornell University, Ithaca, NY 14853
[6]Department of Earth and Environmental Sciences, Wesleyan University, Middletown, CT 06457
[7]United States Geological Survey, 912 National Center, Reston, VA 22092
[8]Department of Geology, George Washington University, Washington, DC 20052
[9]Department of Geology and Geography, University of Massachusetts, Amherst, MA 01003

Tectonic, Depositional, and Paleoecological History of Early Mesozoic Rift Basins, Eastern North America

Gulf, North Carolina, USA to
Parrsboro, Nova Scotia, Canada
July 20-30, 1989

Field Trip Guidebook T351

Editors:
Paul E. Olsen, Roy W. Schlische, and Pamela J. W. Gore

Contributions by:
Bruce Cornet, Patricia Gallagher, William Hoffman, Amy R. McCune, Nicholas G. McDonald, Joseph P. Smoot, Richard P. Tollo, Donald U. Wise, and William K. Witte

Leaders:
Paul E. Olsen and Pamela J. W. Gore

Associate Leaders:
Roy W. Schlische, Joseph P. Smoot, and Richard P. Tollo

American Geophysical Union, Washington, D.C.

2000 Florida Ave., N.W., Washington, D.C. 20009

ISBN: 0-87590-658-3

Printed in the United States of America

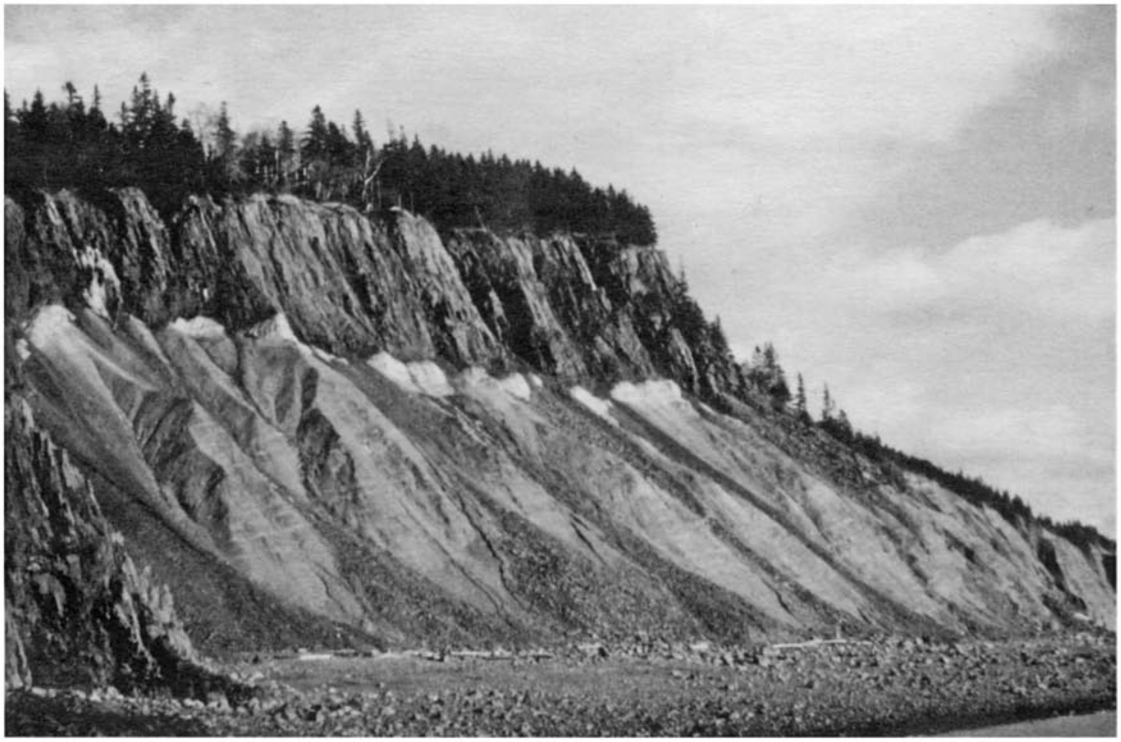

COVER: View toward the northeast from the Old Wife, Stop 11.2, of the Late Triassic-earliest Jurassic Blomidon Formation and Early Jurassic North Mountain Basalt of the Fundy basin along the north shore of the Minas Basin near Five Islands Provincial Park, Nova Scotia. The Blomidon Formation here is visibly cyclic, and the meter-scale cycles are thought to represent the 100,000-year eccentricity cycle according to the Milankovitch theory of orbital climatic forcing. The Triassic-Jurassic boundary is palynologically placed near the base of the light colored layer at the top of the Blomidon Formation. A normal fault which drops down the North Mountain Basalt is visible in the lower left corner. Photo by P.E. Olsen.

TABLE OF CONTENTS

INTERNATIONAL GEOLOGICAL CONGRESS FIELD TRIP T-351

TECTONIC, DEPOSITIONAL, AND PALEOECOLOGICAL HISTORY OF EARLY MESOZOIC RIFT BASINS, EASTERN NORTH AMERICA

JULY 20, 1989-JULY 30, 1989

GULF, NORTH CAROLINA, USA to PARRSBORO, NOVA SCOTIA, CANADA

GUIDEBOOK EDITORS

Paul E. Olsen[1]
Roy W. Schlische[1]
Pamela J.W. Gore[2]

WITH CONTRIBUTIONS BY

Bruce Cornet[3]
Patricia Gallagher[4]
William Hoffman[4]
Amy R. McCune[5]
Nicholas G. McDonald[6]
Joseph P. Smoot[7]
Richard P. Tollo[8]
Donald U. Wise[9]
William K. Witte[1]

FIELD TRIP LEADERS

Paul E. Olsen
Pamela J.W. Gore

ASSOCIATE LEADERS

Roy W. Schlische
Joseph P. Smoot
Richard P. Tollo

[1]Department of Geological Sciences and Lamont-Doherty Geological Observatory of Columbia University, Palisades, NY 10964
[2]Department of Geology, Emory University, Atlanta, GA 30322
[3]Lamont-Doherty Geological Observatory of Columbia University, Palisades, NY 10964
[4]North Carolina Department of Natural Resources and Community Development, Geologic Survey Section, Raleigh, NC 27607
[5]Department of Ecology and Systematics, Cornell University, Ithaca, NY 14853
[6]Department of Earth and Environmental Sciences, Wesleyan University, Middletown, CT 06457
[7]United States Geological Survey, 912 National Center, Reston, VA 22092
[8]Department of Geology, George Washington University, Washington, DC 20052
[9]Department of Geology and Geography, University of Massachusetts, Amherst, MA 01003

PART I: OVERVIEW OF NEWARK SUPERGROUP

INTRODUCTION

Eastern North America includes the classic Atlantic-type passive continental margin formed by the breakup of the supercontinent of Pangaea. The Triassic initiation of the breakup was marked by the formation of rifted crust all along the axis of the future Atlantic, from Greenland to Mexico. In eastern North America, nine major rift basins, mostly half-graben, and several minor basins are exposed from Nova Scotia to South Carolina, with many more buried below the coastal plain and continental shelf (Figure I.1). The exposed rift basins, which closely follow the trend of the Appalachian orogen, filled with thousands of meters of continental sediments and basalt flows over a period of approximately 45 million years. Diabase plutons and dikes, apparently coeval with the basalt flows, extensively intruded and metamorphosed pre-existing strata. The faulted, tilted, and eroded rift strata are termed the Newark Supergroup (Van Houten, 1977; Olsen, 1978; Froelich and Olsen, 1984).

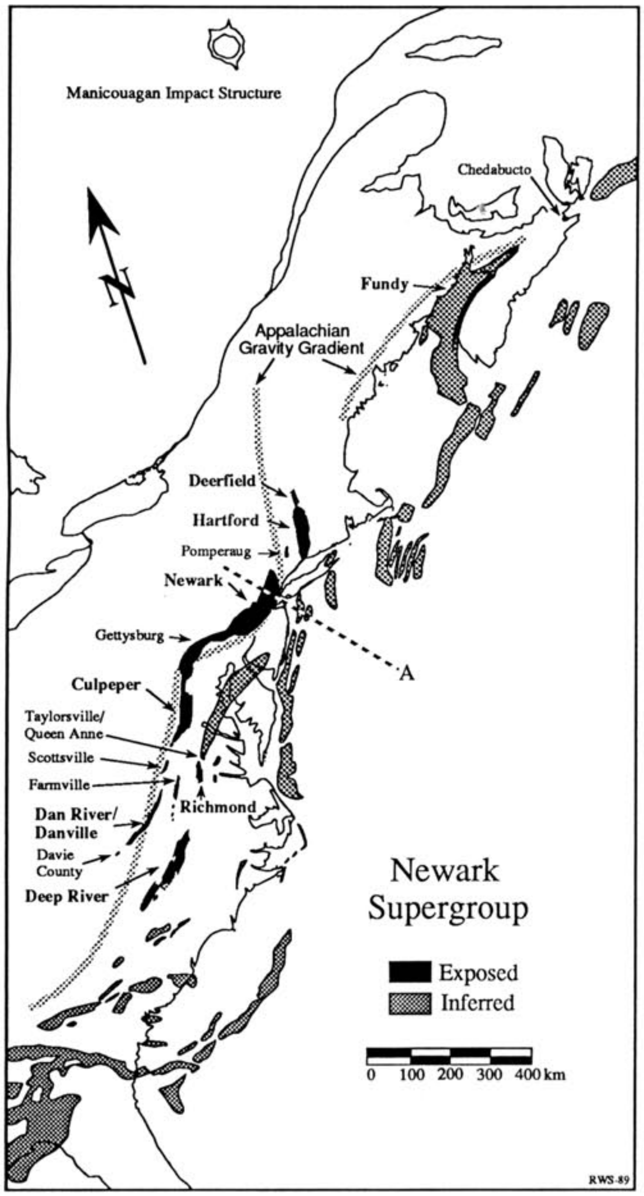

Figure I.1: Newark Supergroup of Eastern North America. Adapted from Klitgord *et al.* (1988). Basins with stops described in this guidebook are shown in the larger, bold-face lettering. Transect of cross section shown in Figure I.2 indicated by A.

The purpose of this field trip and guidebook is to provide a comprehensive overview of the Newark Supergroup with an eye toward understanding some of the basic patterns and processes of rifting dynamics and early Mesozoic biological change. Our main focus is a series of major interrelated problems, around which both the stops and the discussions are centered. These are: 1) How does extension of the crust produce the geometry seen in Newark half-graben and in half-graben in general? 2) What are the underlying general processes which produce the similarities in stratigraphic development among the different basins and are these reflections of rules operating in extensional basins in general? 3) What are the relative roles of intrinsic versus extrinsic controls on ecosystem evolution and the evolution of biological diversity as seen in the Newark paleontological record? Some of the necessary background to these problems as they apply to the rift basins of eastern North America are topically discussed below.

TECTONIC CONTEXT (by P.E. Olsen)

Newark Supergroup rifts lie entirely within the Appalachian orogen, which, as presently understood, is divisible into three broad structural zones (Figure I.2) (generalized from Hatcher, 1972; Cook *et al.*, 1981; Ando *et al.*, 1983; Brown *et al.*, 1983; Williams and Hatcher, 1982; Ando *et al.*, 1984; Nelson *et al.*, 1985; Allmendinger *et al.*, 1987; McBride and Nelson, 1988). The western zone consists of a 2- to 10-km-wide zone of allochthonous slices separated from relatively undeformed North American craton by a low-angle detachment. This thin-skinned zone is separated from the adjacent thick-skinned zone by an east-dipping ramp which may extend to Moho. In proximity to the ramp (but regionally discordant to surface trends) is the Appalachian or Piedmont gravity gradient, which is often considered to mark the approximate edge of the Precambrian-early Paleozoic continent. Above and immediately to the east of this ramp are rooted slices of North American cratonic rocks, followed further to the east by the first of several apparent sutures with exotic accreted terranes. The eastern zone transitional to oceanic crust is as yet poorly known. It lies east of the basement hinge zone of continental crust and probably consists of fragments of continental crust and Mesozoic igneous rocks (Klitgord *et al.*, 1988).

Cook and Oliver (1981) have plausibly argued that development of Precambrian and earliest Paleozoic rifting and of the Iapetus passive margin established the basic configuration of the eastern edge of the North American craton. A succession of Paleozoic accretionary and collisional events activated the old Precambrian-Paleozoic continental margin as a ramp, with repeated emplacement of allochthonous slices to the west in fold and thrust belts. The presumably thickened crust was then thinned in the early Mesozoic during the formation of the present Atlantic margin, with the greatest thinning being manifest in the zone of transitional crust east of the basement hinge zone.

From southern New York State to Georgia, the western-most rift basins lie over the basement ramp with more eastern basins lying at the boundaries between or within accreted terranes (Figure I.2). However, from southern New York State north to Nova Scotia, the western-most rift basins lie east of both the Appalachian gravity gradient and the basement ramp and thus lie in the zone of accreted terranes. Almost all early Mesozoic igneous rocks lie to the east of the basement ramp (McHone and Butler, 1984).

A much less well-known series of early Mesozoic rift basins lie buried below the Gulf Coastal Plain and apparently formed in a similar tectonic setting (Thomas, 1988). Although clearly coeval with (Traverse, 1987) and intimately related to the Newark Supergroup, the history of these basins as well as the entire rifting history of the Gulf of Mexico has been largely ignored in studies of eastern North American rifting.

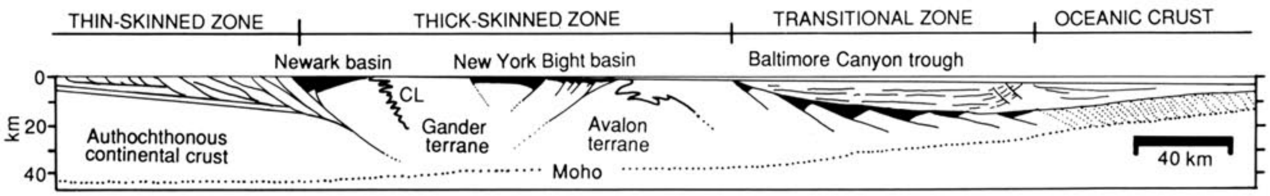

Figure I.2: Cross section across the Appalachian orogen (thin-skinned, thick skinned, and transitional zones) and old oceanic crust along transect shown in Figure I.1. CL is Cameron's line.

Most Newark Supergroup basins are half-graben (Klitgord *et al.*, 1988) with boundary faults which appear in most cases to be reactivated Paleozoic faults (Swanson, 1986). However, the reactivation origin of the boundary faults has been shown definitively only in the Newark basin (sections 5 and 6) (Ratcliffe, 1980; Ratcliffe and Burton, 1985; Ratcliffe *et al.*, 1986) and in the Fundy basin (sections 9, 10, and 11) by Plint and Van de Poll (1984). According to the model of Ratcliffe and Burton (1985), the major direction of slip on reactivated faults and the relative amount of basin subsidence depended on their orientation relative to regional NW-SE σ_3 during early Mesozoic extension and on the dip of the fault. Thus, the deepest parts of the half-graben tend to lie adjacent to faults which are oriented NE-SW, and the shallowest parts of the basins tend to lie adjacent to faults that trend closest to NW-SE. These latter faults sometimes link adjacent basins and are hence transfer faults (Gibbs, 1984) that, unlike those of the East African rifts (Rosendahl, 1987), apparently link basins of similar, not opposing, polarity.

Although most authors (Manspeizer, 1988; Crespi, 1988; Ressetar and Taylor, 1988; Root, 1988) have assumed that most Newark Supergroup basin boundary faults are strongly listric, soling out into sub-horizontal detachments at depths of 5 to 12 km, there is little direct evidence for it. Many such interpretations are based on either unwarranted model assumptions on half-graben mechanics (based on Gibbs, 1984, for example) or on interpretations of seismic profiles in which velocity pull-ups have not been removed by appropriate migration (see Unger, 1988, for explanation). Available published and migrated seismic profiles show faults with variable curvature extending quite deeply, perhaps to Moho (Hutchinson and Klitgord, 1988a,b). Like the Paleozoic faults they reactivated, the early Mesozoic boundary faults probably have a variety of curvatures (flat, concave, or convex), and the assumption of the listric nature of boundary faults for which there is no observational basis is unwarranted. The changing attitude with depth of the major faults and the presence or absence of subhorizontal detachments above Moho obviously remain a contentious and unresolved set of problems.

LITHOSTRATIGRAPHIC, BIOSTRATIGRAPHIC, AND CHRONOSTRATIGRAPHIC FRAMEWORK
(by P.E. Olsen)

Each major basin of the Newark Supergroup has, for the most part, a separate series of lithologically-defined formations which either have no formal inclusive name or are united into one or more groups (Froelich and Olsen, 1984). All told, the Newark Supergroup consists of six formal groups, ten large and five small basins with formations not united into groups, 57 currently recognized formations, and scores of named members (Olsen, in press). This does not include the intrusive units or the very large number of duplicate names for formations and groups.

Once thought to be nearly devoid of fossils, the Newark Supergroup is now known to be one of the world's richest early Mesozoic sequences. Diverse and, in many cases, remarkably well-preserved micro- and macroscopic plants, invertebrates, and tetrapods are known from the oldest to youngest beds from North Carolina to Nova Scotia. These fossils form the basis for a developing sophisticated biostratigraphic correlation. Although correlation with the European standard section still poses numerous uncertainties because of a complete lack of marine invertebrates in the Newark, correlation <u>within</u> the eastern North American rift basins is robust (Figure I.3). The much greater strength of the correlations within the Newark Supergroup, the tremendous thickness and stratigraphic completeness of Newark sections, and the remarkable richness of the sections suggest that it is time to develop a series of local age designations as has proved so useful in the western interior (Berggren *et al.*, 1985). However, that will not be developed in this paper; instead the European standard ages will still be used.

Expressed in terms of the European standard ages, Newark strata range in age from probably Anisian of the Middle Triassic to at least Sinemurian or Pliensbachian of the Early Jurassic (Cornet and Olsen, 1985). However, the bulk of Newark strata are from Carnian to Hettangian in age. The Triassic-Jurassic boundary is present in all of the northern Newark basins and is recognized by palynostratigraphy and vertebrate fossils (Cornet and Olsen, 1985). It should be remembered, however, that there is considerable geographic variation in the Triassic-Jurassic biostratigraphic transitions in Europe. Currently, the most-corroborated hypothesis is that the palynologically-identified boundary in eastern North America may coincide with the base of the pre-planorbis zone (Olsen and Cornet, 1988a). This is an interval of extinctions (Golebiowski and Braunstein, 1988) rather than the traditional Triassic-Jurassic boundary of the European section, which lies at the base of the *Psiloceras planorbis* ammonite zone (Cope *et al.*, 1980; Harland *et al.*, 1982). This hypothesis of correlation has not yet been subjected to any non-biostratigraphic tests, however.

All of the extrusive rocks in the exposed basins are now thought to be of early to middle Hettangian age (Cornet and Olsen, 1985). This represents a revision of previous interpretations which suggested a "Rhaeto-Liassic" age (Cornet *et al.*, 1973; Cornet and Traverse, 1975) or a Hettangian-Sinemurian age (Cornet, 1977a; Olsen *et al.*, 1982). The post-extrusive interval in the Hartford basin was thought to range into the Toarcian; however, recent studies of Hartford basin physical stratigraphy (Olsen *et al.*, 1989) indicate a Pliensbachian age for the youngest palynologically-dated rocks. However, age-level correlation with the European section, based on palynology, is anything but certain.

Milankovitch Cycles and Cyclostratigraphy

Most lacustrine rocks of the Newark Supergroup show a common theme of obvious repetitive and permeating transgressive-regressive lake level sequences called Van Houten cycles (Olsen, 1986) after their discoverer (Van Houten, 1964, 1969; Olsen, Van Houten, *et al.*, 1988). The fundamental Van Houten cycle consists of three divisions, interpreted as lake transgression (division 1), high stand (division 2), and regression followed by low stand facies (division 3) (Figure I.4). These changes are attributed to climatic variations affecting the rate of inflow and evaporation.

Van Houten (1964, 1969) recognized two orders of compound cycles in the Lockatong Formation of the Newark basin (Stop 5.7), and these have since been recognized and described in the other Newark Supergroup basins (Olsen, 1988b). The thinner of the two types of compound cycles consists on the average of five Van Houten cycles, whereas the thicker cycle consists of four of the thinner cycles (Figure I.4). Van Houten calibrated the cycles in the Lockatong in time by using the average thickness of what he assumed to be seasonal couplets in division 2 as an average sedimentation rate for the sections.

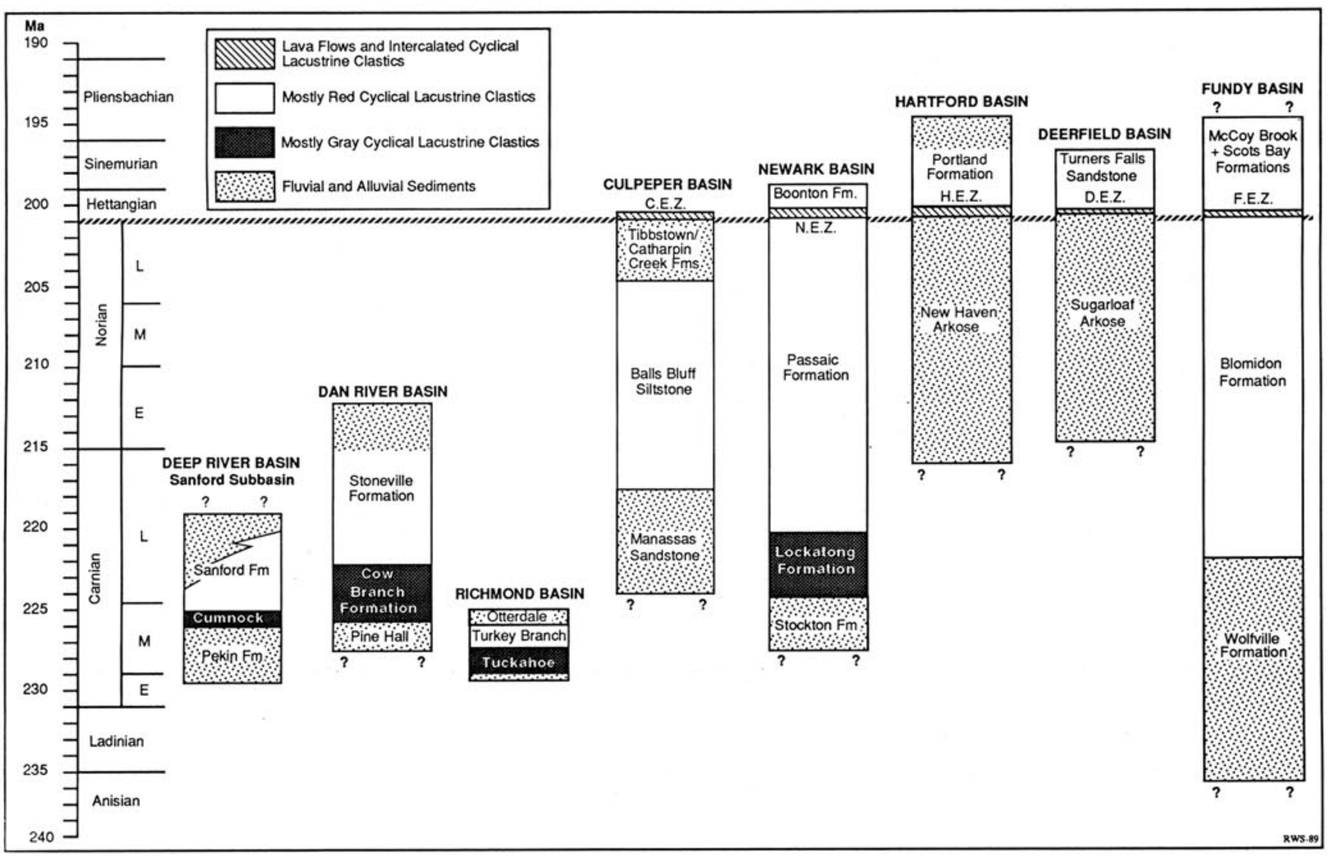

Figure I.3: Correlation of basin sections seen on field stops. Calibration in years is based on tie point at 201 Ma from Newark Supergroup intrusions hypothesized to correlate with lava flows, paleontological correlation of the Ladinian-Anisian boundary, dated according to Webb (1981), and Van Houten cycles from the Newark, Hartford, and Deerfield basins. Overall correlation of sections and age-level correlations based on palynostratigraphy of Cornet and Olsen (1985) and Traverse (1986, 1987). C.E.Z., N.E.Z., H.E.Z., D.E.Z., and F.E.Z. are respectively the Culpeper, Newark, Hartford, Deerfield, and Fundy extrusive zones and consist of lava flows and usually intercalated sedimentary formations.

Thus, Van Houten arrived at values of about 20,000 years for Van Houten cycles, 100,000 years for the thinner compound cycles and 400,000 years for the thicker compound cycles in the Lockatong Formation. Van Houten suggested that the 20,000 year cycles were produced by the cycle of the precession of the equinoxes but did not ascribe an origin to the longer cycles.

The essentially typological approach used by Van Houten suffers from the necessity of identifying the individual cycles so that they can be counted. The rock sequences are complex, however, and different workers choose to demarcate cycles differently, making the procedure highly subjective. The same problem was encountered by early workers on Quaternary $\delta^{18}O$ and terrace stratigraphy (Emiliani, 1966; Broecker *et al.*, 1968). In order to allow quantitative, less subjective analysis, Olsen (1984a, 1984b, 1986) classified the sedimentary fabrics of Van Houten cycles of the Lockatong and Passaic formations into seven categories, ranked in order of water depth: from time-averaged shallowest water (rank 0) to time-averaged deepest water (rank 6) (see Table 2.2). Rock sections were then described bed by bed using this classification scheme (Figure I.4). Following the paradigm set by Hays *et al.* (1976), Fourier analysis was used on these depth rank curves to examine their periodic components in rock thickness (Figure 5.19). Study of the same section originally worked on by Van Houten confirmed the presence of the sets of cycles he described, but also revealed much more periodic structure than could ever be identified typologically. Olsen (1984a, 1984b, 1986) calibrated the sections in time by the same method employed by Van Houten (varve counting), but also used the available published radiometric and biostratigraphic time scales, which gave similar but possibly more reliable results. The results of Olsen's calibration in time not only supported Van Houten's interpretations but also revealed the full spectrum of periods predicted by the orbital theory of climate change (Table I.1). Not only was the double peak of the precession cycle present, but the ~100,000 year cycle was split into two cycles as predicted by Berger (1977). The same pattern is revealed by the study of many other sections in the Newark basin (Figures 5.20, 6.6).

Figure I.4: A) Characteristics of generalized Van Houten cycle based on Figure 5.20A. B) Generalized compound cycles of Newark Supergroup, based loosely on Towaco Formation of Newark basin.

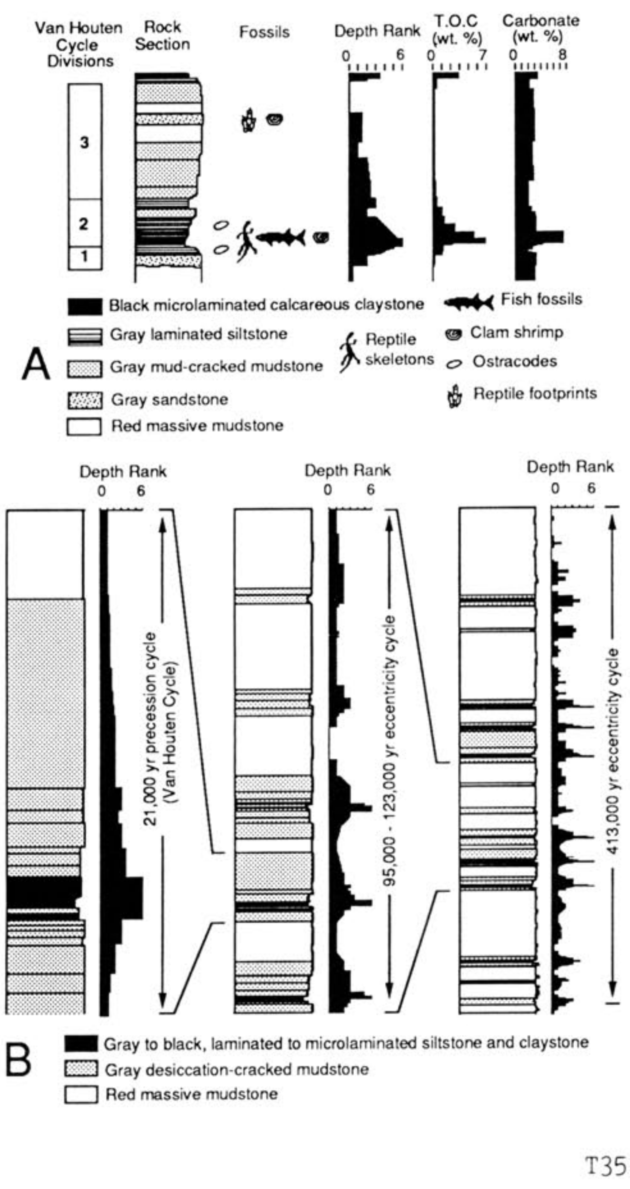

Table I.1: Comparison of present-day orbital cycles with observed and inferred cycles within Newark Supergroup basins.

CYCLES	TERMS[1]	PRESENT[1] PERIODS	NEWARK BASIN	FUNDY BASIN
precession ($e \sin \bar{\omega}$)	3-4 1-2	19,100 23,100	19,100 22,800	~21,000
obliquity (ε)	1, 2, 4, 6, 8, 9	41,000	~35,000*	
eccentricity (e)	2 3 1 6 ??	94,900 123,300 412,900 2,035,400	93,200 120,300 376,800 ~2,000,000 6,000,000	92,000 125,000 413,000 2,064,000

* not statistically significant
[1] From Berger (1984)

More robust than any specific calibration in time are the ratios of higher frequency cycles to the lower frequency cycles, as revealed in the power spectra of the Fourier analysis. This method is based on the strongly hierarchical structure evident in the power spectra and is independent of the vagaries of time scale and sedimentation rate estimates (Table I.1). The modern ratios of precession to the other orbital terms are directly comparable to the data from the Newark basin (Table 2.3). Thus, Fourier analysis of long sections of the Late Triassic Lockatong and Passaic formations of the Newark basin show periodicities in time of roughly 18,000-25,000, ~41,000, 95,000, 125,000 and 400,000 years (Olsen, 1986). These periodicities are in close accord with the orbital theory of climatic change and are strong evidence of orbital forcing of climate in the continental ice-free early Mesozoic (Olsen, 1986).

There can be little doubt that the hierarchical structure seen in Fourier power spectra is characteristic of the entire lacustrine portion of the Newark basin and of other parts of the Newark Supergroup as well. This model for the Newark

Supergroup thus provides an unprecedented opportunity to examine incredibly long intervals preserving a rich record of orbital forcing spanning about 45 million years.

There is some evidence for compound lake level cycles with periods longer than 413,000 years. A roughly 2,000,000-year-long cycle was first noted in the Newark basin (Stops 5.7) but seems to be present in the Fundy basin as well (Stop 10.3). An even longer-period cycle of 6,000,000 years may be indicated by patterns of taxonomic turnover in preliminary compilations of all pollen and spore data from the Newark (Cornet and Olsen, 1985; Olsen and Sues, 1986). The two million year cycle seems to correspond to the 6th term of eccentricity noted by Berger (1977), but the possible six million year cycle has no counterpart in the known range of astronomical forcing. Verification of these longer-term cycles is critical, not only for extending the known range of important astronomical forcing, but also for isolation of new, perhaps tectonically-driven elements of the Mesozoic climate system.

Van Houten cycles, and the compound cycles they comprise, are of great potential geochronologic value. The hierarchy of cycles permits the development of an unprecedented ultra-fine land-based time scale for the Newark Supergroup. The developing cyclostratigraphy for the Jurassic sequences of the Newark Supergroup has already been applied to a correlation over a distance of 700 km through five separate basins with very consistent results. This model allows a precision of less than 10,000 years and and provides an estimate of the duration of the entire Newark extrusive episode (Olsen and Fedosh, 1988; Olsen *et al.*, in prep.). This cycle-based time scale becomes particularly important when testing hypotheses of mass-extinction or climate change (Olsen *et al.*, 1987) as well as other forms of correlation, such as magnetostratigraphy or biostratigraphy.

DEPOSITIONAL ENVIRONMENTS AND EXTENSIONAL BASIN FILLING MODEL

(by R.W. Schlische and P.E. Olsen)

Newark Supergroup basins show two different types of depositional patterns. The first is mostly fluvial and fits an hydrologically-open basin model, characterized by: 1) basin-wide channel systems; 2) large- to small-scale lenticular bedding; 3) conglomeratic intervals which can stretch across the basin; 4) paleocurrent patterns that are often axial or that are dominated by one direction across the basin, indicating through-going drainage; and 5) a lack of evidence for large-scale lakes. However, there is evidence for ponding and the accumulation of palludal deposits. The second is mostly lacustrine and generally fits the accepted criteria for a hydrologically-closed basin model, which according to Smoot (1985), is characterized by: 1) a systematic increase in grain size towards all boundaries of a basin, 2) paleocurrent patterns away from each border of a basin, 3) the local provenance of coarse-grained sediments near the basin's margins, 4) the presence of evaporites or evaporite crystal casts, and 5) the cyclicity of the fine-grained sedimentary rocks in the central portion of the basin. The cyclical lacustrine beds have considerable lateral continuity (Olsen, 1988a), and the basin marginal areas can be dominated by deposits of lake-margin fluvial and deltaic sequences and alluvial fans. Within a basin, these two types of depositional systems have considerable persistence in time and are the largest-scale stratigraphic elements of the stratigraphy.

Newark Supergroup basins tend to display a gross tripartite stratigraphy consisting of a basal fluvial interval, overlain by a deeper-water lacustrine interval in which inferred lake depth generally decreases up-section, which in turn is overlain by a shallower-water lacustrine or fluvial interval. This is apparently a common pattern in many non-marine extensional basin systems (Lambiase and Rodgers, 1988). Traditionally, this stratigraphy has been interpreted in terms of rates of basin subsidence (see references in Lorenz, 1988): initial fluvial sedimentation occurred in a slowly-subsiding, hydrologically-open basin; following rapid subsidence, a deep lake occupied the basin, which then filled with sediment; fluvial sedimentation returned during waning subsidence. Other variants of this type of model are presented by Ressetar and Taylor (1988) and Mickus *et al.* (1988). Such explanations are, however, difficult to accept for the Newark Supergroup, in which the fluvial-lacustrine transition occurred at different times in different basins, implying no evident regional trends or generalities in the controls of basin subsidence.

In contrast to the above approach, Olsen (1988c), Olsen and Schlische (1988a-d) and Schlische and Olsen (in review) interpret the stratigraphy of rift basin deposits in terms of the evolving geometry of the basins. Outcrop studies [*e.g.*, Lyell, 1847; McLaughlin (*in* Willard *et al.*, 1959)] and seismic reflection profiles (*e.g.*, Hutchinson *et al.*, 1986) in some areas suggest a progressive onlap of younger strata onto the hanging wall basement block (Figure I.5), so that the basins were apparently growing in size through time and, more importantly, the depositional surfaces were growing in area. The stratigraphic models presented below assume uniform subsidence and a constant rate of input of sediment and water, and time-averaged dispersal of sediment basin-wide. Although the general conclusions are explained qualitatively, they are based on quantitative three-dimensional modeling discussed in section 5 and in Schlische and Olsen (in review).

If the subsidence rate is slow or the sedimentation rate is high (or both), sediments initially fill the basin, and excess sediment and water leave the basin, forming the fluvial interval. Accumulation rate thus equals subsidence rate. As the basin grows larger, the same volume of sediment added to the basin per unit time is spread over a larger depositional

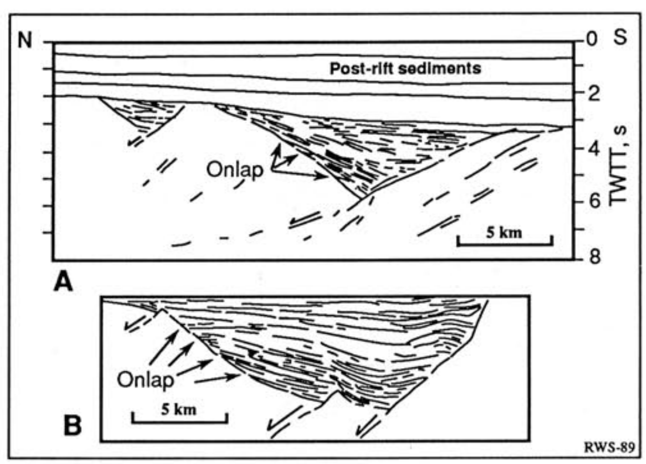

Figure I.5: Line tracings of seismic lines of half graben showing basic geometry of basins and onlap of basin strata onto hanging wall basement. Atlantis basin (A) traced from seismic profile in Hutchinson *et al.* (1986), and Railroad Valley basin (B) based on line drawing in Suppe (1985).

surface area. A point is eventually reached when the sediments just fill the basin. Subsequently, sediments no longer can entirely fill the basin to its outlet(s), and a lake can occupy the volume between the depositional surface and the lowest outlet. During this lacustrine interval, the accumulation rate systematically decreases following an inverse power law. Lake depth first increases as the difference in elevation between the depositional surface and the outlet grows. Excess water continues to flow out of the basin (as well as leave by evaporation) until the basin has grown to such a size that the inflow rate is precisely matched by the evaporation rate with no water flowing out of the basin (basin is hydrologically closed). The deepest lake occurs at this point; thereafter, lake depth decreases as a function of the growing size of the basin and losses to evaporation from a lake whose surface area is continually increasing. Of course, in the Newark, lake depths also fluctuated with Milankovitch periodicities. The above trends in lake depth refer to the deepest lakes during the wettest climate cycles, and we will subsequently call this parameter "maximum" lake depth.

If the subsidence rate is fast or the volumetric sedimentation rate is low (or both), lacustrine deposition occurs from the outset. Trends in accumulation rate and lake depth follow those outlined for the first case above. In both cases, if the subsidence rate slows sufficiently or stops, the basin will fill to its outlet, whereupon fluvial sedimentation will resume at an accumulation rate equal to the subsidence rate.

Even operating under its basic assumptions, the basin filling model can successfully explain the first-order stratigraphic development of the Triassic age portions of the Deep River, Dan River, Culpeper, Newark, Hartford-Deerfield and Fundy basins, each of which will be discussed in more detail in subsequent sections of this guidebook. The onset of lacustrine deposition occurred at different times in different basins (Figure I.3), and this is to be expected: Even if all the basins had started subsiding at the same time, the onset of lacustrine deposition would still be controlled by the basin's geometry and size, its subsidence rate, and the rate of sediment input.

The basin filling model operating under our basic assumptions fails to predict the earliest Jurassic stratigraphic sequences of the northern basins, in which lava flows are intercalated with and overlain by sediments showing a marked increase in accumulation rate and "maximum" lake depth. For reasons more fully developed later (see section 5), we attribute the increases in accumulation rate and lake depth to an increase in the rate of regional extension near the Triassic-Jurassic boundary (because it affected all of the northern basins at the same time), which resulted in a marked increase in basin asymmetry. We propose that this had the effect of shifting water and sediments to the border fault sides of the basins, decreasing the depositional and lake surface areas temporarily.

APPARENT POLAR WANDER PATHS AND PALEOMAGNETISM OF BASIN SEDIMENTARY ROCKS (by W.K. Witte and P.E. Olsen)

Although the North American apparent polar wander path (APWP) is relatively well known, there are discordances of approximately 12° between different interpretations of the APWP's during the latest Triassic and Early to Middle Jurassic (Figure I.6). In part, these differences can be attributed to different methods used in the synthesis of an APWP (Irving and Irving [1982] used a

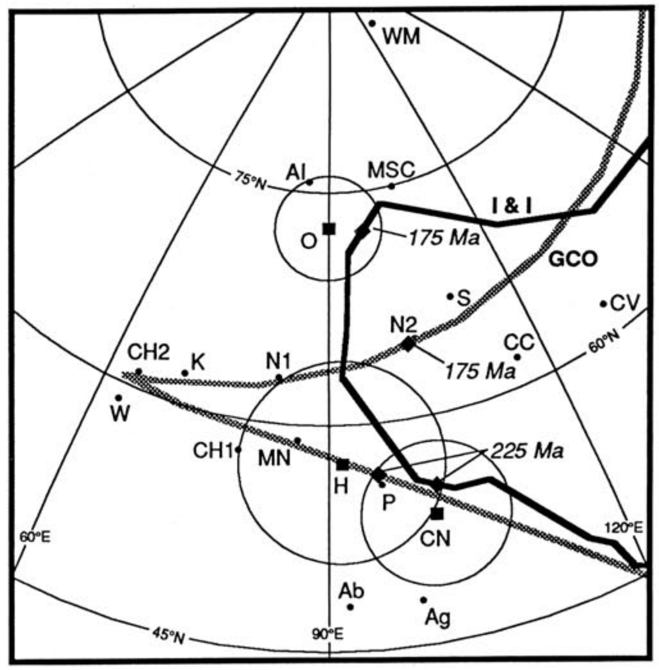

Figure I.6: Newark paleomagnetic pole positions compared to selected Triassic and Jurassic paleopoles and APWP interpretations for North America. Pole positions determined from the study of Late Triassic and Early Jurassic sediments of the Newark basin shown (squares) with their 95% confidence envelopes: CN, the late Carnian/early Norian syndepositional component pole in bedding coordinates; O, the overprint pole isolated in the late Carnian/early Norian study in geographic coordinates; H, the Hettangian syndepositional pole in bedding coordinates. Heavy lines show relevant segments of the APWP interpretations of Irving and Irving (1982) (labeled I&I) and Gordon *et al.* (1984) (labeled GCO), with 175 Ma and 225 Ma points indicated on each. Solid circles denote some of the principal Late Triassic or Jurassic paleopoles used in their syntheses and discussed in the text: AI, Anticosti Island, cited as 178±8 Ma in I&I; CH1, Chinle Formation, Redonda Member, cited as Late Triassic in GCO; CH2, Chinle Formation, Church Rock Member, cited as Norian in GCO; CV, Canelo Volcanics, cited as 151±2 Ma in GCO; K, Kayenta Formation, cited as Pliensbachian in GCO; MN, Manicouagan impact, cited as 215±5 Ma in GCO; MSC, mean southern continent pole position in North American coordinates (from Van Fossen and Kent, 1989); N1, early Newark trend igneous, cited as 195±5 Ma in GCO; N2, late Newark trend igneous, cited as 179±3 Ma in GCO; P, Popo Agie, cited as Norian-Carnian in GCO; S, Summerville Formation, cited as late Callovian in GCO and Pipiringos and O'Sullivan (1978); W, Wingate Formation, cited as Sinemurian in GCO; and WM, White Mountain intrusives, cited as 180 Ma in I&I. Additional poles are from: Ab, Abbott pluton of Maine with a radiometric age of 221±8 Ma (Wu and Van der Voo, 1987); Ag, Agamenticus pluton of Maine with a radiometric age of 228±Ma, respectively (Wu and Van der Voo, 1987); and CC, Corral Canyon in Arizona, cited as 172±5.8 Ma by May *et al.* (1986).

running average method, whereas Gordon *et al.* [1984] used the paleomagnetic Euler Pole method), but most of the difference between the two interpretations can be attributed to the different data sets used by the two syntheses. Late Triassic and Early Jurassic North American paleomagnetic data are primarily available from two geologic settings: the sediments of the southwestern U.S. and the igneous rocks of the Newark Supergroup basins.

Unfortunately, the interpretation of poles from the southwestern U.S. is complicated by the possibility of significant tectonic rotations of the Colorado Plateau (Hamilton, 1981; Steiner, 1986; Bryan and Gordon, 1986) and the presence of local and regional unconformities of uncertain duration in many of the Triassic and Jurassic sections in the southwest (Pipiringos and O'Sullivan, 1978). The igneous rocks of the Mesozoic basins of the Atlantic coast of North America have produced several paleomagnetic poles (*e.g.*, Smith and Noltimier, 1979) that figure prominently in the APWP syntheses of Irving and Irving (1982) or Gordon *et al.* (1984). However, the sediments of these basins have received relatively little attention and could provide an independent source of paleomagnetic poles for this time. The only comprehensive study of the sediments to use the thermal demagnetization technique is that of McIntosh *et al.* (1985). They determined a broadly correlative magnetostratigraphy for the basin but concluded that strong Mesozoic or Cenozoic overprints precluded the determination of useful paleomagnetic poles from the Mesozoic basin red beds. Because Newark Supergroup sedimentation spans a large part of the critical time during which the interpretations of North American APWP are most discordant, we have engaged in further investigations of the reliability of the Newark Supergroup sediments as recorders of the geomagnetic field. The purpose of these investigations and continuing work in the Newark and other basins is twofold: first, to test the possibility of determining reliable paleomagnetic poles for the Late Triassic and Early Jurassic; additionally, to develop a magnetostratigraphic framework within and between the Mesozoic basins of eastern North America.

Our thermal demagnetization experiments on samples from sites in the late Carnian to early Norian Stockton, Lockatong, and Passaic formations of the Newark basin shows that the magnetization of these rocks consists of two significant and consistent components both residing in hematite (Witte and Kent, 1989). A high unblocking temperature (typically above 660°C) magnetization was isolated from samples from 19 sites. The high temperature magnetization occurs in both shallow northerly (normal) and southerly (reversed) directions; samples from any single site are of the same polarity. The pattern of normal and reversed polarity sites forms a correlatable magnetic stratigraphy along three traverses perpendicular to strike (Witte and Kent, 1989). Further sampling at a scale finer than the average 200 meters between sites will resolve the details of the magnetostratigraphy. This magnetization corresponds to a paleomagnetic pole consistent with accepted APWP's for the Late Triassic (Irving and Irving, 1982; Gordon *et al.*, 1984). The similarity of this pole with accepted Carnian and Norian poles and the along-strike continuity of magnetozones leads us to believe this component was acquired nearly simultaneously with deposition.

A low unblocking temperature (typically between 300°C and 680°C) overprint was also isolated in the same study. This magnetization was invariably directed northward and down, significantly steeper than the higher temperature component, but shallower than the present field. In the

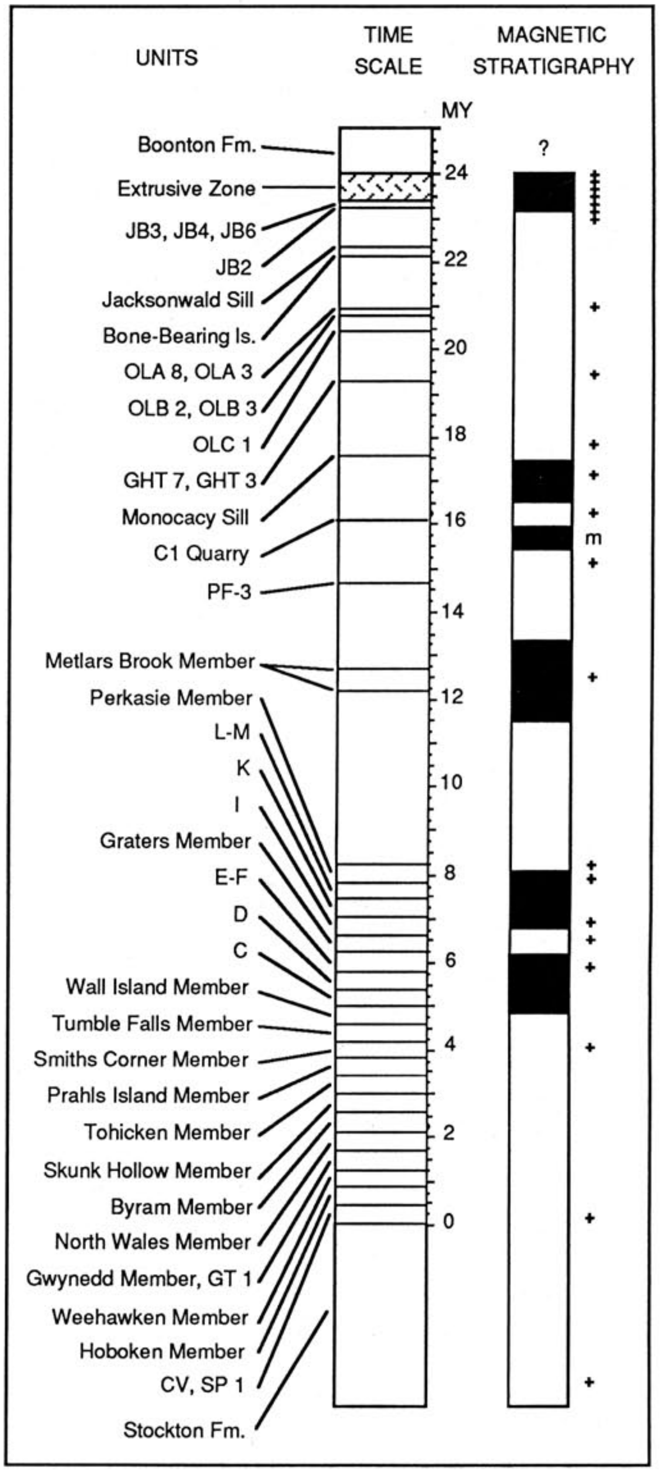

Figure I.7: Consensus magnetic polarity stratigraphy of the Carnian to Hettangian sediments of the Newark basin calibrated in time by Van Houten cycles. Black bars denote normal polarity zones. (+) indicate horizons sampled by W.K. Witte and (m) normal interval identified by McIntosh *et al.* (1985) for which Witte has no data; otherwise data of Witte and McIntosh *et al.* (1985) are in basic agreement. Units names include some abbreviations used by Cornet (1977a) for pollen-bearing levels because there are none available with formal designations.

Jacksonwald syncline a fold test indicates this remagnetization is post-folding (Witte *et al.*, 1989); however, the age of the remagnetization and the folding are poorly constrained. The corresponding paleopole (uncorrected for bedding tilt) lies significantly to the north of the APWP of Gordon *et al.* (1984) and proximal to the APWP of Irving and Irving (1982) at about 175 Ma. This pole is similar to the Middle Jurassic Moat Volcanic pole of the White Mountains and poles from Africa, Eurasia, and South America rotated into Middle Jurassic North American coordinates (Figure I.6) (Van Fossen and Kent, 1989). When considered in tilt-corrected coordinates, our Newark basin remagnetization pole is similar to the Newark igneous trend N2 pole determined by Smith and Noltimier (1979), suggesting a similar time and perhaps cause of acquisition. However, the Jacksonwald fold test indicates our remagnetization is only properly considered in uncorrected coordinates—the same may be true for the N2 pole. Radiometric data from the igneous intrusions of the Newark and Gettysburg basins have been interpreted as indicating a 200 Ma crystallization event and a later 175 Ma hydrothermal event (Sutter, 1988; see below). The remagnetization we observe in the sediments of the Newark basin is perhaps a chemical remnant magnetization acquired during the later hydrothermal pulse which was perhaps also responsible for the N2 magnetization.

Paleomagnetic study of 12 Jurassic sedimentary sites in the Watchung syncline of the Newark basin yields a similar interpretation of a two component magnetization. Sites from the Hettangian Feltville and Towaco formations and from a sedimentary interbed of the Preakness Basalt are all of normal polarity (Witte and Kent, 1988). The lithology and demagnetization behavior of these sediments are very similar to that observed in the Carnian and Norian sections. The pole corresponding to the tilt-corrected high temperature magnetization direction is significantly south of the Newark trend N1 pole of Smith and Noltimier, but falls within 4° of the pole from the Manicouagan impact (Figure I.6). The N1 pole, a compilation of poles from eastern North American Mesozoic extrusive rocks, lies intermediate between the remagnetization pole and the Jurassic sedimentary extrusive zone pole, suggesting that perhaps an overprint similar to that observed in the sedimentary rocks is still contaminating the N1 pole.

Further paleomagnetic study will concentrate on extending the present magnetostratigraphy (Figure I.7) upward through the youngest sediments in the Newark Supergroup, downward into the oldest sediments, and identifying the APWP cusp observed in the earliest Jurassic sediments of the southwest U.S. (Gordon *et al.*, 1984). Toward that goal we are testing the possibility of obtaining reliable data from sediments in other east-coast Mesozoic basins. Although results from the Hartford and Fundy basins indicate the overprints in those basins are more complicated and resistant to magnetic component analysis, it appears that it may be possible to distinguish magnetozones in the sediments of the Fundy basin. Samples from the type area of the Pekin Formation of the Wadesboro basin in North Carolina indicate a two-component magnetization (with an early reversed polarity and a normal overprint) very clearly resolved with thermal demagnetization corresponding to a similar pole position as determined from the Carnian portion of the Newark basin study.

EARLY MESOZOIC EASTERN NORTH AMERICAN MAGMATISM: FIRST-ORDER PROBLEMS AND CONSTRAINTS (by R.P. Tollo)

The numerous petrologic and geochemical studies concerning early Mesozoic eastern North American (ENA) magmatism in the last two decades have elucidated many previously unrecognized characteristics and identified a number of fundamental problems which must be addressed through future research. Perhaps the most fundamental petrologic problem concerns the nature and evolution of primary melts associated with the rifting process. A number of studies (*e.g.*, Weigand and Ragland, 1970; Ragland and Whittington, 1983a; Pegram, 1986; Whittington, 1988) have identified olivine-normative diabase of the ENA dike swarm as the most primitive magma type of the early Mesozoic system but have reached little consensus on the origin and petrogenetic evolution of such melts. Ragland and Whittington (1983a,b) recognized two groups of olivine-normative diabase on the basis of elemental enrichment trends and concentration of large ion lithophilic (LIL) elements. According to this work, all of the major ENA magma types could conceivably have been derived from one of the olivine normative groupings (de Boer *et al.*, 1988). Whittington (1988) revised the olivine-normative classification and proposed that the bimodal grouping of olivine-normative types resulted from melting of different source materials produced at different mantle depths and suggested that each group could be petrogenetically linked to a different ENA magma type.

Geochemical evidence bearing on the ultimate derivation of different ENA magma types from multiple mantle sources is, however, inconclusive. Initial Sr values (Gottfried, unpublished data) show a tendency to cluster in relation to magma type, but the relationship is not unequivocal. On the other hand, incompatible trace element ratios and chondrite- normalized rare earth element (REE) patterns from diabase dikes, chilled margins of diabase sheets, and basalt flows (Ragland *et al.*, 1971; Smith *et al.*, 1975; Froelich and Gottfried, 1988; Pegram, 1986; Tollo, 1988; Tollo *et al.*, 1988 and references therein) do suggest derivation from originally distinct source areas. Results from these studies point out the need for integrated petrochemical investigations capable of delineating source area characteristics and distinguishing from such data the geochemical signature of subsequent crustal fractionation processes.

The petrogenesis of early Mesozoic ENA magmas at relatively high crustal levels is also not presently clearly defined. The voluminous diabase sheets are generally considered to represent hypabyssal intrusions emplaced at high temperatures under relatively low confining pressures (Froelich and Gottfried, 1985), but these interpretations—based primarily on field evidence—remain largely unsubstantiated by rigorous mineralogical and thermochemical studies. In addition, the relationship between these presumably shallow-level magmas and the apparently contemporaneous lava flows remains, for the most part, undocumented. The bimodal chilled margin compositions of diabase sheets in basins with coexisting volcanics correspond to the high-titanium quartz-normative (HTQ) (Mount Zion Church, Orange Mountain, Talcott) and low-titanium quartz-normative (LTQ) (*e.g.*, Sander type D of Tollo, 1988) varieties of basalt (Tollo *et al.*, 1989). This obvious consanguinity notwithstanding, direct physical linkage between the sheets and the flows has been demonstrated possibly only by Ratcliffe (1988) in the Newark basin. As a result, the role of the diabase sheets in the magmatic plumbing system of each basin and the extent to which such bodies may have acted as holding chambers for liquids subsequently erupted as basalt remains unknown.

Petrogenetic relationships between diabase dikes of presumed early Mesozoic age (Figure I.8) and the basalt flows are also, for the most part, unresolved. Philpotts and Martello (1985) proposed that each of the three major dikes within and adjacent to the Hartford basin served as feeders for the three lava flows presently exposed within the basin. Field evidence demonstrating a dike-flow link is, however, available for only the lowermost (Talcott) and the uppermost (Hampden) basalt units; the compositional relations between the second basalt unit (Holyoke) and proposed feeder dikes are unproven. In other basins, field evidence indicates that the dikes are probably of the same general age as the lava flows (Olsen, 1984a; Froelich and Gottfried, 1988), but petrologic systematics have not been established. As a result, unified models describing the relative roles of diabase dikes, sheets, and basalt flows within the magmatic plumbing system of any particular basin are lacking.

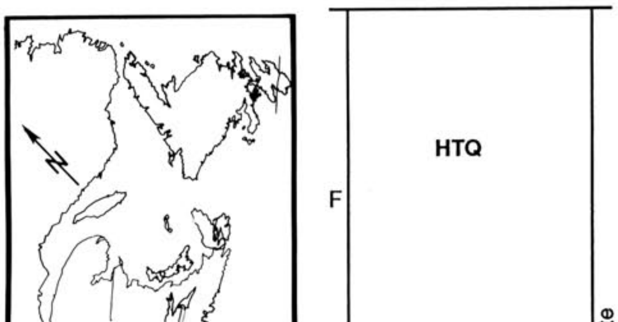

Figure I.8: Diabase dike patterns in eastern North America and proportion of major geochemical types in six broadly defined regions. Abbreviations are: AOD, alkalic to transitional olivine-normative diabase; HLO, high lithophile olivine-normative diabase; HTQ, high-titanium quartz-normative diabase; LLO, low lithophile olivine-normative diabase; LTQ, low-titanium quartz-normative diabase. Map and diabase types adapted from de Boer *et al.* (1988).

Recent studies of the paleontology and stratigraphy of Newark Supergroup sedimentary strata (Olsen, 1984a; Olsen and Fedosh, 1988) and the petrochemistry of the intercalated lava flows (Puffer and Lechler, 1980; Puffer *et al.*, 1981; Tollo, 1988) have raised new questions concerning the timing and geochemical systematics of basalt eruption. Puffer *et al.* (1981) established a geochemical correlation between the three major flow series of the Newark and Hartford basins and subsequent studies (Tollo, 1988; Tollo *et al.*, 1989) have documented further correlation of at least two of these basalt types to the Culpeper basin. The most striking aspect of this work is that the initial eruptions in each basin are nearly identical in composition (Puffer *et al.*, 1981; Tollo, 1988; Tollo *et al.*, 1989) and synchronous within 21,000 years (Olsen and Fedosh, 1988). Furthermore, the second volcanic cycle within each basin is characterized by a nearly identical range in composition defined by a series of flows which show no petrologically-consistent compositional trend and, as a package, are unlikely to represent fractionation products of the first unit (Tollo, 1988; Tollo *et al.*, 1988). Lack of systematic petrochemical variation in time is not uncommon in tholeiitic flood basalt provinces (see, for example, Mangan *et al.*, 1986) and, for the basalt series of a particular early Mesozoic basin, is probably indicative of derivation from short-lived, specially-isolated magma sources. However, the contemporaneous nature of petrochemically-similar eruptives across more than 650 km argues for near simultaneous reiteration of a series of comparable magma generating processes which varied consistently along strike through time. This regional correspondence in both composition and timing of a sequence of eruptive products which may have been derived from separate sources throughout the entire eruptive interval, raises a number of fundamental questions regarding the ultimate derivation of ENA magmas and the subsequent transport, storage, and eruption of such liquids. The present data base is insufficient to adequately quantify such characteristics of early Mesozoic magma genesis, but future investigations incorporating detailed isotopic studies should serve to place important constraints on many dynamic aspects of ENA magmatism and establish a basis for integrated models of large-scale magmatic processes.

DURATION AND AGE RELATIONS OF THE EASTERN NORTH AMERICAN THOLEIITES
(by P. E. Olsen)

Published K-Ar and $^{40}Ar/^{39}Ar$ isotopic dates from igneous rocks within the ENA tholeiite province (of McHone, 1988) show a very wide scatter which some have seen as indicating a protracted history of activity (Sutter and Smith, 1979; McHone and Butler, 1984; de Boer *et al.*, 1988), whereas others have stressed post-cooling alteration (Seidemann *et al.*, 1984; Sutter, 1985, 1988). Presently the "best" ages, in both an analytical and geological sense, are from mineral separates (hornblende) from high-titanium quartz-normative tholeiite diabase plutons which yield ages clustering around 201 Ma (Sutter, 1988). The geochemistry and physical relationships of the plutons suggest they are contemporaneous with the lava flows just above the palynologically-recognized Triassic-Jurassic boundary (Philpotts and Martello, 1985; Ratcliffe, 1988). The 201 Ma date is also probably the best current estimate for the age of the period boundary: the date is younger than the boundary date for most published time scales, although within their error estimates (Olsen *et al.*, 1987). Unfortunately, available

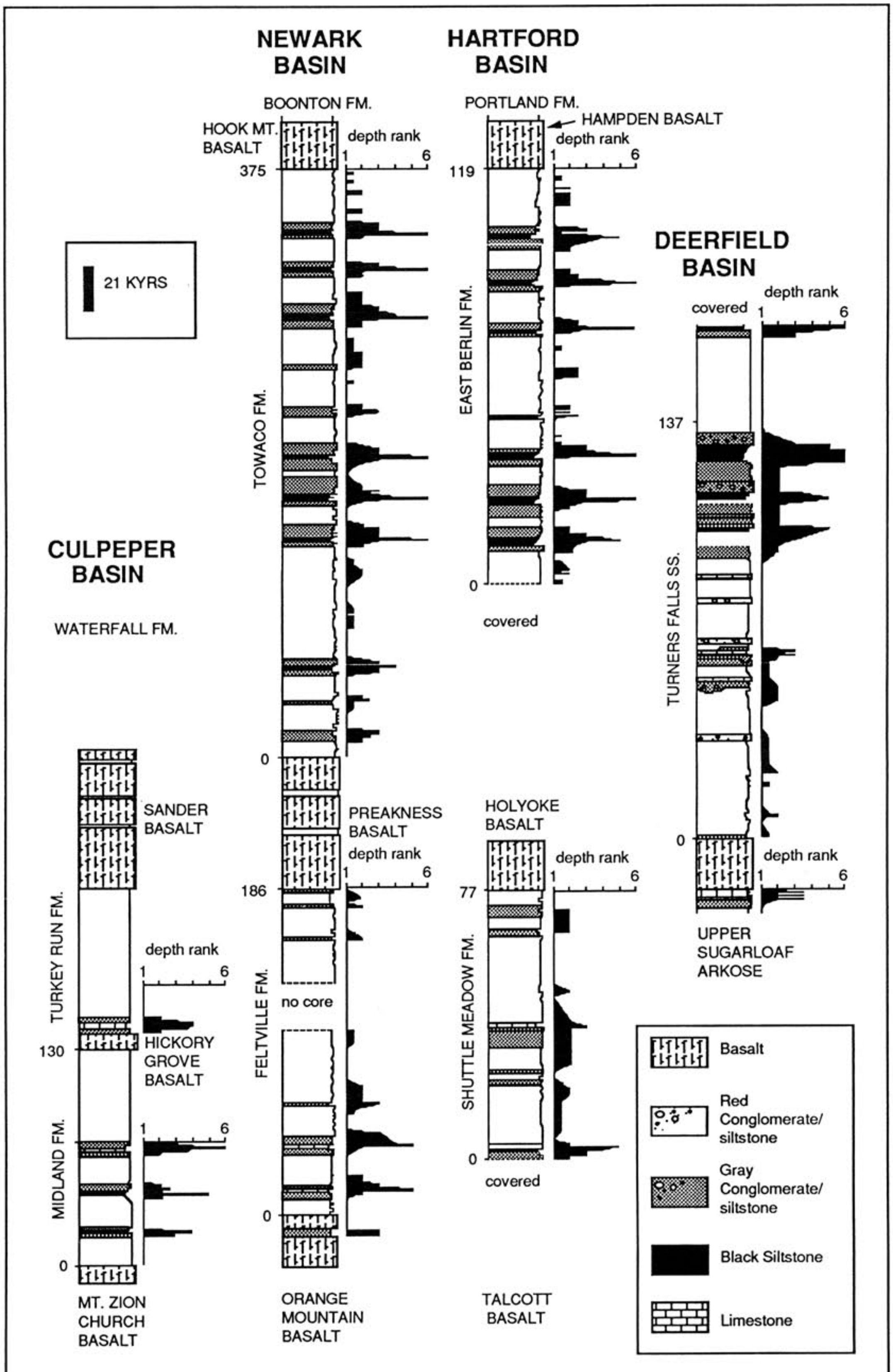

Figure I.9: Correlation of Early Jurassic age strata of Culpeper, Newark, Hartford, and Deerfield basins based on cyclostratigraphy (Olsen and Fedosh, 1988). All sections except for Turkey Run Formation are based on unambiguous outcrops and cores. Turkey Run Formation section is generalized, based on reconnaissance work of A.J. Froelich, G.R. Robinson, and J.P. Smoot. Sections shown as covered are seen at sections at other localities and are in line with the pattern expected for those intervals.

K-Ar and $^{40}Ar/^{39}Ar$ ages on most other ENA tholeiites are unreliable because of common post-crystallization alteration involving argon loss or addition and sometimes low-temperature resetting (Sutter, 1985, 1988).

At least two broad suites of ENA dikes can be recognized on the basis of orientation and composition (Figure I.8). The first is a northern suite stretching from Newfoundland to Virginia with orientations of N30°E to N60°E, with the largest number of these dikes occurring in southeastern Pennsylvania, New Jersey, Delaware, Maryland, and Virginia. Almost all of the dikes with this orientation are quartz-normative, but several are olivine-normative. The second is a southern suite stretching from Virginia to Alabama with orientations ranging from N35°W to N-S (Figure I.8). This suite is mixed olivine- and quartz-normative with no clear relationship between orientation and composition, although there appear to be some geographic groupings (McHone, 1988; *contra* Smith, 1987; and Ragland *et al.*, 1983). The chemistry of the plutons and lava flows tends to follow the geographic pattern of dike compositions with quartz-normative tholeiite sills present in the Danville basin and north and quartz-normative flows present in the Culpeper basin and north. Both olivine- and quartz-normative flows (in the Charleston area—Gottfried *et al.*, 1983) and plutons are present from Virginia to Georgia. Although there is reason to believe that the northern suite of quartz-normative tholeiites represents an event of short duration and consistent style, the duration of the southern suite is less clear.

Despite the apparent great spread of radiometric ages from northern quartz-normative tholeiites, the cyclostratigraphy of sediments interbedded with and surrounding the lava flows indicate a very short time interval, roughly 550,000±50,000 years (Figure I.9; Olsen and Fedosh, 1988). The minimal duration of the sediments between the lava flows can be estimated by counting the the number of 21,000 year cycles (*i.e.*, the Van Houten cycles). The phase relation of longer cycles through the entire igneous event allows for the estimation of the time represented by the lava flows themselves (Figure I.10).

As pointed out by Tollo (above), based on the cyclostratigraphy, the onset of the northern suite of extrusives was synchronous within 21,000 in all of the Newark Supergroup basins. In addition, the base of each major basalt flow formation in each basin correlate in time within 21,000 years, with the exception of the Hickory Grove Basalt in the Culpeper basin (Figure I.9). In other words, the geochemical correlations of flows of the Newark Supergroup by Puffer and Lechler (1980), Puffer *et al.* (1981), Philpotts and Martello (1985), and Tollo (1988) seem to be equivalent to time correlations.

As mentioned by Tollo (above) the connection between intrusive plutons and flows is controversial, and the connection between these and the numerous tholeiitic dikes is more controversial still. Nonetheless, in the northern region (Figure I.8) the match between the chemistry of the exposed flows, sheets, and the northern suite of quartz-normative dikes is so close, and the correlations in chemistry between the time-equivalent lava flows is sufficiently compelling, that a case can be made that most of the northern ENA quartz-normative tholeiites could have been emplaced during a very limited period of 0.5-0.6 million years. Interestingly, a similar short duration has been suggested for the geochemically-similar Deccan Traps of India (0.5 M.yr.; Courtillot *et al.*, 1988) and the Columbia River Plateau Basalts (1.5 M.yr. for >85% of the extrusives; Swanson, 1988).

On the other hand, the southern suite (Figure I.8) and the related Charleston-area flows could conceivably represent a longer interval of intrusion and extrusion, although the supporting data are controversial. Thompson (1968) and Bell *et al.* (1979) have identified a number of olivine-normative tholeiite dikes in South Carolina which exhibit reversed magnetic polarities, as do at least some of the quartz- and olivine-normative Charleston area flows (Phillips, 1983). No examples of primary reversed magnetizations are known from any of the quartz-normative flows (or interbedded strata), dikes or sills of the northern province (McIntosh *et al.*, 1985; W. Witte and D. Kent, pers. comm.). The presence of multiple polarity zones, provided they are not overprints, within the southern suite of dikes and flows indicates that the olivine-normative suite must be of longer duration than the northern quartz-normative suite.

The relative ages of the northern and southern suites remains enigmatic, however. Among authors who have not assumed the two suites are contemporaneous, the olivine-normative suite has usually been regarded as the oldest

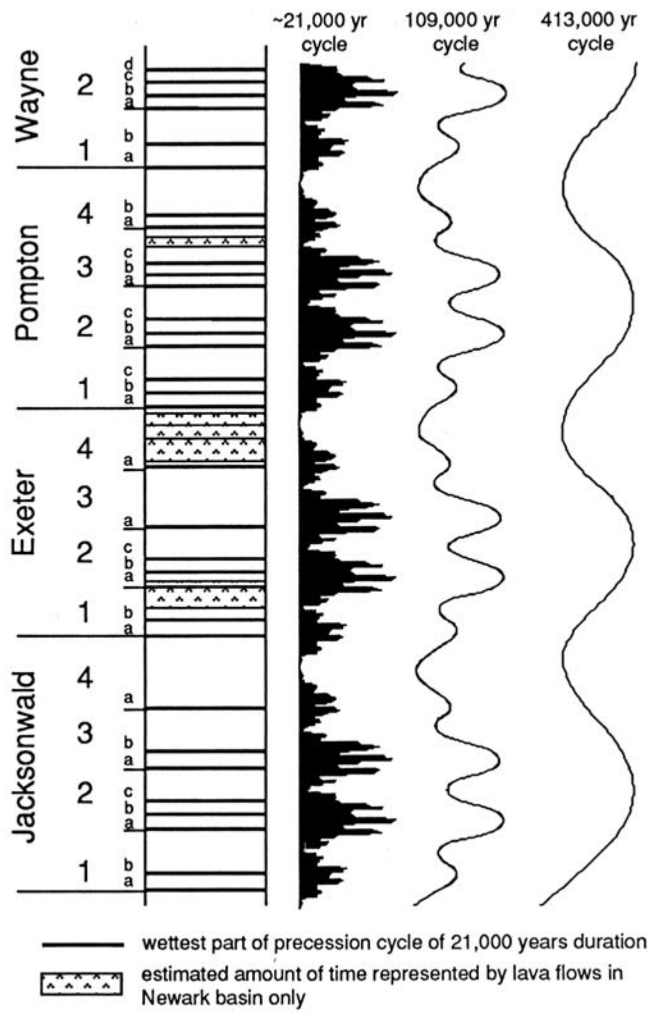

Figure I.10: Definition of time divisions for the extrusive zone in the northern Newark Supergroup showing the composite cyclostratigraphy on which it is based and the generalized interpretation of the cyclostratigraphy as superimposed orbitally-induced climate cycles. Note that the climate signals are considerably more complex than depicted here.

because of its "primitive" composition (Weigand and Ragland, 1970; Deninger *et al.*, 1975; Smith *et al.*, 1975; Ragland and Whittington, 1983a; Pegram, 1986; Whittington, 1988). However, cross-cutting relationships of at least one olivine-normative dike and some quartz-normative flows in the Culpeper basin indicate that the olivine-normative dikes are younger than at least some flows (Froelich and Gottfried, 1988). Because no examples of olivine-normative extrusives have been found within the Culpeper basin (or any exposed basin), the olivine-normative dikes could post-date all of the extrusives within the basin. Some olivine-normative tholeiites are intercalated between the quartz normative flows in the Charleston area (Gottfried *et al.*, 1983), however. This indicates that the production of both olivine- and quartz-normative tholeiite types was cyclic and broadly penecontemporaneous in the south. It should be noted, however, that the quality of the basalt in the cores is so poor that the olivine-normative units could be dikes, intruded into quartz-normative flows, rather than flows (A.J. Froelich, pers. comm.).

Paleomagnetic data of Smith (1987) suggest that the olivine-normative tholeiites of North Carolina are younger than the quartz-normative northern suite because the apparent paleopoles of the former are on the average 30° west of the latter. Some dikes in South Carolina and Alabama, however, have apparent poles indistinguishable from the northern suite. The significant magnetic overprints in most Newark igneous rocks means that each suite of samples must be judged on its own merit.

In summary: 1) The northern suite of quartz-normative tholeiite dikes, sills and flows were emplaced in a very short interval lasting about 550,000 years at about 201 Ma. 2) Paleomagnetic data show that the southern olivine- and quartz-normative tholeiites may have been emplaced over a longer time span than the northern quartz-normative tholeiites, although the northern tholeiites could be synchronous with one of the normally-magnetized zones in the southern suite. 3) Unambiguous cross-cutting relationships in the Culpeper basin show that at least some of the olivine-normative dikes are definitely younger than some of the northern quartz-normative flows. 4) Pole positions of North Carolina olivine dikes suggest they are younger than the northern quartz-normative tholeiites. 5) There is no evidence that any northern quartz-normative flows and intrusives post-date any of the southern suite of flows and dikes. 6) Therefore, it is still possible that most of the ENA series was emplaced in about a half million years, but that some dikes and flows in the south could be younger than those in the north. It must be emphasized that the number of available reliable dates and observed cross-cutting relationships are very few, and therefore any igneous chronology of the ENA systems is still highly speculative.

TECTONIC HISTORY (by P.E. Olsen and R.W. Schlische)

Paleostress Patterns

Dike swarms should be excellent indicators of the direction of principal stresses at the time of intrusion and therefore have been variously used in eastern North America to infer the evolution of the direction of extension during their emplacement (King, 1971; May, 1971; de Boer and Snider, 1979; de Boer *et al.*, 1988; McHone and Butler, 1984; McHone, 1988). The most striking aspect of the ENA dikes is their fanning pattern (Figure I.8): together with dikes in northeastern South America and western Africa, they appear to define a radial system. Considerable speculation has centered on this radial pattern, giving rise to hypotheses of extremely large-scale rift-related regional doming (May, 1971), hot spot activity (de Boer and Snider, 1979), and asteroid impacts (Dietz, 1986). Unfortunately, there has been no agreement on the relative limits or ages of tholeiitic dikes sets within the ENA province, as outlined above, or on the other continents. Obviously, if the dikes making up the apparent radial pattern consist of uniquely oriented sets of different ages, then there is no radial pattern or need to explain it.

The orientation of most of the northern suite of dikes is roughly parallel to the long axes of the Newark Supergroup basins, and those orientations are entirely compatible with the roughly NW-SE extension postulated to have formed the basins (Figure I.8) (Ratcliffe and Burton, 1985; Schlische and Olsen, 1988b). The orientation of the southern suite of dikes, however, is orthogonal or at a high angle to both the trend of the northern suite of quartz-normative dikes and the long axes of the Newark basins and is incompatible with extension in the basins.

The orientations of the southern suite of dikes, perpendicular to the trend of the basins (Figure I.8) argues that the rift basins they cross were essential inactive at the time of intrusion. This is supported by two sets of observations on plutons and flows in the southern basins. First, some of the olivine-normative plutons in the Deep River basin are vesicular even though they intrude stratigraphically low synrift strata (Justus, 1967). Second, the Charleston area basalt flows do not appear to show significant rotation or strong offset along half-graben border faults (Costain and Glover, 1983). Both observations suggest intrusion of the plutons and extrusion of the flows after at least most of the basin subsidence had ceased and perhaps after some erosion of basin strata had occurred. Thus, the entire olivine-normative suite of tholeiites and their associated but less common quartz-normative dikes and flows of the southern province could be post-rift. Unfortunately, with the exception of the Culpeper basin, there are no Jurassic strata in the southern basins cut by the olivine-normative dikes. Furthermore, no olivine-normative dikes are known to cut the youngest Jurassic strata and basalt flows. Therefore, it is still not possible to unequivocally determine either the timing of the cessation of NW-SE extension in the southern basins.

As currently understood the dikes seem to indicate NW-SE extension around 201 Ma (the Triassic-Jurassic boundary) from Newfoundland to Virginia. Close to this time E-W to NE-SW extension predominated in the south (Figures I.8, I.11). Perhaps this variability is related to competing extension fields between the opening of the Atlantic and the opening of the Gulf of Mexico and beginnings of the separation of South America and Africa, but at this time the picture still appears muddled.

Even a cursory examination of faults within Newark Supergroup basins reveals the presence of significant numbers with oblique and subhorizontal striae. These usually have been interpreted as reflecting a major interval of strike-slip or wrench activity within eastern North America (Sanders, 1962; Manspeizer, 1980, 1988; Swanson, 1982; de Boer and Clifford, 1988; Root, 1988; Venkatakrishnan and Lutz, 1988). However, much of the oblique movement appears to be explicable by essentially NW-SE extension acting on pre-existing Paleozoic faults, according to the Ratcliffe-Burton (1985) model (Schlische and Olsen, 1988b). With very few exceptions [*e.g.*, the Chalfont fault and narrow neck between Newark and

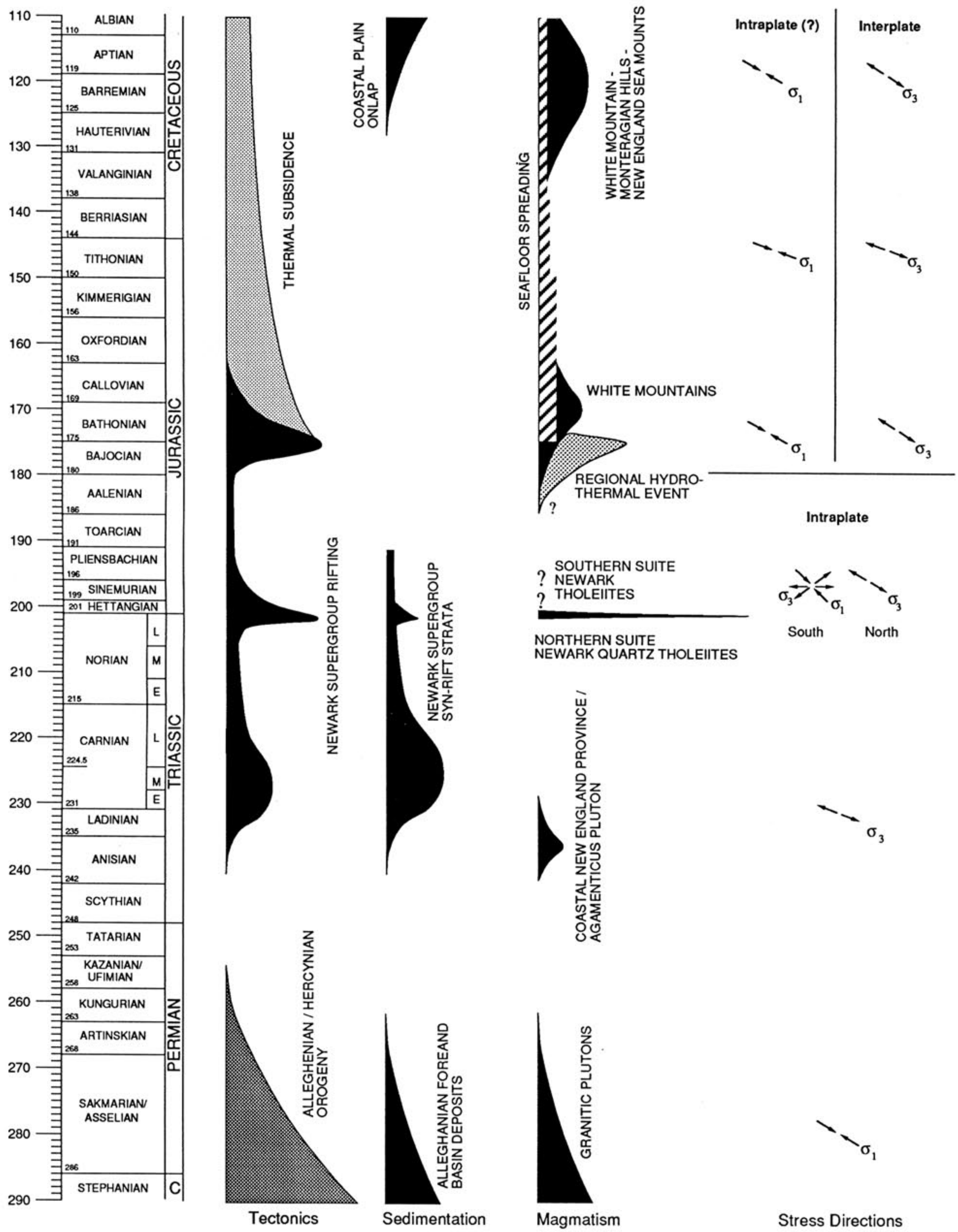

Figure I.11: Summary of events in the late Paleozoic and early to middle Mesozoic history of eastern North America. Numerical time scale adapted from Harland *et al.* (1982) scaled to the Early Jurassic and Late Triassic cyclostratigraphy shown in Figures I.9 and I.10 and the Triassic time scale of Webb (1981). Shaded areas represent relative and qualitative amounts of tectonic, sedimentary, and magmatic activity, increasing in magnitude to the right; no absolute scale implied. Some data from Klitgord and Schouten (1986), de Boer *et al.* (1988), and McHone (1988).

Gettysburg basins (section 5), and Minas fault zone (sections 9-11)], there is virtually no evidence for significant strike-slip offset of marker units or structures which cannot also be explained by normal faulting. Furthermore, the subhorizontal striae often overprint oblique and normal striae on NE-SW trending faults (formed during NW-SE extension) (de Boer and Clifford, 1988; Venkatakrishnan and Lutz, 1988) indicating a relatively young episode of strike-slip reactivation perhaps in response to more recent (Cretaceous and Tertiary) compressional stresses.

A growing body of evidence supports some (apparent?) NE-SW shortening in all Newark Supergroup basins. Again this has been related by some authors to a separate early Mesozoic compressional episode (Sanders, 1962, 1963; Swanson, 1982; Faill, 1973; Faill, *in* Olsen, Van Houten, *et al.*, 1988; Wise, 1988, section 8—this volume). This evidence consists of folds and warps, solution cleavage, thrust and reverse faulting, all of which are oriented consistent with NE-SW shortening (see sections 5, 7, 8, 9). Schlische and Olsen (1987, 1988b) argue that virtually all of this shortening occurs as a result of accommodation related to differential rift basin subsidence during the protracted period of NW-SE regional extension (see section 5). Because similar features appear to be common to a number of less well-known basins (Withjack and Gallagher, 1983), their origin remains one of the most pressing unsolved problems in extensional tectonics.

Summary of Permian-Tertiary History of Eastern North America

Virtually nothing about the history of the Newark Supergroup remains uncontroversial—from the present geometry of the basins to the largest scale rift tectonics. Therefore, the following capsule history of eastern North America and Figure I.11 are presented only as a guide for discussion and not as a summary of results.

1) Formation of strong basement anisotropies by compressional events during the several Paleozoic phases of orogeny responsible for the construction of the Appalachian orogen (700-260? Ma).

2) Intrusion of Coastal New England province of McHone (1988) and initiation of extension in eastern North America (230-240 Ma) perpendicular to the Appalachian orogen.

3) First pulse of extension in eastern North America and deposition of the volumetrically most important syn-rift strata (230 Ma, tapering off in intensity towards 201 Ma).

4) Second pulse of extension in at least northern part eastern North America very close to the Triassic-Jurassic boundary. Dramatic increase in accumulation rate and emplacement of most ENA tholeiites. (Main pulse during 550,000 years at about 201 Ma, tapering off afterwards.) Erosion may have begun by this time in the southern basins.

5) Third pulse of extension in northern basins resulting in intense block faulting, tilting, rotation, and massive hydrothermal alteration producing extensive remagnetization and $^{40}Ar/^{39}Ar$ resetting. Erosional dissection of northern basins begins, possibly during the last phases of rifting. First sea floor spreading and intrusion of Jurassic portion of the White Mountain series also temporally related (185-165 Ma).

6) Thermal contraction becomes main mechanism of subsidence in eastern North America (170 Ma to present).

7) Beginnings of presently-exposed portion of coastal plain onlap; intrusion of series of dikes in New England; second pulse of White Mountain series; New England seamounts; intrusion of lamprophyric "great stone dome" in Baltimore Canyon trough and other plutons off southern Georgia; emplacement of Shenandoah igneous province, kimberlite belt, Notre Dame and Orpheus provinces, and other diverse, poorly-understood igneous events (145-90 Ma).

8) Continuation of thermal subsidence, with apparent NE-SW to NW-SE compression common but not universal in eastern North America (McHone, 1988), occasional intrusive and extrusive events (Eocene Shenadoah igneous province) (90 Ma to present).

Crustal-Scale Tectonics

The controversy and dynamically-evolving concepts of major chronological events affecting the exposed Newark Supergroup translate to apparent chaos in large-scale models of the responsible tectonic processes. There is not even a consensus on the geometry of the basins and their relation to boundary faults and deeper crustal structure. The models of asymmetrical extension of Manspeizer (1987, 1988) and Hutchinson and Klitgord (1988a) are thus not presently testable because there is no first-order observational agreement. In particular, there is no agreement on the presence of a shallow detachment beneath the basins in eastern North America. A comparison of the two leading models of extension (Figure I.12) shows only a superficial resemblance to postulated eastern North American crustal geometry (compare to Figure I.2) Note especially that the simple shear model requires one margin to have a shallow detachment (less than 10 km), and there is very little observational evidence for such a detachment in either eastern North America or Morocco.

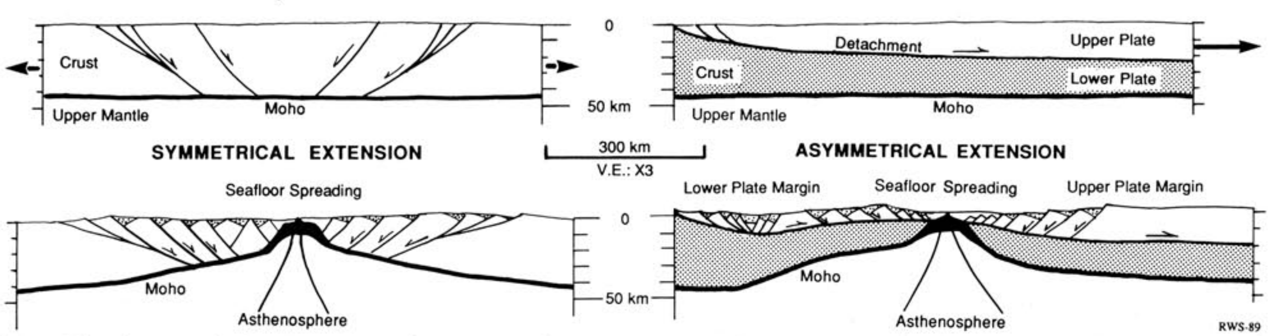

Figure I.12: Symmetrical and asymmetrical models of crustal cross-sectional geometry (vertically exaggerated) at initiation of rifting and initiation of sea floor spreading in eastern North America. Cross-sections based on Hellinger and Sclater (1983) for the symmetrical model and on Klitgord *et al.* (1988) for the asymmetrical models. Models modified to reflect similar thicknesses for lithosphere.

PATTERNS OF BIOLOGICAL CHANGE
(by P.E. Olsen)

Like their modern counterparts, early Mesozoic ecosystems responded to a hierarchy of extrinsic environmental perturbations as well as to intrinsically-caused diversification and extinction of taxa and evolution of new modes of life. The Newark Supergroup is very unusual in richly recording not only the ebb and flow of relatively short-term environmental perturbations but also long-term changes in communities spanning over 45 million years.

The most obvious extrinsic perturbations recorded in the Newark Supergroup are the Van Houten cycles and longer-term cycles so characteristic of the lacustrine sequences. Their effects were obviously most profound for the lacustrine ecosystems, which responded in two fundamentally different ways. First, the dramatic changes in water depth which produced the lake-level cycles were the main controls on lacustrine ecosystem efficiency, which in turn controlled the amount of organic carbon entering the sediments (Manspeizer and Olsen, 1981; Olsen, 1984a). During lake high stands the surface area to depth ratio was relatively low as was ecosystem efficiency and, as a consequence, a proportion of the carbon of organic production in and around the lake escaped to the sediment. This escaped, energy-rich material included fish, reptiles, and large plants as well as the usual microscopic members of the lower food chain. During low lake stands, wind mixing was effective at oxygenating the entire water column and very little organic material was preserved. The most obvious aspect of the Newark lacustrine record—its cyclicity—forces us to recognize that changing climate was the main extrinsic control on the metabolism of lakes (Olsen, 1984a), not ecological succession or eutrophication as is commonly assumed (Wetzel, 1983).

The second way lacustrine ecosystems responded to lake-level changes is by geologically-rapid evolution and adaptation within populations in the lake itself. Some Newark fish assemblages are characterized by closely-related groups of fishes called species flocks which apparently evolved during the high stands of lakes only to become extinct during low stands (McCune *et al.*, 1984—see Stop 6.2). Thousands of fish species evolved and went extinct to the beat of the cycling lakes during Newark history.

Another cyclical ecosystem pattern seen in the Newark Supergroup is a response to the longer-term climate cycles. Within individual Van Houten cycles there is usually a change in dominance of fish genera. These changes seen in individual Van Houten cycles are apparently recapitulated in the longer term cycles (Olsen, 1988b). This is best seen in the Lockatong Formation of the Newark basin (Stop 6.6) but is also seen in the Cow Branch Formation of the Danville-Dan River basin (Stop 2.2). The change seen in dominance is probably a reflection of changes in salinity.

Terrestrial ecosystems also must have felt the pressures of the cyclically-changing climate. However, because terrestrial environments have higher ecosystem efficiency than lacustrine ones and the environments commonly have higher depositional energy, our record of the responses to those changes is very sparse, even where exposure is excellent.

Perhaps the largest perturbation recorded in the Newark Supergroup is the Triassic-Jurassic boundary extinction. On a global basis it is one of the most pronounced of the 13 or so often cited mass extinctions which punctuate the Phanerozoic record. First recognized as a mass extinction in marine sections (Hallam, 1981; Raup and Sepkoski, 1982), roughly 43% of terrestrial vertebrate families were apparently extinguished (Figure I.13) (Olsen and Sues, 1986; Olsen *et al.*, 1987). The Newark Supergroup provides an unprecedented opportunity to examine the fine-scale structure of the Triassic-Jurassic mass extinction in continental environments. Van Houten cycles and the compound cycles they make up provide the time control vital to the understanding of the mechanisms behind mass-extinctions.

In the Newark Supergroup, a large number of at least local vertebrate and palynomorph extinctions are concentrated around the palynologically-identified Triassic-Jurassic boundary, with survivors constituting the earliest Jurassic assemblages, apparently without the introduction of new taxa (Figure I.13). During most of the Newark Triassic record pollen and spore diversity fluctuates between 30 and

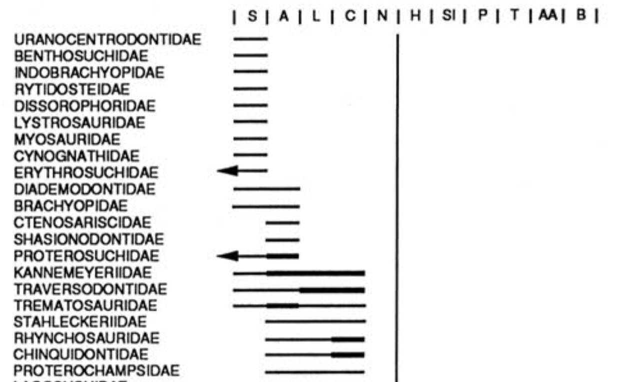

Figure I.13: Range chart for Triassic and Early Jurassic continental reptiles and amphibians. Thin bars indicate compiled global ranges, and thick bars represent ranges in the Newark Supergroup. Abbreviations for standard ages are as follows: S, Scythian; A, Anisian; L, Ladinian; C, Carnian; N, Norian; H, Hettangian; SI, Sinemurian; P, Pliensbachian; T, Toarcian; AA, Aalenian; and B, Bajocian. Adapted from Olsen *et al.* (1987).

40 taxa (Olsen and Sues, 1986). Triassic strata near the boundary have at least 70 pollen and spore taxa (Cornet, pers. comm.). The palynofloral transition is marked by the dramatic elimination of this high-diversity Triassic pollen assemblage, with the survivors making up a Jurassic assemblage of very low diversity overwhelmingly dominated by the conifer pollen type *Corollina*. The extinctions include a large number of species of angiosperm-like pollen (Cornet, 1986), and based on cyclostratigraphy, the transition took place over an interval of less than 40,000 years. During the Early Jurassic, palynofloras never recovered their previous levels of diversity within the region of the Newark Supergroup. The terrestrial vertebrate transition is not so well constrained; however, some dominant taxa of the Late Triassic, such as phytosaurs and procolophonids, are known from osseous remains from strata estimated at about 600,000 years older than the boundary based on Van Houten cycles, and ichnofaunules of "typical" Late Triassic aspect are known from strata about 6,000,000 years older than the palynologically defined boundary (Olsen and Baird, 1986). Newly-discovered ichnofaunules which bridge the temporal gap between those of typical Triassic aspect and the Triassic-Jurassic boundary promise to provide fine-scale control on the rate of the boundary transitions. Several footprint assemblages from just above the palynologically-dated Triassic-Jurassic boundary are already Jurassic in aspect and almost identical to typical Connecticut Valley assemblages.

Rich osseous assemblages from the McCoy Brook Formation of Nova Scotia (Stop 11.3) are characteristically Early Jurassic in aspect and completely lack the dominant "Late Triassic forms", which together with the ichnofossils show that by the earliest Jurassic, the extinctions had already occurred. Based principally on palynological correlations, the hypothesis that these continental taxonomic transitions were synchronous with the massive Triassic-Jurassic marine extinctions seems corroborated. Thus far,

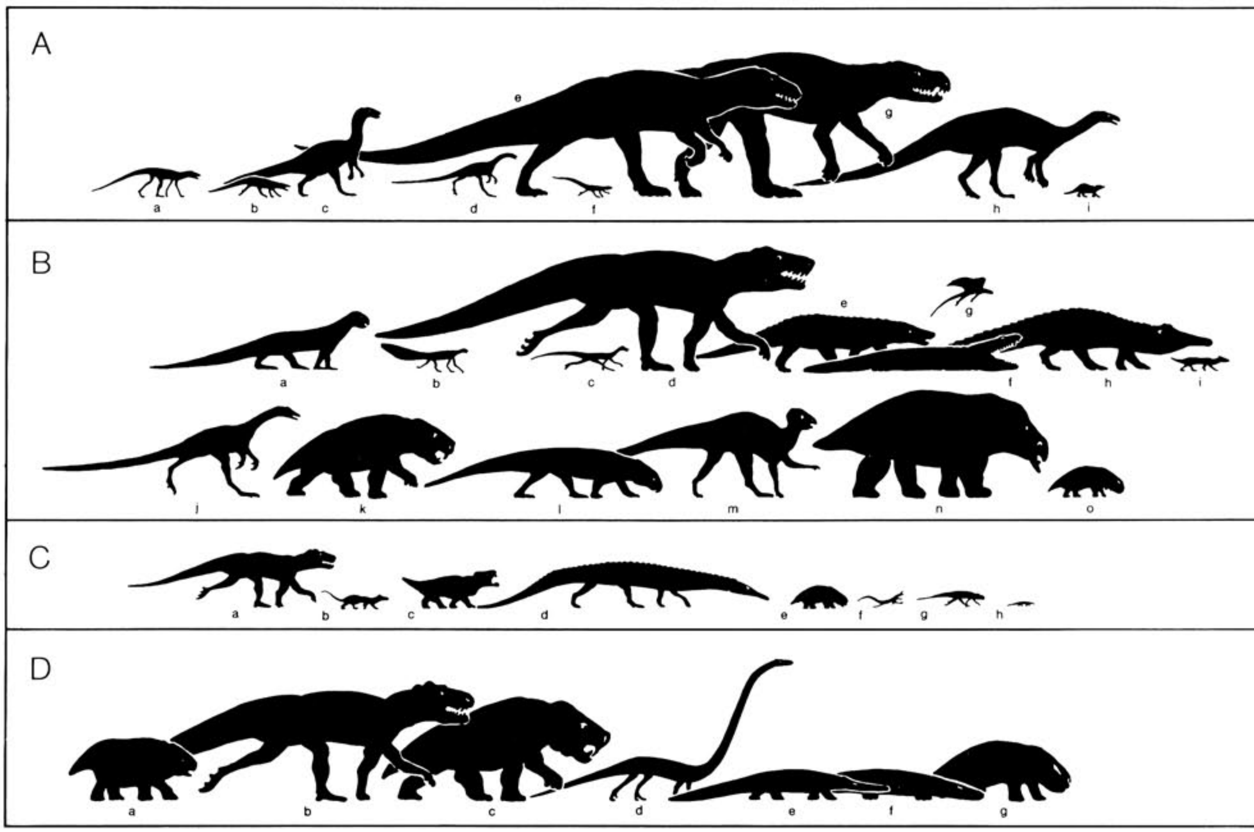

Figure I.14: Representative Triassic and Jurassic age tetrapods from the Newark Supergroup. A) Early Jurassic tetrapods: a, small sphenosuchid crocodylomorph; b, protosuchid crocodylomorph *Stegomosuchus*; c, "fabrosaurid" ornithischian dinosaur; d, small theropod dinosaur *Podokosaurus*; e, large theropod dinosaur (known only from footprints); f, sphenodontid cf. *Glevosaurus*; g, track maker of *Otozoum*-type footprints reconstructed as a large sphenosuchid crocodylomorph; h, prosauropod dinosaur *Ammosaurus*; i, trithelodont mammal-like reptile *Pachygenelus*. B) Late Triassic (middle-late Carnian) tetrapods: a, trilophosaurid archosaur; b, "deep-tailed swimmer"; c, tanystropheid *Tanytrachelos*; d, rauisuchid archosaur; e, aetosaurid archosaur *Stegomus*; f, labyrinthodont amphibian *Metoposaurus*; g, gliding lepidosaur *Icarosaurus*; h, phytosaur *Rutiodon*; i, chiniquodontid mammal-like reptile *Microconodon*; j, small theropod dinosaur cf. *Coelophysis*; k, traversodont cynodont mammal-like reptile *Scalenodontoides*; l, rhynchosaur cf. *Hyperodapedon*; m, small ornithischian ("fabrosaurid") dinosaur; n, dicynodont mammal-like reptile *Placerias*; o, procolophonid *Leptopleuron*. C) Late Triassic (early Carnian) tetrapods: a, small rauisuchid archosaur; b, very advanced mammal-like reptile similar to *Tricuspes*; e, traversodont mammal-like reptile *Massetognathus*; d, armored archosauromorph *Doswellia*; small procolophonid; f, small (?) lizard; g, small sphenodontid; h, (?) salamander. D) Middle Triassic (Anisian) tetrapods: a, dicynodont mammal-like reptile; b, rauisuchid archosaur; c, traversodont mammal-like reptile cf. *Exaeretodon*; d, tanystropheid lepidosaur *Tanystropheus*; e, labyrinthodont amphibian *Aphaneramma*; f, capitosaur labyrinthodont; g, procolophonid *Sclerosaurus*; h, trilophosaurid archosaur; i, aetosaurid archosaur.

the hypothesis of an extremely rapid, perhaps catastrophic, taxonomic turnover at the Triassic-Jurassic boundary, synchronous in continental and marine realms, remains consistent with all the available data.

As is the case for the Cretaceous-Tertiary boundary, plausible causes for the extinctions include: 1) competitive superiority of newly-evolved taxa, 2) climate change, 3) very large-scale volcanic eruptions, and 4) giant bolide impacts. Hypotheses explaining the extinctions as a result of competitive replacement are not supported by the observed pattern of taxonomic change because the surviving taxa coexisted with those that went extinct for millions of years before the boundary. Jurassic strata do seem to indicate changes in climate at many places in the world, but these changes seem neither synchronous with each other nor with the large-scale faunal and floral changes. The northern suite of tholeiitic extrusives which characterize Early Jurassic sequences in the Newark Supergroup, in the rift basins in western Africa, and in the basins of southern Africa **post-date** the Triassic-Jurassic boundary and the associated extinctions by about 60,000±20,000 years (based on Van Houten cycles—Olsen, 1986), which is close in time but hard to understand as a causative agent. A plausible cause could be the great bolide impact which produced the Manicouagan impact structure of Quebec (Olsen *et al.*, 1987). However, the best available dates from Manicouagan range from 206±6 to 215±4 Ma (Olsen *et al.*, 1988), compared to 201±2 Ma for the boundary (Sutter, 1988). This difference may be attributable to excess Ar in the impact melt. Systematic, multiple-system redating of Manicouagan is underway, as is a search for an impact ejecta layer in the Newark Supergroup. Nazarov *et al.* (*in* McLaren, 1988) report a shocked quartz horizon at the marine Triassic-Jurassic boundary in Austria, which supplies some support for the impact hypothesis. Unfortunately, Hallam (1988) has not yet been able to reproduce their results.

Literature tabulations (Sepkoski, 1986) suggest a marine mass extinction at the Carnian-Norian boundary. No interval of comparable taxonomic turnover is apparent in Newark Supergroup strata straddling the Carnian-Norian boundary (as dated by palynostratigraphy), either in vertebrates or palynomorphs. A large faunal and palynofloral turnover is seen, however, within Newark early and middle Carnian age strata. Either Newark strata are misdated or the marine and terrestrial extinctions were not synchronous. Parenthetically, Sepkoski (1986) suggests the apparent marine Carnian-Norian mass extinction could be an artifact of very high ammonite evolution rates during this time. Therefore, evidence from the Newark Supergroup does not suggest a mass extinction event at the Carnian-Norian boundary or anywhere in the Triassic or Early Jurassic, except at the Triassic-Jurassic boundary.

The Triassic-Jurassic faunal and floral extinctions stand in dramatic contrast to the background taxonomic turnover rates during the Triassic and Early Jurassic as seen in the Newark Supergroup (Cornet and Olsen, 1985). In addition, they seem to have occurred during an interval of overall increasing diversity (Olsen *et al.*, 1988). The extraordinarily fine time scale provided by the orbitally-controlled lake-level cycles may provide the basis for rigorous tests of the timing of faunal and floral change across the Triassic-Jurassic boundary and its possible association with the Manicouagan impact.

In addition to the cyclical ecosystem change recorded in the lacustrine strata of the Newark and the apparently abrupt Triassic-Jurassic mass extinctions, there is also a slow accumulation of change through the entire Newark record (Figures I.13, I.14). In the vertebrate assemblages we see the transition between a mammal-like reptile-dominated community in the earliest Late Triassic (Stop 3.2) to the more typical phytosaur-dominated Late Triassic type of assemblage characteristic of the rest of the Triassic (Stop 3.3). The mammal-like reptile-dominated assemblage is unique in the Northern Hemisphere and is more like the Middle and early Late Triassic age assemblages of South America. Dinosaurs become more and more common, as represented by ichnofaunules, towards the Triassic-Jurassic boundary, although apparently without extinction of the typically "Triassic" forms until somewhere close to the boundary itself. In the Jurassic age portions of the Newark there is little apparent change.

PART II: FIELD EXCURSION

1. DEEP RIVER BASIN, NORTH CAROLINA

GEOLOGY OF THE DEEP RIVER BASIN

(by P.J.W. Gore, J.P. Smoot, and P.E. Olsen)

Introduction

The Deep River basin is the southernmost of the exposed rift basins of the Newark Supergroup (Figure I.1). The basin ranges from 9 to 25 km wide and is 240 km long. The Deep River basin is situated near the eastern edge of the North Carolina Piedmont, where it is nearly surrounded by Late Precambrian and Cambrian metasedimentary and metavolcanic rocks of the Carolina slate belt. It is bordered on the northeast by gneiss, schist, and intrusive rocks of the Raleigh belt and is overlapped locally on the southeast by Cretaceous and younger sediments of the Atlantic Coastal Plain (Figure 1.1). The basin is bounded on the east and southeast by the Jonesboro fault system (a steeply-dipping normal fault zone), and on the northwest by a series of minor faults and unconformities (Figure 1.1). The overall structure of the basin is a half-graben in which rocks dip southeastward toward the Jonesboro fault system.

The Deep River basin is comprised of three interconnected sub-basins: from north to south they are the Durham, Sanford, and Wadesboro sub-basins (Figure 1.1). The Durham and Sanford sub-basins are separated by a constriction and basement high called the Colon cross-structure, named for the town of Colon. The Sanford and Wadesboro sub-basins are separated by the Pekin cross-structure and by Coastal Plain overlap.

Sedimentary rocks of the Deep River basin have been correlated with the European section using spores and pollen. The basal Pekin Formation of the Colon cross-structure has produced the oldest palynomorph assemblages, which are dated as early Carnian (Olsen *et al.*, 1982; Traverse, 1986, 1987). The rest of the Pekin Formation and overlying Cumnock Formation of the Sanford sub-basin produce assemblages of middle Carnian age. Younger rocks are probably present in the Sanford sub-basin because more than 1000 m of undated Sanford Formation red beds overlie the uppermost dated beds, which are in the Cumnock Formation. So far, no samples from the Sanford Formation or from the Durham sub-basin have produced spores or pollen. However, microflorules from lacustrine rocks of the Wadesboro basin and fish assemblages from the Durham basin suggest a late Carnian age (Olsen *et al.*, 1982; Cornet, 1977a). An upper age limit may be placed on the sedimentary rocks in the basin using lithostratigraphic inference. The sedimentary rocks of the basin are extensively intruded and metamorphosed by sheets and dikes of predominantly olivine-normative diabase of Jurassic age (see Part I). Many of the larger dikes that trend north and northwest can be traced across the basin and into slate belt rocks and beneath Coastal Plain strata by using aeromagnetic maps (Bond and Phillips, 1988). Basalt flows, however, are absent. In the northern and central basins of the Newark rift system, basalt flows are present just above the Triassic-Jurassic boundary, therefore suggesting that all Deep River basin strata are pre-Jurassic in age.

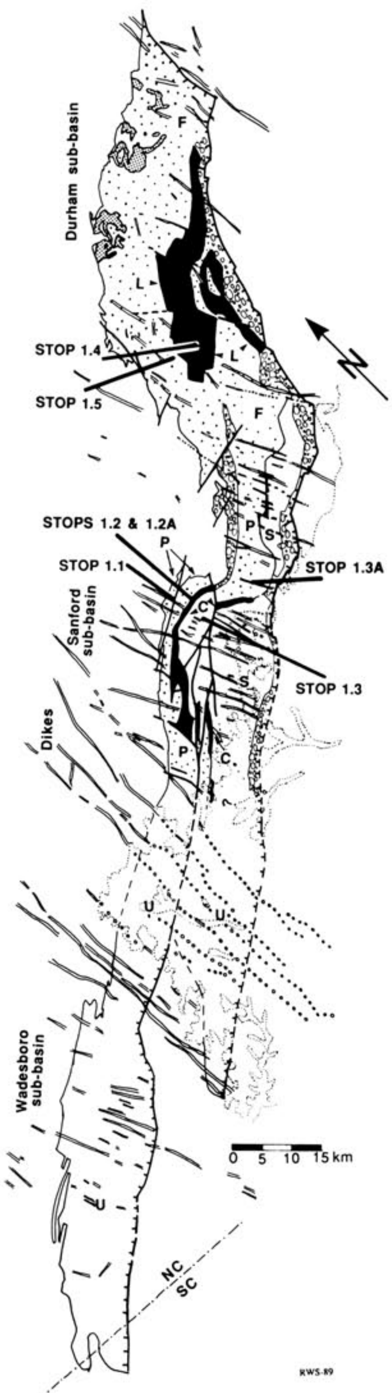

Figure 1.1: Geologic map of the Deep River basin, North Carolina and South Carolina. Thin, double lines represent dikes; regular stipples represent diabase intrusions; and black represents predominantly lacustrine deposits. Abbreviations are: F, fluvial deposits; L, lacustrine deposits; P, Pekin Formation; C, Cumnock Formation; S, Sanford Formation; U, undifferentiated deposits. After Bain and Harvey (1977) and Brown *et al.* (1985).

Table 1.1: Stratigraphy of the Deep River basin, South Carolina and North Carolina (after Emmons, 1856; Reinemund, 1955; Bain and Harvey, 1977; Brown et al., 1985; Gore, 1986a; Traverse, 1986; and Hoffman and Gallagher, 1988, in prep.).

	Units	*Thick-ness (m)*	*Age*	*Description*
Durham sub-basin	Lithofacies Association III	?	?Carnian	Reddish-brown, medium to very coarse fluvial and alluvial clastics
	Lithofacies Association II	?	Late Carnian	Pink to red, medium to coarse feldspathic sandstones and reddish-brown bioturbated siltstone and mudstone with nodular limestone zones; meandering stream, floodplain, and overbank deposits
	Lithofacies Association I	?	?Carnian	Gray feldspathic sandstone and reddish-brown bioturbated siltstone and mudstone; braided stream and floodplain deposits
	Western border conglomerate	?	?Carnian	Buff, coarse fluvial and alluvial clastics; quartz, granite, quartzite, aplite, and slate clasts
	Tan arkosic Ss	?	?Carnian	Tan, medium to coarse fluvial clastics
	Red Ss-mudstone	?	?Carnian	Red to brown, fine to coarse fluvial clastics with caliche horizons
	Chert-Ls-mudstone	?	?Carnian	Fine clastics, carbonates, and cherts deposited in a playa (?) lake
	Eastern border fanglomerate	?	?Carnian	Red, coarse alluvial fan clastics; clasts derived from Piedmont to the east of the Jonesboro border fault
Sanford sub-basin	Sanford Fm.	1240	?? Car.-Nor.	Mostly red to brown, coarse to fine fluvial and alluvial clastics; minor gray, fine to coarse fluvial-deltaic-lacustrine clastics
	Cumnock Fm.	305	Middle Carnian	Mostly gray and black, fine to medium lacustrine and paludal clastics; thin coal seams near base
	Pekin Fm.	1240	E.-M. Carnian	Red to brown, fine to coarse fluvial clastics; distinctive, quartz-rich, alluvial fan conglomerate ("millstone grit") near base
Wadesboro sub-basin contains undifferentiated, Carnian-Norian, coarse to fine terrigenous clastics, including type section of the Pekin Formation (Campbell and Kimball, 1923). Middle lacustrine portion is Late Carnian (Cornet, 1977a).				

Lithostratigraphy

The sedimentary rocks of the Deep River basin, like those of the other Newark rift basins, are dominated by red to brown terrigenous clastics deposited in continental environments. The rocks of the Deep River basin are referred to collectively as the Chatham Group (Emmons, 1856; Olsen, 1978; Froelich and Olsen, 1984; Brown *et al.*, 1985), and the general stratigraphy has been recognized since the 1850's. Emmons (1856, p. 228) divided the rocks of the Sanford sub-basin into three formations: an upper unit and a lower unit of red terrigenous clastics, separated by a unit of gray to black shale, coal, and sandstone. These divisions were formally named by Campbell and Kimball (1923) (in ascending stratigraphic order) the Pekin, Cumnock and Sanford formations (Table 1.1). The distribution and character of these formations has been described in detail by Reinemund (1955) in the Sanford sub-basin, where they are known to vary laterally in lithology, texture and thickness, and to be somewhat intergradational.

The formations in the Sanford sub-basin can be traced northward into the Colon cross-structure, but the Cumnock is apparently replaced laterally by coarser-grained, red to brown or tan sandstones similar to the Pekin and Sanford formations (Reinemund,1955); gray to black siltstones have not been traced northward into the central part of the Durham sub-basin or southward into the Wadesboro basin. The Cumnock is absent throughout most of the Colon cross-structure, and the Pekin and Sanford formations are in direct contact.

Formal stratigraphic subdivision is confined to the Sanford sub-basin. To the north and south, in the Durham and Wadesboro sub-basins, the Triassic age sedimentary rocks are assigned to the Chatham Group, undivided, and consist of conglomerate, arkosic sandstone, siltstone, claystone, and mudstone. In the Durham sub-basin, four lithofacies are designated on the state geologic map (Table 1.1; Brown *et al.*, 1985;), whereas the rocks of the Wadesboro sub-basin are essentially undifferentiated, although the Pekin Formation was named for exposures in the Wadesboro sub-basin (Figure 1.1) (Campbell and Kimball, 1923). The relationships of the type Pekin Formation to the unit bearing its name in the Sanford sub-basin are uncertain, but they are lithologically and biostratigraphically distinct from each other (Olsen *et al.*, 1982) (Table 1.1). Recent mapping of two quadrangles which span an east-west transect across the Durham sub-basin has resulted in a more detailed understanding of the sedimentology (Hoffman and Gallagher, 1988, this volume) and an informal stratigraphic classification has been introduced (Table 1.1).

Depositional History

The Pekin Formation of the Sanford sub-basin is mostly composed of fluvial sandstone, conglomerate, and siltstone. Sandstones are commonly trough cross-bedded, forming fining-upward sequences of pebbly sandstone grading up into bioturbated siltstones. In many places the basal part of the Pekin is a distinctive gray, quartz-rich conglomerate called the "millstone grit" because it was quarried for millstones in the 1800's. The gravel-sized clasts in the millstone grit are 90-95% quartz and 5-10% rock fragments derived from the Carolina Slate Belt (Staggs, 1984) with silicified wood fragments present locally (Reinemund, 1955). Gray and purple flaggy siltstone and shale are locally important in the lower Pekin, particularly in the Colon cross-structure (Bain and Harvey, 1977; Bain and Brown, 1980) and in the middle Pekin in area of Gulf (Stop 1.1).

The Pekin Formation sandstones are interpreted as primarily braided stream deposits because they appear to lack obvious lateral accretion surfaces. However, the abundance of bioturbated siltstone surrounding these sandstones suggest relatively low gradient rivers as in anastomosing streams. Textoris *et al.* (1986) interpreted the "millstone grit" as the deposits of humid alluvial fans due to the maturity of the clasts. Alternatively, the "millstone grit" could have been deposited by higher-gradient streams during the initial stages of basin filling. Individual beds of gray and purple siltstones and shales cannot be traced laterally over a distance of more than about 100 m and may be the deposits of small ponds and shallow lakes on the river flood plains. Intense bioturbation by roots and burrows (mostly *Scoyenia*) and an abundance of *in situ* and transported plant material suggest that the Pekin Formation was deposited in at least a relatively humid climate. Paleocurrent measurements from a limited area by Patterson (1969) suggest the Pekin drainage in the Sanford sub-basin was southwestward from the Durham sub-basin. On the other hand, sparse paleocurrent data and provenance studies reported by Reinemund (1955) from more southern outcrops suggest southeastward flow for the basal Pekin and northwest for the upper Pekin.

Sandstone mineralogy and the character of pollen and spores in the lower Pekin indicate a relatively humid climate during the early history of the basin, and the abundant plant fossils indicate lush vegetation. Streams entered the Sanford sub-basin from the northwest and east (as shown by paleocurrent indicators in the lower Pekin), and alluvial fans were deposited along the faulted northwestern border of both the Sanford and Durham sub-basins. Streams flowing across the basin deposited red and brown terrigenous clastics. Finer sediments were deposited on floodplains and probably in shallow lakes. At this time (early to middle Carnian), the Colon cross-structure was topographically low and the site of shallow lacustrine deposition.

The Cumnock Formation is more or less restricted to the Sanford sub-basin. The lower part of the Cumnock is dominated by gray siltstone and fine-grained sandstone with minor shale and claystone which appear to interfinger with red beds of the Pekin Formation (Reinemund, 1955). Approximately 60-80 m above the base of the Cumnock, two major coal seams and several thinner coal beds are present. The lower Gulf coal seam ranges from a few centimeters to nearly 1 m thick, and the upper Cumnock coal seam consists of three beds which range from 1 to 3 m thick (Robbins and Textoris, 1986). The Cumnock Formation coals are primarily high volatile B bituminous ranging to anthracite; the coals are altered to natural coke near diabase intrusions (Reinemund, 1955). Both seams are underlain by shale, siltstone, and ferruginous shale containing limonite-, siderite-, ammonium- and phosphate-rich nodules. These dark, brittle layers are known as "blackband" (Reinemund, 1955; Krohn *et al.*, 1988). Fish and reptile bones and coprolites are very abundant in the "blackband", perhaps accounting for the high levels of ammonium and phosphate in bulk analyses.

The coal-bearing interval is overlain by about 150-160 m of locally calcareous and organic carbon-rich gray and black shale with minor claystone, siltstone, and sandstone. The upper part of the Cumnock is dominated by gray siltstone and fine sandstone, grading upward into red and brown terrigenous clastics of the Sanford Formation. Some of this fluvial input was from rivers draining southward through the Durham sub-basin (Gore, 1986a).

The Cumnock Formation is interpreted to have been deposited in a lacustrine and swamp environment surrounded by swamps and fed by rivers flowing primarily from the north and northwest (Gore, 1986a). The Cumnock lake was probably hydrologically open because most cores and outcrops do not seem to show well-developed Van Houten cycles characteristic of the more northern Newark rift lakes. This suggests that the lake was not maintained by a delicate balance of inflow and evaporation during most of its history (Langbein, 1961; Richardson, 1967; Smoot, 1985; Gore, in press). In support of this open drainage argument is the absence of evaporite minerals (Gore, in press). The "blackband" siderite deposits probably require at least interstitially anoxic, low-sulfate waters (Berner, 1981). If the siderite is primary, as suggested by its strata-bound occurrence, then the lake must have had low-sulfate and probably low-salinity water. Although there are many cores of the Cumnock and much material still accessible in old mine dumps, the Cumnock completely lacks the microlaminated facies so typical of most other Newark lacustrine sequences. This also suggests a low sill to the lake and open hydrology, even during high stands. Nonetheless, some exposures of the Cumnock do show repetitive alternations of shallower and deeper-water sediments (Olsen, 1980c) suggesting some sort of cyclically changing lake depth or shoreline aggradational sequences. These may reflect the climatic fluctuations responsible for the Van Houten cycles in the more northern basins.

The Sanford Formation of the Sanford sub-basin consists mostly of fluvial deposits nearly indistinguishable from the Pekin Formation. The transition from the Cumnock into the Sanford Formation is gradational and is marked by an increasing frequency of red and gray sandstones and a decreasing frequency of black and gray claystones. Exposures of the lower Sanford Formation still show some lacustrine influence (Stop 1.3) (Gore, 1986a), but stratigraphically-higher exposures consist only of fluvial deposits. Within the Sanford Formation, there are few distinctive beds and no consistently mappable subdivisions (Reinemund, 1955). Lenticular beds of gray, coarse-grained or conglomeratic, arkosic sandstone (probably fluvial channel-fill) are present in the lower 425-490 m of the formation, decreasing toward the southwest (Reinemund, 1955). Red to brown, coarse-grained arkosic sandstone and conglomerate with associated claystone, siltstone, and fine-grained sandstone dominate the upper 300 m of the formation (Reinemund, 1955). Grain size is coarser to the southeast (up section), and poorly-sorted conglomerates are present along the southeastern edge of the basin adjacent to the Jonesboro fault system (Reinemund, 1955). The poorly-sorted, matrix-supported conglomerates are suggestive of debris flows. They were clearly derived from rocks adjacent to the Jonesboro fault system to the southeast. Therefore, they probably represent alluvial fan deposits. It appears that these alluvial fan deposits interfinger with fluvial deposits exhibiting more axial flow orientation. In either case, the final episode of deposition in the Sanford sub-basin was fluvial, supporting the open drainage system model (Smoot, 1985).

A black shale facies similar to the Cumnock Formation has not been found in the central Durham or Wadesboro sub-basins; instead, the latter sub-basins are dominated by sandstones and siltstones with fluvial characteristics. In both basins , however, there are at least some lacustrine deposits sandwiched between the dominantly fluvial intervals.

In the Durham sub-basin the basal part of the section consists of conglomerates and conglomeratic sandstones with clasts reflecting drainage from the west or northwest. Spencer (1985) and Hoffman and Gallagher (1988) have found that litharenites to subarkoses dominate in the lower parts of the section whereas the upper parts of the basin section are dominated by arkoses with pink feldspars, except near the eastern border fault system, where clasts of eastern provenance occur. Three fluvial styles occur in the northern basin: a) lenticular sandstones with well-defined trough cross bedding and overlying tabular sets all of which are surrounded by bioturbated siltstones and sandstones; b) sandstones forming rhythmic fining upward sequences of trough cross beds to ripple cross laminated siltstones; and c) poorly sorted conglomerate to pebbly sandstones with no cross bedding or irregular tabular sets. The changes in provenance and fluvial styles are coincident; the litharenite to arkose transition appears stratigraphically controlled and the arkose to poorly-sorted conglomerate transition appears geographically controlled.

Thin red and green to gray, platy-bedded siltstone and claystone beds are present in the south-central part of the Durham sub-basin. They appear to be lateral equivalents of the arkosic sandstones as suggested by the provenance of the associated sands and their depositional character. They appear to be perennial lacustrine sequences cyclically alternating with meandering stream sequences in the central portion of the Durham sub-basin sequence (Stop 1.4). Wheeler and Textoris (1978) observed limestone, chert, and caliche in some of these lacustrine sequences which they interpreted as indicating playa lakes in a closed basin which responded to alternations from wet to dry climates, as suggested by Textoris and Holden (1986). However, the chert replaces carbonates (Wheeler and Textoris, 1978) and appears not to be parallel to bedding (Hoffman and Gallagher, 1988). No lacustrine fossils occur in the chert or associated carbonates, and because of the extremely irregular and nodular shape of the chert and limestone bodies, these may be silicified caliches as are common elsewhere in this facies (see Stop 1.4). Critically, the caliche nodules, as limestones or chert, have never been found as clasts in sandstones. Therefore, we have no direct evidence that the nodules were synsedimentary. Their distribution and internal fabric is consistent with pedogenic carbonates; however, they appear to not have been available as a source of clasts in the depositional environment. If the nodules were synsedimentary features, they must have been soft or crumbly, which is consistent with our observation of burrows which cross-cut caliche boundaries. We propose that this type of carbonate formation suggest that they formed in perennially-moist soils, not in soils subject to the intense drying characteristic of classic areas of caliche formation (Gile *et al.*, 1966; Reeves,1976). Bioturbation by roots and burrows are extremely abundant in the same horizons. Therefore, we argue that the evidence for playa lakes in an arid setting is weak and possibly only an expression of post-depositional silicification of relatively humid types of caliche.

The stratigraphy of the Wadesboro sub-basin is much more poorly known than either of the other sub-basins. Fluvial sequences clearly dominate the lower, upper, and marginal portions of the section, but a predominantly cyclical gray and red mudstone sequence is at least locally present near the center of the basin. These lacustrine sequences comprise the type Pekin Formation of Campbell and Kimball (1923); they lack black shales and are lithologically more similar to the lacustrine deposits of the central Durham sub-basin than to the Cumnock Formation.

Thus, all three sub-basins, show a tripartite division of stratigraphy, at least superficially. In each basin there are lower and upper mostly fluvial intervals separated by units with at least some lacustrine sequences (Table 1.1). The lacustrine sequences, however, do not appear to be of the same age based on fish and palynomorph assemblages (Cornet, 1977a; Olsen *et al.*, 1982) in each basin. The oldest lacustrine sequence is the Cumnock Formation of Middle Carnian age (Cornet, 1977a; Cornet and Olsen, 1985), whereas the lacustrine units in the Durham and Wadesboro sub-basins appear to be late Carnian in age (Cornet, 1977a; Olsen *et al.*, 1982). This tripartite division in each sub-basin can be explained by the basin filling model (Schlische and Olsen, in review; this volume), with the additional hypothesis that the transition to lacustrine deposition in the Wadesboro and Durham sub-basins began only after the end of most Cumnock deposition in the Sanford sub-basin.

mileage	
0	Leave hotel on Airport Blvd., turning right toward I-40. We are in the Deep River basin (Durham sub-basin).
0.3	Get onto US 40 East, heading toward Raleigh.
2.0	Note outcrops of red Triassic clastic strata on left. We are approaching the Jonesboro fault system which bounds the basin on the east and southeast. The strata are coarser grained near the fault.
2.4	Cross Jonesboro fault system and leave the basin. The rocks southeast of the fault belong to the Appalachian Piedmont province and are Late Precambrian to early Paleozoic in age. In this area, the Piedmont rocks consist of (1) metasedimentary and metavolcanic rocks (phyllite, metaconglomerate, metafelsite, epidote-actinolite greenstone, *etc.*) of the Cary sequence, in a belt 1.5-3 km wide east of the Jonesboro fault system; (2) mica and hornblende gneiss and schist, in part conglomeratic (diamictite?), in a belt 1.5-3 km wide, immediately east of the Cary sequence; (3) felsic gneiss and schist in a belt about 6.5 km wide; (4) mica and hornblende gneisses and schists that have been injected by numerous sills and dikes of granite, pegmatite, and aplite, in a belt 3-6.5 km wide; and (5) the granitic (adamellite) Rolesville batholith, approximately 24 km wide (Parker, 1977). Additional Piedmont lithologies include thick veins of quartz and lenses of amphibolite. In the next few miles, we will cross all of these except the Rolesville batholith. Fresh outcrops are rare, as most of the crystalline rocks are weathered to a very thick saprolite.
8.5	Intersect US 1 south (to I-64), and turn right toward Sanford and Wake Forest. Follow signs to Sanford.
8.9	Turn right at fork, south toward Sanford on US 1 South, and US 64 West.
12.6	US 64 turns off. Stay on US 1.
14.2	Cross Jonesboro fault system and re-enter Deep River basin (Durham sub-basin). (Approximate position of fault.)
15.7	Pass NC 55 overpass and continue southwest on US 1.
23.7	Harris Lake is on the left.
29.2	Cross the Haw River. Leaving the Durham sub-basin and entering the Colon cross-structure, named for the town of Colon, NC.
29.3	Poor exposures on right are of the basal unconformity; gray-blue conglomerates of Pekin Formation rest on Precambrian or Cambrian coarse-grained turbiditic slate belt metasediments. Palynoflorules from shales associated with these Pekin conglomerates indicate an

early Carnian age (Cornet, pers. comm., 1989; Traverse, 1986).

31.3 Cross the Deep River, for which the Deep River basin is named.

38.7 Leaving the Colon cross-structure and entering the Sanford sub-basin.

41.7 Turn right onto exit ramp to US 421, near Sanford.

42.0 End of ramp. Turn left (northwest) onto US 421.

45.4 Outcrops on left are red sandstone and siltstone of the Sanford Formation, the uppermost of the three formations in the Sanford sub-basin.

45.9 Egypt Coal Mine historical marker on right.

46.7 Cross Deep River into Chatham County.

47.8 Clay pit on right is in the Sanford Formation.

49.8 Turn right onto Creosote Road and make an immediate sharp right onto gravel road.

50.2 Park along dirt road adjacent to quarry.

STOP 1.1: BOREN CLAY PRODUCTS QUARRY, GULF, NC (by P.J.W. Gore)

Highlights: Fluvial sequences of Pekin Formation, plant fossils, trace fossils, organic-rich sandstone, diabase dikes.

The Boren pit, about 1.5 km east of the western border of the Sanford sub-basin, exposes strata from the middle Pekin Formation, the lowermost of the three formations in the sub-basin. These rocks are stratigraphically the lowest units that we will examine in the Deep River basin. The rocks in the Boren pit are dug for clay to make bricks. The rocks in the quarry are primarily red, reddish-brown, and gray cross-stratified, rooted, and burrow-mottled sandstone and siltstone. Traverse will begin at southwest end of pit, proceed to the north and then to the northeast corner of the exposures.

The southwest half of the Boren pit exposes approximately 10 m of red beds, overlain by approximately 4-6 m of gray siltstone and sandstone with associated intraformational conglomerate and shale, overlain by approximately 10 m of red beds (Gore, 1986a). The gray siltstone is the source of most of the well-preserved plant material and all of the invertebrates from the Boren pit (see below); unfortunately the section had just been buried at the time of writing.

Exposed grayish-red beds slightly to the north of and ?overlying the plant-bearing gray siltstones consist of a coarsening-upward sequence of wavy-bedded sandstones with mudstone partings. The thickness of the sandstones increase from a few centimeters in the lowest exposed beds to 30-40 cm through a stratigraphic distance of about 2 m. The sandstone at top consists of high-angle climbing ripple cross lamination. Claystone-replaced plant compressions occur in the sandstones and on the mudstone partings. Reptile footprints (Figure 1.5) occur sporadically between ripple-cross laminated beds, and root and burrow (*Scoyenia*) structures are abundant throughout, although not as densely as in the overlying red mudstones and sandstones. The sandstone layers appear to define larger-scale cross strata or low-angle inclined truncation surfaces.

Follow the dirt road which leads west through the center of the pit. Halfway across the pit the road turns to run along an *en echelon* series of mostly thin diabase dikes. Note the color differences between the weathered diabase (yellowish-orange) and the grayish-red to reddish-brown strata that dominate the pit. At the northeastern termination of the dirt road, walk to the north where a sequence of gray to white sandstones is well exposed. The sandstone consists of a single fining-upward sequence erosionally overlying red bioturbated siltstone and fine-grained sandstone. Relief on the erosion surface is at least 2 m. The basal part of the sandstone forms trough cross beds 40-50 cm thick and contains abundant mud intraclasts as much as 10 cm in diameter, marcasite nodules, wood fragments, and abundant plant hash. Some of the cross beds are defined by highly carbonaceous black laminae composed of macerated plant fragments alternating with white quartzose, organic carbon-poor laminae. Cross beds decrease in size to 10-15 cm in the upper sandstone beds. All cross beds appear to indicate northerly flow directions. The top of the sandstone grades upward into bioturbated red and grayish-red fine sandstone and siltstone.

Outcrops on the southeast side of the quarry show the diabase intrusive relationships especially well (Figure 1.2). The dikes are olivine-normative, vertical to subvertical, and the largest shows a distinctive vertical sheeted pattern made up of aphanitic chilled diabase at the edges of the dike surrounding an internal breccia of metamorphosed sediment clasts and diabase matrix. The intruded sedimentary rocks at this spot consist of a coarsening-upward sequence of sandstone beds with deceleration of flow, climbing-ripple cross lamination and mudstone partings. Sandstone beds thicken upward with more low-angle climbing ripples. Bioturbation decreases upward. Long exposure on northeast wall of the quarry consists of highly-bioturbated siltstones and fine-grained sandstones. Some sandstone lenses appear to define meter-scale fining-upward and coarsening-upward sequences.

The coarsening-upward sequences probably represent small crevasse deltas (showing a wide variety of orientations) that possibly entered small ponds or lakes. The grayish-red coarsening-upward sequence could represent the distal deposit of a large crevasse delta into a swampy lowland. The channel sandstone is a fining-upward sequence with no evidence of epsilon-cross beds (*i.e.*, point bars). This would presumably indicate a braided river environment. However, along with the very large amount of fine-grained sediment present, the absence of complex mid-channel bars (tabular sets or several large cross bed sequences perpendicular to small cross bed sequences), suggests that the sandstone represents an isolated channel

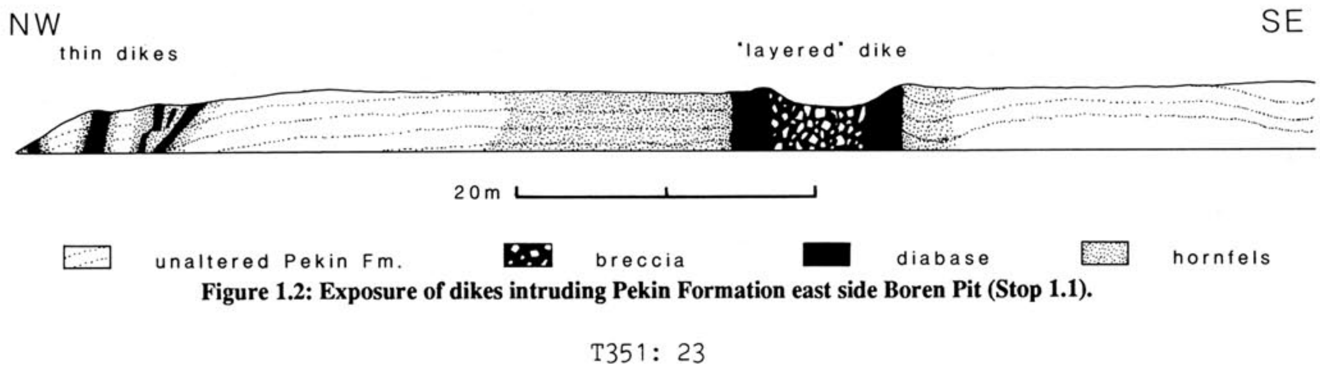

Figure 1.2: Exposure of dikes intruding Pekin Formation east side Boren Pit (Stop 1.1).

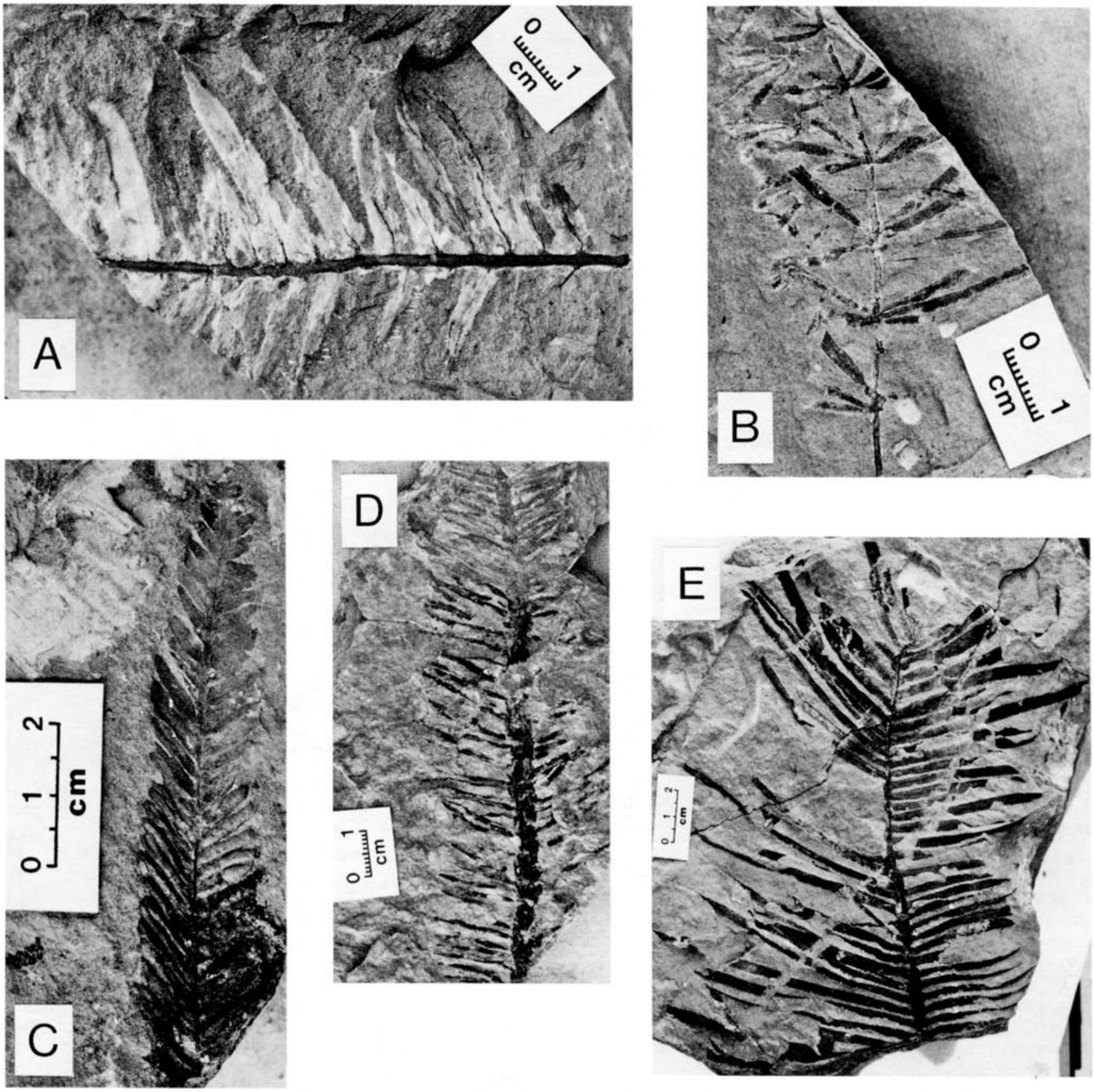

Figure 1.3: Remains of representative plants from the middle Pekin Formation of the Boren Pit (Stop 1.1): A) Portion of leaf of the fern *Pekinopteris auriculata*; B) Part of stem and whorled leaves of the horsetail *Neocalamites* sp.; C) Leaf tentatively assigned to the cycadeoid *Pterophyllum* sp.; D) Unidentified foliage similar to the enigmatic gymnosperm *Dinophyton*. E) Leaf of the common cycadeoid *Zamites*. Photographs courtesy of Patricia Gensel, adapted from Gensel (1986).

fill sequence incised into a wet, swampy, muddy area. It resembles a distributary channel, but it is not related to a large lake. Anastamosing river channels fill these constraints.

Carbonate nodules suggestive of caliche are notably absent at this locality and in adjacent exposures. Instead, small (<2 cm) hematitic nodules are abundant. In the adjacent Pomona pit, immediately on the southwest, wood replaced by hematite is also present. There is nothing in these exposures of the middle Pekin Formation to suggest an arid or even seasonally dry climatic setting.

The Boren pit is well known for the diverse assemblage of plant fossils. These plant fossils include ferns and their relatives (pteridophytes), horsetails, and gymnosperms, including conifers, cycads, and cycadeoids (Figure 1.3, Table 1.2). Stems, roots, leaves, cones, and seeds are preserved as compressions (plant material altered to a carbonaceous residue) and impressions or external molds. Some of the compressions contain well-preserved cuticles (the outer waxy covering of plant parts which retards water loss) and reproductive structures (Delevoryas and Hope, 1973; Gensel, 1986). Cuticle preservation ranges from excellent (*e.g.*, the cycad *Leptocycas*) (Delevoryas and Hope, 1971), to non-existent (most of the ferns)

(Delevoryas and Hope, 1973). In Mesozoic plants, features of the cuticle are also used to distinguish between cycads and cycadeoids, which can be difficult to identify from foliage alone (Gensel, 1986). The megafossil plants from the Boren pit constitute one of the better-known and more recently-studied Upper Triassic floras in eastern North America. This assemblage is placed in the *Eoginkgoites* megafossil floral zone by Ash (1980) , also recognized in the lower Chinle Formation of Arizona (Ash, 1980; Gensel, 1986).

Plant fossils are most abundant and best preserved in olive-gray to yellowish-brown siltstone and very fine-grained sandstone in the southwestern corner of the quarry (Gore, 1986a), not exposed at the time of this writing. Both black and white plant compressions are present. Leaf and stem impressions can be found on some bedding planes of grayish-red to moderate brown siltstone throughout the quarry. The most abundant plant fossils at this locality are leaves of cycads and cycadeoids including the genera *Otozamites*, *Pterophyllum*, and *Leptocycas* or *Pseudoctenis* (Delevoryas and Hope, 1973). Also abundant are leaves of the cycadeoid *Zamites*, and stems and leaves of the horsetail or sphenophyte, *Neocalamites*, as well as ferns (*Cladophlebis*, *Cynepteris* (=*Lonchpteris*), and *Phlebopteris*) and the fern-like plant *Pekinopteris* (Hope and Patterson, 1970; Delevoryas and Hope, 1971; Gensel, 1986). Among the conifer remains are cones belonging to the genera *Voltzia* and *Compsostrobus* (Delevoryas and Hope, 1973, 1975, 1981).

The dominant palynomorphs are fern spores, such as *Neoraistrickia americana* Schultz and Hope, *Triletes klausii*, *Convolutispora* sp., *Cyclogranisporites* sp., and *Cyclotriletes oligogranifer* Mädler (Traverse, 1986). Some conifer pollen is present, such as *Ovalipollis ovali* Krutzsch (Traverse, 1986). Also present is a very odd tetrad which Koob (1961) referred to as "*Placopollis raymondii*", but this palynomorph does not as yet have a validly published name (Traverse, 1986). The palynoflorules are Julian (middle Carnian) in age (Traverse, 1986). The dominance of fern spores suggests moist conditions (although some xerophytic ferns are known) (Traverse, 1986), which is certainly in line with the sedimentological interpretation.

Invertebrates from the gray siltstones of the Boren pit include conchostracans and clams (Table 1.2), and extremely abundant, large backfilled burrows (to 1.0 cm wide and at least 50 cm long) of *Scoyenia* (Gore, 1986a) found in beds of almost all lithologies in this pit (see also Stop 1.4). Vertebrates found in the Boren pit are thus far restricted to small three-toed footprints possibly dinosaurian. The nearby Pomona pit produced a rich vertebrate assemblage including bones of the large dicynodont mammal-like reptile cf. *Placerias*, phytosaurs, and fish, as well as abundant reptile footprints and clams (Table 1.2; Figures 1.4, 1.5). The footprint assemblage is the oldest from the Newark Supergroup and only one known from Newark Middle Carnian age strata; it is distinctly different than any younger assemblages (Olsen, 1988b).

50.6 Return to Creosote Road and turn left (southeast) onto US 421.

51.3 Turn left onto Alton King Road and immediately turn right into gravel driveway to Bethany Church.

51.5 Park in Bethany Church parking lot.

Table 1.2: Fossils from the Boren and Pomona pits (plants adapted from Gensel, 1986). Key as follows: †, ichnofossil; (B), found in Boren pit; (P), found in Pomona pit.

- PLANTS
  - Sphenophytes
    - Equisetales (horsetails)
      - *Neocalamites* (B,P)
  - Pteridophytes
    - Filicales (ferns and fern-like organisms)
      - *Cladophlebis (B)*
      - *Cynepteris* (B)
      - *Danaeopsis* (B)
      - *Phlebopteris* (B)
      - *Clathopteris* (B
      - *Wingatea* (B)
      - *Pekinopteris*
  - Cycadophytes
    - Cycadales (cycads):
      - *Leptocycas* (stems, leaves, cones) (B)
      - *Pseudoctenis* (leaves)(B)
    - Bennettitales (cycadeoids)
      - *Otozamites* (foliage) (B)
      - *Zamites* (foliage) (B,P)
      - *Pterophyllum* (foliage) (B)
      - *Eoginkgoites* (foliage) (B)
      - *Williamsonia* (sterile bracts) (B)
      - *Ischnophyton* (stem) (B)
  - Coniferophytes
    - Coniferales (conifers)
      - *Compsostrobus* (B) (male and female cones and foliage)
      - *Voltzia* (female cones) (B)
      - *Matridiostrobus* (female cones) (B)
  - ?Gnetophytes
    - *Pelourdea* (leaves) (B)
  - Uncertain affinity
    - *Phoenicopsis* (leaves) (B)
- ANIMALS
  - Mollusks
    - Pelecypoda
      - Unionidae
        - undetermined clams (B,P)
  - Arthropoda
    - Crustacea
      - Diplostraca (clam shrimp and water fleas)
        - *Cyzicus* sp. (B)
      - ?Decapoda
        - †*Scoyenia* (B,P)
    - Insecta
      - †undetermined trails (P)
  - Pisces (fish)
    - Actinopterygii (bony fishes)
      - Palaeonisciformes
        - undetermined redfieldiid scales and bones (P)
  - Reptilia
    - Synapsida (mammal-like reptiles)
      - Kannemeyeriidae
        - *Placerias* sp. (P)
    - Archosauria
      - Aetosauridae (armoured herbivorous archosaurs)
        - cf. *Typothorax* (P)
      - Rauisuchidae (carnivorous, usually quadrupedal archosaurs)
        - undetermined teeth (P)
        - †*Brachychrotherium* spp. (P)
        - †*Brachychrotherium* (*Rigalites*) sp. (P)
      - Phytosauridae (crocodile like archosaurs)
        - *Rutiodon* sp. (P)
        - †*Apatopus lineatus* (P)
      - ?Saurischia (lizard-hipped dinosaurs)
        - †(?)*Coelurosaurichnus* spp. (B,P)

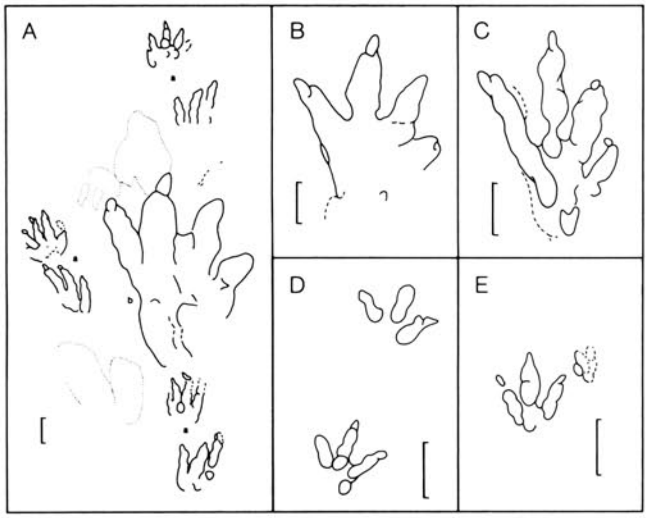

Figure 1.4: Footprints from the middle Pekin Formation of the Pomona Pit, adjacent to the Boren Pit (Stop 1.1) (from Olsen, 1988b): A) Natural cast of right pes impression of very large *Brachychirotherium* sp. with *Apatopus* trackway. B-C) Left pes impressions of *Brachychirotherium* sp. D) Natural casts of successive dinosaurian pes impressions of indeterminate genus; E) Natural cast of ?right pes impression and possible manus impression, possibly dinosaurian. Scale bars are all 10 cm.

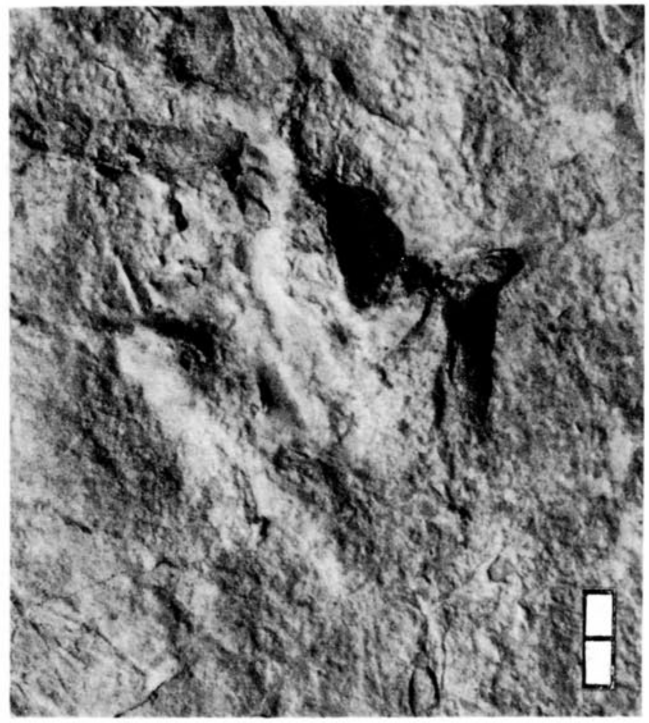

Figure 1.5: Natural cast of dinosaurian right pes impression (genus indeterminate) from the middle Pekin Formation of the Boren Pit, Stop 1.1. Scale bar is 2 cm.

STOP 1.2: CUMNOCK FORMATION AT BETHANY CHURCH, GULF, NC (by P.J.W. Gore)

Highlights: Fossiliferous black shale, coal, siderite nodules.

Proceed down embankment to railroad tracks. Look for small outcrops of the Cumnock Formation coal and black shale near the bridge (Figure 1.6). The shale and shaley coal are extremely fossiliferous, containing a non-marine invertebrate fauna consisting of conchostracans (*Cyzicus* sp.) and several species of smooth-shelled ostracodes in the genus *Darwinula*. Shiny, black, rhombic fish scales, coprolites, reptile bones and teeth, and plant fragments are also present (Table 1.3). The Cumnock coals, unlike the coals of the Richmond basin, are consistently interbedded with shales containing a rich lacustrine fauna. The Cumnock coals themselves apparently contain a large proportion of conifer material rather than cycadeoid material common in the Richmond basin coals.

Walk to the left (northeast) along the railroad tracks for about 100 m and enter the brushy clearing on the right (southeast) side of the tracks. Outcrops of red to brown sandstone, siltstone, and mudstone of the Pekin Formation are present here. These rocks are similar to those seen at the last stop in the Boren pit. According to a paced section presented by Bain and Harvey (1977), approximately 77 m of the Pekin are exposed here. These rocks are massive to poorly bedded, with abundant bioturbation, and local cross-stratification and they are generally non-calcareous. Gray reduction spots are present locally, particularly around root marks and scattered plant remains. There are thin, olive-gray silty to shaley interbeds locally, but thick gray horizons with plant fragments or coarse, organic carbon-rich sandstones are not exposed here. *Scoyenia* burrows with the typical external striations and internal backfilled structure are common but smaller here, with most ranging from 3 to 7 mm in diameter. Carbonate nodules (caliche?) 1-2 cm in diameter are abundant in some layers. This is a pronounced difference from the Boren pit exposures.

Table 1.3: Fossils from the Cumnock Formation at Stop 1.2.

PLANTS
- Sphenophytes -
  - Equisetales (horsetails)
    - *Neocalamites* sp.

ANIMALS
- Arthropods
  - Crustacea
    - Diplostraca (clam shrimp and water fleas)
      - *Cyzicus* sp.
      - ?*Paleolimnadia* sp.
    - Ostracoda
      - *Darwinula* spp.
      - undetermined forms
  - Insecta
    - Coleoptera (beetles)
      - undetermined fragments
- Pisces (fish)
  - Actinopterygii (bony fishes)
    - Palaeonisciformes
      - *Synorichthys* sp
      - *Cionichthys* sp.
  - Sarcopterygii (lobe finned fish)
    - Coelacanthini
      - cf. *Pariostegus* (*Diplurus*) sp.
- Reptilia
  - Archosauria
    - Phytosauridae (crocodile like archosaurs)
      - *Rutiodon* sp.

Proceed downhill to the south in the direction of dip, roughly toward the highway, until reaching a small (nearly dry) stream. Follow the stream downhill to outcrops of bituminous coal and black shale. The coal and black shale belong to the Cumnock Formation and are part of the same unit exposed along the railroad tracks. These beds are in fault contact with the Pekin redbeds, but the fault zone is covered here. The Cumnock Coal exposed here is known to lie about 60-80 m above the base of the Cumnock Formation, but in this area it is only a few meters from the Pekin red beds. A minimum of 50 m of section has been removed by faulting. The strike and dip of the Pekin and Cumnock differ considerably, although both units generally dip southward. For the Pekin, strike and dip are about N79°E, 42°SE (with some variation: locally dips are as shallow as 10°-20°). Strike and dip of the Cumnock are about N46°W, 40°SW (inconsistent due to faulting in the Cumnock). Bedding and possibly stratigraphic order are somewhat obscured by intense small-scale faulting in the Cumnock. A partial measured section in the Cumnock at this locality (Gore, 1986a) is given in Figure 1.6.

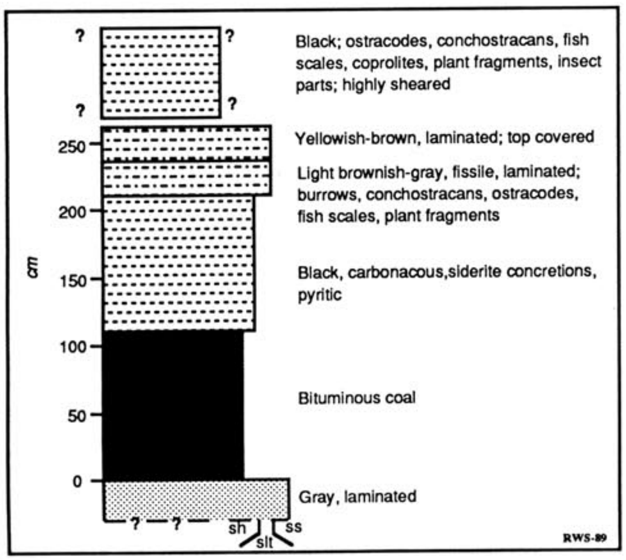

Figure 1.6: Measured section of Cumnock Formation coal (Stop 1.2), exposed south of Bethany Church, Gulf, NC. After Gore (1986).

Pollen and spores extracted from the coal and black shale at this locality are late middle Carnian in age and may indicate considerable drying in the source regions for the palynomorphs (as shown by a substantial decrease in fern spores) since the deposition of the gray Pekin beds at Stop 1.1 (Traverse, 1986). Of course, it is also possible that the advance of the lacustrine environment destroyed the fern-dominated habitats, or perhaps the swamp which produced the coals was dominated by conifers which were Cyprus-like in their adaptations to growing in submerged soils. The most prevalent palynomorphs in the coal include *Patinasporites*-complex (monosaccate conifer pollen), *Pretricolpipollenites ovalis* Danzé-Corsin and Laveine (a sulcate gymnosperm pollen grain), *Camerosporites pseudoverrucatus* Scheuring (a primitive circumpolloid), and *Pseudenzonalasporites summus* Scheuring (Traverse, 1986). Lesser amounts of trilete fern spores and *Cycadopites* spp. (a monosulcate pollen grain more or less identical to modern cycad pollen) are also present (Traverse, 1986). The black shale also contains some specimens of "*Placopollis*" and several types of bisaccate conifer pollen, including *Alisporites* sp. and *Colpectopollis* sp. (Traverse, 1986).

The non-marine fauna and fine-grained sediments indicate deposition in a lake with relatively quiet or deep water. The organic content of the Cumnock black shales is relatively high; total organic carbon (T.O.C.) averages about 1% but locally as much as 5-35% (Ziegler, 1983; Olsen, 1985a; Robbins and Textoris, 1986). The presence of abundant complete ostracodes and complete absence of microlamination indicate that the bottom waters of the lake were frequently oxygenated, however. Hence, the preservation of organics was probably due to high sedimentation rate. The presence of possibly primary siderite nodules in the Cumnock may indicate low sulfate content in the lake waters, at least some of the time (Gore, in press).

51.7 Return to Alton King Road. Turn left, then left again onto US 421 towards STOP 1.3.
OR, to reach Optional Stop 1.2a, continue straight across US 421 to the west, staying on Alton King Road, instead of turning left. Follow Alton King Road approximately 1 mile to strip mine on the left side of the road.

OPTIONAL STOP 1.2A: CHATHAM COAL COMPANY STRIP MINE, GULF, NC (by P.J.W. Gore)

Highlights: Black shales and coal of Cumnock Formation.

Over 2 million tons of coal have been mined in the Deep River basin, and it is calculated that the Sanford sub-basin has about 140,000,000 tons of remaining coal resources (Textoris, 1985). Coal has been mined in the basin since at least 1775, the time of the Revolutionary War (Reinemund, 1955). By 1850, many prospects and small mines had been opened along the coal outcrop belt. The first high production commercial mine was started in 1852, when the main shaft of the Egypt Mine was sunk; the main coal bed (Cumnock Coal) was encountered at a depth of 131 m (Reinemund, 1955). During the Civil War, the Confederate Army took over the mine, using the coal to supply the ships of blockade runners based in Wilmington, NC. Several other mines also operated in this area during the Civil War, including the Black Diamond Mine and the Carolina Mine. An iron furnace was built nearby along the Deep River to forge cannon balls and shot for the Confederate Army (Hetzer, 1987).

Other mines have been operated intermittently and unsuccessfully in the area because of geologic problems (faults and diabase intrusives), transportation problems, gas explosions (which killed over 200 miners), and flooding. The largest single mine disaster in the basin occurred in the Carolina Mine (also called the Farmville or Coal Glen Mine), which opened in 1922; in May of 1925, 53 miners were killed (Reinemund, 1955; Heltzer, 1987). The mine closed four years later due to flooding by the Deep River. The mine was reopened from 1947 to 1951, producing up to 100 tons/day, but failed to turn a profit and was allowed to flood again. Commercial mining in the basin ended in 1953 (Textoris, 1985), but a test pit (approximately 70 m by 30 m) was opened at this site in late 1987 by the Chatham Coal Company as a prelude to strip mining. This is the first attempt at strip mining in the basin, which at the time of this writing has not yet encountered unweathered rock.

The strip mine is near the old Gulf Mine, started during the Civil War and extended during the 1920's, and the old Deep River Mine, which was first opened in 1932 and closed in 1936. In addition, several small surface pits are present nearby. The Deep River lies less than half a mile south of this site. Between the strip mine and the river, about 30 m south of the road, is a large diabase sill. The coal adjacent to the diabase has been metamorphosed to anthracite. The rocks are highly faulted in this area. The Cumnock Coal Bed is repeated here three times by faulting [O. F. Patterson (mine geologist), pers. comm.]. Along the west side of the exploration pit, near a small stream, the coal is exposed at the surface in three places, marked by old hand-dug pits. On the far side of this stream, the coal is displaced to the south by a fault (O. F. Patterson, pers. comm.).

Two facies of shale in the Cumnock Formation similar to what is exposed at Stop 1.2 are present here: (1) black, organic carbon-rich, weathered non-calcareous shale crowded with external molds of ostracode valves, associated with fish scales and abundant powdery brown coprolites, and (2) medium dark gray clay shale with abundant, relatively large conchostracans (whole and fragmented) and plant fragments surrounded by tan oxidation zones, associated with a few ostracodes, fish scales, and coprolites.

From Alton King Road, turn southeast on US 421 (toward Sanford).

52.3 Turn right onto Route 1007 (S. Plank Road).
52.4 Cross the Deep River into Lee County.
55.6 Turn left (east) from Route 1007 onto NC 42 (Carbonton Road).
57.0 Roadcut on left (north) side of NC 42. Park along roadside.

STOP 1.3: SANFORD FORMATION NEAR SANFORD, NC (by P.J.W. Gore)

Highlights: Thin lake bed with conchostracans; cross-bedded red clastics (fluvial); Scoyenia *in laminated strata.*

This road cut (Figure 1.7) exposes 9.5 m of red to brown sandstone, siltstone, mudstone and shale of the lower Sanford Formation, the upper of three formations in the Sanford sub-basin (Gore, 1986a). Bedding in this outcrop tends to be more tabular than in obvious fluvial deposits in the Pekin and Sanford formations, but most of the beds change thickness laterally. The more resistant ledge-forming units are red to brown, non-calcareous, cross-stratified sandstone and massive siltstone. The less resistant beds are massive to poorly-laminated mudstone and shale. Two fining-upward sequences are present, consisting of an abrupt contact (scour surface) overlain by cross-stratified sandstone, grading up into bioturbated siltstone and mudstone (Gore, 1986a).

A convex-upward sandstone lens with rip-up clasts and climbing-ripple cross lamination in the upper part occurs along the left (western) end of the road cut. The morphology, texture, and sedimentary structures of this unit suggest that it may be a crevasse-splay deposit. Approximately 5.5 m above the base of the section is a thin (21 cm) gray bed. The gray bed occurs at the top of a 1.4-m-thick fining-upward sequence (Gore, 1985). The gray bed may be subdivided into three parts: (1) a lower unit, 5 cm thick, of light gray, massive to poorly-laminated, non-calcareous, plant-fragment-bearing siltstone, fining upward into (2) a middle unit, 8 cm thick, of light gray, fissile, non-calcareous clay shale containing closely-packed conchostracans on some bedding planes overlain by (3) an upper unit, 8 cm thick, of laminated, wavy-laminated, and cross-laminated, noncalcareous siltstone with asymmetrical ripple marks (Gore, 1986a). The mineralogy of the gray bed consists of quartz, illite, chlorite, plagioclase, siderite, and possibly ankerite (x-ray diffraction data from Andy Thomas, Texaco). The uppermost beds of the outcrop consist of tabular fine sandstone and interbedded mudstone beds with unidirectional cross beds at the base and abundant possible oscillatory ripples higher up. *Scoyenia* and roots are very abundant and have obscured the ripple cross lamination characteristics of the tabular thin-bedded sandstones.

There is debate about the depositional environments represented by this outcrop with two opposing hypotheses: 1) all of the deposits are related to a fluvial environment with the interbedded lacustrine strata being the deposits of shallow ponds and small lakes on a low relief flood plain; 2) the sequence represents alternating basin-wide shallow lake deposits and fluvial low-stand deposits.

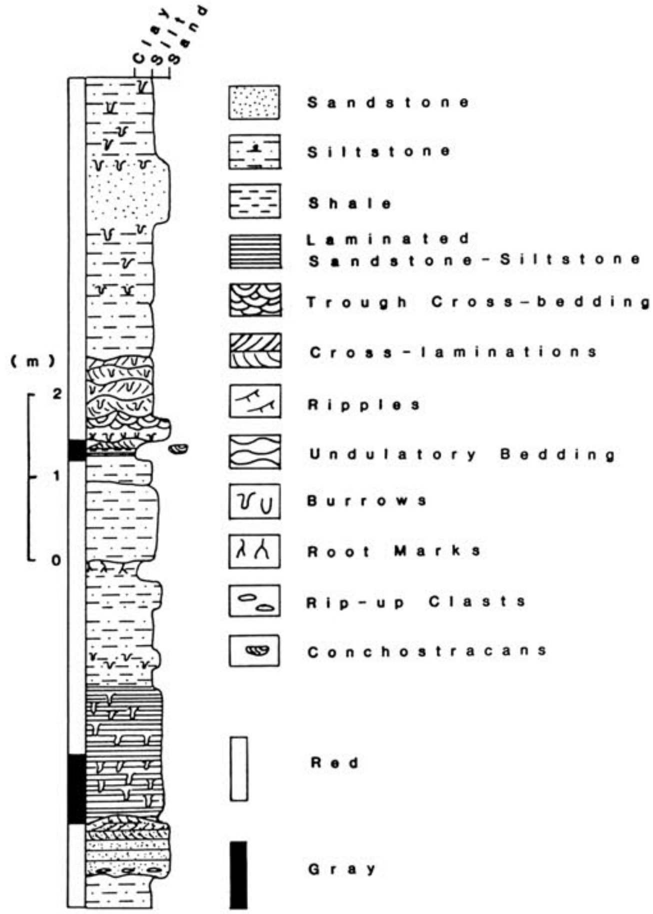

Figure 1.7: Measured section of lower Sanford Formation at Stop 1.3.

Gore (1985, 1986a,b,c) argues that the presence of cross stratification and fining-upward sequences indicates primarily fluvial deposition for the sandstones. The thinness of the lacustrine bed and its position at the top of an apparent fluvial fining-upward sequence suggests that it was deposited in a shallow floodplain lake (Gore, 1985) partially filled by crevasse splays. The presence of oscillatory sandstones associated with the conchostracan-bearing siltstones is not in conflict with this interpretation.

Olsen argues that the conchostracan-bearing siltstone represents substantial lake conditions, and that the associated tabular sandstones are wave-formed beds and associated distributary channels and bars. The associated fluvial beds were deposited during low-stands of the lake and dissection of the lake margin deposits by streams.

According to Olsen, alternations between fluvial and lacustrine deposition would thus be controlled by basin-wide changes in lake level, not lateral migration of channels and floodplains. The sequence appears intermediate in facies between the marginal facies of the Cumnock Formation as exposed near Carthage (Olsen, 1986) and the fully fluvial upper Sanford Formation.

This argument will come up several times during the course of the field trip. Resolution of the arguments rests on determining the regional distribution of beds, which is difficult due to poor exposure.

57.0 Continue east on NC 42 toward Sanford. Small outcrops of the Sanford Formation are present along both sides of the road.
62.6 Intersection with US 1-15-501. Head north on US 1-15-501.
74.6 Cross the Deep River.
90.0 Exit to NC 55, Apex/Fuquay Varina.
90.2 Turn left onto NC 55, heading north toward Apex. Pass through the town of Apex.
93.2 Intersection of NC 55 with US 64.
93.4 Continue north on NC 55.
101.3 Triangle Brick Quarry office. (Stop and ask for permission to enter the quarry).
101.4 Turn left toward quarry.
101.6 Stop sign at Kit Creek Road. Go straight onto quarry entrance.
101.8 Park where directed by quarry personnel. Stay out of the way of the large dump trucks. Descend into the pit beside the white shed.

STOP 1.4: TRIANGLE BRICK QUARRY, DURHAM, NC (by P.E. Olsen, J.P. Smoot, and P.J.W. Gore)

Highlights: Very fossiliferous thin lake bed, fluvial deposits with reptile bones and paleosols.

The Triangle Brick Quarry is on strike with the mudstone facies of Lithofacies Association II of Hoffman and Gallagher (1988). The dominant lithologies in the 60-m-thick exposed section are red-purple to red-brown massive siltstone (Figure 1.8) and gray to brown sandstone. There are subordinate amounts of green and red clay shale and calcareous siltstone to limestone. On the largest scale, the sequence consists of alternating fluvial and apparently lacustrine units (Figures 1.8, 1.9).

Three well-defined channel-fill deposits occur within the quarry. A thick, relatively poorly-exposed gray (weathering yellow) sandstone occurs below the upper lacustrine clay shale (Figure 1.8) and contains large (>20 cm) decimeter-scale trough cross beds fining upward into bioturbated sandy siltstone. Below this are a series of lenticular sandstone beds defining large-scale, low-angle cross strata. In places these strata consist of intensely bioturbated, red-brown, sandy mudstone grading down-dip into ripple cross-laminated fine sandstone and finally into coarser sandstone with trough cross bedding and abundant intraclasts. The sandstone lenses are separated by red-brown mudstones that thin towards the large trough cross-bedded bases of the sandstone lenses. These sequences define lateral accretion beds of a high-suspended load meandering stream (Figure 1.10) (Smoot, 1985) similar to the Barwon River of south Australia (see references in Smoot, 1985).

The lowest channel-fill sequence consists of a single lenticular body with trough cross bedding at the base grading into climbing ripple cross lamination. This sandstone is incised into a tabular sandstone body that

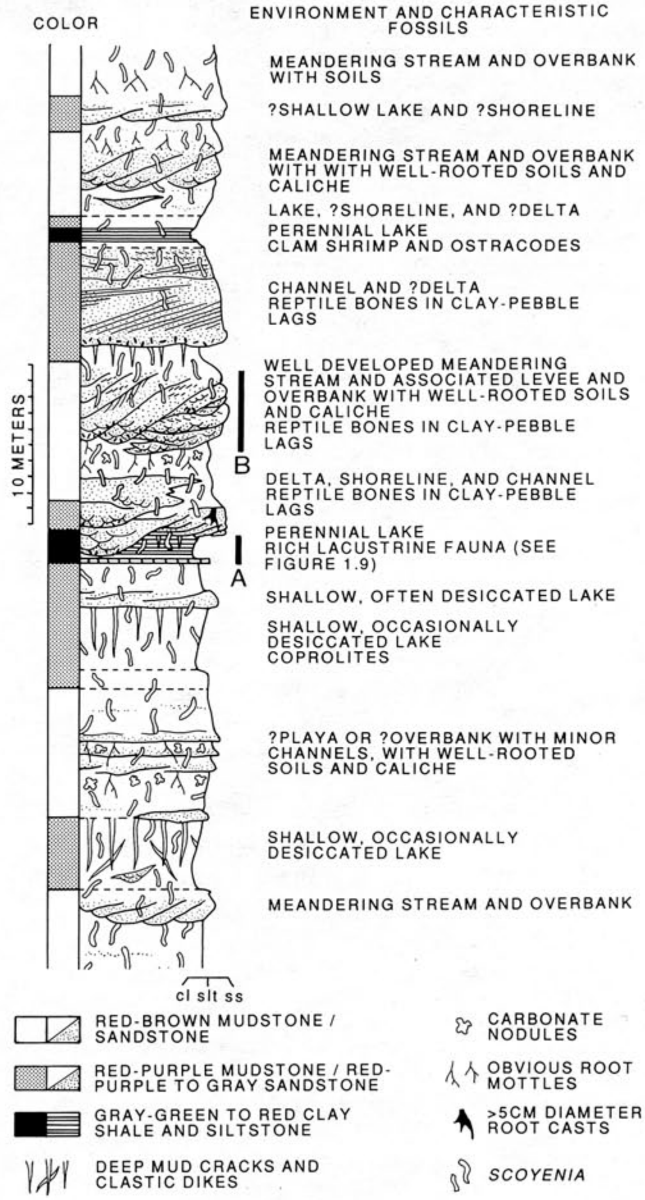

Figure 1.8: Measured section at Triangle Brick Quarry, measured January, 1989. A) Interval of highly fossiliferous clay shale shown in detail in Figure 1.9; B) interval of lateral accretion surfaces shown in detail in Figure 1.10.

gradationally overlies the lower and fossil-rich lacustrine clay shale. The tabular sandstone at the upflow (north) end of the exposure is dominated by planar to wavy lamination, whereas the tabular sandstone at the downflow (south) end of the outcrop contains climbing ripple cross lamination or tabular forsets. In both cases the tabular sandstone grades upward from the clay shales through a thickly laminated siltstone. This association suggests that the tabular sandstone was built out over the shaley sequence as a lobate sheet while the channel sand was cut into it as a crevasse delta or distributary mouth bar.

Most other sandstone bodies are thin and broadly lenticular. They are heavily bioturbated, particularly by *Scoyenia* and roots, and internal bedding and bed boundaries are indistinct. Most of the deposits around the sandstones are reddish brown mudstone or muddy siltstone similarly bioturbated with several horizons bearing irregular spongy appearing carbonate nodules that in places define portions of root-tubules. As described in the introduction to this section, these nodules do not appear to have been available for transport in the channel deposits and were probably not solid at the type of formation. This implies wetter conditions than usually assumed for caliche formation.

There are four distinctive mudstone beds that are traceable as tabular beds across the outcrops and represent lacustrine or possible lacustrine deposits. Most spectacular is the lower laminated clay shale which contains abundant fossils and underlies the tabular sandstone unit (Table 1.4; Figures 1.11); the distinctive distribution of the various types of fossils remains consistent across the quarry. The base of the fossiliferous part of the sequence is a calcareous ostracodal siltstone or limestone with abundant fish fragments and coprolites (see Figure 1.9). This is abruptly overlain by a finely-laminated (but not microlaminated) claystone with abundant small conchostracans (cf. *Palaeolimnadia*) and partially associated fish remains. The better than usual (for the Deep River basin) fish preservation and the preserved laminations suggest deposition in perennially poorly-oxygenated water. This is followed successively upward by clay shale showing a progressive decrease in lamination and an increase in the diversity of body fossils of infauna (Figure 1.9). Several thin (< 5 cm) green siltstone beds near the top of the clay shale are traceable across the quarry except where truncated by channels.

The lateral continuity of thin beds in the clay shale interval and the consistency of the faunal zonation suggest that the lake was considerably larger than the size of the quarry. The lake also had to have negligible bottom relief over the area of the quarry. The succession of fossils is similar to sequences seen in division 2 of Van Houten cycles in the Cow Branch Formation of the Dan River-Danville basin (Stop 2.2) and the lower Lockatong of the Newark basin (Stops 6.6-6.8), and at least the latter units demonstrably have great lateral extent.

The uppermost lacustrine clay shale is similar to the lower but is much thinner, lacks a basal calcareous bed, is less well laminated, and is less fossiliferous. Two other mudstone units contain almost no fossils (a few small coprolites have been found) and are not bedded. They are distinguished from the more typical mudstones by their color (purple-red) and in containing large (23 cm) and deep (>1 m) sandstone and siltstone-filled mudcrack polygons

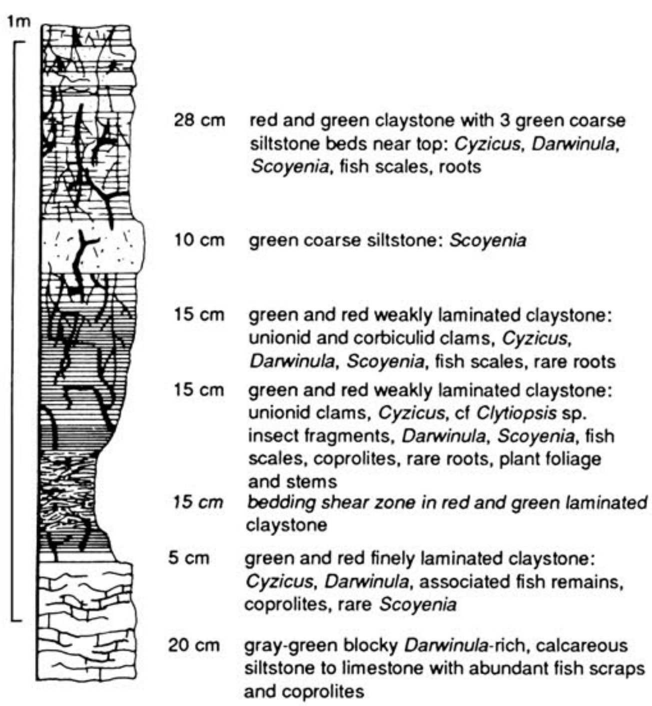

Figure 1.9: Section through highly fossiliferous clay shale ("A" of Figure 1.8). Adapted from Olsen (1977). Thick black branching lines represent *Scoyenia*; thin downwardly branching lines are roots; closeness of parallel lines indicates degree of lamination.

Table 1.4: Fossils from the Triangle Brick Quarry, Stop 1.4. All fossils from middle lake bed except as noted. † Indicates an ichnotaxon.

- PLANTS
  - Sphenophytes -
    - Equisetales (horsetails)
      - *Neocalamites* sp.
      - *Equisetales* sp.
  - Pteridophytes
    - Filicales (ferns and fern-like organisms)
      - *Cladophlebis sp.*
  - Coniferophytes
    - Coniferales (conifers)
      - *Pagiophyllum cf. simpsoni*
- ANIMALS
  - Mollusks
    - Pelecypoda
      - Unionidae
        - undetermined aragonitic clams
      - ?Corbiculidae
        - undetermined calcitic clams
  - Arthropods
    - Crustacea
      - Diplostraca (clam shrimp and water fleas)
        - *Cyzicus* sp.
        - ?*Paleolimnadia* sp.
      - Ostracoda
        - *Darwinula* spp.
      - ?Decapoda
        - cf. *Clytiopsis* sp
        - †*Scoyenia*
    - Insecta
      - Coleoptera (beetles)
        - undetermined fragments
    - undetermined large arthropod fragments
  - Pisces (fish)
    - Actinopterygii (bony fishes)
      - Palaeonisciformes
        - *Turseodus* spp.
        - *Cionichthys* sp.
      - Semionotidae
        - *Semionotus* sp.
    - Sarcopterygii (lobe finned fish)
      - Coelacanthini
        - cf. *Pariostegus* sp.
        - *Osteopleurus* sp.
  - Reptilia
    - Archosauria
      - Phytosauridae (crocodile like archosaurs)
        - *Rutiodon* sp. (sandstone channel lags)
      - Aetosauridae (armoured herbivorous archosaurs)
        - *Stegomus* sp. (sandstone matrix, bed unknown)

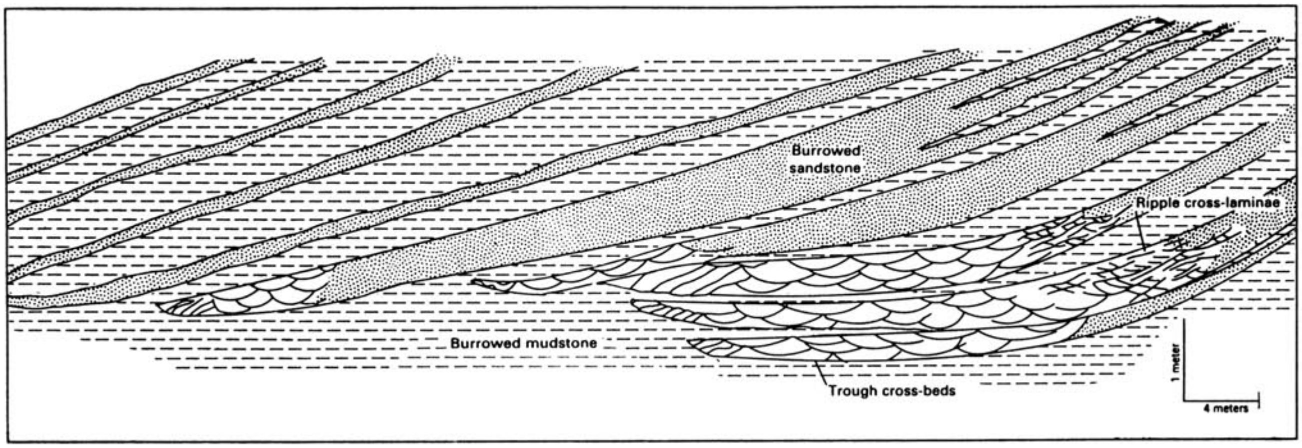

Figure 1.10: Simplified sketch of sedimentary features in the bed marked "B" in Figure 1.8 (from Smoot, 1985). Trough cross-bedded areas are coarse-grained sandstone with mud intraclasts, and the ripple cross-laminated areas are medium- to fine-grained sandstone. The stippled areas represent internally massive, burrowed, muddy sandstones, and the dashed areas represent internally massive, burrowed mudstones. Vertical exaggeration (X 4) has increased the apparent dip of bedding, which is actually ~ 5°. Paleocurrent direction, as indicated by the trough cross beds, is out of the page and to the right.

that become asymmetrically wider and more abundant upward. The association suggests that these mudstones were deposited in slightly more water-logged conditions than the other mudstones and that they may have accumulated in shallow lakes.

As in the Pekin and Sanford formations, *Scoyenia*-type burrows are exceedingly common, often obliterating any other textures. *Scoyenia* are burrows with external, longitudinal striations and a meniscate or tangential internal backfilling. They range here from approximately 0.5-1.0 cm in diameter. In general, the smaller burrows are sub-horizontal, and the larger burrows are sub-vertical, locally cutting or intersecting the smaller burrows. Knot-like and club-shaped terminations occur, as does branching. The branching indicates that the burrows remained open for some before being backfilled.*Scoyenia* puncture beds with the crayfish-like *Clytiopsis* in the lacustrine shale and have been interpreted as the burrows of crayfish or crayfish-like decapods (Olsen, 1977; *contra* Frey *et al.*, 1984). *Scoyenia* has been interpreted by Frey *et al.* (1984) as an indicator of moist or wet non-marine substrates, either shallow aquatic deposits which are periodically exposed, or low-lying subaerial deposits which are occasionally flooded. The fine sculptural details of *Scoyenia* are best preserved in clay shale, although *Scoyenia* are also preserved in siltstone and sandstone.

The overall environmental context and cause of the fluvial and lacustrine alternations are as unclear here as they were in the Sanford Formation at Stop 1.3. Gore (1985, 1986a) sees the alternations as due to the lateral migration of rivers and shallow flood plain lakes, whereas Olsen sees the alternations as reflections of cyclically-changing climate affecting lake depth in a closed basin with a low outlet or just a restricted outlet. Once again, observations of the lateral continuity of the putatively deeper water units are critical to testing these hypotheses. If the basin was open all during deposition, then the lake deposits should be of limited areal extent and the fluvial deposits could stretch across the entire basin. On the other hand, if the basin was hydrologically closed, the lacustrine intervals should be present over the center of the basin and the fluvial intervals should somewhere pass laterally into lacustrine strata in the deepest part of the basin (Smoot, 1985).

Whatever the cause, a vague 20 m alternation of red-purple and red-brown mudstone intervals seems apparent. If the cause of the apparent cyclicity is climate acting on lake level in a closed or semi-closed basin, the 20 m cycles could be due to the cycle of the precession of the equinoxes, although the number of cycles at this outcrop is certainly too small to obtain the full Milankovitch-type spectrum of small and larger-scale cycles even if they are present.

102.0 Leave quarry. Turn left onto Kit Creek Road as you exit the gate.
102.2 Turn left (north) on NC 55.
104.4 Intersection with NC 54. Turn left (west) toward Chapel Hill.
106.3 I-40 overpass over NC 54.
106.6 Turn left onto Fayetteville Road (NC 1118).
108.1 Bridge over abandoned railroad cut. Park.

STOP 1.5: RAILROAD CUT, DURHAM, NC

(by W. Hoffman and P. Gallagher)
Highlights: Fluvial sequences, diabase dike.

A 200-m-long by approximately 10-m-high cut along an abandoned section of the Norfolk and Southern Railroad exposes a large sequence of interbedded sandstone and mudstone of Lithofacies Association I (Hoffman and Gallagher, 1988, in prep.). This section has been subdivided into four units which are described below. The southeastern end of the exposure is terminated by a diabase dike; a normal fault is exposed near the southeastern end of the outcrop (Figure 1.12).

Unit 1 is a muddy sandstone with resistant lenses of coarse feldspathic sandstone. The unit is graded with coarser sandstone at the base and finer sandstone towards the top. The resistant lenses near the base of unit 1 are internally cross-stratified and the boundaries are gradational into the muddy sandstone which has similar grain sizes. The muddy sandstone underlying those lower resistant lenses in places consists of pebble-sized mud clasts in a coarse sand matrix. All layering is indistinct, possibly due to bioturbation. In the upper part of unit 1 burrows and root structures are evident and carbonate nodules are present.

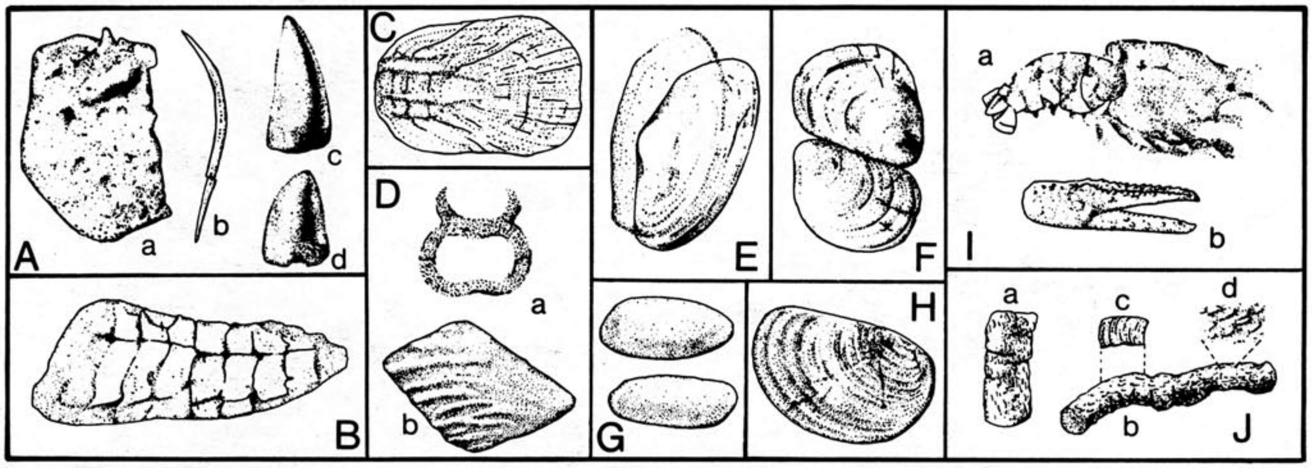

Figure 1.11: Vertebrate and invertebrate fossils from the Triangle Brick Quarry. A) Bones and teeth of the phtyosaur *Rutiodon* sp.: a, dorsal scute (X 0.13); b, gastralia element (X 0.19); c and d, posterior teeth (X 1.0). B) Ventral view of fragment of tail cuirass of armored archosaur *Stegomus* sp. (X 0.25). C) Scale of coelacanth *Osteopleurus* (*Diplurus*) sp.(X 3). D) Centrum and scale of palaeoniscoid fish *Turseodus* sp. (X 3). E) Undetermined unionid clam (X 2.5). F) Undetermined ?corbiculid clam (X 3). G) Ostracode *Darwinula* sp. (X 20). H) Clam shrimp *Cyzicus* sp. (X 5). I) Crayfish-like decapod crustacean cf. *Clytiopsis* sp.: a, specimen missing front claws (X 1.5); b, isolated front claws (X 1.6). J) *Scoyenia* burrows: a, segment pf large vertical burrow (X 0.5); b, segment of horizontal burrow (X 0.5); c, longitudinal section showing meniscus-type infilling; d, enlargement of "prod" marks on burrow exterior (X 2). From Olsen (1977).

Unit 2 is a silty mudstone with carbonate nodules, root structures, and abundant *Scoyenia* burrows. The lower contact of this bed is gradational with unit 1, and the upper contact with unit 3 is a scour surface.

Unit 3 consists of medium- to coarse-grained, trough cross-bedded feldspathic sandstone overlain by medium to coarse-grained, planar-tabular cross-bedded feldspathic sandstone. Large mud clasts occur along the bases of the lower, large-scale trough cross beds which grade upward into smaller-scale trough cross beds which lack mud clasts. Within the planar-tabular cross-bedded portion of the unit, large tabular sets grade vertically and laterally into small tabular sets. Paleoflow, determined from the troughs, is S50°W-S60°W. The planar-tabular cross beds yield a S70°W paleoflow direction. This unit is cut by a normal fault.

Unit 4 is a burrowed and rooted silty mudstone in fault contact with Unit 3. It closely resembles unit 2.

The rocks at this outcrop are interpreted as sandy braided stream system deposits within a muddy floodplain. The sequence of structures in unit 3 is similar to the sandy braid stream deposits described by Cant and Walker (1976, 1978). As in this type of braid stream, large-scale (>20 cm) trough cross beds form in the deepest part of the channel while smaller scale trough cross beds form in shallow water as the channel fills. Tabular forsets of a variety of thicknesses are produced by barfront accretion. These are oriented at considerably different angles than the trough cross beds which they typically overlie. On the other hand, the thick sequences of mudstone surrounding the channel fill sandstone (units 2 and 4) are not like the braided river model of Cant and Walker. This suggests that the river was incised into a low gradient muddy plain, more like anastamosing rivers of Smith and Smith (1980). The swampy wet conditions envisioned for this model are consistent with the abundant root and burrow structures. Unit 1 is a problem because it is unclear what effects bioturbation and/or modern weathering have had on the present appearance. The sequences of grain sizes and structures in unit 1 are consistent with a channel-fill sequence similar to unit 3 but thinner and without tabular sets. This may represent a shallow side branch of the braid river that was covered by vegetation during periods between high flood stages. We see no need to call upon climatic fluctuations (as in Textoris and Holden, 1985). As in the previous stop, the carbonate nodules are conspicuously absent from the sandstones. The random interbedding of channel fill sandstones with braid river characteristics and bioturbated mudstones is characteristic of the stratigraphically-lower outcrops of the northern Durham sub-basin. This is in contrast to the rhythmic fining-upward sequences in channel sandstones, similar to the previous stop, that characterize the overlying middle belt. This fluvial style suggests a possible change from anastomosing to meandering rivers as the basin developed. This change is accompanied by a change in provenance, this stop being very close to the boundary. There is no evidence to suggest the change is related to climate, although stream gradients may have been reduced by lake transgressions. Another possibility is that the source drainage areas changed in response to tectonic activity also changing the character of the rivers.

108.3 Turn around and return north on Fayetteville Road to NC 54.
109.8 Turn left (west) onto NC 54 toward Chapel Hill.
114.9 Chapel Hill city limits.
115.6 Turn right onto US 15-501 north toward Durham.
119.3 Durham city limits—"City of Medicine".
121.0 Turn right onto US 15-501 Bypass.
125.4 Intersect I-85. Roads merge.
128.0 Exit on US 501 North to Roxboro, NC. Leave Durham sub-basin of Deep River basin. Enter an area underlain by felsic volcanic rock (metamorphosed dacitic to rhyolitic flows and tuffs) interbedded with mafic and intermediate metavolcanic rock, and metasediments of

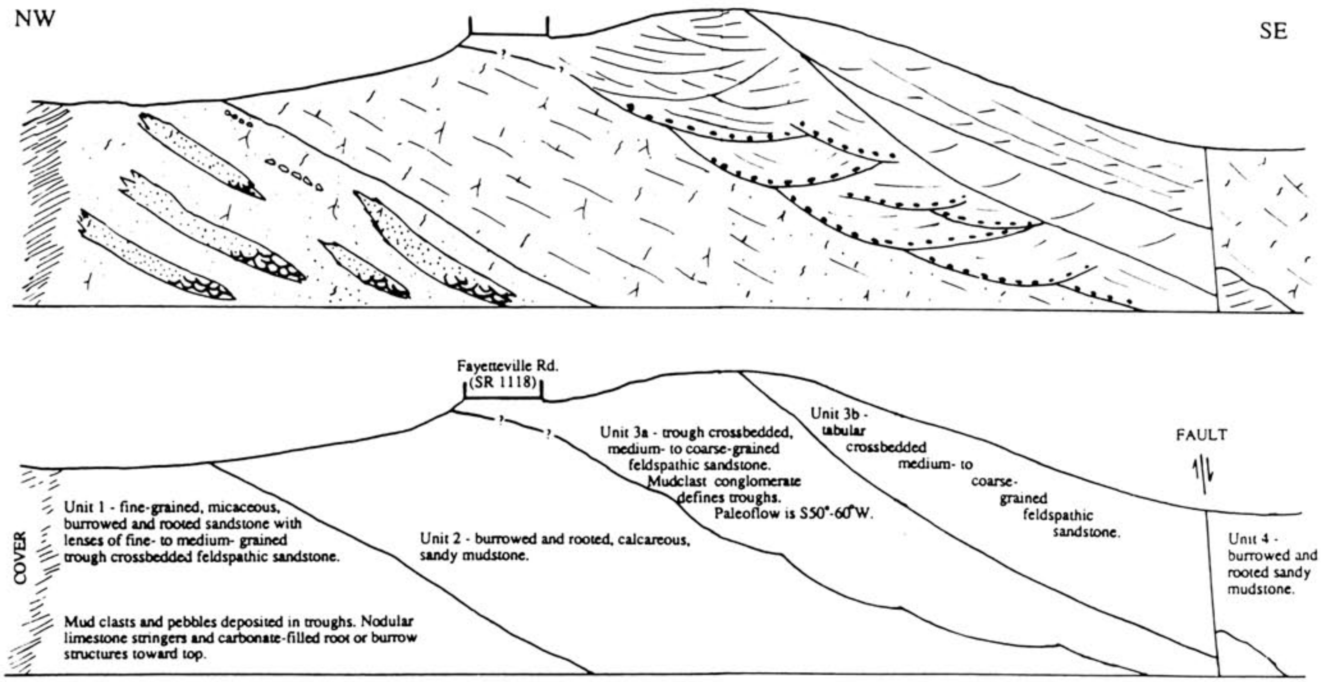

Figure 1.12: Generalized sketch of section exposed along abandoned railroad grade at Stop 1.5. Vertical exaggeration is about X 15; length of section is about 150 m.

the Carolina Slate belt (Late Precambrian to lower Paleozoic).
153.8 Roxboro city limits.
155.1 Turn left onto North 57-South 49-West 158.
155.5 Turn right onto Route 57 North.
161.0 Boulder-like outcrops of Late Proterozoic to Late Cambrian metamorphosed granite in and near Roxboro.
167.5 Intersection with NC 119. Continue north on NC 57. This area is underlain by Late Precambrian and Lower Paleozoic biotite gneiss and schist, and felsic mica gneiss.
172.5 Intersection with NC 62 at Milton, NC. Continue north on NC 57.
172.6 Cross the Dan River.
172.9 Virginia state line.
176.8 Turn left on US 58 West to Danville, VA.
183.7 Turn left onto Business Route 29 (N. Main Street).
183.8 Cross Dan River, home of Dan River Fabrics.
184.6 Last Confederate capital building.
184.8 Fork right onto West Main Street (South Business 29).
184.9 Turn right onto Route 86 North-Bypass 29.
185.2 Cross Dan River.
186.1 Exit right at Riverside Drive (US 58 west) going west.
187.3 Arrive at stop for evening.

2. DAN RIVER-DANVILLE BASIN, NORTH CAROLINA AND VIRGINIA

GEOLOGY OF THE DAN RIVER-DANVILLE BASIN
(by P.J.W. Gore and P.E. Olsen)

Introduction

The Dan River-Danville basin, approximately 167 km long and from 3 to15 km wide, is an exceptionally narrow and long basin (Figure 2.1). The basin is bounded on the northwest by a southeast-dipping normal fault system, referred to as the Chatham fault zone, toward which the sedimentary rocks in the basin steeply dip (20°-45°). The fault zone strikes approximately N30E°-N35°E, and dips approximately 44° SE (S.E. Halladay, unpublished manuscript). The southeastern edge of the basin is predominantly an unconformity, but a northwest-dipping normal fault is present locally (S.E. Halladay, unpublished manuscript). The basin straddles the North Carolina-Virginia state line, and the rocks in each state have been described in separate publications. Meyertons (1959, 1963) mapped the rocks in Virginia (Danville basin), and Thayer (1967, 1970) and Thayer *et al.* (1970) mapped the rocks in North Carolina (Dan River basin). Although there is only one basin, a dual system of nomenclature arose, and the basin is referred to as the Dan River-Danville basin (Robbins and Traverse, 1980). The rocks in the basin have been defined as the Dan River Group (Thayer, 1970), but lithostratigraphic nomenclature changes across the state line. Late Triassic (late middle and late Carnian) pollen, spores, and vertebrates have been found in the Cow Branch Formation of the Dan River Group (Olsen *et al.*, 1978, 1982; Robbins and Traverse, 1980; Thayer *et al.*, 1982). The total stratigraphic thickness of sedimentary rocks in the basin is estimated at 1100 m in the narrowest part of the basin, and may be more than 4000 m in the widest part (Henika, 1981).

Lithostratigraphy

In Virginia, three formations are recognized: (1) the mostly lacustrine Leakesville Formation, (2) the fluvial Dry Fork Formation, and (3) the fluvial and lacustrine Cedar Forest Formation (Table 2.1A; Meyertons, 1963). These formations are differentiated primarily on the basis of grain size. The Leakesville Formation is dominated by shale and siltstone, the Dry Fork Formation is dominated by sandstone, and the Cedar Forest Formation is dominated by conglomerate. As originally defined, these three formations all intertongue with each other and are at least in part lateral equivalents (Thayer, 1970). In North Carolina, a three-part stratigraphy is also present, but the nomenclature differs. Thayer (1970) divided the rocks into the following units: (1)

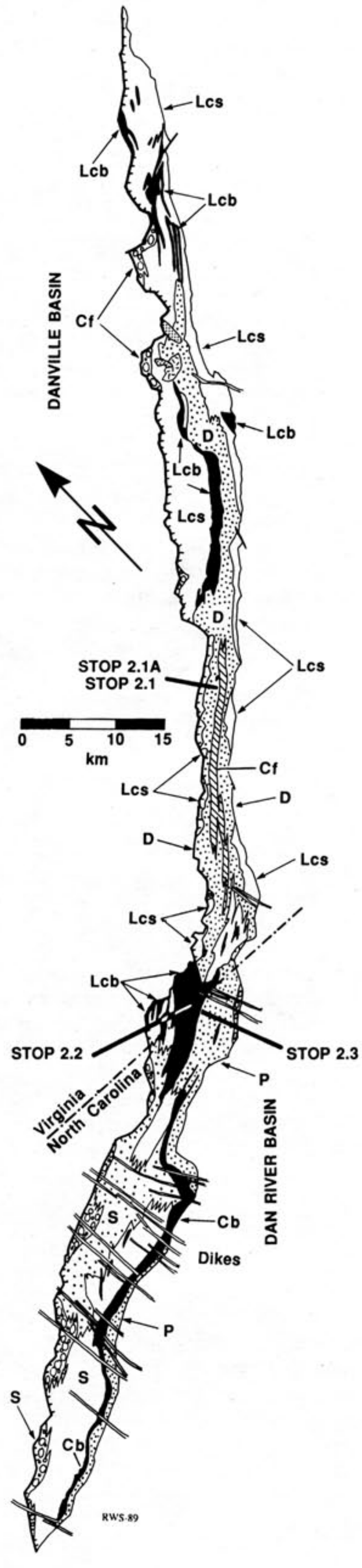

Figure 2.1: Geologic map of the Dan River-Danville basin, North Carolina and Virginia. Thin, double lines are dikes; regular stipple represents diabase intrusions; and black indicates predominantly lacustrine deposits. Abbreviations are: in Dan River basin—P, Pine Hall Formation; Cb, Cow Branch Formation; S, Stoneville Formation; in Danville basin—D, Dry Fork Formation; Lcs, Cascade Station Member of the Leakesville Formation; Lcb, Cow Branch Member of the Leakesville Formation; and Cf, Cedar Forest Formation. Modified from Meyertons (1963) and Thayer (1970).

Table 2.1A: Stratigraphy of the Dan River basin, North Carolina (after Thayer, 1970; Cornet, 1977a)

Units	*Thick-ness (m)*	*Age*	*Description*
Stoneville Fm.	?	Norian	Coarse to fine fluvial and alluvial clastics
Cow Branch Fm.	183	M.-L.Carn.	Gray to black, fine to coarse cyclical lacustrine clastics; thin coal seams at base
Pine Hall Fm.	2133	Carnian	Mostly tan, brown and red, coarse to fine fluvial and alluvial clastics

Table 2.1B: Stratigraphy of the Danville basin, Virginia (after Meyertons, 1963; Cornet, 1977a)

Units	*Thick-ness (m)*	*Age*	*Description*
Cedar Forest Fm.	?	Norian	Red, coarse to fine, basin margin, alluvial and fluvial clastics
Dry Fork Fm.	2438	?Car.-Nor.	Red to gray/green, fine to coarse fluvio-lacustrine graywackes and arkoses
Leakesville Fm.	?	L. Carnian - ?Norian	Red (Cascade Station Mb.) and gray to black (Cow Branch Mb.), fine to coarse, fluvial and cyclical shallow-water lacustrine clastics

the fluvial Pine Hall Formation, (2) the lacustrine Cow Branch Formation, and (3) the fluvial Stoneville Formation (Table 2.1B). The Pine Hall Formation is the lowermost unit and crops out along the southeastern basin margin. The Cow Branch Formation conformably overlies the Pine Hall but interfingers with it near the state line (Stop 2.3). The Stoneville Formation conformably overlies and interfingers with the Cow Branch-Pine Hall sequence (Thayer, 1970). We suspect that part of the rather choppy distribution of units apparent on the map (Figure 2.1) is due to intrabasinal faults, not interfingering, as does Weems (1988).

mileage

0 Begin mileage at 3020 Riverside Drive (US 58), Danville, VA.

0.8 At cloverleaf intersection of US 58 and US 29, get onto US 29 North.

10.5 Continue past VA 863 on left.

11.4 Entering Dan River-Danville basin. The basin is only about 3.2 km wide here. White Oak Mountain, just ahead, is a large northeast-trending ridge underlain by lithic arkoses and feldspathic litharenites (Thayer *et al.*, 1970). This is the mountain made famous in the ballad "Wreck of the Old 97". The railroad is less than a mile west of US 29 at this point.

12.1 Note roadcut on the left near top of White Oak Mountain off US 29. Pull off the road and park in dirt lot on the right side of the road. Cross the road with caution.

OPTIONAL STOP 2.1A: WHITE OAK MOUNTAIN NEAR DRY FORK, VA (by P.J.W. Gore)

Highlights: Coarse-grained fining-upward cycles in Dry Fork Formation

The outcrops on the west side of US 29 at White Oak Mountain, north of Danville, Virginia, are primarily red beds, which belong to the Dry Fork Formation, but they may be lateral equivalents of the Cow Branch Formation, which we will see later today. This locality was described by Meyertons (1963) in his report on the Triassic formations of the Danville basin and is also described by Thayer *et al.* (1970) in his field guide on the Dan River basin (Figure 2.2). The descriptions of this outcrop are from Meyertons (1963) and Thayer *et al.* (1970).

This site is located approximately in the narrowest part of the Dan River-Danville basin, and coarse-grained clastics extend across the basin here. These rocks are predominantly lithic arkoses and feldspathic litharenites, and they are arranged in thick, well-indurated, fining-upward cycles (7-10 m thick) consisting of sandy pebble conglomerates grading up to sandstone and in places capped by thin siltstone beds. The sandstones are characteristically poorly-sorted, have angular grains, and are commonly in grain-to-grain contact, with suturing and concavo-convex contacts (Thayer *et al.*, 1970), suggesting high pressures or temperatures. The high contact index and abundance of secondary overgrowths of calcite, chlorite, quartz, and albite are responsible for the hardness of these rocks (Thayer *et al.*, 1970).

An ideal fining-upward cycle at this locality consists of poorly-sorted pebble and cobble conglomerate overlying an erosional contact. The conglomerate, which actually consists of gravel lenses with low-angle cross beds to large trough cross beds (J.P. Smoot, pers. comm.), fines upward into dark gray, massive-appearing or trough cross-bedded, very coarse-grained sandstone, commonly containing scattered pebbles and cobbles (Thayer *et al.*, 1970). This sandstone grades upward into red or gray fine-grained sandstone, and the top of the cycle consists of red, massive, very fine-grained sandstone or siltstone (Thayer *et al.*, 1970). The presence of fining-upward cycles, possible channel lag conglomerates, and dune-scale cross bedding suggests fluvial deposition (Thayer *et al.*, 1970). The cycles are interpreted as the result of channel filling and migration in a braided stream environment because of the high ratio of coarse-to fine-grained rock, the wide range of grain sizes, and the presence of fining-upward sequences (Thayer *et al.*, 1970).

Leave Optional Stop 2.1A and continue north on US 29 for 0.6 miles.

12.7 Turn left into Vulcan Materials Corporation (first left going down the mountain from roadcut).

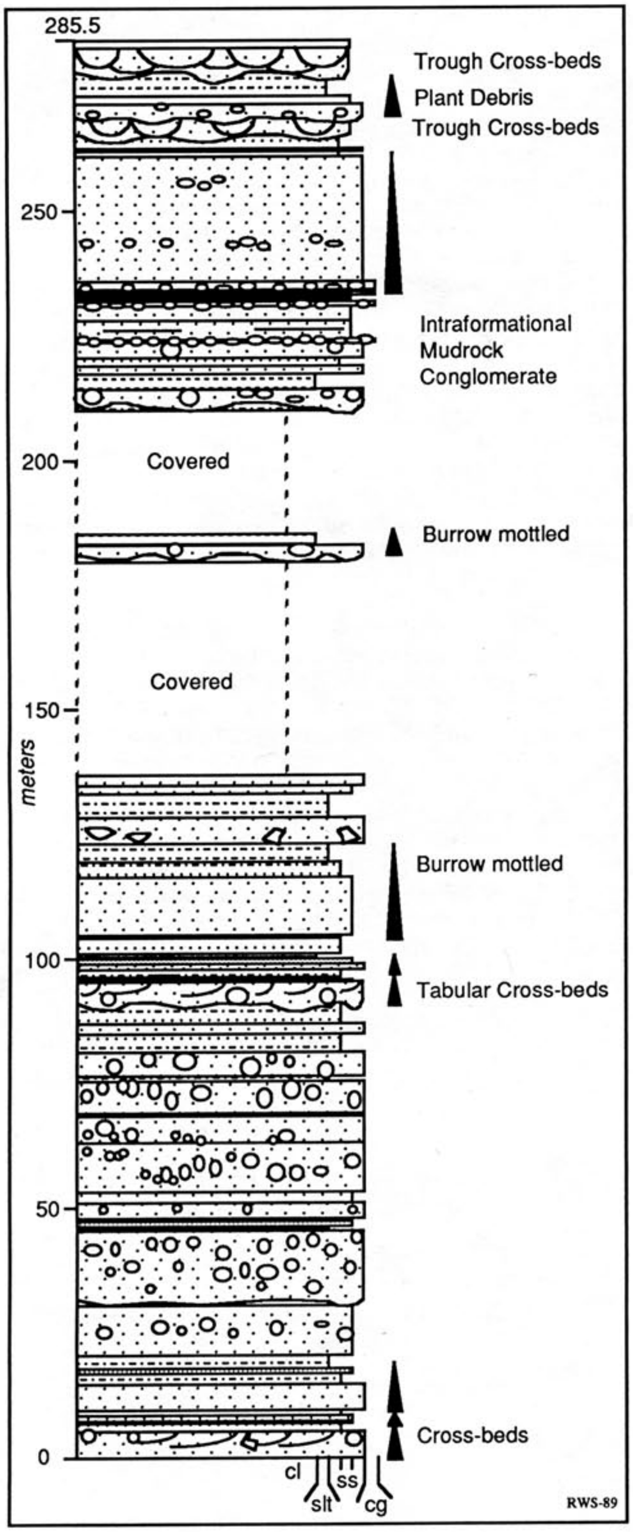

Figure 2.2: Measured section of the Dry Fork Formation along US 29, Stop 2.1A, showing several fining-upward cycles. Data for stratigraphic section from Thayer *et al.* (1970).

STOP 2.1: DRY FORK FORMATION AT CHATHAM QUARRY, CHATHAM, VA

(by P.E. Olsen and P.J.W. Gore)

Highlights: Large scale fluvial channels, intense bioturbation, conglomerates with unweathered feldspar.

The rocks exposed in this quarry are similar to those exposed in the White Oak Mountain roadcut on US 29, less than a mile away (see description of Optional Stop 2.1a). Note that the bedding is irregular and difficult to trace laterally due to large-scale channeling and faulting. Some of the conglomerates contain remarkably fresh pink feldspar (or feldspar overgrowths), suggesting deposition in an arid climate, rapid uplift and downcutting by streams, or retrograde weathering due to diagenesis.

The Chatham Quarry of the Vulcan Materials Corporation exposes more than 100 m of Dry Fork Formation. These beds lie stratigraphically below the Cow Branch Formation and are equivalents of the outcrops along US 29 described by Meyertons (1963) and Thayer *et al.* (1970). Large-scale tilted surfaces and large channel-form lenses can be seen in the quarry wall; however, small-scale sedimentary structures appear to be mostly obliterated by intense bioturbation or diagenetic overprints. Little detailed study has been made of these outcrops.

13.7	Leave Chatham Quarry. Turn right onto US 29 (heading south).
22.1	Follow US 29 South Truck Route. At the intersection of US 29 Bypass (Truck Route South 29) to US 58 West, fork to the right by cemetery (exiting basin).
25.8	Turn right onto US 58 West.
29.9	Crossing southeastern border and re-entering Dan River-Danville basin.
30.9	Turn left onto VA 863 to Eden, N.C. Note exposures of Dry Fork Formation on both sides of road. Ridges on right (northwest) for the next several miles are underlain by lithic arkoses and feldspathic litharenites of the Dry Fork Formation.
38.4	North Carolina state line. Road becomes NC 770.
40.7	Webster Brick Company quarry on right, lower Cow Branch Formation.
41.1	Cross the railroad tracks and turn right immediately into the Solite Quarry.

STOP 2.2: SOLITE QUARRY, LEAKSVILLE JUNCTION, VA (by P.E. Olsen and P.J.W. Gore)

Highlights: Cyclical lacustrine sequence; insect and reptile fossils; bedding plane shear zones; "syneresis cracks".

Quarries of the Virginia Solite Corporation on the border between North Carolina and Virginia expose a substantial portion of the Cow Branch Formation laterally equivalent to the type section of that unit. At these outcrops, the Cow Branch is highly cyclical and exceptionally fossiliferous. These exposures constitute one of the most important paleontological sites in North America.

This quarry and plant produce lightweight aggregate from shales in the Cow Branch Formation. Lightweight aggregate is any lithic substance that has been expanded by heating and can be used in place of sand, gravel, or crushed stone in mixtures of portland cement or in construction materials (Kirstein, 1970).

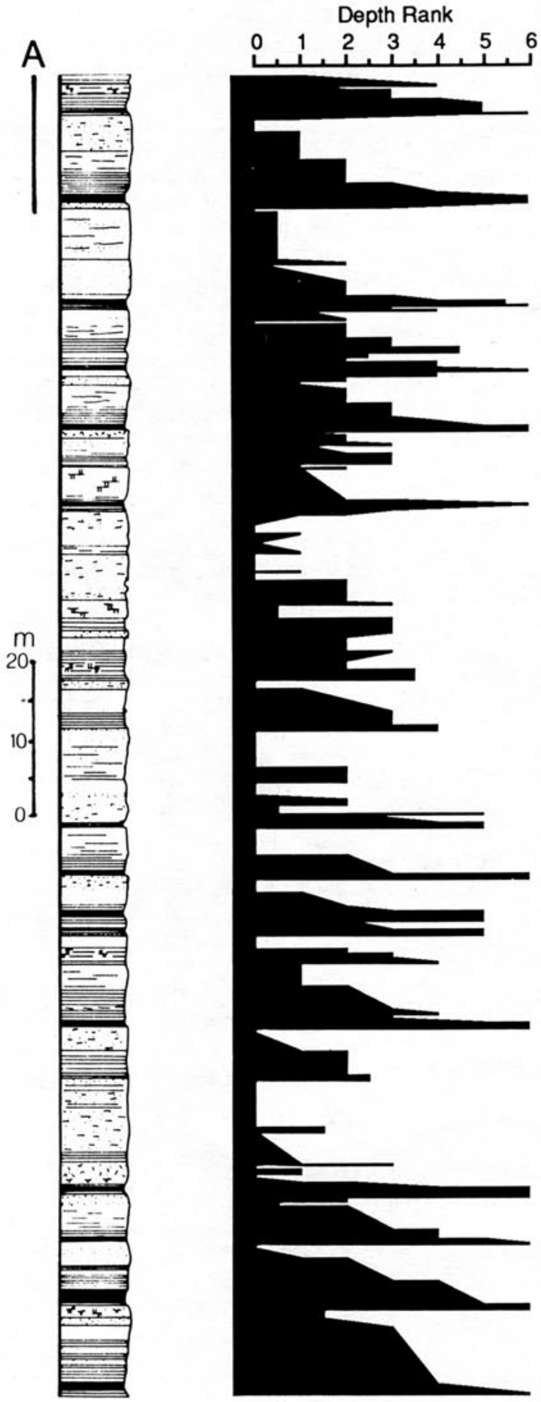

Figure 2.3: Measured section and depth ranks of the cyclical lacustrine Cow Branch Formation at the Solite Quarry, Stop 2.2. Black represents gray to black, finely-laminated calcareous siltstones; thin black lines represent gray, laminated siltstones; white represents gray, massive siltstone; and irregular stipple represents gray sandstone. Upper two lacustrine cycles labeled A are detailed in Figure 2.4. Modified from Olsen (1984a).

Cyclostratigraphy

One hundred and sixty meters of section, which dip at 30° NW (Kirstein, 1970), are exposed in the southern quarry (Figure 2.3) (not active at the time of writing). The main rock types present are: 1) black to gray, calcareous, laminated, clayey siltstone; 2) gray, mudcracked, massive mudstone; and 3) gray, ripple cross-laminated sandstone to cross-bedded conglomerate. All of the deposits appear to be lacustrine in origin with few fluvial channels.

The Cow Branch Formation is strikingly cyclical at a number of levels. These cycles can be analysed quantitatively by Olsen's (1986) depth rank classification and Fourier methods. The fine-grained lithologies can be broken down into a number of sub-categories which can be ordered by their interpreted depositional environment and used in quantitative analysis of cycle periodicities as shown by Olsen (1986) for the Lockatong Formation of the Newark basin (see Stop 5.7). These categories are called depth ranks because they are ranked by the time-averaged depth of water in which they were presumably deposited. In the Solite Quarry, as in the Lockatong Formation, the depth-rank categories described in Table 2.2 can be recognized. Chemical data correlate well with depth rank (Figure 2.4), and the correlation is especially strong between total organic carbon (T.O.C.) and depth rank (Figure 2.5). Depth ranks are based on several bedding and layering characteristics and are probably a more sensitive indicator of lake depth than any single chemical parameter.

The power spectrum of the Solite Quarry section (Figure 2.6) shows a number of significant peaks, the most prominent of which are at 8.9 m, 12.0 m, 41.0 m, 68.3 m, and 208.8 m. There are also significant peaks at 5 m to 6.6 m and a less significant peak at 22.8 m. Visual examination of the actual section shows that the 8.9 and 12 m cycles correspond to the types of cycles described by Van Houten

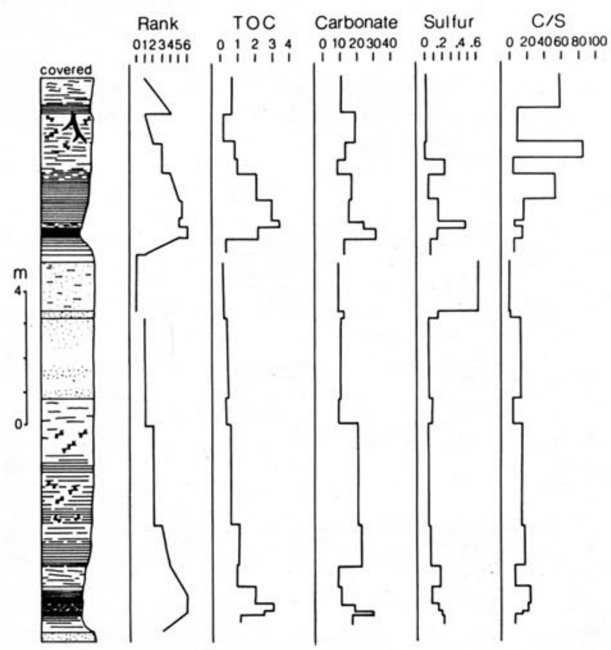

Figure 2.4: Depth ranks and chemical data from the upper two cycles (A in Figure 2.3) of the Cow Branch Formation exposed in the Solite Quarry. Note particularly the positive correlation between depth ranks and total organic carbon (T.O.C.). From Olsen (1984a).

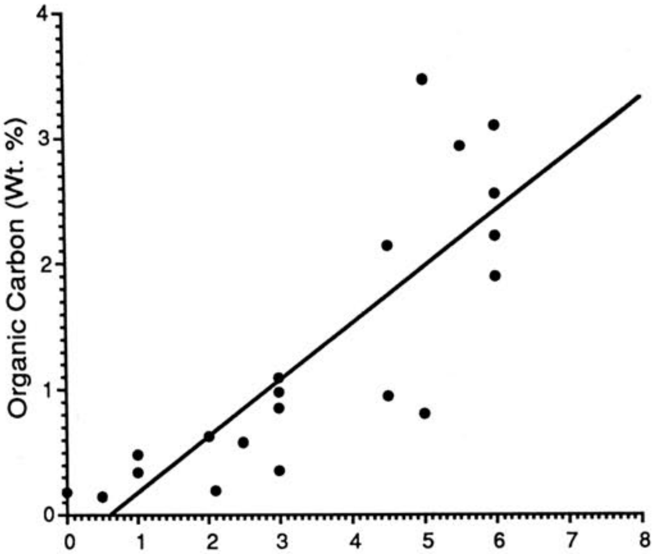

Figure 2.5: Correlation of depth rank and organic carbon content from the two cycles shown in Figure 2.4. $R^2 = 0.7$. Data from Olsen (1984a).

(1964) from the Lockatong Formation of the Newark basin (see Stop 5.7). These sorts of cycles are common in most Newark Supergroup basins.

In the Solite Quarry, the closest match between the ratios of the modern orbital periods and the periods in thickness are seen if the 8.9 and 12.0 m peaks are hypothesized to represent the precession cycles of 19,000 and 23,000 years, respectively (Table 2.3). If we set the average of these two periods in thickness to 21,000 years, corresponding to a sedimentation rate of 0.304 mm/yr, the durations in years of the main periods seen in the Solite section are shown in Figure 2.6. These periods are in rather close agreement with both the predictions of the orbital theory and the periods seen in the Lockatong and Passaic formations of the Newark basin.

Paleontology and Environments

The fossils follow a predictable sequence tracking the lithological changes seen through Van Houten cycles (Olsen *et al.*, 1978). Articulated fish and reptiles and complete insects occur only in the finest laminated (depth rank 6), organic carbon-rich (T.O.C. 2%) portions of division 2. Plant foliage compressions occur in these units and in surrounding slightly less well-laminated but still organic carbon-rich units. Root structures, burrows and casts of *in situ* plant stems occur in poorly-laminated units (depth rank 3-0) as do carbonized scraps of mostly conifer wood and foliage. Reptile footprints and plant fragments are present on surfaces of low depth rank (2-1) mudstones and sandstones that have polygonal cracks on thin bedding planes. Isolated bones and teeth of phytosaurs can occur in all lithologies. Besides producing extremely large numbers of articulated skeletons of the little reptile *Tanytrachelos* (Figure 2.7), the Solite Quarry has yielded some of the very oldest true flies and the oldest true water bugs (Figure 2.8). A faunal and floral list is given in Table 2.4.

The taphonomic pattern seen in division 2 of Van Houten cycles fits a chemically-stratified lake model (Bradley, 1929, 1963; Ludlam, 1969; Boyer, 1981), in which bioturbation is perennially absent from the deeper parts of the lake bottom because the bottom waters lack

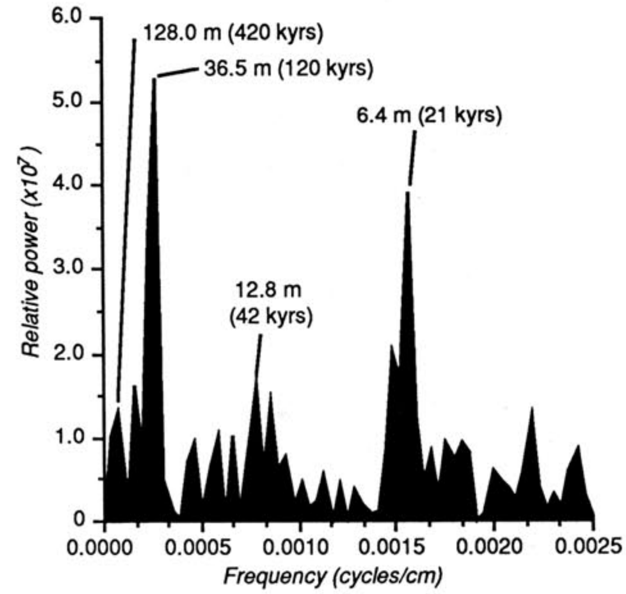

Figure 2.6: Power spectrum of depth rank curve (Figure 2.3) at the Solite Quarry, illustrating prominent periodic thicknesses. The sedimentation rate is .304 mm/yr.

Table 2.2: Description of depth ranks for fine-grained lacustrine sediments (from Olsen, 1986).

Depth Rank	*Description*	
0	Massively bedded calcareous claystone and siltstone with root, tube, crumb, and vesicular fabric; faint remnant parent fabric present; abundant clay cutans; intensely desiccated fabric	Shallow Oxygenated High-Energy Lake
1	Intensely brecciated and cracked calcareous claystone and siltstone; burrows can be common but obvious remnant parent fabric present; mud curls and cracks with vesicular fabric sometimes present	↑
2	Thin-bedded calcareous claystone and siltstone with desiccation cracks; large patches of uncracked matrix preserved; reptile footprints and burrows often present; infrequent desiccation cracks	*Time-Averaged Conditions*
3	Thin-bedded calcareous claystone and rare siltstone with very small scale burrows; rare to absent desiccation cracks; pinch and swell lamination often present	
4	Evenly laminated calcareous claystone with some small-scale burrows; abundant discontinuous laminations; no desiccation cracks	↓
5	Evenly and finely laminated calcareous claystone or limestone; abundant discontinuous laminations; no desiccation cracks	Deep Anoxic Low-Energy Lake
6	Microlaminated calcarous siltstone with only rare disruptions; no desiccation cracks	

Table 2.3: Ratios of periodicities in thickness compared with the ratios for the modern orbital periods. P is precession; O is obliquity; E1-3 are first three terms of eccentricity

	P	O	E1	E2	E3
Modern Periods	1.0	1.9	4.4	5.8	19.0
Lockatong Formation Average	1.0	1.8	4.3	5.5	16.3
Cow Branch Formation	1.0	2.0	—	5.7	20.0

oxygen, necessary for almost all macroscopic benthic organisms. Chemical stratification, often called meromixis, can arise by a number of mechanisms, but the main physical principle involved is the exclusion of turbulence from the lower reaches of a water column. This tremendously decreases the rate at which oxygen diffuses down from the surface waters and retards the upward movement of other substances. The main source of water turbulence is wind-driven wave mixing. This turbulence usually extends down about one-half the wavelength of surface wind waves, which depends on the fetch of the lake, wind speed, and wind duration. If the lake is deeper than the depth of the turbulent zone, the lake becomes stratified with a lower non-turbulent zone and an upper, turbulently-mixed zone. The thickness of the upper mixed zone is also dependent on density differences between the upper waters (epilimnion) and lower waters (hypolimnion) which can be set up by salinity differences (saline meromixis) or by temperature differences as in many temperate lakes. In the absence of saline or temperature stratification, chemical stratification can still arise in a deep lake with relatively high levels of organic productivity. Because oxygen is supplied slowly by diffusion, consumption by bacteria of abundant organic matter sinking into the hypolimnion plus oxidation of bacterial by-products eliminates oxygen from the hypolimnion. Lakes Tanganyika and Malawi in East Africa are excellent examples of very deep lakes in which there is very little temperature or density difference between the epilimnion and hypolimnion, but still chemical stratification occurs with the exclusion of oxygen below 200 m. Such a pattern is common in deep tropical lakes. The preservation of microlaminations and fossils in Cow Branch cycles may have been a function of great water depth relative to a small surface area of the lake.

An alternative explanation is that the Cow Branch lakes exhibited saline meromixis, in which a low-density, relatively dilute epilimnion floated on a highly-saline, high-density hypolimnion. Although probably not stable over long periods of time, a shallow body of water could be chemically stratified in this way, possibly decoupling inferred "depth ranks" from depths (*e.g.*, Bradley and Eugster, 1969). Berner (1979) and Berner and Raiswell (1983) have documented a relationship between salinity and pyrite sulfur content (water sulfate content related to salinity) and this should allow us to tell whether or not the bottom waters of the Cow Branch lakes were saline. Dissolved sulfate is limiting to the growth of sulfate-reducing bacteria until roughly 14 ppt (1100 mg/l sulfate) is reached, and at higher salinities, the amount of metabolizable organic matter is limiting. Thus, under low sulfate concentrations, as in most non-saline lakes, there is no correlation between T.O.C. and pyrite sulfur. Carbon and sulfur data (Figure 2.9) from the two Van Houten cycles shown in Figure 2.4 show essentially no correlation and fall in the fresh water field of Berner *et al.* (1979) and Berner and Raiswell (1983). It is, of course, possible that the sulfates have been removed diagenetically or that the bottom waters could have been saline without being enriched in sulfate, but the compositions of the rocks surrounding the Dan River-Danville basin would appear to

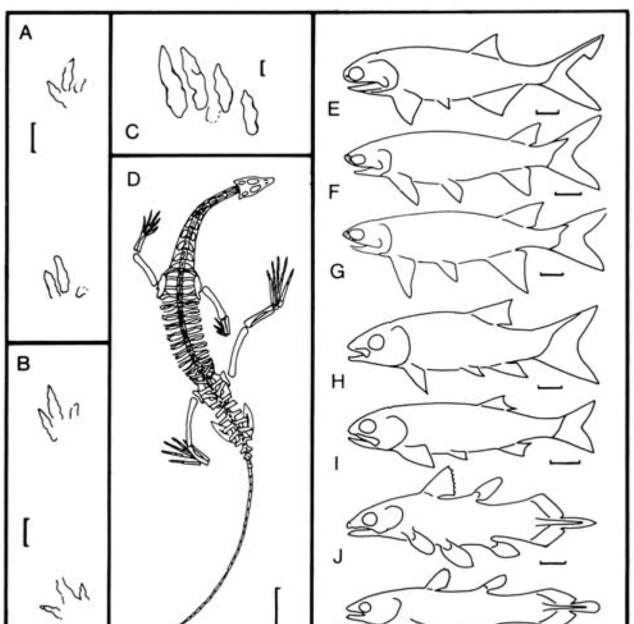

Figure 2.7: Vertebrate fossils from the Solite Quarry. A-B, cf. *Atreipus* sp. trackways; C, left pes impression of *Apatopus* sp.; D, *Tanytrachelos ahynis*; E, palaeoniscid *Turseodus*; F, redfieldiid palaeonisciform *Synorichthys*; G, redfieldiid palaeonisciform *Cionichthys*; H, holostean of the *Semionotus brauni* group; I, undetermined holostean; J, coelecanth *Osteopleurus newarki*; and K, coelecanth *Pariostegus*. Scales are all 1 cm. Modified from Olsen (1988b).

Table 2.4A: Plants from the Solite Quarry, Stop 2.2.

PLANTS
- Lycopodiales (lycopods)
  - cf. Grammaephoios sp.
- Sphenophytes -
  - Equisetales (horsetails)
    - *Neocalamites* sp.
- Pteridophytes
  - Filicales (ferns and fern-like organisms)
    - *Lonchopteris virginiensis*
    - cf. *Acrostichites linnaeafolius*
    - *Dictyophyllum* sp.
  - Caytoniales (Mesozoic seed ferns)
    - cf. *Sagenopteris* sp.
- Coniferophytes
  - Coniferales (conifers)
    - *Pagiophyllum* spp.
    - *Glyptolepis* cf. *G. platysperma*
    - cf. *Compsostrobus neotericus*
    - cf. *Dechellyia* sp.
    - *Podozamites* sp.
- Cycadophytes
  - Cycadales (cycads):
    - *cf. Zamiostrobus lissocardus*
    - *Glandulozamites* sp.
    - large androsporophylls
  - Bennettitales (cycadeoids)
    - *Zamites powelli*
    - *Pterophyllum* cf. *Ctenophyllum giganteum*

be capable of producing high-sulfate brines (Robbins, 1982). Thus, the bottom waters of the Cow Branch lakes were probably not saline, and chemical stratification probably developed as a consequence of great water depth and stratification of turbulence (Olsen, 1984a).

Van Houten cycles with a microlaminated division 2 thus reflect the alternation of shallow, ephemeral lakes or subaerial flats and deep perennial lakes with an anoxic hypolimnion set up by turbulent stratification under conditions of relatively high primary productivity and low organic consumption (*e.g.*, low ecoystem efficiency). The low organic content of divisions 1 and 3 of the cycles probably reflects higher ecosystem efficiency caused by shallow water depths rather than lower total organic productivity.

Table 2.4B: Animals from the Solite Quarry, Stop 2.2. † indicates an ichnotaxon.

- ANIMALS
  - Arthropods
    - Crustacea
      - Diplostraca (clam shrimp and water fleas)
        - *Cyzicus* sp.
        - ?*Paleolimnadia* sp.
      - Ostracoda
        - *Darwinula* spp.
      - Decapoda
        - cf. *Clytiopsis* sp.
    - Insecta
      - Blattaria (roaches)
        - several genera
      - Heteroptera (true bugs)
        - cf. Hydrocorisiae (water bugs)
          - new genus
      - Coleoptera (beetles)
        - cf. Nitidulidae (sap beetles)
          - several genera
        - cf. Buprestidae (metallic wood-boring beetles)
          - several genera
      - Psocoptera
        - new genus
      - Diptera (true flies)
        - Tipulidae (crane flies)
          - several genera
        - Bibionidae (March flies)
          - several genera
        - cf. Glosselytrodae
          - undetermined genus
  - Pisces
    - Actinopterygii (bony fishes)
      - Palaeonisciformes
        - *Turseodus* spp.
        - *Cionichthys* sp.
        - *Synorichthys* sp.
      - Semionotidae
        - *Semionotus* sp.
      - ??Pholidophoridiformes
        - new genus
    - Sarcopterygii (lobe finned fish)
      - Coelacanthini
        - cf. *Pariostegus* sp.
        - *Osteopleurus* sp.
  - Reptilia
    - Lepidosauromorpha
      - Tanystropheidae
        - *Tanytrachelos ahynis*
    - Archosauria
      - Phytosauridae (crocodile like archosaurs)
        - *Rutiodon* sp.
        - †*Apatopus* sp.
      - ?Ornithischia
        - †*Atreipus* cf. *A. mifordensis*
      - Saurischia
        - †?*Grallator* sp.

A large (*ca.* 10 m^2) excavation in cycle CB1-2 (Figure 2.10) produced over 150 skeletons of *Tanytrachelos*, dozens of fish, and over 300 insects, as well as abundant conchostracans and plant foliage. The microstratigraphy of this excavation reveals details of the lake transgression and regression. Many details of the pattern seen in the microstratigraphy and taphonomy of cycle CB1-2 are seen not only in other Cow Branch Van Houten cycles but in many other places where Van Houten cycles are recognized in the Newark Supergroup (see Stops 5.7, 6.2, 6.6-6.8). Normally, however, the occurrence of articulated reptiles is not symmetrical but rather limited to the lower few centimeters of division 2. The reasons for this common asymmetry are not clear but might involve increasing salinity as the lake evaporated.

"Syneresis Cracks"

Well-laminated, organic carbon-poor portions of Van Houten cycles in the Newark Supergroup often show small (<1 cm) to large (>10 cm) structures on bedding planes which have variously been referred to as subaqueous shrinkage cracks or syneresis cracks. These are especially well developed in the Solite Quarry section (Figure 2.11).

In plan view, these structures appear as elongate, lozenge-shaped impressions. Some appear to have a preferred orientation. Recent examination, at this section and also in the Jurassic Portland Formation of the Hartford basin, reveals that these structures are mechanically similar to the half-graben structures described by Shelton (1984) and Barnett *et al.* (1987). As seen in cross section and plan view, the structures are bounded on one side by a low-angle normal fault in which the net slip appears to be maximized at the center and dies out in all directions through just a few millimeters in the vertical direction and larger amounts in the horizontal direction (Figures 2.11, 2.12). The hanging wall adjacent to the fault is depressed in proportion to the relative amount of slip on the fault, producing a micro-half-graben. The footwall adjacent to the fault is similarly uplifted. Thus, the structures appear similar regardless of whether they are right-side up or up-side down. There is no evidence for filling of the micro-half-graben during deformation; instead adjacent material seems to have flowed. Therefore, the formation of these micro-half-graben seems to have been a process occurring below the sediment-water interface, within the sediment layers.

The net effect of many of these micro-half-graben is that bedding is thinned. In tectonics, such thinning and faulting is usually thought of as a consequence of stretching. However, the beds which appear to show a random orientation of these structures show that, because stretching cannot take place in all directions at once, the bed itself must have shrunk in volume. These micro-half-graben are thus evidence of a volume change within the bed. Compaction compensates for shrinkage in the vertical direction. Because the structures formed within the bed, there is no reason to suspect that the shrinkage occurred subaqueously. All we can infer is that shrinkage occurred, perhaps by water loss and/or clay mineralogy change, and there are no compelling reasons why such structures should be characteristic of any specific environment.

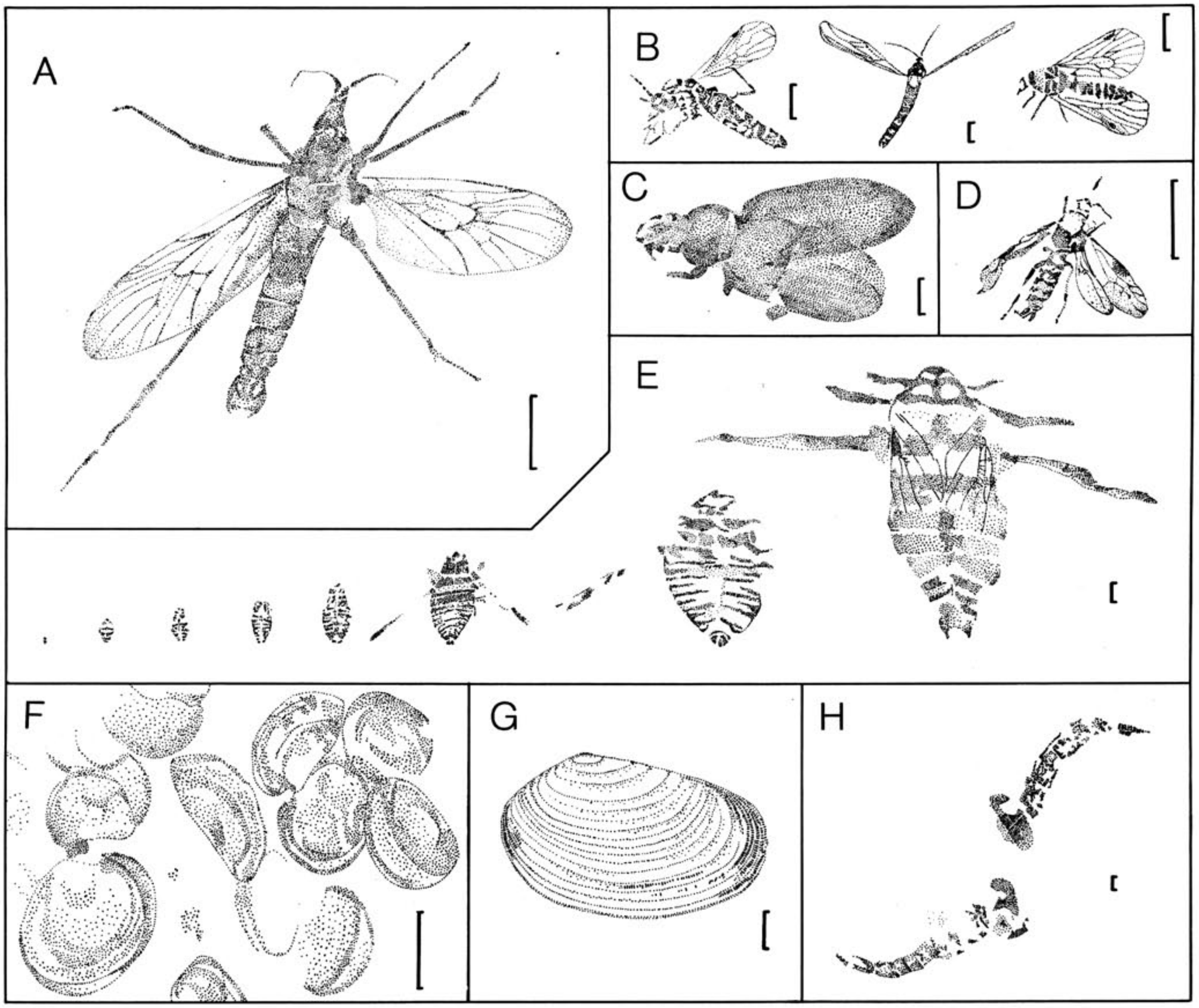

Figure 2.8: Insect fossils from the Solite Quarry. A and B, true flies (Diptera, ?Tipulidae); C, beetle; D, psocopteran; E, partial growth series of ?hydrocoricid water bugs. Scales are all 1 mm. From Olsen (1988b).

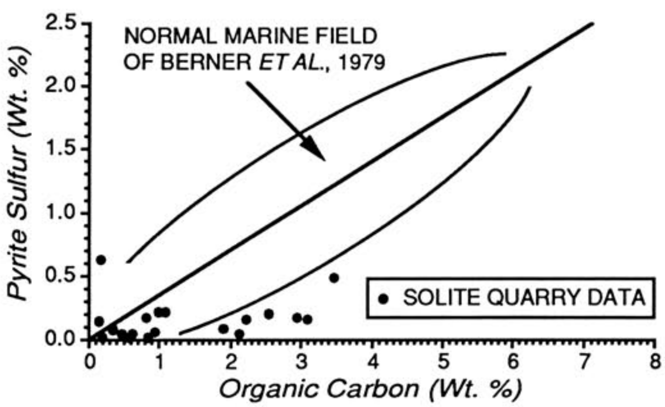

Figure 2.9: Correlation of weight percent organic carbon and weight percent pyrite sulfur from the Solite Quarry in relation to the marine fields. Note that there is no correlation between the variables which is characteristic of continental environments. From Olsen (1984a).

Deformation

Two partially gradational styles of deformation are evident in the Solite Quarry section which are also characteristic of the Newark Supergroup in general. Brittle deformation is concentrated in bedding plane shear zones and occasional high-angle faults, and ductile deformation is especially noticeable in the beds adjacent to the bedding plane shear zones. The bedding plane shear zones most often invade division 2 of Van Houten cycles, usually within more clastic portions and often in the best-laminated intervals (Figure 2.13). Slip can be concentrated along single bedding planes or sets of bedding planes with the development of slickensides, polished surfaces, and well-organized duplexes. Folds are often present both within and outside the duplexes. Sometimes there are voids, filled with evidently liquefied sediments, and clastic dikes, which probably formed quite early in the burial history. On the other hand, slip can involve decimeters of section, with the development of complex zones of polished and slickensided flakes and plates, almost totally decalcified. Duplexes consisting of coherent phacoids, themselves made up of

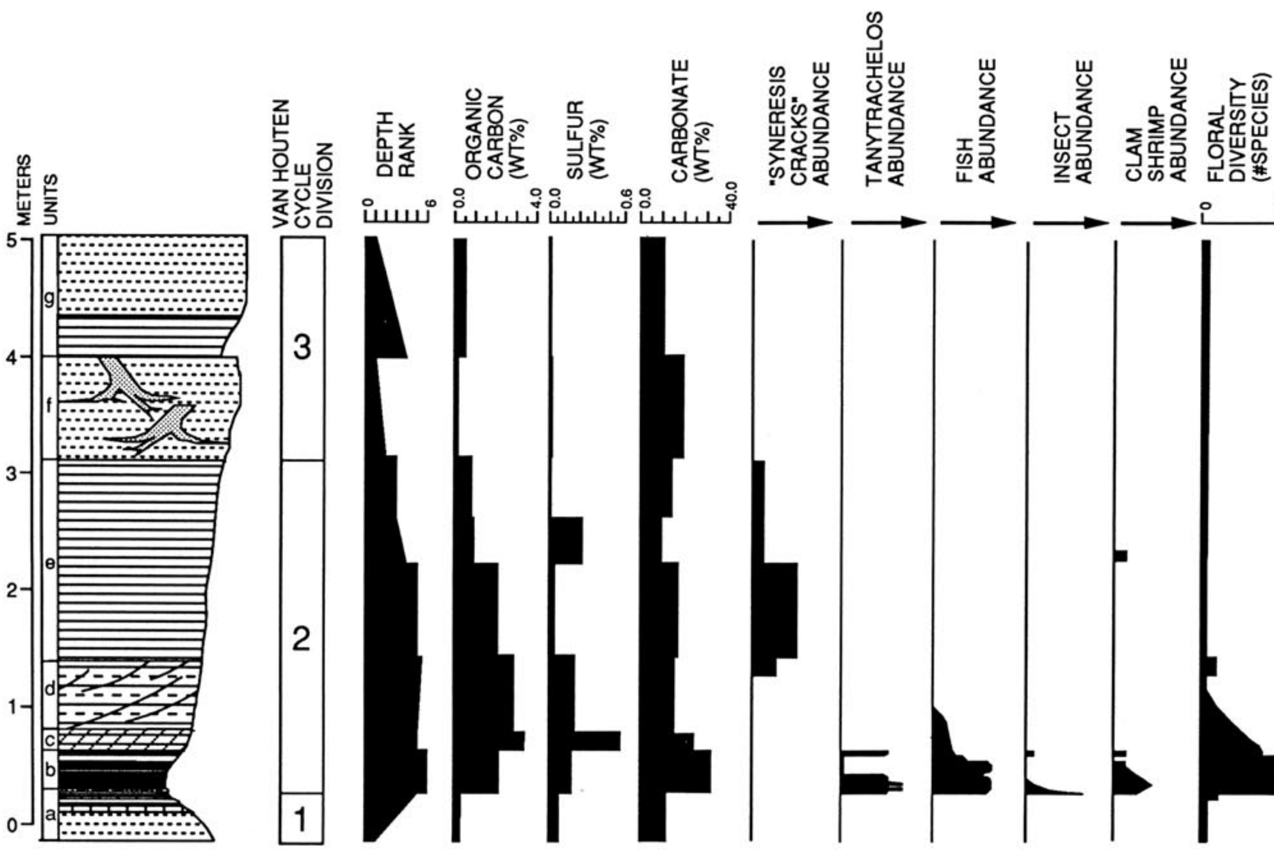

Figure 2.10: Microstratigraphy of the uppermost cycle of the Solite Quarry section. Modified from Olsen (1984a).

Figure 2.11: Oriented "syneresis cracks" surrounding a root cast from the Solite Quarry. Photo by P.E. Olsen.

slickensided flakes and plates, are often present, as are mineralized voids and gouge. The absence of liquefied sediment and the presence of mineralized zones suggest that these features formed later in the burial history of the sequence.

Many bedding planes in division 2 also show bedding plane-parallel ductile deformation which is especially obvious in deformed fossils, such as skeletons of reptiles (*Tanytrachelos*—Figure 2.13) and as a lineation caused by numerous deformed fossils, such as conchostracans. Small-scale folds are also present, commonly associated both with bedding-parallel shortening and the development of duplexes. Polygonal cracks within divisions 1 and 3 of Van Houten cycles do not show evidence of this kind of ductile deformation, as is seen in the Jacksonwald syncline of the Newark basin (see Stop 5.1).

We can imagine a sequential development of deformation styles in bedding shear zones from ductile deformation in water-rich sediments at shallow burial depths to brittle deformation in the same strata with additional shear under greater burial depths. There have been no systematic studies of bedding plane shear zones in the Newark Supergroup, and thus this scenario of progressive deformation remains untested. At least in part, these shear zones are related to the mechanism of accommodation within half-graben sediments, necessary because of rotation and thinning of strata.

42.7	Leave quarry, turn right (west) onto NC 770/VA 863.
43.7	Welcome to Eden, NC.
47.0	Turn right onto NC 14-87-770.
47.3	Cow Branch Formation with *Diplurus* fish fossils is exposed on left in ditch.

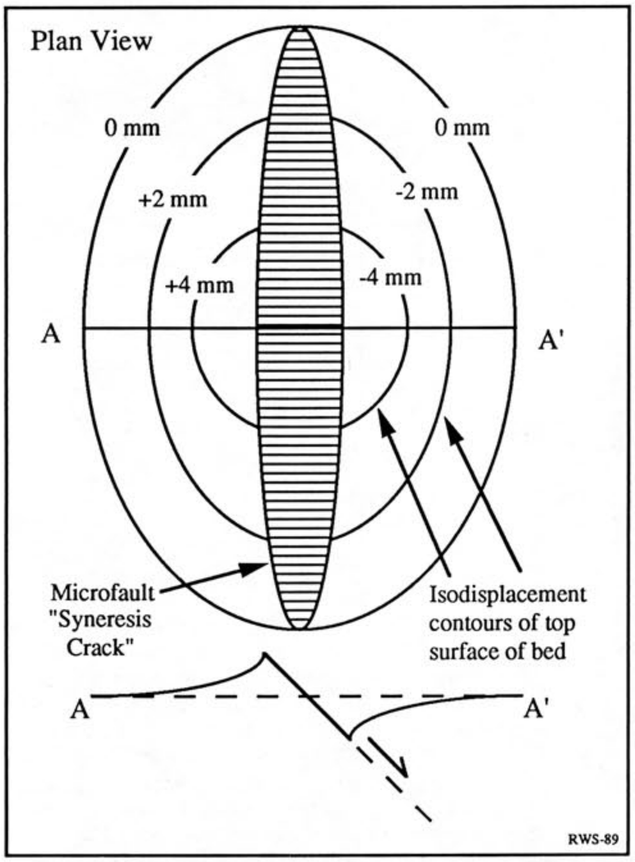

Figure 2.12: **Conceptual diagram of a "syneresis crack" based on models of faults of finite length (Shelton, 1984; Barnett *et al.*, 1987). Note that the "cracks" are miniature half-graben.**

47.9 Turn around and go back to NC 770-700.
48.1 Exit right onto ramp at and go east on NC 700-770. (Just past Cow Branch outcrop).
52.6 Railroad tracks and Solite Quarry entrance.
53.0 Left into old Webster Brick Quarry (now abandoned).

STOP 2.3: WEBSTER BRICK COMPANY QUARRY, EDEN, NC (by P.J.W. Gore and P.E. Olsen)
Highlights: Black shale, tan cross-bedded sandstone, and red beds of Pine Hall Formation.

The Pine Hall Formation is thickest in this part of the basin and exceeds 2100 m. It is much thinner in the southern part of the outcrop belt, being only about 75 m (Thayer, 1970). The formation coarsens southeastward toward the basin margin, and a conglomeratic lithofacies unconformably overlies pre-Triassic basement rocks in a narrow belt along the southeastern edge of the basin about 3.5 km from here (Thayer, 1970).

Maroon claystones and shales were quarried here from the uppermost part of the siltstone facies of the Pine Hall Formation for the manufacture of brick (Thayer *et al.*, 1970). Most of the rocks exposed here are red, but cross-bedded tan sandstone and black, laminated shale are also exposed. This exposure is in the siltstone facies of the Pine Hall Formation, which is composed of reddish-brown siltstone, claystone, and shale that form planar, thin-bedded

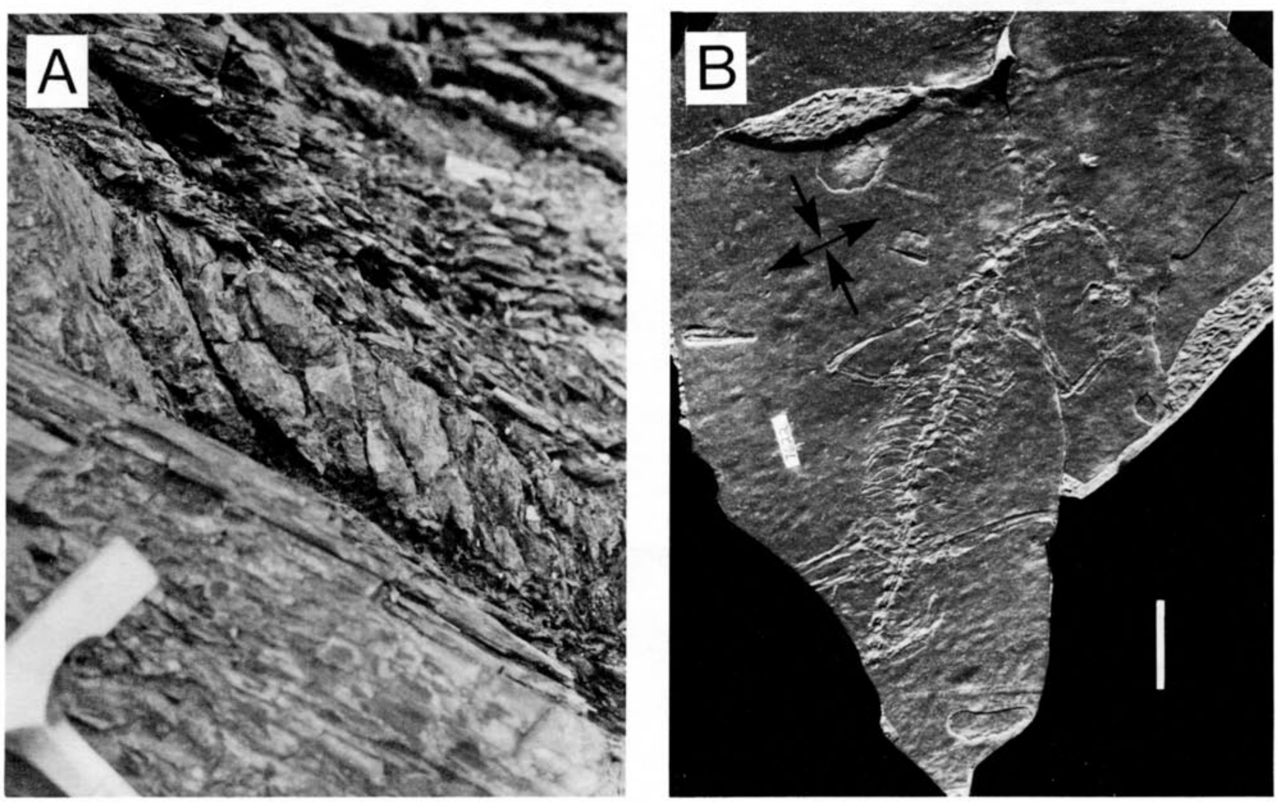

Figure 2.13: A) Bedding plane-subparallel shear zone and fault-bound slivers of rock (phacoids) forming what appears to be a duplex within laminated siltstone of the Solite Quarry. Sense of shear is top to the left. B) Deformed *Tanytrachelos* associated with shear zone similar to that shown in (A); scale bar is 2 cm. Photos by P.E. Olsen.

to thick-bedded (decimeter) units and less common grayish-orange, poorly sorted arkosic sandstone that also forms thin to thick beds (Thayer, 1970). The strata are characterized by mottled and disturbed bedding, calcareous concretions, cut-and-fill structures, current lineation, graded bedding and *Scoyenia*-type burrows (Thayer, 1970).

The upper contact of this formation is gradational into the Cow Branch Formation, the base of which is placed at the lowest persistent dark colored shale (Thayer, 1970). The black shale present in this quarry is not microlaminated, as is typical of the transition between the Pine Hall and Cow Branch formations. Fossils from the black shale include the fish *Turseodus*, *Synorichthys*, and *Diplurus*, as well as phytosaur teeth, coprolites, conchostracans, and extremely abundant darwinulid ostracodes. Large inclined sandstone and siltstone beds that were formerly exposed above the black shale may have been delta foresets.

53.4 Leave Webster Brick Quarry. Turn left (east) onto NC 770.

55.6 Virginia state line.

61.1 Oak Ridge Estate on right

63.1 Turn right onto US 58 East.

68.4 Cross US 29 and continue east on US 58.

71.6 Intersection of Main Street and US 58.

78.6 Intersection of US 58 and the road to Milton, N.C.

101.3 Turn left onto US 360 East toward Richmond (at flashing yellow light).

117.1 Cross Staunton/Roanoke River.

127.6 Lookout tower.

134.9 Exit onto Business US 360-US 15 to Keysville, VA.

138.7 Exit onto US15 North to Farmville, VA.

150.8 Cross Briery Creek. We are now in the Briery Creek basin.

The Briery Creek basin is one of the smallest basins of the Newark rift system, a maximum of 2 km wide and 7 km long (Figure I.1). Several other small basins lie a few kilometers to the south in this area, including the Roanoke Creek, Randolph, and Scottsburg basins. The Farmville basin, which is somewhat larger, lies a few kilometers to the north. The Briery Creek basin is a graben in which the rocks dip toward the western faulted margin (Wilkes, 1987) which occurs in an epidote-rich, Paleozoic mylonite zone up to 91 m wide, adjacent to feldspar-rich amphibolite gneiss. The eastern margin of the basin is in fault contact with garnetiferous schist (Wilkes, 1986, 1987). The sedimentary rocks in the basin have been dated as Carnian based on palynomorphs and megafossils (E.I. Robbins, personal communication, *in* Wilkes, 1987).

The rocks in the Briery Creek basin include breccia, conglomerate, sandstone, siltstone, mudstone shale, coal, and diabase (Wilkes, 1986, 1987). Coal was discovered in the southern part of the basin in 1833, and a coal seam about 60 cm thick was mined during the middle 1800's (Wilkes, 1987).

150.9 Pass sign to Chesapeake Nature Trail.

153.4 Pass VA 133

The Farmville basin is the largest and northernmost of a line of several small basins clustered in the south-central Virginia Piedmont, southwest of Richmond (Figure I.1). The basin is approximately 37 km long, and about 7 km wide, elongated in a northeast-southwest direction, similar to the other basins of the Newark rift system. The western border of the basin is a high-angle normal fault associated with a Paleozoic? mylonite zone, and the rocks in the basin dip westward toward the fault at 30°-35°. The eastern border of the basin is also faulted. Diabase dikes cut across the basin and its border faults. Although the dikes are only a few feet wide, many are mappable for kilometers (Wilkes, 1986). The present basin is probably a small erosional remnant of a formerly much larger basin. In all probability, the Farmville basin and the cluster of smaller basins to the south were originally part of one larger basin. Exposures in all of these basins are poor, and we will not visit them on this trip.

156.3 Arrive at stop for evening.

3. RICHMOND BASIN, VIRGINIA

GEOLOGY OF THE RICHMOND BASIN
(by P.J.W. Gore and P.E. Olsen)

The Richmond basin is located in east-central Virginia, approximately 19 km west of Richmond, near the eastern edge of the Piedmont (Figures I.1, 3.1). The basin is surrounded by igneous and metamorphic rocks of the Piedmont Province and bounded on the west by a normal fault believed to be a reactivated portion of the Hylas zone (Goodwin *et al.*, 1985), a Paleozoic thrust fault (Taylor and Ressetar, 1985) or Alleghenian strike-slip fault (Manspeizer and Gates, 1988). The basin is approximately 53 km long and 15 km wide at its widest point (Goodwin *et al.*, 1985). The dated sedimentary rocks in the basin range from early to middle Carnian (early Late Triassic) (Traverse, 1987; Cornet, in press), and a few Jurassic diabase dikes intrude both the rocks in the basin and the surrounding Piedmont (Goodwin *et al.*, 1986). The thickness of the sedimentary fill in the Richmond basin has been determined by drilling in several locations. Depth to basement reaches 2177 m in the south central part of the basin (Goodwin *et al.*, 1986). Five small outlier basins are present near the northeastern edge of the Richmond basin and were probably once continuous with the main basin, but were later isolated from it by erosion (Goodwin *et al.*, 1985). Based on trends of maturation and porosity, Cornet and Ziegler (1985) stated that more than 2100 m of sediment have been eroded from the Richmond and Taylorsville basins. If so, the total thickness of sedimentary basin fill in the Richmond basin may have been as much as 4300 m.

The similarity of the fossil assemblages and facies patterns (Olsen *et al.*, 1982) and the proximity of the two basins suggest that the Richmond basin was once continuous with the Taylorsville basin, which lies just 11 km to the north. The Taylorsville basin extends in the subsurface to the northeast and according to Hansen (1988) is continuous with the recently discovered Queen Anne basin of the Delmarva Peninsula, and possibly its equivalents in southern New Jersey (Sheridan *et al.*, 1988, pers. comm., 1988). Far from being small isolated remnants, the Richmond-Taylorsville-Queen Anne sub-basins constitute one of the largest divisions of the Newark Supergroup, one with a very distinctive stratigraphic and sedimentologic pattern.

Shaler and Woodworth (1899) established the first formal stratigraphic classification of the Richmond basin (Table 3.1). Recent exploratory drilling and field work by a number of workers have shown the need for revision of their system, including the need for several new unit names. Herein, the revised nomenclature of Ediger *et al.* (in prep.) is used (Table 3.1).

RICHMOND BASIN LITHOSTRATIGRAPHY AND PALEOENVIRONMENTS (by B. Cornet)

The small size of the Richmond basin relative to other basins of the Newark Supergroup is deceiving, because the basin occupies the southwestern side of an elongated rift valley area and the distribution of its sedimentary facies suggest that this basin may preserve only a part of the original rift valley fill south of the Taylorsville-Queen Anne basins. Based on the literature (*e.g.*, Taylor, 1835; Clifford, 1887; Shaler and Woodworth, 1899; Goodwin and Farrell, 1979), the basin was thought to contain no more than 1067 m of basin-restricted fluvial, lacustrine, and coal swamp strata. Well and seismic data acquired since 1980 have greatly expanded our knowledge of the stratigraphy and structure of the basin. To date at least 17 shallow wells (under 1000 m) and 3 deep wells have been drilled for oil

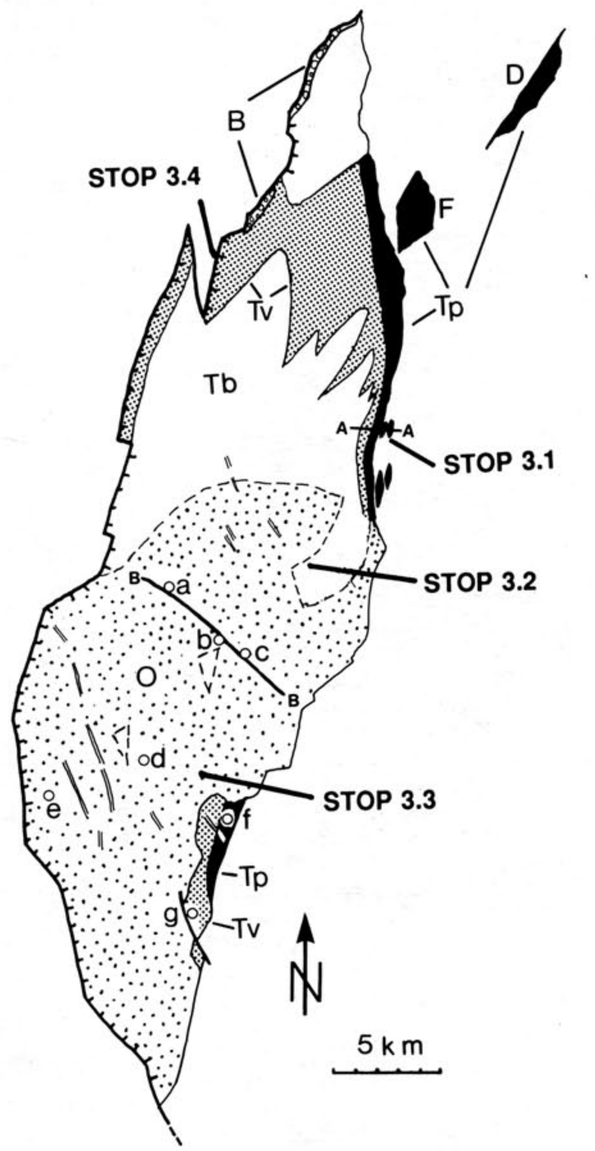

Figure 3.1: Geologic map of the Richmond basin and its outlier or subsidiary basins (D, Deep Run basin; F, Flat Branch basin), Virginia. Thin, double lines represent dikes; black represents coal measures and interbedded strata. Abbreviations are: Tp, Productive Coal Measures Member and underlying Lower Barren Beds Member of the Tuckahoe Formation; Tv, Vinita Beds Member of the Tuckahoe Formation; Tb, Turkey Branch Formation; O, Otterdale Formation; and B, Boscabel Formation. Wells are indicated by open circles: a, Horner; b, Hicks; c, Chesapeake; d, Bailey and Turner; e, Hudgins; f, Adamson; and g, Chalkey. B-B' represents transect of seismic reflection profile on which cross-section in Figure 3.2 is based. Cross-section A-A' shown in Figure 3.7. Based on Cornet (1977a) and Ediger (1986).

and gas within the basin, with three of them reaching pre-Triassic basement at 363 m (Chalkey No. 1), 1369 m (J.R. Hicks No. 1), and 2177 m (Bailey No. 1). The Adamson No. 1 was thought to have reached basement at 844 m, but recent seismic interpretation and analysis of bottom hole samples (metasedimentary) suggest that the well terminated at the top of a probable diabase sill in the upper Productive Coal Measures. These wells have all yielded oil and gas shows. One well (Chesapeak No. 1) pumped oil at 5 bbls. (110 bbls water) per day, but commercial production has yet to be established. A major conclusion from data of two of the deep test wells (Horner No. 1 and Bailey No. 1) is that the basin is more than twice as deep as previously thought.

Three major revisions in our knowledge of the stratigraphy and structure of the basin have occurred since exploration for hydrocarbons in the basin began in 1980 (Figures 3.2 and 3.3): 1) the basin contains an additional sequence of strata (Turkey Branch Formation), which has limited surface exposure and was misidentified as Vinita Beds (*q.v.* the Turkey Branch section) by Shaler and Woodworth (1899); 2) the Otterdale Formation unconformably overlies and hides much of the older Triassic sequence and is a separate geologic unit depositionally unrelated to older facies or sequences; and 3) the basin deepens rapidly south and southwest of Midlothian, Virginia, with the oldest strata cropping out mostly in the northern part of the basin rather than just along the eastern side as in a typical half-graben model (*cf.* Venkatakrishnan and Lutz, 1988).

Our new understanding of the structure and stratigraphy of the basin is based on the study of seismic, gravity, aeromagnetic, well, and outcrop data (Cornet and Ziegler, 1985). Early Carnian strata lie unconformably upon metamorphic and igneous basement (lower unconformity, Figure 3.3). A syndepositional unconformity (middle unconformity, Figure 3.3) separates an underlying sequence (Tuckahoe Formation) consisting of about 975 meters of folded, faulted, and rotated deltaic-lacustrine strata (*i.e.*, Vinita Beds Member, Productive Coal Measures Member, and Lower Barren Beds Member) from an overlying sequence (Turkey Branch Formation) consisting of as much as 1128 meters of deltaic-lacustrine and fluvio-deltaic strata. The middle unconformity is best developed in up-dip areas of rotated fault blocks, where it is angular, but may disappear in synclines where deposition was probably continuous (Figure 3.2). Vinita Beds eroded from the tops of anticlines and steeply-dipping fault blocks were redeposited in synclinal and fault-controlled lows as the Hidden Member, so named because it has no known surface exposure.

Seismic, well, and outcrop data indicate the presence of an erosional unconformity between the Otterdale Formation and the underlying Triassic (upper unconformity, Figures 3.2 and 3.3). This unconformity can be traced due to the incision of deep canyons separated by buttes and plateaus. The Hicks and Turner wells, for example, penetrated a 344-415 m deep canyon system with 26-36 m of talus at its base. Palynomorphs present in shale clasts of this talus indicate a source from the canyon walls. The erosional contact between the Otterdale and the upper Turkey Branch formations can be seen along Old Hundred Road at Stop 3.2 (Figure 3.1). Black shale clasts from just above the unconformity contain a palynoflora that correlates with lithologic zone C3 (Figure 3.3).

The Horner and Bailey Wells

During the Summer of 1981 the Horner and Bailey wells (Figures 3.3, 3.4) were drilled about 9.7 km apart (Figure 3.1) and tested the stratigraphic sections in the central and southern thirds of the basin. Since they were drilled in the deeper parts of separate fault blocks, they contain the most complete stratigraphic sequences yet recognized in the basin. The SEPCO J.R. Hicks No. 1, for example, which was drilled on the up-dip edge of a rotated fault block, contains a condensed lower section with all of the Lower Barren Beds and most of the Productive Coal Measures members missing (non-deposition), as well as the uppermost part of Vinita Beds Member, which was apparently eroded. A condensed Turkey Branch Formation unconformably overlies the Vinita Beds (seismic interpretation), since most of the Hidden Member is not present (*cf.* Figure 3.2).

Environmental interpretation using only well cuttings and electric logs leaves considerable latitude for differences of opinion because these data lack valuable depositional features visible in outcrop, such as cross bed types, trace fossils, and mud cracks, which enable geologists to interpret environments of deposition without the aid of paleontology. The study of palynofloral and kerogen facies for the Horner

Table 3.1: Stratigraphy of the Richmond basin, Virginia.

Units: Shaler and Woodworth (1899)	Units: Ediger et al. (in prep.)			Thickness (m)	Age	Description
Otterdale Sandstone Fm	Otterdale Fm.			415 m	L.Trias.-E.Jur?	Mostly coarse, buff and red fluvial clastics
Vinita Beds Fm	Boscabel Formation	Turkey Branch Fm	Tomahawk Creek Mbr	950 m	M. Carnian	Gray to black, fine to medium lacustrine, deltaic, and brown to red fluvial clastics
Vinita Beds Fm	Boscabel Formation	Turkey Branch Fm	Hidden Mbr	244 m	? E.-M. Carnian	Gray to black, fine to medium lacustrine clastics and turbiditic sandstones; (subsurface unit)
Vinita Beds Fm	Boscabel Formation	Tuckahoe Fm	Vinita Beds Mbr	640 m	Early Carnian	Gray to black, fine to medium deep-water lacustrine clastics at base, passing upward into deltaic clastics
Productive Coal Measures Fm	Boscabel Formation	Tuckahoe Fm	Productive Coal Measures Mbr	180 m	Early Carnian	Coal measures interbedded with gray to black, fine to medium fluvio-lacustrine clastics
Lower Barren Beds Formation	Boscabel Formation	Tuckahoe Fm	Lower Barren Beds Member	185 m	Early Carnian	Brown to black, fine to very coarse fluvial clastics
Boscabel Boulder Beds Formation	Boscabel Formation			?	?	Very coarse, angular fault talus slope breccias

and Bailey wells made it possible to recognize depositional facies and interpret at least the general type of environment. Certainly the addition and correlation of outcrop data and observations will help refine the interpretations given below.

Palynofloral and kerogen composition of the shales and siltstones reflect the cyclic waxing and waning of a large fresh-water and possibly alkaline lake and the progradation of large deltaic complexes during three different periods of basin history (Figure 3.3; Cornet and Olsen, 1985). A graph of the relative percentage of amorphous kerogen (mostly algal debris) in the Horner samples records major lacustrine cycles as zones of high amorphous kerogen content (Figure 3.3, column seven). A second graph (Figure 3.3, column eight) shows the relative abundance of palynomorphs in the palynological preparations (*i.e.*, number of palynomorphs per traverse of a slide). That graph tends to track the curve for amorphous kerogen; the correlation between the curves reflects the finer grain size of the sediments yielding the higher concentrations of kerogen and palynomorphs. Higher than normal percentages of palynomorphs occur in prodeltaic facies underlying prograding deltaic complexes and in swamp facies that lie on top of deltas. A third graph (Figure 3.3, column nine) tracks the relative percentage of pollen versus spores in the Horner No. 1. Intervals dominated by spores are interpreted to reflect either swampy or lacustrine facies, whereas intervals dominated by pollen are believed to reflect either prodeltaic or fluvio-deltaic facies. Swampy conditions correlate with the presence of coals, whereas strictly fluvial conditions correlate with very low palynomorph abundances, a strong dominance by pollen, and an abundance of sandstone.

A fourth graph (Figure 3.3, column 10) gives a summary of lacustrine transgressions and regressions in proximity to the Horner No. 1 well, based on the data in Figure 3.3. Deltas prograding in one part of the basin may be replaced by lacustrine or prodeltaic facies in another part; the deltaic complex present in the Horner No. 1 near the top of the Vinita Beds Member, for example, is represented by shallow lacustrine and delta-margin deposits with high palynomorph abundance in the Bailey No. 1 well. The fourth graph portrays the major trends in lake history for the center of the basin and does not reflect short-duration fluctuations in water depth (*i.e.*, precession cycles) that may have occurred from orbital forcing of the climate. Short-duration depositional cycles are apparent in the Horner and Bailey wells, but water depth apparently did not fall to the extent that it did in the Newark basin, where the lake actually dried up about every 21,000 years (Olsen, 1986). The lacustrine history as presented in Figure 3.3 reflects both long term climatic cycles on the order of 1.6 million years (see below; Cornet, in press) and local tectonic subsidence mediated by structural deformation.

Two types of depositional cycles are recognizable in the Richmond basin wells: 1) very thick, generally coarsening-upward cycles of approximately 838 m in thickness, consisting of swamp and shallow lacustrine deposits dominated by cryptogam spores in the lowest part, mostly lacustrine facies in the middle, and fluvial-deltaic facies dominated by pollen in the upper part of the cycle, and 2)

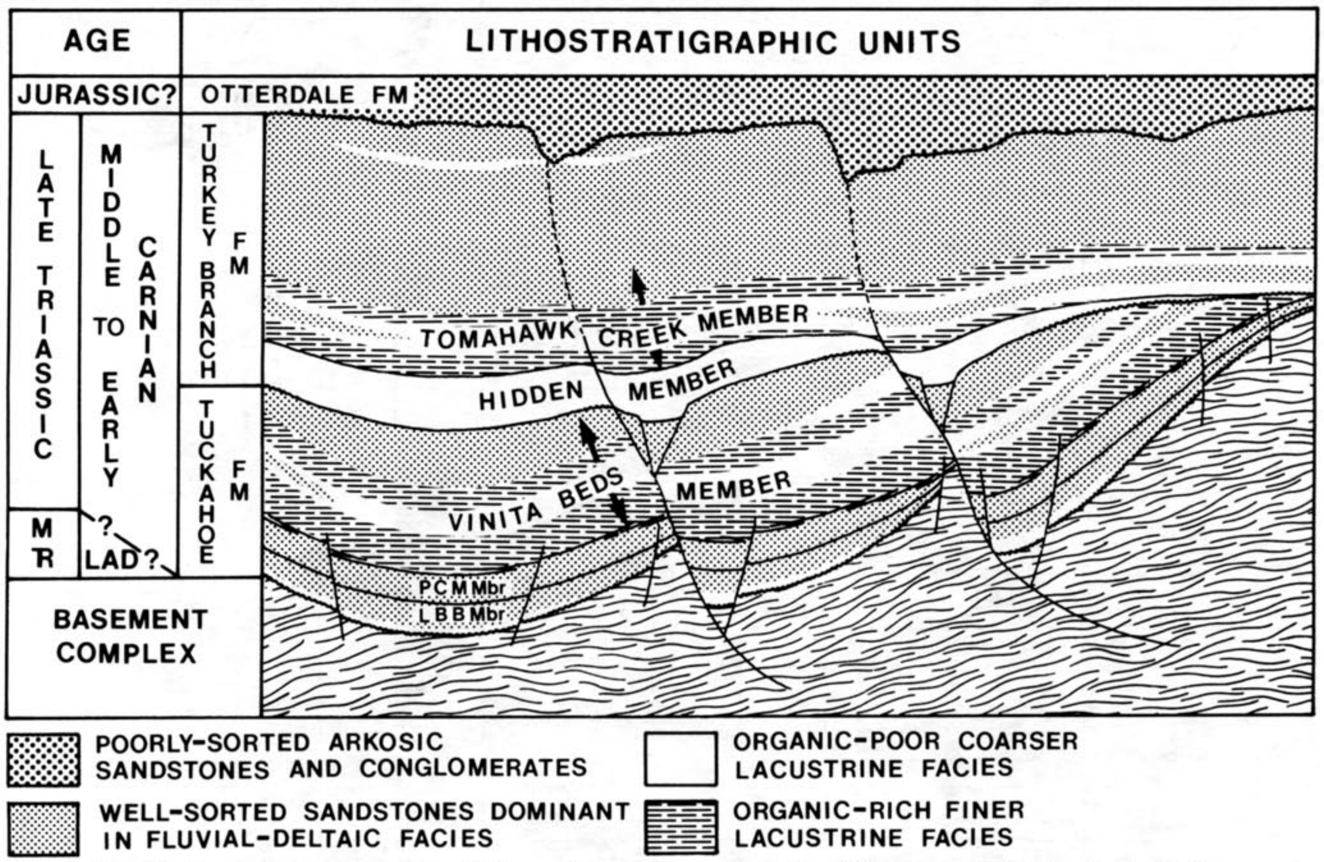

Figure 3.2: Idealized cross section of the Richmond basin along seismic line B-B' (Figure 3.1). The similarity in general lithostratigraphy between the Tuckahoe and Turkey Branch formations is a reflection of long-term climatic cycles, whereas the up-dip truncation of the Tuckahoe Formation and the wedge shape of the Hidden Member are the direct results of tectonism. Formation names and ages are from Ediger *et al.* (in prep.). PCM Mbr. = Productive Coal Measures Member; LBB Mbr. = Lower Barren Beds Member.

smaller-scale coarsening-upward cycles averaging 28 m in thickness (Cornet, in press). The smaller cycles range from 15-45 m in thickness, with organic carbon-rich shale intervals usually separated by more than 9 m and typically by at least 18 m of sandstone and siltstone.

The smaller cycles are believed to be double cycles (*i.e.*, two cycles of 21,000 yr., or 42,000 yr.), because they frequently have a shalier or siltier bed near their middle and sometimes are divisible into two coarsening-upward cycles of similar thickness (*cf.* Ediger, 1986). Palynofloral change through these double cycles sometimes shows a high fern spore count near the center, suggesting that the most obvious cycles are not the smallest ones (*i.e.*, equivalent to the 21,000 year precession cycles; Olsen, 1986). Every other cycle in the Horner and Bailey wells may have been masked to a greater or lesser extent by the movement of coarse sediment into the deeper parts of the basin (via gravity slides and turbidites?) when lake level was high.

Two complete large-scale cycles (*i.e.*, 838 m) and the top and bottom portions of two others are preserved. The two

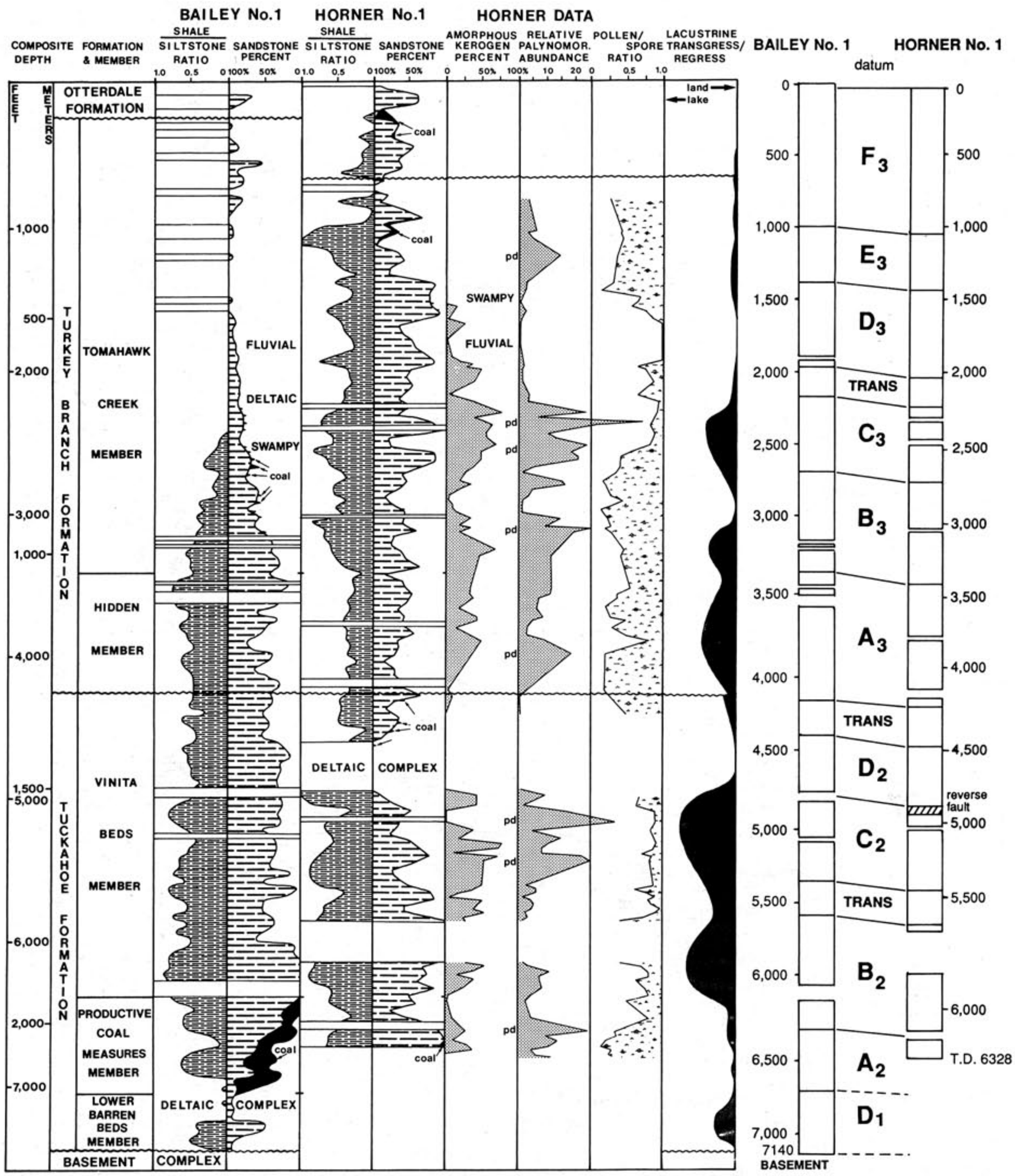

Figure 3.3: Properties, interpretations, and lithozone correlation of the sections in the Horner No. 1 and Bailey No. 1 wells, Richmond Basin.

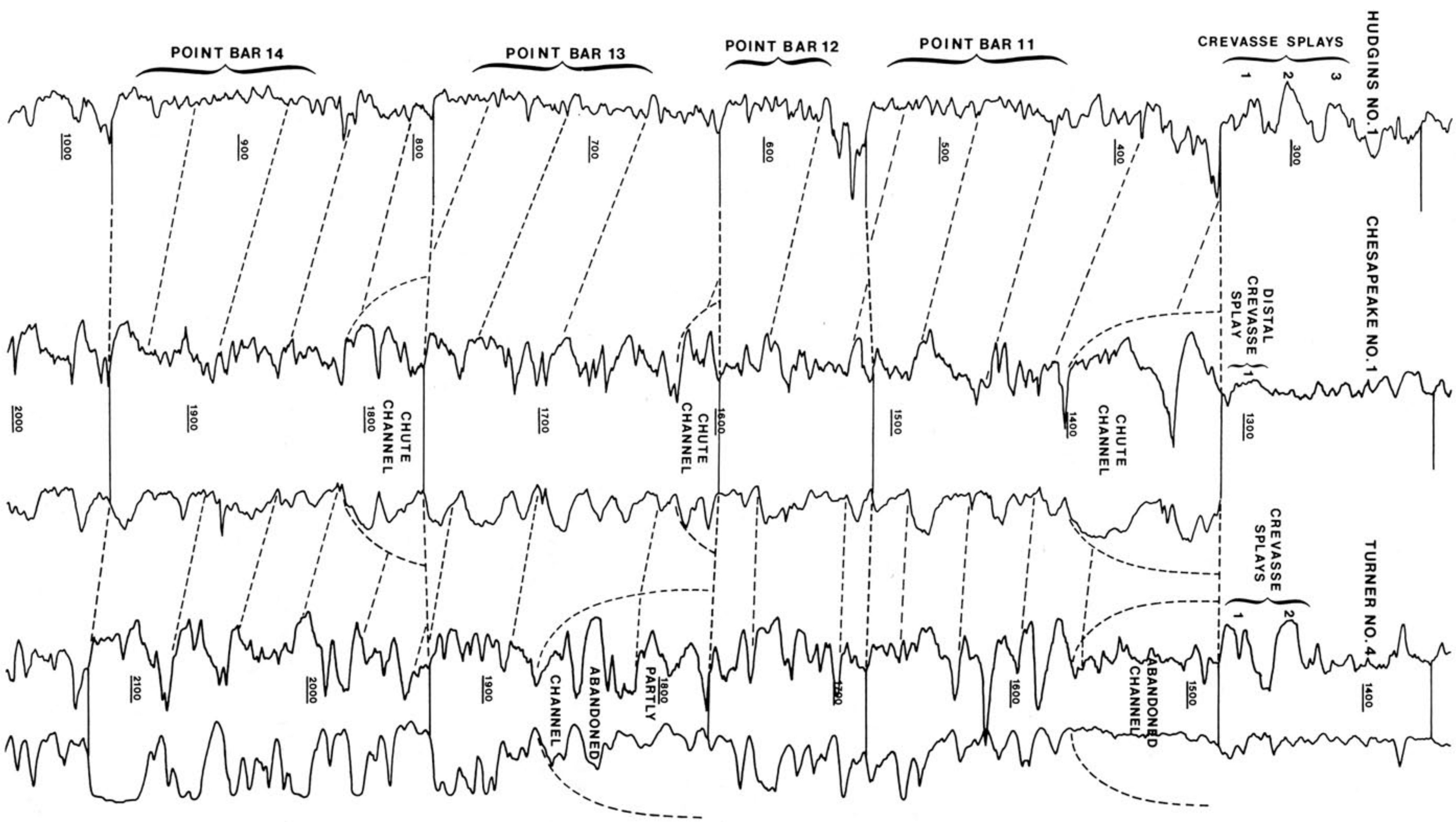

Figure 3.4: Correlation of gamma and induction logs and facies interpretation for lithologic zone D3 in the Hudgins No. 1, Chesapeake No. 1, and Turner No. 4 wells. The close spacing of these three wells (Figure 3.1) and the sudden transition to overbank facies in all three wells at the top of the channel fill sequence made it possible to recognize these channel forms as different parts of a very large meander set. See Cossey and Frank (1983) for electric log responses in an Eocene deltaic point bar.

complete cycles are depicted by lithologic zones A2 to D2 and A3 to D3, respectively, in Figure 3.3. Portions of the two additional (incomplete) cycles are depicted by lithologic zones D1 (only penetrated by the Bailey No. 1 well) and E3 to F3 (present in both the Horner No. 1 and Bailey No. 1 wells). The youngest cycle (E3-F3) shows no return to basin-wide lacustrine conditions and lithologically appears to be a continuation of the preceding cycle (cycle 3), but palynoflorules from that part of the section show a distinct return to wet climatic conditions with the dominance of the local flora by hydrophytic cryptogamous plants (Figure 3.3, swampy in column 6) and the formation of local coal beds (Figures 3.3). The fact that the lake did not return in the upper Tomahawk Creek Member is consistent with models of rift basin filling, where the deepest lakes and most organic carbon-rich shales occur early in basin history, and fluvial environments with common red beds dominate the stratigraphy late in basin history (Lambiase and Rodgers, 1988; Schlische and Olsen, in review; this volume).

The eastern and northeastern parts of the basin experienced significant uplift and erosion during the deposition of the Hidden Member, which reaches 244 m in the Horner and Bailey wells. Evidence for such erosion comes from the sandstones in this member, which are better sorted and more porous than older and immediately younger sandstones of the basin. These sandstones are probably the result of recycling of eroded Triassic sands and are organized into about 30 well-sorted sandstone beds, interpreted as turbidites, and two thick poorly-sorted slumps (*e.g.*, core #1, Horner well), separated by discrete shale beds. The turbidites become thinner and finer towards the south, become more closely spaced upwards in the Hidden Member as the rate of sedimentation decreased, and are capped by a thick shale unit. The restricted development of strata younger than the Vinita Beds Member in the northern part of the basin may be due to syndepositional erosion and non-deposition following deformation.

River Size and Form

The fluvial environments established during lithologic zone D3 can be identified and mapped, because many of the wells drilled in the basin (Figure 3.1) penetrated this sequence. The Horner No. 1 and Gordon No. 1 show mainly overbank and crevasse splay deposits, whereas the three Turner wells, the Chesapeake No. 1, the Hudgins No. 1, and the Bailey No. 1 show mainly point bar and channel deposits (*cf.* Figure 3.1). The point bars can be identified on electric logs as fining-upward sequences of sandstone and siltstone and are very thick for a basin as small as the Richmond, ranging from 26 m to over 46 m in thickness. These point bars are stacked as a sequence of upper point bar sandstones in the Hudgins No. 1, whereas the sequence is mainly middle point bar sandstones containing clay drapes in the Chesapeake No. 1, and conglomeratic lower point bar sandstones in the Turner No. 4 (Figure 3.4) and in the Hicks No. 1, located at the up-dip edge of a rotated fault block. The similarity of the dominantly shale channel-fill sequences to the correlative overbank sequence in the Horner No. 1 is noteworthy.

The repetition of similar sedimentary structures in each well suggests a strong degree of structural control for the path of the river. It would appear that a large river traversed the basin from southwest to east toward the end of Triassic deposition, probaby continuing into the Taylorsville part of the rift valley. Because of the narrow width of the meander belt and the large size of the river, the channel form was repeated in successive sequences, resulting in the stacking of similar facies to form repetitious sequences in the closely-spaced wells (Figure 3.4). By contrast, the west central part of the basin received mainly overbank deposits during this time.

Lake Duration

The Richmond-Taylorsville basins represent the oldest rift valley deposits currently recognized south of Nova Scotia and developed at a time when the North American plate was near the paleo-equator (Cornet and Olsen, 1985; Cornet, in press). A humid tropical climate and the presence of large rivers that emptied into the rift valley created lakes that frequently filled and interconnected the basins, and existed for long periods of time, much like lakes Tanganyika and Malawi of East Africa. The dominance of lacustrine environments despite climatic fluctuations is a pattern very different from that of the Newark, Gettysburg, and Culpeper basins, where lakes dried up periodically, and lake margin facies were reworked into the basin. Depositional topography is therefore much more likely to be preserved in the Richmond-Taylorsville rift, as deltaic sands became encapsulated by lacustrine shales.

mileage	
0	Leave previous night's stop, turning left onto VA 15 South.
0.2	Turn onto US 460 east (toward Richmond).
1.6	Cross Briery Creek downstream of the Briery Creek basin.
7.0	Turn left onto VA 309 East toward US 360 (about 9 miles).
16.1	Turn left on US 360 toward Richmond and Amelia.
41.9	Clover Hill. A major coal mine once existed near here in the Richmond basin.
46.8	Powhite Parkway overpass. Follow US 360 east.
48.7	Intersection of US 360 and VA 604.
49.8	Turn left onto Courthouse Road (VA 653) heading north.
54.4	Intersection with US 60, begin North VA 147. Continue straight on VA 147 for 0.3 mi.
54.7	Turn left on Old Buckingham Road (VA 677).
55.4	Turn right onto Old Blackheath Road (Road 1482).
55.9	Turn right onto Deerhurst Drive (Road 1232) in a housing subdivision.
56.1	Follow to *cul-de-sac* and park.

STOP 3.1: BLACKHEATH MINE (by P.J.W. Gore and P.E. Olsen)

Highlights: Productive Coal Measures; structure at the updip edge of the Richmond basin.

Follow path to railroad tracks on the left (northwest) side of Deerhurst Drive. Walk along railroad tracks approximately 145-150 paces to the left (southwest), and follow a path into the woods on the right (northwest) to a stream. [The path can also be reached by walking straight back behind the house at 11808 Deerhurst Drive]. Tuckahoe Group coals and associated sedimentary rocks are exposed in the banks of the stream (Figure 3.5).

Coal was mined in the Richmond basin from the early 1700's until the 1930's (Goodwin *et al.*, 1985, 1986). Five major mining centers were present in the basin: (1) the Midlothian District south of the James River along the eastern edge of the basin, part of which we will see here, (2) the Gayton or Carbon Hill District north of the James River

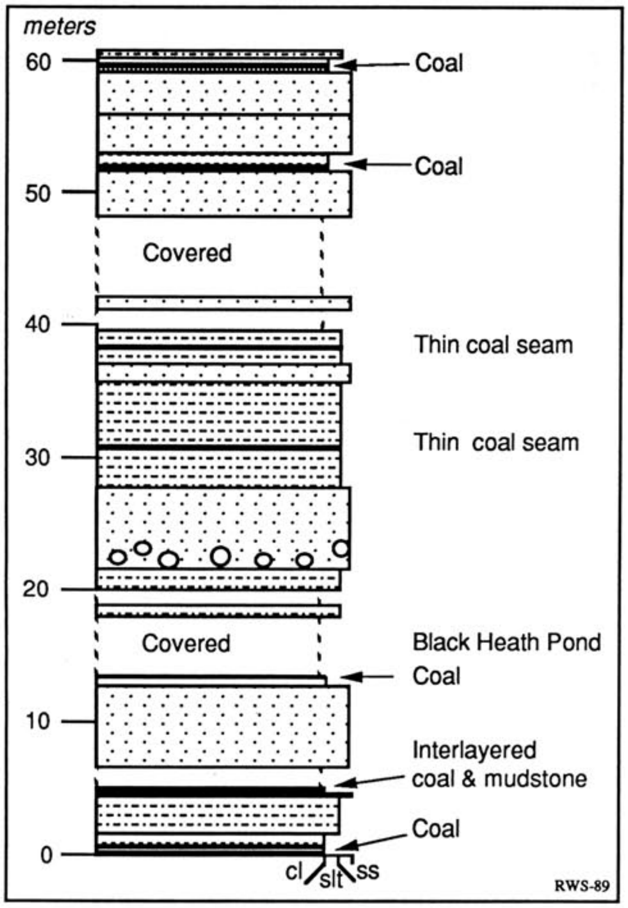

Figure 3.5: Measured section of the Productive Coal Measures Member of the Tuckahoe Formation within the Blackheath sub-basin, Stop 3.1. Data for stratigraphic column from Goodwin *et al.* (1985).

along the eastern edge of the basin, (3) the Winterpock or Clover Hill District in the southeastern part of the basin, (4) the Manakin District north of the James River at the western edge of the basin, and (5) the Huguenot Springs District south of the James River along the western edge of the basin (Goodwin *et al.*, 1985, 1986). At least 2,892,645 tons of coal were mined between 1780 and 1840 (Brown *et al.*, 1952), and a total of more than 8 million tons of coal have mined in the basin (Robbins *et al.*, 1988).

The rocks at this locality occur in a small structural trough or sub-basin just to the east of the Richmond basin, called the Black Heath sub-basin. The nonconformity between the underlying Petersburg Granite and the Triassic sediments is not exposed. Boulders of porphyritic Petersburg Granite can be seen in the stream near the *cul-de-sac* at the end of Deerhurst Drive.

The Black Heath mine was opened near here around 1788 by the Heath Mining Company (Goodwin *et al.*, 1986). Four seams of high volatile A bituminous coal were reported in this area; the lower two seams form a unit 12 m thick with a shaley parting 4.6 m thick. The two upper seams are 0.3 m and 1.5 m thick, respectively. The mine began with a 240-m-deep-shaft with side galleries. As with the mines in the Deep River basin, this mine (and others in the Richmond basin) were continually plagued by gas explosions which killed many miners over the years. Sir Charles Lyell visited the mine in 1844, and published his findings in 1847. By the early 1860's, all the mineable coal had been removed, and the mine was flooded. By 1887, all that remained of the mine was a pond.

The coal mines of the Richmond basin produced a spectacular assemblage of plant fossils, which has been documented by Fontaine (1883) and Ward (1900). In addition, the dumps of the Black Heath mine have produced the type specimen of the guide vertebrate of the Richmond and related basins, the subholostean fish *Dictyopyge macrurus*, collected by Charles Lyell and others (N.G. McDonald, pers. comm.), as well as conchostracans, unionid clams and the rare beetle elytra (Olsen, 1988b). The vertebrates and invertebrates appear to come from strata above at least the main coal seams of the Productive Coal Measures.

Unlike the coals of the Cumnock Formation (Stop 1.2), those of the Richmond basin, as exemplified by this stop (Figure 3.5), are not interbedded with vertebrate- and conchostracan-bearing shales. The fish fossils from the mine dumps appear to come from beds transitional into the overlying Vinita Member. In addition, the coals of the Richmond and Farmville basins are made up of mostly cycadeoid, fern, and equisetalian remains, whereas those of the Deep River basin are predominantly made up of conifers. This difference is reflected in the associated palynofloras which are spore-dominated in the Richmond basin and pollen-dominated in the Deep River basin (Olsen and Cornet, 1988a). This difference is probably related to a difference in climate, with the Richmond coals having formed under more humid conditions.

The structure of this portion of the eastern edge of the Richmond basin show an onlap pattern typical of half-graben. The Lower Barren Beds Member is absent here and the Productive Coal Measures Member rests directly on basement. Seismic lines and drill holes show a progressive thickening of the Lower Barren Beds Member to the west. In the area of Black Heath, the basal contact and enclosed coals form a series of "flexures" or "troubles" (Figure 3.6) of overall synclinal form. These could be interpreted as compressional folds, with structural thickening of the hinges. However, it seems more likely that they represent small graben developed in the hinge area of the larger Richmond half-graben perhaps in a manner similar to crestal collapse structures of McClay and Ellis (1987). The flexures would be tiny graben growing during deposition and influencing sedimentation. This would explain the presence of thickened coal seams only in the trough and not on the crests of the "flexures". Overall symmetrical structural thickening would be expected of compressional folds.

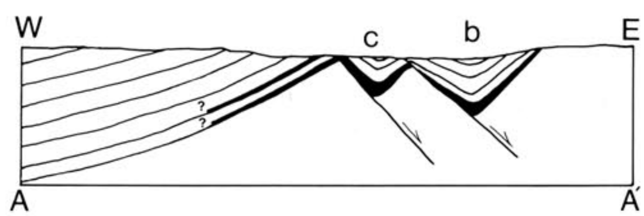

Figure 3.6: Structure of the hinge area of the Richmond basin in the vicinity of Stop 3.1 (see Figure 3.1 for location) based on data and figure from Shaler and Woodworth (1899). Black represents coal measures and interbedded strata; C, Cunliffe basin; b, Black Heath basin. The E-dipping limbs of the "flexures" might be a result of normal drag along the faults; the increased thickness of the coal measures within the "flexures" strongly suggests synsedimentary faulting.

56.1 Leave *cul-de-sac*.
56.4 Pass Blackheath Road.
56.5 Turn left onto Olde Coalmine Road (Road 1265).
57.0 Turn right onto VA 677 (Buckingham Road).
58.0 Turn right onto US 60 (Midlothian Turnpike) at shopping center.
58.5 Turn left on Coalfield Road (VA 754), just past the high school. Turn right (west) at T-junction.
62.0 Turn right (northwest) onto VA 652, Old Hundred Road. Road will turn to left and become a dirt road.
62.5 Outcrop of Vinita (?) Beds.
63.2 Stop and park.

STOP 3.2: TOMAHAWK TETRAPOD QUARRY
(by P.E. Olsen)
Highlights: One of the richest vertebrate localities in Triassic rocks in North America.

Because of a lack of exposures, the vertebrate paleontology of the early Carnian portion of the Newark Supergroup has been very poorly known, but recently joint teams from Columbia University (Olsen), the Smithsonian Institution (Hans-Dieter Sues), Rutgers University (ShayMaria Silvestri) and the Virginia Museum of Science (Noel Boaz) have excavated a spectacularly rich reptile assemblage in the Turkey Branch Formation which should shed considerable light on this time period. Unlike all other North American Triassic age assemblages, this one is dominated by mammal-like reptiles and is closely comparable to those known for many years from southern Africa, Brazil, and Argentina. Most common is an advanced traversodont mammal-like reptile almost identical to *Massetognathus* (Figure 3.7 A), otherwise known only from Argentina. Most of the other reptiles present were previously unknown from North America but resemble southern hemisphere forms, whereas others appear to be completely new. A faunal list as of February 1989 is given in Table 3.2. A major discovery is excellent jaw and skull material of what appears to be a form similar to *Microconodon* (from the Cumnock Formation of the Sanford sub-basin) and one of the closest reptilian forms to mammals (Figure 3.7 B). For the first time it is clear that the differences between the Carnian assemblages of Laurasia and Gondwanaland were due to differences in age rather than geographic isolation.

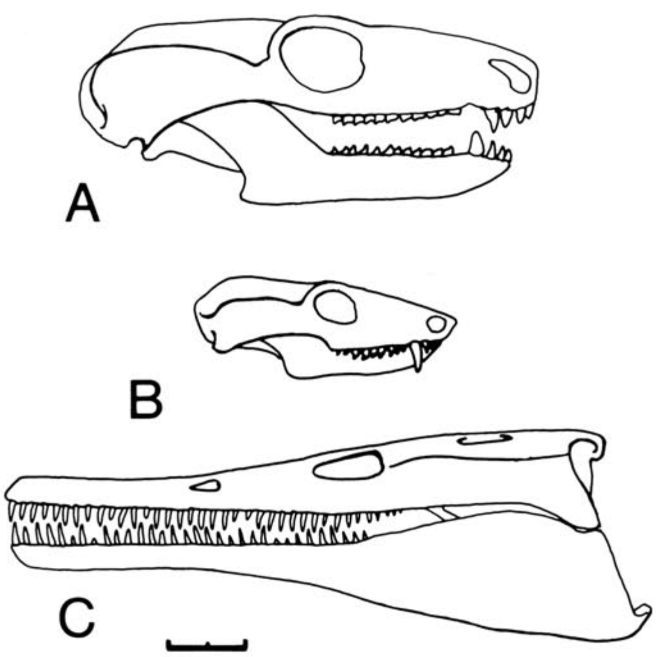

Figure 3.7: Vertebrates from the Tomahawk tetrapod quarry, Turkey Branch Formation, Stop 3.2: A) *Massetognathus* (redrawn from Jenkins, 1970); B) speculative reconstruction of cf. *Microconodon* (adapted from Romer and Lewis, 1973); C) *Doswellia kaltenbachia* (adapted from Weems, 1980). Scale is 2 cm.

Table 3.2: Vertebrates and invertebrates from the Richmond basin. Lithologic units: CM) productive coal measures of Tuckahoe Formation; V) Vinta beds of Tuckahoe Formation; T) Turkey Branch Formation; O) Otterdale Formation. Field stop occurences: b) Boscabel Quarry (3.4); t) Tomahawk Quarry (Stop 3.2); bh) Blackheath (Stop 3.1).

- Mollusks
  - Pelecypoda
    - Unionidae
      - undetermined clams [V,bh]
- Arthropods
  - Crustacea
    - Diplostraca (clam shrimp and water fleas)
      - *Cyzicus* sp. [V, bh; T, t]
      - ?*Paleolimnadia* sp. [V, bh; ?V, b]
    - Ostracoda
      - *Darwinula* spp. [V, bh; T,t]
    - ?Decapoda
      - †*Scoyenia* [?PM, bh; T; O]
  - Insecta
    - Coleoptera (beetles)
      - undetermined fragments [V, bh]
- Pisces (fish)
  - Actinopterygii (bony fishes)
    - Palaeonisciformes
      - *Tannaocrossus sp.* [V]
      - *Dictopyge macrusus* [V, bh, b; T, t]
      - *Cionichthys meekeri* [V, b]
- Amphibia
  - ?Urodela?
    - undientified jaws and vertebrae [T, t]
- Reptilia
  - Procolophonia
    - Procolophonidae
      - unidentified form [T, t]
  - Synapsida
    - Traversodontidae
      - aff. *Massetognathus* [T, t]
    - ?Chiniquodontidae
      - new genus near *Microconodon* [T,
  - *incertae sedis*
    - 2 new taxa near *Tricuspes* [T, t]
  - Lepidosauromorpha
    - Sphenodonta
      - unidentified form [T, t]
    - ?Lacertilia
      - unidentified form [T, t]
  - Archosauria
    - ?Proterochamsidae
      - *Doswellia kaltenbachia* [T, t]
    - Phytosauridae (crocodile like archosaurs)
      - ?? teeth [T, t]
    - Archosauria *incertae sedis*
      - bilaterally compressed teeth [T, t]
      - small recurved conical teeth [V, b, bh; T, t]

The outcrops occur along the northeast bank of Old Hundred Road, just east of the east branch of Tomahawk Creek, on what was the Tomahawk Plantation. The section consists of a poorly-exposed sequence of laminated conchostracan-bearing claystone grading up into massive mudstone and nodular limestone with root structures, in which the tetrapod bones are found. The bones occur as disarticulated but partially associated skulls and skeletons, as well as small isolated bone fragments. Unlike virtually all of the other Newark bone localities, the bone is hard, almost uncrushed, and separated easily from the rock. Microvertebrates are recovered by bulk processing in kerosene and hot water and sieving. Microvertebrate remains found so far include more mammal-like reptile teeth, and bones and jaws of lizard-like and salamander-like forms.

63.2 Continue northwest on Old Hundred Road.
64.6 Turn left on Otterdale Road (VA 667).
66.2 Cross Swift Creek.
66.6 Weathered exposure of Vinita Beds in road cut on left side of the road, according to Goodwin *et al.* (1985).
66.8 Cross VA 604 (Genito Road). Continue south on VA 667.
67.2 Cross Otterdale Branch. Conglomerate is exposed in the creek bed on the right. Continue to a T junction 2 miles after crossing creek.
68.2 Near here, three wells were drilled by Merrill Natural Resources and Shore Petroleum between1980 and 1985.
69.2 Turn left at T junction (staying on Otterdale Road).
71.0 Turn right (west) onto US 360 (Hull Street Road).
72.3 Turn left onto VA 730, Baldwin Creek Road.
73.6 Stop sign at Beach Road (VA 665). Park.

STOP 3.3: OTTERDALE FORMATION NEAR WINTERPOCK, VA (by P.J.W. Gore)
Highlights: Sandstone with petrified wood in saprolite and liesegang banding.

The Otterdale Formation is the uppermost unit in the Richmond basin. This outcrop is a conglomeratic, coarse-grained, arkosic sandstone with associated siltstone altered to saprolite, but the overall geometry, sedimentary structures and textures of the Otterdale Formation are well exposed.

Four lithologies are present in this exposure: (1) poorly-sorted, matrix-supported, pebbly conglomerate in lenticular beds 30-60 cm thick with poorly defined planar bedding; (2) poorly-sorted, sandy to clayey siltstone in beds 60-180 cm thick, which vary in thickness laterally; (3) cross-bedded, pebbly, coarse arkosic sandstone in beds 30-150 cm thick; and (4) cross-bedded, planar-bedded, or graded, coarse arkosic sandstone in beds 30-60 cm thick (Roberts, 1986). The sandstone consists of quartz, highly-weathered feldspar (now clay), and muscovite (Roberts, 1986). Channel forms and dune-scale trough cross-beds are visible in the sides of the pit (Goodwin *et al.*, 1986). Boulders and cobbles overlie distinct erosional surface-truncated cross-bedded sandstone. Most clasts are subrounded to subangular, but a few are angular and some are rounded (Roberts, 1986). There is a varied suite of clast lithologies in the Otterdale, including muscovite schist, granite gneiss, quartzite, vein quartz, cataclastic rock, and granite (which is the most common), derived from nearby Piedmont rocks, but many of the clasts are highly weathered and difficult to identify (Roberts, 1986). Weathering has produced liesegang banding in the sandstone, which locally obscures primary sedimentary structures.

On the basis of lithologies and sedimentary structures, the Otterdale could be interpreted as a braided stream (Goodwin *et al.*, 1985) or alluvial fan deposit (Roberts, 1986). Smoot (pers. comm.) argues that the dominance of dune-scale cross bedding points more towards a large-scale braided river. The scale of the system is clearly larger than most fluvial systems in the Newark Supergroup, and because the Otterdale appears to blanket much of the Richmond basin, the rivers were probably through-flowing and the basin hydrologically open. Smoot (1985) argues that either the Otterdale represents a through-going drainage system in a small basin or that the Richmond basin is an erosional remnant of what was a much larger basin. Interpreted in terms of the basin filling model outlined in the Overview, the fluvial Otterdale would be a consequence of slowing basin subsidence so that the depositional surface reached the hydrologic outlet (Schlische and Olsen, in review). This is not incompatible with the Richmond basin having been part of a larger basin system.

Fossils are not common in the Otterdale, but petrified wood (*Araucarioxylon*) has been found at this locality. Without other fossils (primarily pollen and spores), it is difficult to date the Otterdale. It has been assumed that the Otterdale Formation overlies the Vinita Beds (Shaler and Woodworth, 1899), but if the Otterdale interfingers with the Vinita Beds (*cf.* Roberts, 1986) it is Carnian in age (*cf.* Goodwin *et al.*, 1986). However, if an unconformity separates the Otterdale from the Vinita Beds, as Cornet and Ziegler (1985) suggested (see Figure 3.2), the Otterdale may be younger. The Otterdale is cut by diabase dikes, suggesting that it can be no younger than earliest Jurassic.

It is difficult to distinguish between weathered early Mesozoic conglomerates and Tertiary or Quaternary upland gravels, which are also highly weathered in this area (Goodwin *et al.*, 1986). The main distinction between the two is geomorphic. The lower contact of the Cenozoic gravels is an eastward-dipping surface, which in this area should be at an elevation of 100-106 m (Goodwin *et al.*, 1986). The elevation of this exposure is 81 m, which is much lower than the predicted elevation of the younger upland gravels (Goodwin *et al.*, 1986). Clast composition may also be useful in distinguishing between the two conglomerates. The Cenozoic conglomerates appear to have a greater abundance of quartz, sandstone, and quartzite clasts, some of which contain *Skolithus* (vertical burrows), derived from Cambrian rocks in the Blue Ridge Province (Goodwin *et al.*, 1986). These clasts are only known to be present in Miocene and younger conglomerates (Goodwin *et al.*, 1986). In contrast, most of the clasts in the Triassic conglomerates are locally derived igneous and metamorphic lithologies.

Turn around and return to intersection with US 360.
74.8 Turn right on US 360 toward Richmond. (We will be staying on US 360 for about 15 miles).
88.1 Exit onto VA 150, Chippingham Parkway (to I-95).
89.9 Pass over Midlothian Turnpike.
91.4 Veer right toward I-64 and I-95 onto Powhite Parkway (VA 76). (This is a toll road).
93.5 Cross the James River.
93.8 Road forks. Go left toward Charlottesville and Washington, D.C. (I-195 North, to I-64 and I-95 North.)
94.5 Exit onto VA 147, Cary Street/Floyd Avenue. Go west (left) onto VA 147 at end of ramp.
(Alternate Route - take the next exit, Patterson Avenue, VA 6 west; stay on VA 6 to Manakin, VA and quarry.)

95.1 Go right onto Cary Street at T junction (VA 147 west).
97.2 Veer right onto Three Chopt Road.
97.7 Note sign to University of Richmond.
98.8 Turn left onto Patterson Avenue, VA 6. (10 miles to Manakin).
108.5 Turn left into Luck Stone Quarry.

STOP 3.4: BOSCABEL QUARRY, MANAKIN, VA

(by P.E. Olsen)

Highlights: Petersburg Granite and Vinita Beds; deep-water black shales; fish fossils; normal faults.

The Boscabel Quarry of the Luck Stone Company is a large, deep, active pit operated for cut and crushed granite. The west wall exposes a spectacular saprolite profile in granite, whereas on the east side there is a fault contact with black claystones, siltstones, and sandstones of the Richmond basin. According to Goodwin *et al.* (1985), the granite represents a small horst, with the main border fault of the basin being about 2.5 km to the west in the Hylas zone (Goodwin *et al.*, 1985). The dip of the beds is gently eastward on the east quarry wall but swings to the west along the northwest-trending road at the main entrance to the quarry.

According to Goodwin *et al.* (1985) the attitude of the fault between Newark sedimentary rocks and granite varies from N10°W, 57° NE to N-S, 65° E (Goodwin, 1970) and seems to have many small splays which ramify through the sedimentary rocks. In places sandstone and siltstone show boudinage bounded by low-angle normal faults. Bedding plane faults are common, and it is normal for fresh laminated black siltstone to break out as large (1 m) polished phacoids. In general, the direction of strike of the normal faults parallels the local boundary between granite-metavolcanic and sedimentary rocks.

Most authors (Cornet, 1975; Schaeffer and McDonald, 1978; Olsen *et al.*, 1982; Goodwin *et al.*, 1985) have assumed that the sedimentary rocks of the Boscabel Quarry belong to the Lower Barren Beds, because coal-bearing strata, usually identified as Productive Coal Measures, crop out to the east and dip to the east. However, the broad synclinal cross section of the local exposures suggests that they could represent a small graben, down-dropped against the fault (an interpretation first suggested by Bruce Cornet). As pointed out by Goodwin *et al.* (1985) the strata exposed in the Boscabel Quarry are indistinguishable from Vinita Beds; similar strata have not been seen below the Productive Coal Measures where penetrated by drill holes (Cornet, pers. comm.), and pollen assemblages from the quarry outcrops are most similar to those from the Vinita Beds (Cornet, pers. comm.). In total, the sedimentary rocks exposed in the quarry appear to be Vinita Beds rather than Lower Barren Beds.

Sedimentary rocks include microlaminated black shale, thin-bedded graded sandstones and siltstones, and gray coarse sandstones and conglomerates. Sedimentary structures include load casts, tool and groove marks, current ripples, normally-graded beds (at several scales), and possible oscillatory ripple cross-lamination and hummocky cross stratification. In 1976 about 35 m of section were exposed (Figure 3.8), and in contrast to the cyclical strata seen in the Cow Branch Formation of the Dan River-Danville basin and virtually all other lacustrine rocks of the Newark Supergroup, these beds showed no sign of subaerial exposure (desiccation cracks, roots, or tracks). Virtually all fine-grained beds are microlaminated and contain articulated fish, abundant clam shrimp, and occasional coprolites. Apart from fine-coarse alternations, no obvious cyclical pattern presents itself. Although we have no time control in this section, the great thickness of beds with no signs of desiccation suggests that deep water persisted for much longer periods of time than in most other Newark Supergroup basins. Ressetar and Taylor (1988) placed this section in the "coal measures" rather than the Vinita Beds and suggested that the sedimentary environment was fluvial to paludal. The complete lack of root structure or any evidence of subaerial exposure as well as the preservation of articulated fish in microlaminated black shales, strongly argue against their interpretation. In addition, we have been unable to find any coal in the outcrops.

Fossils from this quarry include abundant and very well-preserved examples of the subholostean fishes *Dictyopyge macrurus* and *Cionichthyes* (*Dictyopyge*) *meekeri* (Schaeffer and McDonald, 1978), the clam shrimp *Palaeolimnadia*, and small (1 cm) conical and slightly recurved reptile teeth. Fossils are universally common in the fine grained rocks. However, fresh rock tends to fracture along the abundant low-angle slickensided faults, and therefore almost all of the good fossils have been recovered from the weathered zone, where the microlaminated beds split along bedding planes. In these cases, although the bone or coprolite material has disintegrated, a high fidelity mold of the external surface remains for study.

109.2 Leave quarry. Turn left and continue west on VA 6. The rolling hills between Richmond and Culpeper are typical of the Piedmont region, which is underlain by saprolite developed from metamorphic and igneous rocks.
116.5 Pass Department of Corrections and VA 645.
119.9 Fork to the right onto US 522 North. (Goochland 1 mile).
121.7 Turn right onto US 522, Sandy Hook Road toward Gum Spring and Culpeper.

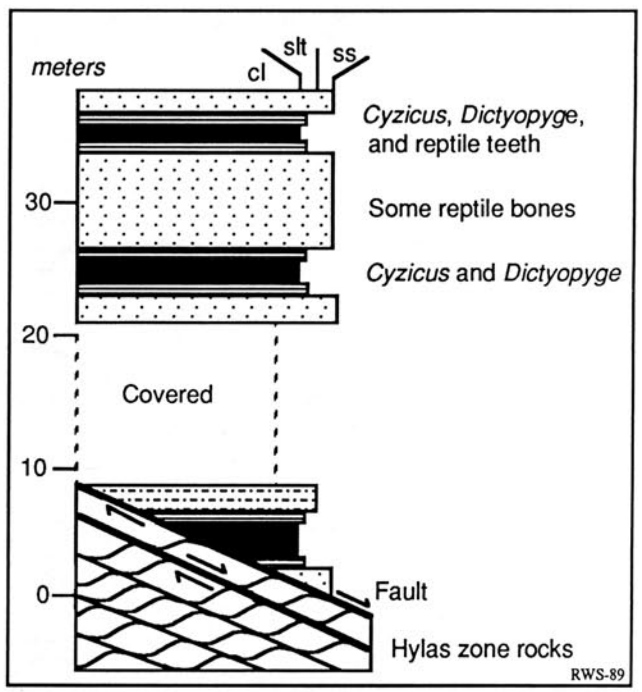

Figure 3.8: Measured section at the Boscabel Quarry, Stop 3.4. Black represents gray to black microlaminated siltstones; thin black lines represent gray laminated siltstones; and stipple represents gray sandstone. The faulted contact with and structures within the Hylas zone are idealized.

126.3 Sandy Hook.

128.1 Pass intersection with US 250. Go straight on US 522 North to I-64.

128.8 Turn onto I-64 West.

150.6 Exit onto US 15 (Exit 27) toward Gordonsville and Orange.

161.0 Pass intersection with US 33.

161.5 Gordonsville, VA.

About 8 km to the west is Barboursville, Virginia, located in the small, elliptical Barboursville basin. The basin is located about 2.5 km southwest of the southern end of the Culpeper basin, of which it is probably an erosional outlier. It is about 16 km long and 4 km wide, with a normal border fault on the western flank and strata dipping moderately to the west (Lee, 1980), beginning at the Rapidan River and extending to the southwest. The sediments consist primarily of red terrigenous clastics 330-576 m thick (Lee and Froelich, in press), and are probably entirely Late Triassic in age. The rocks belong to the lower part of the Culpeper Group (nomenclature extended from Culpeper basin), and consist of three formations (from the bottom up): Manassas Sandstone with basal greenstone conglomerate (Rapidan Member), Balls Bluff Siltstone, and Tibbstown Formation with conglomerate member (Haudrickes Mountain Member) (Lee and Froelich, in press). Unlike the Culpeper basin, there are no known igneous rocks in the Barboursville basin (Lee and Froelich, in press).

162.5 Turn right, staying on US 15.

170.8 Turn right, staying on US 15 North in Orange, VA.

174.2 Rapidan River. Madison Mills. Entering the southern tip of the Culpeper basin. Note the rich, dark red color of the soil. This is typical of the southern Culpeper basin, especially where basal greenstone conglomerate underlies the margin, but is not common in most of the southern basins.

178.8 Robinson River (Jackson's Crossing).

188.0 Turn south onto US 29.

188.9 Turn right into parking lot for overnight stop, Culpeper, VA.

4. CULPEPER BASIN, VIRGINIA

GEOLOGY OF THE CULPEPER BASIN
(by P.J.W. Gore, P.E. Olsen, and R.W. Schlische)

The Culpeper basin is an elongate-half graben more than 180 km long and as much as 20 km wide located in northern Virginia and Maryland (Figure 4.1). The basin is bounded on the west by a major zone of east-dipping normal faults, which separate the early Mesozoic strata from Precambrian and lower Paleozoic metasedimentary, metavolcanic, and granitic rocks of the Blue Ridge Province. The rocks in the basin, called the Culpeper Group (Lindholm, 1979), dip westward toward the border fault. The eastern border of the basin is predominantly an unconformable onlap of Triassic sedimentary rocks onto Precambrian and lower Paleozoic crystalline rocks of the Appalachian Piedmont Province and in part bounded by minor faults. The Culpeper basin is the southernmost Newark Supergroup basin known to contain sedimentary rocks and basalt flows of Early Jurassic age. It contains the longest depositional record of any of the basins in the southern part of the rift system, ranging from Carnian to late Hettangian-early Sinemurian?, an interval of about 25 million years (Figure I.3). Maximum thickness of sedimentary basin fill is calculated at about 7900-9000 m, although nowhere is such a thickness preserved.

The Culpeper basin forms the southern part of the Newark-Gettysburg-Culpeper basin system, which probably represents a single rift basin with subsidiary sub-basins, all of which have the same polarity (*i.e.*, the master faults are all on the northwest or west side of the basin) and similar sedimentary sequences (compare Figures I.1, 4.1 and 5.1). In size, this basin system is comparable to the Tanganyika rift of East Africa, although the latter is distinguished by being divided into many more sub-basins of alternating polarity (Rosendahl, 1987). The overall stratigraphic pattern is similar in the Culpeper, Gettysburg, and Newark basins, and there is little question that they were all onced interconnected; the Newark and Gettysburg basins are connected still, but there is a 3.2-km-wide gap between the Gettysburg and Culpeper basins.

Stratigraphic nomenclature of the Culpeper Group has had a long and complicated history. At present, two systems of stratigraphic nomenclature are in use (Table 4.1): that of Lindholm (1979) and that of the U.S. Geological Survey (Lee and Froelich, in press). Both systems are used in this report for clarity and for better comparison with recently published literature. The synonymy, age and description of these units is shown in Table 4.1. The rocks of the Culpeper basin were deposited in a number of lacustrine (Gore, 1983, 1988a, 1988b, 1988c, in press; Hentz, 1985; Smoot, 1989), fluvial (Sobhan, 1985), and alluvial fan environments (Lindholm *et al.*, 1979).

The first-order stratigraphy of the Culpeper basin can easily be explained in terms of the basin filling model (Schlische and Olsen, in review, this volume). The fluvial

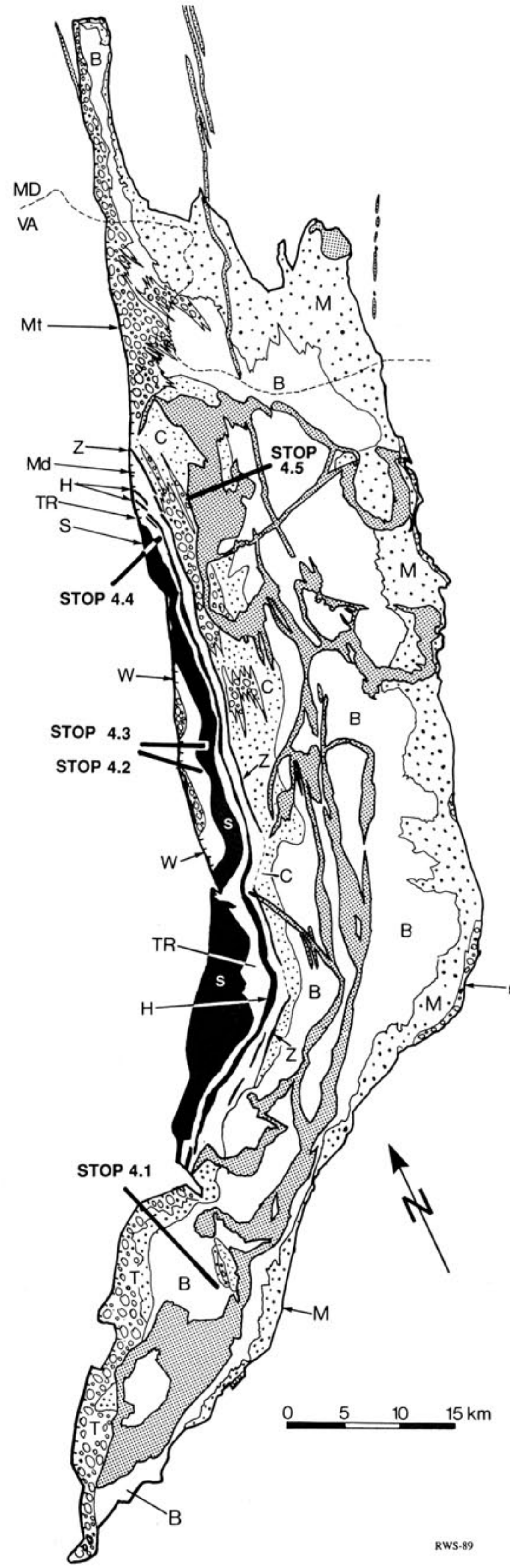

Figure 4.1: Geologic map of the Culpeper basin, Virginia and Maryland. Regular stipple represents diabase intrusions; black represents lava flows. Abbreviations are: M, Manassas Sandstone; Mre, Reston Member; Mt, Tuscarora Member; B, Balls Bluff Siltstone; C, Catharpin Creek Formation, T, Tibbstown Formation, Z, Mt. Zion Church Basalt; Md, Midland Formation, H, Hickory Grove Basalt; TR, Turkey Run Formation, S, Sander Basalt; and W, Waterfall Formation. After Leavy *et al.* (1983).

Manassas Sandstone was deposited when the basin was hydrologically open. It is overlain by the predominantly lacustrine Balls Bluff Siltstone. Our data are still too sparse to determine trends in accumulation rate. The Balls Bluff Siltstone is overlain by the Catharpin Creek and Tibbstown formations, which appear to contain a large quantity of coarse clastics (at least to the north), which may mark a gradual return to predominantly fluvial accumulation (A.J. Froelich, written comm.). This may be due to a decrease in subsidence rate or as a consequence of a widened basin in which fluvial systems had a longer distance to go before ponding (J.P. Smoot, pers. comm.). In other parts of the basin, these formations constitute cyclical lake sequences up until the first basalt flow (J.P. Smoot, written comm.). The syn- and post-extrusive formations again show marked increases in accumulation rate and "maximum" lake depth, apparently reflecting an increase in half-graben asymmetry.

The Triassic strata are extensively intruded and thermally metamorphosed by a complex network of quartz normative diabase sheets (as much as 600 m thick). Olivine- and quartz-normative dikes trend N, NNE, and NW and locally intrude basalt flows and interbedded Early Jurassic-age sedimentary rocks.

mileage

0 Leave Culpeper, VA.
0.1 Turn left at stop sign at end of driveway.
0.3 Turn left (north) onto Bypass 29.
2.5 Exit to US 522 heading east.
2.7 Turn right onto US 522 at end of exit ramp.
3.1 Continue straight on this road. Road becomes VA 3.
3.9 Mount Pony is on the right. This mountain is underlai by diabase and bordered by thermally altere sedimentary rocks (hornfels).
6.9 Turn right into office of Culpeper Crushed Ston Company Inc.

STOP 4.1: CULPEPER CRUSHED STONE QUARRY, CULPEPER (STEVENSBURG), VA

(by J.P. Smoot and P.E. Olsen)

Highlights: Lacustrine cycles in thermally-altered rock, mineralized siltstone, dinosaur tracks, öolitic limestone.

Lithostratigraphy and Cyclostratigraphy

The Culpeper Crushed Stone Company quarry expose about 80 m of thermally-altered mudstone and siltstone c the Balls Bluff Siltstone. These deposits can be divided int nine lithologic types, which are shown in the stratigraphi column and key (Figure 4.2): 1) Dark gray to blacl laminated shaley mudstone without mudcracks. Th lithology is interpreted as the deposits of a deep, perenni lake. 2) Dark gray or purplish red, platy mudstone wit internal pinch-and-swell layering reflecting oscillator ripples, and large sinuous mudcracks. This lithology i interpreted as shallow lake deposits that were intermittentl subaerially exposed. 3) Gray or purplish red mudstone wit layering similar to lithology 2 but broken into breccia-lik blocks by numerous polygonal mudcracks. This i interpreted as a subaerially-exposed lake deposit which wa

Table 4.1: Stratigraphy of the Culpeper basin, Virginia and Maryland (age data from Cornet, 1977a).

Units				
Lindholm (1979)	Lee and Froelich (in press)	*Thick-ness (m)*	*Age*	*Description*
Waterfall Fm.	Waterfall Fm.	1500-1719	Hettan.	Mostly red, fine to coarse, cyclical shallow-water lacustrine clastics; some gray to black deep-water lacustrine clastics and minor limestone
	Millbrook Quarry Mb.	450	Hettan.	Alluvial fan conglomerate; contains Jurassic basalt clasts
Buckland Fm.	Sander Basalt	140-600	Hettan.	Tholeiitic basalt flow (high Fe); interbedded sediments
	Turkey Run Fm.	150-330	Hettan.	Mostly red and gray, fine to coarse fluvio-lacustrine clastics; one gray to black lacustrine claystone and limestone
	Hickory Grove Basalt	80-212	Hettan.	Tholeiitic flows; interbedded clastics and basalt-clast conglomerate
	Midland Formation	150-300	Hettan.	Mostly red and gray, fine to coarse fluvio-lacustrine clastics; some gray to black cyclical lacustrine claystone and limestone
	Mt. Zion Church Bst.	3-180	Hettan.	Tholeiitic basalt flows; interbedded red clastics
Bull Run Fm.	Catharpin Creek Fm.	500	L. Nor.	Red to gray, fine to coarse fluvial (?) clastics
	Goose Creek Mb.	500	L. Nor.	Fluvial conglomerate; greenstone clasts derived from Blue Ridge
	Tibbstown Fm.	300-640	L. Nor.	Fluvial (?) arkosic sandstone
	Mountain Run Mb.	0-640	L. Nor.	Fluvial and alluvial conglomerate containing greenstone clasts
	Haudricks Mtn. Mb.	500	L. Nor.	Fluvial and alluvial conglomerate
	Balls Bluff Siltstone	80-1690	Norian	Mostly red, fine to coarse, cyclic shallow-water lacustrine clastics; some gray to black, cyclic deep-water lacustrine clastics and carbonates
	Leesburg Mb.	40-1070	Norian	Fluvial and alluvial conglomerate; predominantly carbonate clasts
Mannassas Ss.	Mannassas Ss: Poolesville Mb.	200-1000	L.Car?	Red, fine to coarse, arkosic fluvial clastics
	Tuscarora Creek Mb.	21-67	L.Car?	Fluvial/alluvial conglomerate; predominantly carbonate clasts
	Rapidan Mb.	70-140	L.Car?	Fluvial/alluvial conglomerate; clasts derived from Blue Ridge
Reston Fm	Reston Mb.	3-100	L.Car?	Fluvial/alluvial conglomerate; clasts derived from Piedmont

wetted and dried repeatedly without much net sediment accumulation. 4) Thin beds of tan-weathering siltstone with mudstone partings that are disrupted into polygonal, concave-upward curls. This lithology is interpreted as shallow lake or sheetflood deposits which were desiccated, causing the coarser material to curl away from the finer-grained sediments. 5) Massive, red or gray mudstone with abundant narrow, jagged mudcracks and spheroidal to flattened, albite-, K-feldspar- and dolomite-filled vugs. This type of deposit is interpreted as a product of an aggrading playa-like mudflat. The vugs are probably vesicles formed from air trapped during flooding events which brought in the sediments. 6) Massive, red or gray mudstone similar to lithology 5 but also containing abundant cement-filled tubes which are root structures. This lithology is interpreted as a playa-like deposit disrupted by roots. 7) Massive, red or gray mudstones with abundant millimeter- to centimeter-scale, albite-, K-feldspar-, Fe-calcite-, dolomite-, or mudstone-filled tubes (root structures) and deep, narrow, sinuous mudcracks. This is interpreted as the deposit of a vegetated mudflat with the deeper cracks suggesting the mudflat was wetter than that of lithology 5. 8) Massive, gray to black sandy mudstone or siltstone with abundant albite- and Fe-calcite-filled tubular root structures; some deep, narrow, sinuous mudcracks; large carbonate, Fe-calcite, dolomite, or epidote nodules; and sulfide mineralization. This lithology is interpreted as a vegetated shallow water shoreline deposit that was intermittently subaerially exposed. 9) Undifferentiated, massive, red or gray mudstone, inaccessible and examined by binoculars only, appears to be combinations of lithologies 5, 6, and 7.

Another important lithologic type is marked "c" on the stratigraphic column. It is a lenticular öolitic limestone with stromatolitic micrite lamination and abundant sulfide minerals. This is the unit described by Young and Edmundson (1954) and Carozzi (1964), and it is interpreted as a shoreline tufa deposit, probably related to spring activity.

The lithologies are organized into cyclic patterns with layering that grades upward into massive rocks. Nineteen cycles are shown on the stratigraphic column with two end-member types: 2-1-2-3-4-6-7-8 (thick gray cycles) and 4-5-6-7 (thin red cycles). The contacts between cycles are abrupt, whereas the boundaries between lithologic types are gradational. The cycles appear to be the product of the transgression and regression of a lake, probably driven by climate changes (Olsen, 1986). The thinner red cycles represent drier conditions and shallower lakes than the thicker gray cycles.

If the above lithologies are ordered by inferred lake depth, the section can be subjected to Fourier analysis in the same manner as the Solite section (Stop 2.1). We have ordered these lithologies as follows with the number in parentheses corresponding to the assigned depth rank: 5, 9 (0); 6 (0.5); 3 (1); 7 (1.5); 4, b, c, e (2); 2, d (2.5); 1 (3); a (no rank). There are no lithologies at this outcrop with a depth rank greater than 3. When subjected to Fourier analysis a strong hierarchy of cycles, comparable with those seen in the Cow Branch Formation, is evident (Figure 4.3). Most important are the peaks at 4.7 m and 20.9 m which correspond, respectively, to one mode of the precession cycle (23,000 years) and the average of the high-frequency elements of the eccentricity cycle (109,000 years), if a

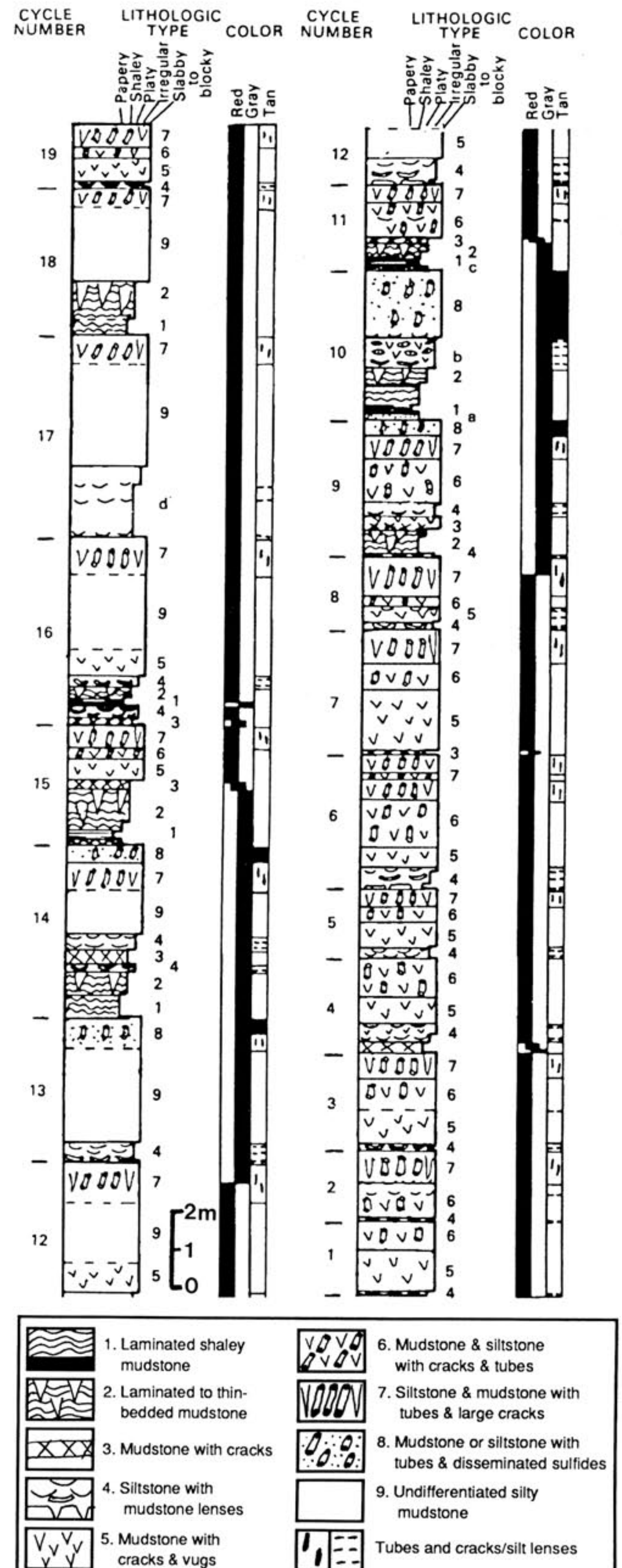

Figure 4.2: Stratigraphic column illustrating lithologic types and cycles within the Balls Bluff Siltstone, Culpeper Crushed Stone Quarry, Stop 4.1. From Smoot and Robinson (1988).

sedimentation rate of 0.19 mm/yr is assumed. A peak at 51.2 m is present which probably corresponds to the 413,000 year cycle of eccentricity, but the section is too short (80 m) to resolve it. Interestingly, a peak at 6.8 m is present in the spectrum, but no corresponding cycle is obvious in the outcrop. This peak could correspond to the obliquity cycle of 41,000 years, although the match is not especially good. A longer section is needed to resolve the periodic elements present; however, considering the short length of the section, the correspondence with the predictions of orbital forcing is rather good.

The type of sequence at the Culpeper Crushed Stone Quarry exposures of the Balls Bluff Siltstone appears to be restricted to the southern part of the Culpeper basin. The cycles here are generally thinner and have much more evidence of prolonged desiccation than the deposits of the northern part of the basin. The lacustrine deposits at this stop may represent the sediment-starved margin of the lakes forming the cycles to the north, or they may represent a different climatic setting in a sub-basin of the Culpeper. These lake deposits are probably older than any exposed to the north in the basin, and the style of sedimentation is similar to late Carnian and early Norian age mudstones in the Newark basin.

Base metal mineralization, including zinc and copper as sphalerite and chalcopyrite respectively, is restricted to lithology 8 at this exposure. This lithology was probably mineralized because it contained woody roots, the sediments remained water-saturated, the sediments were buried beneath organic lake deposits, and the diagenetic fluids could pass though the slightly sandy, relatively porous matrix. A similar deposit is seen at Stop 5.1 in the Passaic Formation of the Newark basin. The copper and zinc sulfides appear to be replacing pyrite and carbonate that grew around the roots during their decay. It is not clear what, if any, effect the thermal alteration of the mudstone had on the mineralization.

The Balls Bluff Siltstone, as exemplified by this outcrop, is comparable to the Gettysburg Shale of the Gettysburg basin and to the Passaic Formation of the Newark basin. This resemblance extends to the details of Van Houten cycles and to overall facies trends. The ages of the units are comparable as well. These resemblances suggest the similarity and probable former connection of the Newark, Gettysburg and Culpeper basins. There are no other units quite like the Balls Bluff-Gettysburg-Passaic formations elsewhere in the Newark Supergroup.

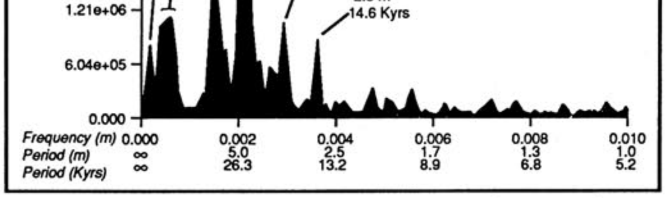

Figure 4.3: Power spectrum for Culpeper Crushed Stone Quarry based on data in Smoot and Robinson (1988). * denotes periods labeled but not significant at the 95% level.

Paleontology

Lithology 8, just below the horizon marked "c", produces a large number of poorly-defined reptile footprints recently described by Weems (1987). The footprints vary in length from 8 to 28 cm and are generally very deep (3-10 cm), decreasing in density down-dip (Smoot, pers. comm.). According to Weems (1987) there are six ichnogenera (Figure 4.4) in the Culpeper track assemblage, two of which Weems designated as new genera (*Gregaripus* and *Agrestipus*) and four of which he referred to Connecticut Valley genera (*Apatichnus*, *Eubrontes*, *Anchisauripus*, and *Grallator*). Unfortunately, the Culpeper Crushed Stone Quarry tracks seem completely indeterminate and should not have been assigned to existing genera or named as new taxa. They completely lack pad impressions, show a very large amount of individual variation, and have no diagnostic characters which can not be attributed to substrate effects.

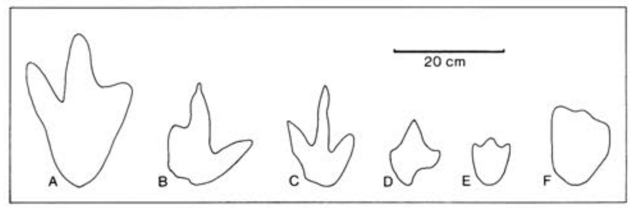

Figure 4.4: Footprints from the Culpeper Crushed Stone Quarry (Stop 4.1): A-D) possible *Grallator* spp.; E-F) indeterminate ?non-dinosaurian forms. Adapted from Weems (1987).

7.0 Turn around and turn left (west) on VA 3 back toward Culpeper.

10.8 VA 3 becomes US 522.

11.1 Turn right onto US 15-29 North. The road passes through the Culpeper basin for about 20 miles.

11.7 Near Opal, a few miles south of Warrenton, VA, the road leaves the Culpeper basin for a few miles and enters the Blue Ridge Province, which is underlain by Late Precambrian-Lower Paleozoic metasedimentary rocks and greenstones (Catoctin metabasalt). In many places, the Blue Ridge is represented by a prominent ridge or series of ridges, but south of Warrenton, the topography consists of low rolling hills, and the basin margin is ill-defined.

32.7 At Warrenton, fork right toward Leesburg and Washington, DC, on Bypass Route 15-29 North.

37.0 Continue on Route 15-29. Look for intersection with Route 600, which marks the approximate position of the western border fault of the Culpeper basin. At this point, the road re-enters the Culpeper basin. Note the low ridge on the left (north) side of the road. The steep eastern side of this ridge marks the western border fault.

39.8 to 41.8 Note the presence of small ridges marking the position of Early Jurassic basalt flows in the Buckland Formation (terminology of Lindholm, 1979), or Sander Basalt, Hickory Grove Basalt, and Mount Zion Church Basalt (terminology of Lee and Froelich, in press). The Culpeper basin is the southernmost exposed basin which contains basalt flows, the Triassic-Jurassic boundary (located just below the base of the lowest basalt flow), and Jurassic sedimentary rocks sandwiched between basalts. The road has been cut through the basalt flows, making mound-like features in the median strip and along the sides of the road. At least four distinct ridges can be seen. The valleys between the ridges are underlain by Jurassic sedimentary rock. It is interesting to compare the low relief of the basalt flows in this area with the considerably higher relief of the flows in the basins to the north, reflecting the higher rate of chemical weathering in the warmer southern basins *vs.* the predominance of mechanical weathering in the northern basins.

42.4 Town of Buckland.

42.9 Turn left on US 15 North toward Leesburg. This road passes along sedimentary rocks belonging to the Midland Formation between the first and second basalt flows in the basin (Mount Zion Church Basalt and Hickory Grove Basalt).

45.3 On the right is an outcrop of the lowermost basalt flow (Mount Zion Church Basalt), just before the stream and railroad crossing at Haymarket. At this point, the road passes through the lowermost basalt and into the underlying sedimentary rocks of the Bull Run Formation (Lindholm, 1979) or Catharpin Creek Formation (Lee and Froelich, in press).

45.6 Turn left (west) onto VA 55. The road will be passing up section through the basalt flows and intervening sedimentary units. The basalt flows do not have as much topographic expression here as they do near Buckland. Ahead, you will see a gap through a prominent mountain range. This is Thoroughfare Gap, passing between the Pond Mountains on the left (south) and Bull Run Mountains on the right (north) reaching an elevation of 400 m above sea level. Both mountains belong to the Blue Ridge Province, and the steep slope on the eastern side of these mountains marks the border fault at the western edge of the Culpeper basin.

47.6 Town of Thoroughfare. Cross railroad tracks.

48.4 Turn right onto road F723. Cross I-66.

48.5 Turn right onto Beverly Mill Road. Park. (Beverly Mill is the name of an old mill which lies just east of Thoroughfare Gap.)

STOP 4.2: THOROUGHFARE GAP, VA

(by P.E. Olsen and P.J.W. Gore)

Highlights: Unusually thick gray to black lacustrine sequences with turbidites of Waterfall Formation; fish and conchostracan fossils.

The late Hettangian-early Sinemurian? Waterfall Formation is unusual because it contains some of the thickest lacustrine sequences in the Newark Supergroup, some of which contain turbidites and channel-fill conglomerates.

This section is a partially overgrown road cut which was measured by Tucker Hentz in 1979 when I-66 was under construction. At that time, the road cut was approximately 0.5 km long, with over 140 m of section exposed (Hentz, 1981). According to Hentz (1981), several angular unconformities are present in this cut, all of which are overlain by relatively coarse-grained sandstone or conglomerate, and differences in dip across the unconformities are as much as 20°. Olsen suspects that these unconformities may be small-scale sequence boundaries rather than tectonically-induced rotations. In addition, several high-angle faults are present near the western end of the original exposure (Hentz, 1981). Most of these features are presently obscured by vegetation.

As categorized by Hentz (1985), five distinct lithofacies are present in the Waterfall Formation:

1) Laminated mudstones are medium- to dark-gray or black, highly-calcareous, pyritic shales with interlaminated lighter-colored, silty calcilutite or microspar, and darker-colored, calcareous, organic carbon-rich clayshale. There are two types of laminated mudstones, "unevenly laminated mudstones", and "finely laminated mudstones", differentiated on the basis of lamina thickness and morphology, contacts between laminae, and diagenetic features (Hentz, 1985).

The laminae in the "unevenly laminated mudstones" are thicker (0.1-18.0 mm thick), and consist of silty calcilutite grading up into calcareous mudshale or clayshale. Soft-sediment deformation features are common. There are two types of "unevenly laminated mudstones", and both are graded or structureless. One has erosional contacts between laminae and is interpreted to have been deposited by currents (possibly distal ends of turbidity flows) (Hentz, 1985). The other has sharp, planar contacts between laminae and is interpreted to have been deposited by settling (Hentz, 1985). Fossils in the "unevenly laminated mudstones" include fish, conchostracans, and ostracodes. These mudstones are interpreted as deposited in anaerobic waters on profundal slope and basin plain environments of a lake (Hentz, 1985). Down-slope movement is interpreted to have produced the soft-sediment deformation structures.

The laminations in the "finely laminated mudstones" are thinner, (0.08-0.90 mm thick), and consist of thinly-laminated or lenticular-laminated ferroan calcite (microspar) and clayshale or mudshale. Phosphate nodules (most of which are coprolites according to Gore and Olsen) and chert nodules are present locally, and fossils include well-preserved conchostracans (*Cornia* sp.), fish, ostracodes, and plant fragments. Contacts between laminae are abrupt. These mudstones are interpreted as deposited on the shore terrace and lake slopes below wave base, but above the anaerobic profundal region according to Hentz (1985), based on supposed burrows. According to Olsen, the structures described by Hentz as burrows are mostly diagenetic and deformational features. In plan views of laminae no burrows are visible and this is the facies in which completely articulated fish occur most commonly. Olsen interprets this facies as deposited in the anaerobic zone of the lakes.

2) Wavy-bedded sandstones are light gray and consist of silt to very coarse-grained sand with rare granules and small pebbles. Sedimentary structures include wavy bedding, ripples with mud drapes, channel-forms, burrows, and rare desiccation cracks and clastic dikes. These rocks are interpreted as littoral shore terrace deposits above wave base (Hentz, 1985).

3) Thinly-bedded sandstones are light- to dark-gray and consist of silt to very coarse-grained sand with some clay. The basal contacts of the beds are erosional, and the beds are graded or massive (structureless). Sedimentary structures include flame structures, flute casts, graded bedding with coarse fossil debris concentrated near the bottoms of the beds, ripple cross lamination, and wavy and parallel lamination. These rocks are interbedded with sublittoral and profundal mudstones and are interpreted as turbidity current deposits. The sand grains are probably derived from the shallow water wavy-bedded sandstones (Hentz, 1985).

4) Conglomerates are gray, with clasts ranging in size from granules to boulders. Both clast- and matrix-supported conglomerates are present. Some of the clasts in the conglomerate were derived from the Blue Ridge to the west, but others are derived from Jurassic basalt flows in the Culpeper basin. The lower contacts of the conglomerate beds are erosional and channel-form in shape, and most of the beds are graded. Channel-forms are as much as 120 m

wide and 10.5 m deep, comparable to slope channels in modern lakes (Hentz, 1985). The conglomerates are interbedded with fine-grained lacustrine deposits and turbidites and are interpreted as subaqueous lacustrine channel-fill deposits on a sloping bottom. However, Hentz's sections show a number of these conglomerates to be associated with units containing desiccation cracks, indicating subaerial exposure; therefore the conglomerates cannot be associated with any single environment.

5) Red interbedded siltstones and intraclastic sandstones are burrowed and mudcracked, with mudshale intraclasts and cross-laminated sandstones. This facies consistently occurs between fluvial deposits and littoral to sublittoral lacustrine deposits and is interpreted as deposits of the lake margin mudflat and shallow shore terrace (Hentz, 1985).

Sedimentary sequences in the Waterfall Formation consist of alternating shallow water to fluvial and deeper water lacustrine deposits making up the thickest Van Houten cycles in the Newark Supergroup. There are at least ten episodes of lake expansion and contraction, and the average thickness of a combined fluvial-lacustrine cycle is 150 m according to Hentz (1985). Individual gray lacustrine sequences range in thickness from about 7 m to more than 38 m (based on section descriptions in Hentz, 1981). Most of these sequences are not entirely exposed (top or bottom covered), but of nine lacustrine sequences described by Hentz (1981), mean thickness of the partial sections is at least 20 m. Hentz reported an average thickness for complete gray lacustrine sequences of about 35 m (Figure 4.5). The lacustrine sequences are separated by 5 to 240 m of red beds (Hentz, 1985).

Hentz (1985) has provided a reconstruction of Waterfall lake physiography (Figure 4.6). In this model, laminated mudstone units surround a thin-bedded sandstone unit deposited on the lake plain. The thin bedded sandstones, however, occur interspersed in the laminated mudstone

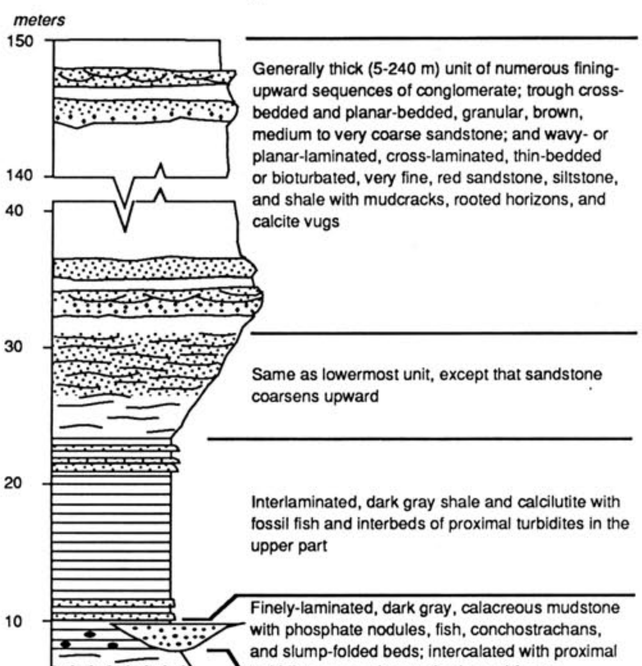

Figure 4.5: Generalized lacustrine cycle of the Waterfall Formation, Stop 4.2. Modified from Hentz (1985).

sequences both laterally and in vertical section. There is, therefore, no reason to assign them to a particular physiographic position on the lake floor. Instead, Olsen regards the laminated mudstone intervals as the deepest facies produced in Waterfall lakes and regards the thin bedded sandstones primarily as "randomly dispersed" turbidite lobes. Closely associated desiccation-cracked intervals indicate that most (but definitely not all) of the thick conglomerate sequences were deposited in shallow water, not deep subaqueous channels as inferred by Hentz. If the laminated mudstones and thin-bedded sandstones of Hentz are the deepest water units and the mostly conglomeratic units and red clastics are the shallowest, the Waterfall Formation shoaling-upward sequences are comparable to Van Houten cycles (except in thickness) seen in other basins.

Hentz (1985) also regarded the shoaling-upward sequences of the Waterfall as a lake-filling sequence and ascribed the deepening of the lake to intervals of accelerated subsidence. As filling sequences, the maximum depths of the lakes need not have been greater than 35 m (Hentz, 1985). If the same filling argument were applied to the microlaminated beds in the Lockatong Formation (Stop 5.7), those fish-bearing mudstones would be interpreted as deposited in 2 m of water over an area of more than 7000 km^2! It thus seems reasonable to assume that the lake cycles were driven by orbitally-induced climatic fluctuations, as has been proposed for much of the Newark Supergroup (Olsen, 1986). However, the hypothesis that the Waterfall cycles were produced by climate cycles rather than tectonic events cannot be tested directly at these outcrops because of lack of data on the lateral continuity of beds and lack of long sections suitable for Fourier analysis.

Hentz's average 150-m-thick lacustrine to fluvial sequences show great variability individually and appear to Olsen to be mixtures of several orders of cycles. Alternations of fish-bearing, laminated units and subaerially-exposed desiccated units average about 70 m in the I-66 cuts. These are interpreted as Van Houten cycles. These very thick Van Houten cycles are directly comparable, facies-for-facies, to Van Houten cycles in the Towaco Formation adjacent to the border fault in the Newark basin (see Stop 6.2), where the cycles average 25 m. Compound cycles should average roughly 350 m thick for the 100,000 year cycle and roughly 1400 m thick for the 400,000 year cycle. The estimate for the 100,000 year cycle is in line with the thickness of the thickest red sequences (240 m) cited by Hentz (1985), which represent the driest parts of the 100,000 year cycle in the driest portions of the 400,000 year cycle.

Although the details of Waterfall Formation stratigraphy have yet to be worked out, Olsen postulates that the I-66 outcrops of lacustrine cycles correlate mostly with the middle Towaco Formation (Hettangian; time intervals P2a,b,c; Figures I.9, I.10) and represent the same climatic events.

Fossils are exceedingly abundant in the Waterfall Formation, especially at these outcrops, not only in the dark laminated mudstones but also in sandier units. Most notable are the fossil fishes (Figure 4.7), which are potentially more diverse here than anywhere else in the Newark Supergroup, and the gastropods which occur in gray muddy sandstones.

48.7 Turn around and head back to VA 55.
48.8 Turn left (east) onto VA 55.
49.6 Turn left on Antioch Road (VA 681) toward Silver Lake Campground.

50.9 Turn right onto dirt road to Haymarket Quarry and Silver Lake Campground.
51.4 Stop at gate to the quarry and park.

STOP 4.3: HAYMARKET QUARRY (by R.P. Tollo)

Highlights: Tholeiitic Sander Basalt with lenticular sedimentary interbeds.

This quarry exposes a cross section through the lower portion of the second lava flow of the Sander series. This represents the geochemical type locality of Sander type B basalt, defined by Tollo (1988) as one of five petrochemical varieties comprising the Sander series in the Culpeper basin. This basalt type, which corresponds to the broad HTQ category of ENA magma types defined by Weigand and Ragland (1970), is characterized by higher MgO contents and lower concentrations of incompatible minor and trace elements than the type A basalt that forms the regionally-extensive first flow of the series. This lack of progressive fractionation in stratigraphically successive flows is typical of the Sander series and suggests that basalt petrogenesis involved episodic tapping of multiple parental sources.

Redbeds underlying the basalt are exposed in the southeast portion of the quarry. They form part of a mappable unit intercalated between the first and second Sander flows in this part of the basin (Lee, 1979) and consist of thin- and thick-bedded shales and siltstones and relatively thin (<10 cm) lenses of quartz and lithic granule conglomerate.

This locality is particularly noteworthy because of the abundance of medium- to coarse-grained gabbroids which occur locally as isolated pods and veins cutting the basalt. These gabbroids are characterized by coarse plagioclase and clinopyroxene with the latter occurring as prominent, herringbone-twinned prisms ranging to 2 cm in length. The veins range from approximately 1 to 50 cm in width and are characteristic of the Sander/Hickory Grove sequence in the Culpeper basin and have been observed in the compositionally similar Preakness (Newark basin), Holyoke (Hartford basin), and Deerfield (Deerfield basin) basalts. The gabbroids typically contain higher concentrations of TiO_2 and other incompatible elements than the surrounding basalt and have been interpreted as late-stage, relatively chemically-evolved, auto-intrusions of fractionated basaltic liquid (Tollo, 1988).

A series of closely-spaced, north-striking fractures occurs in the northwest portion of the quarry. These fractures contain locally prominent mineralized zones, including prehnite, quartz, calcite, and a variety of zeolite group minerals, all of which show abundant textural evidence for precipitation as open-space fillings. Although relatively common in many localities in the Newark basin, such mineralized zones are somewhat rare in the volcanic units of the Culpeper basin. Prominent columnar joints occur throughout the quarry and are characteristic of all the volcanic units of the basin. The curved jointing defining splintery columns of the entablature of this flow in this quarry is particularly striking and is similar to patterns seen in the Preakness Basalt of the Newark basin (Stop 6.4) and the North Mountain basalt of the Fundy basin (Stop 11.2), and are interpreted as post-cooling deformation related to faults and mega-kink banding due to bending of the thickest flows.

51.5 Turn around and leave the quarry.
52.0 Turn left (southeast) at Antioch Road (VA 681).
53.3 Turn left (east) onto VA 55.
54.2 Turn left onto US 15 North toward Leesburg.
66.6 Turn left into driveway of Oak Hill Plantation, home of James Monroe.

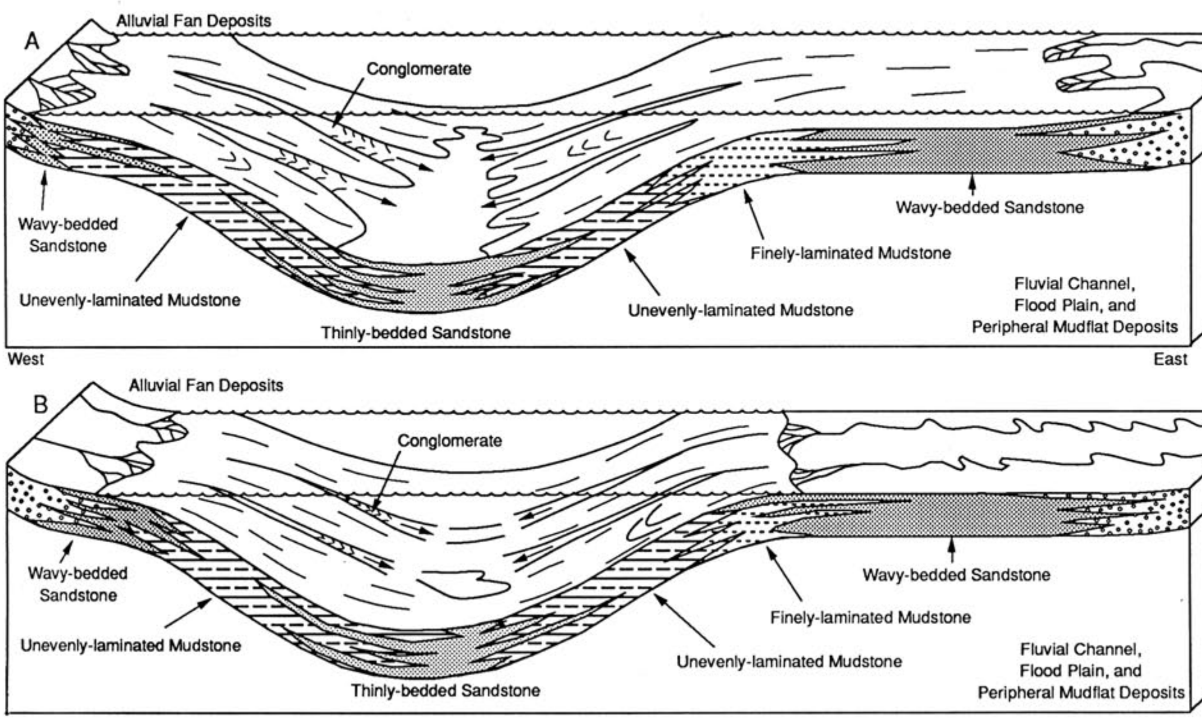

Figure 4.6: Reconstructed physiographic profiles of the Waterfall lake at (A) high-water level and (B) low-water level, showing the interpreted distribution of lithofacies within the lake basin. Modified from Hentz (1985).

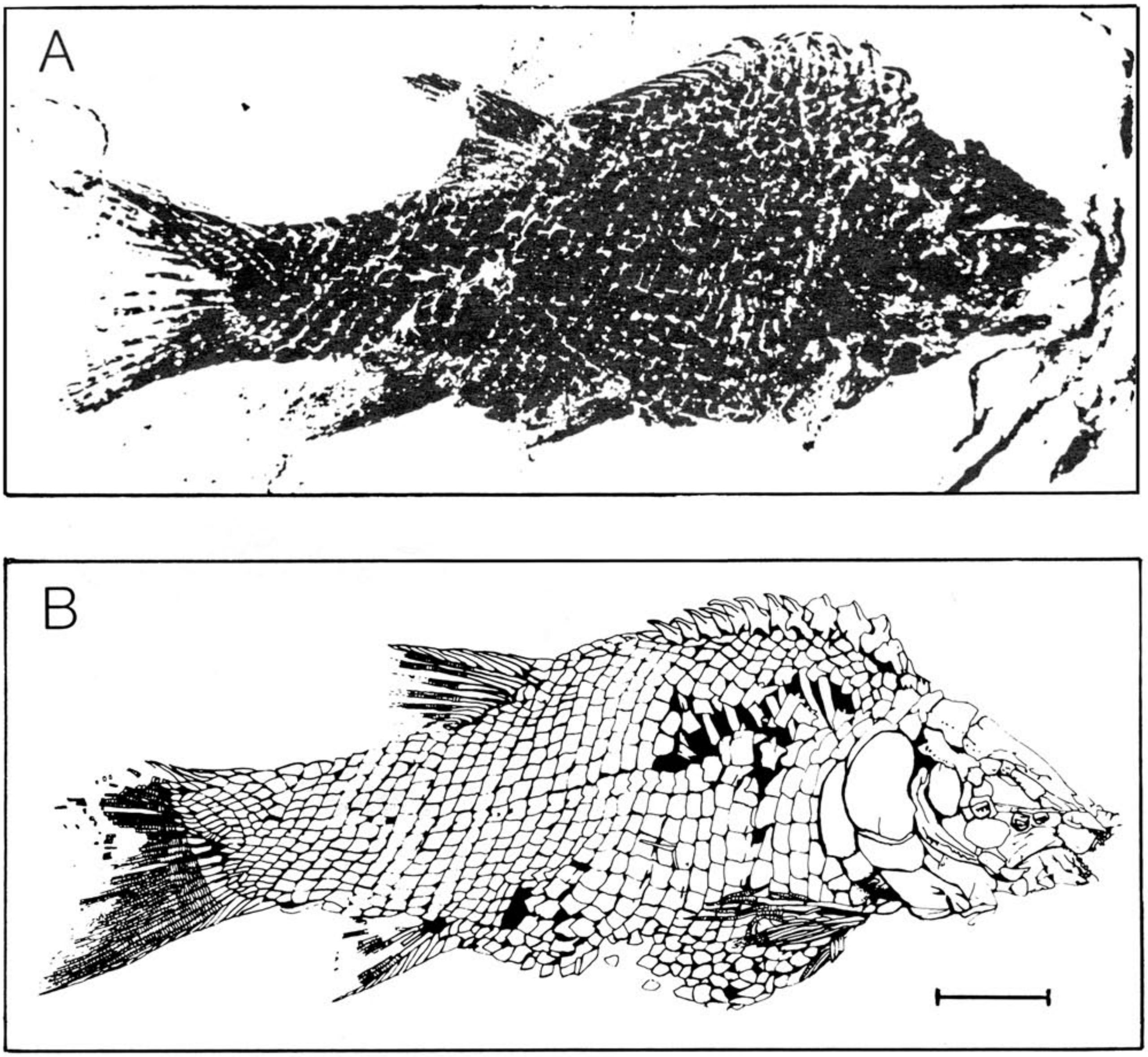

Figure 4.7: A) Semionotid fish of the *Semionotus tenuiceps* group from the Waterfall Formation of Stop 4.2 (courtesy of Tucker Hentz); B) member of the *Semionotus tenuiceps* group from the Turners Falls Sandstone of Sunderland, Massachusetts (from Olsen *et al.*, 1982). Scale is 2 cm.

STOP 4.4: DINOSAUR TRACKS AT OAK HILL

(by P.J.W. Gore)

Highlights: Dinosaur tracks in paving stones (Turkey Run Formation) around the house.

Oak Hill is a privately-owned home which was built about 1818-1821 by James Monroe, 5th President of the United States. The famous "Monroe Doctrine" is said to have been written at Oak Hill. Lafayette was entertained here in 1824. Monroe lived here most of the time from his retirement in 1821 to his death in 1831.

The flagstones in the formal gardens surrounding the house were quarried in the 1920's as part of a historical renovation (Ridky and O'Connor, 1979). Both isolated footprints and a trackway are present in the stones around the house. Well-preserved positive and negative prints are present in the pantry, and a side porch contains a trackway consisting of four tracks. (One visitor to the site is reported to have remarked that she was surprised that they let the dinosaurs roam so close to the house!)

The stone was obtained approximately 1.6 km north of the mansion along the north side of the Little River. This quarry lies in the sedimentary sequence between the second (Hickory Grove) and third (Sander) basalt flow units, which Lee and Froelich (in press) have designated as the Turkey Run Formation (see geologic map of Leesburg Quadrangle by Lee, 1979). The footprints come from a section about 62 m thick, containing a 42 m covered interval (Pannell, 1985). The tracks are from a bed of red siltstone and shale with wavy bedding, ripple marks, and slump features, which appears to be of fluvial origin (Pannell, 1985), unlike the rocks with tracks at the Culpeper Crushed Stone Quarry, which are lacustrine deposits. Olsen, however, believes them to be marginal lacustrine and shallow-water lacustrine.

Here at Oak Hill, two ichnospecies of *Eubrontes* (*E. giganteus and E. approximatus*) and two of *Grallator* (*G. cuneatus* and *G. formosus*) were identified by Pannell (1985) (Figure 4.8). The largest tracks at Oak Hill are at least 32.6 cm long and 22.5 cm wide, are three-toed, and were identified by Pannell (1985) as *Eubrontes*, a theropod track (Figure 4.9). The trackway belongs to *Grallator* and consists of four well-preserved three-toed footprints (Pannell, 1985). The length of the stride was a little over a meter. *Grallator*-type tracks were probably produced by a raptorial small theropod, capable of high speed and sudden turns without skidding on a very soft substrate (Pannell, 1985; Weems, 1987). Calculations of size and speed of the *Grallator* track-maker by Pannell (1985) suggest that the reptile was running at 6.5 km/hour, and was 52 cm from the hip to the ground. This is a typical Connecticut Valley-type assemblage of footprints, typical of the Early Jurassic (Figure 4.9).

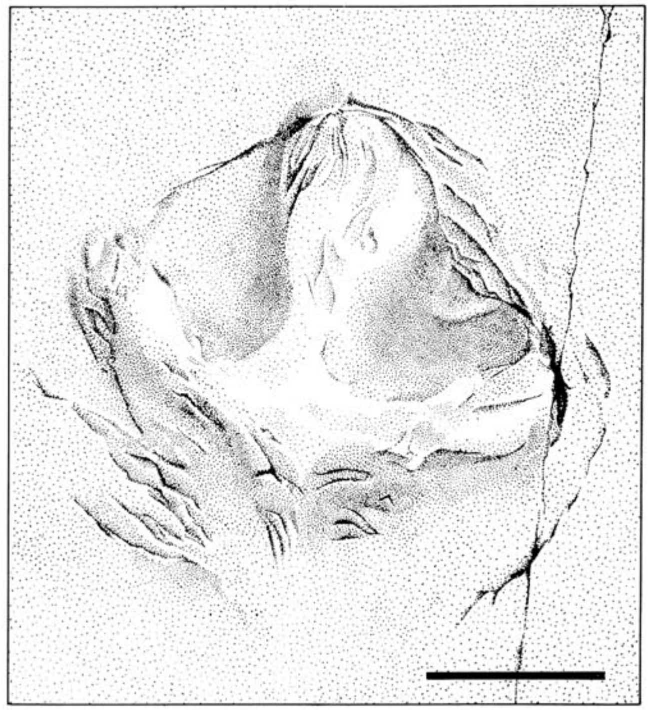

Figure 4.8: Dinosaur footprint from Oak Hill, Stop 4.4. Scale is 10 cm. Drawing by P.E. Olsen from a photo by P.J.W. Gore.

66.8 Turn around. Turn right (south) onto US 15.
68.7 Turn left (southeast) onto US 50 at Gilbert's Corner.
74.7 Turn left (north) onto VA 659 to Arcola.
74.8 Turn left (north) onto VA 621 in Arcola.
80.1 At the intersection with VA 860 at bridge over Goose Creek, park on shoulder of the road.

STOP 4.5: EVERGREEN MILLS AT GOOSE CREEK, SOUTH OF LEESBURG, VA (by R.P. Tollo)

Highlights: Mineralized contact metamorphic zone.

This locality provides an opportunity to examine the upper portion of the Belmont diabase sheet and the contact metamorphic effects of this intrusion on the overlying sedimentary rocks. The contact between the diabase and the west-dipping strata is located along Goose Creek approximately 50 m downstream from the VA 621 bridge (Lee, 1979). The clastic sedimentary rocks exposed in the road cuts at the intersection of VA 621 and 860 have been assigned to the Goose Creek Member of the Catharpin Creek Formation (Lee and Froelich, in press). Here, this unit is composed mainly of thick-bedded to massive siltstone with several discontinuous(?) lenses of intercalated pebbly conglomerate containing limestone, quartz, and fine-grained lithic fragments in a clay-silt matrix. The metamorphosed siltstones are locally spotted, a feature that can be best observed in the road cut on the east side of VA 621. The conglomeratic units show more obvious evidence of the thermal metamorphism with the development of prominent reaction zones around and replacing some of the clasts. Lee (1982) and Lee and Froelich (1985) have reported the development of a variety of minerals including andraditic garnet, diopside, serpentine, wollastonite, idocrase, and scapolite in such rocks surrounding diabase intrusions in the Culpeper basin. Amethyst is also relatively common in the conglomerate units at this locality.

The contact between the metamorphosed sedimentary

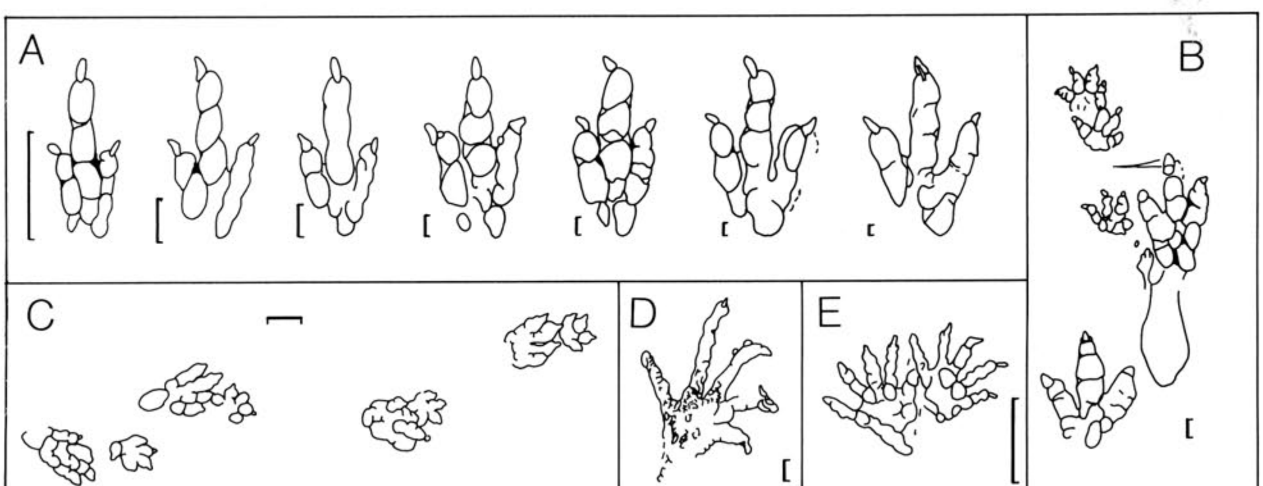

Figure 4.9: Early Jurassic track types from the Newark Supergroup. A, *Grallator* spp. (theropod dinosaurs); B, *Anomoepus scambus* sp. (ornithischian dinosaur); C, *Batrachopus deweyii* (crocodylomorph); D, *Rhynchosauroides* sp. (?sphenodontid); and E, *Ameghinichnus* sp. (trithelodont mammal-like reptile). Scales are all 2 cm. From Olsen (1988b).

rocks and the diabase is located along the southern bank of Goose Creek. The diabase is fine- to medium-grained with plagioclase and pyroxene visible in hand specimens. Geochemical data for chilled margin samples (Lee *et al.*, 1984; Mihm, 1986; Froelich and Gottfried, 1988) indicate that the Belmont sheet is composed of HTQ diabase compositionally similar to the York Haven type identified in Pennsylvania by Smith *et al.* (1975). Mihm (1986) has demonstrated that this sheet includes at least four petrographic types including chill, orthopyroxene, inverted pigeonite, and augite diabase. Froelich and Gottfried (1988) have shown that the diabase encloses ferrodiorite, ferrogabbro, and granophyric/granitic differentiates. They have suggested that the distribution of these lithologies and the lack of chemical mass-balance throughout the sheet can best be explained by process of lateral flow differentiation modified by gravitational settling and late-stage filter pressing.

Leave by heading north on VA 621, toward Leesburg, VA.

85.2 Leesburg city limits.

86.2 Turn right (north) onto US 15 into Leesburg.

87.5 Continue north on US 15, toward Frederick, Maryland. Between Leesburg and Frederick, note the carbonate-clast conglomerates with red mudstone matrix exposed in road cuts and in isolated outcrops in the fields on both sides of the road. These conglomerates have been quarried locally and are referred to as "puddingstone", "Potomac marble" or "Calico marble" (Froelich *et al.*, 1982). The carbonate clasts are derived from Cambrian and Ordovician carbonates which mantled the Blue Ridge in this area during the Late Triassic.

99.1 Cross the Potomac River at the town of Point of Rocks and enter Maryland. Note that the road is parallel to the main western border fault of the Culpeper basin. Goethite specimens of unusual quality consisting of black, lustrous, botryoidal and stalactitic masses to over a meter across have been found here, apparently occurring along the fault zone.

Catoctin Mountain is on the left. In this area, the Blue Ridge is a northward-plunging anticlinorium overturned to the west. The two limbs of the fold consist of Late Precambrian and Cambrian metasedimentary rocks (quartzite and phyllite) overlying an older unit of schistose Catoctin metabasalt. The anticlinorium is cored by Precambrian Grenville granitic basement rock. The Appalachian Trail passes through this area on the mountain marking the western limb of the anticlinorium (South Mountain).

On the right (east), the isolated mountain is Sugarloaf Mountain. It rises about 245 m above the surrounding countryside to an elevation of 390 m and is underlain by quartzite similar to the Weaverton Quartzite exposed along the crest of Catoctin Mountain to the west. Sugarloaf Mountain is a doubly-plunging anticline; the southern nose of the anticline is unconformably overlain by rocks of the Culpeper basin.

110.8 In Frederick, turn to continue north on US 15 to Gettysburg, PA. The Culpeper basin is separated from the Gettysburg basin to the north by approximately 3.2 km (Figure I.1), underlain by Cambrian Frederick Limestone. US 15 runs through the Gettysburg basin from just north of Frederick all the way to Gettysburg. If road construction is continuing at the time of the field trip, continuous exposures of red beds and diabase can be seen for kilometers.

The Gettysburg basin of Maryland and Pennsylvania is over 100 km long and 25 km wide. Like the Newark and Culpeper basins, it is a half-graben bounded on its northwestern margin by a predominantly normal fault system toward which the strata dip. Only two formations are recognized within the basin: from the bottom up, these are the New Oxford Formation (fluvial at its base and fluvio-lacustrine in its middle and upper portions) and the cylically lacustrine Gettysburg Formation. The Heidlersburg Member of the Gettysburg Formation contains more gray and black cyclical lacustrine strata than "typical" Gettysburg. The strata range in age from middle Carnian to Hettangian (Cornet, 1977a) and attain a maximum calculated stratigraphic thickness of 9.5 km (Root, 1988), although nowhere is such a thickness preserved. Two thin basalt flows, intercalated with the youngest sediments of the basin (Cornet, 1977a), are preserved within a transverse syncline adjacent to the border fault. The Triassic rocks of the basin are intruded and thermally metamorphosed by a series of quartz-normative diabase plutons. Quartz-normative dikes intrude the basin's strata and the surrounding pre-Triassic rocks.

135.5 Series of red and gray beds of the Heidlersburg Member just past the cloverleaf turnoff to Emmitsburg. These form cyclic sequences nearly identical to those of the Culpeper Crushed Stone Quarry (Stop 4.1; J.P. Smoot, written comm.). These gray beds are reported to contain lacustrine fossils. A number of dinosaur footprints have been found in sandstone quarried from the Gettysburg Shale near Emmitsburg.

147.2 At Gettysburg, exit to York, PA on US 30.

154.0 Enter New Oxford, PA on US 30. (The type area for the Triassic New Oxford Formation.)

158.8 Continue on US 30 through circle intersection with PA 194. Leave the Gettysburg basin; enter the western part of the Piedmont.

166.0 Enter Thomasville, PA. Thomasville is situated in an area underlain by metamorphosed Cambrian carbonate rocks, basically equivalent to those in the Frederick Valley. The Thomasville Stone and Lime Company quarries the Thomasville Member of the Lower-Middle Cambrian Kinzers Formation, which contains limestone breccias with clasts of shallow water lithologies (öolitic limestone, *etc.*), intertonguing with black limestones. These deposits are interpreted to represent mass flows off the Cambro-Ordovician carbonate platform margin into an anoxic basinal environment.

169.0 Fork right toward Lancaster on US 30 East.

176.2 Cross Susquehanna River. Up the river to the left (north) is Chickies Rock, an outcrop of Chickies Quartzite along Chickies Ridge. Middle Cambrian and younger carbonate rocks are exposed north of Chickies Ridge and are unconformably overlain by the Triassic rocks of the Gettysburg basin.

About 8 km to the south is the controversial Martic line, which marks a transition from slightly-metamorphosed early Paleozoic shallow water carbonates and sandstones to highly-metamorphosed, structurally-contorted, deep-water flysch deposits and volcanics. Rapid facies changes and structural telescoping occur along this line. The Martic line extends southward into Maryland and marks the eastern edge of the Cambro-Ordovician carbonates exposed in the Frederick Valley. It is probably the southern continuation of Cameron's line and seems to mark the Taconic suture.

183.2 Exit right to Centerville Road.

5. NEWARK BASIN, PENNSYLVANIA AND NEW JERSEY

GEOLOGY OF THE NEWARK BASIN

The Newark Basin (Figure 5.1) is the largest of the rift sequences exposed in the United States, covering over 7000 km^2 and with a preserved stratigraphic thickness of more than 6 km. It is a block-faulted, deeply-eroded, half-graben (Figures I.2 and 5.2). Most strata dip 5°-15° NW. Most of the basin's northwestern margin is bound by normal faults, whereas the southeastern margin consists of an unconformable contact with Paleozoic rocks or is marked by overlap of coastal plain sediments.

Stratigraphy (by P.E. Olsen)

Nine formations are presently recognized in the Newark basin section (Table 5.1). These are, from the bottom up: Stockton Formation, Lockatong Formation, Passaic Formation, Orange Mountain Basalt, Feltville Formation, Preakness Basalt, Towaco Formation, Hook Mountain Basalt, and Boonton Formation. The upper seven formations were originally included in Kümmel's (1897) Brunswick Formation and Darton's (1890) Watchung Basalt. The present revision has been accepted by most authors in recent years (Smoot, 1985; Van Houten, 1987; Manspeizer and Cousminer, 1988; Parker *et al.*, 1988); however, a formal Brunswick Group is recognized by Lyttle and Epstein (1987) for Pennsylvania where most of the Jurassic basalt flows and intercalated sedimentary rocks are absent. I feel that the use of Brunswick is not a particularly natural grouping of formations because it precludes an inclusive group name for all the formations of the Newark basin, as has proved useful in several other basins (*e.g.*, Fundy Group, *etc.*). The Hammer Creek Conglomerate of Glaeser (1963) is recognized by some authors (Lyttle and Epstein, 1987), but I feel that the Hammer Creek is best regarded as a coarse-grained facies of the Passaic Formation (Olsen, 1980a, 1980b).

The subdivisions of the Lockatong and Passaic Formations also require note. McLaughlin (1943, 1945) mapped the distribution of the red portions of the 400,000 year cycles (Olsen, 1986) in the Lockatong Formation of the Hunterdon Plateau fault block and gave most of them informal member names. The gray portions of the cycles in the Lockatong were not named with the exception of Members A and B. Because of the intense interest in many of the gray portions of these same cycles, it makes sense to apply some kind of informal, consistently-applied name to each. It is simplest to revise the nomenclature of the Lockatong so that each member consists of a lower gray portion and an upper red portion, making up a single 400,000 year cycle and receiving the same member name (Figure 5.3). McLaughlin's place names are retained where possible, but new names are needed where he used letter or descriptive designations and for the unnamed units (in accordance with the North American Commission on Stratigraphic Nomenclature, 1983). Most of these names have already been used informally in previous works (Olsen, 1984a, in press). In the central Newark basin, the Lockatong Formation is 1100 meters thick and is thus divided into eleven 400,000 year cycles, each about 100 m thick (Figure 5.3). These names will be used throughout this guidebook.

McLaughlin (1944, 1946) subdivided the Passaic Formation (Brunswick of Kümmel, 1897) of the Hunterdon Plateau fault block into members differently from the system he used in the Lockatong and named the gray

Table 5.1: Stratigraphy of the Newark basin (from Darton, 1890; Kümmel, 1897; Cornet, 1977a; Olsen, 1980a)

Units	*Thick-ness, (m)*	*Age*	*Description*
Boonton Fm.	500	Hettangian-Sinemurian	Mostly red, cyclical lacustrine clastics; some gray and black lacustrine (rarely deep) carbonates and clastics; minor red fluvial sandstones and alluvial fan conglomerates
Hook Mt. Bst.	110	Hettangian	Tholeiitic basalt flows
Towaco Fm.	340	Hettangian	Mostly red, cyclical lacustrine clastics; some gray and black lacustrine (often deep) carbonates and clastics; minor red fluvial sandstones and alluvial fan conglomerates
Preakness Bst.	250	Hettangian	Tholeiitic basalt flows and interbedded sediments
Feltville Fm.	170	Hettangian	Mostly red, cyclical lacustrine clastics; some gray and black lacustrine (often deep) carbonates and clastics; minor red fluvial sandstones and alluvial fan conglomerates
Orange Mt. Bst.	150	Hettangian	Tholeiitic basalt flows and interbedded sediments
Passaic Fm.	3300	L. Carnian-Hettangian	Mostly red, cyclical shallow-water lacustrine clastics; some gray and black lacustrine (often deep-water) clastics with minor limestone; minor red fluvial and alluvial coarse clastics
Lockatong Fm.	1100	L. Carnian	Mostly gray and black, fine, cyclical lacustrine carbonates and clastics with deep water intervals; some red, fine cyclical lacustrine clastics; very minor fluvial clastics
Stockton Fm.	1800	?M. Carnian-L. Carnian	Mostly coarse brown, fine red, and very minor gray fluvial and alluvial clastics


RWS-89
A
B
0 5 10 15 20 km
N

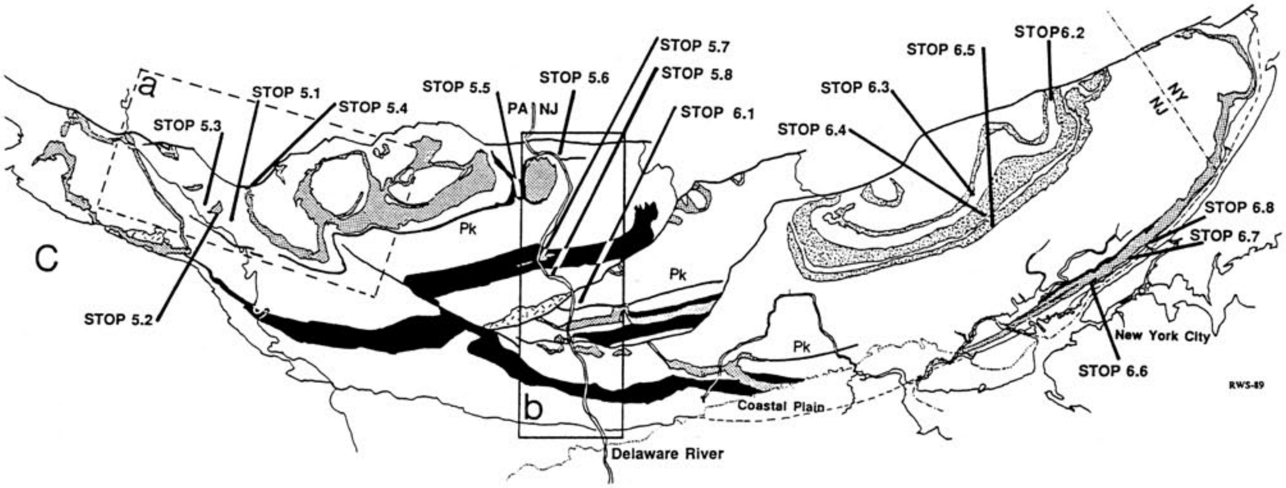

Figure 5.1: A) Geologic map of the Newark basin of Pennsylvania, New Jersey, and New York. Regular stipple represents diabase intrusions, irregular stipple represents lava flows. Dotted lines are form lines of bedding, and thin black lines are gray and black units in the Passaic Formation. Abbreviations are: S, Stockton Formation; L, Lockatong Formation; P, Passaic Formation; Pk, Perkasie Member of Passaic Formation; O, Orange Mountain Basalt; F, Feltville Formation; Pr, Preakness Basalt; T, Towaco Formation, H, Hook Mountain Basalt; B, Boonton Formation; J, Jacksonwald Basalt; Pd, Palisades diabase; and I, basement inliers. B) Structural map of the Newark basin and surrounding area, illustrating the close correspondence in attitude between the border faults and Paleozoic thrust faults. Thin double lines represent dikes. Abbreviations are: r, Ramapo fault; h, Hopewell fault; f, Flemington fault; c, Chalfont fault; z, zone of intense normal faulting (shown schematically); cl, Cameron's line; w, Watchung syncline; j, Jacksonwald syncline; bd, Birdsboro dike; da, anomalous NW-striking dike (Solebury dike); and db, dike apparently offset by Chalfont fault. Paleozoic structures after Lyttle and Epstein (1987) and Ratcliffe (1980). C) Location map of the Newark basin, showing field trip stops. Box a shows area detailed in Figure 5.6; box b shows area detailed in Figure 5.17.

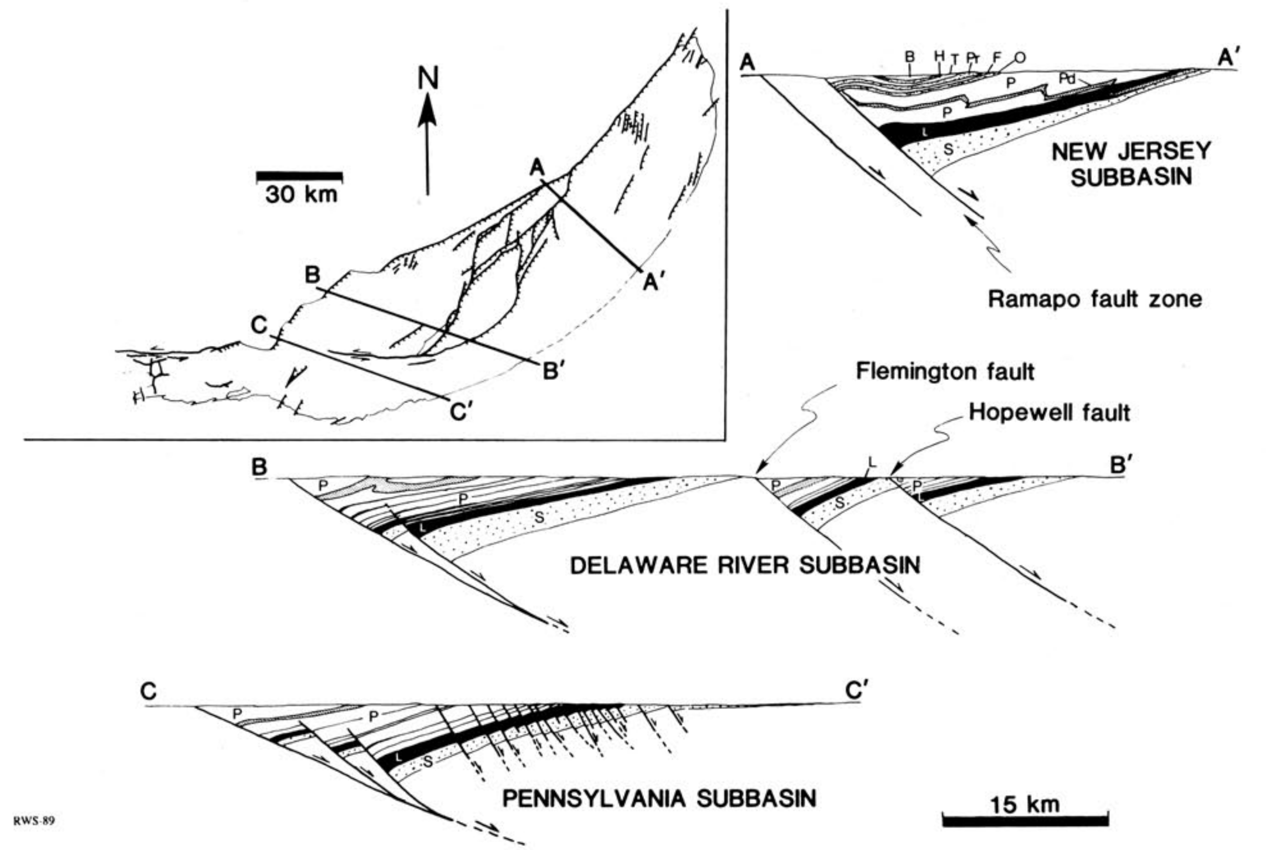

Figure 5.2: Representative cross sections through the three Newark sub-basins. Faulting within the Pennsylvania sub-basin is diagrammatic. From Schlische and Olsen (1988b).

portions of the 400,000 year cycles, not the red. Pending detailed revision, we use McLaughlin's member names for the Passaic, but include the overlying red half of each 400,000 year cycle in the named unit. McLaughlin (1946) and McLaughlin *in* Willard *et al.* (1956) also provided the alternative names, Graters Member and Perkasie Member for his members G plus H and members N plus O, respectively, because of their distinctiveness and great lateral continuity.

The Lockatong and Passaic formations together make up a natural facies package united by repetitive and permeating Van Houten cycles (Van Houten, 1964, 1969, 1980; Olsen, 1980a, 1980c, 1984a, 1988a). Because of the great thickness of the two formations, presence of very large exposures, relatively common small exposures, and a long history of detailed mapping, it is in these two formations that the evidence for Milankovitch-type climatic forcing is

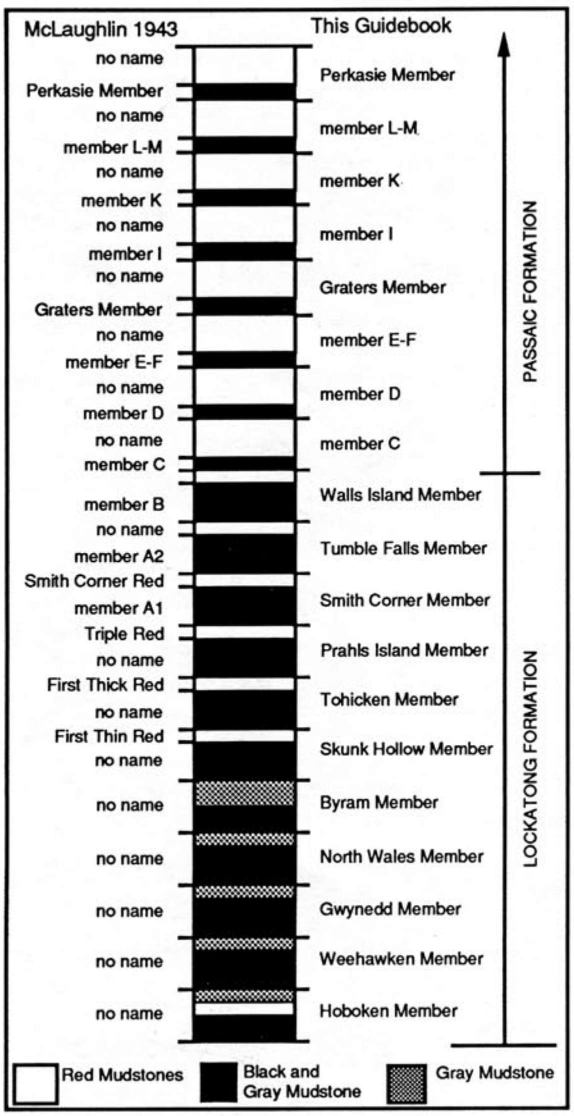

Figure 5.3: Nomenclature and stratigraphy of the Lockatong and lower Passaic Formations.

the strongest (Olsen, 1986) (see Stops 5.5 and 5.7, below). The hierarchy of Van Houten cycles of 21,000-year-duration and higher order cycles of 100,000- and 400,000-year-duration is obvious at virtually all relatively fine-grained outcrops, and even many of the coarsest (see Stop 5.6). Similar sequences of sedimentary cycles similar to those in the Lockatong and Passaic formations occur throughout the Jurassic portions of the Newark basin (Stop 6.2).

Basin Filling Model (by R.W. Schlische and P.E. Olsen)

The Newark basin exemplifies the stratigraphic pattern seen in the northern basins of the Newark Supergroup (Figure 5.4) and provides the best example of the basin filling model (Olsen and Schlische, 1988a-d) outlined in the Overview. The lower (Late Triassic age) sequence consists of a basal fluvial interval (Stockton Formation) overlain by a largely gray and black lacustrine sequence (Lockatong Formation), which is succeeded by an upper, mostly red, lacustrine interval (Passaic Formation). Based on a combination of transects across the Newark basin, accumulation rates seem to show a slow decrease after the onset of lacustrine deposition (see Figure 5.4). Maximum lake depth (during the wettest portions of division 2 of Van Houten cycles; see Figure 5.4) began shallow, rapidly deepened, and then slowly and systematically shallowed through the close of the Late Triassic. The overlying Early Jurassic sequence carries on the principally lacustrine pattern seen in the Lockatong and Passaic but shows a marked increase in accumulation rate and "maximum" lake depth just prior to and during the extrusive episode (Figure 5.4); thereafter, both decreased.

We have quantitatively modeled the filling of the Newark basin by using equations developed for the filling of full-graben and selecting parameters based on the actual geometry of the basin (Schlische and Olsen, in review) (Figure 5.5). Despite its oversimplifications, the model correctly predicts the switch from fluvial to lacustrine deposition 3 M.yr. after subsidence began, the systematic decrease in accumulation rates after the onset of lacustrine deposition, the occurrence of the deepest lake in the lower Lockatong Formation, and the overall decrease in "maximum" lake depth thereafter.

Deviations from the model's predictions also reveal important information. For example, one Van Houten cycle high in the Passaic Formation (Figure 5.5) stands out as anomalous compared to the rest of the upper Passaic because it has a microlaminated, carbonate-rich division 2 comparable to the deepest water units in the lower Lockatong. Prior to this type of analysis, the "excursion" would simply have been interpreted as one of the many climatic changes thought to have influenced the basin's stratigraphic development. With the basin filling model and Milankovitch-period modulation accounting for most of the changes in the stratigraphic sequence, this anomaly stands out as something unique, attributable to a "super-wet" climatic anomaly.

Major deviations from the model's predictions are the marked increases in accumulation rate and "maximum" lake depth in the Early Jurassic sequences. In the full-graben model, once lacustrine deposition began and the deepest lake had been achieved, no change in subsidence rate couldincrease both accumulation rate and "maximum" lake depth. These are governed solely by the area of the depositional and lake surfaces, respectively, which would not change even if subsidence were grossly increased.

In half-graben, however, maximum subsidence occurs adjacent to the border fault and decreases systematically toward the basin's hinge. An increase in the subsidence rate (a deviation from the model's assumption) results in an increase in basin asymmetry. As a result, sediments and water are preferentially shifted to the deepest portion of the basin. A rapid increase in basin asymmetry could therefore lead to (temporary) decreases in the areas of the depositional and lake surfaces, resulting in increases in accumulation rate and "maximum" lake depth. It is not yet clear if the basin asymmetry was the result of accelerated basin tilting, in which significant tectonic unconformities should be present, or if it was the result of movement on antithetic faults, creating an Early Jurassic sub-basin. Neither the unconformities nor major antithetic faults have yet been identified in outcrop.

A dramatic increase in the volume of sediment added to the basin per unit time would also increase the accumulation rate. However, this added volume of sediment would elevate the depositional surface and thereby displace the volume of water upward. In a concave-upward basin, this has the effect of increasing the lake's surface area, thereby decreasing "maximum" lake depth. An increase in the volume of water added to the basin during the wettest climate cycles would increase "maximum" lake depth and presumably also would bring in more sediments, increasing the accumulation rate. However, this would imply that the accumulation rate would be slower in the drier portions of the lake cycles. In fact, in a systematic study of the dependence of accumulation rate on sedimentary facies within the lacustrine cycles of Newark Supergroup basins, Kominz and Bond (1988) found that the wettest (deepest water) facies had slower accumulation rates when compared to the drier (shallower water) facies. It therefore appears likely that the observed Early Jurassic increases in accumulation rate and "maximum" lake depth were the result of an increase in basin asymmetry. Because the observed increases in accumulation rate and "maximum" lake depth occurred simultaneously in all of the northern rift basins (Figure I.3) we attribute the Jurassic "event" to a marked increase in regional extension, which significantly coincided with the brief but voluminous Newark Supergroup igneous activity.

Structural Evolution (by R.W. Schlische)

The border fault system of the Newark basin consists of reactivated Paleozoic thrust faults formed during the Appalachian orogenies (Ratcliffe, 1980; Ratcliffe and Burton, 1985; Ratcliffe *et al.*, 1986). The border fault system dips 60° SE at the New York and New Jersey border and only 30° SE or less in Pennsylvania (Ratcliffe and Burton, 1985). However, in the area of Boyertown, Pennsylvania (Stop 5.4), the generally NE-striking border fault changes to a more E-W trend, and also becomes more steeply dipping (~80°S). A similar attitude is suggested for the border fault at the Jacksonwald syncline, west of Boyertown (Lucas *et al.*, 1988). According to the Ratcliffe-Burton (1985) model, an east-southeasterly regional extension direction would have produced predominantly dip-slip on the majority of the NE-striking border faults as well as the NE-trending Flemington and Hopewell faults, and predominantly left-lateral strike-slip on E-striking

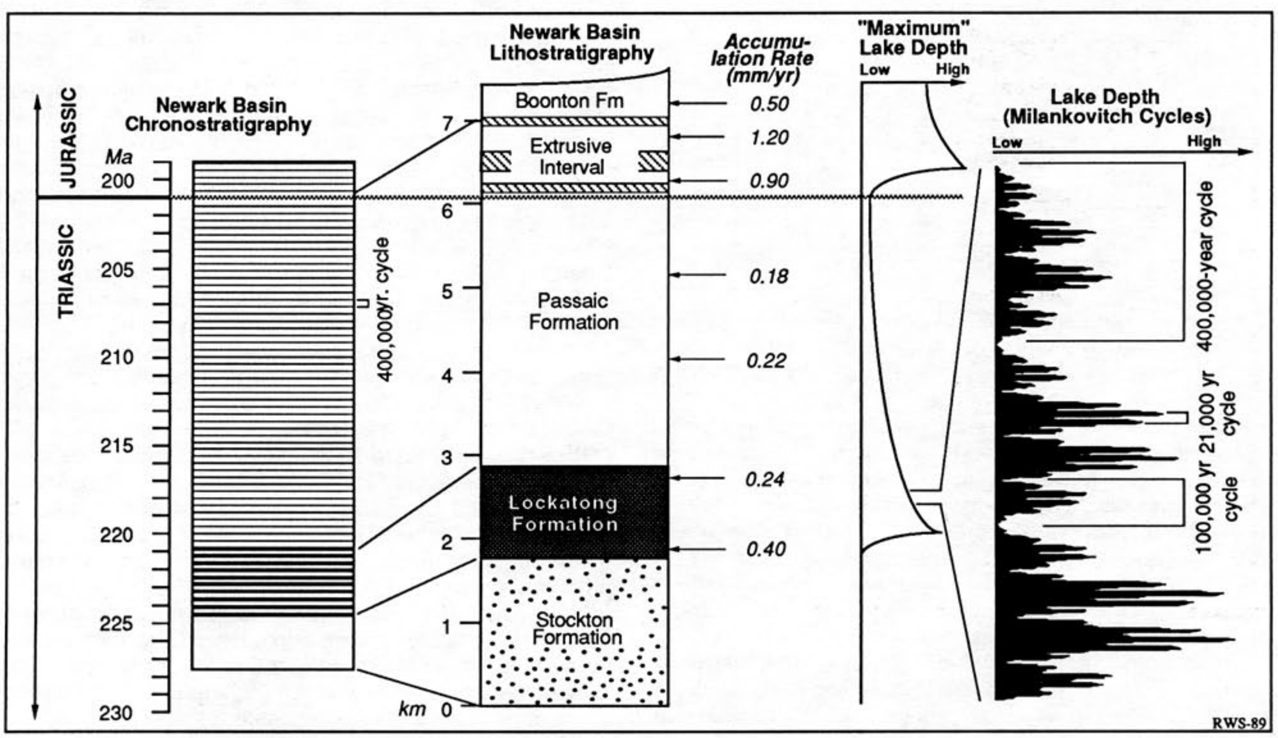

Figure 5.4: Stratigraphic framework of the Newark basin. Accumulation rates were calculated using Fourier analysis of representative stratigraphic sections. "Maximum" lake depth is the enveloping surface of inferred lake depth, shown schematically here. Extrusive zone consists of Orange Mountain Basalt, Feltville Formation, Preakness Basalt, Towaco Formation, and Hook Mountain Basalt. From Schlische and Olsen (in review).

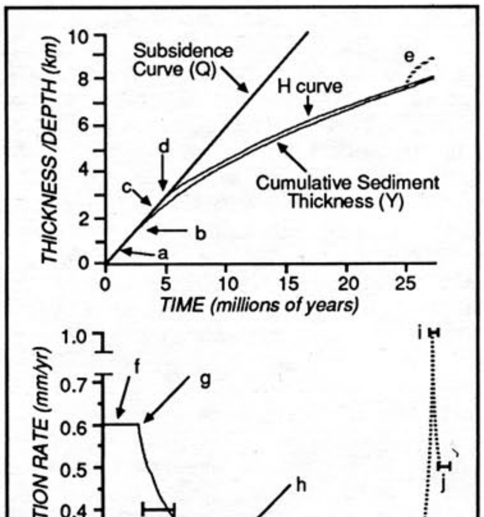

Figure 5.5: Predictions of the full graben basin filling model (solid lines) compared to data from the Newark basin (dashed lines and bars). Abbreviations are: a, filling equals subsidence resulting in fluvial sedimentation; b, onset of lacustrine deposition; c, rapid increase in lake depth as depositional surface subsides below hydrologic outlet; d, deepest lake predicted by model; e, major deviation from cumulative thickness curve in Early Jurassic; f, constant accumulation rate in fluvial interval; g, onset of lacustrine deposition, corresponding to b above; h, hyperbolic decrease in accumulation rate predicted by model; bars represent data on accumulation rates from outcrops in center of the basin; i, anomalously high accumulation rate in extrusive zone, a deviation from the model's predictions; j, decreasing accumulation rate in the Boonton Formation; k, 200-m-depth line corresponding to wave base, above which microlaminated sediments cannot be deposited; l, rapid increase in lake depth corresponding to c above; m, deepest lake predicted by model corresponding to d above; n, slow decrease in lake depth; o, "superwet" climatic anomaly; p, anomalously deep Jurassic lakes. From Schlische and Olsen (in review).

faults, such as the border fault in the narrow neck between the Newark and Gettysburg basins in Pennsylvania.

Mesozoic strata of the hanging walls of faults which experienced predominantly dip-slip are characterized by folds whose axes are nearly perpendicular to the fault. The high angle that the axes make with the fault makes it unlikely that the folds formed as a result of strike-slip; typically strike-slip related folds make an angle of 45° or less with the associated fault. The transverse folds do not extend into the footwall, they do not fold the fault, and they die out away from the fault in the hanging wall. Hence, these folds appear to be intimately tied to the faults and the faulting responsible for basin subsidence (Schlische and Olsen, 1987).

In the Sassamansville area (Figure 5.6), diabase plutons are generally concordant and sill-like in the synclines, but generally discordant in the anticlines, suggesting that intrusion may have been influenced by some folding of strata, which preceded or was contemporaneous with intrusion. Two diabase bodies whose geometry suggests that they are phacoliths are restricted to the axis of the Jacksonwald syncline (Stop 5.2). The phacoliths were intruded during or after some folding of the enclosing Late Triassic strata, while at the same time, the coeval Jacksonwald Basalt was extruded onto a nearly flat surface. Folding continued after the extrusion, because both the lava flow and the overlying sediments are folded. Stratigraphic patterns of onlaps and pinchouts and the presence of ductilely-deformed mudcracks and fossils (detailed at Stop 5.3) in the Jacksonwald syncline also suggest folding during sedimentation. Hence, the Jacksonwald and Sassamansville folds are partly growth structures, having begun to form during sedimentation of the preserved strata.

The axes of the transverse folds trend NW and are generally perpendicular to the strike of a majority of the region's Early Jurassic diabase dikes, which likely formed normal to the regional extension direction at that time (Figure 5.6). A pervasive set of joints, often most strongly developed in hornfels adjacent to the diabase intrusions (Stops 5.2, 6.1), also formed perpendicular to this direction. Interestingly, the fold axes are also parallel to the large dikes at either end of the basin, the Birdsboro dike in Pennsylvania (separating the Newark basin from the narrow neck) and the dike-like extension of the Palisades sill in New York. Apparently, σ_1 and σ_3 were parallel immediately adjacent to each other and at the same time (for intrusion and some of the folding were coeval). Another NW-trending dike (Solebury dike) crops out in the footwall of the Flemington fault; a set of joints parallels the dike in this region as well.

Many structural models have been proposed to explain the origin of these structures, especially the folds. Models calling for post-basin-subsidence compression or synrift strike-slip (Sanders, 1963; Swanson, 1982; Manspeizer, 1980; Burton and Ratcliffe, 1985) can be ruled out because the evidence suggests that the folds were forming during basin subsidence along faults which experienced predominantly dip-slip. Wheeler (1939) proposed that the folds formed as the hanging wall slid down a corrugated fault surface, although the geometry of the faults has not borne this out. The following model not only may explain the origin of growth folds along dip-slip faults but the origin of the anomalous extensional structures as well.

The model (Schlische and Olsen, 1988b) is based on the notion that the amount of dip-slip on the border fault system decreases away from a maximum at the center of the basin to nearly zero at the ends of the basin. This displacement geometry results in a basin which resembles a giant synform plunging toward the border fault system (Figure 5.7). The lower convex surface of this synform would experience maximum fault-parallel extension and could account for the anomalous NW-trending Solebury dike (intruded low in the stratigraphic section) and the joint set parallel to it. The upper concave surface of the synform would have been extended least and might have been subjected to fault-parallel shortening, producing transverse folds (Schlische and Olsen, 1988b). Alternatively, the transverse folds may have formed as a result of local variations in fault slip (*i.e.*, the synclines formed in areas of localized higher fault displacement than surrounding areas). The dike-like and discordant intrusions preferentially intruded at or near the crestal areas of anticlines might be related to the fault-normal extensional structures required in the fault displacement model.

The patterns of intrabasinal faulting suggests that the Newark basin can be divided into three structural sub-basins informally named the New Jersey, Delaware River, and Pennsylvania sub-basins (Figure 5.2; Schlische and Olsen, 1988a,b). In the New Jersey sub-basin, extension was taken up almost exclusively on the moderate to steeply-dipping (50°-70°) border fault. In the Delaware River sub-basin, extension was taken up partly on the shallow-dipping (~30°) border fault and partly on the more steeply-dipping (~45°, Ratcliffe and Burton, 1988) Flemington and Hopewell faults, which twice repeat the Triassic stratigraphic section. In the Pennsylvania sub-basin, extension was partly taken up along very shallow-dipping (25°) border fault system and partly along a series of closely-spaced normal faults.

The Chalfont fault (Figure 5.1) accommodates the variation in strain between the Delaware River and Pennsylvania sub-basins (Schlische and Olsen, 1988a,b) and hence is a transfer fault (terminology after Gibbs,

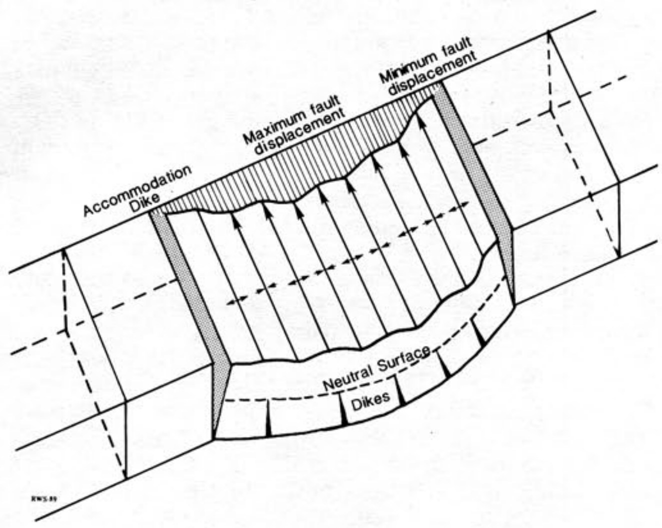

Figure 5.7: Highly simplified model illustrating the relationship between compressional and extensional structures in the Newark basin, based on a variable displacement field for the border fault, which produces a synform-shaped basin plunging toward the border fault. In this down-plunge view, the basin fill has been omitted for clarity of presentation. The lower surface has been extended the most and may account for the orientation of the Solebury dike (see Figures 5.1 and 5.17). Extensional collapse accommodation structures are developed at the lateral edges of the basin. The folds may develop as a result of local variations in fault displacement and die out in amplitude up-plunge. From Schlische and Olsen (1988b).

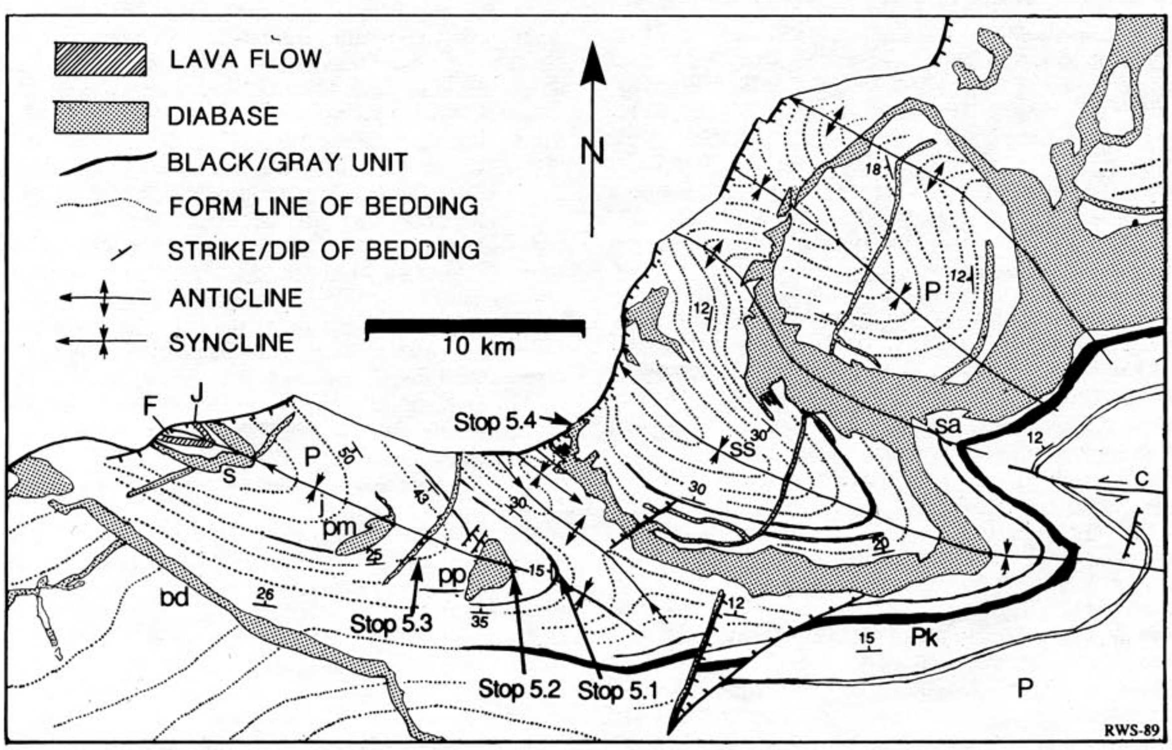

Figure 5.6: Geologic map of the southwestern corner of the Newark basin in Pennsylvania (see Figure 5.1C for location). Abbreviations are: P, Passaic Formation; Pk, Perkasie Member; J, Jacksonwald Basalt; F, Feltville Formation; bd, Birdsboro dike; j, Jacksonwald syncline; s, Jacksonwald sill; pm, Monocacy Station phacolith; pp, Pottstown phacolith; ss, Sassamansville syncline; sa, Sassamansville anticline; and c, Chalfont fault. From Schlische and Olsen (1988b).

1984). South of the transfer fault, the basin fill is extended by numerous small normal faults. These small faults are not observed north of the Chalfont fault. The Chalfont fault dies out to the west, as do the number and spacing of minor faults, until at the Chalfont fault's termination, the rocks on either side are relatively unextended. As the Chalfont fault is kinematically analogous to transform faults, it yields an east-southeasterly extension direction (Schlische and Olsen, 1988a), the same as given by the NE-striking Early Jurassic diabase dikes.

The timing of intrabasinal faulting appears to post-date the earliest Jurassic because none of the strata preserved within the hanging walls, including the Early Jurassic-aged Feltville Formation, shows any evidence of syndepositional faulting (Olsen, 1985b; see Stop 6.1). The timing of the faulting may coincide with a period of extensive hydrothermal alteration which reset the age of the 201 Ma igneous rocks to 175 Ma (Sutter, 1988). It therefore appears likely that the intrabasinal faults developed late in the history of the basin. As slip was reduced on the shallow-dipping and shallowing (as a result of isostatic uplift) border fault in Delaware River sub-basin, it was transferred to two new, more steeply-dipping (Ratcliffe and Burton, 1988) intrabasinal faults, whose hanging walls suffered additional tilting over that of the border fault (Schlische and Olsen, 1988a,b). Indeed, strata dip more steeply in the hanging walls of the Flemington and Hopewell faults. Folding of the hanging wall strata of these intrabasinal faults by variations in fault displacement probably occurred at this time.

The following, then, is a structural history of the Newark basin as I presently see it: [1] gentle syndepositional tilting of sediments in the developing half-graben, in which subsidence was greatest adjacent to the border fault (this continued throughout the history of the Newark basin); [2(a)] gentle syndepositional folding of relatively unlithified sedimentary strata adjacent to the border faults in Pennsylvania, as indicated by pinchouts and onlap relations in the synclines; [2(b)] NE-SW-directed shortening with concomitant NW-SE extension in relatively unlithified sediments, producing deformed mudcracks and ductilely-deformed fossils, such as those observed at Stop 5.3; [2(c)] intrusion of diabase into slightly folded strata in Pennsylvania, the intrusion of a majority of the dikes perpendicular to the regional extension direction, and extrusion of lava flows onto relatively unfolded strata; [2(d)] baking and lithification, coupled by hydrofracting, produced closely-spaced fracture cleavage adjacent to diabase intrusions; [3] folding of lava flows in Pennsylvania and New Jersey; [4] development of axial planar cleavage late in the history of folding in the Jacksonwald syncline because the cleavage does not fan about the fold (Lucas *et al.*, 1988); [5] intrabasinal faulting and associated tilting and folding of the hanging wall strata and development of a widespread set of joints perpendicular to the regional extension direction, in response to the late stage brittle release of accumulated strain in the rocks.

mileage

0.0 Mileage begins at the entrance ramp for US 30 East at Centerville Road. Head toward Lancaster, PA.

4.1 Fork right on US 30 East towards Coatesville.

6.8 Exit to PA 23, Lancaster. Turn left on PA 23 East, New Holland Pike,

17.8 Town of New Holland, PA.

20.1 Town of Blue Ball, PA, and intersection of US 322 and PA 23. We are skirting the southern edge of the broad part of the narrow neck between the Newark and Gettysburg basin (Figure 5.1). Holotype and only specimen of skeleton of *Sphodrosaurus pennsylvanicus* (Colbert, 1960) found in hornfels of Passaic-Gettysburg-Hammer Creek Formation about 9.7 km north of here in old quarry in Bowmansville, PA. Originally thought to be a procolophonid closely related to *Hypsognathus* (Price, 1956; Colbert, 1960), *Sphodrosaurus* has turned out to be a rhynchosaur (Baird, pers. comm., 1987).

23.4 Morgantown, PA. From here to PA 100, we will be traveling along the contact between the Stockton Formation and Paleozoic and Precambrian basement as well as a diabase body (Morgantown sheet) which intrudes the contact zone. Basement rocks (mostly Cambrian carbonates) are exposed to the north of this diabase and the Stockton-basement contact is repeated.

Cornwall-type iron ore bodies occur at the Grace Mine, located just north of Morgantown. Cornwall-type ore bodies are mineralized carbonates (either Paleozoic limestone or early Mesozoic limestone conglomerate) adjacent to diabase sheets. The ore is magnetite replacing Cambrian Buffalo Springs Formation at the faulted contact between the diabase and Stockton Formation (Sims, 1968). Pyrite, chalcopyrite, pyrrhotite, and sphalerite also occur (Sims, 1968). No exposures were present at the surface and the mine was operated from a deep shaft until 1977. Estimated reserves are about 40-50 million tons (Robinson, 1988, and pers. comm.).

34.3 Intersection with PA 345; continue straight on PA 23.

41.2 Bucktown, PA, in Stockton Formation. Turn left onto PA 100 North, heading towards Pottstown. Proceed up section into main part of Newark basin.

41.7 Mapped position of most western portions of Lockatong Formation. The mapped extent of the Lockatong terminates about 1.6 km to west at the southern termination of the massive Birdsboro dike, the western great dike intruded along the hinge zone on the western side of the Jacksonwald syncline (see Schlische, above).

42.2 Lower Passaic Formation sandstones and conglomerates in this area are the lateral equivalents of the middle and upper Lockatong Formation, to the east and north.

43.9 Upper parts of large tongue of conglomerate may underlie in part the lateral equivalent of the Graters Member of the Passaic Formation.

45.1 Outcrops of sandy facies of Perkasie Member of Passaic Formation. The Perkasie is the most widely-mapped gray and black unit within the Newark basin. In this area it changes facies dramatically along strike from relatively fine-grained rocks at the Sanatoga Quarry of Pottstown Trap Rock Company (see Stop 5.5), about 3.2 km east of here, to gray conglomerates and sandstones exposed on the dip slope of the large conglomerate tongue mapped to the immediate west of here.

45.9 Crossing Schulkill River. Entering Pottstown, PA.

46.3 Turn right on PA 663.

46.5 Cross Manatawny Creek.

46.6 Turn left on Manatawny Road, heading north parallel to Manatawny Creek.

47.3 Pass under PA 100.

47.6 On left is bridge for Glasgow Street passing over Manatawny Creek and Reading Railroad tracks. Cut below bridge exposes excellent >20 m section shown in Figure 5.8. This sequence of gray and black units is exposed at several places along strike in the Jacksonwald syncline (Figure 5.6), including Stop 5.1.

48.0 Sign for West Pottsgrove Township. Park in open area on right after sign and walk along road to abandoned quarry on right.

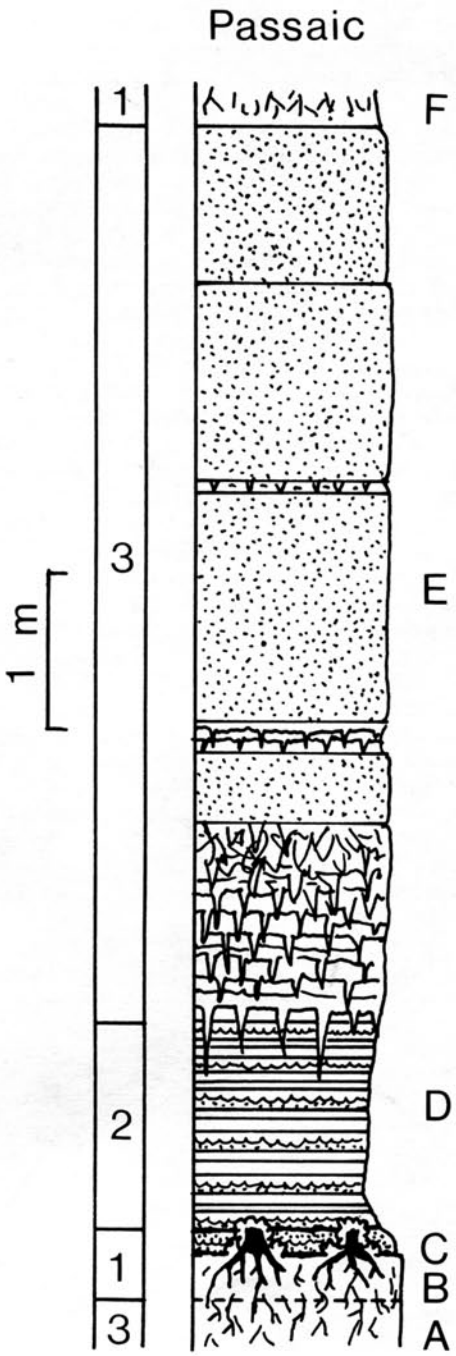

Figure 5.8: Measured section of one complete Van Houten cycle and two partial cycles within the Passaic Formation exposed at Stop 5.1. Key to section as follows: A, rooted, massive red mudstone of division 3 of lowermost cycle; B, rooted, massive gray mudstone of division 1 (transgressive unit) of middle cycle; C, öolitic sands encasing stromatolitic tufa-coated tree stumps; D, black and gray mudstone interbedded with burrowed oscillatory-rippled sandstone, with mudcrack density increasing upsection; E, red massive sandstone with minor massive, mudcracked mudstone; and F, rooted, red massive mudstone of division 1 of overlying cycle.

STOP 5.1: PASSAIC FORMATION, WEST POSTGROVE TOWNSHIP, PA (by P.E. Olsen)
Highlights: Compressional deformation.

This abandoned quarry exposes about 10 m of section (Figure 5.8) of parts of what appears to correlate with the Metlars Brook Member of the northern Newark basin in the axis of the Jacksonwald syncline (Figure 5.6). The upper portions of a red Van Houten cycle are exposed in a spectacular dip slope showing strong deformation of desiccation polygons (Figure 5.9). Lucas *et al.* (1988) have described the deformation patterns seen in the Jacksonwald syncline, all of which can be seen at this outcrop.

1) A shape lineation is marked by mudcrack polygons elongated sub-parallel to the axis of the Jacksonwald syncline, as first noted by Stringer and Lajtai (1979).

2) Spaced, axial planar cleavage marked by penetrative (at the outcrop scale), anastomosing fractures which weather to produce short "pencils" of siltstone.

3) *En echelon* calcite and quartz-filled vein systems cut all other structures and trend perpendicular to the fold axis.

According to Lucas *et al.* (1988), the solution cleavage is defined by dark, opaque phyllosilicate-rich seams usually 1 mm thick and 2 to 3 cm in length, terminating in feathery splays. The cleavage planes are vertical and apparently do not fan about the Jacksonwald syncline axis. Because of the

Figure 5.9: Deformed mudcrack polygons exposed on the dip-slope at Stop 5.1. The polygons can be circumscribed by ellipses, the long axes of which are parallel with the Jacksonwald syncline fold axis. Photo by P.E. Olsen.

constant orientation relative to the fold axis, Lucas *et al.* believe that the cleavage developed late in the structural history of the rocks but before the development of the quartz- and calcite-filled veins. Variations on this pattern of deformation are present at most outcrops in the Jacksonwald syncline (see Stops 5.2 and 5.3).

The red mudcracked massive mudstone forming the main dip slope surface is overlain by a gray massive mudstone with a well-developed rooted fabric superimposed on a breccia fabric massive mudstone (Figure 5.8). About 25 cm of oscillatory ripple-bedded öolitic sand follows. Small coalified tree stumps and roots project upward from the underlying rooted unit and are covered by stromatolitic tufa in the öolitic zone. The overlying black shale at the top of exposure consists of over 1 m of black and dark gray mudstone with pinch and swell laminae interbedded with centimeter-scale beds of oscillatory-rippled fine sandstone with burrows. Despite the proximity of the Rattlesnake Hill (Pottstown) diabase to the northwest, residual hydrocarbons stain most joints (L. Pratt, pers. comm, 1988).

Evidently, transgression of the lake which deposited the black shale drowned an area of low trees, probably conifers. Wave erosion exposed some of the roots. The trees died, and as they rotted they were coated with tufa, while öolitic sand accumulated around them. Finally, the water depth increased with consequent accumulation of the black shale.

Walk back to car and turn around, heading south on Manatawny Road.

49.5 Pass through intersection with PA 663.
49.6 Turn right on High Street (old PA 422) heading west and cross over Manatawny Creek.
52.3 Turn right (north) on Squirrel Hollow Road.
52.5 Exposures of gray and black Passaic Formation dipping 42° N mapped by Longwell and Wood (1965) as the same unit examined at Stop 5.1.
52.7 Squirrel Hollow Road ends and merges with with Rattlesnake Hill Road; proceed on latter.
53.1 Cross railroad tracks and park at office of Pottstown Trap Rock Quarry.

STOP 5.2: DOUGLASVILLE QUARRY OF POTTSTOWN TRAP ROCK COMPANY

(by P.E. Olsen and R.W. Schlische)

Highlights: Fracture cleavage in Passaic Formation hornfels and contact with Rattlesnake Hill (Pottstown) phacolith.

The quarry exposes about 100 m of pervasively fractured Passaic Formation hornfels and about 30 m of the base of the Rattlesnake Hill diabase pluton (often called the Pottstown pluton). The pluton is coarse-grained above the aphanitic to finely-crystalline basal chilled zone and is a high-titanium, quartz-normative diabase which here is an orthopyroxene cumulate with about 35% orthopyroxene, 25% clinopyroxene, and 45% plagioclase. The hornfels belong to the upper Passaic Formation, about 650 m above the black shale units of Stop 5.1. Highly-indurated strata of three strongly-altered Van Houten cycles are evident near the contact, and the underlying, less metamorphosed section consists of the dry portion of a 400,000 year cycle.

The dense fracturing at this locality is typical of the hornfels adjacent to the diabase bodies in this part of the Newark basin. Most systematic fractures in the hornfels strike northeast (Figure 5.10), and are thus parallel to the main set of joints and perpendicular to the cleavage at Stop 5.1. As exposed in the summer of 1988, the fracture system passes with full intensity into the fine-grained lower few meters of the diabase but dies out further up. Because of the apparent incompatibility of strain between the fractured and unfractured portions of the diabase, the lack of a fault between the two zones, and the close spatial relationship between the diabase, hornfels, and dense fracturing, the fracturing must have been synchronous with intrusion. The main mass of the diabase was unaffected by the fracturing because it may have been still molten during the fracturing process. Hydrofracturing due to massive fluid migration during intrusion seems a likely origin (Schlische and Olsen, 1988b). Under these conditions the fractures should have been oriented perpendicular to the regional extension direction. The quartz- and calcite-filled veins present at Stop 5.1 may be reactivated, less densely-spaced examples of the same syn-intrusion joint system present here.

A few blocks of hornfels seem to show elongated polygonal desiccation cracks similar to those at Stops 5.1 and 5.3. The dense fracturing clearly cuts the apparently ductilely deformed mud cracks. Thus, the ductile deformation preceded diabase intrusion. This needs to be tested by more extensive observations.

Return to cars and turn around, heading south on Rattlesnake Hill Road.

53.3 Turn left onto Squirrel Hollow Road.
53.9 Turn right onto High Street (old PA 422).
52.4 Hornfels at southern tip of Rattlesnake Hill pluton on right in back of stores on right.
54.8 Merge with new PA 422; continue west. Creek and tributary to north expose well-developed cyclic strata of Passaic Formation with at least one footprint-bearing horizon which has produced *Rhynchosauroides* sp.
55.2 Intersection with PA 662; continue west on PA 422.
55.9 Crossing over unnamed creek.
56.0 Turn right (north) on Parklane Road.
56.1 Turn right (east) onto Lake Drive.

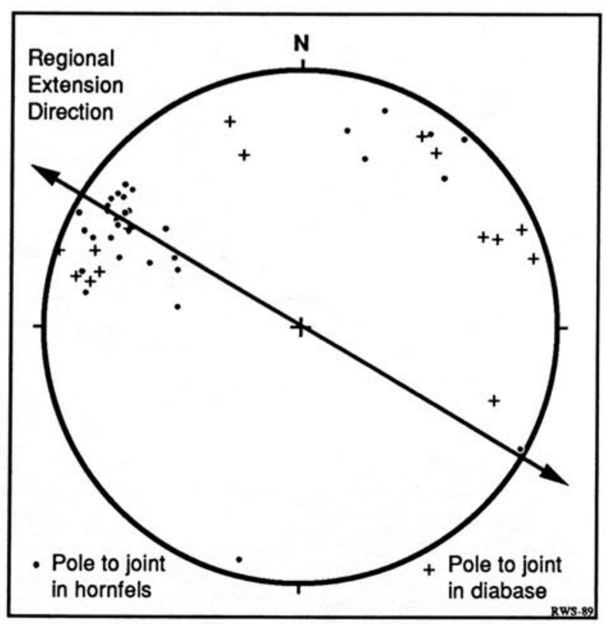

Figure 5.10: Poles to joints within the hornfels and diabase of the Pottstown Traprock Quarry, Stop 5.2. Most joints are oriented normal to the regional extension direction. Modified from Schlische and Olsen (1988b).

56.2 Cross creek and turn left into lot for recreation area and park. Walk east back over creek and turn right onto dirt path. Follow path about 500 m to intersection of creek and tributary.

STOP 5.3: DOUGLASVILLE FOOTPRINT QUARRIES (by P.E. Olsen)

Highlights: Cyclic Passaic Formation, penetrative deformation, and Triassic vertebrate footprints.

Extensive outcrops along the creek expose a >100-m-thick cyclic sequence of mostly fine-grained lacustrine clastics. Like Stop 5.1, these rocks are deformed with strong stretching parallel to the axis of the Jacksonwald syncline (Lucas *et al.*, 1988). The section is roughly 2.7 km above the Perkasie Member.

Stratigraphy and Evidence for Syndepositional Folding

The hierarchical pattern of Van Houten cycles is present in this section (Figure 5.11), with cycle modes at 8.5 m (the Van Houten cycle), 17.1 m (?obliquity cycle), and 51.2 m (eccentricity cycle). A cycle of 4.7 m is also suggested by the power spectrum; however, this is probably similar to the higher-frequency cycles present in the Cow Branch Formation of the Dan River basin and are probably non-periodic aggradational cycles (see Stop 2.1).

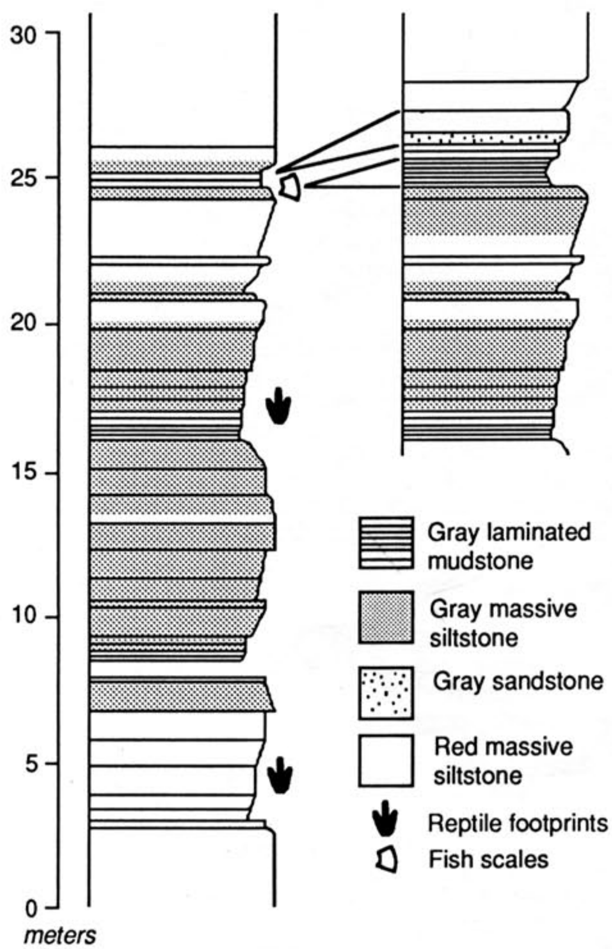

Figure 5.11: Measured sections of the Passaic Formation, Stop 5.3. The upper laminated mudstone of the section on the right is absent in the section located 300 m to the south. See text for discussion.

The top-most cycle shown in Figure 5.11 is unusual because it changes dramatically along strike over a relatively short distance. The well-developed black part of division 2 at the northern exposures is absent at the exposure about 300 m to the south. In addition, the southern exposure lacks the cross-bedded sandstone present to the north, and the gray portion of the massive mudstones below division 2 of this cycle thins from 2 m in the north to 50 cm at the southern exposures. Among other possible explanations, this change may reflect progressive onlap of units onto a gently tilted surface, or it may represent the local erosion of previously deposited beds during a period of tilting. In any case, we take the pinch out of units away from the axis of the Jacksonwald syncline as evidence of folding during Passaic Formation deposition. We have observed similar pinch-outs of units towards the south limb of the syncline in units slightly higher in the section. At the time of writing, however, we have not yet observed this pattern on the north limb of the syncline.

We predict that Fourier analysis of cyclic sequences in the Jacksonwald syncline will show a systematic pattern of Van Houten cycles thickening toward the axis of the fold along a transect parallel to the paleo-basin margin. Such thickening could be due to post-depositional structural thickening in the fold axis, or the thickening could be a consequence of a higher rate of accumulation in the axis because of folding during deposition, or both. In order to factor out the effects of structural thickening, bedding-perpendicular strain indicators (such as desiccation cracks) will be examined in the fold limbs for passive systematic rotation due to compression at an oblique angle to bedding.

Shallow Ductile Deformation

Dip-slope exposures of mudcracked massive mudstone show the same degree of fold-axis-parallel elongation as seen at Stop 5.1. The abundant reptile footprints found here show similar strain (Figure 5.12). There is a slight crenulation present and, a lineation is obvious on surfaces with rain drop impressions. Cleavage, however, is very poorly developed, and most very thin beds shown no hint of it. In fact, the rock shows no tendency to break along surfaces parallel to the axial plane of the syncline. We suspect that this indicates that the deformation was ductile and penetrative at the hand-sample scale. We predict that most detrital fragments will show little or no deformation in thin section. We hypothesize that this ductile deformation took place at shallow crustal levels prior to complete dewatering. The prominent joint system present at this site was imposed later, perhaps at the same time as the dense fracturing present at Stop 5.2 or later yet. Similar deformation patterns are present at most outcrops in the Jacksonwald syncline, whether or not cleavage is developed. We thus postulate that some of the shortening seen in the Jacksonwald syncline is not due to solution along cleavage planes late in the history of folding, but rather is ductile and early in origin.

As outlined by Schlische (above), this site provides evidence of syndepositional folding beginning as early as Passaic Formation deposition (Norian) and subsequent ductile deformation during relatively shallow burial. Diabase intrusion (earliest Jurassic) during continued folding followed, and this was followed by more folding and the development of axial planar cleavage by dissolution.

Footprints

A series of excavations for footprints (still underway at the time of writing) resulted in the uncovering of a very rich footprint assemblage from these beds; the footprints reflect the plastic deformation (Figure 5.12). The footprint quarries themselves were opened in a cluster of well-developed Van Houten cycles (Figure 5.11) exposed near the junction of the tributary and the main stream. Characteristic of these Van Houten cycles is the extensive development of thin-bedded, oscillatory-rippled siltstones and very fine-grained sandstones with claystone partings, and these tend to be the units with the most abundant footprints. Brecciation by desiccation cracks is not as intense in these units as elsewhere in the Passaic Formation.

The assemblage from these quarries is the youngest from the Triassic portions of the Newark Supergroup for which we have a large sample of well-preserved material, and the assemblage as a whole is very similar to those from older parts of the Newark basin section (Silvestri and Olsen, 1989). It bears directly on the rate of taxonomic turnover through the Triassic and hence on the rate of change across the Triassic-Jurassic boundary.

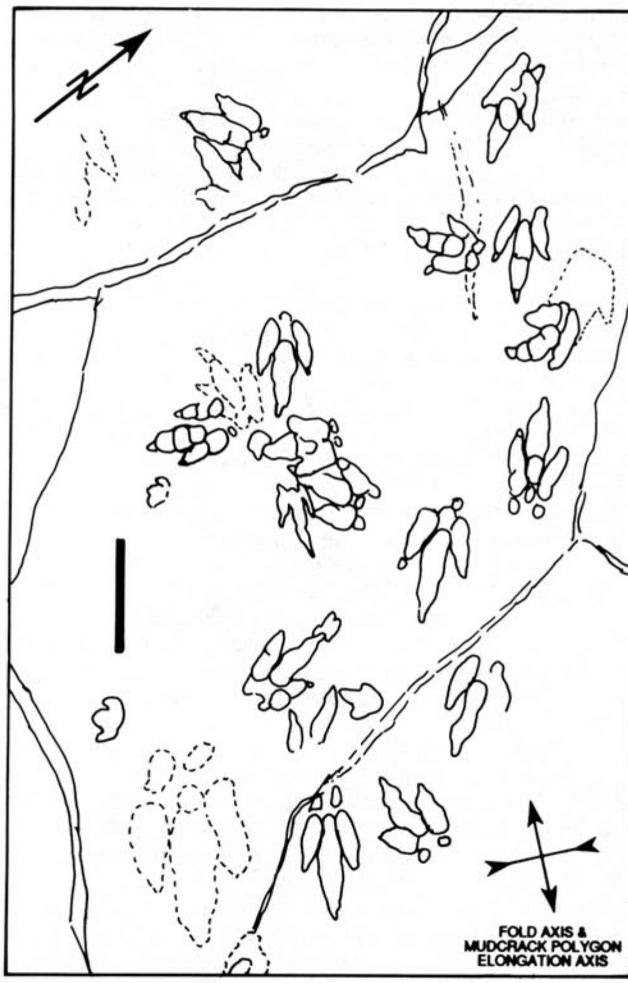

Figure 5.12: Deformed footprints at Stop 5.3. Note that the footprints have been shortened perpendicular to the fold axis of the Jacksonwald syncline and/or extended parallel with the axis. Scale is 10 cm. Slab on which drawing is based collected by SM. Silvestri.

Vertebrate Ichnological Succession in the Newark Supergroup

The until recently poorly-known Lockatong and Passaic formation footprint fauna are very rich compared with classic Jurassic assemblages of the Connecticut Valley type. Recent taxonomic revisions have whittled down the number of Early Jurassic valid ichnogenera from the 47 cited in Lull's (1953) compendia to 8 (Figure 4.9) (Olsen, 1980c, 1980d; Olsen and Galton, 1984; Olsen and Baird, in press; Olsen and Padian, 1986): *Grallator* spp., *Anomoepus* spp., *Batrachopus* spp., *Otozoum*, *Rhynchosauroides* sp. (Olsen, 1980c), *Ameghinichnus* sp. (Olsen, 1980c), and two uncertain but possibly valid forms, *Hyphepus* and *Gigantipus*. Two of these, *Rhynchosauroides* and *Ameghinichnus*, were until recently (Olsen, 1980c; Olsen and Galton, 1984), unknown in Connecticut Valley-type faunules. The number of ichnospecies is completely muddled; there could be as few as 10.

In contrast, Triassic footprint assemblages from the Lockatong and Passaic contain at least 10 ichnogenera collected from far fewer localities: *Procolophonichnium* (Baird, 1986b), *Gwyneddichnium* (Baird, 1986b), *Rhynchosauroides*, *Apatopus*, *Chirotherium*, *Brachychirotherium*, *Atreipus*, *Coelurosaurichnus*, *Grallator* (Figure 5.13), and equivalent beds in the Gettysburg basin have produced *Dicynodontipes*. There are several valid species of *Rhynchosauroides*, *Brachychirotherium*, *Coelurosaurichnus*, probably *Grallator*, and *Atreipus* making up at least 15 ichnospecies (Figure 5.13).

Even at this early stage of sampling, when footprint faunules are examined from the Lockatong through Passaic, there appears to be a marked increase in taxonomic diversity through the Late Triassic. This is punctuated by a dramatic drop in diversity at or closely below the palynologically-defined Triassic-Jurassic boundary in the uppermost Passaic Formation. Newark ichnological assemblages never recover their previous levels of diversity. Global compilations of osseous taxa show the same basic pattern around the Triassic-Jurassic boundary (Olsen and Sues, 1986; Olsen *et al.*, 1987) suggesting the possibility of a catastrophic extinction event.

The ichnotaxa recovered here (Silvestri and Olsen, 1989) show unambiguously no evidence for extinctions from the lower Lockatong Formation to the upper Passaic Formation, a thickness of 4.9 km. Translated into time, using the lacustrine cycle chronometer, this interval represents 14.7 million years.

	Return to cars, turn left and head east on Lake Drive.
56.5	Turn left onto Briarwood Road.
56.6	Turn right onto Nicholson Road.
56.8	Turn left onto PA 662 (Old Swede Road).
59.4	Amityville, PA.
60.3	Low exposures of coarse limestone conglomerate.
61.4	Turn right onto PA 562 (Oley Line Road) going east. Exposures along this road to west contain Cornet's (1977a) "Oley Line Road" localities which are the best documented palyniferous sections through the upper parts of the Passaic Formation.
62.1	Hills on left are composed of Cambrian Hardyston Quartzite and Precambrian gneiss.
66.9	Turn left into lot for West Motor Freight Inc.

STOP 5.4: BORDER FAULT AT BOYERTOWN, PA

(by P.E. Olsen and R.W. Schlische)

Highlights: Hanging and footwall outcrops of border fault; Cornwall-type mineralization.

An abandoned gravel pit and limestone quarry comprise the best existing exposures of a part of the Newark basin border fault system. Here both hanging wall and footwall rocks can be seen at the border fault and associated splays. This portion of the border fault is critical because it marks the transition from the dominantly low-angle (20°-35°), NE-SW striking faults to the northeast to the dominantly high-angle (60°-80°), E-W striking faults characterizing the narrow neck between the Newark and Gettysburg basins.

The fault zone shows the following characteristics:

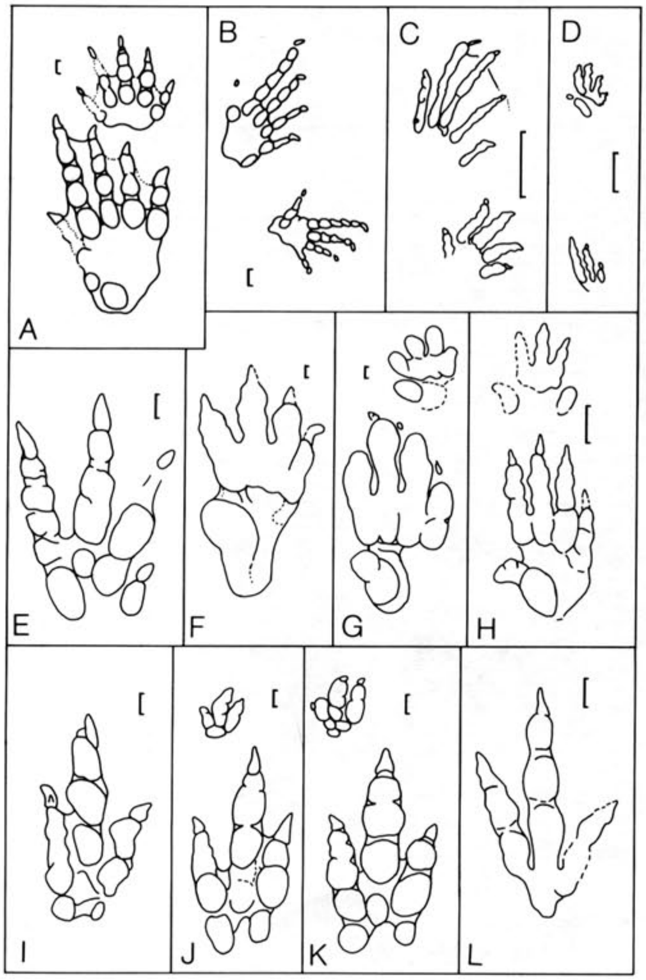

Figure 5.13: Late Triassic (Carnian-Norian) footprint types and their likely trackmakers, principally from strata of the Newark basin: A, *Apatopus lineatus* (phytosaur); B, *Rhynchosauroides hyperbates* (sphenodontid); C, *Gwyneddichnium majore* (tanystropheid Tanytrachelos); D, *Rhynchosauroides brunswickii* (?sphenodontid or lacertilian); E, *Coelurosaurichnus* sp.2 (?dinosaur); F, *Brachychirotherium eyermani* (?rauisuchid archosaur); G, *Brachychirotherium parvum* (?aetosaur archosaur); H, *Chirotherium lulli* (?rauisuchid archosaur); I, *Grallator* sp. (theropod dinosaur); J, *Atreipus sulcatus* (?ornithischian dinosaur); K, *Atreipus milfordensis* (?ornithischian dinosaur); L, *Coelurosaurichnus* sp.1 (?dinosaur). Scales are all 1 cm. From Olsen (1988b).

1. Footwall of the border fault fault consists of strongly-deformed Cambrian Leithsville Dolomite showing a cohesive, well-developed, intensely-folded brecciated foliation marked by slickensided calcite veins.
2. Steeply-dipping (70°-80°) fault with gouge between dolomite and Newark rocks.
3. Intensely-brecciated, slickensided, silty hornfels to metaconglomerate of Passaic Formation in hanging wall.
4. Subsidiary, steeply-dipping (70°-80°) faults with large phacoids and sub-horizontal slickensides in the hanging wall of the border fault.
5. Footwall dolomite as exposed in the old quarry is broken into many horses which appear to be in a series of oblique duplexes.

Evidence for reactivation of Paleozoic faults by Mesozoic structures is not obvious here, although the border fault in this area is clearly parallel to the nearby Paleozoic thrusts.

The Boyertown area was for a while among the most important late 18th and 19th century iron mining districts in Pennsylvania. The first operating blast furnace in Pennsylvania was constructed and operated by Thomas Rutter around 1720 in Boyertown, which was then called Colebrookdale Furnace after the English iron town of the same name. The mines were closed shortly before the turn of the century and have not been reopened. Relevant papers on the history of mining and the local geological relations are D'Invilliers (1883), Spencer (1908), Hotz (1953) and Hawkes *et al.* (1953).

The ore bodies are Cornwall-type (magnetite replacing carbonates adjacent to diabase bodies) and occur adjacent to the border fault in altered carbonates, apparently slivers of footwall rocks invaded by diabase. At the north end (Gabel Hill) of the diabase body coursing to the east of this stop is the subsurface Gabel-Warwick ore body. Hawkes *et al.* (1953) provided a cross section of this body which dips 35°SW. The main portion of the Gabel-Warwick ore body occurs at the contact between Passaic Formation metamorphosed conglomerate and diabase with fault slivers of early Paleozoic Leithsville Dolomite?, some of which are over 30 m thick. These relations suggest that the diabase invaded the border fault zone much as Ratcliffe (1980, 1988) described for parts of the northern Newark basin.

Return to cars and turn right onto PA 562 East.

67.1 Entering Boyertown, Pennsylvania.

68.3 End PA 562, turn right onto PA 73 East.

69.1 Cross PA 100.

69.2 Sweinhart Road on right. Excavation at end of road revealed several Van Houten cycles (gray shales and conglomerate) with reptile footprints (*Atreipus sp.* and *Rhynchosauroides* sp.) as well as a small fault.

70.4 Take left turn, staying on PA 73 East.

70.8 Crossing position of axis of New Hanover syncline.

71.5 Intersection with PA 663 South.

71.6 Turn left onto PA 663 North. About 4 km to the southeast are excellent outcrops in the bed of Swamp Creek that extend across several hundred meters of the middle to upper Passaic Formation. These outcrops show the typical hierarchy of Van Houten and compound cycles in this part of the Passaic Formation better than any other exposures of this part of the formation because of the great length of the section. Fourier analysis of depth ranks reveals prominent peaks with the typical Milankovitch-type ratios as seen at Stops 2.1 and 5.7.

73.7 "Fingers" of west dipping diabase.

74.4 Crest of Sassamansville anticline. Site of Parestis # 1 drilled by North Central Oil in winter of 1987-1988 to a total depth of about 3.2 km.

74.8 Diabase sill dipping to east.

75.6 Passaic Formation hornfels dipping to east.

79.4 Pennsburg, PA, center; intersection with PA 29. Continue straight on PA 663 North.

81.2 Crest of anticline. Exposures on left have produced indeterminate fish scales, conchostracans, phytosaur teeth indistinguishable from *Rutiodon* sp., and disarticulated bones of what appears to be *Tanytrachelos*. The fish and conchostracans occur in a greenish siltstone, whereas the reptile bones occur in an algal tufa conglomerate, a very common lithology for disarticulated tetrapod material throughout the Newark Supergroup. This appears to be the youngest occurrence of *Tanytrachelos*.

82.3 Road cut exposing east-dipping lacustrine Passaic Formation hornfels and a discordant contact with a diabase sill. The contact is faulted, which is common for sills and sheets and is a consequence of the mechanics of intrusion (Pollard, 1973). Site has produced conchostracans and shows mineralization of hornfels with sulfides and possibly hornblende (A.J. Froelich, pers. comm.).

About 5.3 km to the west the partial skeleton of the phytosaur *Clepsysaurus pennsylvanicus* was found by Issac Lea along Hosensack Creek (Lea, 1851). This occurrence, probably near the Ukrainian Member of the upper Passaic, is certainly one of the youngest osseus record of phytosaurs in the Newark basin and the Newark Supergroup.

83.6 East-dipping thick red and thin gray beds of Passaic Formation.

84.7 Crossing northeast extension for Pennsylvania Turnpike. Large road cut on turnpike to north is in hornfels of the upper Passaic Formation between two limbs of a diabase sheet. The hornfels sequence is highly cyclic and must represent a relatively major black and gray sequence high in the Passaic Formation.

87.8 Quakertown, PA. Turn right onto PA 309 South.

89.8 Crossing upper mapped contact with Quakertown sheet.

90.2 Crossing lower mapped contact with Quakertown sheet.

93.5 Exit right for PA 563—Perkasie.

93.7 Turn right.

93.8 Turn right onto PA 563 North.

94.0 Crossing over PA 309. From here until Stop 5.5, the field trip route follows crest of ridge made by the Perkasie Member of the Passaic Formation, the most extensively mapped gray and black sequence in the Newark Supergroup (Figure 5.1).

95.2 Perkasie, PA. Crossing over railroad tunnel which exposes both the type section of the Perkasie Member itself at the south portal and another series of black and gray Van Houten cycles (informally called "post-Perkasie member").

98.8 Intersection with PA 313; PA 563 turns left (North) here. Proceed straight onto South Park Road.

105.0 1.5 km to north are spectacular exposures of unit O of Perkasie Member in spillway for Noximixon Reservoir.

105.3 Crossing Tinicum Creek.

106.4 Turn left on PA 611 North. About 300 m south of this intersection along PA 611 are outcrops of lower parts of the Perkasie Member (unit N). McIntosh *et al.* (1985) reported the transition from a lower, normally-magnetized interval and an upper, reversed interval at this outcrop.

107.5 Turn right onto Quarry Road.

107.8 Turn right into lot for Buck County Crushed Stone Quarry. Walk west into quarry.

STOP 5.5: BUCKS COUNTY CRUSHED STONE QUARRY, HARROW, PA (by P.E. Olsen)

Highlights: Cyclic Perkasie Member of the Passaic Fm.

Quarry on west side of Rapp Brook exposes unit O of Perkasie Member (Figure 5.14). Compared to the exposures at Milford (Stop 5.6), a much finer-grained facies of the Passaic is present here with extensive development of massive mudstones. At the far east side of the quarry and along Rapp Brook, the lower red beds between units N and O are exposed.

Two prominent black siltstone-bearing cycles are exposed within the quarry. Division 2 of these cycles shows intense bioturbation, pinch-and-swell lamination, and thin graded silt beds which are probably distal turbidites. Division 1 of the lower cycle bears poorly-preserved dinosaur footprints. Other than the bioturbation and the tracks, no fossils have been found at these outcrops and this is typical of the finer-grained intervals of the Passaic Formation. Fossils of all forms are much more common in the coarser-grained facies of the Passaic.

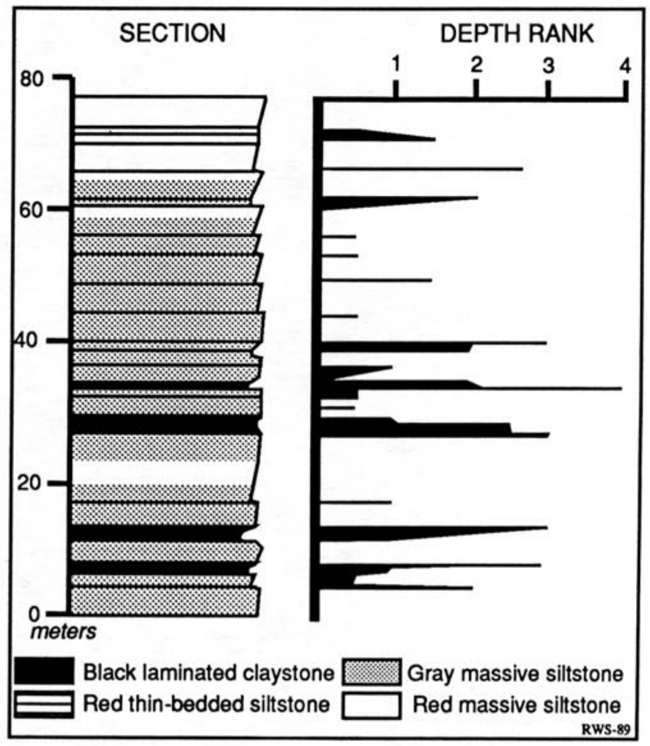

Figure 5.14: Measured section and depth ranks of the Perkasie Member of the Passaic Formation exposed at Stop 5.5. Modified from Olsen (1986).

The trend towards more abundant fossils in coarser facies, we reason, is related to a higher variance in sedimentation rates at the margins of the basin compared to the center, which results in a higher preservation potential in the marginal facies. In the Lockatong and Passaic formations in the more central parts of the basin, most sedimentation was by suspension, and the range in sedimentation rates was probably relatively restricted. There was ample time for destruction by biological and chemical means of most organic and osseus material, and even ichnofossils. In contrast, at the basin margins, even suspension deposition was probably much more variable, and other forms of deposition with much higher short term rates of sedimentation were dominant. Biological remains might thus have been buried and protected more often and more quickly, even though the frequency of sedimentation events might be lower on the basin margins than in the center. A contributing effect, especially to the poor preservation of pollen and spores in the more central areas, might be the presence of corrosive interstitial alkali fluids, whereas the pore fluids near the basin margins might be buffered by spring water. We consider it less likely that the lack of fossils in the central basin facies reflects a lack of organisms.

Stratigraphy of the Perkasie Member

The Perkasie Member consists of strata that exhibit Van Houten cycles and compound cycles showing the same pattern as the Lockatong (Olsen, 1988a; Olsen and Baird, in press). It consists of two sequential 100,000 year cycles, each containing two well-developed Van Houten cycles and one weakly developed red and purple Van Houten cycle, succeeded upwards by red clastics (Figure 5.14). McLaughlin named the lower set of gray beds member N and the upper set member O. Most, if not all, of the classic fossil material described by Eyerman (1886), Bock (1952), and Baird (1957) apparently came from division 3 of the second gray and black Van Houten cycle of member O at a locality near Stop 5.6 (Olsen and Flynn, 1989).

Once thought to be the youngest strata in the basin, it is now clear that the Perkasie Member actually lies in the lower Passaic Formation far below the top of the formation. All of the overlying strata have been eroded in this area. Correlation of the strata in the Milford area with that in other fault blocks of the Newark basin where these younger beds are still preserved is afforded by magnetostratigraphy, lithological matching, and a palynological correlation web (Olsen, 1988a).

Fourier analysis (Figure 5.15) of depth ranks as described for Stops 2.2 and 4.1 shows the usual strong hierarchical pattern of cycles. Thus at this outcrop, the interval between the two black shales low in the section would correspond to a 21,000 year precession cycle.

Return to Quarry Road and turn left.
108.2 Turn right on PA 611 North.
109.7 About 1.6 km southeast is site of a 4000-m-deep hydrocarbon test well drilled in 1985. Proprietary drill hole records show that individual Van Houten cycles as well as the compound cycles present in outcrops to south east can be traced at least to this area across most of the basin and thus represent basin-wide events. This new bore hole is close to the position of the Revere well drilled in 1891 to a depth of 635 m (McLaughlin, 1943). Stay on PA 611.
111.7 Ferndale, Pennsylvania.
112.4 Type specimen of *Rhynchosauroides (Kinternia) brunswickii* (Ryan and Willard, 1947) found in cut on right side of road.
113.5 Kintersville, PA, exposures of Passaic members L and M in local streams.
113.7 Junction with PA 32. Veer right on PA 32 going south.
114.8 Cliffs of lower Passaic Formation (between Perkasie Member and members and L and M).
117.5 Extensive exposures visible from here on east bank of river, along Spring Glen Road [described in Stop 5.6, Van Houten (1969, 1980), and Manspeizer and Olsen (1981)].
118.2 Upper Black Eddy, PA. Turn left onto Bridge Street over Delaware River.

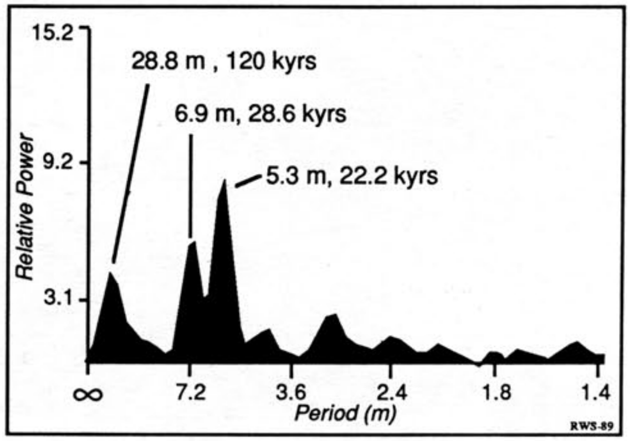

Figure 5.15: Power spectrum of depth rank curve from Figure 5.14, Stop 5.5. Modified from Olsen (1986).

118.3 Crossing Delaware River, entering Milford, Hunterdon County, New Jersey.
118.4 Left onto Church Street.
118.5 Left on Church Street.
118.6 Right onto Spring Glen Road. (Hunterdon Co. 627). *THIS ROAD IS VERY NARROW AND HAZARDOUS; BEWARE OF ONCOMING VEHICLES.*
118.9 Culvert on right and adjacent exposure of Passaic Formation member M. Gray shale at base of division 2 of Van Houten cycle at this outcrop has produced disarticulated *Semionotus* and *Cyzicus*.
119.3 First of eight small faults downthrow to the east. Cumulative throw exceeds 500 m.
119.8 Cyclical mudstone beds of Passaic Formation below members L and M.

Cycles are obvious at several scales. Picard and High (1963) reported that this exposure shows an alternation of massive ledge-forming units of poorly-sorted siltstone with less resistant, finer-grained units, with the couplets ranging from 1.1 to 4.8 m and averaging 2.6 m thick. Most units show intense bioturbation and common desiccation cracks merging into breccia fabrics. The thinner of these alternations seem to us to be grouped into larger cycles averaging 5 to 7 m thick. We hypothesize that these larger cycles are probably homologous to the Van Houten cycles in the more arid portions of the 400,000 year cycles as seen at Stop 5.7, whereas the shorter alternations correspond to the "aggradational cycles" also seen in the Lockatong. This hypothesis needs testing by careful measurement of this section combined with Fourier analysis. This section is also described by Van Houten (1969, Stop 5).

120.2 Park in dirt area off road to right at milepost 37 (adjacent to tracks).

STOP 5.6: PEBBLE BLUFF, NEAR MILFORD, NJ

(by P.E. Olsen and J.P. Smoot)

Highlights: Interbedded conglomerates and lacustrine strata at border fault basin margin.

These outcrops [also described by Van Houten (1969, Stop 6; 1980, Stop 1) and Arguden and Rodolpho (1987) and Olsen, Van Houten, *et al.* (1988)] consist of thick sequences (>20 m) of red conglomerate and sandstones alternating with cyclical black, gray, and red mudstone and sandstone. Dips average 10-15° NW, and there several faults, downthrowing to the east, between the largest outcrops. The thickest gray beds (see Figure 5.16) appear to be the Perkasie Member.

Conglomerates at Pebble Bluffs occur in three basic styles. 1) Poorly-bedded boulder-cobble conglomerate with pebbly sandstone interbeds. Matrix rich conglomerates are in places matrix-supported. These appear to define lenses that are convex-upward and bounded by the largest clasts at their edges and tops. These lenses appear to be debris flow lobes, in which some of the matrix may have been partially washed out by rain during periods of non-deposition. If correctly identified, the flow lenses are typically less than 30 cm thick and less than 5 m wide, similar to debris flows formed on mid to lower portions of steep fans. Pebbly sandstone and muddy sandstone include "trains" of isolated cobbles often oriented vertically. These cobble trains represent thin, low viscosity debris flows that are stripped of their matrix by shallow flash-flood streams. The sandstones appear to be broad, shallow stream deposits that may include hyperconcentrated flow as indicated by flat layering defined by the orientation of granules.

2) Well-defined lenticular beds of pebble-cobble conglomerate separated by pebbly muddy sandstones with abundant root structures. The conglomerate beds are channel-form with abundant imbrication. Some internal coarsening and fining sequences are consistent with longitudinal bars (Bluck, 1982). Finer grained deposits resemble less-incised channels and overbank deposits. There are some hints of thin debris flow sheets. Abundant root structures filled with nodular carbonate (caliche?) suggest soil development.

3) Grain-supported cobble-pebble conglomerate with sandy matrix. Granules and coarse sand show high degree of sorting suggesting wave reworking of finer fractions (LeTourneau and Smoot, 1985; Smoot and LeTourneau, 1989). These are associated with gray and black shales and oscillatory-rippled sandstones in Van Houten cycles (Figure 5.16). No unequivocal bar-form structures or imbricate ridges have been observed.

Laterally-continuous black and gray siltstones and claystones within division 2 of Van Houten cycles (Figure 5.16) contain pinch-and-swell laminae, abundant burrows, and rare conchostracans. These are definitely lacustrine deposits, almost certainly marginal to the finer-grained facies more centrally located in the basin. These lacustrine sequences mark transgressions of perennial lakes over the toes of alluvial fans, much as LeTourneau and Smoot (1985) and LeTourneau (1985a) described in marginal facies of the Portland Formation in the Hartford basin of Connecticut. Division 2 of cycles comprising the Perkasie Member were produced by lakes which were almost certainly shallower than those which produced the microlaminated, whole fish- and reptile-bearing units in other parts of the Newark basin section. They evidently were deep enough, however, to transgress over at least the relief caused by the toes of alluvial fans. To what degree have more subtle transgressions of shallower lakes modified clastic fabrics elsewhere in this section?

The restriction of the conglomerate facies to the vicinity of the border fault and the association of debris flow and shallow stream deposits is consistent with an alluvial fan model (*i.e.*, Nilson, 1982). Channel-form conglomerates suggest flash-flooding streams that are still consistent alluvial fans; but the abundance of interbedded fine sandstone suggest lower slopes than for the debris flow deposits. All of the deposits resemble distal low-slope fans or in the case of the coarse debris flow conglomerates, more distal parts of steep fans. Intercalation of lacustrine shales would appear to demand low slops. Coarsening up sequences of wave-formed deposits suggest intermittent introduction of material in receding lakes. This is probably a climatic as opposed to tectonic response because the shallowing is recognized basin-wide. Therefore, even the coarsest deposits accumulated on relatively low slopes. The requirement of low slopes means the present basin fault does not necessarily mark the apex and more likely the fans extended several miles beyond the present basin boundary (Smoot *et al.*, in press). The fans could have extended away from the present basin as thin veneers on pediment surfaces on basement, with fan material being continuously recycled basinward. This is consistent with the observations of a number of workers (Van Houten, pers. comm.; Manspeizer, pers. comm.) who noted that many of the clasts in the debris flow and poorly-sorted stream deposits are relatively well-rounded and mixed with highly-angular clasts.

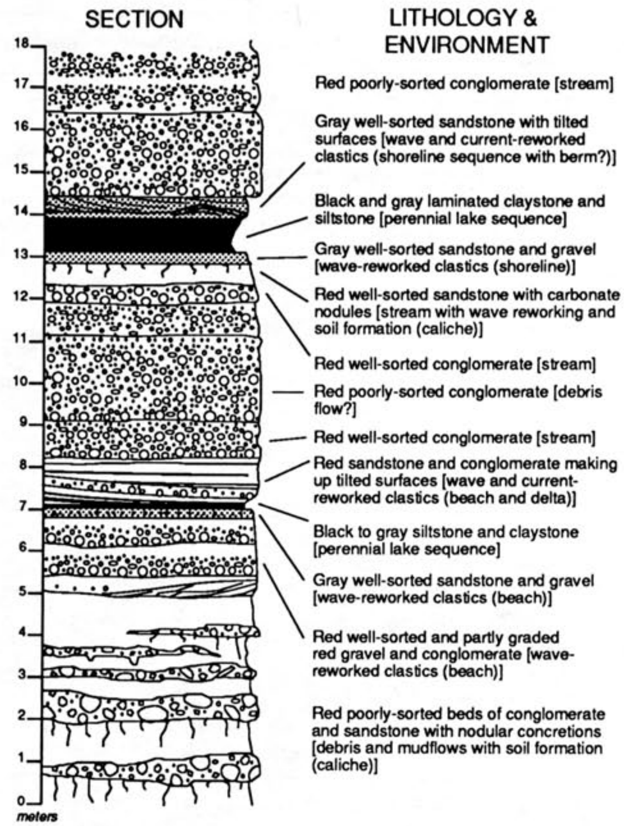

Figure 5.16: Measured section of the Passaic Formation at Pebble Bluff, Stop 5.6, showing the interfingering of debris flow, shoreline, and perennial lake deposits. Modified from Olsen, Van Houten, *et al.* (1988).

Individual Van Houten cycles of the Perkasie Member in this area average 7 m thick, as compared with a mean of 6.5 m for the same cycles at the Bucks County Crushed Stone Quarry (Stop 5.5). The thickness of the 100,000 year cycles increase as well from 20.3 m at Stop 5.5 m to 28.1 m in this area. At New Brunswick, New Jersey, near the east side of the basin, the cycles are a mean of 4.4 m. This thickening towards the border fault is typical of most of the Newark Supergroup and dramatically illustrates the asymmetrical character of the half-graben. The trend to greater fossil richness is evident at this outcrop as is typical for more marginal facies of the Passaic Formation. The conchostracans present in the upper parts of division 2 in the upper black shale cycle in member O are absent in the more basinward exposures.

The black siltstones of division 2 in this area are thicker than in more basinward outcrops and contain numerous graded siltstone layers 0.1-1.0 cm thick, all punctured by abundant tubes (burrows and roots). Organic carbon content exceeds 5%, and fresh rock has a strong odor of hydrocarbons. Based on pyrolysis studies, these rocks are apparently still in the oil window (L. Pratt, pers. comm.)

The border fault is less than 2.4 km to the northwest of this series of outcrops. As mapped by Ratcliffe (1986) on the basis of surface geology, drill cores, and a Vibroseis profile, the border fault in this area is a reactivated imbricate thrust fault zone dipping 32°SE. Core and field data reveal Paleozoic mylonitic fabrics of ductile thrust faults in Precambrian gneiss and early Paleozoic dolostone overprinted by brittle cataclastic zones of Mesozoic normal faults which form the border fault system of this part of the Newark basin. According to Ratcliffe *et al.* (1986, p. 770), "Field evidence indicates reactivation of the imbricate thrust faults in an extensional mode, a dominant extension direction being S40° to S50°E. These data suggest strongly (1) that reactivation of Paleozoic thrusts controlled the formation of the border fault in eastern Pennsylvania and (2) that fault patterns may have formed by passive response to extension rather than by active wrench fault tectonics as proposed by Manspeizer (1980)".

A series of very gentle but rather complex folds are present in this area close to the border fault (Figure 5.17). On the New Jersey side of the Delaware River their axes are parallel to the fault but at high angles with the border fault on the Pennsylvania side of the river. What might this transition have to do, if anything, with the origin of folds in the basin? The fault-parallel folds may be drag folds, whereas the fault-perpendicular folds are fault-displacement folds; complexity is introduced when these two styles interfere with one another.

Turn around and head back east along Spring Glen Road.
121.7 Turn left on Church Street.
121.8 Turn right on Church Street.
121.9 Turn left on Bridge Street.
122.0 Intersection with Water Street (Hunterdon Co. 515) at traffic light.
About 1.3 km to the north are several good exposures of the richly-fossiliferous Perkasie Member and adjacent beds (see Olsen and Flynn, 1989)
128.5 Small quarry on right in Passaic Formation. Much burrowing by *Scoyenia* and some very poorly preserved footprints are present (aff. *Brachychirotherium*). Outcrop described by Van Houten (1980, Stop 3).
129.7 Turn left onto 8th Street, Frenchtown, NJ.
129.8 Turn right onto Milford Road and head south.
130.1 Merge right onto Race Street.
130.2 Intersection with NJ12, go straight and follow road around to right onto Bridge Street.
Excellent outcrops to northeast along Nishisackawick and Little Nishisackawick creeks are of coarse-grained facies of Graters Member (members G and H), members E and F, and member D of the Passaic Formation. Stratigraphy and abundant fossils from these exposures are described in Olsen and Baird (1985) and Olsen and Flynn (1989).
130.3 Turn left onto NJ 29 and head south.

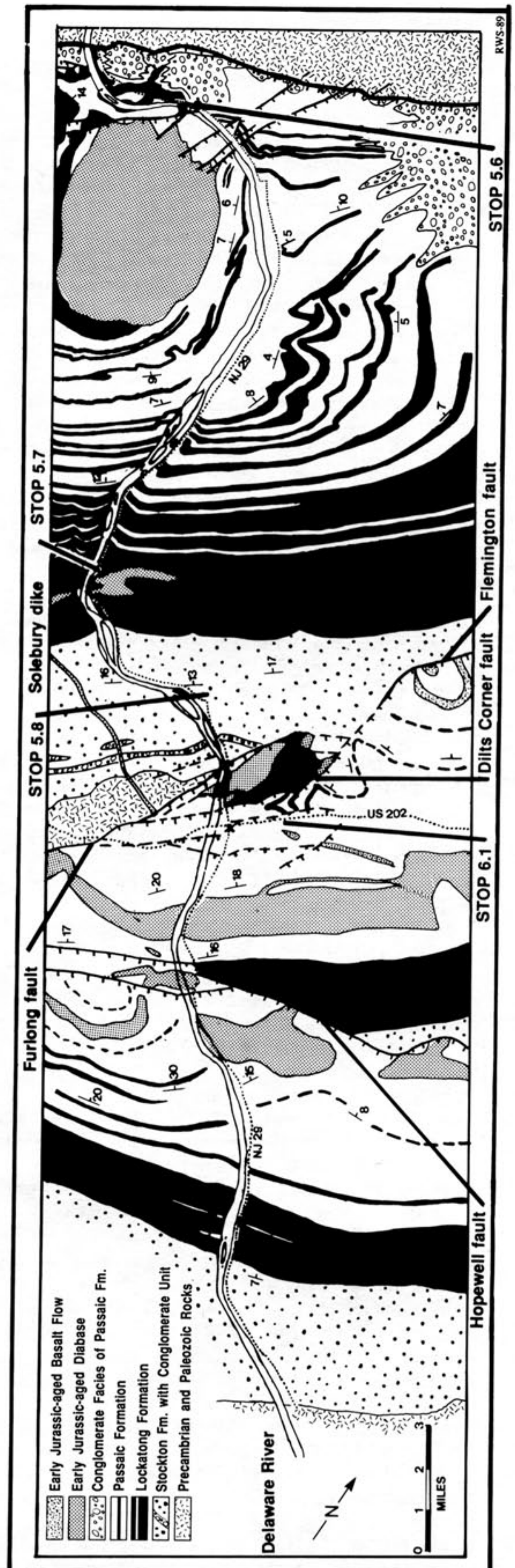

Figure 5.17: Geologic map of the Delaware River region (see Figure 5.1 for location). Modified from Olsen, Van Houten, *et al.* (1988) and Ratcliffe and Burton (1988).

130.4 Crossing Copper Creek, with exposures of red beds above the Graters Member.

130.8 Members G and H of Mclaughlin are poorly exposed in hills on left.

133.7 Excellent exposures of members E and F in creek to left.

130.3 Crossing Warford Creek. Extensive outcrops of a single Van Houten cycle in the lower part of Member D of the Passaic Formation extend for over 0.8 km upstream (Olsen, Van Houten, *et al.*, 1988, Stop 5). The lower part of division 2 of this cycle is microlaminated and contains articulated and disarticulated *Semionotus* cf. *braunii* and *Paleolimnadia*-type clam shrimp. Division 3 contains *Scoyenia*, abundant tool marks, and possibly poor *Rhynchosauroides*. This same cycle crops out ~4.8 km to northeast along the east branch of Nishisackawick Creek where it contains fish, although they are disarticulated (Olsen, 1988a). Although mapping is as yet incomplete, member D evidently is traceable to Linfield, Pennsylvania, near the Limerick nuclear power plant. At a small exposure along Longview Road the lower part of division 2 of the same cycle exposed along Warford Creek consists of black siltstone with well-developed oscillatory ripples. Articulated and disarticulated *Semionotus* cf. *braunii* are common in calcareous nodules in the black claystone laminae. Oscillatory ripples adjacent to the fish are also carbonate cemented and much less compacted than other ripples showing the nodules to be of early diagenetic origin.

134.5 Large exposures of upper red beds of member C of Passaic Formation showing continuation of pattern of Van Houten cycles expressed as variations in red mudstone fabric resembling the red mudstone cycles described in detail at Stops 4.1 and 5.7. *Rhynchosauroides* cf. *brunswickii* occurs in some of the red, thin-bedded mudstones of division 2 of these cycles.

135.0 Exposures of gray and red Van Houten cycles of McLaughlin's member C. Section described by Van Houten (1969, Stop 4; 1980, Stop 4).

135.3 Upper red beds of Walls Island Member (member B plus High Rocks member of McLaughlin *in* Willard *et al.*, 1959). These red beds have usually been considered the basal beds of the Passaic Formation even though they are mineralogically more similar to the Lockatong (Van Houten, 1969). They are regarded here as the uppermost beds of the Lockatong.

135.7 Tumble Falls Road. Stream on right exposes most of the Tumble Falls Member of the upper Lockatong Formation, the upper red parts of which correspond to McLaughlin's member B. Minor transgressive interval in middle of division 3 of a gray Van Houten cycle exposed in stream at road level contains abundant and well-preserved *Rhynchosauroides* sp. tracks.

135.9 Red and gray Van Houten cycles comprising the upper parts of the Smith Corner Member.

136.0 Ravine on left exposes lower parts of Smith Corner Member with well-developed black and gray Van Houten cycles. The lowest outcrop produces *Cyzicus* and indeterminate fish scraps.

136.3 Old Busik Quarry on left is in the upper part of Prahls Island Member (McLaughlin's "Triple Red") of the Lockatong Formation. Section in quarry has been described by Van Houten (1969, Stop 3).

136.5 Upper red portions of Tohicken Member of Lockatong Formation.

136.7 Begin 410 m of almost continuous section of middle Lockatong Formation. Ravine on left exposes upper 100 m of section; the rest is exposed along the road and in an old abandoned quarry.

137.8 50 mph sign on right, falling rock sign facing south on left. Pull over and park. Walk north along east side of road.

STOP 5.7: MIDDLE LOCKATONG FORMATION AT BYRAM, NJ (by P.E. Olsen)

Highlights: Classic field locality of cyclic Lockatong lacustrine strata.

Exposed along the east side NJ 29 and along the ravine at its north end are more than 400 m of middle Lockatong Formation (Figure 5.18). These are the exposures on which Van Houten based most of his original interpretations and the exposures most often seen by visiting geologists. About 99% (405 m) of this section consists of fine calcareous mudstone and claystone with the remaining 1% (5 m) consisting of very fine sandstone. These exposures include the North Wales, Byram, Skunk Hollow, and Tohicken members. McLaughlin's (1944) "First Thin Red" makes up the upper part of the Skunk Hollow Member and the "First Thick Red" makes up the upper part of the Tohicken Member.

Because of its fine-grained nature, fossils are very rare in this section, with only two cycles producing vertebrates to our knowledge. Unfortunately, this is the section most often examined by visiting paleontologists and it is, at least in part, responsible for the undeserved opinion that the Newark Supergroup is poorly fossiliferous.

Fourier analysis of this depth-ranked section (Figure 5.19) and calibration by varve-based sedimentation rates and radiometric time scales show the main thickness and time periodicities typical of both the Lockatong and Passaic formations in this part of the basin.

In order to illustrate the wide range of variation exhibited by these cycles, we will compare two end-members of the range of sequences of sedimentary fabrics present in this section (Figure 5.20). These two end-members correspond, in part, to Van Houten's (1962, 1964, 1969) detrital and chemical short cycles. Figure 5.20a shows a single Van Houten cycle (a in Figure 5.18) in the lower part of the Skunk Hollow Member. This is the most fossiliferous cycle exposed in this outcrop. Division 1 is a thin sand overlain by thin-bedded mudstone with an upward increase in total organic carbon (T.O.C.). This represents the beginning of lake transgression over the mostly dry playa flat of the preceding cycle and this is followed by deposition under increasing water depth.

Following the pattern seen at Stop 2.2 in the Cow Branch Formation of the Dan River basin, the transition into division 2 is abrupt and is marked by the development of microlaminated calcareous claystone consisting of carbonate-rich and carbonate-poor couplets an average of 0.24 mm thick. The basal few couplets of this interval contain articulated skeletons of the aquatic reptile *Tanytrachelos*, infrequent clam shrimp, and articulated fossil fish (*Turseodus* and ?*Synorichthys*). Abundant conchostracans occur in the middle portions of the unit. In its upper part, the microlaminae are very discontinuous, perhaps due to microbioturbation. No longer microlaminated, the succeeding portions of division 2 become less organic carbon-rich and less calcareous upward, and there is an upward increase in pinch and swell lamination. Deep, widely-spaced, sinuous desiccation cracks propagate down from the overlying unit. The average T.O.C. of division 2 (83 cm thick) of this cycle is 2.5%, a rather common value for black siltstones and limestones of the Lockatong. Studies of similar microlaminated units in other parts of the Lockatong suggest deposition in water in excess of 100 m deep, below wave base, and in perennially anoxic water (Manspeizer and Olsen, 1981; Olsen, 1984a).

Division 3 is characterized by an overall upward increase in the frequency and density of desiccation-cracked beds and a decrease in thin bedding. Reptile footprints (?*Apatopus*) are found near the middle of the sequence (Figure 5.21). T.O.C. decreases through division 3 and is low (1.3%-0.5%). This interval shows the greatest evidence of subaerial exposure in the cycle and represents the low stand of the lake. However, as evidenced by the relative rarity of desiccation-cracked intervals and the generally wide spacing of the cracks themselves, submergence was much more frequent than emergence during deposition.

Figure 5.20b shows a Van Houten cycle in McLaughlin's "First Thin Red" (b in Figure 5.18) about 55 m above the cycle shown in Figure 5.20a. This cycle contrasts dramatically with the Upper Skunk Hollow Fish Bed in consisting of 75% red massive mudstone and completely lacking a black organic carbon-rich division 2. Division 3 of the previous cycle (also mostly red) consists of red, massive, almost homogeneous-appearing mudstone with a faint but highly vesicular crumb fabric, which according to Smoot and Olsen (1985) formed by repeated desiccation of slowly aggrading mud in a playa lake, with the vesicular fabric representing air bubbles trapped in sediments during floods and hardened by desiccation. The vesicles do not seem to be related to an evaporitic texture.

The overlying massive mudstone of division 1 is gray and contains a better-developed crumb fabric. This unit was probably deposited under much the same conditions as the unit underlying it. Its iron was reduced, however, by the interstitial waters from the lake which deposited the overlying gray unit. The transition from an aggrading playa to a short-lived perennial lake is marked by an upward increase in lamination, a disappearance of the crumb fabric and a decrease in the density of desiccation cracks.

Division 2 of this cycle consists of red and green laminated to thin-bedded claystone lacking desiccation cracks. This is the lake's high stand deposit of this cycle and is most comparable to the fabric seen in the lower part of division 3 of the cycle shown in Figure 5.20a.

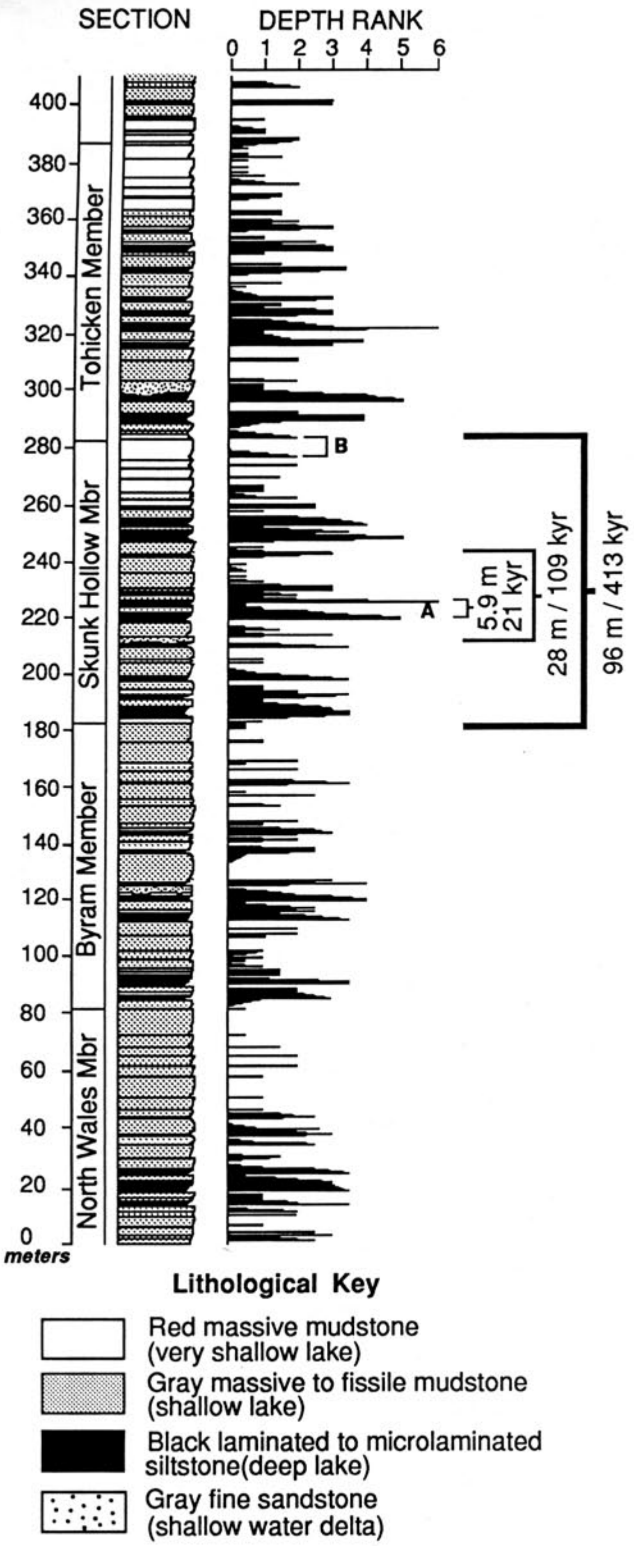

Figure 5.18: Measured section and depth rank curve of the middle Lockatong Formation at Byram, NJ, Stop 5.7. Cycles designated A and B are detailed in Figure 5.20. Modified from Olsen (1986).

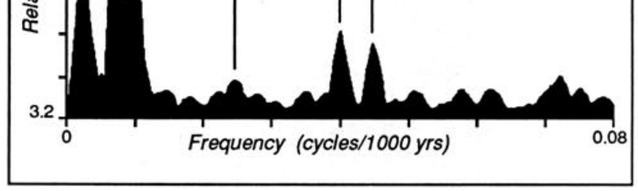

Figure 5.19: Power spectrum of the depth rank curve of the Byram section of Figure 5.18. The varve-calibrated sedimentation rate is .24 mm/yr. Modified from Olsen (1986).

Division 3 consists of massive mudstone (argillite) sequences consisting of a basal green-gray mudstone grading into a very well-developed breccia fabric (Smoot and Olsen, 1985) and then upwards into a well-developed crumb fabric. Breccia fabrics consist of densely-spaced anastomosing cracks separating non-rotated lumps of mudstone showing some remnant internal lamination. They are very common in the Lockatong Formation and are directly comparable to fabrics produced by short periods of aggradation separated by longer periods of desiccation and non-deposition (Smoot and Katz, 1982). The breccia fabric passes upward into a well-developed vesicular crumb fabric. The transition into the overlying similar sequence is abrupt. These thin sequences, several of which here make up division 3 of a Van Houten cycle, are very common in the fine-grained facies of the Newark Supergroup.

The upper half of these thin sequences are cut by dish-shaped, concave-upward clay-lined surfaces with radial slickensides. These "dish structures" were described by Van Houten (1964, 1969) and interpreted as a possible gilgai-type soil feature (Van Houten, 1980). A mechanical analysis of these structures suggests they are coulomb fractures produced in relatively rigid, but not lithified, mud by more or less isotropic expansion in a three-dimensional analogue of Davis *et al.*'s (1983) "bulldozer" model for the development of thrust faults in accretionary wedges. The volume increase was probably due to eolian deposition of mud in desiccation cracks followed by rewetting. Because the bed was confined laterally, it fractured along listric, dish-shaped faults and compensated for increased volume by increasing in thickness. As a mechanical consequence of volume increase, the dish-structures are probably not specific to any particular environment in larger sense, but could be indicative of a limited range of environments in a particular basin setting such as the Lockatong (J. Smoot, pers. comm.).

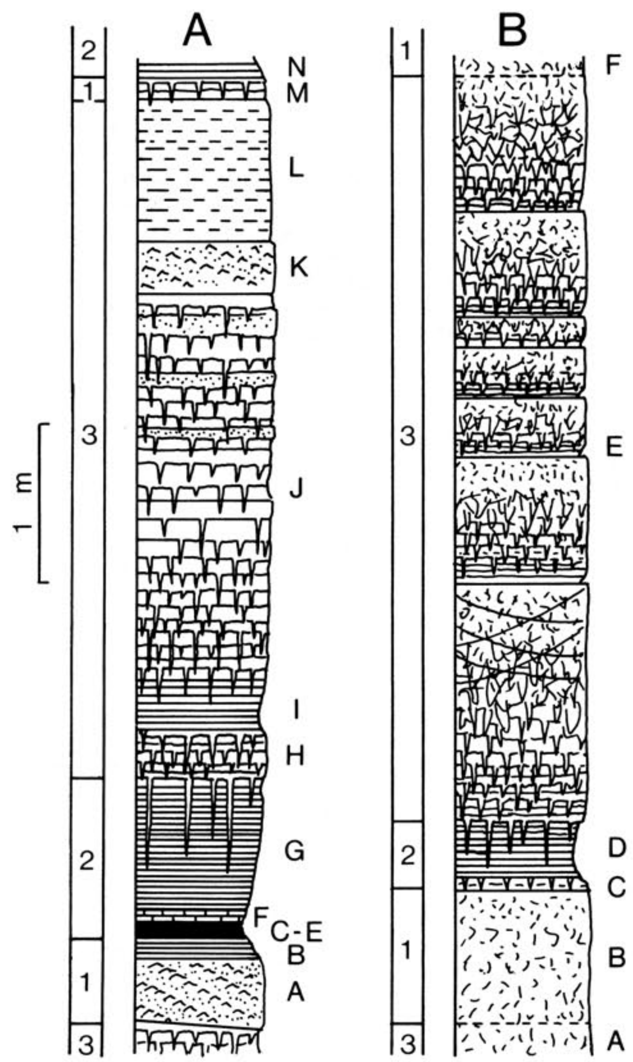

Figure 5.20: Two end members of the cycle types seen at Stop 5.7. (A) Corresponds to Van Houten's (1964) detrital cycle type, whereas (B) corresponds to Van Houten's chemical cycle type. Key to lithology in Table 5.2. From Olsen and Smoot (1988).

Table 5.2: Key to lithologies in Figure 5.20.

Figure 5.20A	
N	+30 cm black laminated claystone (2.9% TOC).
M	10 cm gray mudstone with widely-spaced desiccation cracks.
L	96 cm massive, seemingly structureless, monosulfide-bearing gray mudstone (0.6% TOC).
K	30 cm gray fine-grained, oscillatory-rippled sandstone.
J	240 cm gray decimeter-scale siltstone and fine sandstone beds with abundant contorted desiccation cracks, soft sediment deformation, reptile footprints (*Apatopus*), and rare clam shrimp (*Cyzicus*)(0.5% TOC).
I	30 cm dark gray, laminated mudstone with rare fish bones (0.1% TOC).
H	30 cm dark gray, centimeter-scale mudstone beds with widely-spaced, deep, contorted desiccation cracks (1.3 % TOC).
G	83 cm black, laminated, organic-rich (5.0% TOC) limestone (77% carbonate) grading up into less calcareous (34% carbonate) and less organic rich (1.6% TOC) siltstone with deep, widely-spaced, and sinuous desiccation cracks originating in the overlying beds. Abundant pinch and swell laminae present. Clam shrimp (*Cyzicus*) and ostracodes (*Darwinula*) abundant at the base but absent at top.
F	3 cm black, laminated, organic-rich (6.6% TOC) blebby limestone (76% carbonate) with occasional microlaminae. Abundant ostracodes (*Darwinula*) and clam shrimp (*Cyzicus*) present.
E	8 cm black, microlaminated limestone with even microlamination and some pronounced stylolites passing up into limestones with very discontinuous blebby microlaminae. Clam shrimp (*Cyzicus*), ostracodes (*Darwinula*), fish (*Turseodus* and *Synorichthyes*), and coprolites present.
D	3 cm black, microlaminated blebby calcareous siltstone with extremely abundant clam shrimp (*Cyzicus*), articulated fish (*Turseodus*), and coprolites.
C	4 cm black, microlaminated calcareous claystone (1.4% TOC, 33% carbonate). Basal few couplets with articulated reptiles (*Tanytrachelos*) and rare clam shrimp (*Cyzicus*).
B	12 cm black well-bedded mudstone showing an upward increase in thin-bedding and total organic content. Rare fish bones (?*Diplurus*) and clam shrimp (*Palaeolimnadia* and *Cyzicus*).
A	39 cm gray, climbing ripple-bedded fine sandstone (0.3% TOC), Desiccation cracks are absent in contrast to underlying division 3 of the preceding cycle.
Figure 5.20B	
F	+20 cm gray massive mudstone with crumb fabric.
E	491 cm consisting of 7 massive mudstone sequences, each 150 to 20 cm thick, showing upwards transition from thin-bedded claystone to breccia fabric to crumb fabric.
D	31 cm red and green laminated to thin-bedded claystone with widely-spaced desiccation cracks projecting down from overlying unit.
C	8 cm gray claystone becoming laminated upwards with widely-spaced desiccation cracks at top.
B	82 cm gray massive mudstone with well-developed crumb fabric with analcime filled vesicles.

Clearly, this particular Van Houten cycle represents the transgression and regression of a lake which never became as deep as the cycle shown in Figure 5.20a and when lake level dropped, the lake desiccated for longer intervals. Unfossiliferous here, cycles of this type contain clam shrimp in division 2 and sometimes abundant reptile bones in division 3 in coarser facies (see Stop 5.6). Most of the other cycles at this stop fall somewhere between these two extremes.

At the north end of the exposure is a creek with excellent outcrops of an additional 100 m of section of the upper Tohicken and lower Prahls Island Member (Figure 5.18).

Return to vehicle and head south on NJ 29.

137.4 Old Quarry in upper part of North Wales and lowermost part of Byram members, Lockatong Formation. Quarry in this interval at Point Pleasant has produced slab of large but sloppy *Apatopus* (D. Baird, pers. comm.).

137.7 Byram sill on right intruding beds between lower and middle Lockatong Formation. Igneous layering is apparent at several places in the diabase sill. The Byram sill may not extend down dip in this area, as revealed by proprietary seismic reflection studies in Pennsylvania.

137.9 Poor exposures on right of upper part of lower Lockatong Formation (upper ?Gwynedd Member).

138.5 Stumphs Tavern Road. Stream along north side of road exposes gray and red beds of the ?Weehawken Member of the lower Lockatong Formation. The Weehawken and succeeding Gwynedd Member of the lower Lockatong are the most fossiliferous portions of the Lockatong. Precisely equivalent cycles are exposed in creeks which cut through cliffs on opposite side of river at Lumberville, PA. Here a microlaminated and strongly metamorphosed limestone (by the overlying Byram sill) of division 2 of a Van Houten cycle produces complete *Turseodus* and abundant conchostracans. Presumably-equivalent beds produce copious fossils in the Princeton, Weehawken (Stop 6.6), and North Bergen areas of New Jersey to the northeast. Unfortunately, exposures of this part of the Lockatong are very poor in this part of the Newark basin.

138.9 Low exposures in hill on right show cyclic sequence of thin gray and thick red beds in uppermost Stockton Formation.

139.1 Cliffs of red mudstones and sandstones of upper Stockton Formation on right.

139.4 Old quarry in woods on right in Raven Rock Member of Stockton Formation. Lower parts of quarry expose gray, slightly uraniferous sandstones and siltstones which were the site of a uranium prospect during the 1950's (Turner-Peterson, 1980).

140.6 Crossing Lockatong Creek - extensive outcrops of middle and upper Stockton Formation and type section of Lockatong Formation are found upstream (McLaughlin, 1945).

141.8 Turn left onto open dirt area and park.

STOP 5.8: QUARRY IN PRALLSVILLE MEMBER OF STOCKTON FORMATION, STOCKTON, NJ

(by P.E. Olsen and R.W. Schlische)

Highlights: Large fluvial cycles; orthogonal joint sets.

Quarry in upper part of the Prallsville Member of the Stockton Formation exposes about 60 m of section and begins about 760 m above the base of the formation (Van Houten, 1969, 1980).

Four main lithologies are obvious at these outcrops: 1) massive, well-sorted, medium gray to buff arkose with faint to prominent large-scale cross bedding; 2) massive to crudely cross-bedded (2 m) arkosic conglomerate units, some of which are kaolinized and have small to large rip-up clasts; 3) well-bedded, red, coarse siltstone with small dune-scale cross bedding, ripple cross lamination, and parallel lamination; 4) blocky, massive, red mudstone intensely bioturbated by *Scoyenia* and roots and slickensided dish structures. These sediment types make up thick (>10 m),

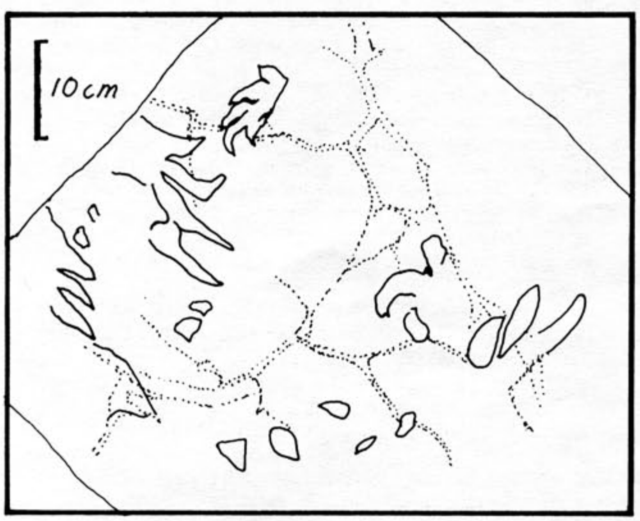

Figure 5.21: Poor footprints apparently belonging to *Apatopus*, produced by a swimming phytosaur in shallow water, from division 3 of cycle A in Figure 5.20. About 10 cm above this bedding surface is a unit with irregular parting planes covered by small conchostracans. From Manspeizer and Olsen (1981).

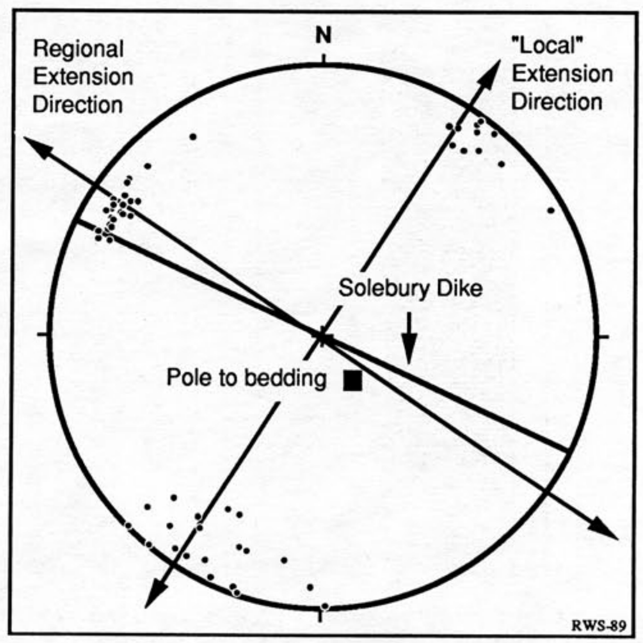

Figure 5.22: Poles to sets of orthogonal joints from quarry in Stockton Formation, Stop 5.8. Modified from Schlische and Olsen (1988b).

fining-upward cycles composed of: 1) pebbly trough cross beds at base passing upwards into sandy compound cross-bed sets; 2) thick interval of climbing ripple cross lamination and planar lamination with bioturbation and siltstone partings increasing up section; 3) climbing ripple siltstone with intense bioturbation by *Scoyenia* and roots, and slickensided dish structures. The sequence of structures in the fining-upward sequences are consistent with large, perennial meandering river deposits. In addition, lateral accretion surfaces of point bars are suggested by the lateral fining of cross-bedded structures in the up-dip direction. The large river systems implied by these outcrops are incompatible with a closed basin model for the Newark basin (Smoot, 1985) and indicate an open basin for this part of the basin's history. This is in accord with the predictions of the basin filling model outlined by Schlische and Olsen (in review; this volume) and Olsen and Schlische (1988a-d).

Other items of note include: (1) Na-feldspar to K-feldspar ratio is commonly 2:1 (Van Houten, 1969); (2) this interval is part of a large magnetically-reversed interval (Witte and Kent, 1987); (3) micro-placers of specular hematite (after magnetite) grains locally outline thin bedding. Probable implications for detrital remnant magnetism (Van Houten, 1969); and (4) small to large root mottles and goethite stain weathered vertical trains of nodules, probably following roots (Van Houten, 1969).

This is particularly good place to see the two main mutually perpendicular joint sets outlined by Schlische (structural evolution section, above). Note especially that the NW-striking set parallels the nearby Solebury dike (Figures 5.1, 5.18, and 5.22), and both are thought to be related to the overall bending and downwarping of the Newark basin as a result of a variable slip on the border fault system.

The Stockton Formation remains almost entirely unprospected for vertebrates. Nonetheless, important osseous remains have been found (Olsen, Van Houten, *et al.*, 1988).

Return to vehicles. Continue south on NJ 29.

142.2 Crossing Wickecheoke Creek at junction with Route 515 in Prallsville, NJ, with extensive exposures of Stockton and Lockatong formations upstream. Lower Lockatong is well exposed and typically fossiliferous. Old quarries along road and canal in vicinity are in Prallsville Member of Stockton Formation.

142.8 Stockton, NJ: type area of the Stockton Formation (Kümmell, 1897; McLaughlin, 1945).

143.0 Exposures of cross-bedded conglomeratic Solebury Member of Stockton Formation (McLaughlin *in* Willard *et al.*, 1959) on left.

143.6 Crossing Flemington fault. Entering northern or Hunterdon Plateau fault block. Across the river in Pennsylvania is uplifted basement consisting of Precambrian metamorphic rocks, Cambro-Ordovician limestones and phyllite, all overlain by basal Stockton Formation.

144.4 Quarry in Mount Gilboa diabase, gabbro, and metamorphosed Lockatong Formation (see Husch *et al.*, 1988).

144.9 Crossing Dilts Corner fault.

145.2 Intersection with US 202.

146.4 Turn right on NJ 179 South (Bridge Street), Lambertville, NJ.

146.6 Turn left into entrance for overnight stop next to Delaware River.

6. NEWARK BASIN, NEW JERSEY

mileage

0 Turn right onto NJ 179 North from the hotel.

0.2 Turn left onto NJ 29.

1.2 Right to US 202.

1.4 Right onto US 202 N ramp. First of a series of four large exposures of Passaic Formation stratigraphically close to the Perkasie Member of early Norian Age. These exposures show a number of Van Houten cycles which are extensively faulted at several scales, with considerable duplication of section. Division 2 of the most prominent Van Houten cycle at this outcrop is uraniferous.

1.8 Second set of exposures.

2.6 Pull off on right next to large exposure.

STOP 6.1: PASSAIC FORMATION ADJACENT TO DILTS CORNER FAULT

(by P.E. Olsen and R.W. Schlische)

Highlights: Cyclical lacustrine strata, fracture cleavage.

This is the largest road cut of hornfels along US 202 in this area, exposing more than 40 m of section in 5 fault blocks (Figure 6.1). According to Hozik (1985), these exposures of thermally-metamorphosed Passaic Formation provide ample evidence of normal faulting specifically associated with movement on the Flemington-Furlong-Dilts Corner fault system. Fewer than 10 of 150 of the small faults measured by Hozik (Figure 6.2) show a significant strike-slip component of movement (based on slickenlines). He notes that most of the faults strike northeasterly and dip steeply either to the northwest or to the southeast. Faults that strike N40°E and dip 70° to the northwest or southeast appear to define a conjugate set which would require σ_1 to be nearly vertical, σ_2 to be nearly horizontal and trending N40°E, and σ_3 to be horizontal and trending S50°E.

As pointed out by Hozik (1985), both Sanders (1962) and Manspeizer (1980) have argued that the intrabasin faulting was essentially strike-slip in origin and specifically that the Flemington fault should be a right lateral fault (Figure 5.1). Hozik's data suggest dominantly normal motion on the Flemington-Dilts corner system which is much more in line with the predictions of the Ratcliffe-Burton (1985) and Schlische and Olsen (1988b) models of regional NW-SE extension (Figure 6.2). Recent mapping and coring by Ratcliffe and Burton (1988) have shown that the Flemington-Furlong fault system strikes N45°E and dips 42°-50°SE with slickenlines recording a number of slip vectors averaging around S45°E.

The bulk of the joints at this outcrop strike northeasterly and are subvertical. The high density of the jointing may again reflect hydrofracturing associated with the intrusion of diabase bodies (located to the southeast of the outcrops) in a regional NW-SE extensional stress regime (see also Stop 5.2).

These cyclical lacustrine strata (Figures 6.1, 6.3) of the Passaic Formation are located stratigraphically near the Perkasie Member. Fourier analysis of the depth-ranked section reveals periodicities in thickness of 5.5 m for the Van Houten cycles (precession cycle) and 25.6 m for the ~100,000-year eccentricity cycle (Figure 6.4). Similar periodic thicknesses were obtained for the Perkasie in New Brunswick, NJ (Olsen and Schlische, unpub. data), an area relatively undisturbed by intrabasinal faulting. These observations therefore suggest no appreciable thickening of strata within the hanging wall of the Flemington-Furlong fault system, suggesting no fault movement during Perkasie deposition. Based on the mineralization of the fault system and the geochemistry of a horse of Early Jurassic diabase within the fault system, Ratcliffe and Burton (1988) concluded that significant motion post-dated intrusion. These observations support a growing body of evidence that the intrabasinal faulting occurred late in the history of the Newark basin (Olsen, 1985; Faill, 1988; Schlische and Olsen, 1988a,b; Schlische, this volume).

The thinness of the cycles here and at New Brunswick is in full accord with the predictions of the basin filling model.

Return to vehicles and continue north on US 202.

3.3 Sections on both sides of highway expose faulted red beds of the Passaic Formation from a stratigraphic position somewhat above the previous outcrops. This exposure reveals roughly 64 m of section. Fourier analysis of this sections shows cycles at about 4.5 m (Van Houten cycle) and 21.3 m (~100,000-year eccentricity cycle).

4.5 The ridge on the right is underlain by the Perkasie Member of the Passaic Formation.

26.2 Get onto I-287 North toward Morristown (keep left). Ridges on the right are underlain by Jurassic rocks in the Watchung Syncline.

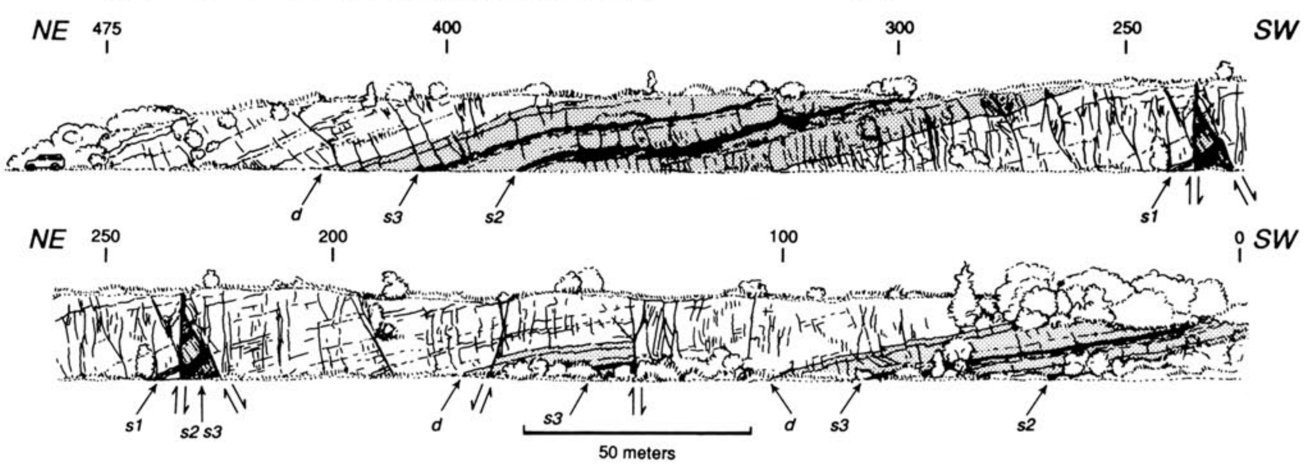

Figure 6.1: Sketch of outcrop along north-bound side of US 202, Stop 6.1. Symbols are: s1-s3, gray and black shales; d, doublet of thin gray siltstones. Note the repitition of units by faulting. Drawing by P.E. Olsen.

Figure 6.7: Nappe-like folds associated with bedding plane-subparallel thrust faults in Towaco Formation, The Glen, Stop 6.2. Photo by A.R. McCune.

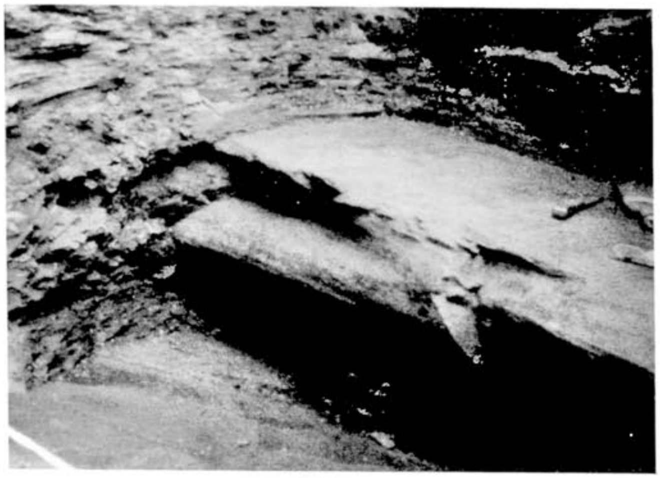

same age. The cyclostratigraphic interpretation is also crucial to interpretations of the duration of the Newark extrusive interval and micro-correlation of cycles between basins. Fourier analysis of the complete Towaco section in the cores (Figure 6.6) shows the characteristic pattern seen much lower in the Newark basin section. It is the resemblance in the hierarchical structure of these cycles to those seen in the Lockatong and Passaic which is the best evidence for their origin. The Van Houten cycles are much thicker than anything in Lockatong or Passaic formations, averaging 25 m. The 100,000 year cycles average about 125 m. There are three 100,000 year cycles in the Towaco; the middle 100,000 year cycle has the best developed (and deepest water) cluster of Van Houten cycles. These are the cycles exposed at this stop.

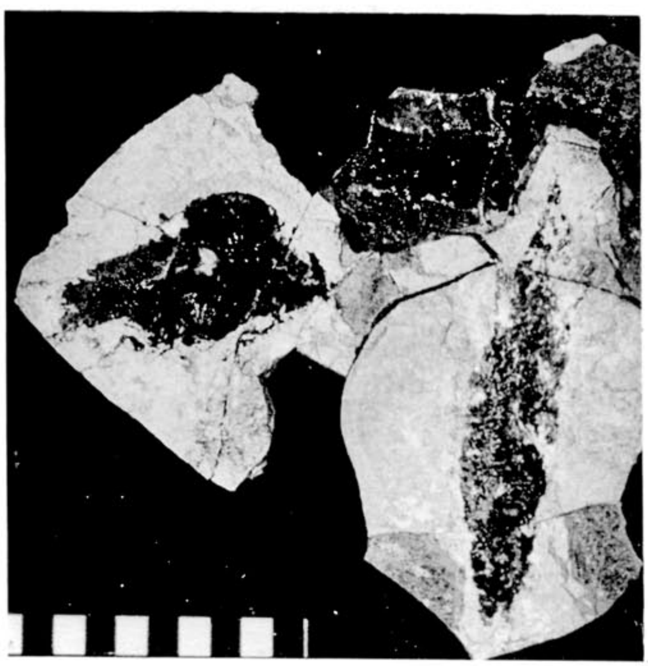

Figure 6.8: Deformed *Semionotus* fish fossils from the hinge of the fold in Figure 6.8. Fish have either been shortened perpendicular to the fold axis or stretched parallel with it or both. Scale in centimeters. Photo by A.R. McCune.

Stratigraphy and Structure of Cycle P4

The three cycles exposed in The Glen have been designated P-3, P-4, and P-5, from the top down (time intervals P2a,b,c) (Figures 6.5, I.9, I.10). A quarry was developed in division 2 of cycle P-4 by A. R. McCune (see below) for collection of fossil fish. Division 1 is characterized by an overall fining-upward trend from wave-reworked conglomerates into oscillatory rippled sandstones and siltstones. Division 2 begins with oscillatory-rippled siltstones, passes rapidly into laminated siltstones with pinch-and-swell laminae, and then up into a very thick microlaminated interval showing silt-carbonate couplets and many sub-millimeter to decimeter thick graded beds that we regard as distal lacustrine turbidites, much as at Stop 4.2 in the Culpeper basin. One turbidite has occasional 1-2-cm-diameter pebbles at its base. The T.O.C. of these beds is relatively low compared to the finer facies of the Towaco, averaging less than 2% by weight. Complete, well-preserved fossil fishes are abundant in these beds (see below). The transition into overlying non-microlaminated silts is abrupt, as is the correlative disappearance of fish. Sandstone and conglomerate at the transition into division 3 show a number of features suggesting wave reworking (Smoot, pers. comm., 1984), including virtually all the features of LeTourneau's (1985a) "lithic unit 7", such as oscillatory ripples, "fitted fabric" of pebbles and cobbles (LeTourneau, 1985b), oriented plant debris, and well-sorted layers and patches of sand, granules, and pebbles. Also present are small lenses of oscillatory-rippled sandstone nestled in well-sorted conglomerate beds, coalified roots, and dinosaur footprints. Higher in division 3, the conglomerates appear fluvial in origin, although they have been examined only superficially.

Decimeter-scale folds are prominent in the microlaminated portions of division 2 of cycle P-4 (Figure 6.7). At first we thought these were subaqueous slump folds, but additional work shows they are nappe-like drag folds of thrust faults propagating upward through major portions of the microlaminated unit. These folds show large amounts of thickening in their hinges, which are often cut by small faults. The fault-adjacent limbs are often sheared out, although completely overturned bedding is locally present. Fish are deformed within these folds: shortened where they are perpendicular to the fold axis and elongated when they are parallel to it (Figure 6.8). The thrusts themselves are slickensided and sometimes polished, and they sole into bedding plane shear zones. The ductile behavior of the beds and the extremely low thermal maturity of the contained hydrocarbons (Pratt *et al.*, 1988) demands that this thrust faulting and folding be early in the burial history of the units, prior to complete lithification, but after significant burial.

SEMIONOTID SPECIES FLOCKS IN THE NEWARK BASIN (by A.R. McCune)

In eight basins of the Newark Supergroup, there are abundant fossils of a primitive ray-finned fish called *Semionotus* (Figure 6.8). *Semionotus* was first discovered in Newark sedimentary rocks in the early 19th century by Benjamin Silliman Sr. (1816), and since that time thousands of specimens have been collected by both amateur and professional paleontologists.

In recent years, evolutionary biologists have become interested in *Semionotus* because the evolution of its diversity and domination of ancient Newark lakes provide a

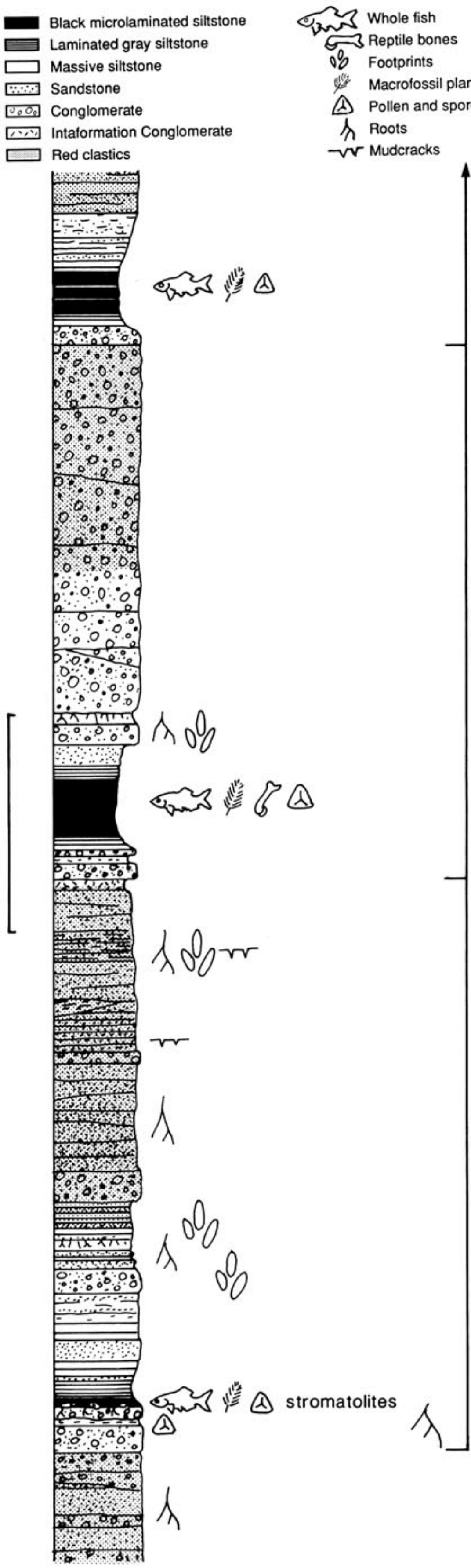

Figure 6.5: Measured section of the middle Towaco Formation at The Glen, Stop 6.2. From Olsen (1984a).

Figure 6.6: Power spectrum of depth rank curves of the Towaco Formation (see Figure I.9) compiled from U.S. Army Corps of Engineers drill cores. Note the four-fold increase in Van Houten cycle thickness over that in Late Triassic rocks (*cf.* Figures 5.15, 5.19, 6.4).

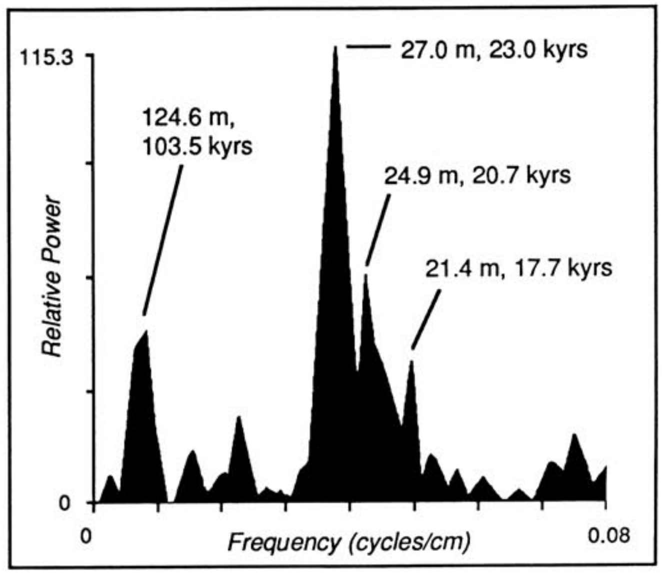

64.3 Turn right onto Alternate Route 511.
65.1 Turn right onto Riverdale Road (Route 651 North).
65.3 Turn left onto Ramapo Avenue.
65.5 Turn right onto Riverview Road (Pompton Plains). At the intersection, Hook Mountain Basalt and conglomeratic strata of the Boonton Formation can be seen.
65.7 Turn right at T-junction onto Hamburg Pike (Pompton Falls).
65.8 Turn left onto Terhune Drive (US 202). Pompton Lake on the left. Most of the lakes in the area are the result of glaciation.
66.1 Turn right onto Colfax Road.
66.5 Turn left onto Vale Road.
66.6 Park.

STOP 6.2: THE GLEN NEAR PINES LAKE, POMPTON, NJ (by P.E. Olsen)

Highlights: Lacustrine cycles and fish fossils of Towaco Formation; white coprolites.

A stream connecting Pines Lake and Pompton Lake and a tributary to this stream provide the best outcrops of the Early Jurassic Towaco Formation (Figure 6.5). About 65 m of the middle of the Towaco Formation are exposed, comprising two complete and one partial Van Houten cycles (each about 25 m thick).

Stratigraphy of the Towaco Formation

Like the rest of the post-Stockton Newark basin section, the Towaco Formation is made up of Van Houten cycles (Figure 6.5). Recent drilling by the Army Corps of Engineers (Fedosh and Smoot, 1988; Olsen and Fedosh, 1988) produced cores of the entire Towaco Formation within comparatively fine-grained facies (Figure I.9). The cored sections have allowed the complete cyclostratigraphy to be worked out and serves as a standard of comparison for all the other intervals in other basins we believe to be of the

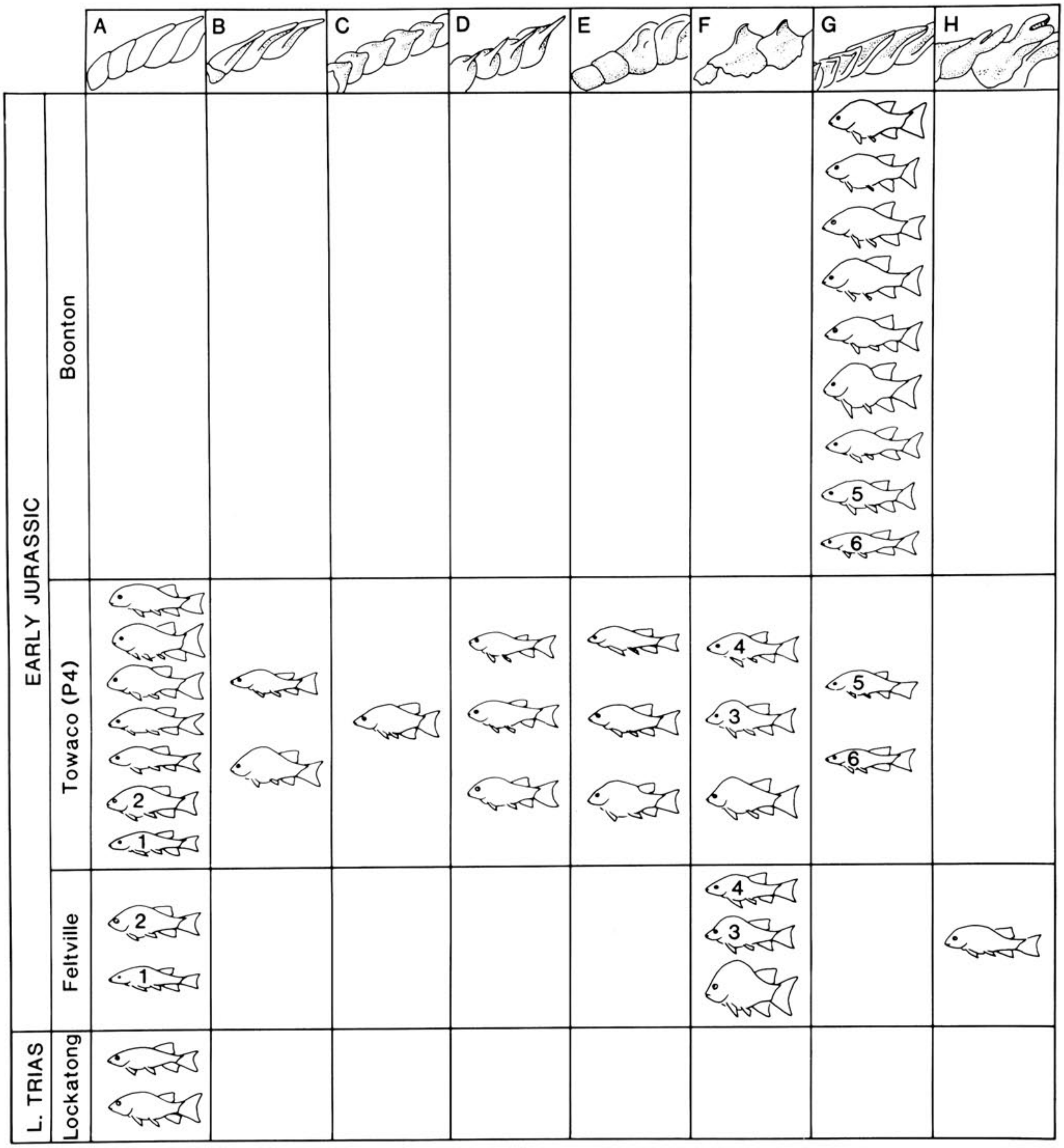

Figure 6.9: Pattern of distribution of *Semionotus* species through the history of the Newark basin. The diversity of *Semionotus* found in the Late Triassic Lockatong Formation (cycle 5 of Olsen, 1984a), and three Early Jurassic sedimentary formations: the Feltville, Towaco (cycle P4), and the Boonton formations. Each of these four faunas is from a single sedimentary cycle. Each fish represents the occurrence of a species. Thus, in the Lockatong Formation, there are 2 species of *Semionotus*; there are 6 in the Feltville, 21 in the Towaco and 9 in the Boonton. Species in each cycle are further grouped by their morphology of dorsal ridge scales as illustrated in the column headings: A, simple scale group; B, modified simple scale group; C, small scale group; D, thin-spined scale/*S. micropterus* group; E, globular scale; F, robust scale/*S.tenuiceps* group; G, concave scales/*S. elegans* group; H, dorsal ridge scale group. Species occurring in more than one cycle are numbered 1-6 and are presumed colonists. Unnumbered species in each cycle are unique (thus far) and are tentatively considered to be endemic.

fascinating fossil analogue to an important evolutionary phenomenon—profuse, and possibly rapid, speciation in geographically-confined areas such as oceanic islands or inland lakes. The best known examples of this phenomenon are the finches from the Galapagos Islands that so influenced Charles Darwin in formulating the theory of natural selection, the more than 400 species of *Drosophila* inhabiting the Hawaiian Islands, and the 800+ species of cichlid fishes that dominate the great lakes of East Africa. These closely-related groups of species, endemic to geographically-restricted areas are often termed "species flocks." The localized high diversity of species flocks poses challenges to some of the basic tenets of evolutionary theory (Mayr, 1984), and therefore evolutionary biologists are particularly interested in understanding the pattern and process of speciation in these groups.

Repeated episodes of lake formation and evaporation in the Newark Supergroup (Olsen, 1984a, 1986) provide a uniquely detailed record of colonization and speciation in semionotids, something that is not available for any living species flocks. Ongoing studies of taxonomy, phylogenetic (genealogical) relationships, colonization, speciation, and morphological change in *Semionotus* (Olsen *et al.*, 1982; McCune *et al.*, 1984; McCune, 1982, 1986, 1987a,b) are directed towards understanding the evolution of the group, especially in relation to the regular cycles of environmental change worked out by Olsen (1984a, 1986).

The best-known semionotid faunas are from the Newark basin. Here the Late Triassic semionotids show rather little species diversity, whereas the Early Jurassic faunas are considerably more diverse (McCune *et al.*, 1984). Morphological variation in *Semionotus* is concentrated in overall body shape and the morphology of the series of spined scales, called dorsal ridge scales, that rim the dorsal midline. Well-studied deposits from the Early Jurassic Feltville, Towaco, and Boonton formations contain 6, 21, and 9 species of *Semionotus*, respectively (McCune, 1987b). The pattern of species distribution (Figure 6.9) suggests that as many as 5 species from the Feltville, 17 in cycle P4 of the Towaco, and 7 in the Boonton Formation could have speciated *in situ*, in well under 10,000 years (the first half of a Newark sedimentary cycle). This hypothesis is based on knowledge of the Newark basin faunas, and is subject to test by extensive large-scale biogeographic studies and detailed microstratigraphic studies (within individual sedimentary cycles) currently underway.

66.7 Turn around and leave. Retrace back to US 202. Turn right onto Colfax Road.
67.1 Turn left onto Terhune Drive (US 202).
67.3 Hook Mountain Basalt on left.
67.4 Turn left onto US 202 (Hamburg Pike).
68.1 Stay on US 202 South. Veer right onto Black Oak Ridge Road.
70.4 Turn right onto NJ 23 South just before a large intersection.
74.2 Turn right onto US 46 West. Follow signs.
79.7 Type section of Hook Mountain Basalt on I-80 to the north. Some outcrops of the basalt on the right.
80.1 Turn right at New Road, then turn left at stop sign. Follow signs to I-280 East.
81.0 Cross over and get on I-280 East toward Newark. Keep right onto exit ramp.
83.2 Exit to Eisenhower Parkway and Chatham (Exit 4A).
83.7 Cross Eagle Rock Avenue. Get in left lane.
83.9 Turn left after railroad tracks into Nob Hill Condominiums.

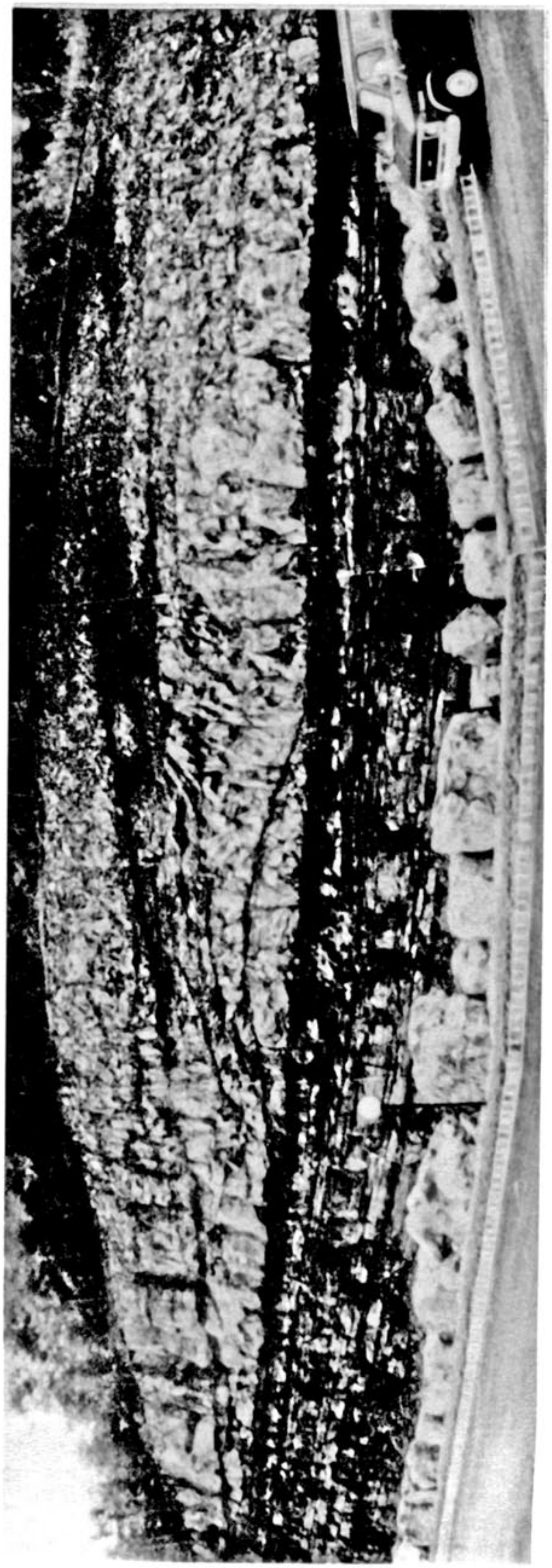

Figure 6.10: Composite photograph of the contact between the fluvio-lacustrine red beds of the Towaco Formation and Hook Mountain Basalt at Riker Hill, Stop 6.3. Note the numerous low-angle fractures within the basalt.

STOP 6.3: RIKER HILL, ROSELAND, NJ
(by P.E. Olsen)
Highlights: Towaco Formation; Hook Mountain Basalt.

The cut on north side of Riker Hill adjacent to Nob Hill Condominiums exposes about 20 m of red, fine-grained sandstone and siltstone and nearly the full thickness of both flows of the Hook Mountain Basalt (Figure 6.10). The upper parts of the sequence are somewhat bleached by low-grade thermal metamorphism like that seen at Stop 7.2.

The Hook Mountain Basalt is a high-TiO_2, high-Fe, quartz-normative tholeiite which in this area consists of two flows (Olsen, 1980a,b) both fitting Long and Wood's (1986) criteria for Type I flows of the Columbia Plateau basalts except that they are somewhat thicker. As is true for the Type I flows the bulk of the flows here consists of irregular tapering columns that are 1 to 2 m in diameter, with no distinct entablature. However, at the type section of the Hook Mountain Basalt, the lower flow has a distinct entablature and fits Long and Wood's Type III category. At Millington, 15 km to the southwest, several flows are present according to Faust (1975, 1978).

Pipe vesicles near the base of the flow indicate southerly flow of the basalt over the basin floor (Manspeizer, 1980). In contrast, pipe vesicle data from the Orange Mountain and Preakness basalts indicate northeasterly flow.

In addition to the poorly-developed cooling fractures, a series of large, low-angle, weathered fractures cut down section to the east (Figure 6.10). Are these related to the Mesozoic history of this flow or are they glacial loading, unloading, or shear features?

Return to cars and head back to Beaufort Avenue and turn right.

84.2 Leave condominium parking lot and turn right. Cross railroad tracks. Get back on Eisenhower Parkway.

84.5 Cross Eagle Rock Avenue.

84.7 Get back onto I-280 East (exit ramp). The road is going up the dip slope of the Preakness Basalt.

88.0 Stop.

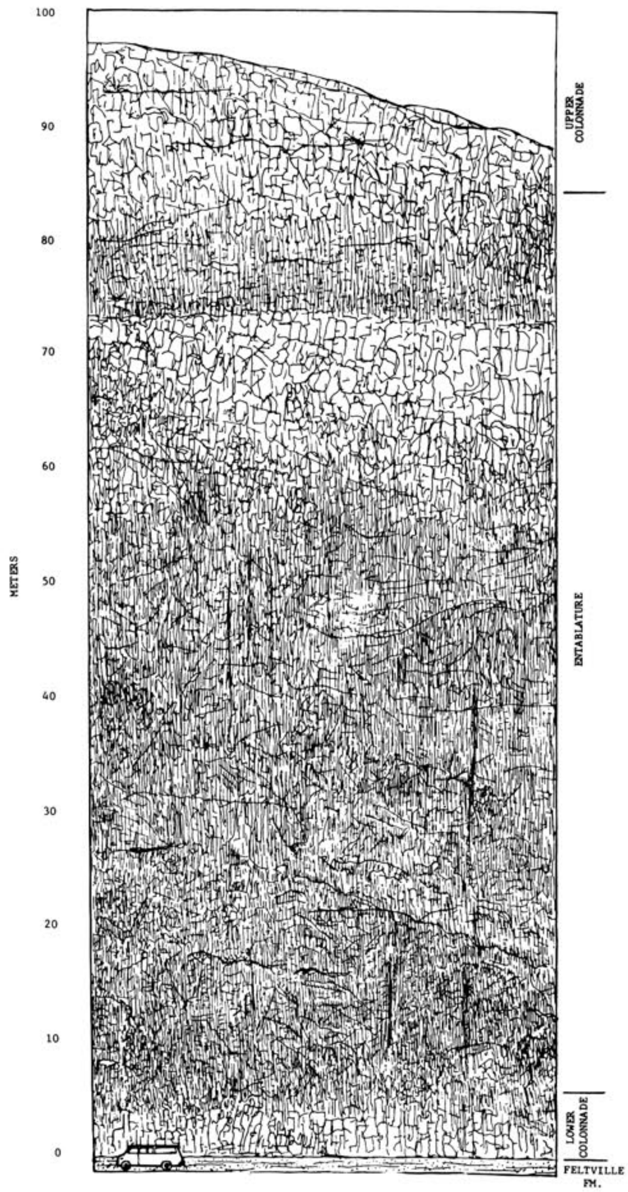

Figure 6.11: Composite sketch of the type section of the Preakness Basalt along I-280, Stop 6.4. From Olsen (1980a).

STOP 6.4: PREAKNESS BASALT, WEST ORANGE, NJ (by P.E. Olsen and R.W. Schlische)
Highlights: Splintery jointing.

This type section exposes about 100 m of the lowest flow of the Preakness Basalt, the thickest extrusive multiple flow unit in the Newark basin section (Figure 6.11). It is a high-Ti, high-Fe quartz-normative tholeiite indistinguishable from the Holyoke Basalt of the Hartford basin. The lowest flow is characterized by a thin lower colonnade; a massive, thick, and coarse-grained entablature with very characteristic splintery columns; a massive upper colonnade; and a comparatively thin vesicular flow top. It does not closely resemble any of the flow types of Long and Wood (1986), but it is obviously similar to the second flow of the Sander Basalt of the Culpeper basin (see Stop 4.3), the Holyoke Basalt of the Hartford basin, and some parts of the North Mountain Basalt of the Fundy basin (Stop 11.2).

The splintery columns are defined by what Faust (1978) calls a platy prismatic joint system, and it is characteristic of the lower flow throughout the areal extent of the Preakness Basalt. The joint system is not hexagonal and does not appear to be a faulting phenomena (although faulting does exaggerate it). Its origin remains a mystery.

Several faults cut the rocks at this exposure (Schlische, 1985). The largest fault zone strikes N05°W, dips 85°E and is marked by a gulley 1.5 m wide. The zone of brecciation varies in width from 40 to 60 cm. Slickenlines are curved from more steeply-plunging to more shallow-plunging attitudes. Another major fault strikes N35°W and dips 83°NE and is marked by a breccia zone (with clasts 2 to 5 cm in size) 35 to 40 cm wide. Slickenlines rake 35°N. Three other macroscopic faults have orientations N10°W, 82°NE; N40°W, 82°NE; and N20°E, 83°NE; brecciated zones are 10 to 15 cm wide. A systematic study of minor fault populations showed that, although most of the faults followed pre-existing joints within the basalt, the slickenside striae strongly indicated strike-slip on NW-striking planes (Schlische, 1985), consistent with the larger faults at this exposure. The faulting here is consistent with the postulated young episode of NE-SW compression responsible for strike-slip faulting in many of the Newark Supergroup basins (see Tectonic Setting under Geological Overview and Stop 8.4).

At this locality the contact with the underlying Feltville

Formation is simple, with massive basalt of the lower colonnade in direct contact with sedimentary rocks. At other localities thin flow units, pillow lavas or rubble flows are present (Olsen, 1980a).

Continue east on I-280. The road is going up the dip slope of the Orange Mountain Basalt.

89.2 Stop.

STOP 6.5: ORANGE MOUNTAIN BASALT, WEST ORANGE, NJ (by P.E. Olsen, R.W. Schlische, and P.J.W. Gore)

Highlights: Columnar jointing.

When this road was constructed in 1969, this roadcut was the deepest federally financed highway cut east of the Mississippi River (Manspeizer, 1980). The roadcut is about 33 m high and exposes a complete section of the lower flow unit of the Orange Mountain Basalt (Figure 6.12) (Olsen, 1980a; Manspeizer, 1980). Unusual curved patterns of columnar joints are present in the cut, described as chevrons, oblique and reverse fans, and rosettes. This flow overlies red beds of the Passaic Formation.

At this outcrop of the type section, the west-dipping lower flow of the Orange Mountain Basalt is almost completely exposed (Olsen, 1980a; Puffer, 1987). The Orange Mountain Basalt is an HTQ basalt (Puffer and Lechler, 1980) which at this exposure shows a complete, beautifully displayed Tomkeieff (1940) sequence (Olsen, 1980a; Puffer, 1987) almost exactly comparable to Long and Wood's (1986) Type III flows. The thin (6 m) lower colonnade is fine-grained with large columns, the entablature is thick (35 m) with very well-developed curvicolumnar jointing, and the upper colonnade (10 m) is massive with poorly-developed columns.

The largest fault in this exposure strikes N05°E, dips 80°E, and does not visibly offset subhorizontal cooling joints, suggesting that it is a predominantly strike-slip fault (Schlische, 1985). Another fault with a 25-cm-wide breccia and gouge zone strikes N30°E and dips 70°NW. Although slickensides suggest that the last slip on the fault was predominantly dip-slip, this fault may have originated as a normal fault during NW-SE extension. Several minor slickensided surfaces, mostly reactivated cooling joints in the basalt, show evidence of an earlier period of predominantly normal-slip and a later period of predominantly strike-slip (Schlische, 1985).

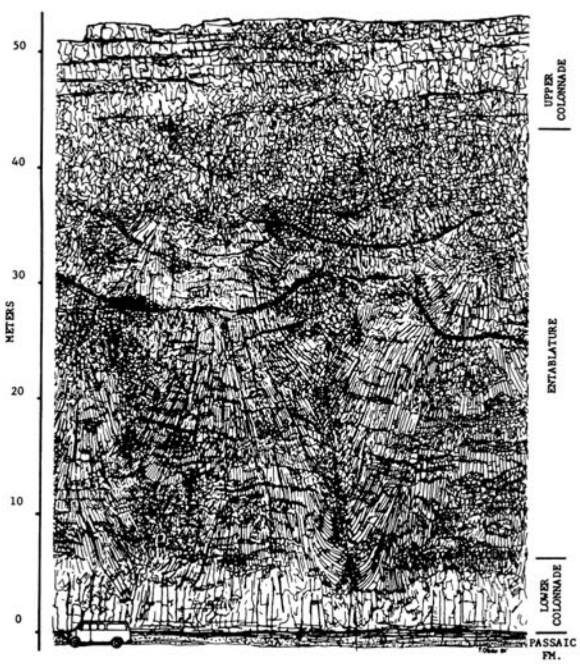

Figure 6.12: Composite sketch of the type section of the Orange Mountain Basalt along I-280, Stop 6.5. From Olsen (1980a).

Continue east on I-280. We will be going through Newark and crossing the Passaic River. Note outcrops of Passaic Formation red beds along the road.

97.1 Get on the New Jersey Turnpike (I-95), heading north.

97.8 Toll Booth. Get ticket.

97.9 Cross to the right and get on the Lincoln Tunnel approach. The ridges in this area are landfills.

99.6 Snake Hill diabase plug on the left. Ridge ahead is the Palisades sill (diabase) and beyond is Manhattan (downtown New York City).

Take exit 16E, Lincoln Tunnel.

103.0 Toll.

103.1 Take the right exit to Lincoln Tunnel and NJ 495, and keep left to NJ 495 East, Lincoln Tunnel.

104.4 Roadcut through Palisades sill.

104.9 Take exit to right "Last exit in New Jersey", to Pleasant Avenue, Weehawken. Get immediately in right lane after exit.

105.0 Veer right onto ramp.

105.2 Turn right to Boulevard East. Immediately get in the left lane.

105.4 Turn left at the traffic light at Baldwin Avenue. Go under ramp for NJ 495. Cross railroad and follow road around to left. Watch out for trucks and trains. Park.

STOP 6.6: YALE QUARRY, KINGS BLUFF, WEEHAWKEN, NJ (by P.E. Olsen)

Highlights: Thin lake cycles of Lockatong Formation in the hinge of the Newark basin.

Beds of the Lockatong and Stockton Formation and their contacts with the overlying Palisades sill are exposed at numerous places from Hoboken to Alpine, NJ. Because of the abundance of outcrops, the very thin Van Houten cycles, and fossil richness of many of the lacustrine units, it has been possible to develop a very robust cycle-by-cycle correlation of the Lockatong in this very densely populated area (Olsen, 1980c, 1988c). These cycles have been designated by informal codes as shown in Figure 6.13.

The cliffs at Kings Bluff, on the east face of the Palisades escarpment, expose a long series of Van Houten cycles, tongues of Stockton-like arkose, and alternating concordant-discordant contacts with the Palisades sill. The details of stratigraphy, physical relationship to the Palisades intrusion, and paleoecology are known in more detail here than in any other portion of the Lockatong Formation.

At Hoboken, the Palisades sill rests near the base of cycles 5 and 6. To the north, towards the Lincoln Tunnel toll plaza, the contact drops more than 25 m into the Stockton Formation (Figure 6.14). At Kings Bluff, this contact abruptly rises again to cycle 0 of the Lockatong Formation, staying within division 2 of this cycle for at least 300 m north. An olivine zone about 10 to 15 m above the base of the Palisades diabase produces an obvious bench along the escarpment, essentially paralleling the lower contact of the sill, as observed by Walker (1969) (Figure 6.14). A thin subsidiary sill was intruded between cycles a and b. This sill definitely runs north for at least 400 m and was encountered during the excavation for the ventilation buildings for the Lincoln Tunnel (Figure 6.14a,b) (Fluhr, 1941). It may extend at least another 200 m north.

About 30 m south of the ventilation buildings for the tunnels, P.E. Olsen, A.R. McCune, and other colleagues opened a quarry (Figures 6.15, 6.16, 6.17) for Lockatong fossils in cycles 5 and 6 as part of a larger project on fish evolution headed by K.S. Thomson (then at Yale). Over 4000 fish and reptiles have been recovered from the two quarried Van Houten cycles. The stratigraphic and bedding-plane position of all the collected vertebrates was carefully noted, with the results shown in Figure 6.15. Note the very specific sequence in which various kinds of fossils appear and disappear through the section. Each cycle has its own particular lithological and biological characteristics and these allow the cycles to be recognized elsewhere.

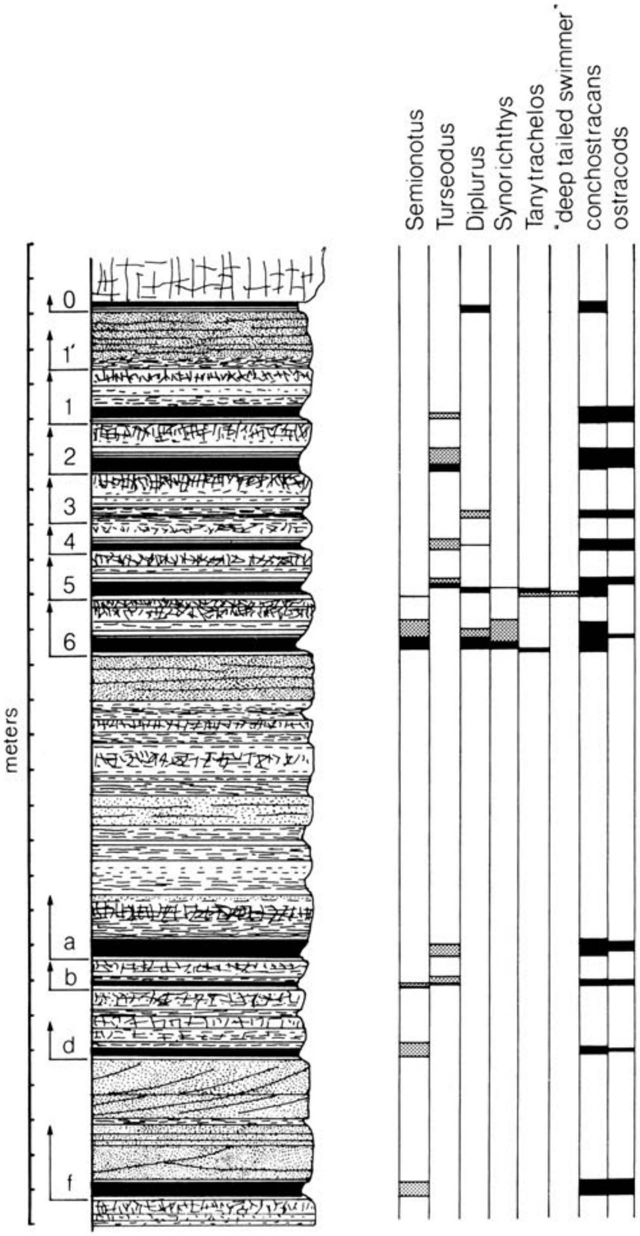

Figure 6.13: Measured section showing stratigraphic nomenclature and position and nature of fossils at Kings Bluff, Stop 6.6. From Olsen (1980c).

However, each cycle also repeats a general pattern of fossil preservation very similar to that seen in the Cow Branch Formation Van Houten cycles at Stop 2.2 and in the middle Lockatong at Stop 5.7.

The microlaminae of division 2 of cycle 6 are subtle and show up as relatively minor differences in Ca-rich silicates *vs.* K-rich silicates. Prior to metamorphism, these were probably calcium carbonate-rich *vs.* silicate- and dolomite-rich laminae (Figure 6.18). The dominant fish taxon is *Semionotus brauni*, which is very well preserved in the microlaminated beds (Figure 2.7). The overlying Van Houten cycle (5) has a microlaminated unit in which the laminae stand out boldly as white and black laminae which differ in composition. In marked contrast to 6, the microlaminated portion of 5 is dominated by the coelacanth fish *Diplurus* and the paleoniscoid fish *Turseodus* (Figure 2.17). Apart from one possible scale, *Semionotus* is absent from 5 and there is no evidence for *Turseodus* in 6. In addition, bones of the peculiar reptile dubbed the "deep tailed swimmer" (Figure 6.19) are entirely restricted to 5. There are many other finer-scale paleontological and lithological differences between 5 and 6 (Figure 6.16). All of the cycles at Kings Bluff and elsewhere are characterized by their own peculiarities. These differences are the basis of a fine-scale ecostratigraphic correlation (Cisne *et al.*, 1984) of these cycles along strike (Olsen, 1988c) (Figures 6.16, 6.17).

Although each cycle has its unique properties, as in the Cow Branch Formation (Stop 2.2), there are prominent general paleontological patterns repeated in most cycles, which are well shown in cycles 5 and 6. The most obvious and least surprising pattern is seen in the correlation between the degree of fish preservation and the degree of lamination of the sediments (Figure 6.15). Microlaminated beds (depth rank 6) tend to preserve beautifully articulated fish. Mudcracked mudstones (depth rank 2-0) have only dissociated scales and skull bones. Laminated mudstones (depth rank 3) produce disarticulated but still associated fish. This correlation almost certainly reflects the often quoted dependence of fish preservation on a lack of oxygen, bioturbation, macro-scavenging, and physical disturbance.

Inversely correlated with this fish-preservation trend is one which at first appears very peculiar: a trend to lower fish diversity in the beds with the best fish preservation, and vice versa (Figure 6.15). This trend is all the more surprising because many more fish are identifiable from the beds producing the best-preserved fish. The pattern is similar to that seen at the Solite Quarry in the Cow Branch Formation (Stop 2.2) and can be similarly explained. The highest diversity of lake zones tend to be near the shores, whereas the deeper-water zones tend toward low diversity (this is especially true for lakes with anoxic bottom waters, because they lack benthic forms). Thus the cycle in diversity is a consequence of proximity to the shore which varies as a function of depth, which in turn controls the degree of lamination and absence of bioturbation (see Stop 2.2).

106.1 Turn around and retrace route. Pass the point where we exited from the ramp to the tunnel.
106.8 Turn right onto Boulevard Road.
107.3 Turn right onto Highwood Terrace. This area is an old dueling grounds, where Alexander Hamilton was shot by Aaron Burr on the morning of July 11, 1804.
108.5 Turn right onto 60th Street which follows the edge of the Hudson River.

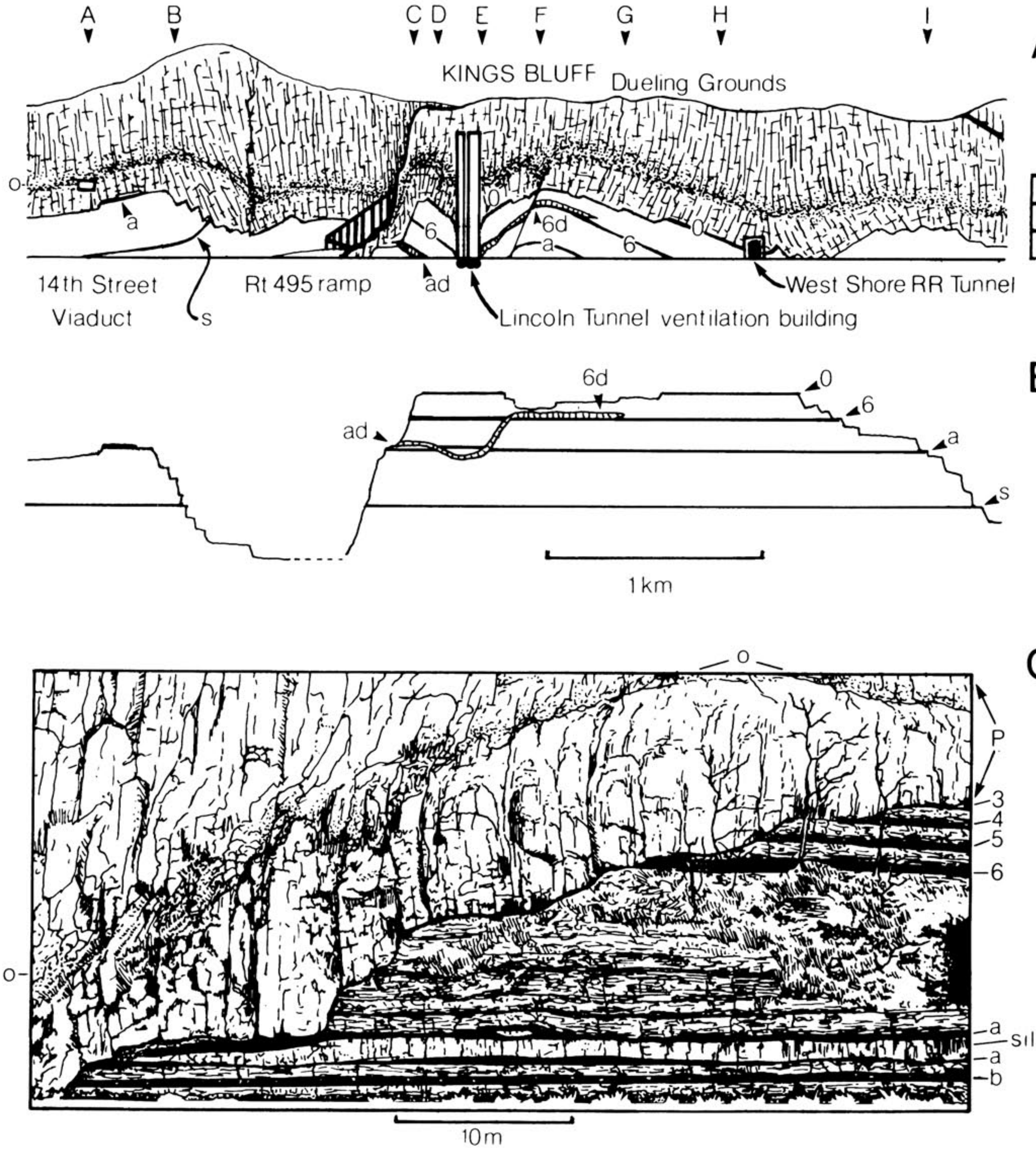

Figure 6.14: A) View of Palisades escarpment looking NW; note vertical exaggeration. Abbreviations are: A, exposure below west portal of 14th Street Viaduct, Hoboken; B, exposures west of west end of Chestnut Street, Hoboken; C, Kings Bluff, Weehawken; D, Yale Quarry in cycles 5 and 6; E, exposures of cycles 0-6 at north side of ventilation building; F, "two runs" exposures of cycles 4-f; G, position of Weehawken fossil fish locality; H, exposure of cycle 0 at south side of west portal of the southern tunnel of New York, Susquehana, and Western Railroad; I, area where diabase cuts down into Stockton Formation; S, Stockton-Lockatong contact; ad, thin diabase sill intruding cycle a; 6d, thin diabase sill intruding cycle 6; O, olivine zone of Palisades sill. B) Section from Hoboken to West New York, NJ, reconstructed with fault displacement removed, showing large irregularities of hornfels-diabase contact. Abbreviations as in (A). C) Section exposed on east face of Kings Bluff shows diabase cutting obliquely across cycles 3-b and thin sill intruding cycle a. P is Palisades sill. From Olsen (1980c).

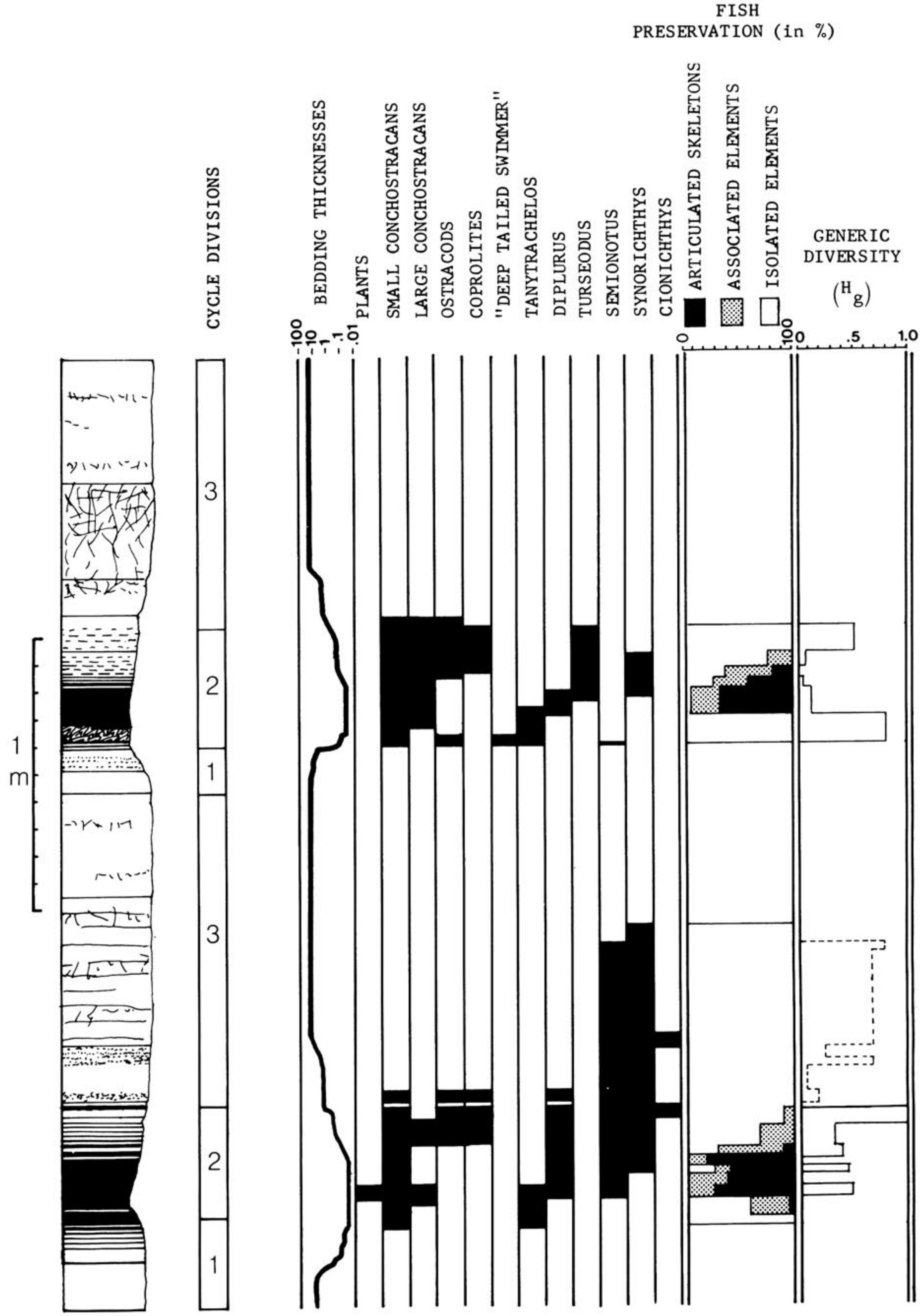

Figure 6.15: Results of paleontologic excavations in cycles 5 and 6, Kings Bluff, Stop 6.6. Generic diversity is the Shannon-Weaver (1949) information index. From Olsen (1980c).

109.5 Outcrops of Stockton Arkose below Palisades sill.

110.4 Outcrops of Lockatong Formation at Gorge Road and River Road.

Cycles 1'-6 are exposed along Gorge Road and cycles a-c on the west side of River Road opposite service station (Figures 6.16, 6.17). These are the same cycles as seen at Stop 6.5a. Cycles 5 and 6 are virtually unchanged with the exception of an increase in ostracode density in the upper parts of division 2 of both cycles, fewer fish in division 2 of cycle 6, minor color changes, and the presence of calcareous nodules in division 2 of cycle 5. Cycles 1, 3, and 4 appear unchanged from Stop 6.5, while cycle 1' is less disturbed and cycle 2 has more fish than at Stop 6.5.

In contrast with the relative lack of change from Stop 6.6 in cycles 1'-6, the siltstone units between cycles 6 and cycle a are nearly completely replaced by 5.5 m of arkose with some unidirectional cross bedding indicating transport to the west and southwest (Van Houten, 1969). Some wave influenced sandstones are also present (Smoot, pers. comm.). I believe the arkose tongue and the thin siltstones present in this interval to be the lateral equivalents of low-depth-rank cycles present in the central Newark basin. Cycles a and b appear virtually the same as at Stop 6.6.

The detailed correspondence between beds and vertical changes in lithology and paleontology in cycles 5 and 6 between Stop 6.6 and here is illustrative of the large area over which the factors responsible for the details of the cycle operated. The region represented by Stop 6.6 and here was evidently far enough from shore (during the deposition of division 2) that the normal heterogeneous depositional environments of the shore had virtually no influence on cycles 5 and 6. This, in turn, is indirect evidence that the size of the lake which produced cycles 5 and 6 was considerably larger than the 5 km traced so far.

Note that Gorge Road follows a fault-line ravine north of the Lockatong exposures; the eastern block is downthrown about 53 m (Van Houten, 1969).

110.7 Entrance to tunnel for former New York Susquehanna and Western Railroad. Directly under River Road is a complete section of Lockatong cycles 1-6.

110.9 Exposures in railroad cut.

111.1 Exposures on the left at welding shop.

112.1 Turn left at Anchor Bank.

112.2 Turn right at the T-junction and park in front of the small playground on Undercliff Road. Uphill on west side of road is a long series of exposures along an abandoned trolley route.

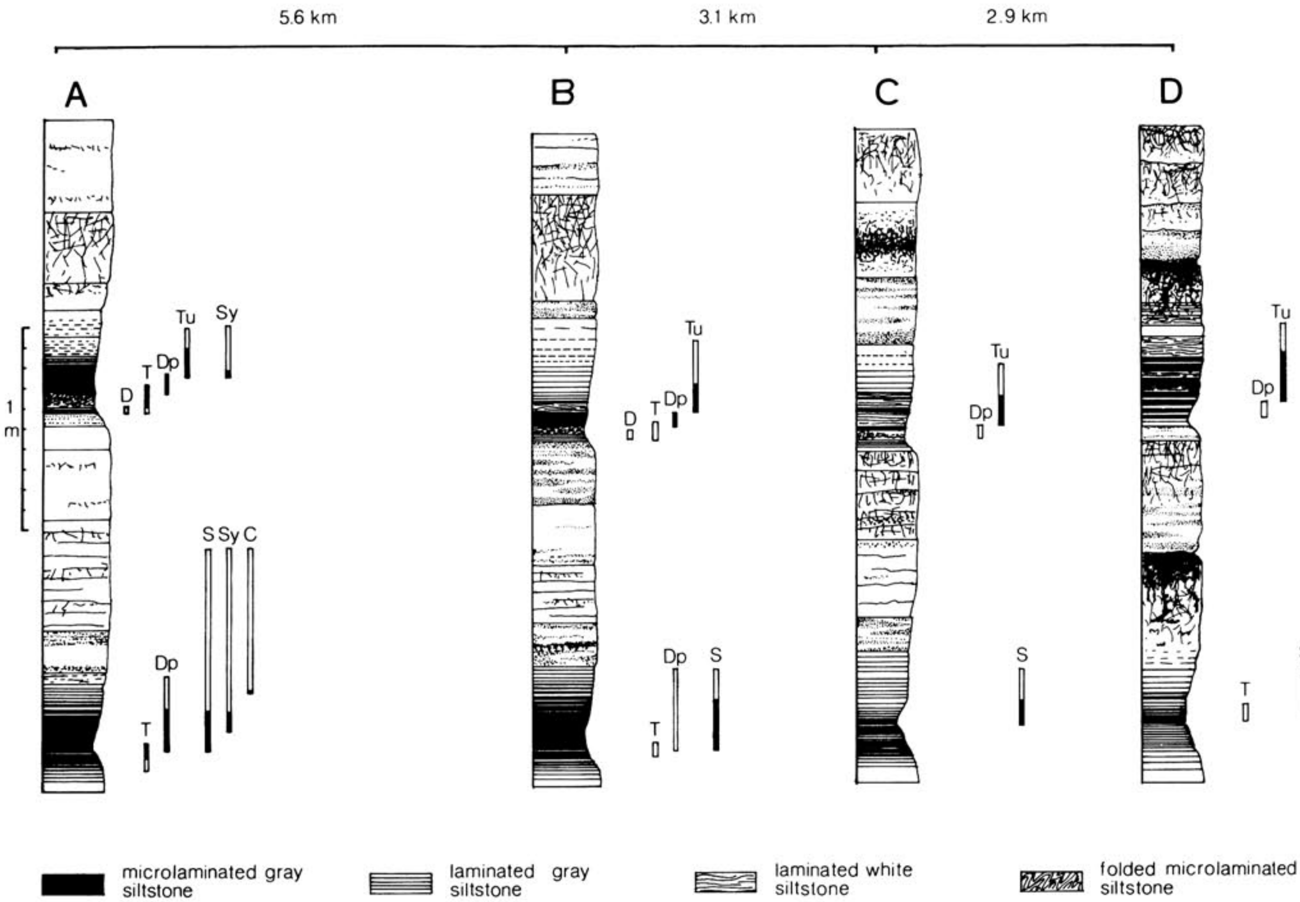

Figure 6.16: Comparison of cycles 5 and 6, showing distribution and preservation style of fish at A) Kings Bluff (Stop 6.6), B) Gorge and River Roads (mileage 110.4), C) Undercliff Road trolley cut (Stop 6.7), and D) Ross Boat Dock (Stop 6.8). Abbreviations for fossils are: D, "deep-tailed swimmer"; Dp, *Diplurus*; C, *Cionichthys*; T, *Tanytrachelos*; TU, *Turseodus*; Sy, *Synorichthys*; and S, *Semionotus*. Open column indicates disarticulated fish; solid column represents complete specimen. From Olsen (1980c).

STOP 6.7: UNDERCLIFF ROAD TROLLEY CUT, FORT LEE, NJ (by P.E. Olsen)

Highlights: Sandstone appears in Lockatong lake cycles.

Exposures include upper Stockton and lower Lockatong formations including cycles 5 and 6 and a-c (Figures 6.16, 6.17). The base of the Palisades sill is well-exposed with a large xenolith of cycle 5 suspended above the Lockatong-diabase contact. Cycle 5 below contains scapolite, aegerine, and Na-feldspar-rich hornfels, whereas the xenolith of the same unit consists of very coarse-grained biotite-Na-feldspar-rich hornfels with minor pyroxenes, and beds of cordierite-biotite-Na-feldspar hornfels (Van Houten, 1969).

At this outcrop the Lockatong is noticeably coarse-grained, with both an increase in the number of sandstone beds and a decrease in the degree of lamination in division 2 of the Van Houten cycles. This can be seen especially well in cycles 5 and 6 (Figure 6.16). Despite this coarsening, the same kinds of fossils, in the same order, occur here as at the more southern outcrops. One prominent sandy unit in division 3 of cycle 6 has a band of calcareous nodules which may represent a caliche zone, better developed at Stop 6.8.

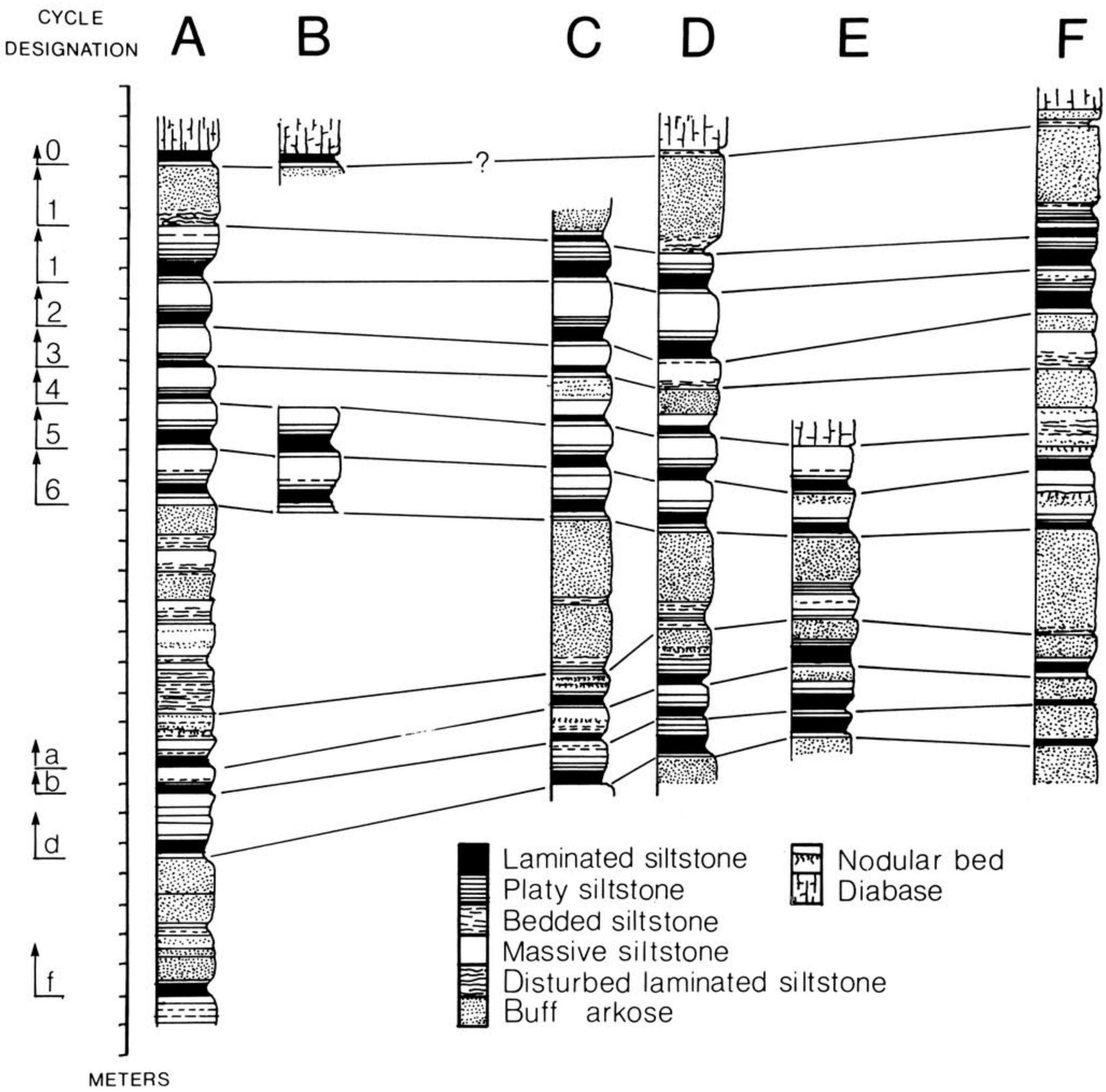

Figure 6.17: Correlation of cycles from Kings Bluff (Stop 6.6) to Ross Boat Dock (Stop 6.8). A, Kings Bluff; B, Weehawken; C, Gorge and River Roads (mileage 110.4); D, west shore railroad tunnel; E, Undercliff Road trolley cut (Stop 6.7); and F, Ross Boat Dock. A and F are 12 km apart; the others are scaled accordingly. From Olsen (1980c).

112.2 Continue to the right (north) on Undercliff to first right.
112.3 Turn right onto Hudson Avenue, the next street.
112.5 Turn left (north) onto River Road.
113.9 Entrance to Ross Dock portion of Palisades Interstate Park System. Turn right into the entrance and STOP. Passengers get off and walk along series of outcrops downhill to the right of the road through the park. The bus will meet them 1.2 miles down the road.

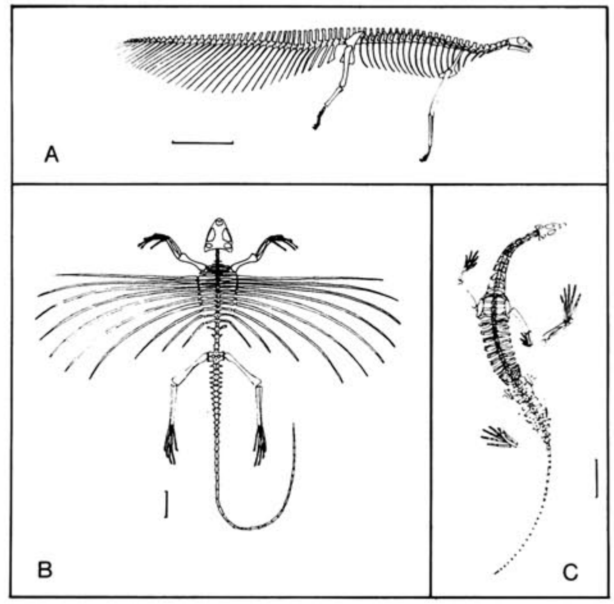

Figure 6.19: Reptiles from the hinge area of the Newark basin (Stops 6.6-6.8). A) "Deep-tailed" swimmer; B) *Icarosaurus siefkeri*; and C) *Tanytrachelos* cf. *ahynis*. Scale bars are all 2 cm. Modified from Olsen (1980c).

STOP 6.8: ROSS BOAT DOCK, PALISADES INTERSTATE PARK (by P.E. Olsen)

Highlights: Contact between Palisades sill and thermally-metamorphosed sedimentary rocks; arkosic sandstone in Lockatong Van Houten cycles.

Proceed north along road, slowly walking down section (Figures 6.20-6.22). Cycle 1' and overlying 4 m of arkose are present, with no sign of cycle 0 which presumably has pinched out or was cut out south of here. Cycle 1 is present but poorly exposed. Cycle 2 is very well exposed and contains the fossils *Turseodus* and *Diplurus*. Cycles 3 and 4 are evidently replaced by wave-influenced buff, cross-bedded arkose. Cycles 5 and 6 are very well exposed. Middle part of division 3 of cycle 6 contains a distinctive nodular calcareous bed resembling caliche which was first seen at Stop 6.9. Cycle 5 still shows the same basic sequence of beds and vertebrates as at previous stops, but cycle 6 is noticeably coarser with fewer less well-developed laminations and fewer fish. Articulated *Tanytrachelos* skeletons are still present, however. Upper division 1 of cycle 6 has produced a 20-cm-long partial arthropod of uncertain relationships.

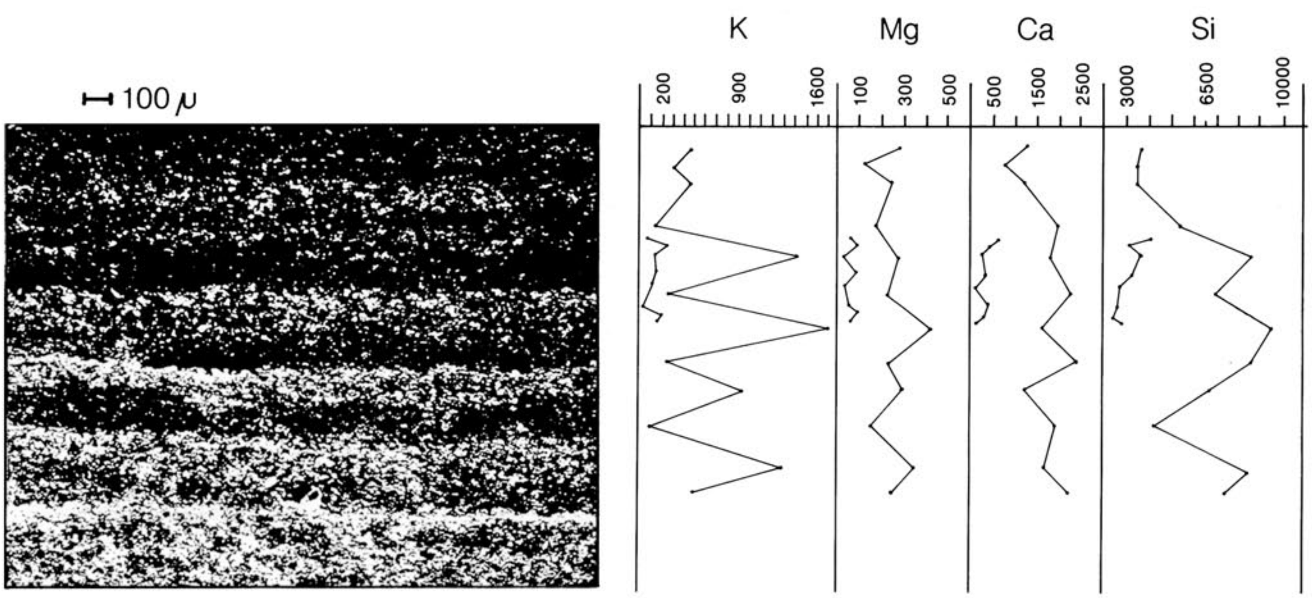

Figure 6.18: Scanning electron photomicrograph of microlaminated part of cycle 6 (Stop 6.6) and relative concentration of selected elements derived through an E.D.A.X. system. The numbers indicate only relative concentrations for a given element and are not comparable between elements. Counts have been integrated along the total length of the image of the couplet at the sampling horizon and are not point samples. Longer, very jagged lines are sampled only at the bottom and top of each couplet. Shorter, less jagged lines are closely-spaced sampling intervals which overlap a portion of the coarser line. K is in K-feldspar, whereas Ca and Mg are mostly in the form of albite which, prior to metamorphism, was calcite and probably ferroan dolomite. The K-rich layers were originally clay-rich, and Ca-rich layers were originally carbonate layers. Based on thin section examination of the same couplets, the K-rich layers have more organic carbon in them than the Ca-rich layers. From Olsen (1984a).

Figure 6.20: A) Sketch of discordant contact of Palisades sill and Lockatong Formation along Palisades Interstate Park road south of the George Washington Bridge near Ross Boat Dock, Stop 6.8. B) Outcrops of Palisades sill and cycles 0-d west of Ross Boat Dock. From Olsen (1980c).

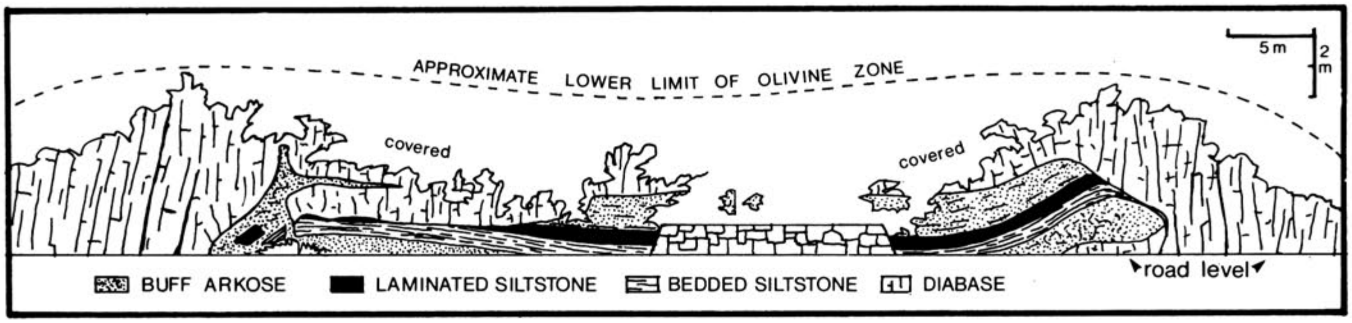

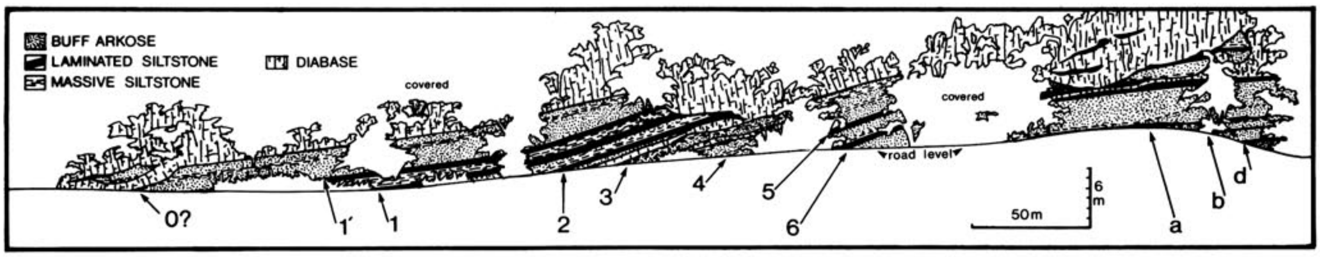

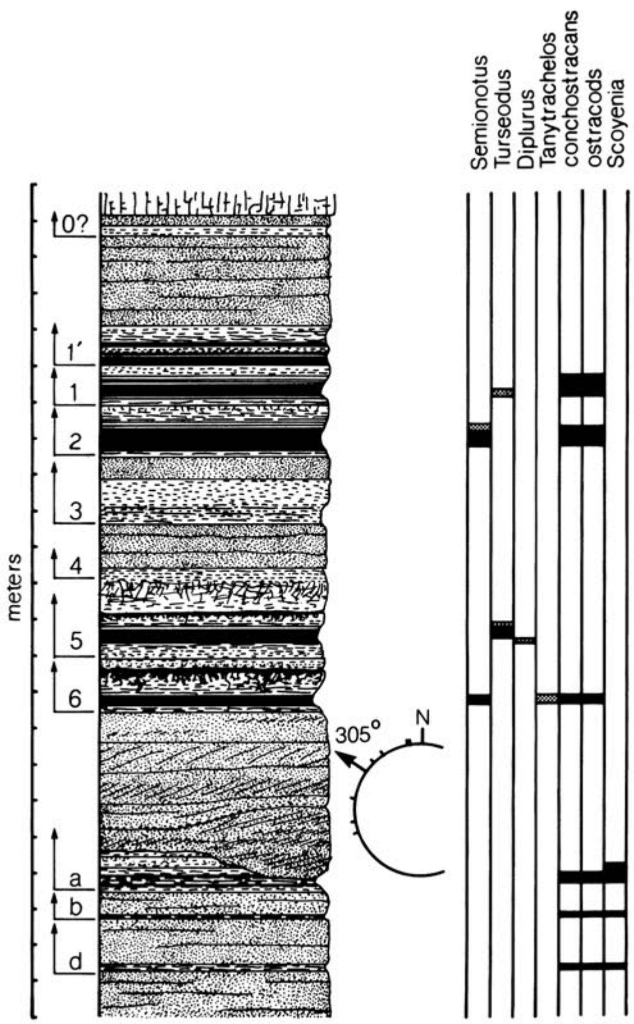

Figure 6.21: Measured section of outcrops west of Ross Boat Dock, Stop 6.8, showing distribution of major fossils and paleocurrent data (n=7) for cross-bedded buff arkose between cycles 6 and a. From Olsen (1980c).

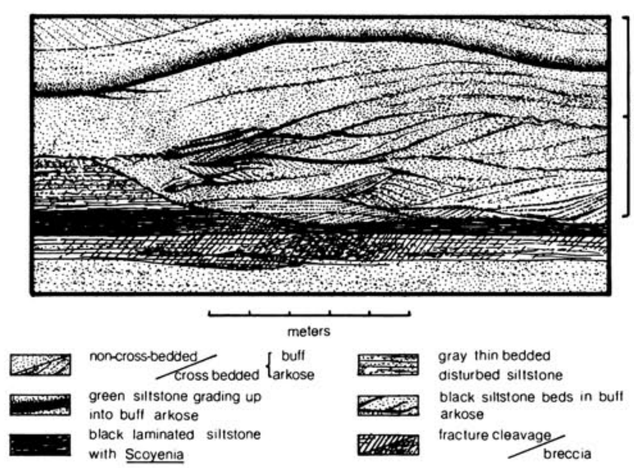

Figure 6.22: Sketch of downcutting cross-bedded arkose that eliminates most of cycle a (black laminated siltstone). Outcrop is northernmost of those sketched in Figure 6.21B. From Olsen (1980c).

The tongue of buff arkose between cycles 6 and a is slightly thinner than at Stop 6.6 and diplays unidirectional, oscillatory, and possibly hummocky cross stratification, suggesting wave reworking of very low relief deltas. Division 2 of unit a is cut out by the lower arkose beds of this sequence by a channel-fill sandstone with mudcracked mudstone interbeds. Mean paleocurrent direction for these cross-beds is N59°W (based on 8 readings) (Figure 6.22).

Cycle a is penetrated by numerous *Scoyenia* burrows (which were definitely not present at Stop 6.6) as are what appear to be cycles b and c. We are clearly in the shallow water facies of division 2 of cycles a-c at this point but only just leaving the deep water facies of division 2 in cycles 2, 5, and 6. Cycles 5 and 6 are punctured by *Scoyenia* in outcrops about 2 km to the north along the park road.

Cycle a shows well developed fracture cleavage in division 1. Cleavage dips 25-30° and strikes N78°E. Cleavage is strata-bound but discontinuous, passing laterally into breccia or non-cleaved beds. What is the significance of these structures?

The facies trend in the Lockatong Formation from Stops 6.5 to 6.7 is from a more central basin facies to a marginal facies. The previously seen monotony in horizontal continuity gives way laterally to heterogeneity. Those cycles with the best developed microlaminae and the best preserved fish at Stop 6.6 are also those which persist the furthest laterally with the least change.

Return to park entrance.

115.1 Leave park and turn right onto River Road which then becomes Main Street and then Hudson Terrace.

115.3 Turn left onto Plaza Road (Bergen County Route 12), proceed west.

115.45 Turn right onto extension of Hudson Road and entrance for George Washington Bridge to New York City.

116.1 Enter New York State and New York City at midspan of George Washington Bridge. Approximate contact of Stockton Arkose and metamorphic basement of the Manhattan prong; leave Newark basin.

116.7 Exit for West Side Highway and Northern Bus Terminal of Port Authority of New York and New Jersey. Keep left for Bus Terminal.

116.9 George Washington Bridge Bus Terminal.

7. HARTFORD BASIN, CONNECTICUT AND MASSACHUSETTS

GEOLOGY OF THE HARTFORD AND DEERFIELD BASINS (by R.W. Schlische and P.E. Olsen)

Structural Geology

The Hartford basin of Connecticut and Massachusetts is an east-tilted half-graben, 140 km long and 30 km wide, bounded on its eastern side by a predominantly normal fault system (Figure 7.1). The border fault system generally parallels the N-S structural fabric of the Devonian mantled gneiss domes, suggesting that the border faults may be reactivated structures (Wise and Robinson, 1982). Notably, most of the eastern border fault system is oblique to the early Mesozoic extension direction given by Early Jurassic diabase dikes; if the Ratcliffe-Burton (1985) model holds, a component of right-lateral shear is predicted for the N-S trending faults. The N60°W extension direction did produce a series of N30°E-striking normal faults east of the Connecticut River, giving the border fault system in that region a jagged nature (Wise and Robinson, 1982). In addition, gravity studies indicate the eastern border fault system may consist of a series of "riders", with the deepest portion of the basin occurring somewhat west of the mapped border fault near the Connecticut-Massachusets state line (Eaton and Rosenfeld, 1960; Chang, 1968;Wenk, 1984a,b,c). The western edge of the basin consists of a number of minor antithetic (?) normal faults and unconformable onlap with basement rocks.

Numerous intrabasinal faults that generally strike N30°E cut the Hartford basin (Figure 7.1). Many of the faults have subhorizontal slickenlines and show apparent left-lateral or normal offset, although slickensides indicate both left- and right-lateral movement. Sanders (1963) suggested that these faults were primary strike-slip faults with real horizontal displacements of as much as 30 km. On the basis of subhorizontal slickenlines overprinting subvertical slickenlines, de Boer and Clifford (1988) argued that NE-striking faults formed during NW-SE extension and were later reactivated with relatively minor lateral movement during NE-SW compression.

A series of transverse folds characterizes the hanging wall of the border fault system. As in the Newark basin, these folds die out away from the fault in the hanging wall, they do not fold the fault, they do not extend into the footwall, and they are associated with principally normal-slip faults. Although the precise timing of the folding is not known in the Hartford basin, these folds may owe their origin to a similar mechanism as that proposed for the Newark basin (section 5).

A 5-km-wide neck joins the Deerfield basin of Massachusetts with the Hartford basin to the south. Like the Hartford basin, the Deerfield basin (Figurer 7.1) is an east-tilted half-graben bounded on its eastern side by a

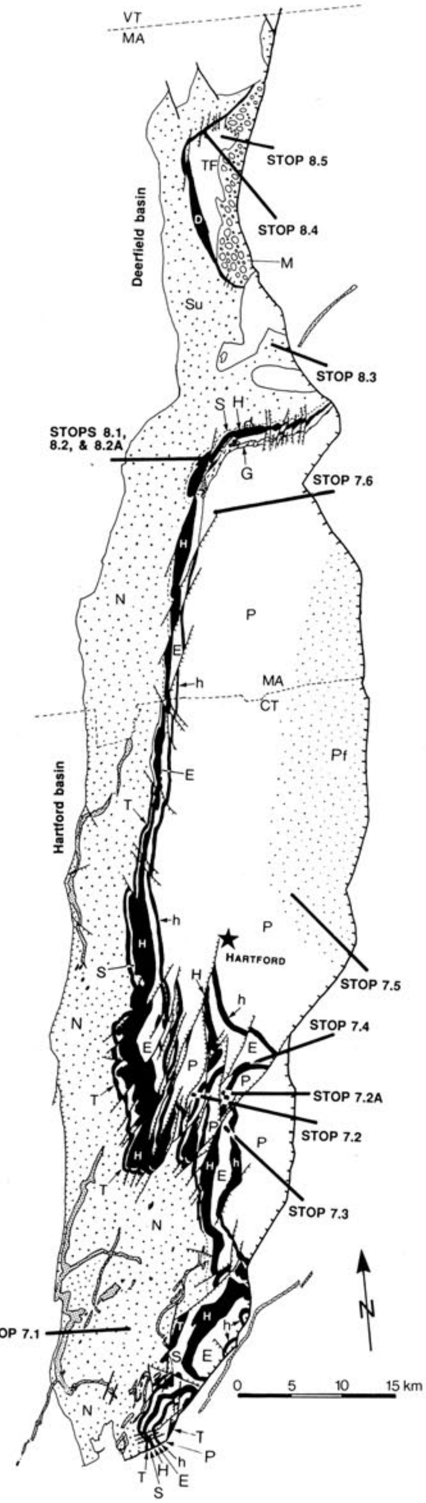

Figure 7.1: Geologic map of the Hartford and Deerfield basins, Connecticut and Massachusetts. Regular stipple represents diabase; black represents basalt flows. Abbreviations are: N, New Haven Arkose; T, Talcott Basalt; S, Shuttle Meadow Formation; H, Hampden Basalt; E, East Berlin Formation; h, Holyoke Basalt; G, Granby Tuff; P, Portland Formation; Pf, fluvial Portland Formation; Su, Sugarloaf Arkose; D, Deerfield Basalt; TF, Turners Falls Sandstone; and M, Mt. Toby Conglomerate. Based on Rodgers (1985) and Zen (1985).

Table 7.1: Stratigraphy of the Hartford basin, Connecticut and Massachusetts (after Krynine, 1950; Lehman, 1959; Cornet, 1977a)

Units	*Thick-ness (m)*	*Age*	*Description*
U. Portland Fm.	1000	Pleinsbach.	Red, coarse, fluvial and alluvial clastics
L. Portand Fm.	1000	Hettangian-Sinemurian	Mostly red, cyclical, shallow water lacustrine clastics; some gray and black lacustrine (some deep-water) clastics with minor limestone; minor red fluvial and alluvial clastics
Hampden Bst.	60	Hettangian	Tholeiitic basalt flows
East Berlin Fm.	150	Hettangian	Mostly red, cyclical shallow water lacustrine clastics; some gray and black lacustrine (often deep-water) clastics with minor limestone; minor red fluvial and alluvial clastics
Holyoke Bst.	100	Hettangian	Tholeiitic basalt flows
Shuttle Meadow Fm.	100	Hettangian	Mostly red, cyclical shallow-water lacustrine clastics; some gray and black lacustrine (often deep-water) clastics with minor limestone; minor red fluvial and alluvial clastics
Talcott Bst.	65	Hettangian	Tholeiitic basalt flows
New Haven Arkose	2250	L. Carnian-Hettangian	Red and brown, coarse, soil-modified fluvial clastics

predominantly normal-slip fault (dipping 30°W), which closely follows the trend of the west flank of the Devonian Pelham dome (Wise, 1988). NNE-striking normal faults have been ascribed to NW-SE extension; thrust faults, recumbent folds, and conjugate strike-slip faults (see Stop 8.4 and 8.5) are interpreted by Wise (1988) as indicating a later period of NE-SW compression.

Stratigraphy and Basin Filling Model

The Hartford basin contains approximately 4 km of basin fill divided into seven formations (Table 7.1). From oldest to youngest, these are the New Haven Arkose, Talcott Basalt, Shuttle Meadow Formation, Holyoke Basalt, East Berlin Formation, Hampden Basalt, and Portland Formation. The New Haven Arkose is primarily fluvial, in accord with the predictions of the basin filling model (see overview), although the Hartford basin appears to have remained an open basin for a much longer time than the Newark basin. It is also possible that the basin grew to such a size that rivers had to flow a long distance before ponding (J.P. Smoot, written comm.) and that lacustrine deposits are located up-dip of exposed fluvial strata and now eroded. The predominantly lacustrine strata in the sedimentary formations between the Jurassic basalt flows show the same characteristics as in the Newark basin: deep lake deposits and high accumulation rates. The fluvial deposits in the upper Portland Formation suggest a return of open-basin sedimentation perhaps because subsidence had slowed sufficiently or stopped.

Four formations comprise the approximately 3.75-km-thick Deerfield basin section (Table 7.2). The Deerfield basin basically mirrors the stratigraphic pattern of the Hartford basin and its agreement with the basin filling model, except that only one basalt flow sequence is present. The Deerfield basalt is essentially equivalent to the Holyoke Basalt of the Hartford basin.

Broad Terrane Hypothesis

Russell (1879) and Sanders (1963), among others, suggested that the Hartford and Newark basins are erosional remnants of a once much larger full-graben (the broad terrane hypothesis), the basins being separated by a very broad post-depositional longitudinal arch. Evidence in support of this hypothesis includes: (1) the Newark basin is a NW-tilted half-graben bounded on the NW by a SE-dipping normal fault; (2) the Hartford basin is an E-tilted half-graben bounded on the E by a W-dipping normal fault; and (3) the lava flows and interbedded sediments of both basins form similar sequences (compare Tables 5.1 and 7.1). Arguments against the broad terrane hypothesis are: (1) provenance studies by Abdel-Monem and Kulp (1968) and Ratcliffe (1980) which suggest that sediments were

Table 7.2: Stratigraphy of the Deerfield basin, Massachusetts (after Emerson, 1891; Cornet, 1977a).

Units	*Thick-ness (m)*	*Age*	*Description*
Mt. Toby Cgl. Turners Falls Sandstone	2000	Hettangian	Mostly red, coarse alluvial clastics; lateral equivalent of Turners Falls Ss. Mostly red, cyclical, shallow-water lacustrine clastics; some gray to black, cyclical lacustrine limestones with deep water intervals
Deerfield Bst.	50	Hettangian	Tholeiitic basalt flows
Sugarloaf Arkose	1700	Norian?	Red, buff, and minor gray, coarse to fine fluvial and alluvial clastics

derived from crystalline rocks to the northeast and southeast of the Newark basin, indicating that the longitudinal arch was a high even during deposition; (2) significant differences in thickness between homotaxial formations of the two basins; (3) paleontologic studies showing fish populations unique to each basin (Olsen *et al.*, 1982); and (4) identification of east-flowing paleocurrents and deltaic units in the Hartford basin by LeTourneau and McDonald (1985) and McDonald and LeTourneau (1988). However, although the Newark and Hartford basins were not connected, both were influenced by coeval tectonic and climatic events.

mileage

From George Washington Bridge Bus Terminal of the Port Authority of New York and New Jersey in northern Manhattan (end of Day 6), enter onto I-95 North (Cross Bronx Expressway) and proceed on I-95 North to Intersection with I-287, where mileage begins.

0	At intersection of I-287 and I-95, continue north on I-95.
0.9	Connecticut state line. Note outcrops of high-grade metamorphic rocks.
8.5	Stamford, CT.
29.0	Bridgeport, CT.
45.0	Enter Hartford basin.
47.2	At New Haven, CT, enter I-91 North toward Hartford (Exit 48). Fork to the right and then to the left.
48.5	East Rock (diabase) is on the left protruding through New Haven Arkose.
53.3	Take Exit 10, CT 40 towards Hamden and Cheshire (northwest).
55.5	Park at outcrop along road.

STOP 7.1: NEW HAVEN ARKOSE, HAMDEN, CT

(by J.P. Smoot and P.E. Olsen)

Highlights: Paleosol caliche and braided stream deposits.

This outcrop reveals about 70 m of New Haven Arkose (Figure 7.2) that is near the middle of the 1950-2250-m-thick interval in this vicinity. Hubert *et al.* (1978) interpreted this deposit as representing flash-flooding braided river deposits in a semi-arid flood plain. The outcrop is dominated by pale red conglomerate, pebbly sandstone, and arkosic sandstone that contain a complex mixture of scour surfaces, planar stratification, and cross bedding. This outcrop is typical of the New Haven Arkose in showing extreme bioturbation, not only by roots, but also the ubiquitous *Scoyenia*.

Hubert *et al.* (1978) envisage this deposit as consisting of a series of channel scours filled with longitudinal and transverse bar structures. Planar lamination in pebbly sandstone is common and is interpreted as upper flow regime deposits. Tabular cross beds and low-angle inclined beds are believed to be bar front deposits formed during waning flow. Less common small-scale trough cross bedding and ripple cross lamination represent low flow stage deposits around bar forms. Thin mudstone partings

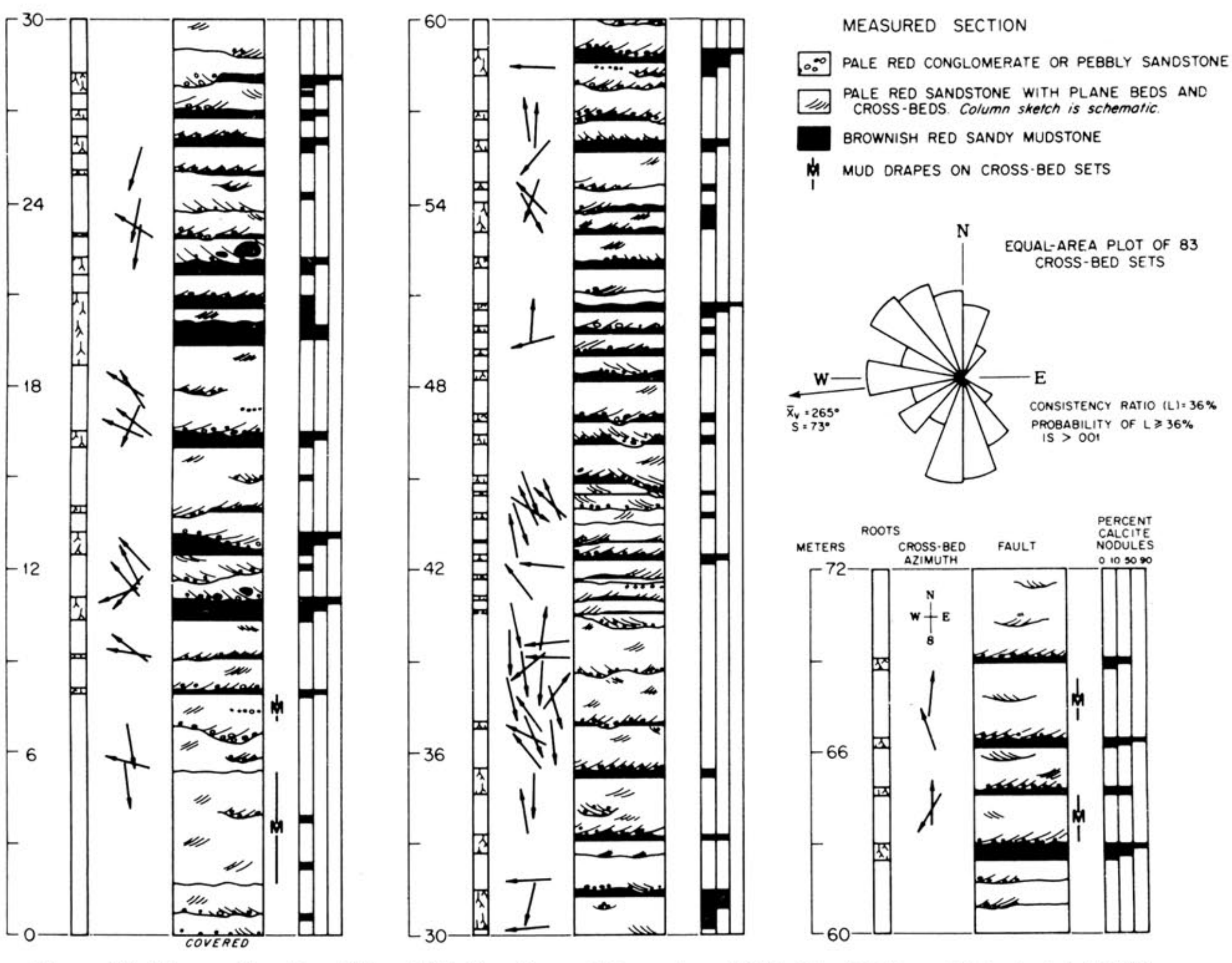

Figure 7.2: Measured section of the middle New Haven Arkose along CT 40, Stop 7.1. From Hubert *et al.* (1978).

may directly overlie planar-bedded pebbly sandstone, suggesting rapid fluctuations in discharge. Paleocurrent roses by Hubert *et al.* (1978) based on measurements of all inclined beds show a wide scatter that is consistent with the interpretation of mixed bar deposits and low flow-stage bed forms. The vector mean for their measurements is S85°W with a 99% statistical confidence level. The signficance of this, however, is unclear since bar aggradation is not necessary in the down-flow direction, and low-stage bed forms will orient around the bar shapes.

Thicker beds of sandy mudstone commonly contain root casts, and carbonate nodules, and tubules that form discrete layers (Figure 7.3). The carbonate layers are interpreted by Hubert *et al.* (1978) as caliche horizons formed on the flood plains. They believe that the caliche profiles are indicators of semi-arid conditions after Gile *et al.* (1966).

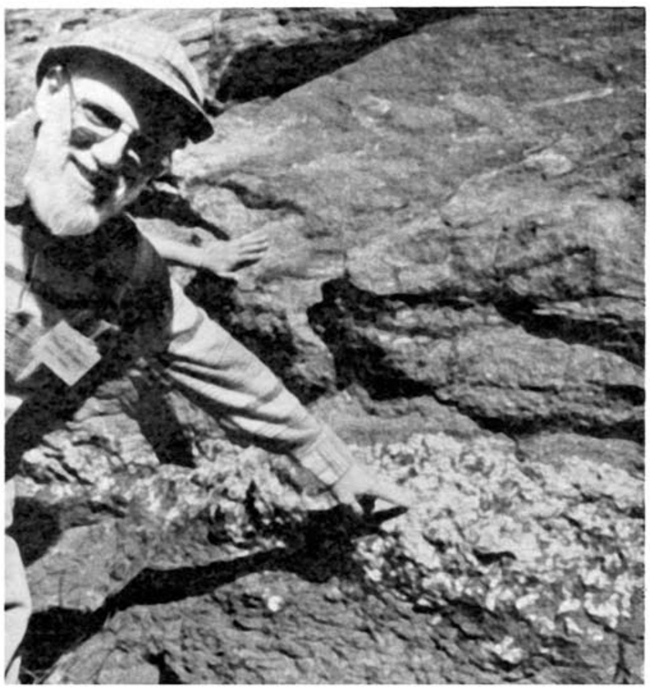

Figure 7.3: John Hubert pointing to a particularly well-developed caliche horizon in New Haven Arkose at Stop 7.1. Photo by P.E. Olsen.

The New Haven Arkose, quite unlike coeval coarse-grained facies in the Culpeper, Gettysburg, and Newark basins, apparently does not grade laterally into lacustrine deposits, and paleocurrent data indicate through-flowing streams. The only gray deposits in the formation are definitely fluvial (such as those at Forestville, CT; Krynine, 1950). Transgressive-regressive cycles are thus absent from the New Haven Arkose. Nonetheless, if periodic climate change was responsible for the Van Houten cycles in the contemporary strata of the Newark and other basins, then those climate fluctuations must have influenced the Hartford basin as well. Because the duration of the climate cycles may be similar to the amount of time it supposedly takes to form the caliche profiles (Hubert *et al.*, 1978), no single climate type can be assigned the caliches and associated strata of the New Haven Arkose; the caliches may have formed only during the drier parts of climate cycles.

56.3 Continue northwest on CT 40. Fork to the left onto CT 10 South. Turn left at the end of ramp and left again to get onto CT 40 East (*i.e.*, turn around and get back on CT 40, heading in the opposite direction).

58.9 Get back onto I-91 North. Go to the left (toward Meriden).

64.0 Outcrops of New Haven Arkose on the left.

65.9 Outcrops of New Haven Arkose in the median on the left.

72.4 Outcrops of uppermost New Haven Arkose. The ridges ahead are the Hanging Hills of Meriden, tilted fault-blocks of basalt and interbedded sedimentary units.

73.1 Outcrops of pillow basalt of the Talcott Basalt on the right. The Talcott Basalt is apparently a time equivalent of the Orange Mountain Basalt in the Newark basin (Figure I.9).

73.3 Outcrops of lowermost Shuttle Meadow Formation on right. Higby Mountain on the right.

73.9 Outcrops of lower to middle Shuttle Meadow Formation in the creek to the left and in the bank to the right. The lower two lacustrine cycles of the Shuttle Meadow with fish-bearing black shales are exposed in the stream. A lacustrine calcareous sandstone in the middle Shuttle Meadow Formation on the right produces disarticulated fish and clams. The cycles of the Shuttle Meadow Formation match those in the Feltville Formation of the Newark basin exactly (Figure I.9) and represent Jurassic time intervals E2c,d and E3a (Figure I.10).

75.0 Faults and Holyoke Basalt with splintery fractures. The Holyoke Basalt is thought to be a time and geochemical equivalent to the Preakness Basalt of the Newark basin (Figure I.9).

75.6 Glacial scour on the right.

77.3 Exit right to CT 72 at Exit 21. On the right side of the exit ramp is an exposure of Hampden Basalt. Turn right (west) on CT 72 toward Berlin.

79.2 Outcrop of Hampden Basalt on CT 72. The Hampden Basalt is a geochemical and time equivalent of the Hook Mountain Basalt of the Newark basin (Figure I.9).

80.2 Outcrop of Hampden Basalt.

80.3 Type section of East Berlin Formation. Red beds and black shales.

80.8 Exit right onto CT 15 South (Berlin Turnpike) toward Meriden and New Haven.

81.0 Turn right following CT 15.

81.1 Turn left onto Mill Street.

81.15 Turn right onto CT 15 (follow signs).

81.3 Make a U-turn. Go to the new road cut (under construction in early 1989).

STOP 7.2: CT 9 ROAD CUT, EAST BERLIN, CT

(by P.E. Olsen, N.G. McDonald, and R.W. Schlische)

Highlights: Upper 3/4 of East Berlin Formation, Westfield fish bed, hydrocarbons, lake cycles, dinosaur tracks.

Stratigraphy

In the Fall of 1988, these exposures at the intersection of CT 9, CT 15, and CT 72 revealed over 120 meters of the upper two-thirds of the East Berlin Formation and almost all of the Hampden Basalt. The exposure consists of cyclical red, gray, and black lacustrine units and subordinate fluvial strata. The presence of lacustrine cycles in the East Berlin Formation was first recognized by Krynine (1950), with later work carried on by Klein (1968), Hubert and Reed (1978), Hubert *et al.* (1978, 1976), and Demicco and Gierlowski-Kordesch (1986). These cycles are virtually

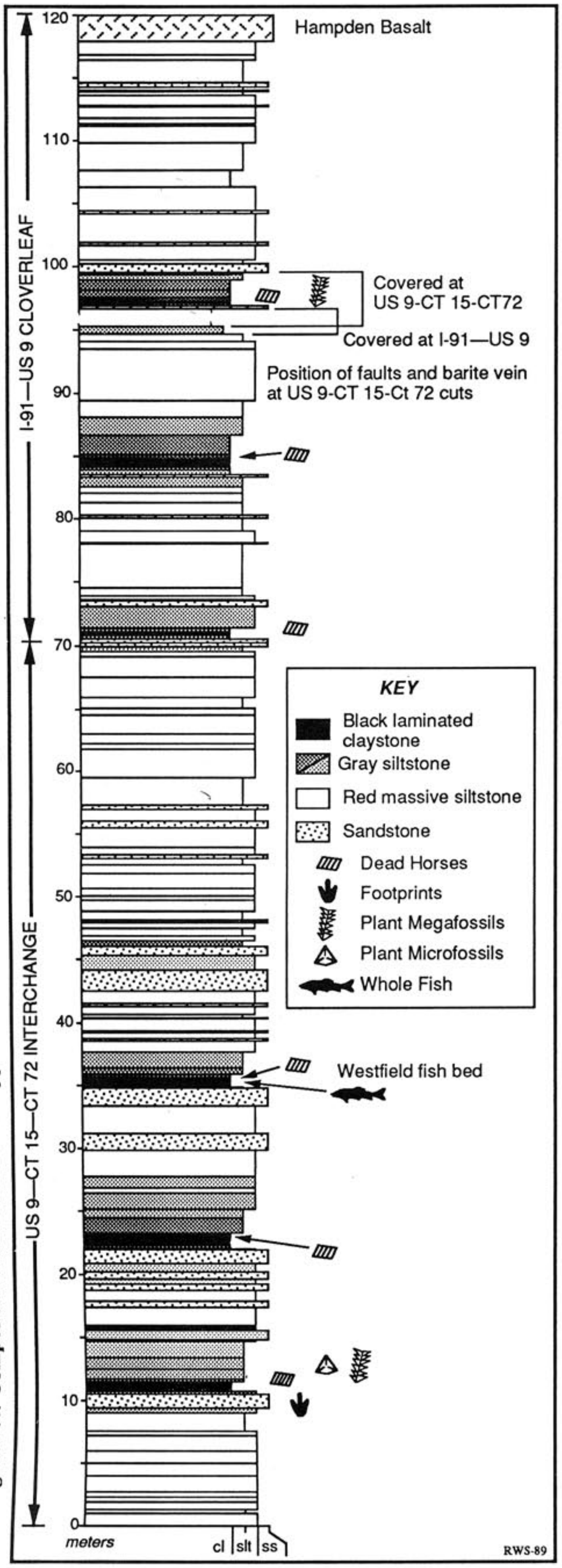

Figure 7.4: Composite measured section of upper East Berlin Formation at Stops 7.2 and 7.2A. See Figure I.9 for a depth rank curve for this section.

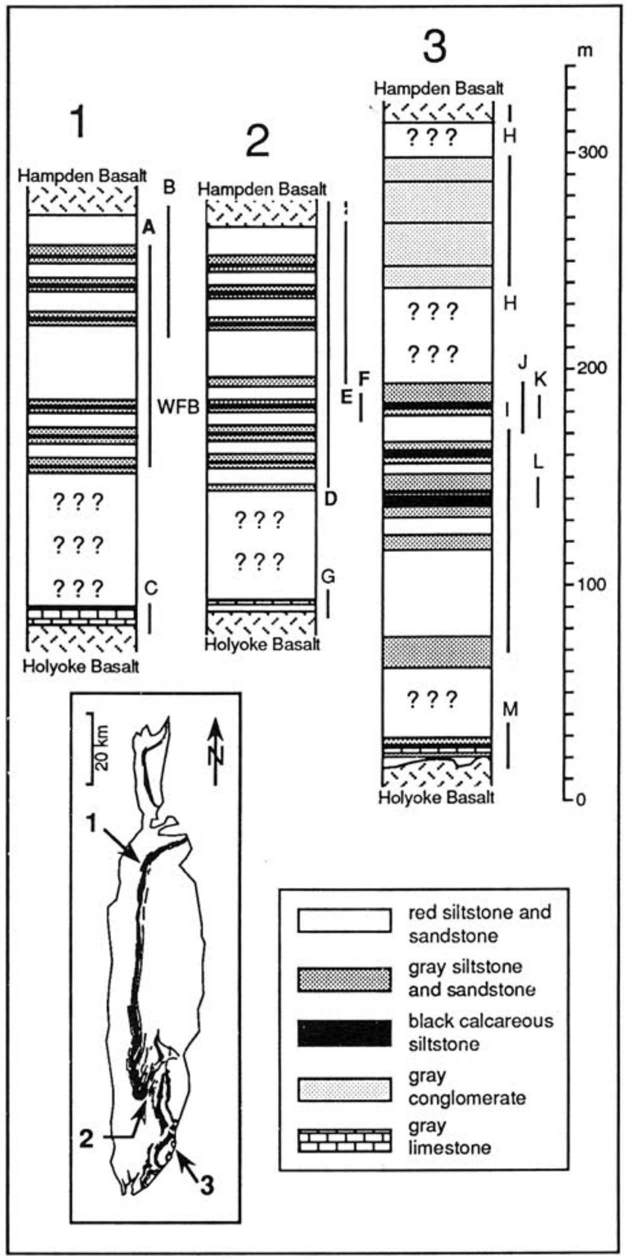

Figure 7.5: Correlation of the East Berlin Formation at three major areas of exposure: 1) Mt. Tom area, near Holyoke, MA; 2) East Berlin-Westfield area, central Connecticut; 3) Gaillard syncline area, southern Connecticut. Sections 1-3 are composites based on individual sections indicated to the right of each column as follows (sections seen as field stops indicated by a bold-face letter): A) Mt. Tom Ski Area, (Stop 8.1); B) I-91 cut, Mountain Park, MA; C) railroad cut at Ashley Pond, Holyoke, MA; D) US 9, Ct 15, Ct 72 cuts, East Berlin, CT (Stop 7.2); E) I-91, US 9 cuts, Cromwell, Connecticut (Stop 7.2A); F) Miner Brook outcrops, Westfield, CT (Stop 7.3); G) Spruce Brook outcrops, East Berlin, CT; H) Lake Quonnipaug outcrops (note that horizontal black lines denote valleys with no exposure, possibly underlain by shales); I) section in Sugar Loaf tunnel measured by Thorpe (1929); J) section measured at Lake Gaillard dam by Thorpe (1929); K) section along tributary of Branford River, North Branford, CT (see Figure 7.8); L) Roses Brook, east side of along tributary of Lake Gaillard; M) outcrop along creek on south side of Bluff Head, North Guilford, CT.

identical in form, but not in all fabrics, to the Van Houten cycles described by Olsen from the Towaco Formation (Olsen, 1980c). Jurassic time intervals P2a - P3d are represented here (Figures 7.4, I.9, I.10).

The lateral continuity of Van Houten cycles in the East Berlin Formation was demonstrated by Hubert *et al.* (1976) who showed the strong stratigraphic relationship between the mapped distribution of the Hampden Basalt and the underlying Van Houten cycles (Figure 7.5). Three Van Houten cycles are present in the upper part of this section and these correlate with the three cycles exposed on CT 72 a few hundred meters to the north as well as the three cycles exposed at the I-91/CT-9 cloverleaf, about 2 km to the east (Stop 7.2a) (Hubert *et al.*, 1978). A 35-m-thick section of red and minor gray and purple clastics separates the upper cycles from three more cycles in the middle East Berlin visible at this stop and CT 72. The uppermost of these three middle cycles contains a black, microlaminated carbonate correlative with the Westfield fish bed (Stop 7.3) (Figure 7.5). The Westfield fish bed is the most distinctive in the East Berlin Formation, and at all outcrops it contains a characteristic assemblage of fishes. Correlation of the microlaminae and turbidites in polished slabs from the middle of the fish-bearing carbonate leaves little doubt of the lateral continuity of this units (Olsen, 1988a). All six cycles, however, are well exposed at a number of places in the Hartford basin.

Fourier analysis of depth ranks of this section and exposures at Stop 7.2b reveals a clear hierarchy of periodicities in thicknesses of 12.0 m and 68.3 m. Assuming the 12.0-m-thick cycles to be the 21,000-year precession cycles, the 68.3-m-thick cycles have periodicities in time of 119,000 years. There are not, as stated by Demicco and Gierlowski-Kordesch (1986), 15 black-shale bearing cycles in the East Berlin. Rather, there is a clear hierarchy of cycles similar to that seen in the Lockatong and Passaic Formations and elsewhere.

This and the succeeding outcrop (Stop 7.2a) are unambiguous exemplars of the stratigraphy of the upper two-thirds of the East Berlin Formation. They show clear and precise homotaxiality with the Towaco Formation of the Newark basin (Figures I.9, 7.4). The lower three Van Houten cycles at this outcrop, for example, are correlative with the three exposed at The Glen in the Towaco Formation of the Newark basin (Stop 6.2). Nonetheless, the fish assemblages of the two formations are quite distinct (Olsen *et al.*, 1982; Olsen, 1983). The lakes which produced these cycles in the Newark and Hartford basins rose and fell synchronically, controlled by regional climate change, without being contiguous bodies of water.

Almost the entire thickness of the Hampden Basalt is exposed here. It is a high-TiO_2, high-Fe, quartz-normative tholeiite identical in composition to the Hook Mountain Basalt (see Overview) to which it appears to exactly correlate in time. According to Chapman (1965), there may be as many as eight flow units, although Gray (1982) suggested that the maximum may be closer to two flows. The basalt is typically massive but is very vesicular at the base. Tilted pipestem vesicles are common at the lower contact and indicate a northeasterly flow direction (Gray, 1982). The Hampden is the thinnest of the extrusives in the Hartford, reaching a maximum thickness of 30 m, and thinning and disappearing near the Massachusetts border, reappearing again on the back slope of the Mount Tom and Holyoke ranges at the northern end of the Hartford basin.

"Dead Horses"

Small-scale thrust fault complexes associated with bedding-parallel shear zones are commonly developed in the microlaminated black shales of division 2 of the Van Houten cycles as described at Stop 2.2. At this outcrop and elsewhere in the East Berlin and Towaco formations, black mudstone units above and sometimes within the microlaminated intervals contain what we call "dead horses", small (<20 cm long) quadrangular pods of rock composed of laminae and layers oblique to the bedding surface (Figure 7.6). Similar structures occur in the Eocene Green River Formation and in a variety of other laminated shale sequences (J. Stanley, pers. comm., 1988). We interpret the "dead horses" as compacted and dissociated blocks, after the term "horse" for a fault-bounded sliver of rock and their "dead" or dismembered condition. Most

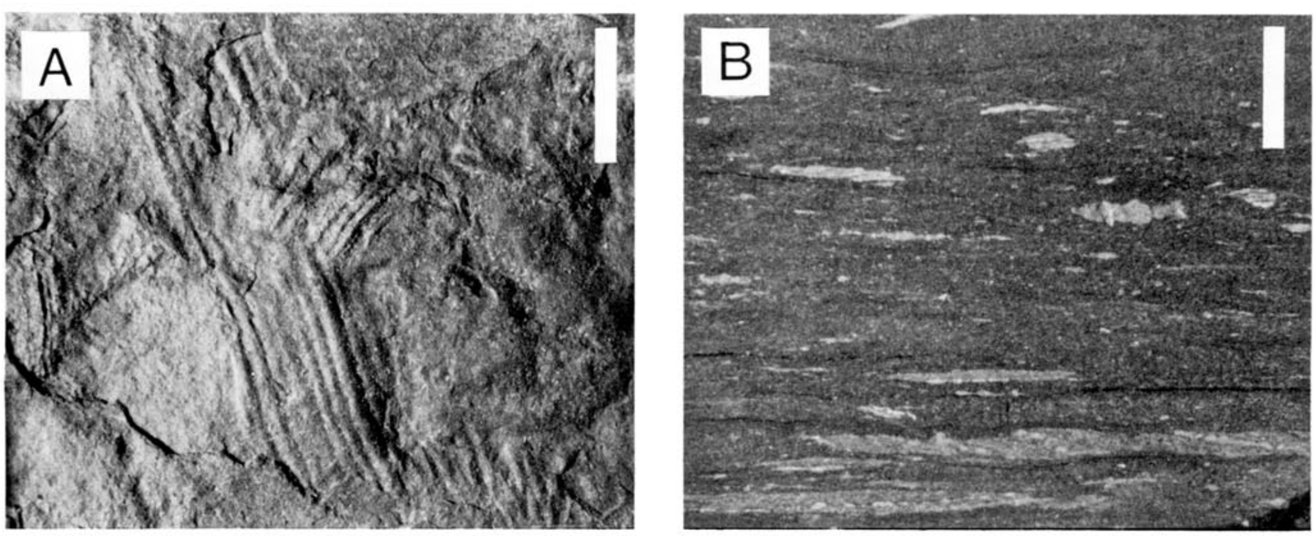

Figure 7.6: "Dead horses" from laminated siltstones at Stop 7.2: A) plan view (scale bar is 2 cm); B) cross-section in which the carbonate-rich "dead horses" show up as the lighter patches with oblique lamination (scale bar is 1 cm). Photo by P.E. Olsen.

commonly, these "dead horses" float in a matrix of massive black mudstone; however, there is a progression from jumbled and partly associated masses of these blocks with no matrix, to isolated blocks in layers composed mostly of matrix. The associated massive mudstone suggests that partial liquefaction accompanied the deformation which produced the dead horses. Beds composed of these black massive mudstones and "dead horses" have usually been interpreted as depositional units, but we interpret them as a form of low-pressure structural mélange.

We suggest that bedding plane-parallel shear lead to three intergradational types of deformation depending on depth of burial and pore-fluid pressure: 1) shallow bedding plane shear with the development of plastic folds, duplexes, considerable liquefaction, and the production of "dead horses "; 2) intermediate depth bedding-plane shear with abundant slickenside formation, some brecciation, some mineralization of voids, and small amounts of liquefaction; 3) completely brittle shear with extensive slickensiding and decalcification, with the production of platy, polished horses. All of these structures involve at least small-scale thrust faults and concomitant fault-bend folds. They can easily be confused with "slump" structures, which require a free upper surface, and are usually interpreted as indicators of paleoslope. Although the ultimate tectonic origin of these bedding-parallel shear-related structures is not understood, they cannot be assumed to be related to paleoslope.

Figure 7.7: Barite vein within fault zone at Stop 7.2. See Figure 7.4 for location within section. Scale bar is 1 cm. Photo by P.E. Olsen.

Hydrocarbons

Hydrocarbon staining is ubiquitous at this outcrop. Most joints and minor faults show some staining and many sandstone beds show matrix staining. The thermal maturity of these outcrops is quite low (0.5 R_o, T_{max} 439°C, Pratt *et al.*,1988), falling in the upper part of the oil window. The black shales are mature source rocks (Pratt and Burruss, 1988) yielding a mature oil extraction. A small fault is present in the East Berlin Formation close to and paralleling the surface trace of the contact with the Hampden Basalt. This fault is mineralized primarily with barite and sulfides but also shows early oil staining and some fluorite (Figure 7.7).

Paleontology

The gray mudstones and gray-black shale beds have generated most of the fossils at these outcrops. The gray units are palynologically productive and have also yielded carbonized leaf and twig fragments of the conifers *Brachyphyllum* and *Pagiophyllum* and the cycadophyte *Otozamites* (Cornet, 1977a). Other fossils include the conchostracan *Cornia* sp., coprolites, articulated but dephosphatized *Semionotus* and *Redfieldius* (in the equivalent of the Westfield fish bed), dinosaur tracks, and burrows and invertebrate trails in various gray and red lithologies (McDonald, 1982; McDonald and LeTourneau, 1988a).

81.4	Turn right onto CT 72 East.
84.4	Turn left at the traffic light onto Coles Road, heading north.
85.0	Turn left onto North Road Extension.
85.2	Pass under I-91.
86.1	Park.

OPTIONAL STOP 7.2a: I-91/CT 9 INTERCHANGE
(by R.W. Schlische)
Highlights: Upper East Berlin Formation; Hampden Basalt.

A series of four major exposures along the interchanges (first exposed in 1963 and under final construction at the time of writing) between I-91 and US 9 display the upper 70 m of the East Berlin Formation, including three gray and black units (for a more complete discussion, see previous stop description). The top of the section contains the contact with the overlying Hampden Basalt. The uppermost black shale-bearing Van Houten cycle is better exposed here than at Stop 7.2.

	Turn around and leave, heading south on North Road Extension.
87.6	Turn right (south) at stop sign onto Coles Road, and go back the way we came.
88.2	Cross CT 72. Stay on Coles Road, heading south. (Road becomes East Street.)
88.25	Cross Mattabesset River.
89.0	Turn right into Town Colony Drive Condominiums. Go down the road to the creek (Miner Brook) with exposures of Westfield fish bed.
89.1	Park.

STOP 7.3: MINER BROOK, WESTFIELD, CT

(by N.G. McDonald and P.E. Olsen)

Highlights: Westfield fish bed, conchostracans, "dead horses", folds and small thrust faults.

In one of the earliest references to Mesozoic fossils in North America, Silliman (1816) described fish from the "Westfield fish bed", and since that time the locality has been one of the most productive sites in the Newark Supergroup (McDonald, 1983). The holostean *Semionotus*, the palaeonisciform *Redfieldius*, and the large coelacanth *Diplurus* occur here. Typically, the abundant fish are preserved whole but are usually dephosphatized, with only an organic film remaining (McDonald and LeTourneau, 1989). Hence, this locality is probably in part responsible for the older reputation of Connecticut Valley fossils as being poorly preserved. The degree of fish dephosphatization decreases systematically with increasing terrigenous content. Thus, fish in the basin center, such as those here or at Stop 7.2, are almost completely dephosphatized and poorly preserved, whereas those found in the same unit but adjacent to the border fault show almost no dephosphatization and are very well preserved. This dephosphatization was probably microbially mediated under conditions of low sedimentation rates (McDonald and LeTourneau, 1989).

Four meters of the East Berlin Formation, including the Westfield fish bed, are exposed for a distance of 50 m along Miner Brook (see measured section in Figure 7.8). The hard, platy to flaggy, distinctly microlaminated black dolomitic limestone of the Westfield fish bed has also produced possible charophytic algae, vascular plants, clam shrimp (*Cornia* sp.), and coprolites (McDonald, 1982).

As at Stop 7.2, "dead horses" are common. Here we can see undisturbed microlaminated units passing abruptly laterally into aggregates of "dead horses", always adjacent to a bedding plane thrust fault or between two of them.

At times during the year, hydrocarbon "seeps" produce oil slicks in the stream. Pratt *et al.* (1988), Pratt and Burruss (1988), and Kotra *et al.* (1988) have studied the organic geochemistry of the Westfield fish bed at this outcrop and concluded that it is a mature source rock in the upper part of the oil window [0.6 R_o, T_{max} 440°C].

	Turn around and return to East Street (Coles Road).
89.3	Turn left (north) onto East Street (Coles Road).
90.0	Turn left (west) onto CT 72.
90.4	Turn right onto I-91 North.
92.0	Pass under interchange for CT 9 road cuts.
93.6	Exit right to West Street at Exit 23.
94.0	Turn right (east) onto West Street.
94.2	Hampden Basalt exposed at Corporate Ridge Building (on the flanks of an anticline). The anticline strikes east-west.
94.8	Turn right into Dinosaur State Park. Stop.

STOP 7.4: DINOSAUR STATE PARK, ROCKY HILL, CT (by N.G. McDonald and P.E. Olsen)

Highlights: Bedding plane covered with 500 tracks of carnivorous dinosaurs.

This site was discovered in 1966 during excavation for the foundation of a state building. Exposures here have revealed nearly 2000 reptile tracks, most of which have been buried for preservation and future exhibition. The

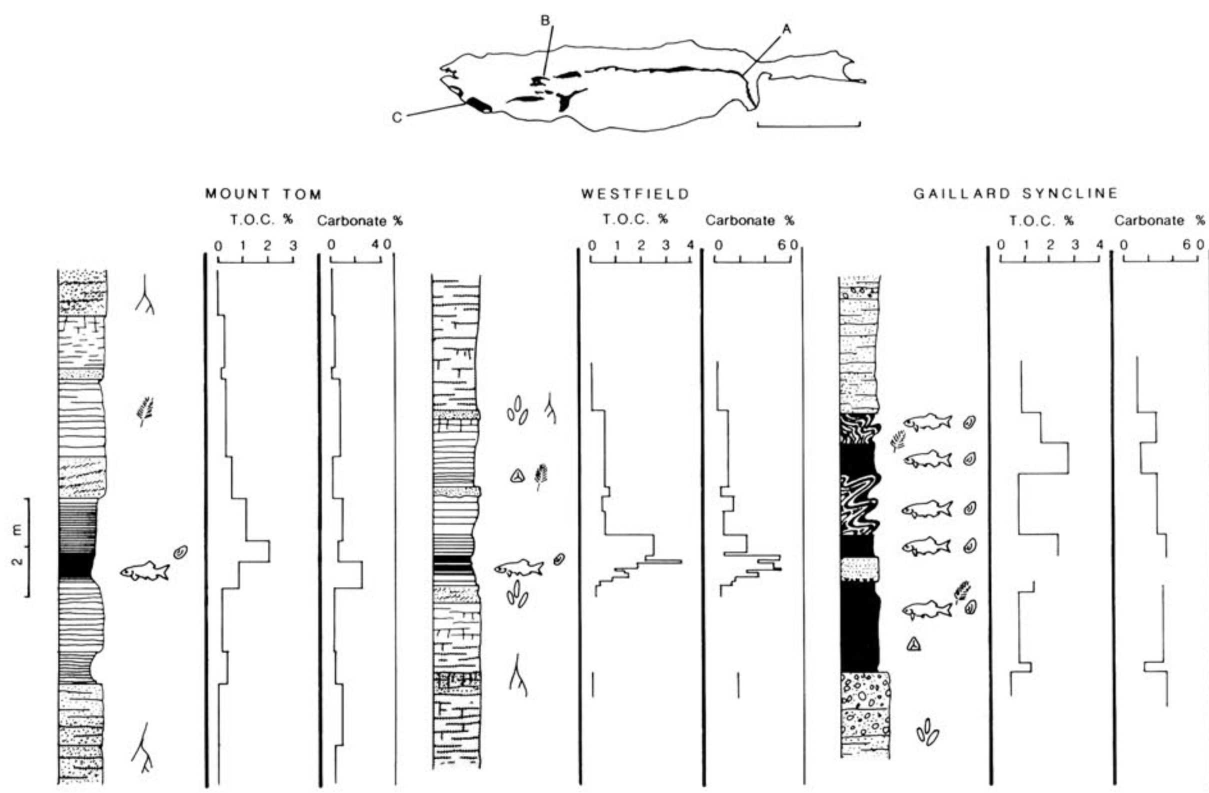

Figure 7.8: Measured sections of Westfield Fish Bed of the East Berlin Formation outcropping in three areas: Mt. Tom is Mt. Tom Ski Area (Stop 8.1); Westfield is Miner Brook outcrops (Stop 7.3), and Gaillard Syncline is section along tributary of Branford River, North Branford, CT. Key to symbols as in Figure 7.4. From Olsen (1984a).

present geodesic building at the park houses approximately 500 tracks. The tracks are found in the gray arkoses, siltstones, and mudstones of the East Berlin Formation, about 20 m below the contact with the Hampden Basalt. Ripple marks, raindrop impressions, mudcracks, and the footprints indicate shallow-water conditions deposition and some subareal exposure.

The ichnogenera *Grallator (Eubrontes)*, *Grallator (Anchisauripus)*, *Grallator* (*Grallator*), and *Batrachopus* have been identified at this locality (Ostrom and Quarrier, 1968) (Figure 4.9). However, large *Grallator* (*Eubrontes*) tracks are by far the most common and are the only tracks visible *in situ* within the geodesic dome. The width and spacing of tracks suggests that the track maker of *Eubrontes* was more than 2 m tall at the hip and 6 m long, but no osseous remains assignable to this animal have been recovered from the Hartford basin. The skeletal remains of the theropod dinosaur *Dilophosaurus*, known from the Early Jurassic Kayenta Formation of Arizona, are the best match for *Eubrontes*. Based on what appear to be claw drags without any pad impressions, Coombs (1980) suggested that some of the track-makers were swimming. The marks were probably made as the half-submerged reptile pushed itself along the bottom with the tips of its toes (Figure 7.9).

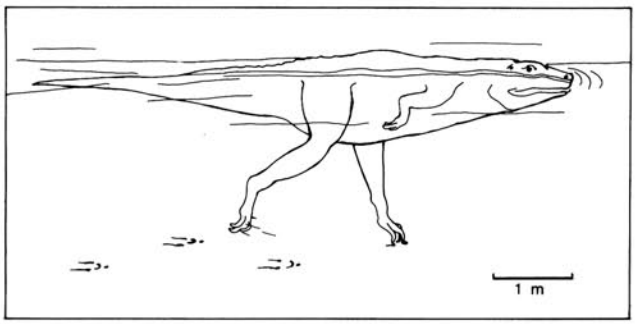

Figure 7.9: Reconstruction of swimming theropod dinosaur based on peculiar tracks found on the main *Grallator* (*Eubrontes*)-bearing bedding plane at Rocky Hill Dinosaur State Park, Stop 7.4. Traced and simplified from Coombs (1980).

95.0 Leave Dinosaur State Park. Go left on West Street.
95.8 Turn onto I-91 North.
96.3 Exposures of East Berlin Formation on right.
96.7 More exposures of East Berlin Formation on right.
97.5 Unfinished cloverleaf has cuts in Holyoke Basalt with faults mineralized with calcite and solid bitumen. Originally described as solid bitumen (Dana, 1878) and later as a coal (Nelson, 1964) and pyrobitumen (Grew, 1965), more recent geochemical work by Pratt and Burruss (1988) has shown that the material is a low temperature hydrocarbon with extracts almost identical to hydrocarbons extracted from the overlying black units of the East Berlin Formation.
98.2 Fossil fish in gray-black shale in stream bed on right (next to motel).
104.6 Get on I-84 East (right lane), Exit 30 in Hartford, CT.
105.2 At Exit 2, fork right to get on I-84 East, after crossing Founder's Bridge.
110.1 Note outcrops on left side of interstate. We will take the next exit and turn around to reach outcrops.
111.6 Exit at Buckland Road, Exit 62.
111.7 Turn left onto Buckland Road. (Outcrops of Portland Formation straight ahead.)
112.1 Turn left towards I-84 West (making a U-turn). The exposures on the right, once part of a quarry for building and dimension stone, produced 5 partial skeletons of the prosauropod dinosaurs *Anchisaurus* and *Ammosaurus* during the late 1800's (Galton, 1976).
112.3 Turn left onto I-84 West.
113.6 Road forks to the left.
113.8 Stop at outcrops on the right.

STOP 7.5: UPPER PORTLAND FORMATION, BUCKLAND, CT (by P.E. Olsen)

Highlights: Fluvial deposits, paleosol caliche.

Huge road cuts for I-84 near Buckland expose about 100 m of red, fluvial, conglomeratic arkose of the Early Jurassic Portland Formation, superficially resembling the New Haven Arkose. As in the New Haven Arkose, braided river sequences predominate, and some caliche is present. These strata may be the youngest in the Newark Supergroup, and unlike older Portland sequences (Stop 7.6) there are no indications of cyclic lacustrine deposits. If their apparent absence is real, these upper Portland fluvial strata may record a late part of Hartford basin history in which through-flowing rivers again dominated basin sedimentation. This facies package may be fundamentally different than the types of fluvial, alluvial and lacustrine Portland conglomerates and pebbly sandstones described by (LeTourneau, 1985b; LeTourneau and McDonald, 1985). According to our basin filling model, these units would have resulted from a decrease in basin subsidence rates.

Several faults (slightly recessive) cut the outcrops. The most prominent set is NE-striking and NW-dipping and can probably be attributed to NW-SE extension.

113.8 Continue west on I-84 back to Hartford.
119.3 Continue on I-84, cross the Connecticut River.
119.4 Exit onto I-91 North.
138.7 Massachusetts state line.
144.0 Springfield, MA. Continue north on I-91.
147.0 Cross Connecticut River.
152.2 Get off I-91 at Exit 16 to US 202 North, Holyoke, MA.
152.3 Turn right onto US 202.
153.5 Turn right onto Cabot Street toward downtown Holyoke.
153.8 Turn left onto High Street.
154.0 Turn right onto Appleton Street.
154.3 Turn left on Race Street (becomes North Canal Street).
154.9 Turn left onto MA 116 North. Cross canal.
155.0 Just before the big green bridge, turn left into parking lot.

STOP 7.6: HOLYOKE DAM, HOLYOKE, MA (by P.E. Olsen)

Highlights: Thrust faults, folds; evaporite pseudomorphs and abundant conifer fossils in lacustrine lower Portland Formation.

Descend hill from parking lot toward the river. Head upstream toward the dam. Beware of sirens which will signal that the floodgates are about to be opened. If so, head immediately to high ground.

Exposures below the Holyoke Dam on the Connecticut River provide the best outcrops of the fine-grained, lacustrine lower Portland Formation (see also LeTourneau and McDonald, 1985). The section consists mostly of thin-bedded gray siltstones, claystones, and carbonates, with a

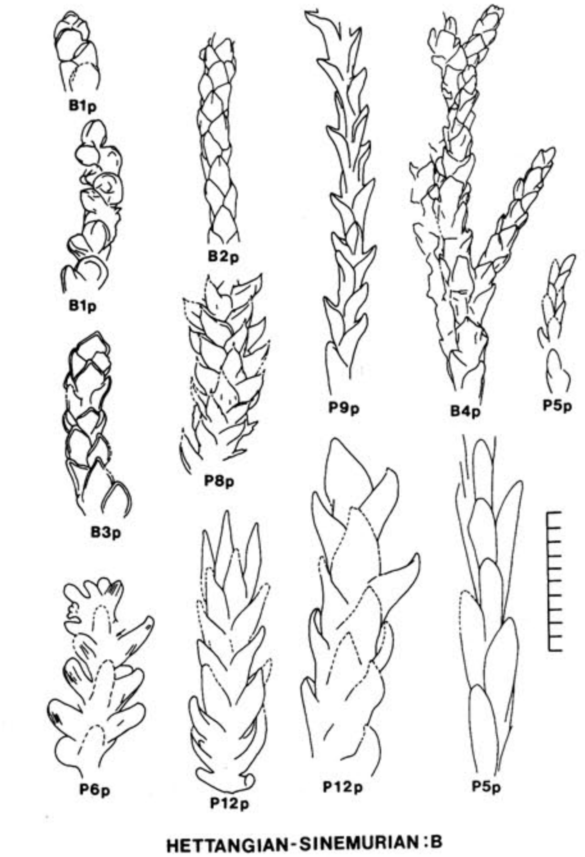

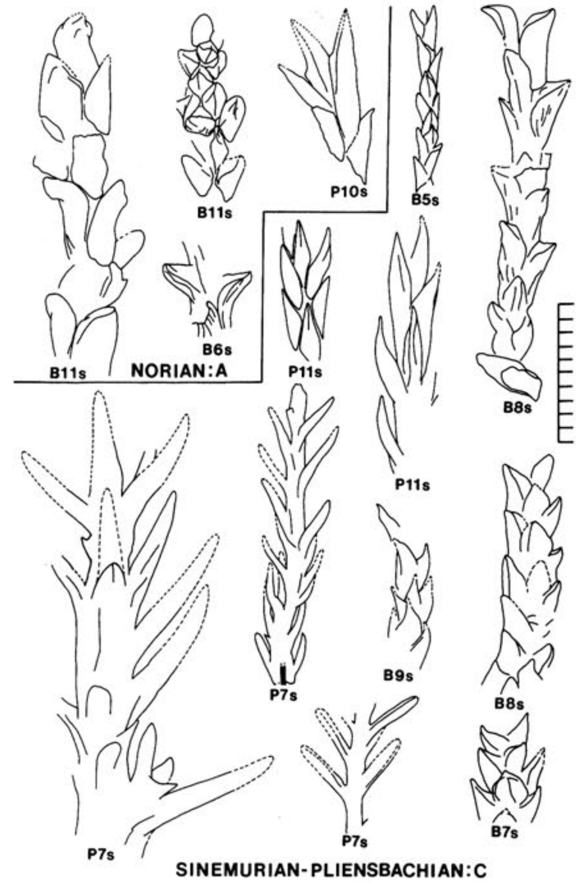

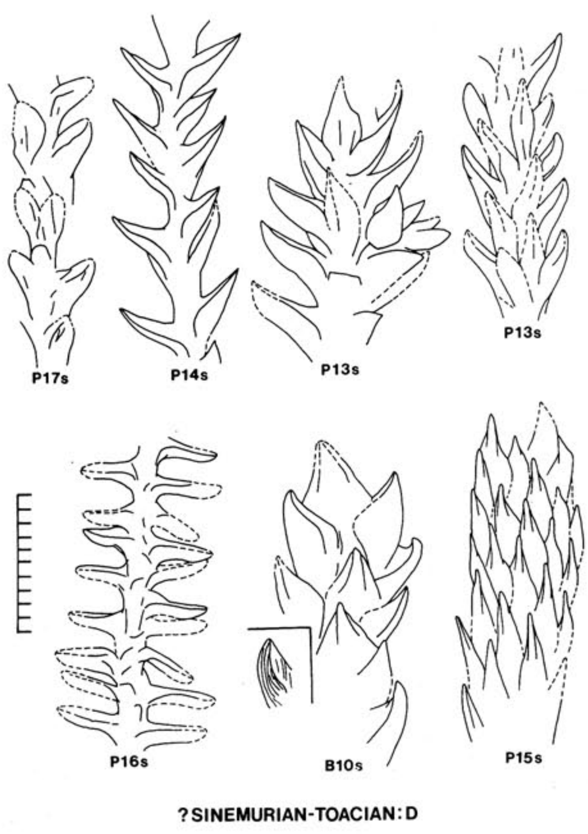

Figure 7.10: Jurassic conifer assemblages. Scale in millimeters; all figures drawn to same scale. Conifer Assemblage B: abbreviations are—B, *Brachyphyllum*; P, *Pagiophyllum*; 1-12, species number; p, papillate cuticle with slightly sunken stomata. Conifer Assemblages A and C: abbreviations as above and 5-11, species number; s, non-papillate or smooth cuticle. Conifer Assemblage D: abbreviations as above and 10-17, species number.

general trend to red beds higher in the section. Characteristic of these strata are very large cubes of pyrite, possible pseudomorphs after ?halite in gray and red-brown siltstones, and abundant conifer remains in gray claystones.

According to Wise (pers. comm., 1988) these outcrops show thrust faults and associated folds superimposed on very low-angle dip-slip detachments. This relationship can be seen in the west-facing exposure on the east side of the canal. Prominent recumbent folds and trains of recumbent folds are present adjacent to the larger thrust faults. The details of the stratigraphy are strongly disturbed by these faults and have yet to be worked out.

Leafy shoots, male cones, and cone scales of cheirolepidaceous conifers are abundant in gray silty claystones. This is one of the most prolific plant fossil localities in the Newark Supergroup and illustrates one of the major floral assemblage types found in these basins. The plant-bearing units also produce occasional disarticulated *Semionotus* sp., and reptile footprints occur in some gray and red platy, mudcracked siltstones.

JURASSIC CONIFER ASSEMBLAGES AND THEIR PALEOCLIMATIC IMPLICATIONS (by B. Cornet)

Unlike latest Triassic floral assemblages which are very heterogeneous and were comprised of a diversity of plant taxa (based on palynological study), Early Jurassic assemblages of the Newark Supergroup are relatively homogeneous and strongly dominated by one major group of conifers, the Cheirolepidaceae, and their pollen, *Corollina* spp., which make up usually at least 90% of most Jurassic palynoflorules (Cornet and Traverse, 1975; Cornet and Olsen, 1985). The greatest morphological diversity in this group appears to be among seed-cone scales, of which ten types have been found (Cornet, 1977a).

Small leafy shoots of *Brachyphyllum* and *Pagiophyllum* make up the majority of Jurassic megafossil floras in the Newark Supergroup (Figure 7.10) including the remains found at the Holyoke Dam. Within latest Triassic through Early Jurassic strata of the Newark Supergroup about 13 *Pagiophyllum* species and 11 *Brachyphyllum* species are

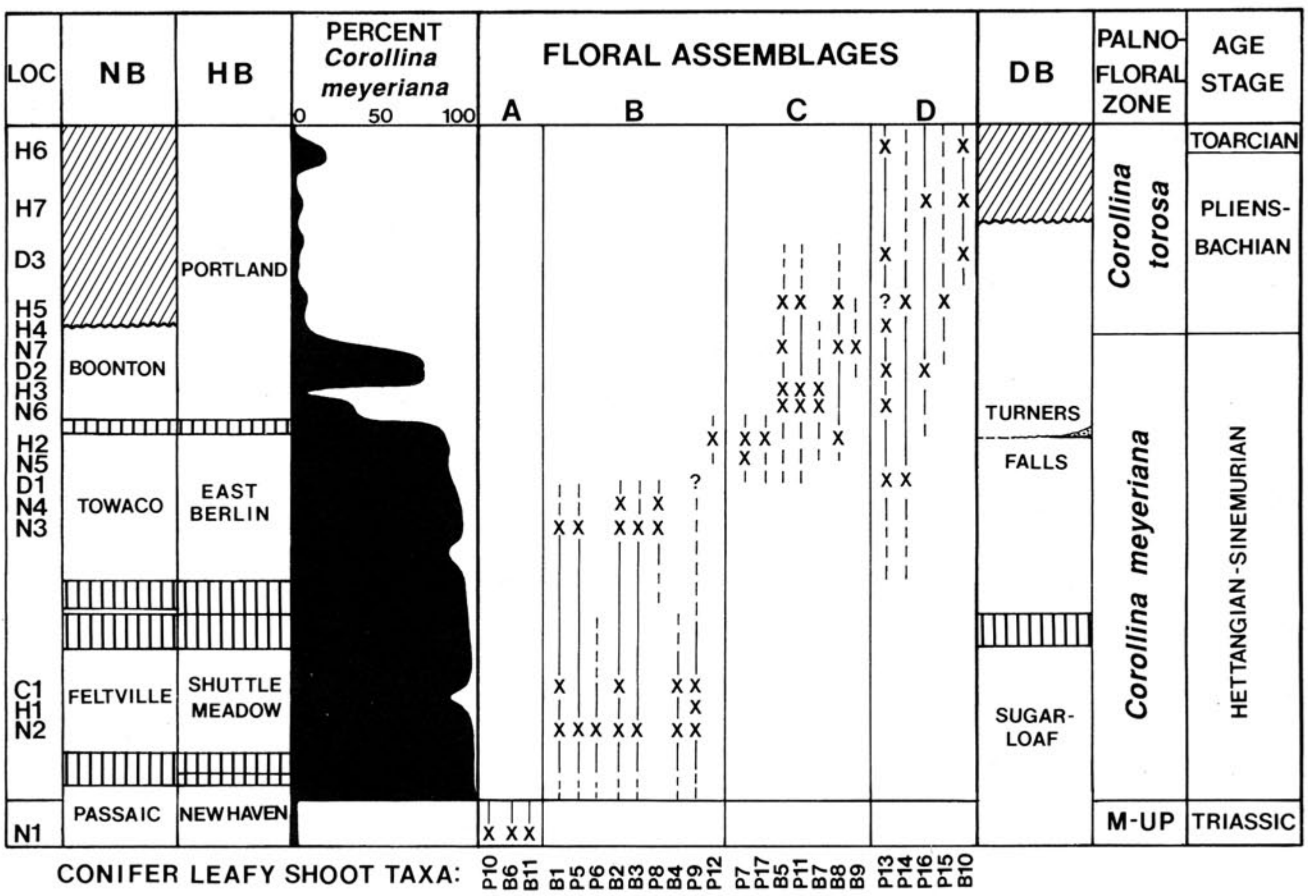

Figure 7.11: Distribution of Conifer Assemblages A-D within the uppermost Triassic and Jurassic sections of the Newark (NB), Hartford (HB), and Deerfield (DB) basins of the Newark Supergroup. Conifer taxa are illustrated in Figure 7.11 (X) indicates presence at the localities listed; (?) indicates presence of a similar but unnamed taxon. Newark basin: N1, Upper Passaic Formation; N2, middle Feltville Formation; N3, middle Towaco Formation (Pompton, NJ); N4, upper Towaco Formation; N5, upper Towaco Formation; N6, lower Boonton Formation; N7, upper Boonton Formation. Hartford basin: H1, lower Shuttle Meadow Formation; H2, upper East Berlin Formation; H3, lower Portland Formation; H4, Hadley Falls; H5, lower Portland Formation (Holyoke Power Co. dam, South Hadley Falls, Stop 7.6); H6, middle Portland Formation; H7, middle Portland Formation (Chicopee Falls at dam). Deerfield basin: D1, lower Turners Falls Sandstone (at dam; Stop 8.4); D2, middle Turners Falls Sandstone (Montague Falls); D3, upper Turners Falls Sandstone (Horse Race). Culpeper basin: C1, Midland Formation. Data from Cornet (1977a).

currently recognized, including *Hirmeriella muensteri* (Schenk) Jung, *Brachyphyllum scottii* Kendall, and possibly *Pagiophyllum peregrinum* (Lindley and Hutton) Schenk (Cornet, 1977a). Most of the 24 species of superficially similar leafy shoots are discriminated by one or more distinctive characteristics (for details, see Cornet, 1977a).

The 24 species can be divided into four assemblages based on association, leaf size and cuticular features (Figure 7.11). Each taxon has been given a code designation for simplicity and because many of the species have not yet been formally named. Assemblage A is the oldest (late Norian = Rhaetian) and has been recognized in the Passaic Formation of the Newark basin. All the leaf taxa in this assemblage have thin smooth cuticles and normal unsunken stomata. Assemblage A is important because it represents a group that survived the mass extinctions at the end of the Triassic in North America (Olsen and Cornet, 1988a, b). The members of assemblage B have thick papillate cuticles and slightly sunken stomata (*e.g.*, Cornet and Traverse, 1975), indicative of common ancestry. This group may have been derived from an unidentified member of Assemblage A or from a survivor of some Triassic community external to the Newark. These cuticular features are important, because they are considered adaptations for high insolation and dry air that would enable this plant to survive brief periods of climatic adversity.

Assemblage B persists in the Newark Supergroup through most of the zone of extrusives (Hettangian-Sinemurian) before it is replaced by Assemblage C in the upper Towaco Formation (Newark basin) and upper East Berlin Formation (Hartford basin) (Figure 7.11). However, megafossil remains of ferns, cryptogams, and their spores are more common and diverse in Assemblage B than in Assemblage C, suggesting that the climate was generally wetter in the zone of extrusives than for the overlying lower Portland Formation, despite the dominant type of conifer cuticle.

Assemblage C is dominated by conifer shoots with thin smooth cuticles, however. Yet, the presence of *Hirmeriella muensteri* (P11's; Cornet *et al.*, 1973), which in Europe is a coastal inhabitant possibly adapted to saline "mangrove" environments (Jung, 1968), and of common cycadophyte pollen (Cornet, 1977a) is consistent with lake beds of this zone which contain common crystal casts of gypsum and halite (Lorenz, 1988), possibly indicating a shift to drier conditions within the basins. An abundance of small leafy shoots and a scarcity of specimens showing more than one branch order in these lake beds suggests a physiological adaptation to annual periods of aridity by the deciduous loss of individual leafy shoots. The transition from Assemblages B to C roughly correspond to the transition from the *Corollina meyeriana* to the *Corollina torosa* palynofloral zones (Cornet and Olsen, 1985).

Assemblage D is found mainly within the Deerfield basin of Massachusetts (Figure 7.11) and differs from the other assemblages by a two to five times increase in size of leafy shoots (Figure 7.10), probably indicating large tall trees. The cuticles are thin and smooth, although they sometimes possess parallel grooves (Figure 7.10, B10's). Overall conifer diversity is higher than in assemblage C and associated plants include *Elatides falcifolia* (P16's) and *Araucaria imbricata* (B10's), which are non-cheirolepidaceous conifers.

Assemblage D existed at the same time that Assemblages B and C were dominant in more southern basins (Figure 7.11). Bain (1932) presented evidence that considerable relief in the form of high mountains probably existed to the north and east of the Deerfield basin, and Assemblage D could represent an allochthonous upland or even mountainous flora (*i.e.*, mist forest) that enjoyed a cooler and much wetter climate. The unusually intense bioturbation by *Scoyenia* and roots in red and gray Deerfield shallow-water lacustrine and fluvial deposits associated with Assemblage D, but not in correlative Hartford or Newark shallow lake and fluvial deposits (Olsen, pers. comm.), supports a more humid climate for the Deerfield basin than the Hartford or Newark basins. Differences in fish faunas for correlative lacustrine strata of the Deerfield and Hartford basins (Olsen, 1984a) may also be due to climate or isolation. The regional gradient seems to have been towards aridity in the north throughout the early Mesozoic (Cornet, 1977a; Hubert and Mertz, 1980, 1984; Olsen, 1981), and therefore, the anomalously wet Deerfield basin conditions were probably due to local orographic effects.

Assemblage D replaces Assemblage C in the middle Portland Formation (Hartford basin), although the extent of this replacement (displacement?) cannot be determined due to the limited geographic distribution of strata younger than Sinemurian (Cornet and Olsen, 1985). The transition correlates with an increase in araucarian pollen (*e.g.*, *Callialasporites* spp.) in the upper part of the *Corollina torosa* palynofloral zone, and indicates a shift to more humid and possibly cooler conditions within the northern part of the Hartford rift valley during the late Pliensbachian-Toarcian. A similar age for the breakup unconformity offshore on the continental shelf (Manspeizer and Cousminer, 1988) may indicate regional uplift for the continental Newark Supergroup during plate separation.

Turn around and leave.

155.3 Turn right onto MA 116 (south).

155.4 Cross canal and turn right.

155.6 Turn right onto Lyman Street. Cross canal.

156.2 Turn left onto US 202 South. (Keep left)

156.5 Turn right onto 202. (Follow signs.)

156.7 Turn left onto MA 141, Hampden Street. Follow signs to I-91.

157.4 Turn right onto ramp to I-91 North, toward Northampton, MA. Driving north through the Connecticut Valley, the wooded mountain range on the left and ahead is the Mount Tom Range. Ahead and to the right is the Holyoke Range. These spectacular ridges are capped by Jurassic Holyoke Basalt. (Note the difference in relief compared to the basalt flows in the Culpeper basin.)

159.6 Outcrops of East Berlin Formation on the right (east).

159.7 Outcrops of diabase intrusives on left (west).

160.3 Exposures of the Early Jurassic Granby Tuff (palagonite; equivalent to the Hampden Basalt) on the left (west). Scenic area on the right (east).

162.6 Outcrops of Holyoke Basalt on the left with splintery fracture.

164.9 Get off I-91 at Exit 18 and onto US 5 North (King Street) into Northampton.

165.6 Arrive at overnight stop.

8. HARTFORD AND DEERFIELD BASINS, MASSACHUSETTS

mileage

0 Begin at stopping point from Day 7. Go south on US 5 toward I-91.
0.7 Continuing south on US 5, pass under I-91.
2.6 Contact between New Haven Arkose and Shuttle Meadow Formation on the right. Note that the Talcott Basalt, which separates the two formations in most of the Hartford basin, is absent from this area.
2.7 Approximate location of fish-bearing units beds in the Shuttle Meadow Formation (exposed along strike on I-91, southbound).
3.1 Holyoke Basalt exposed on the right. Coal-fired electrical plant on the left.
3.4 On left and right, exposures of Hampden Basalt and intrusive complex.
3.8 Granby Tuff exposed on right.
4.2 Pass entrance to Mt. Tom State Reservation.
5.0 Exposures of Hampden Basalt.
5.9 Dinosaur footprints described by Ostrom (1972) at Smiths Ferry on left along the Connecticut River.
6.2 Exposures of Granby Tuff and Portland Formation.
6.5 Turn right to Mt. Tom Ski Area, Mountain Park. (Passing through Granby Tuff, heading up section).
7.0 Bridge over I-91. Exposures of East Berlin Formation overlain by Hampden Basalt at top. Follow road to the right to Mt. Tom Ski Area.
7.5 Exposures of East Berlin Formation and intrusives in the woods on the right.
7.6 Dike.
7.8 Fault between Holyoke Basalt and East Berlin Formation.
7.9 Park.

STOP 8.1: MT. TOM SKI AREA, HOLYOKE, MA

(by P.E. Olsen)

Highlights: Well-laminated and microlaminated lacustrine beds including Westfield fish bed; diabase intrusions.

The upper two Van Houten cycles of the middle three cycles in the East Berlin Formation (time intervals P2b,c) are well exposed at this locality (Figure 8.1). The uppermost is the Westfield fish bed and contains the characteristic fauna seen in the southern Hartford basin. Poorly-preserved fossil fish are abundant, as is the conchostracan *Cornia*. The sequence contains a well-developed turbidite resembling that seen at Miner Brook (Stop 7.3). A diabase dike parallels the strike of the beds and forms the backbone of the hill behind these outcrops.

Walk on the road to the south side of the hill where extensive outcrops of red beds overlie the three middle cycles. At the top of the red bed sequence is a single Van Houten cycle, the lowermost of the uppermost three cycles in the formation, which is intruded by a slightly vesicular diabase sill. The sill and dikes are feeders to the Hampden Basalt and the Granby Tuff. Reptile footprints are abundant in the rubble along the slope.

Turn around and return to US 5.
8.2 Pass Westfield fish bed.
8.9 Cross bridge over I-91 again.
9.4 Turn left (north) onto US 5 at T-junction with traffic light.
11.7 Turn left into Mount Tom State Reservation.
11.9 Go under bridge of I-91.

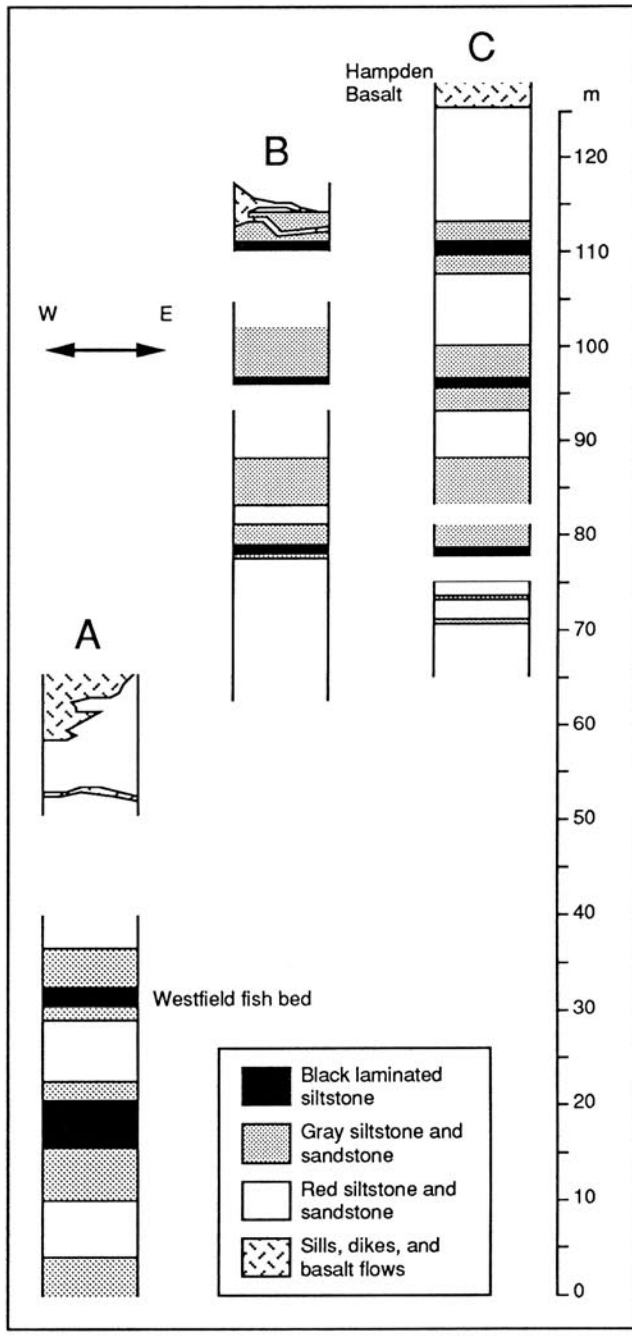

Figure 8.1: Measured section of the East Berlin Formation at Mt. Tom, Stop 8.1: A) exposures on west side of Little Mountain adjacent to road for Mt. Tom Ski Area; B) outcrops on south side of Little Mountain; C) exposures on cut on I-91 on the west face of Cedar Knob [section from Hubert *et al.* (1976) modified by data from P.J. Carey, pers. comm.].

12.1 Lake Bray on left has an extensive outcrop of the East Berlin Formation. (Road goes up the eastern dip-slope of the Holyoke Basalt.)

12.4 Exposure of Holyoke Basalt.
13.5 Outcrops on left are probably Shuttle Meadow Formation.
13.6 T-junction. Turn right then fork to right toward Goat Peak and Mount Nonotuck.
14.2 Turn into parking area and road with a gate. Park and follow road up to lookout tower.

OPTIONAL STOP 8.2: GOAT PEAK LOOKOUT TOWER, MT. TOM STATE RESERVATION, HOLYOKE, MA (by P.E. Olsen)

Highlights: Pillow basalts.

Well-developed pillows in the basal Holyoke Basalt are exposed along the path to the Goat Peak lookout tower. Such pillowed horizons are absent from the basal Holyoke to the south but are present in the lower part of the geochemically-identical Deerfield Basalt in the Deerfield basin.

Return to bus and continue northeast along road toward Mount Nonotuck.
14.8 Outcrops on right are Shuttle Meadow Formation and Holyoke Basalt.
14.9 Drive to the end of the road near the top of Mount Nonotuck. Park.

OPTIONAL STOP 8.2A: SCENIC OVERLOOK OF MT. NONOTUCK, MT. TOM STATE RESERVATION, HOLYOKE, MA (by P.J.W. Gore)

From this point, you are looking towards the northwest from an elevation of approximately 230 m near the top of Mount Nonotuck in the Mount Tom Range. The Connecticut River Valley below contains a large oxbow lake. The town of Northampton is visible in the distance. The large highway below is I-91. The ridges to the west and northwest are underlain by Ordovician-Devonian metamorphic basement rocks west of the Deerfield basin.

Turn around at lookout area and return toward US 5.
16.1 Turn left at fork in road.
17.5 Toilets at park facilities.
18.1 Turn left onto US 5, heading toward Amherst, MA.
21.2 Turn left onto I-91 North.
23.3 Exit to MA 9, and head east to Amherst (5 miles.)
23.5 Cross Connecticut River on Calvin Coolidge Memorial Bridge. Pass through the town of Hadley, MA, and continue toward Amherst on MA 9 East/116 South.
27.9 Enter Amherst, MA. The University of Massachusetts on the left (towers).
29.3 Turn right onto South Pleasant Street (MA 116 South).
29.4 Turn left into the campus of Amherst College. Go right around circle. Park in front of Pratt Museum.

STOP 8.3: PRATT MUSEUM AND HITCHCOCK FOOTPRINT COLLECTION, AMHERST COLLEGE (by P.E. Olsen, N.G. McDonald, and P.J.W. Gore)

Highlights: Fossil vertebrates, invertebrates, and geology exhibits; lower level of museum contains largest fossil footprint collection in the world.

The Pratt Museum of Natural History, on the campus of Amherst College, contains a large collection of fossil vertebrates and invertebrates and exhibits on the geology of Massachusetts. The Hitchcock footprint collection of the Museum is the largest fossil footprint collection in the world and is named for Professor Edward Hitchcock, president of Amherst College and State Geologist of Massachusetts during the early to middle 1800's. Following the discovery of Connecticut Valley fossil footprints in 1835, Hitchcock began a career of collection and study of the tracks of the Hartford and Deerfield basins, culminating in the publication of *Ichnology of New England* in 1858. The footprint collection of the Pratt Museum is the fruit of Hitchcock's labors consisting almost entirely of tracks collected from the Lower Jurassic rocks of the two basins. The footprints comprise the basis of the Connecticut Valley-type assemblage.

Originally, the footprints were housed in a building named the Appleton Cabinet, erected specifically for that purpose in 1855. The footprints were oriented to the large windows so they could be viewed with the appropriate oblique lighting. But several decades later the space was required for another purpose, and the tracks were moved into the basement, the so-called "tombstone room" of the new Pratt Museum. Fortunately, most of the collection remains intact, although it is still largely unstudied.

Hitchcock began applying scientific names to footprints almost as soon as they were first discovered, which had a very unfortunate and far-reaching effect on the study of vertebrate ichnology. The earlier specimens were of relatively poor quality, but these were the ones described and figured by Hitchcock in his many publications. Most of the thousands of spectacular and beautifully-preserved tracks in the Museum were collected after the publication of the *Ichnology* (Hitchcock, 1858; Deane, 1861). As a consequence, there is little recognition of the very high quality of Connecticut Valley material in the older literature, and most of the the type specimens of most of Hitchcock's taxa are indeterminate by modern standards. Some indication of the quality of the later material is in the posthumously published *Supplement to the Ichnology of New England* (1865), in which all of the footprints in the collection at that time were catalogued by Charles H. Hitchcock (his son). In many ways this is the most useful of the elder Hitchcock's publications because it synthesizes much of the previous work of 25 years and attaches specimen numbers to what were only names and/or crude drawings in previous reports. Unfortunately, the taxonomic status of most of Hitchcock's taxa was completely muddled by repeated renaming of forms and seemingly endless numbers of different names applied to specimens of the same taxon.

The sorry state of Connecticut Valley footprint taxonomy unfortunately has not been appreciated by most workers, and most ichnological studies since Hitchcock have only made matters worse. An excellent example of the confused state of affairs is the history of the ichnotaxon *Sauropus barrattii*, which started out as an isolated, indeterminate manus impression from an unknown locality (Hitchcock, 1837) and ended up as a fancifully "reconstructed" sitting trackway complete with a trackmaker which was used to infer how Cretaceous hadrosaurs sat (Lull, 1953)! From 1837 "Sauropus" went through seven invalid name changes, three invalid changes of type specimens, and four crude redrawings in which dotted lines were slowly replaced with solid ones. The final result was complete fiction, repeated in every major ichnological compendium to this day (see Olsen and Baird, 1986, for a full history). That is just one taxon out of the 47 listed by Lull (1953).

The Hitchcock collection, however, is a remarkable, priceless archive and resource. Ichnology is beginning to contribute to critical areas in paleobiology and stratigraphy, and no worker on early Mesozoic ichnology can claim to have even a rudimentary of knowledge of Connecticut Valley footprints unless he has examined the Hitchcock collection.

29.9 Leave Amherst College and turn right on South Pleasant Street.
30.5 Turn left on Triangle Street at Bay Bank, following sign to University of Massachusetts.
30.8 Turn right at the entrance to the University of Massachusetts.
32.6 At fork in road, bear right on MA 63 North (Long Plain Road) toward Mt. Toby, after which the Mt. Toby conglomerate is named.
33.9 Entering Leverett, MA.
36.1 At this point the road is paralleling the eastern border fault along the basin edge.
38.4 On the left is a path leading to Roaring Brook Falls in Mt. Toby State Forest. Exposures of silicified splays of the border fault can be seen along the path. At the falls, the Jurassic Mt. Toby Conglomerate unconformably overlies Paleozoic high-grade metamorphic rocks of the hanging wall basement of the Deerfield basin half graben.
42.7 Turn left at the tractor dealership toward Lake Pleasant.
44.8 Turn left and follow signs to Turners Falls.
46.0 Town of Montague. Hills to the west (left) are the Pocumtuck Range underlain by Deerfield Basalt.
48.2 Town of Turners Falls.
48.4 Turn right and cross the Connecticut River. Viewed from the bridge heading northeast, the dam is to the right under the bridge.
48.7 Turn left (west) onto MA 2 at end of bridge. Immediately after turning, bear left into an overlook lot along the river, and park.

STOP 8.4: TURNERS FALLS DAM, TURNERS FALLS, MA

Highlights: Evidence for multiple episodes of deformation; clastic dike; fossiliferous lacustrine shale.

Begin by walking west along the south side of MA 2 (Figure 8.2), and cross the bridge of Fall River to the end of the outcrops where the stratigraphic and structural transect will begin. Walk east along exposures (Location 1) to Fall River Bridge (Location 2) then cross road to the section on the north side of MA 2 (Location 3). Descend the hill between the parking area and the river to look at the outcrops upstream (Locations 4-9). The latter exposures are immediately downstream of the Turners Falls dam, and are inaccessible when the dam gates are open. *Water rises rapidly when the dam gates are opened.*

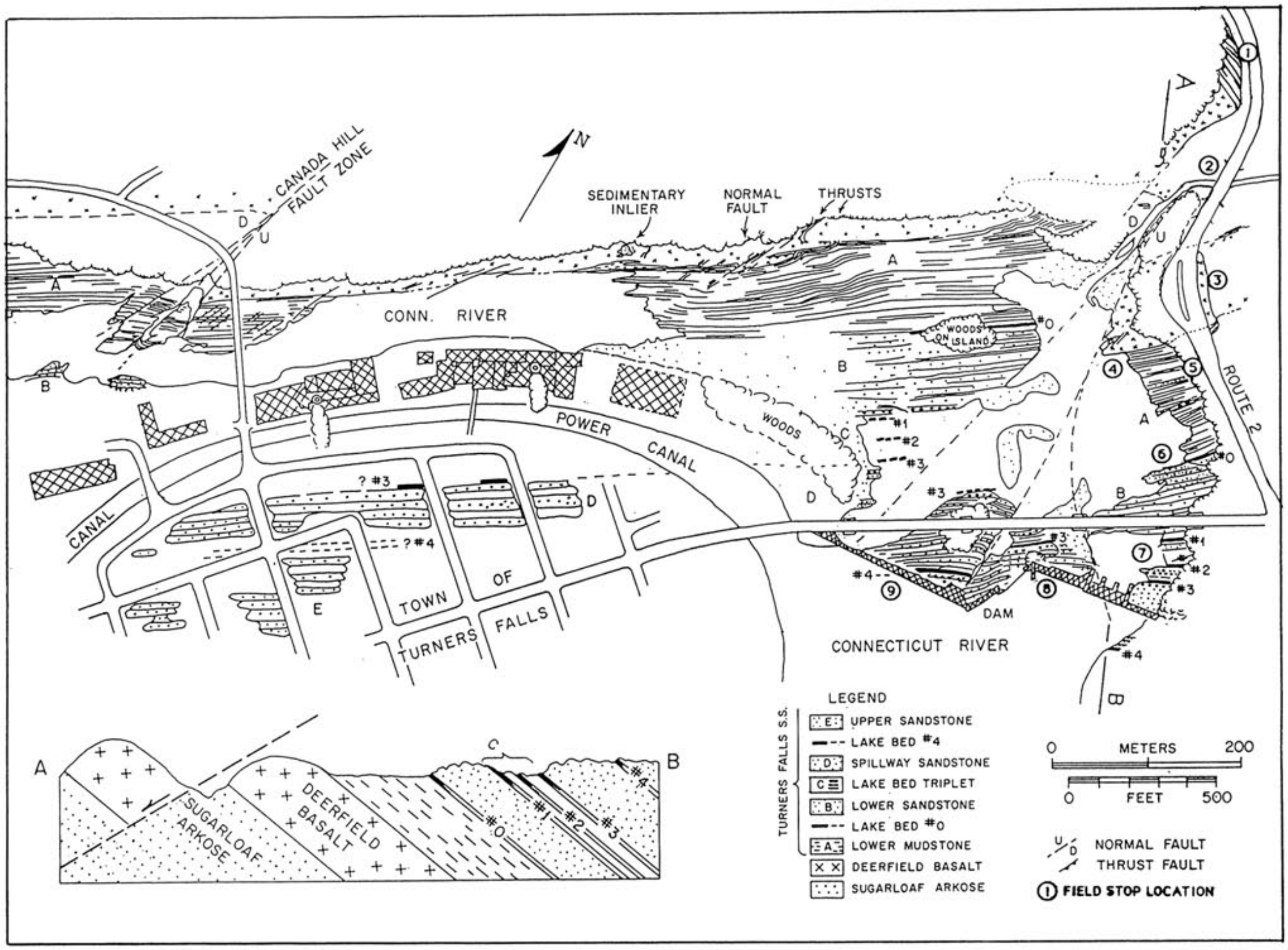

Figure 8.2: Geologic map of the Turners Falls area, showing localities for Stop 8.4. Modified from Wise (1988).

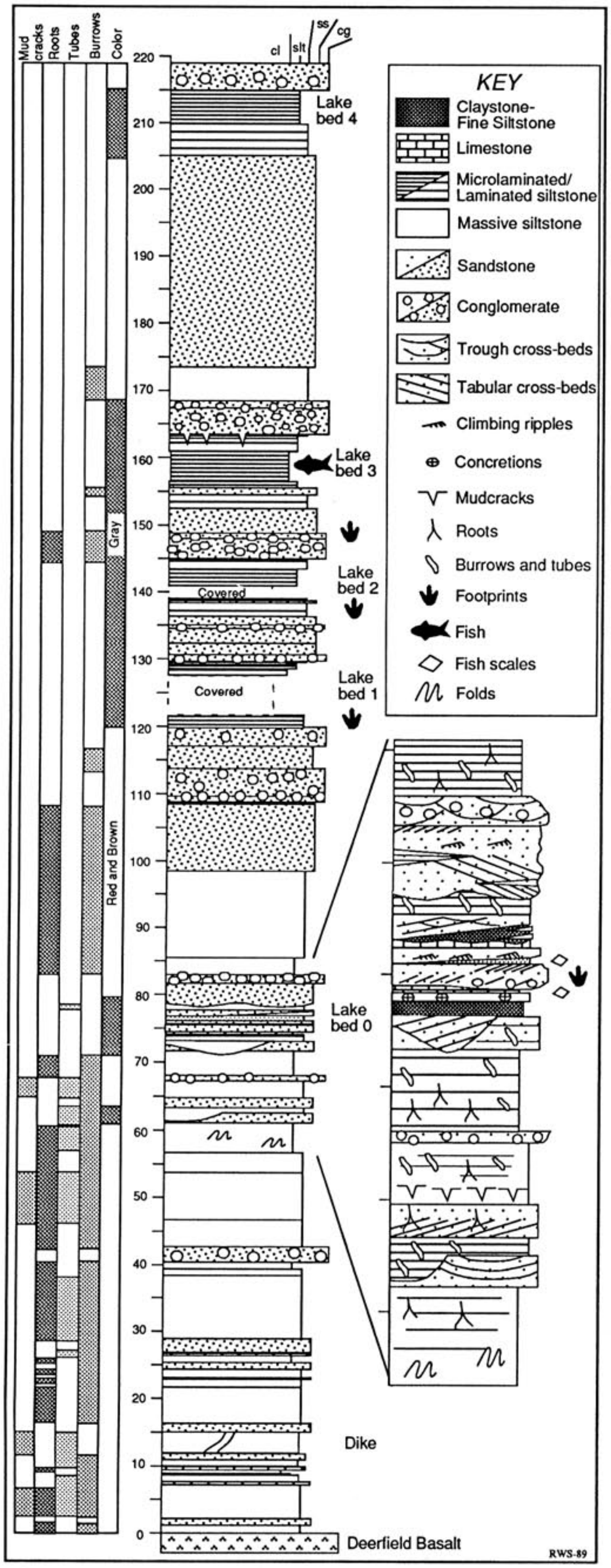

Figure 8.3: Measured section of the Turners Falls Sandstone at Turners Falls, Stop 8.4, showing interbedded perennial lake and fluvio-deltaic sequences. Depth rank curve appears in Figure I.9. Note that the distribution of mudcracks and roots is shown only where they are very common. Some data from Wise (1988).

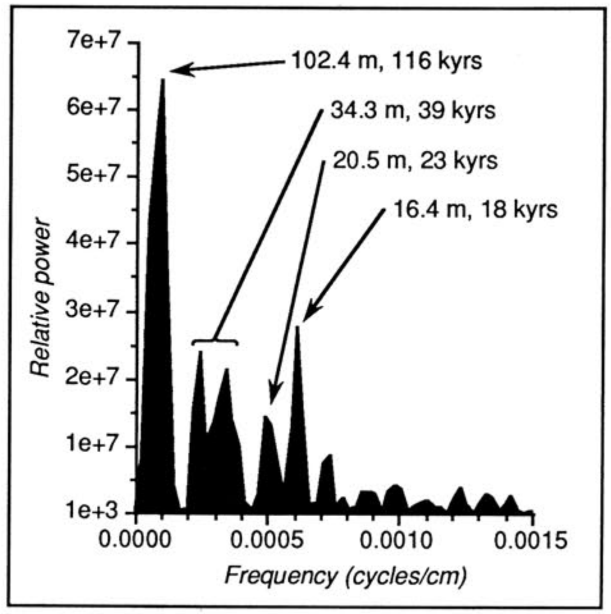

Figure 8.4: Power spectrum of depth rank curve of Turners Falls Sandstone shown in Figures 8.3 and I.9.

Stratigraphy and Paleontology (by P.E. Olsen, R.W. Schlische, and N.G. McDonald)

These outcrops reveal 16 m of the uppermost Sugarloaf Arkose, the full 80 m of the Deerfield Basalt, and 250 m of the Turners Falls Sandstone. The Turners Falls Sandstone (Figures 8.2, 8.3) consists of red, gray, and whitish fluvial to lacustrine sandstone and minor conglomerate; red brown fluvial to lacustrine sandstone and siltstone; brick red to maroon lacustrine siltstone and mudstone; and five gray to black lacustrine shale and siltstone beds which commonly contain calcareous siltstone concretions.

Fourier analysis (Figure 8.4) of depth ranks of the Turners Falls Sandstone (Figure 8.3) shows significant peaks at an average of 18.5 m, 34.3 m, and 102.4 m. If the 18.5 m set of peaks corresponds to the 21,000 year precession cycle, then the 34.3 m peak has a periodicity of 39,000 years, and the 102.4 m peak has a periodicity in time of 116,300 years. Jurassic time intervals (Figure I.10) P1a-P3a are represented, but only intervals P1c, P2a,b,c, and P3a have well-developed black and gray shale-bearing Van Houten cycles (Figure I.9). The triplet of Van Houten cycles so prominent in this outcrop (Location 7, Figure 8.3) are hypothesized to be time equivalents to the three cycles in the middle East Berlin Formation seen at East Berlin and Mt. Tom (Stops 7.2, 8.1), the three cycles in the Towaco Formation at The Glen (Stop 6.2), and the exposures of the Waterfall Formation (Stop 4.2).

Turners Falls is one of the premier fossil localities in the Connecticut Valley. Fishes from this site were first described by Emmons (1857), but the locality was probably known much earlier (see McDonald, 1975, 1982). Fish are most abundant in the microlaminated shale beds (preserved whole but flattened), and in the center of calcareous siltstone concretions (somewhat dissociated but more three-dimensional). Better preserved, more robust specimens are occasionally found in siltstsone beds. All of the articulated fish found so far come from the dark gray to black portions of division 2 of the Van Houten cycles marked 2, 3, and 4 (Figure 8.3) corresponding to time intervals P2b, P2c, and P3a. By far the most common fish are semionotids of the "*Semionotus tenuiceps*" (Figure 4.6) and "small scale" groups of Olsen *et al.* (1982). The fish average 7-15 cm in length but can attain sizes up to 40 cm. Much less common are the subholostean *Redfieldius* and the coelacanth *Diplurus*. Even though many hundreds of museum specimens of *Semionotus* have been obtained from this locality, definitive examples of the former two genera were found only recently (by McDonald and Olsen).

In the mid 1800's, Turners Falls was one of the most productive footprint localities in the Connecticut Valley and was a favorite of Edward Hitchcock and fellow collectors Deane, Marsh, and Field. Tracks are now uncommon on the mainland, but the islands in the river occasionally yield fine specimens. *In situ* footprints are most common in transgressive portions (division 1) of Van Houten cycles; poorly-preserved examples are also present in the red beds. The most common ichnotaxa are *Grallator* (*Eubrontes*) spp. and *Grallator* (*Anchisauripus*) spp.

Structural Geology (by D.U. Wise)

The outcrops at Turners Falls show a far more complex series of structures than those usually ascribed to the Mesozoic of this region. Such structures include significant normal faults reflecting NW-SE extension and younger conjugate strike-slip faults indicative of NE-SW compression.

Several populations of faults, many of which utilize pre-existing joints, have been identified in the Turners Falls outcrops (Figure 8.5, 8.9, 8.15, 8.16). The earliest formed faults are NE-striking normal faults of the A_1 group (subsequently tilted to the present shallow dips), related to NW-SE extension. The A_2 group has identical slickenlines, steep dips to the west, and right-lateral motion. It is interpreted to be a result of oblique strain produced by the interaction of the N15°E border fault and the Falls River fault with the average regional NW-SE extension direction. The A_3 group is a product of the younger reversal of motion on these NE-striking fracture planes. The V group of faults (with slickenlines approximately vertical) may be partly a conjugate pair to the A_1 extension faults subsequently tilted from a 60°SE dip and plunge to the present vertical. B_1 (NE-striking, NW-dipping, sinistral slip) and C (NNE-striking, WNW-dipping, dextral slip) are the fault groups associated with the younger NE-SW σ_1 orientation. Groups B_2 and B_3 represent shallow to moderately west-plunging, right- and left-lateral motions on NW-dipping planes. Some of the reverse and right-oblique motions may be part of the B_1 conjugate system. The normal, left-oblique motions may be variations on the older extension pattern. Group F are bedding plane parallel faults attributed to down-to-the-southeast shear (*i.e.*, down-dip).

Mineralization on the A set of faults is largely calcite with some quartz. On the B set, minerals are similar but more sparse. The C set is marked by polished surfaces and hematitic stains. Cross-cutting or overprinting relations of slickensides are not common but locally show the C_2 set to be relatively young.

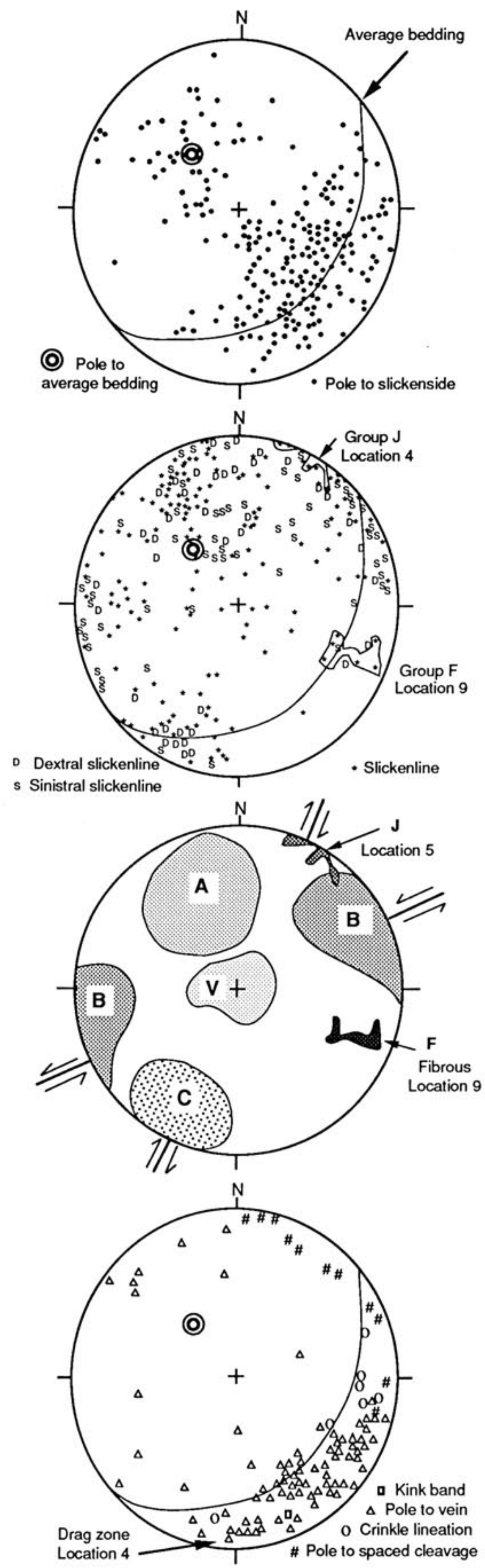

Figure 8.5: Cumulative plots of all brittle fracture data at Turners Falls, Stop 8.4., and grouping of Turners Falls faults based on orientations of slickenlines. Modified from Wise (1988).

Local thrusting and small-scale compressional folding are in part younger than the normal faulting extensional episode. Several periods of jointing and veining were associated with these events, especially with normal faulting and extension. The transition from extension to compression might be correlated with the change from rifting to drifting as the Atlantic Ocean opened (Wise, 1988; de Boer *et al.*, 1988). It is important, however, to note that the orientation of the inferred later NE-SW compression is compatible with the direction of shortening for virtually all of the transverse folds and associated structures in the Newark Supergroup and probably calls for a comprehensive explanation.

Field Stop Transect (by D.U Wise, P.E. Olsen, and R.W Schlische)

Location 1: Uppermost Sugarloaf Arkose and lower Deerfield Basalt. Gray, tan, and red micaceous siltstones and sandstones comprise the upper 16 m of the Sugarloaf Arkose at this locality (Figure 8.6). Lithologically the sequence is unlike any known lower in the Sugarloaf Arkose and much more closely resembles the strata of the upper Shuttle Meadow Formation in the Hartford basin. Based on the cyclostratigraphy of the overlying Turners Falls Sandstone (Figures 8.1, I.9), this outcrop should be the time equivalents the upper Shuttle Meadow Formation, the upper Feltville Formation of the Newark basin, and the upper Turkey Run Formation of the Culpeper basin (time division E4a).

Stevens and Hubert (1980) described this section (Figure 8.6) and interpreted the thin, even beds of pyritic gray mudstone as the deposits of the deepest water sediments of a perennial lake. The red units were interpreted as shallow water deposits and contain caliche. According to Stevens and Hubert (1980) the lake originated as a playa and later expanded to a closed, alkaline perennial lake with substantial amounts of dissolved sodium, calcium, magnesium, and bicarbonate.

Abundant megafossil plants occur in muddy gray siltstone about 8.75 m below the Deerfield Basalt (Cornet, 1977a; Stevens and Hubert, 1980). *Equisetites* sp. is the most common plant, but a large three-dimensional *Clathropteris meniscoides* in growth position was found (Figure 8.7) in a fallen block from this zone in 1988.

The basal 17 m of the 23-m-thick lower basalt flow complex consists of well-developed pillows which then pass upward into a 6-m-thick reddened vesicular zone, poorly exposed at this locality. The upper flow complex of the Deerfield Basalt is exposed in the woods to the southeast. The Deerfield Basalt is a high-titanium, quartz-normative basalt, compositionally similar to the Holyoke Basalt of the Hartford basin, Preakness Basalt of the Newark basin, and Sander Basalt of the Culpeper basin.

Location 2: Bridge over Fall River and Fall River fault zone. The offset in the basalt ridge is caused by the Fall River fault zone which displaces the upper contact of the Deerfield Basalt about 200 m to the south. Displacement is probably due to normal faulting, as shown at location 9, a continuation of the same zone.

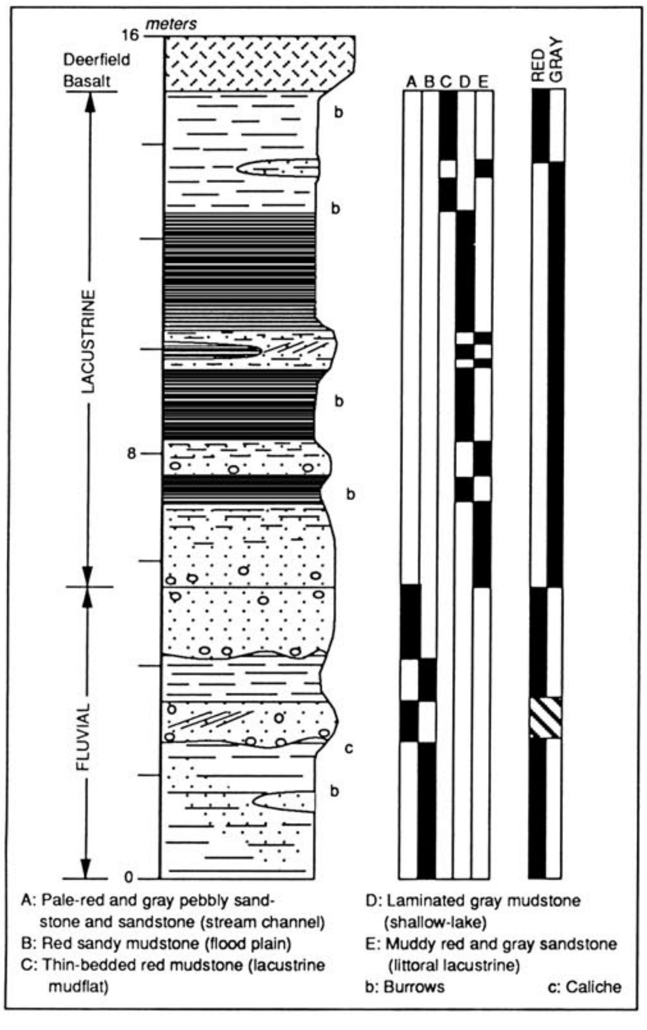

Figure 8.6: Measured section of the uppermost Sugarloaf Arkose, location 1, Stop 8.4. Modified from Stevens and Hubert (1980).

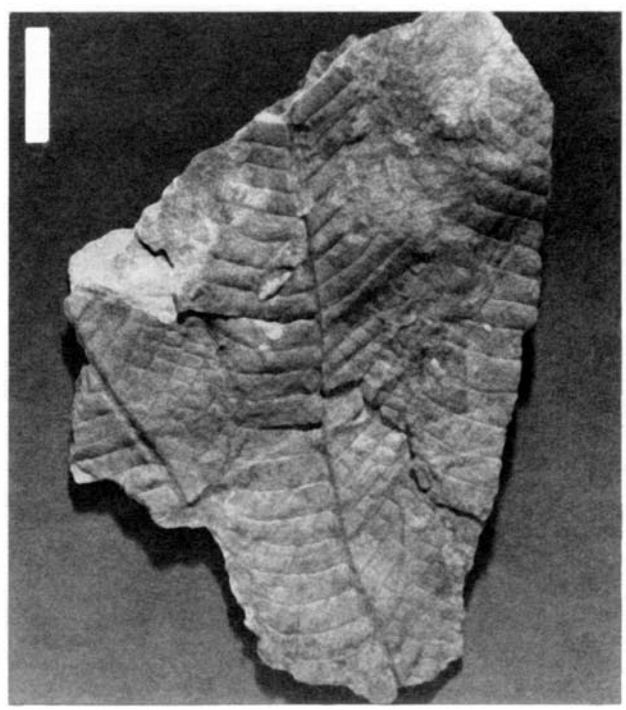

Figure 8.7: Partial palmate leaf of the fern *Clathropteris meniscoides* found in growth position at location 1, Stop 8.4. Scale is 1 cm. Photo by P.E. Olsen.

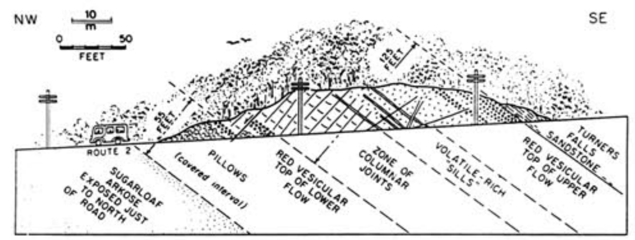

Figure 8.8: Diagrammatic sketch of outcrop along US 2, location 3, Stop 8.4, showing fault contact between Deerfield Basalt and Turners Falls Sandstone. Modified from Wise (1988).

Location 3: Road cut on Route 2 with Deerfield Basalt. The top of the flow is visible at the east end of the outcrop (Figure 8.8), and the base can be seen on the east bank of the river in the woods to the northwest. The upper reddened zone of the lower flow complex is well displayed here as is the upper flow complex. Several sill-like gabbroic zones 5-10 m thick are present; these are typical of the middle extrusive complex in the Newark Supergroup (see Stop 4.3). These gabbroids have higher concentrations of TiO_2 and other incompatible elements than the surrounding basalt and are late-stage, relatively chemically-evolved, auto-intrusions of fractionated basaltic liquid (Tollo, 1988). Alteration to near greenstone condition is common throughout this outcrop of the flow. Note the gradation of texture and grain size in the upper flow complex, changing from fine at base, through medium, to very coarse grained and finally to vesicular at the top. Volatiles from the basalt may be responsible for the reddened, oxidized tops of both flows, or the reddening could be due to oxidizing water moving through the porous sediment-basalt contact or along the basalt-basalt contact.

Large columnar joints in the middle section of basalt (Figure 8.8) show excellent arrest marks in paleo-horizontal orientation. Columnar joints cut and thus post-date the gabbroids. Note the superimposed slickenlines with strike-slip motion close to present day horizontal; which can be interpreted as a post-tilting, strike-slip phase.

Tectonic joints, most striking N45°E, are mineralized with calcite and some quartz (Figure 8.9). Some fractures show pull-apart structures indicative of down to the NW faulting during deposition. These were probably caused by the general extension and tilting of the basin.

A normal fault at the west end of the outcrop (Figure 8.8) strikes N30°E and has several meters of predominantly dip-slip displacement with relatively few mineralized fractures. Complex families of minor slickenside motions are separated and designated by letter in Figure 8.9.

Location 4: Faulting in upper part of Deerfield Basalt and contact with Turners Falls Sandstone. Proceed down the path on the basalt to the river's edge (Figure 8.10). Beds visible on island along strike are 90 m higher in section, and thus the Falls River fault zone must pass directly off the bank from basalt outcrop. A prominent joint set (oriented about N10°E, 40°W) marking the ridge line for the descending path is most strongly developed in basalt and overlying strata adjacent to the normal fault zone. Locally the joints are listric, opening toward the fault, and are products of the extension process which produced the main fault.

A remnant of infaulted sedimentary rock and the contact with basalt is exposed at very low water and is bounded by shallow-dipping faults with shallow-plunging slickenlines (Figure 8.10). The faults curve back and forth between the main west-dipping joint set and a moderately NW-dipping set of faults (fault groups A_1 and A_2). The parasitic nature of the faults is obvious, as they make alternate use of the two joint sets. The average slip direction of the faults is about 30° toward N20°W. The faulting involved little rotation of blocks.

Gabbroic sill-like zones similar to those seen at Location 2 are present in the basalt. However, they break upward irregularly at a few places. Neptunian dikes of red mudstone are locally visible in the basalt along the contact.

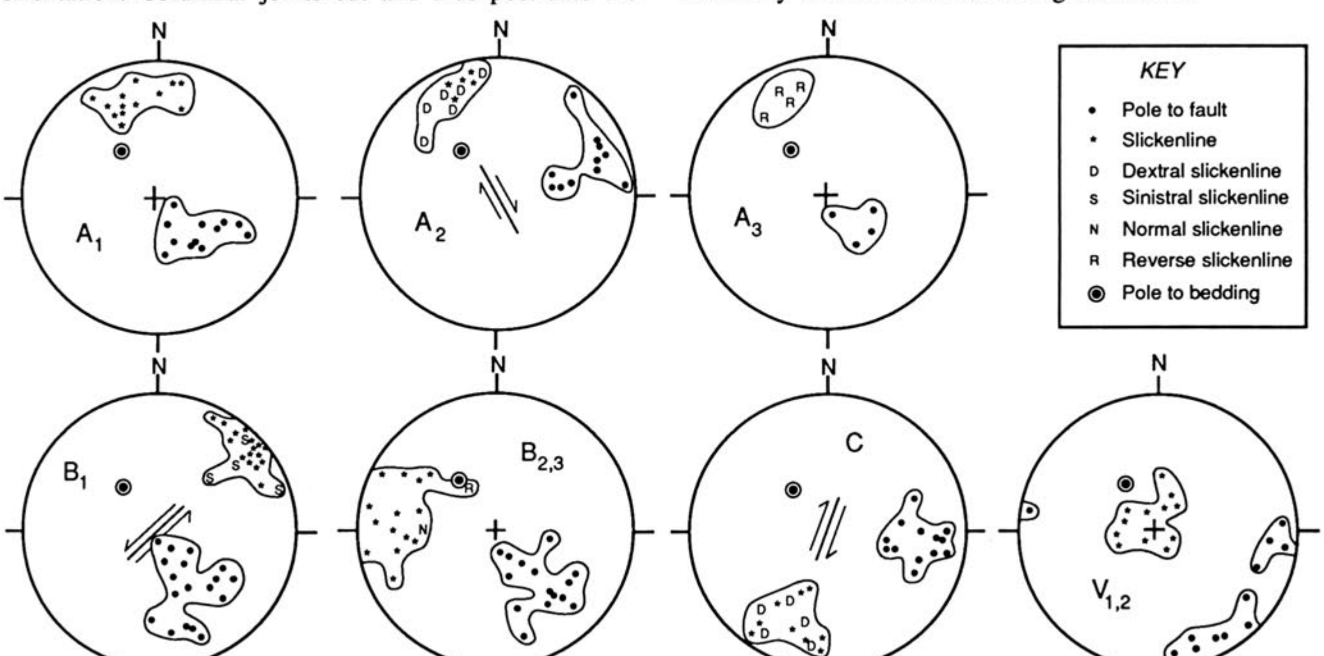

Figure 8.9: Families of faults at location 3, Stop 8.4. Modified from Wise (1988).

Location 5: Basal Turners Falls Sandstone and large clastic dike. The red siltstones and fine sandstones of the Turners Falls Sandstone commonly show intense bioturbation by roots and burrows, some of which appear to be *Scoyenia*. In the lower 70 m of the Turners Falls Sandstone, intervals of mudcracked massive mudstone alternate with lightly-burrowed to densely-burrowed and rooted strata and outline a vague cyclic pattern. Some units show considerable relief and some of the sandy and gravelly units display dune-scale trough cross bedding. This section is a mixed fluvial-shallow water lacustrine system which, by cyclostratigraphic correlation, represents time zones ?E4d, P1a and P1b (Figure I.10). The cyclic pattern, so obvious in the correlative lower Towaco Formation of the Newark basin, is rendered somewhat obscure by the abundance of coarse-grained fluvial and deltaic strata.

A large clastic dike, cutting red sandstone and mudcracked massive mudstone, is present about 14 m above the base of the section. The dike (Figure 8.11) appears to have no connection with the beds above it or below it at this level of exposure. A bedding-parallel septum in the middle of the dike may be a remnant of a sand bed located down-dip which was mobilized by the injection of the sand. The dike is segmented with mudstone septa constricted between growing dike segments. The dike appears to be the result of lateral injection within mudstone units. A likely scenario is seismically triggered fluidization of an unconsolidated sand; the sand was prevented from dewatering by enclosure in the less permeable mudstone.

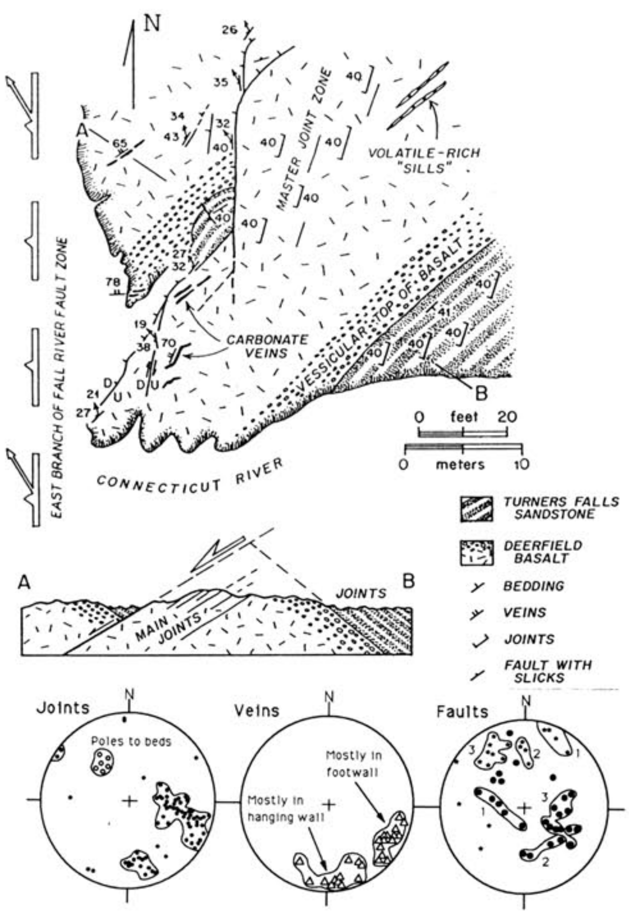

Figure 8.10: Detailed geologic map of the vicinity of the Fall River fault, location 4, Stop 8.4 (see Figure 8.2) and structural data. Modified from Wise (1988).

Location 6: Van Houten cycle #0. Cycle #0 contains carbonate concretions and sparse organic matter in a fine-grained matrix. The gray limestone near the base of the gray interval (74.9 m above the base of formation) and a nodular calcareous siltstone about 30 cm higher have dissociated fish (*Semionotus* sp.). The weathered color of the fish bones is white and blue (from vivianite). A gray sandy siltstone just below the upper fish-bearing unit has abundant poor *Grallator* (*Anchisauripus*) spp.-type tracks. About 1 m above the base of the lower limestone is an upward-coarsening sequence of sandstone and siltstone with large, north-tilted surfaces. Individual sandstone beds thin down-the-paleoslope and pass into gray siltstone. The geometry suggests a small, shallow water delta. However, at least some groove marks and current lineations trend E-W, appropriate for a current tangential to the downstream portion of a point bar of a meandering stream. Along-strike color changes toward the river suggest oxidation or reduction reactions from circulating fluids. Cyclostratigraphic correlation with the Towaco Formation indicates this Van Houten cycle represents time interval P1c.

The lake bed has many small-scale bedding plane faults and fold structures. Strike-slip faults cut the overlying sandstones and penetrate into lake beds. Transtensional

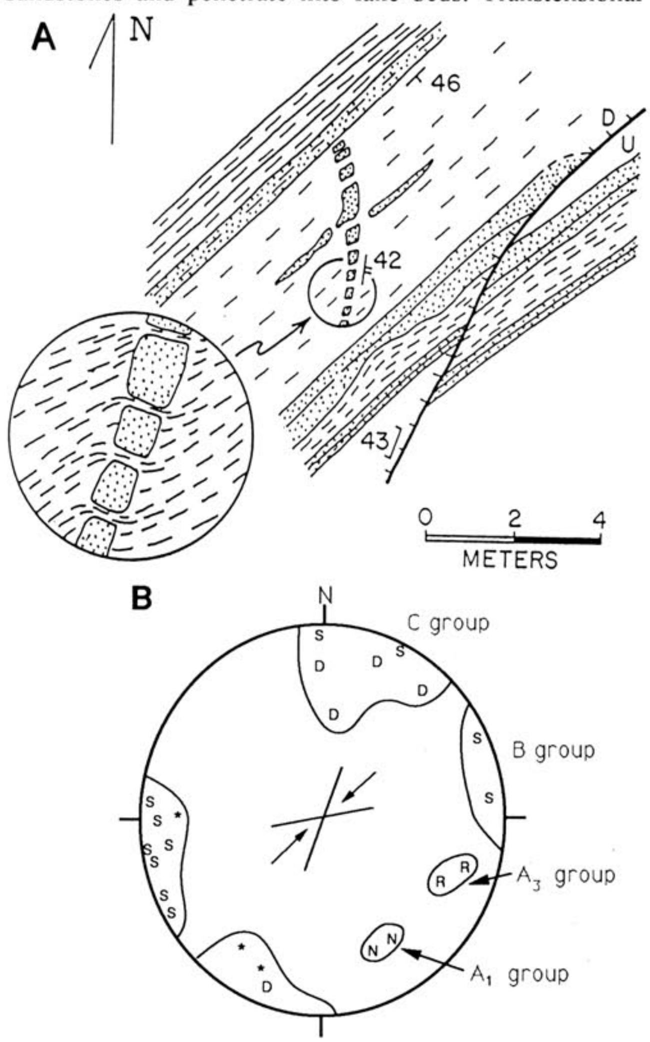

Figure 8.11: A) Sketch of clastic dike at location 5 and B) fault families at locations 6 and 7, Stop 8.4. Modified from Wise (1988).

Figure 8.12: Fault-bend fold in gray sandstone and siltstone at Stop 8.4, location 7. Photo by P.E. Olsen.

movements permitted by local stress fields are demostrated by curvature of some strike-slip slickenlines into more dip-slip displacements. The plot (Figure 8.11) of the faults from this location to the dam shows conjugate groups B and C with appropriate left- and right-lateral displacement. The faults are typically polished and little mineralized. Minor drag folds, crude cleavage development, and minor breccia can be seen at the intersections or splays of some faults. Some of the faults disappear up-section into zones of more intense jointing.

About 25 m downstream from the bridge is an inconspicuous 1-m-wide kink band orientated N70°E, 75°NW, which can be traced for about 20 m. It folds and hence postdates the N45°E-striking joint set. Formation of the kink band requires compression within about 30° of a prominent, pervasive anisotropy—bedding in this case.

Location 7: Triplet of gray lacustrine cycles. The prominent ledge-forming sandstone of Van Houten cycle #1 lies under the bridge. Lack of outcrop immediately above marks the trace of the overlying black shale, exposed only during very low water levels. The second and third Van Houten cycles are well exposed, the third being at the foot of the dam. Reptile footprints occur in many of the gray sandstones and siltstones in division 1 and 3 of all three cycles. Thick black shale with dolomitic laminae in cycles #2, #3, and #4 contain articulated fish; however, fish are most abundant from cycle #3. At very low water, silty limestone nodules washed out of cycle #3 can be found, each of which has fish or coprolites inside. Bedding plane faults and veins with fibrous calcite and bitumen are common in the black shale units. In the upper parts of division 2 of cycles #2 and #3 are abundant tan-weathering, septarian, dolomitic concretions. Cycle #3 has deep, conglomerate-filled desiccation cracks where black shale is in contact with the overlying conglomerate bed.

An excellent example of the transpressional mode of part of a strike-slip fault is visible at about 137 m above the base of the section (division 1 of cycle 2) where a superb example of a small fault-bend fold is exposed (Figure 8.12).

Location 8: NE end of spillway island; lake bed #3. The dam foundations are in the resistant spillway sandstone (Figure 8.2). This unit also forms the resistant base for the north end of the dam and for the next bridge pier to the south. Correlation with lake bed # 3 on the mainland is based on matching of thicknesses, lithology, deep clastic-infilled mudcracks, and septarian concretions comprised of dolomite (Wise, 1988).

The "island" is a fault block splay of the Falls River fault (Figures 8.13, 8.14, 8.15). The fault must pass very close to the bridge pier and very close to the south end of the spillway gates. At extreme low water, the disturbed beds are visible next to the gates. Much of the surface of the island is a large, curving, normal (?) fault surface (Figure 8.13). With present dips, the fault would be regarded as normal, but it is essentially perpendicular to bedding, a paleovertical structure. At the contact with the underlying dark shales, the fault and others parallel to it bend and drag the lake beds (Figures 8.13, 8.14). One small graben drops the overlying clastics about 0.5 m into the lake beds with the line of intersection of the conjugate faults plunging at 10° towards 215°. Fault motions on the island are indicated on Figure 8.15. Group A_1 normal faults dominate, but some probable reverse motions of group A_3 type can be found, possibly a reflection of a younger compressional phase (Figure 8.15). Present but not so prominent are strike-slip and oblique faults of group C.

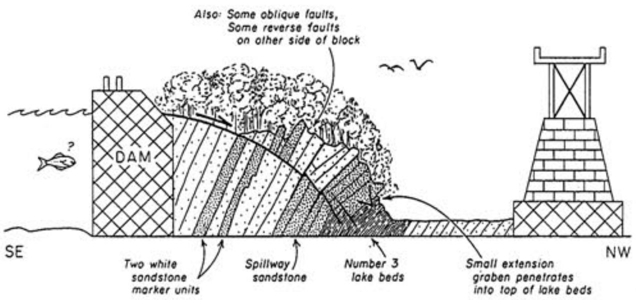

Figure 8.13: Geologic relations on northeastern block of Spillway Island, location 8, Stop 8.4. Modified from Wise (1988).

Location 9: Lake bed #4. Cross with care onto concrete apron of dam. The largest of the Falls River fault splays passes under concrete here (Figure 8.14). Immediately next to the main fault is a concentration of small A_1, A_2, and A_3 faults in the sandstone (right hand net of Figure 8.15); note breccia and mineralized fractures.

Lake bed #4 (Figures 8.13, 8.14) differs from those exposed on the mainland in having a more finely-laminted dolomitic unit with fewer coarse interbedded siltstone beds. Jointing is well developed in the adjacent sands but rare to completely absent in lake beds. This probably reflects the very slow lithification of the water-rich lake beds. Van Houten cycle #4 corresponds to time interval P3a (Figures I.9, I.10).

The sequence of structural events recorded in the pace and compass map of Figure 8.15 and the net plots of Figure 8.16 are as follows:

a. Isoclinal folds formed with axes plunging shallowly at S30°W. The best example of these folds is visible under the concrete at the SW end of the exposure. Cleavage is present in the axial plane regions of some of the folds, but isoclinally-folded calcite veins or other indications of mineralizing fluids are rare or absent. Fold asymmetry suggests that the top moved toward the NW. An early compressional phase seems likely because the motion sense is opposite that expected for gravity sliding in a SE-tilting basin (Wise, 1988).

b. Bedding plane faults (Group F) developed. Here they are associated with fibrous calcite with fibers plunging shallowly toward the NW. Slickenlines on the faults rake at S70°E. The extension direction of the calcite fibers clearly indicates a down to the SE or normal sense of displacement.

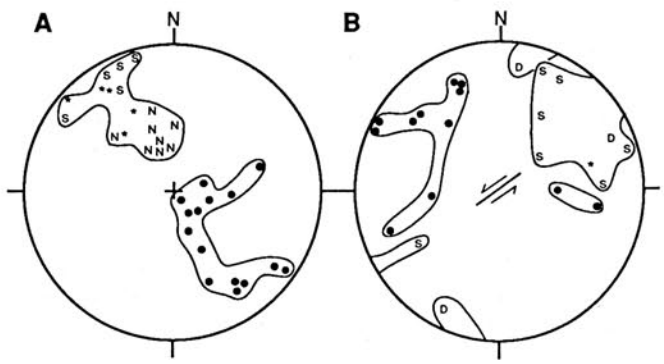

Figure 8.15: Fault families at location 8, Stop 8.4. A) A group normal faults, and B) B_1 group (sinistral) and minor C group (dextral) faults. Modified from Wise (1988).

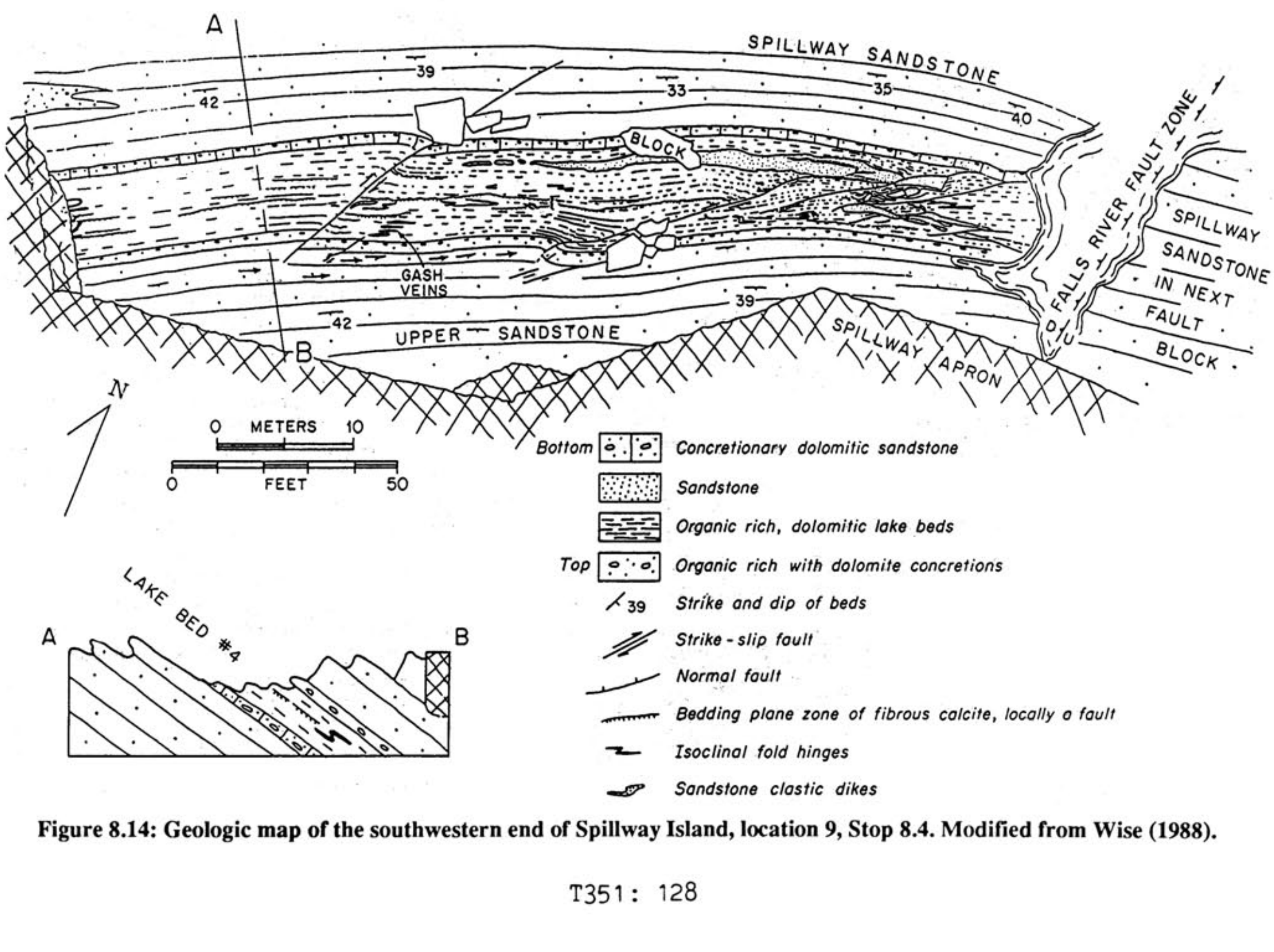

Figure 8.14: Geologic map of the southwestern end of Spillway Island, location 9, Stop 8.4. Modified from Wise (1988).

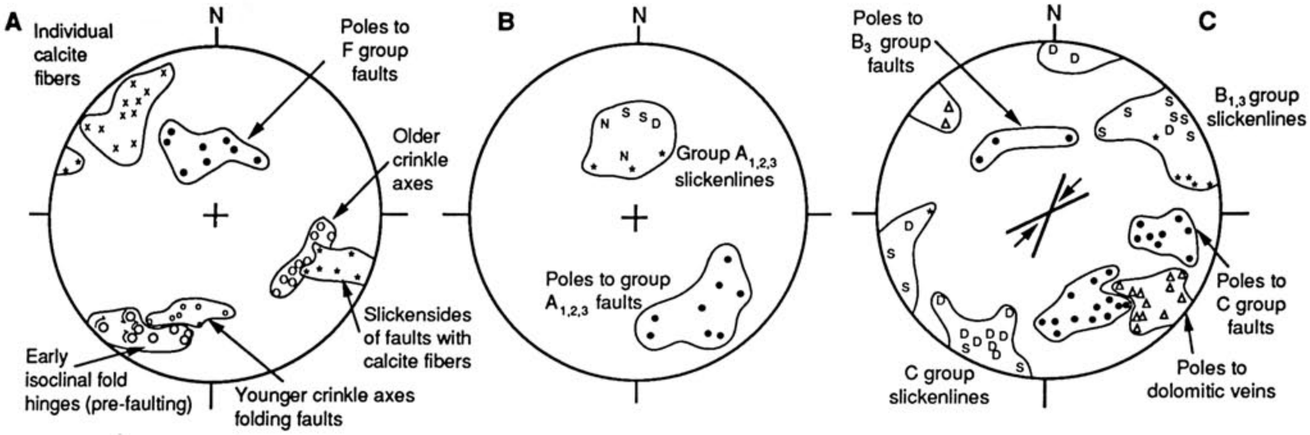

Figure 8.16: Structural relationships at location 9, Stop 8.4. A) Early structures; B) structures in the vicinity of the Fall River fault; and C) conjugate strike-slip faults. Modified from Wise (1988).

A reasonable origin is slow gravity sliding to the SE of the entire mass of basin fill. Movements were complex, however, as the fibrous veins, faults, and some thin beds are mildly folded and crinkled about axes plunging S20°W.

c. A normal faulting phase, expressed throughout much of the Turners Falls region, has left little effect at this location except immediately adjacent to the Falls River fault splay. Development of well-defined joints must have taken place in the well-lithified sandstones and conglomerates because these structures were used for parasitic faulting in the next phase, and many pebbles are fractured.

d. Lastly, conjugate strike-slip motion occured on both the B and C groups of faults. These motions are prominently displayed on the many large slickensided joint surfaces of the overlying sandstone and in faults crossing the lake beds (Figure 8.16). Associated dolomitic veins with *en echelon* arrangements show a properly oriented S50°E σ_3 to be in accord with a N40°E σ_1. The faults are mineralized with calcite, dolomite, quartz, siderite, pyrite, chalcopyrite, and galena. Hydrocarbon coatings on veins and open-space fillings are common, suggesting that this phase may have been at the height of organic matter maturation. Breccias are common and show evidence of multiple motions.

Figure 8.17: Breccia at Barton Cove, Stop 8.5. Photo by P.E. Olsen.

49.5 Turn around and head east on MA 2 toward Boston.
50.6 Barton Cove. Turn right onto park road and continue to parking area.

STOP 8.5: BARTON COVE, GILL, MA (by P.E. Olsen)

Highlights: Tectonic or slump deformation; historic footprint locality.

The extensive exposures of gray and red lacustrine siltstones and sandstones of the Turners Falls Sandstone in the Barton Cove area show complex structural features and include a classic footprint locality which produced many of the footprint slabs in the Hitchcock collection.

The most distinctive deformation at these exposures consist of resistant ledge-forming (up to 10 m thick) beds of coarse breccia. The breccia is composed of 2-100 cm blocks of gray and black to reddish dolomitic siltstone and fine sandstone in a muddy matrix of dark sandy siltstone (Handy, 1976) (Figure 8.17). Small coalified logs are locally present. Both clasts and matrix weather gray white. The breccia supports a ridge jutting into the Connecticut River. Handy (1976) was able to trace both the ridge and the breccia to south of Montague, about 4 km. On a smaller scale, the breccia units are discontinuous and pass laterally into relatively undisturbed beds. High-angle thrust faults and associated (in some places, recumbent) folds are present in beds below and adjacent to the breccia.

The origin of these breccia bodies and thrust faults is presently enigmatic. Handy (1976) and Cornet (1977a) described the breccia and thrust faults as a large-scale sedimentary slump. The rounding of clasts, plastic folding adjacent to faults, lack of mineralized fractures argue for a

Figure 8.18: Type slab with two trackways of *Anomoepus curvatus*. Note that all but the middle part of the slab is covered by dense rain drop impressions which are superimposed on the footprints. The smooth swath across the middle of the slab must have been covered by a puddle at the time of the shower. Scale is 20 cm. Photo by PEO.

relatively early origin. However, the lateral passage of breccia zones into undisturbed beds and associated thrust faults suggests a tectonic origin for both. The lateral extent of the zone indicates a rather large structural feature, although stresses may have been localized within the incompetent gray and black shale sequence.

Cornet (1977a) recovered a palynoflorule ("LP") dominated by *Corollina meyeriana* from the breccia and a different assemblage dominated by *Corollina torosa* was recovered from an overlying undisturbed gray unit. This led Cornet (1977a) to infer that the breccia represented a hiatus. However, alternating zones dominated by *C. torosa* and *C. meyeriana* are present in the broadly correlative lower Portland Formation of the Hartford basin and upper Boonton Formation of the Newark basin in intervals not thought to contain a hiatus (Cornet (1977a).

Table 8.1: Footprint taxa from Lily Pond listed by Lull (1953) and reclassified according to Olsen (1988b).

Crocodiliomorphs	
Batrachopus deweyi	
Batrachopus bellus	
Batrachopus gracilior	
Batrachopusgracilis	
Batrachopus (Comptichnus) obesus	
Otozoum minus	
Ornithischian Dinosaurs	
Anomoepus curvatus	
Anomoepus (Pleisiornis) pilulatus	
Saurischian Dinosaurs	
Grallator (Eubrontes) gigateus	
Grallator (Eubrontes) approximatus	
Grallator (Eubrontes) divaricatus	
Grallator (Eubrontes) tuberatus	
Grallator (Anchisaurips) hitchcocki	
Grallator (Anchisaurips) exterus	
Grallator (Anchisaurips) minusculus	
Grallator (Anchisaurips) parallelus	
Grallator (Anchisaurips) sillimani	
Grallator (Anchisaurips) tuberosus	
Grallator (Grallator) cursorius	
Grallator (Grallator) cuneatus	
Grallator (Grallator) formosus	
?Grallator (Stenonyx) lateralis	
Dinosaur footprints of uncertain position	
Hyphepus fieldi	
Gigandipus caudatus	
Indeterminate footprints	
Chelonoides incendens	*Corvipes lacertoideus*
Exocamope ornata	*Harpedactylus gracilior*
Harpedactylus tenuissimus	*Lacunculapes latus*
Palamopus gracilipes	*Palamopus palmatus*
Palamopus rogersi	*Platypterna concamerata*
Platypterna digitigrada	*Platypterna gracillima*
Platypterna delicatula	*Plectropterna angusta*
Plectropterna gracilis	*Plectropterna lineans*
Selenichnus breviusculus	*Shepardia palmipes*
Sillimanius tetradactylus	*Steropoides diversus*
Steropoides elegans	*Steropoides ingens*
Steropoides infelix	*Steropoides uncus*
Tarsodactylus caudatus	*Ammopus marshi*
Arachichnus dehiscens	*Argoides minimus*
Anticheiropus hamatus	

Thin-bedded, red-gray siltstones and sandstones underlie the gray sequences. These units are rich in reptile footprints. A quarry was opened next to what was called Lily Pond (now a small cove off Barton Cove) which became a major source of tracks for the Hitchcock collection. A nearly complete suite of Connecticut Valley tracks was recovered from this quarry. Valid taxa include *Batrachopus* spp., *Anomeopus* spp., and *Grallator* spp. (Figure 8.18), although Lull (1915) lists 46 ichnospecies in 25 genera (Table 8.1).

Return to vehicles and continue east on MA 2.

50.9 Outcrop with footprints on the left.

51.2 Outcrop with footprints and plant fossils on the left.

52.0 Conglomerate on the left.

52.8 Cross Connecticut River, leaving the basin. We are just a few miles south of Vermont.

From here to the International Ferry in Portland, Maine, take MA 2 to I-495 North. Take Exit 4 onto US 1 at Portland. Take Truck Route 1A to the waterfront. Follow signs to International Ferry to Nova Scotia. Travel time from Portland, Maine to Yarmouth, Nova Scotia is 11 hours.

9. FUNDY SUB-BASIN, SOUTHEAST SHORE OF FUNDY BASIN, NOVA SCOTIA

GEOLOGY OF THE FUNDY BASIN

Stratigraphy, Depositional Environments and Paleontology (by P.E. Olsen)

The Fundy basin of Nova Scotia and New Brunswick, Canada, is the largest of all the exposed Newark Supergroup basins (Figure 9.1). It underlies the Minas Basin, Annapolis Valley, and Bay of Fundy and extends into the Gulf of Maine. Exposures, many very large and spectacular, extend almost all around the shore line in Nova Scotia but are restricted to a few small series of coves and points in New Brunswick and on Grand Manan Island.

Fundy basin strata are divided into five formations (Table 9.1; Powers, 1916; Klein, 1962; Keppie, 1979). Like the Newark basin, the pre-basalt section consists of a basal fluvial interval (Wolfville Formation, Stops 10.2, 10.2, 11.1) succeeded by a lacustrine sequence (Blomidon Formation, Stops 9.1, 10. 2, 10.3, 11.2) in which the lower portions were apparently deposited in the deeper lakes. Again like the Newark basin, the lacustrine rocks (Scots Bay Formation, Stop 10.4; McCoy Brook Formation, Stops 11.2, 11.3) above the basalt (North Mountain Basalt, Stops 10.3, 11.2, 11.3) appear to have been deposited in deeper and less ephemeral lakes than those of older strata. The Fundy basin therefore seems to be another basin fitting the predictions of the basin filling model (Schlische and Olsen, in review; see also Geological Overview).

An abundance of sedimentary fabrics indicating arid depositional environments, such as sand-patch fabrics (see below), evaporites, or eolian dunes, characterize the Fundy basin section (Stops 9.1, 10.3, 11.2, 11.3). Unlike all other major Newark Supergroup basins, there are virtually no organic carbon-rich shales exposed, even in what appear to be strata deposited in the deepest water. The style of cyclic deposition is notably different from the more southern basins; a meter-scale 100,000 year cycle is the most obvious periodic sequence, with the 21,000 year cycle being suppressed or expressed only in the deepest water intervals (Stops 10.3, 11.2). In addition, the cumulative thickness of the exposed strata is only about 1 km. Well and seismic data (Brown, pers. comm.) show, however, that the total thickness beneath the Bay of Fundy is greater than 4 km. In most respects the sedimentary facies of the Fundy basin more closely resemble the pattern seen in the Argana basin of Morocco (Smoot and Olsen, 1985, 1988) than they do the rest of the Newark Supergroup.

The overall arid depositional environments indicated for much of the Fundy basin sequence and the presence of coals in the Triassic-age portions of most of the southernmost exposed Newark basins has been interpreted as indicating a strong N-S climatic gradient (Cornet, 1977a; Hubert and Mertz, 1980, 1984; Olsen, 1981; Cornet and Olsen, 1985). As Manspeizer (1982) has pointed out, there may have been a very strong orographic effect as well, with the more southern basins perhaps being at a higher altitude than the Fundy basins or closer to a large rain-shadow-producing mountain front.

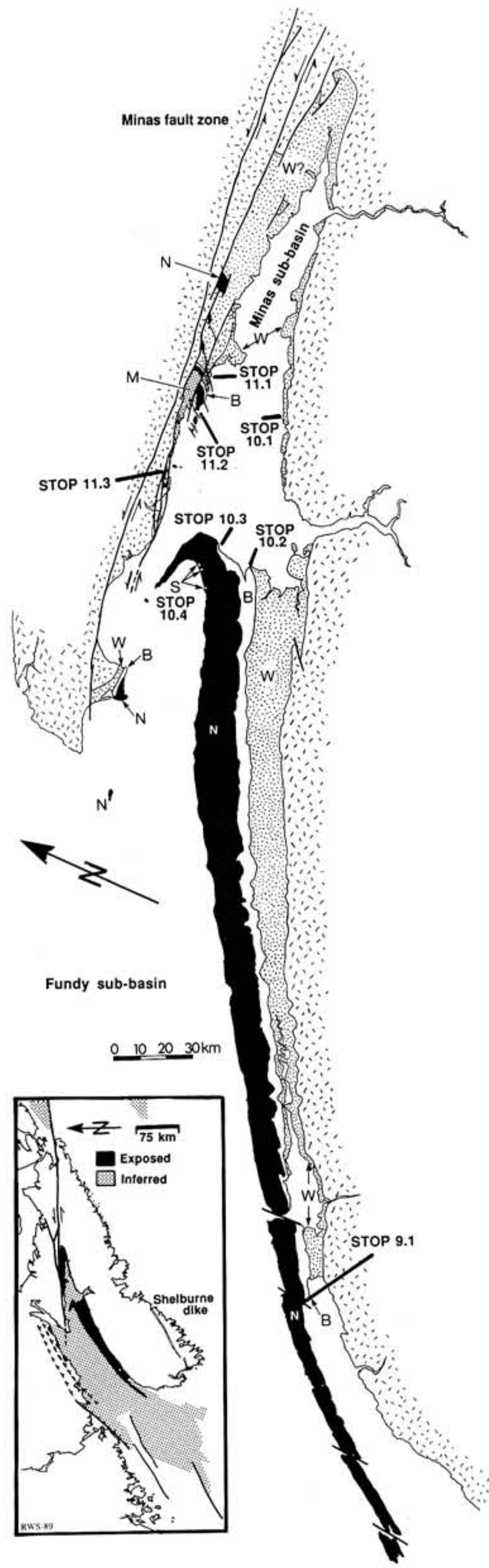

Figure 9.1: Geologic map of exposed rocks of the Fundy basin, Nova Scotia. Inset shows entire basin and Shelburne dike. Black represents basalt flows. Abbreviations are: W, Wolfville Formation; B, Blomidon Formation; N, North Mountain Basalt; S, Scots Bay Formation; M, McCoy Brook Formation. Modified from Keppie (1979).

Table 9.1: Stratigraphy of the Fundy basin, Nova Scotia (after Powers, 1916; Keppie, 1979; Cornet, 1977a).

Units	*Thick-ness (m)*	*Age*	*Description*
McCoy Brook Formation	+200	Pleinsbachian Hettangian	Red and brown, coarse to fine, fluvial, deltaic, and lacustrine clastics with locally developed eolian sandstones; purple, green, and white lacustrine limestones; and basalt agglomerates (lateral equivalent of Scots Bay Fm.)
Scots Bay Fm.	<40	Hettangian	White, green, and red lacustrine limestones (partially bioclastic); chert; and minor brown, fluvial sandstone
North Mt. Bst.	270	Hettangian	Tholeiitic basalt flows
Blomidon Fm.	200	Carnian-Hettangian	Red, brown, and green cyclic lacustrine and deltaic claystones to sandstones with locally developed brown eolian sandstones and conglomerates. Laterally persistent gray, green, and black claystone beds in upper few meters
Wolfville Fm.	300	Anisian-Norian	Brown and red fluvial sandstones and conglomerates; subordinate red mudstones with locally developed red and brown deltaic-lacustrine deposits; and thick, brown eolian sandstones

Despite the apparent aridity of many Fundy basin depositional environments, vertebrate fossils have proved unusually common (Baird and Take, 1959; Baird, 1986a; Baird and Olsen, 1983; Olsen and Baird, 1982, 1986; Sues *et al.*, 1987; Olsen *et al.*, 1987; Olsen, 1988b). Anisian, Carnian, and Hettangian assemblages have produced more than 24 skeletal taxa of reptiles and amphibians identifiable at the genus or better level and several more identifiable at the family level, nine ichnogenera, and representatives of at least four families of fish (Olsen, 1988b). The Fundy basin is unique in producing abundant terrestrial vertebrates from both Triassic and Jurassic deposits. It is thus of great importance in studies of faunal change across the Triassic-Jurassic boundary (Olsen *et al.*, 1987).

Structural Geology (by R.W. Schlische and P.E. Olsen)

The Fundy basin consists of two sub-basins (Figure 9.1) with markedly different structural and stratigraphic styles, influenced by the attitude of Paleozoic structures with respect to the early Mesozoic extension direction. In the larger, NE-trending Fundy sub-basin, NE-striking, SE-dipping thrust faults form the dominant Paleozoic fabric. A NW-SE extension direction, taken to be normal to the strike of the Early Jurassic (Papezic and Barr, 1981) Shelburne dike, reactivated these thrust faults as low-angle dip-slip normal faults (Plint and van de Poll, 1984). The Fundy sub-basin is therefore a half-graben with at least 2 km of synrift strata preserved below the Bay of Fundy, and 1 km of exposed strata in outcrops along the Annapolis Valley (Stops 10.1-10.4).

Structure contour mapping of distinctive reflectors from seismic profiles (D. Brown, Mobil Canada, pers. comm., 1988) reveals a series of folds oriented nearly perpendicular to the normally-reactivated, NE-striking Paleozoic thrust faults on the basin's northwestern margin. Again, these structures may be fault-displacement folds (see section 5). These folds are orthogonal to small amplitude, NE-trending folds identified by Stringer and Lajtai (1979) at Point LePreau, New Brunswick. Based on the highly indurated nature of these rocks compared to Newark age rocks in the area, the lack of definitive age control, and the presence of well-developed axial planar cleavage (Stringer and Lajtai, 1979), we suspect that these rocks and the folding may be Carboniferous in age.

The smaller E-trending Minas sub-basin was influenced by the Minas fault zone, the boundary between the northern Avalon and southern Meguma terranes. The Minas fault zone has had a long history of strike-slip, predominantly right-lateral in the Paleozoic associated with the convergence marking the closure of the Iapetus Ocean (Keppie, 1982), and many Carboniferous strike-slip pull-apart basins are inferred to have formed along it and its numerous subparallel splays (Bradley, 1982). In response to the NW-SE extension which opened the Fundy sub-basin, the Minas fault zone probably experienced left-oblique slip [although in the two localities they studied, Mawer and White (1987) could find no evidence of left-lateral motion]. Hence, the Minas sub-basin is a transtensional rift. In contrast to the relative simplicity of the Fundy sub-basin, the Minas sub-basin consists of a complex series of horsts, graben, and half-graben (Stops 11.1, 11.3). Hence, immediately adjacent to the splays of the Minas fault zone (Stop 11.3), stratigraphic thickness is much less when compared to equivalent strata deposited in the Fundy sub-basin half-graben (Stops 9.1, 10.1-10.4).

mileage	
0	Arrive in Yarmouth, Nova Scotia.
0.1	Turn left onto Main Street, and proceed through downtown Yarmouth.
4.2	Turn right onto Collector Highway 340 North.
5.6	Take Provincial Arterial Highway 101 East (north) to Digby.
6.4	Medulla Gap. Cambro-Ordovician flysch with Devonian plutons. We will see exposures of these rocks all the way to Digby.
24.4	Highway ends. Turn left onto Truck Highway 1 to Digby.
45.4	Turn left towards Digby on Provincial Arterial Highway 101.
63.7	Take Exit 26 to Digby, Collector Highway 303 North.
66.4	Continue on NS 303 leaving downtown Digby.
66.6	Turn left onto NS 217 West.
66.7	Turn right following NS 217 West.
75.9	Pull off to the left side of the road going downhill toward the cove. Park.

STOP 9.1: ST. MARY'S BAY, ROSSWAY, NS

(by P.E. Olsen)

Highlights: Fluvial channel sequence and lacustrine red beds of Blomidon Formation.

A long series of sea cliffs expose middle Blomidon beds at Rossway along the north shore of St. Mary's Bay, Digby County. These outcrops have been studied by Hubert and Hyde (1982), who described the sequence as made up of 10% fissile claystone deposited in playas, 64% sandy mudstones formed on playa mudflats, 25% graded sandstone beds of sand flats deposited at the toes of alluvial fans, and 1% meandering channel sandstones. Hubert and Hyde (1982) recognize 32 thinning- and fining-upward cycles averaging 4.6 m (1.3 to 13.3 m) thick grouped into megacycles 60 to 70 m thick, which they attribute to lateral movement of channels on the fan toes for the small cycles and to deposition resulting from border fault rejuvenation for the megacycles (Figures 9.2, 9.3). Olsen suspects that 1.3 m is closer to the mode for the small-scale cycles, that the larger-scale thinning and fining-upward cycles are compound cycles, and that the 1.3 m cycles are themselves made up of smaller-scale cycles.

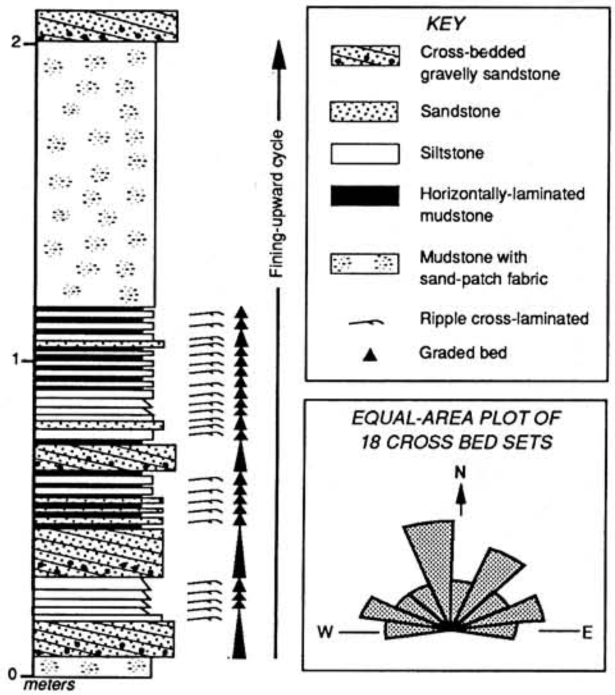

Figure 9.2: Typical thinning- and fining-upward cycle in the Blomidon Formation, St. Mary's Bay, Stop 9.1. Adapted from Hubert and Hyde (1982).

The shore exposures are comprised of three large sections, which from east to west Hubert and Hyde (1982) designated I, II, and III. Although Hubert and Hyde (1982) treated these sections as continuous, they are, in fact, each isolated by faults with at least some component of normal (down-to-the east) slip. The sections could be duplicated by this faulting, and although the sections are similar, they differ enough so that correlation is ambiguous. We enter from the west side and will examines sections III and II (Figure 9.3). Small-scale cycles are obvious on the cliff face as is an isolated channel fill, with well-exposed point bar slip-off faces.

At this outcrop, the base of small-scale cycles consists of a variety of sandy sequences ranging from gray-buff, trough cross-bedded pebbly sandstone to red, ripple cross-laminated, fine-grained sandstones, which locally have reptile footprints preserved at their bases as casts of the underlying mudstones or as poor impressions on their tops (Figure 9.4). The reptile footprint assemblage thus far consists of *Rhynchosauroides* sp. and a number of grallatorids including cf. *Grallator* (*Anchisauripus*) *hitchcocki* and *Grallator* (*Anchisauripus*) *sillimani*.

The mudstones that comprise 64% of combined sections I, II, and III are poorly sorted with abundant small lenses or pods of well-sorted sandstone apparently of eolian origin

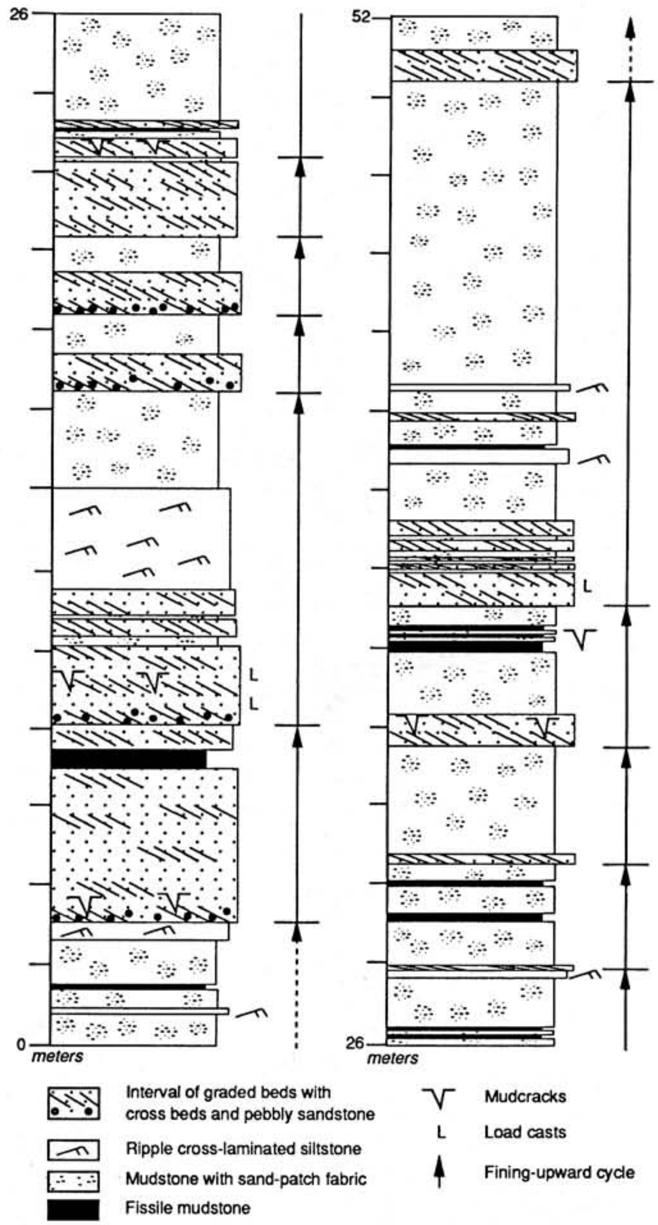

Figure 9.3: Measured section of the Blomidon Formation at Section II, St. Mary's Bay, Stop 9.1. The section consists of 10 thinning- and fining-upward cycles, portions of two others, and 11 playa lake beds (fissile claystone). An upward increase within the cycles of the ratio of playa sandy mudstone to sandflat graded beds defines a fining-upward megacycle from 3.1 m to 50.2 m. Adapted from Hubert and Hyde (1982).

(Hubert and Hyde, 1982). Hubert and Hyde describe these sand pods as adhesion ripples, but this type of unit is described by Smoot and Olsen (1988) as their sand-patch fabric (Figure 9.5). Sand-patch fabric consists of irregular pods of sandstone and siltstone with cuspate contacts with surrounding mudstone, internal zones of different grain sizes, and sometimes cross-laminae showing no consistent orientation relative to other pods. The sand-patch fabric may be cut by jagged-edged, mudstone-filled cracks. Sand-patch fabrics have been identified with certainty only in the Fundy basin of the Newark Supergroup and the Bigoudine Formation of the Argana basin of Morocco (Smoot and

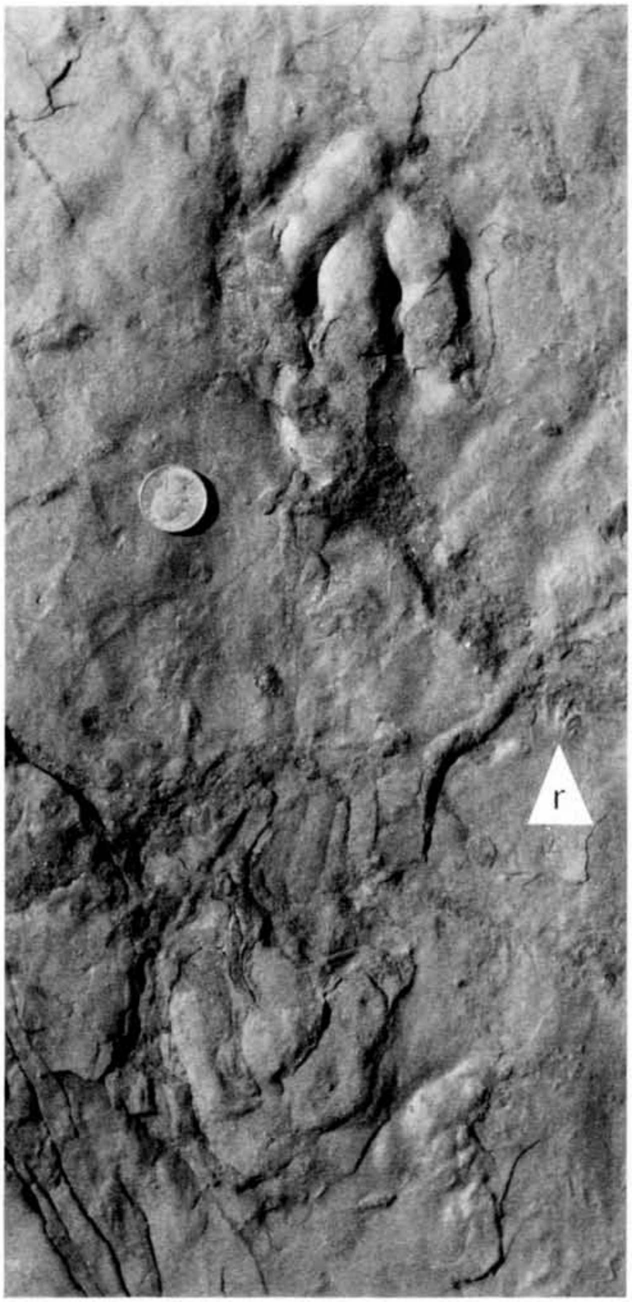

Figure 9.4: Natural casts of two *Grallator* (*Anchisauripus*) *sillimani* tracks from the Blomidon Formation at Rossway, St. Mary's Bay (Stop 9.1). (r) shows *Rhynchosauroides* sp. manus. U.S. quarter (2.4 cm) for scale. Photo by P.E. Olsen.

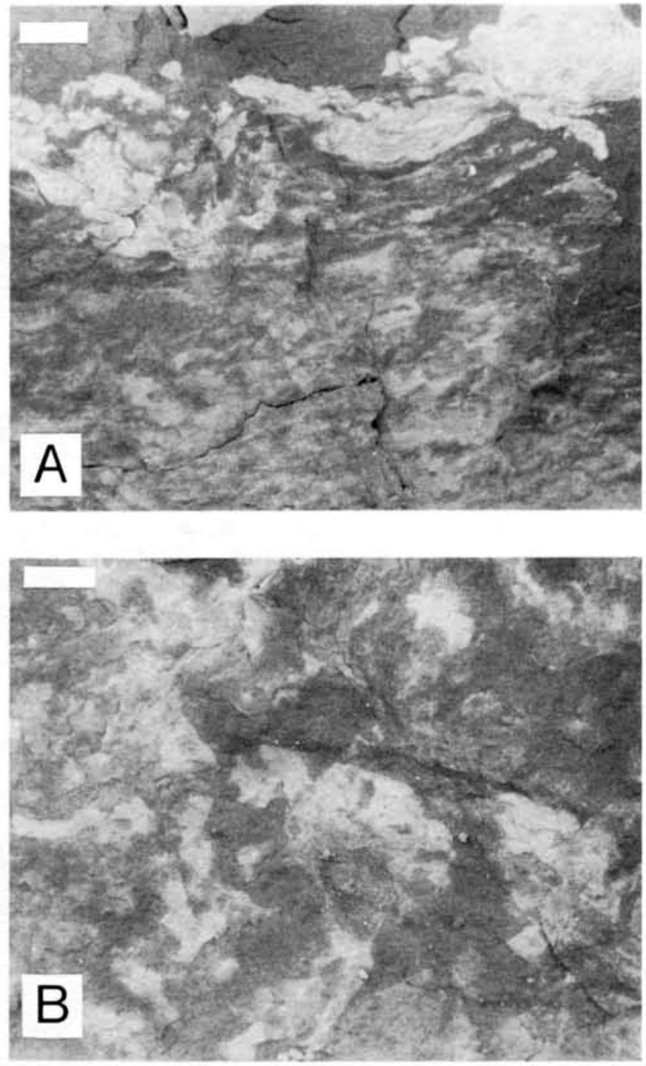

Figure 9.5: Sand-patch fabric within the Blomidon Formation, Stop 10.3: A) cross section; B) plan view. Scale is 2 cm. Photo by P.E. Olsen.

Olsen, 1988). Some beds in the lower Boonton Formation of the Newark basin also appear to have this fabric. Beds containing the sand-patch fabric are part of the playa sequence itself.

In the Fundy basin the sand-patch fabric commonly occurs in meter-scale cycles termed sand-patch cycles (Figure 9.6), which make up larger cycles. Most sand-patch cycles (Smoot and Olsen, 1985, 1988) consist of a lower massive red mudstone with irregular wispy sandy pods succeeded by a red brown massive mudstone-sandstone showing a very well-developed sand-patch fabric. Above the unit with a sand-patch fabric is often a faintly ripple-bedded sandstone. Some cycles may begin with a laminated claystone or fine siltstone, in some places underlain by a thin oscillatory-rippled sandstone or siltstone. Irregular tabular zones at various intervals in the cycles are riddled with euhedral crystals or pods of gypsum, which produce vugs where weathered.

Between sections II and III are a series of intensely faulted beds, one isolated block of which is composed of a white to buff and red granule-bearing sandstone which is probably part of a channel system. This exposure produced the rostrum of the phytosaur *Rutiodon* (Figure 9.7) as well as scutes and a mandibular fragment. This is the only phytosaur known from Canada.

76.3	Leave and return the way we came, back toward Digby.
85.0	Turn right onto NS 303 South at the edge of Digby.
85.5	Turn right onto NS 303 South, NS 101.
86.2	Fork left, following NS 303 South, NS 101.
86.9	Turn left onto Provincial Arterial Highway 101 East toward Halifax.
103.8	Get off NS 101. Turn left toward Annapolis Royal. Leave Annapolis Royal and follow NS 1 toward Wolfville.
121.6	Bridgetown.
123.0	Turn left onto Provincial Arterial Highway 101 East.
163.0	Kentville.
170.6	Take exit 11, NS 358, toward Greenwich and Wolfville (Land of Evangeline).
170.8	Turn right onto Ridge Road. Note apple orchard.

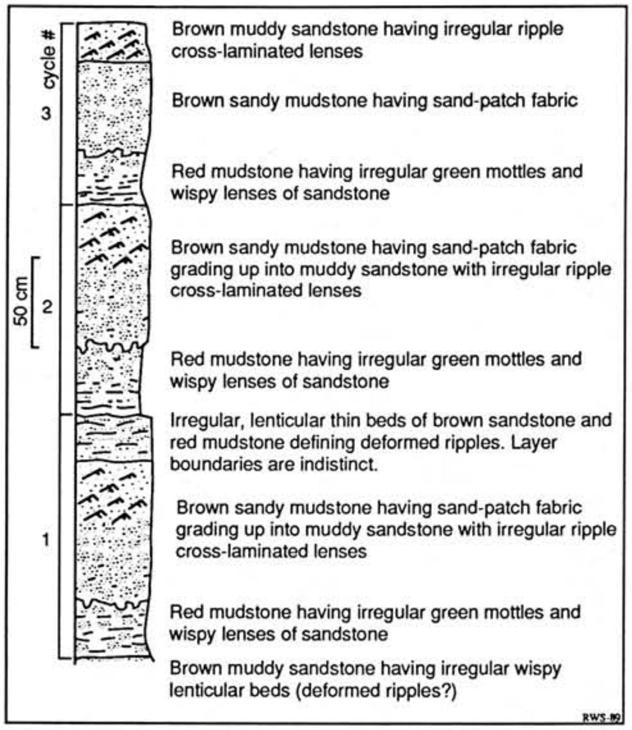

Figure 9.6: Typical sand-patch cycles of the Blomidon Formation. Modified from Smoot and Olsen (1988).

Figure 9.7: Ventral view of rostrum of a phytosaur skull (*Rutiodon* sp.). Scale is 10 cm. Photo by P.E. Olsen and W.K. Sacco.

10. FUNDY SUB-BASIN, SOUTH SHORE OF MINAS BASIN, NOVA SCOTIA

mileage

0	Leave hotel. Turn left onto Ridge Road. View of Minas Basin of the Bay of Fundy. (Note: The term "Minas Basin" is a geographic term used to refer to the large eastern branch of the Bay of Fundy. It refers to a present-day body of water and is not to be confused with a geologic basin.)
0.2	Turn right onto Provincial Arterial Highway 101 East.
16.5	Windsor Mud Flats.
19.5	Take Exit 5 to NS 14 East toward Rawdon and Chester. Turn left at end of exit ramp onto NS 14 East toward Milford and Truro.
20.1	Note gypsum mines on left (Mississippian Windsor Group).
21.3	Gypsum mines on left. Windsor Group.
22.8	Gypsum outcrops in cliffs on right along the St. Croix River. Another gypsum mine is visible in the distance on the left.
25.1	Turn left (northwest) at the service station onto NS 215 East toward Walton.
25.6	Turn left on NS 215 at the service station.
26.2	Turn left onto NS 215 East to Walton.
26.25	Fork right immediately toward Walton.
26.6	Fork right again. Stay on main road.
27.3	Outcrops of the Horton Group (Mississippian) along cliff to the left. Kennetcook River.
27.6	Go right at fork onto Woods Road, toward Walton.
28.4	Turn right at stop sign at Upper Burlington Baptist Church. Stop sign at T-junction, go left on Walton Woods Road toward landfill.
34.5	Dirt road begins.
43.2	Walton, Nova Scotia.
43.4	Very sharp right turn at wharf. Still on NS 215, Glooscap Trail.
47.7	Tennycape.
47.7	Look for an inconspicuous dirt road on the left between a pinkish tan house and a white house. Dirt road descends to shore line along a creek. Park and walk down the road.

STOP 10.1 (OPTIONAL): TENNYCAPE (by P.E. Olsen)

Highlights: Angular unconformity between Triassic Wolfville Formation and Mississippian Horton Group.

Vertical lacustrine strata of the Horton Group are overlain with a profound angular unconformity by the basal Wolfville Formation of the Fundy Group at this stop. The basal contact is irregular on a small scale but dips to the north at a slightly higher angle than the Wolfville strata. This conforms to the general pattern of onlap at the up-dip edges of half-graben as seen in seismic lines (Figure I.5).

Lower Wolfville strata consist of thick fining-upward cycles (2-10 m) of dune-scale trough cross-bedded conglomerate, grading upwards into sandstone and some mudstone with caliche (Hubert and Forlenza, 1988). Some of the conglomerates had a completely open framework, now filled with calcite. This section has produced no fossils to our knowledge, but sightly finer-grained facies in the middle Wolfville have produced a wide range of bones and some clams (Olsen, 1988a). According to Hubert and Forlenza (1988), the Wolfville at these outcrops represents deposits of large-scale braided rivers in a semi-arid setting. The presence of large clams at other Wolfville outcrops, however, argues for wet conditions for long periods of time, as does the large scale and coarse grain size of the trough cross-bedded units which seem more compatible with long periods of sustained flow (J. Smoot, pers. comm.).

Bone- and clam-bearing units in the Wolfville tend to be open framework, calcite-cemented intraformational conglomerates with dune-scale cross bedding, where the bones are clasts. However, some well-preserved skulls have been found in fine-grained sandstones as well. A complete faunal list for the middle Wolfville is given in Table 10.1. Correlation with the middle to late Carnian age Dockum Group is supported by the presence of *Metoposaurus bakkeri* and the rest of the assemblage (Baird and Olsen, 1983; Olsen and Galton, 1984; Olsen and Sues, 1986).

Table 10.1: Faunal assemblage from the middle (M) and upper (U) Wolfville Formation. † indicates an ichnotaxon; assignment to higher (osteological) taxon is tentative.

- Mollusks
  - Pelecypoda
    - Unionidae
      - undetermined clams (M)
- Arthropods
  - Crustacea
    - Diplostraca (clam shrimp and water fleas)
      - *Cyzicus* sp. (M)
    - ?Decapoda
      - †*Scoyenia* (M,U)
- Amphibia
  - Metoposauridae
    - *Metoposaurus bakeri* (M)
- Reptilia
  - Procolophonia (Procolophonids)
    - *Leptopleuron* sp. (M)
    - 3 new genera (M)
    - *Hypsognathus* sp. (U)
  - Synapsida (mammal-like reptiles)
    - Traversodontidae (chisel-toothed mammal-like reptiles)
      - *Scalenodontoides* sp. (M)
    - Kannemeyeriidae (dicynodont mammal-like reptiles)
      - indeterminate (M)
  - Lepidosauromorpha
    - Sphenodontidae
      - †*Rhynchosauroides* sp. (U)
  - Archosauromorpha
    - Trilophosauridae (chisel-toothed archosauromorphs)
      - indeterminate (M)
    - Rhynchosauridae (split-beaked archosauromorphs)
      - *Hyperodapedon* (M)
    - Aetosauridae (armored herbivorous archosaurs)
      - cf. *Stagonolepis* sp. (M)
      - *Stegomus* sp.
      - †*Brachychirotherium* cf. *parvum* (U)
    - Rauisuchidae (carnivorous, usually quadrupedal archosaurs)
      - undetermined teeth (M)
    - Theropoda (carnivorous bird-like dinosaurs)
      - cf. *Coelophysis* sp. (M)
    - 'Fabrosauridae' (poorly defined bird-hipped dinosaurs)
      - new genus (M)
    - Dinosauria incertae sedis
      - partial skeleton (M)
      - *Atreipus acadianus* (U)
      - †(?)*Coelurosaurichnus* sp. (U)

48.0 Turn around and head back toward Walton.
51.5 Enter Walton.
52.3 Sharp turn to the left by the water.
52.4 Turn right on NS 215. Cross Walton River.
55.6 Outcrops of Horton Group (Devonian?-Mississippian) lacustrine strata which contain amphibian tracks and fish fossils. The Mississippian evaporites which we saw earlier are younger than these beds.
68.9 Enter Lower Burlington on NS 215.
71.2 Central Burlington.
76.6 Outcrops of Mississippian Windsor Group—limestone, clastics, evaporites, marine carbonates. Cross Kennetcook River.
77.9 Veer left to NS 236 East toward Stanley.
78.0 Veer right onto NS 215.
78.4 Cross Herbert River (tiny bridge).
78.6 Turn right onto NS 14.
79.0 Turn right on NS 14 (leave NS 215).
80.3 Cross Meander River.
82.8 Gypsum mine.
84.3 Turn onto NS 101 West.
87.4 Windsor Tidal Flats.
98.2 Take Exit 10 to Grand Pré and Wolfville, NS 1.
99.2 Grand Pré Road leading to the Shrine of Evangeline.
102.3 Acadia University.
104.0 Turn right onto NS 358 North toward Canning (10 km).
110.2 Canning. Turn right onto NS 358 North, Glooscap Trail, towards Scots Bay. Continue toward Blomidon.
111.0 Turn left, following signs to Blomidon Provincial Park (14 km).
112.7 Turn right onto Weaver Road just past an orchard.
114.4 Turn left at the T-junction.
115.0 Turn right at the T-junction onto North Medford Road.
115.3 Turn into a small gravel drive going into a field toward the bay. Park.

STOP 10.2: PADDY'S ISLAND NEAR MEDFORD, NS

(by P.E. Olsen)

Highlights: Contact between Blomidon and Wolfville Formations; reptile tracks.

The sea cliffs in the vicinity of Paddy Island, West Medford, Kings County, display the upper Wolfville Formation and its transition into the lower Blomidon Formation (Figure 10.1).

At this locality, 1-2 m intervals of brown, dune-scale, trough cross-bedded conglomerate and sandstone, passing upward into smaller-scale, cross-bedded and ripple-bedded sandstone and planar-bedded red mudstone comprise 4- to 10-m-thick fining-upward cycles. Over all, these sequences resemble those described by Hubert and Forlenza (1988) in other parts of the Wolfville. However, some intervals of low-angle inclined beds of ripple-bedded sandstone with red clay interbeds resemble the deltaic sequences in the Passaic Formation of the Newark basin.

The transition into the Blomidon is marked by the first appearance of laterally continuous (10-100 m) claystone and siltstone beds, with reptile footprints at the top of 4- to 10-m-thick fining-upward sequences followed by the disappearance of dune-scale trough cross-bedded units and conglomerate (Figure 10.1). The basal Blomidon beds are marked by planar, ripple-bedded, or massive, laterally-continuous (at the outcrop scale) sandstone beds, and higher in the section by laminated to massive red claystones and mudstones and by massive sand-patch fabric.

Sand-patch cycles occur at this exposure (Figure 10.1), but are best seen higher in the Blomidon, such as at Stop 10.3. A higher order cyclicity can also be seen at these outcrops, consisting of intervals with well-developed sand-patch cycles alternating with intervals of sandstone and mudstone without sand-patch fabric. The cycles average 6.6 m thick at these outcrops. These larger Blomidon cycles seem to pass, in phase, into the predominantly fluvial cycles of the uppermost Wolfville Formation (Figure 10.1). The middle portions of the dune-scale cross-bedded conglomerate and pebbly sandstones appear to be the

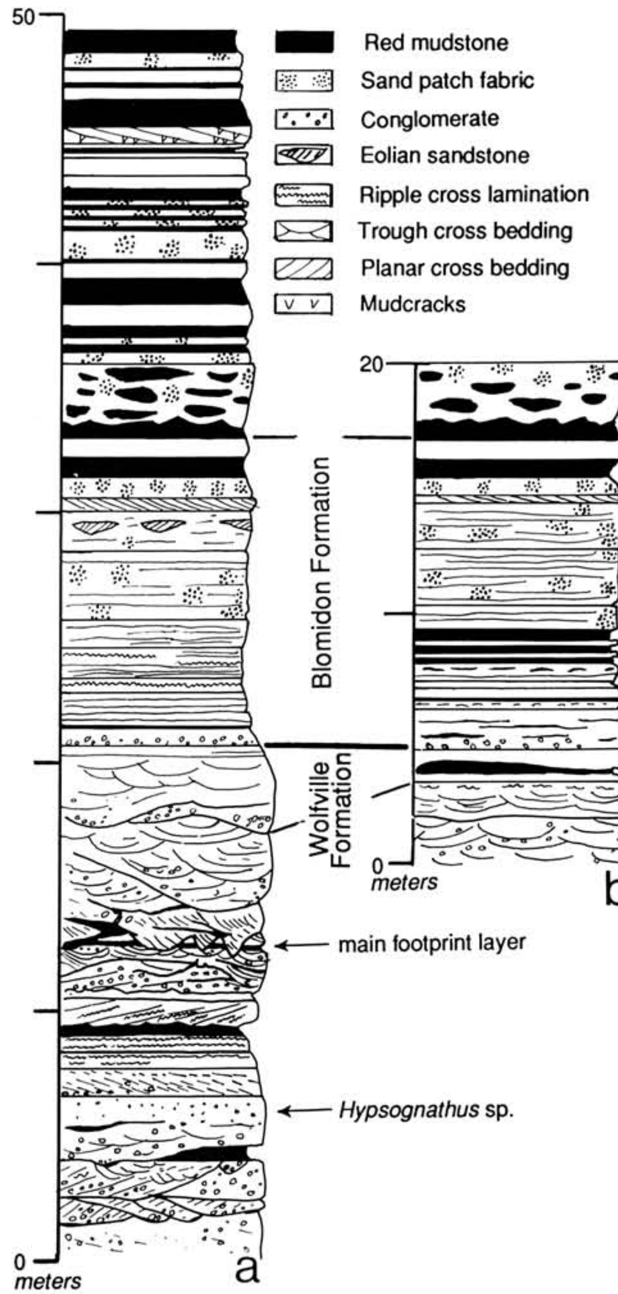

Figure 10.1: Measured sections of the uppermost Wolfville Formation and lowermost Blomidon Formation adjacent to Paddy Island, Stop 10.2: a) section on mainland south east of Paddy Island; b) section covering the same interval as (a) but repeated by a normal fault and lying about 600 m to the north.

homotaxial equivalent of the sand-patch intervals, whereas the red, footprint-bearing mudstone intervals appear equivalent to the mudstone intervals in the Blomidon which mostly lack the sand-patch cycles. If true, this would imply a climatic control of the large-scale fluvial cycles, rather than an origin from the lateral migration of channel systems. On the other hand, it is possible that the sand-patch fabrics have no counterpart at all in the fluvial cycles.

A fault opposite Paddy Island repeats the basal Blomidon section and gives us a chance to see the lateral change in facies toward the basin interior (Figure 10.1). As we might expect, the frequency of mudstone beds in the basal Blomidon increases basinward, and the upper portions of a conglomerate in the uppermost Wolfville in the southern outcrops is replaced by a mudstone and sandstone sequence in the northern outcrops (Figure 10.1).

Well-preserved reptile footprints are abundant in the laterally-continuous claystone and siltstone beds in the uppermost Wolfville at this locality (intervals 10.5 m, 12.8 m, Figures 10.1, 10.2, 10.3). The most abundant taxon is cf. *Rhynchosauroides* sp., followed by numerous and well-preserved *Atreipus acadianus* (Olsen and Baird, 1986). The brachychirotheriid *Brachychirotherium* cf. *parvum* is relatively rare as is *Coelurosaurichnus* sp. 2 (of Olsen, 1988b). In total, the assemblage is directly comparable to that seen in the Lockatong Formation and lower to middle Passaic Formation of the Newark basin.

A skull and disarticulated skeleton of the procolophonid *Hypsognathus* was found at the 6 m position in poorly-sorted pebbly sandstone in 1983 by Alton Brown (then of Arco Petroleum). The skull is smaller and less completely ossified than the existing specimens of *Hypsognathus fenneri* known from the uppermost Passaic Formation and New Haven Arkose, and horns on the sides of the head are very much smaller in the Nova Scotian form. Pending detailed anatomical comparisons, it is unclear whether taxonomic, sexual, or ontogenetic differences account for these differences.

Figure 10.3: Slab bearing natural casts of three manus-pes sets of *Atreipus acadianus*, 5 pes impressions of *Atreipus acadianus*, manus-pes set of *Brachychirotherium* cf. *parvum*, and several poor *Rhynchosauroides* sp. manus impressions. Scale is in cm. Photo by Donald Baird.

Figure 10.2: Sketches of vertebrate tracks from the Wolfville Formation adjacent to Paddy Island, Stop 10.2: A) *Atreipus acadianus* (from Olsen and Baird, 1986); B) *Coelurosaurichnus* sp. B; C) cf. *Brachychirotherium parvum*; D) *Rhynchosauroides* sp. Scale is 1 cm.

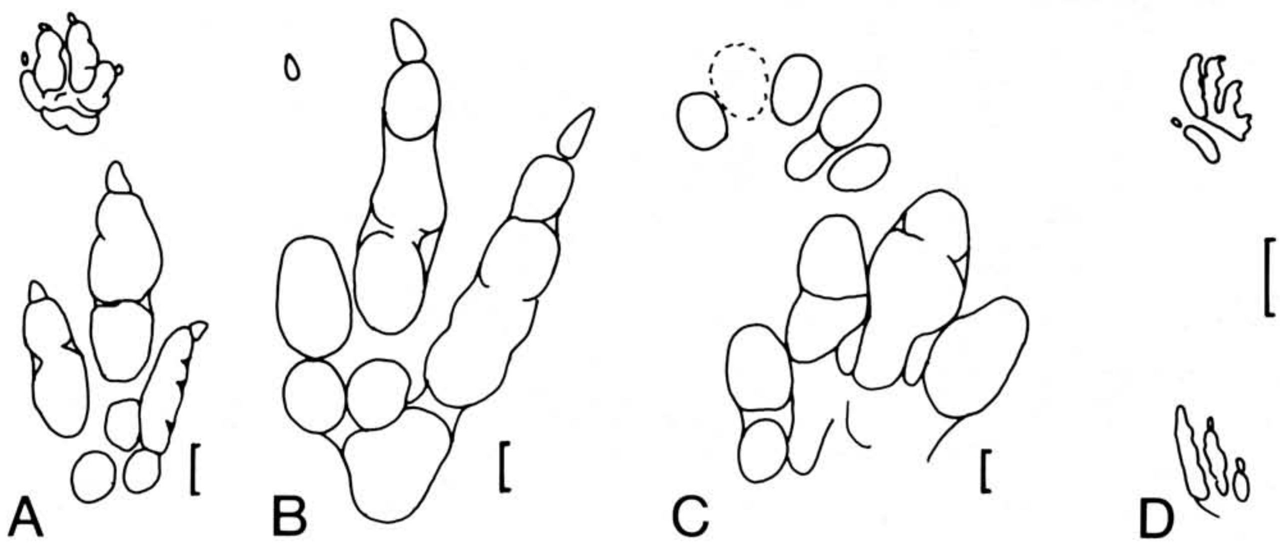

Paddy Island is on the north side of the fault and consists totally of upper Wolfville Formation. Footprint-bearing claystone and siltstone layers are more numerous on the island and surrounding flats than in the corresponding horizon at the mainland cliffs, but the quality and density of the tracks is much lower.

115.6	Leave. Go straight ahead on road to Medford.
116.4	Turn right onto Jackson Barkhouse Road to Pereau.
117.0	Turn right onto Pereau Road.
118.4	Welcome to Blomidon.
121.8	Blomidon Provincial Park. Turn into lot and park.

STOP 10.3: BLOMIDON PROVINCIAL PARK, CAPE BLOMIDON (by P.E. Olsen)

Highlights: Gypsum nodules and veins, sand-patch cycles, synsedimentary? deformation.

This stop consists of a 4.2 km walk down section through about 150 m of middle Blomidon Formation, beginning at the White Water picnic area of the Blomidon Provincial Park and ending at the tidal channel of Mill Creek.

View north from the stairs leading to the beach at the east end of the picnic area shows the spectacular cliff outcrops of the upper Blomidon Formation and lower part of the lower flow of the North Mountain Basalt. Most of the Blomidon Formation outcrops consist of cyclic red and brown lacustrine sequences producing almost no fossils. The uppermost Blomidon, however, consists of a sequence of four red to black cycles, which despite their proximity to the North Mountain Basalt, are sparsely palyniferous. The uppermost black unit produces a palynoflorule dominated by *Corollina meyeriana* (Cornet, 1977) and indicates the Triassic-Jurassic boundary is probably below this level. Palynoflorules from the uppermost Blomidon at other localities in the Fundy basin show that the boundary must lie within the uppermost few meters of the formation (Olsen *et al.*, 1987).

Talus of the lower flow of the North Mountain Basalt is a popular area for mineral collecting, especially for amethyst, agate, and zeolites.

Walk down steps to beach and proceed south, following cliffs. Distances are measured cumulatively southeastward from the foot of the stairs. Distances were originally measured in paces by Olsen with one pace = 0.9448 m.

62 m: Borden Brook—well-developed sand-patch cycles. At these outcrops the sand-patch cycles average about 1.5 m thick. Sand-patch cycles can be generally traced at least the length of outcrops (300-1000 m).

213 m: Very thin (20-30 cm) sand-patch cycles with well-developed claystone bases make up marker beds which can be traced to cliffs on north side of steps from the picnic area allowing sections to be correlated unequivocally. Clusters of such thin sand-patch cycles often underlie clusters of three or four thicker (1-2 m) sand-patch cycles, making a higher-order cycle.

499 m: Mudstone cycles consisting of about five 20-to-40-cm-thick beds of laminated claystone and siltstone grading upward into massive mudstone, with sand-patch fabrics becoming common in the upper beds. Such cycles increase in frequency lower in the Blomidon Formation, and these mudstones are the main source of fossils. Alternations of two or three of these cycles with two or three sand-patch cycles make up larger cycles similar to those made solely of sand-patch cycles (as at 144 m).

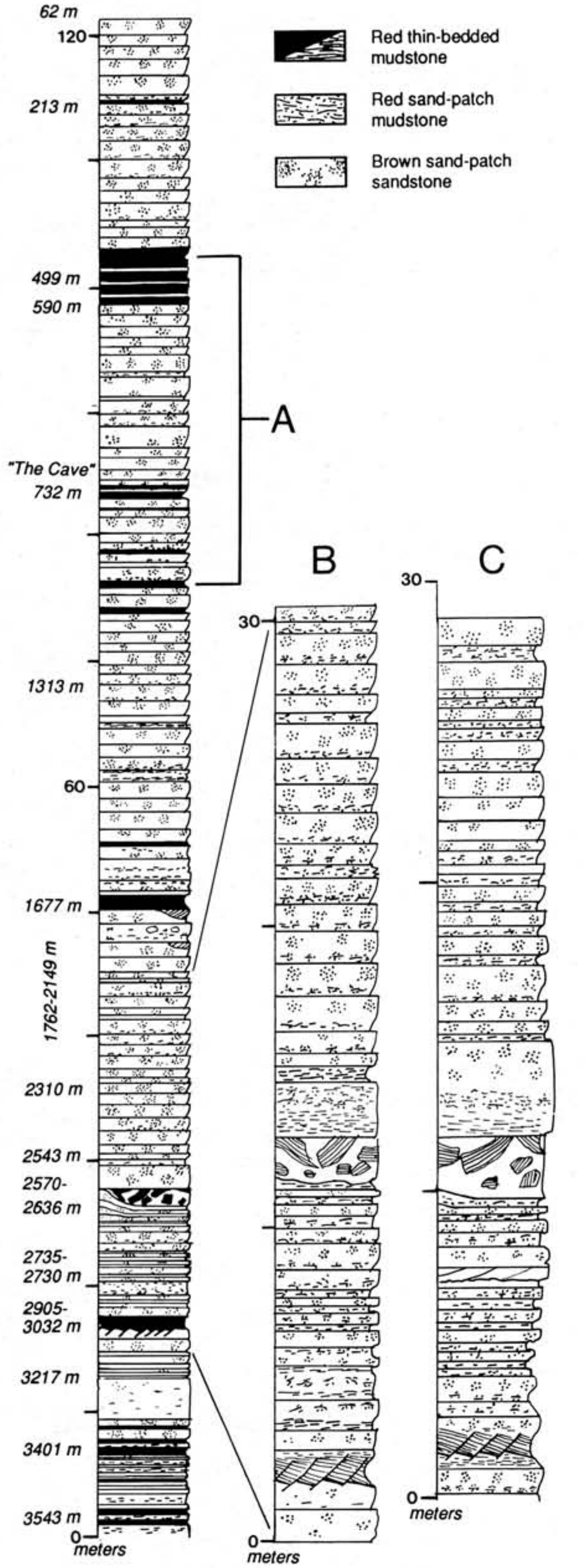

Figure 10.4: Measured section of the Blomidon Formation at Cape Blomidon Provincial Park, Stop 10.3. (A) Location of section illustrated in Figure 10.5; B) enlargement of section at meter-marks 1782-3032; C) same stratigraphic interval as (B) but repeated by faulting about about 1 km to southwest (visible from southwest end of traverse).

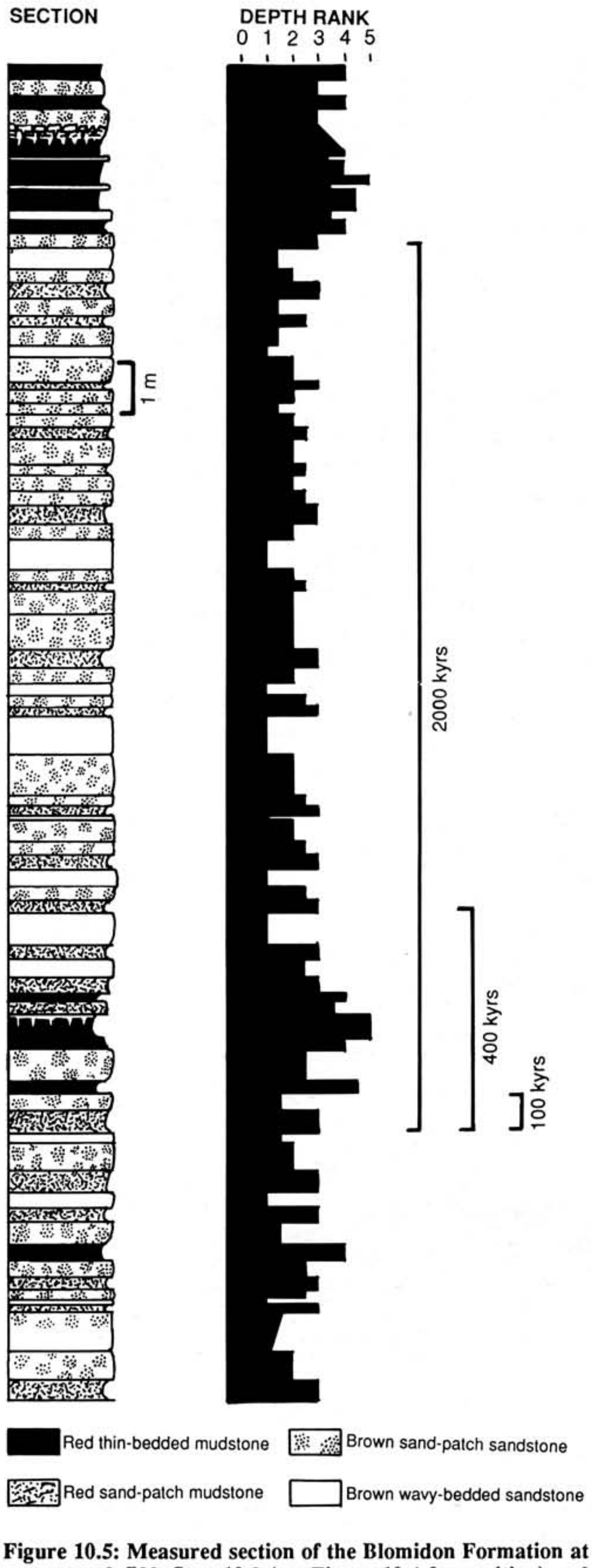

Figure 10.5: Measured section of the Blomidon Formation at meter mark 732, Stop 10.3 (see Figure 10.4 for position) and depth rank curve. Indicated 2 M.yr. cycle is based on power spectrum (Figure 10.6).

590 m: Long, thin sandstone lenses, possibly eolian, crop out in cliff face in lower beds of mudstone cycles. These lenses pinch out down-dip to beach level.

732 m: Two well-developed mudstone cycles are overlain by a series of well-developed sand-patch cycles making a yet higher-order cycle. Fourier analysis of this section (Figures 10.4, 10.5, 10.6) shows prominent compound periods of 0.91 m, 1.24 m, 4.10 m, and 20.48 m. The well-developed mudstones cycles correspond to the 1.24 m thick cycles in the power spectrum. The alternation from these mudstone rich layers to the next cluster up the cliff (at 499 m) corresponds to the 4.1 m cycle.

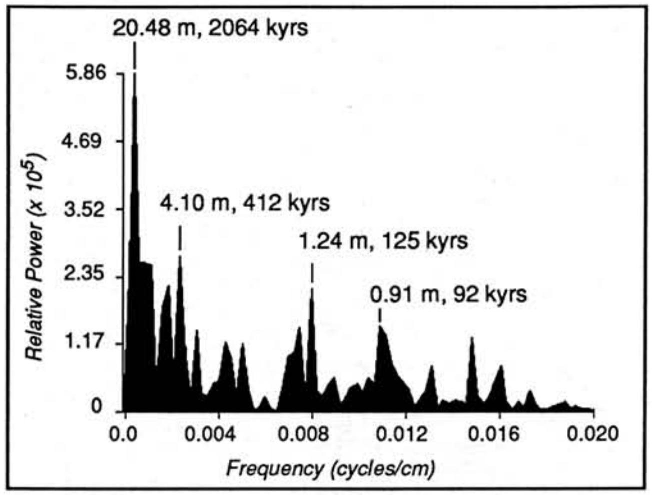

Figure 10.6: Power spectrum of the depth rank curve from Figure 10.5. The 20.48 m cycle may correspond to the 2 M.yr. eccentricity cycle if the sedimentation rate in this portion of the Blomidon is only .01 mm/yr.

1162 m: Hanging outlet of Straddle Leg Brook. More sand-patch cycles.

1313 m: Very clear, well-developed sand-patch cycles.

1677 m: A well-developed mudstone cycle is on the west, with finely-laminated clam shrimp (*Cyzicus*) and ostracode-bearing claystone with pinch-and-swell siltstone laminae. On the south is a "reef" of eolian sandstone.

1708 m: Steel stairs from Glooscap Lane development.

1762-2149 m: Bowl-shaped deformation pods within well-developed sand-patch cycles are well displayed here. Asymmetrical fanning, isolated beds of very well-sorted sand, and lack of associated or compensating uplift suggest progressive subsidence and filling of a very small basin, perhaps by dissolution of underlying evaporites or by small-scale thinning by surface extension or earthquake liquefaction.

2244 m: Stream entering Lyons Cove.

2310 m: Prominent cliff of sand-patch cycles. The red mudstone beds at the top of the cliff correlate with those at 1677 m.

2543 m: Base of long sequence of sand-patch cycles. There are no comparable long sequences better exposed below this stratigraphic interval.

2570-2636 m: Brick red mudstone sequence 1.9 m thick with a flat bottom overlies a strongly lenticular (0-2 m) chaotic-looking unit consisting of decimeter- to meter-scale irregular pods and fissures of brown mudstone to coarse sandstone with internal bedding and abundant small (< 1 cm) to large (> 1 m) clasts of deeply mudcracked, finely-laminated red, green-gray, purple, and yellow claystone containing fish scales, sparse articulated fish, and abundant clam shrimp (*Cyzicus*) and ostracodes. Clasts seem to be derived from the bed that is occasionally present **at the top** of the lenses. The lower contacts of the lenses are **conformable** with underlying mudstone and sand-patch-bearing beds (Figure 10.7), which are warped into gentle anticlines and synclines (or domes and bowls) that decrease in amplitude down-section. The whole section below the brick red unit is riddled with pods and euhedral crystals of gypsum. Pods and fissures in lenses containing clasts derived from overlying beds suggest progressive erosion and deposition below the sediment surface mostly prior to the deposition of the flat-bedded brick red mudstone. A meter-scale bed of salt could have been dissolved in stages and replaced by subsurface channels and fissures, or space for subsurface deposition could have been created by earthquake-induced surface ruptures, blowouts, and fissures. However, because no evidence of upward movement of material has been found, we favor the salt dissolution model. It should be noted that similar sand-patch facies are associated with substantial halite beds in basins of Morocco (Lorenz, 1988; Smoot and Olsen, 1988).

Carroll *et al.* (1972) reported the occurrence of *Semionotus* (erroneously referred to as a redfieldiid) found by William Take and Edwin H. Colbert in 1962 at this locality in a block of loose rubble (Olsen *et al.*, 1982).

2735-2830 m: A sequence of sand-patch cycles about 8 m thick has a higher percentage of mud and gypsum than usual. Many low-angle faults are present.

2905-3032 m: Outcrops of red to greenish-gray, finely-laminated claystone (90 cm thick) with thin pinch-and-swell siltstone laminae. The unit is deeply and polygonally-cracked and produces clam shrimp (*Cyzicus*), darwinulid and other ostracodes, and semionotid and possibly redfieldiid fish scales. The unit apparently forms the base of a well-developed 2-m-scale mudstone cycle.

The fossil-bearing unit is cut by east-trending listric and planar faults which rotate the units downward to the north. There is some evidence of rotation and syn-faulting deposition of eolian sandstone in one or two of the mini-half-graben. Although there is no distinct upper erosional surface, the faulting appears not to penetrate more than 4 m above the fossil-bearing unit, either soling out into roof faults or dying out as growth faults. Lower parts of faults appear to sole out into underlying sand-patch and gypsum-rich unit. Deformation is consistent with **a period** of **repeated** earthquake events.

3217 m: Sand-patch cycles.

3401 m: Two well-developed mudstone cycles, each about 2 m thick (1.9-2.1 m) consisting of five 20- to 40-cm-thick cycles of laminated to thin-bedded claystone, grade upward into massive mudstone beds. The pattern of about five thin cycles making up a larger cycle which in turn makes up larger cycles is very suggestive of the Van Houten and higher-order cycles seen in the southern Newark Supergroup basins. In this case, the thin decimeter-scale cycles would appear to be the 21,000 year precession cycle. The 1-2 m cycles might then be the 100,000 year eccentricity cycle. The larger cycles made up of clusters of four, meter-scale cycles could be the 400,000 year eccentricity cycle. The largest cycles could reflect the as yet very poorly known eccentricity cycles of ~ 2,000,000 years (Berger, 1977). Following this hypothesis, the approximately 200-m-thick Blomidon Formation would represent about 20 million years, comparable to the duration of the Lockatong plus Passaic formations (Olsen, 1986). If, on the other hand, the meter-scale cycles were assumed to be produced by the precession cycle, the duration of the Blomidon would be only about 4.2 million years, comparable to the duration of the upper Passaic Formation. The presence of unusually thin (for the Newark Supergroup) magnetically-reversed intervals in this section (W.K. Witte, pers. comm.), the presence of Carnian vertebrates in the underlying middle Wolfville Formation (Baird and Olsen, 1983), and the presence of Middle Triassic vertebrates in the lower Wolfville at Lower Economy (Stop 11.1), all suggest a long duration for the exposed Fundy basin section, which favors the former hypothesis. It is also possible that the sand-patch cycles represent aggradational events, unrelated to climatic changes.

Fourier analysis of the section seen at 732 m supports the

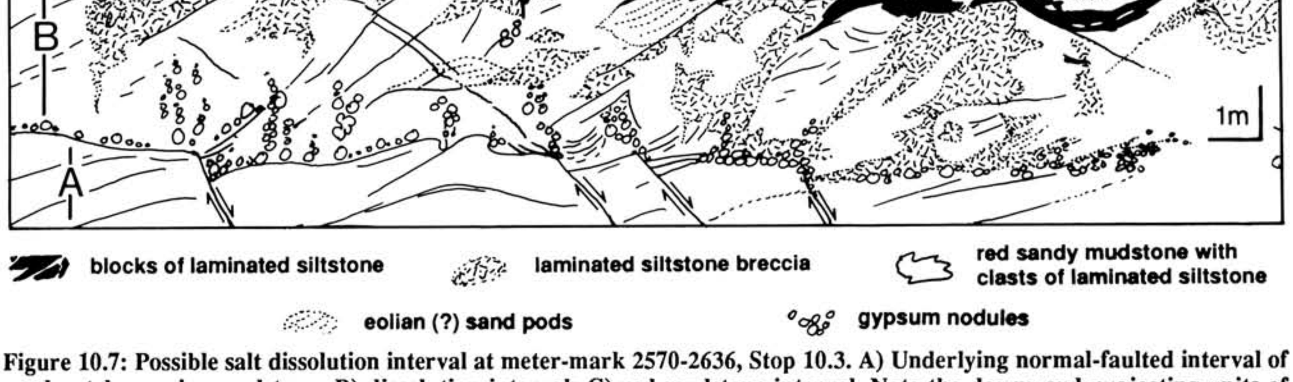

Figure 10.7: Possible salt dissolution interval at meter-mark 2570-2636, Stop 10.3. A) Underlying normal-faulted interval of sand-patch massive mudstone; B) dissolution interval; C) red mudstone interval. Note the downward projecting units of laminated shale breccia, apparently originating from collapse of the overlying units.

astronomical interpretation of the cycles. If we assume the meter-scale cycles are the 100,000 year cycles, Fourier analysis yields significant periods at 92,000, 125,000, 413,000, and 2,064,000 years (Figure 10.6). Modern orbital periods are 95,000, 123,000, 413,000, and 2,035,000 years (Berger, 1977). Despite the somewhat large amount of noise in this spectrum, the very close correspondence between the modern and model periods seen in the Blomidon Formation indicates that we should be optimistic in testing the hypothesis that orbital variations were responsible for the Blomidon cycles.

3543 m: The stratigraphically-lowest outcrops of the Blomidon Formation which can be unambiguously tied to overlying outcrops consist of a single sand-patch cycle. About 10 m of underlying section can be seen in the beach, but the lithology is hard to work out because of poor exposure.

3765 m: Ravine in cliff face. No fault is present here.

3822 m: A steeply S-dipping, E-W striking fault zone drops the section down to the south. Steeply-dipping beds adjacent to the fault apparently involve the lenticular and brecciated unit (seen at 2905-3032 m) and underlying units. A tight anticline can be seen in the fault zone.

4039 m: Gently-dipping sequence of sand-patch cycles that correlate with those seen at 2310 m.

4228 m: Pilings for abandoned wharf at tidal channel of Mill Creek. View to the south is of a large cliff of sand-patch cycles that correlate with those seen at 2310 m and 4039 m. Equivalents of the entire section corresponding to 2310 to about 2950 m at this stop are repeated by a major fault that must lie in the channel of Mill Creek.

Turn west and follow the path on north side of Mill Creek toward main road and rejoin vehicle.

Table 10.2: Faunal list for Scots Bay Formation. Gastropod and ostracode udentifications from Cameron (1986). † Designates an ichnotaxon.

Mollusks
  Pelecypoda
    ??Unionidae
      undetermined very small clams
  Gastropoda
    Planorbidae
      Gyraulus sp.
    Valvatidae
      Valvata sp.
    Hydrobiidae
      Hydrobia sp.
Arthropods
  Crustacea
    Ostracoda
      Darwinula sp.
      Metacypris sp.
Pices
  Actinopterygii
    Semionotidae
      Semionotus sp.
Reptilia
  Archosauria
    Protosuchidae
      isolated bones and scutes
    Theropoda
      †*Grallator (Anchisauripus) minusculus*
      †*Grallator (Anchisauripus) tuberosus*
      †*Grallator (Anchisauripus) sillimani*

122.0 Head south on Pereau road. Mileage at this point will have advanced to 123.0 because the vehicle will have turned around at Blomidon Park and driven the distance we walked.

125.1 Intersection with Stewart Mountain Road and road to beach. Outcrops from here to Delhaven expose sequence of sand-patch cycles and underlying fossil-bearing lensing unit of 2570-2636 m of Stop 10.3. Lensing unit is here associated with well-developed sandstone channels. There must be a fault in marshy zone at this mileage to repeat the section.

127.1 Turn right onto Medford Road at Pereau-Delhaven Community Hall.

128.1 Turn right on NS 358 to Lookoff and Scots Bay.

129.6 Outcrop of North Mountain Basalt.

129.7 T-junction. Turn left toward Glenmont (Gospel Woods Road).

130.8 Turn right onto Ross Creek Road at Bethel Church. Dirt road. Ridges here are the massive parts of basalt flows and valleys are underlain by the vesicular tops of flows.

133.6 Stop at end of road and park.

STOP 10.4: COVES ALONG SCOTS BAY

(by P.E. Olsen)

Highlights: Lacustrine stromatolites around tree trunks in Scots Bay Formation; amygdaloidal North Mountain Basalt; mineral collecting.

Caution*: Long walk over difficult basalt terrane. Do not walk on boulders covered by slippery sea weed.*

A series of small coves expose remnants of the Jurassic sedimentary sequence overlying the North Mountain Basalt. These sedimentary sequences consist mostly of limestone and chert and were named the Scots Bay Formation by Powers (1916). The Scots Bay Formation is a local, lateral equivalent of the basal part of the predominantly red clastic McCoy Brook Formation of the north shore of the Minas Basin (see Stops 11.2 and 11.3) and apparently underlies most of the Bay of Fundy (Brown, pers. comm.). The principal workers on the Scots Bay other than Powers have included Haycock (1900), Klein (1960, 1962), Crosby (1962), Palmer (1971), Olsen *et al.* (1982), Birney (1985), Cameron (1986), and Suchecki *et al.* (1988).

The sedimentary rocks of these sequences can be divided into six categories, each with characteristic fossils, as follows: 1) brown quartz-rich sandstone with dinosaur footprints; 2) thick-bedded, sometimes cross-bedded chert and limestone with clastic textures; 3) crudely-bedded, commonly silicified limestones with large desiccation cracks and few fossils; 4) stromatolitic limestones and cherts with domed heads and tufas around trees; 5) red and green, crudely to thin-bedded snail and clam coquinas with probable charophyte debris; and 6) laminated green-gray calcareous siltstones with ostracodes, probable charophyte debris, and fish fragments, articulated remains and coprolites. A faunal list is given in Table 10.2.

Walk to the northeast from road and cross the outlet of Ross Creek. To the southwest of this point and around the basalt point are the Scots Bay Formation outcrops at Woodward Cove, described by Haycock (1900), Klein (1960), and Birney (1985). To the northeast, are the outcrops at Lime, West Broad, East Broad, Central Broad, and Davidson Coves. As we proceed along the basalt note the abundant neptunian dikes in the basalt filled with zones of red and green partly silicified mudstone and locally cut by faults with mineralized and slickensided surfaces.

Figure 10.8: Impression of *Grallator* (*Anchisauripus*) cf. *tuberosus* from the uppermost brown sandstone at Central Broad Cove in the Scots Bay Formation, Stop 10.4. Scale bar is 5 cm. Photo by P.E. Olsen.

Going to the northeast along the shore, the first good outcrops of Scots Bay Formation are in Lime Cove. Outcrops along the entire inside of the cove contain abundant silicified tufa-coated logs (Birney, 1985). The logs are almost always completely gone, with the resulting cavity filled with botryoidal quartz and sometimes a geopetal fabric. In one very large log, Olsen found slivers of silicified wood with cells preserved, surrounded by puffy outwardly-radiating tufa fabrics.

The next cove to the northeast has a major stream entering it and is called West Broad Cove (Birney, 1985; Suchecki *et al.*, 1988). The most distinctive aspects of West Broad Cove are the well-developed domed stromatolites exposed near the mouth of Black Brook at the center of the cove.

Further to the northeast is what Birney (1985) and Suchecki *et al.* (1988) called Central Broad Cove. Distinctive to this outcrop is the thick brown sandstone near the middle of the section, large blocks of which lie strewn about the cove. This sandstone has dune-scale trough cross-bedding with chert clasts capped by a veneer of thin beds bearing abundant dinosaur footprints (Figure 10.8)

Birney (1985) and Suchecki *et al.* (1988) called the most northeastern in the series East Broad Cove. This is the most fossiliferous of the sections, with articulated and disarticulated fish common in one bed and silicified clams and snails common in another (Figure 10.9). *Semionotus* is the only fish so far recognized (Olsen *et al.*, 1982). However, large, *Semionotus*-containing coprolites suggest the presence of a large coelacanth or a shark as at Wasson Bluff (Stop 11.3) in what is probably the lateral equivalent of these beds in the McCoy Brook Formation.

Two large-scale cycles (3-4 m) are obvious at this outcrop (Figure 10.9) (Suchecki *et al.*, 1988), each

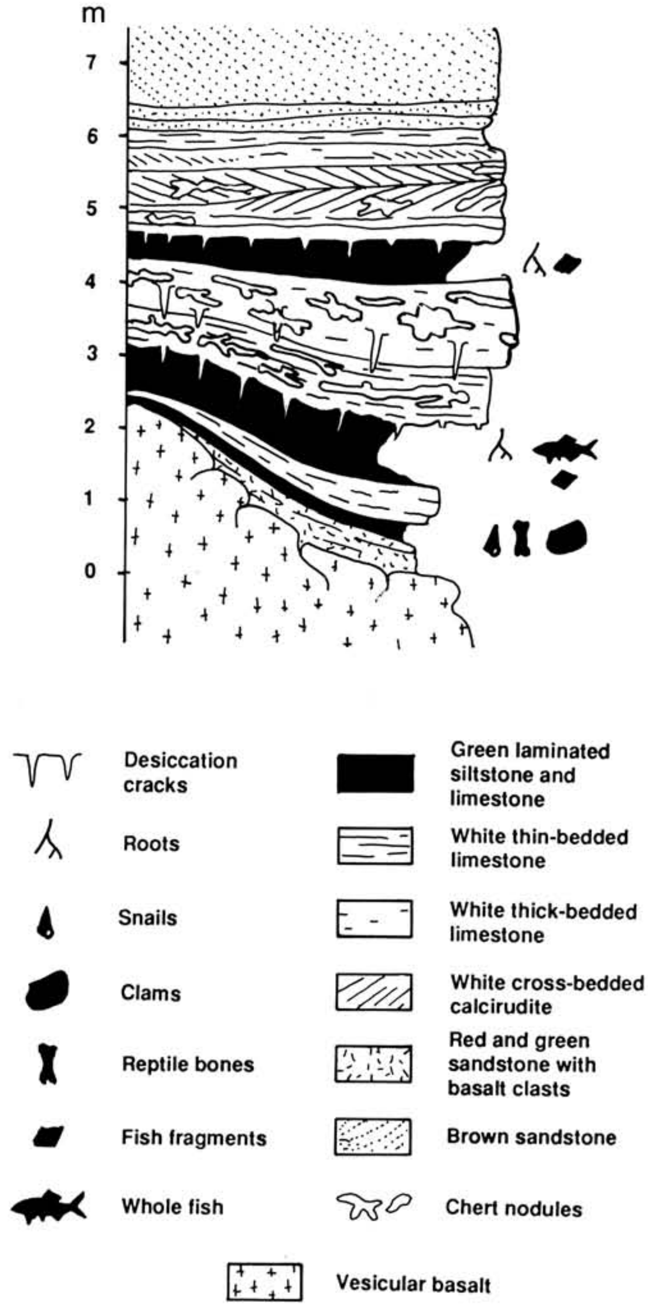

Figure 10.9: Measured section of the Scots Bay Formation at East Broad Cove, Stop 10.4.

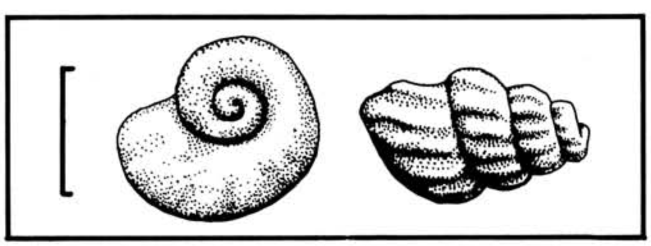

Figure 10.10: Tiny snails (cf. *Hydrobia* sp., right; cf. *Gyraulus* sp. left) from the Scots Bay Formation, Stop 10.4 . Scale is 1 mm. Adapted from Olsen (1988b).

consisting of a lower laminated, green, calcareous siltstone overlain by massive limestone and chert with abundant desiccation cracks. Each large cycle is composed of several shoaling-upward sequences marked by desiccation-cracked horizons suggestive of the smallest (decimeter-scale cycles) within the laminated clay-rich portions of the Blomidon Formation.

A red and green silicified clam and snail coquina (Figure 10.10) occurs low in the section at the northern edge of the outcrop in the "cave" about 44 cm above the basalt. Also present are possible charophyte debris and sparse crocodile (protosuchid) bones. The clam and snail coquinas lap onto the basalt to the southwest.

133.6 Turn around and go back the way we came.
137.5 Turn left at Bethel Church.
137.6 Turn right onto NS 358.
140.7 At statue of Borden, turn right, following NS 358 South.
141.1 Turn left following NS 358.
146.3 Intersection with NS 1. Pass through Greenwich on NS 358, toward Provincial Arterial Highway 101.
147.3 Intersect Provincial Arterial Highway 101. Keep going straight on 358, past intersection. Turn onto Greenwich Road and then right into hotel parking lot.

11. MINAS SUB-BASIN, NORTH SHORE OF THE MINAS BASIN, NOVA SCOTIA

***Please note**: The actual order in which the field stops are run will depend in large measure on the times of high tide. All of the stops are along the coast, and most of the outcrops are not accessible during high tide.*

mileage

0	Leave Hotel.
0.2	Get on Provincial Highway 101 East toward Truro.
16.5	Windsor Mudflats.
19.5	Exit 5 onto NS 14 East, toward Truro. Turn left at the end of the exit ramp onto NS 14 East toward Milford and Truro.
23.4	Fork right to Truro.
25.2	Turn left at intersection toward Truro.
25.6	Turn right on NS 14 toward Truro.
59.2	Get on Provincial Arterial Highway 102 and go north.
65.7	Road sign indicates that we are now halfway between the North Pole and the Equator at 45° north latitude.
82.2	Truro.
85.2	Take exit 15W to Trans Canada Highway 104 West toward Amherst and New Brunswick.
92.5	Take Exit 11 to NS 2 west toward Parrsboro. (Glooscap Trail.)
113.9	Carrs Brook. Turn left into driveway just past bridge over Carrs Brook.

STOP 11.1: CARRS BROOK NEAR LOWER ECONOMY, NS (by P.E. Olsen)

Highlights: Fluvial and eolian strata of Wolfville Fm.

From the beach at Ross Creek walk west. Steeply dipping (20-50°) beds of brown, calcite-cemented intraformational conglomerate with a few lithic clasts alternate with orange eolian sandstone, fluvial sandstone and minor red mudstone. The intraformational conglomerate produce a wide range of scrappy bones and rare, thick-shelled clams. These bone-bearing units are comparable to the bone-bearing fluvial units from the south shore of the Minas Basin which produce a taphonomically-similar reptile and amphibian assemblage of apparently much younger age (see Stop 10.1).

The vertebrate assemblage is apparently dominated by labyrinthodont amphibians, notably capitosaurs and the long-snouted *Aphanerama*, known from Early Triassic beds from Madagascar, Spitzbergen, Greenland, and the Moenkopi Formation of Arizona. A complete faunal list is given in Table 11.1. On the whole, the assemblage most closely resembles faunules of Early Triassic to early Middle Triassic age, especially the upper Buntsandstein of Germany (Olsen and Baird, 1986). These beds thus represent the oldest dated strata in the Newark Supergroup.

The eolian sandstones (Hubert and Mertz, 1984) suggest an arid environment, but both the aquatic herpetiles and the clams suggest perennial water for the intraformational conglomerates. Perhaps this is again an example of the

Table 11.1: Faunal list for Anisian age portion of the Wolfville Formation at Lower Economy (Carrs Brook) Stop 11.1.

- Mollusks
  - Pelecypoda
    - ??Unionidae
      - undetermined clams
- Arthropoda
  - Crustacea
    - ?Decapoda
      - †*Scoyenia*
- Amphibia
  - Labyrintodontia
    - Trematosauridae
      - *Aphanerama* sp.
    - cf. Captiosauridae
      - undetermined skull parts
- Reptilia
  - Procolophonia
    - cf. *Sclerosaurus* sp.
    - *Anomoiodon* sp.
  - Synapsida (mammal-like reptiles)
    - Traversodontidae
      - aff. *Exaeteodon* sp.
    - Dicynodontia
      - undetermined bones
  - Lepidosauromorpha
    - Tanystropheidae
      - *Tanystropheus* sp.
  - Archosauria
    - cf. Proterosuchidae
      - undetermined jaw
    - ?Aetosauridae
      - undetermined scute
    - Rauisuchidae
      - large undetermined teeth
    - Trilophosauridae
      - undetermined teeth and bones

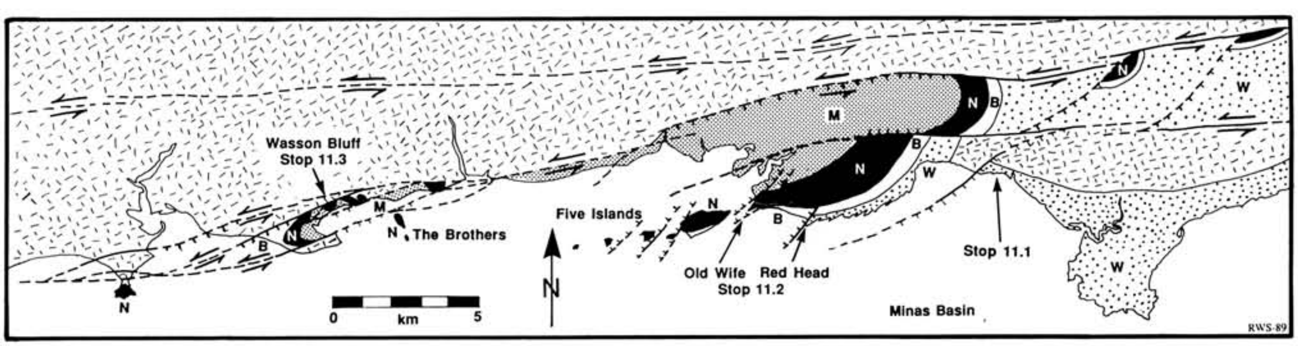

Figure 11.1: Geologic map of the Five Islands area, north shore of Minas Basin, Nova Scotia. Abbreviations are: W, Wolfville Formation; B, Blomidon Formation; N, North Mountain Basalt; and M, McCoy Brook Formation. The Cobequid-Chedabucto fault system forms strike-slip extensional duplexes near Stops 11.1 and 11.3. Base map from Donohoe and Wallace (1982).

effects of cyclically-changing climate on a highly erratic "recording" system.

To the west, the Mesozoic rocks are in high-angle fault contact with Pennyslvanian Riversdale Group fluvial and lacustrine strata. The Riversdale Group has here produced a small aquatic scorpion as well as common pteridosperm foliage and amphibian footprints. These Paleozoic beds constitute a large horst inlier surrounded by the Wolfville Formation (Figure 11.1). We believe this area to consist of a series of syndepositionally developed basins and horsts along the transtensional margin of the Fundy basin, much like what can be seen in more detail at Stop 11.3.

The gently-dipping unconformity with the overlying Wolfville Formation crops out at the west end of the Riversdale outcrops. The basal Wolfville at this outcrop is mostly a conglomerate with abundant angular clasts, predominantly of Riversdale Group. The conglomerate beds alternate with apparently eolian sandstones (Hubert and Mertz, 1984), and there are abundant ventifacts at the contacts between the fluvial and eolian units. A minor fault isolates these conglomeratic and eolian beds from the beds transitional between the Wolfville and Blomidon formations visible to the west.

114.0 Get back onto NS 2 heading west toward Parrsboro.
117.5 Turn left onto Bentley Branch Road to Five Islands Provincial Park.
119.3 Park in lot near shore.

STOP 11.2: FIVE ISLANDS PROVINCIAL PARK

(by P.E. Olsen)

Highlights: Large exposures of eolian sandstones at far point of traverse; fish fossils in sandstone.

Outcrops at Five Islands Provincial Park, along the south face of Economy Mountain display more than 50 m of the McCoy Brook Formation, a structurally-truncated section of the North Mountain Basalt, the entire Blomidon Formation, and most of the Wolfville Formation. This description follows from the Five Islands tidal flat viewing area, along the beach to the east, around Old Wife Point to Red Head, and back (Figure 11.1). This section is a stratigraphic complement to the stratigraphic transect at Stop 10.3.

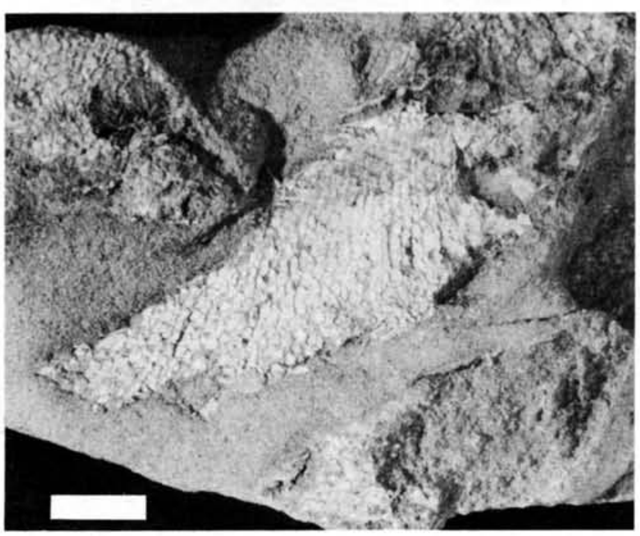

Figure 11.2: Examples of four semionotids from fish-kill layer, McCoy Brook Formation, Stop 11.2. All were complete prior to surface weathering. Scale is 1 cm. Photo by P.E. Olsen.

1) Poorly-exposed lacustrine strata of McCoy Brook Formation, with limited development of sand-patch fabric. Units resemble Blomidon Formation, which they were once thought to be (Klein, 1963).

2) Channel-fill and lacustrine sandstones with fish bone- and coprolite-bearing intraformational conglomerate at base. The intraformational conglomerate is apparently the lateral equivalent of or derived from the fish-bearing, thin-bedded sandstone exposed in the cliff face to the east. The only identifiable remains consist of scales and a ceratohyal of a large *Semionotus* sp.

3) Thin- to thick-bedded, climbing-ripple cross-laminated sandstone alternating with red fine mudstone and claystone with widely-spaced desiccation cracks and reptile footprints. The structural analysis of Liew (1976) and these footprints provided some of the first evidence of the Jurassic age of these strata. Ichnotaxa identified so far include *Grallator (Anchisauripus) minusculus*, *Grallator (Anchisauripus) parallelus*, *Grallator (Anchisauripus) sillimani*, *Grallator (Anchisauripus) hitchcocki*, *Grallator (Grallator)* sp., and *Batrachopus* sp. (Figure 4.9).

4) Location of common rock falls from fish-bearing sandstone in cliff. Fish-bearing unit consists of a climbing-ripple cross-laminated or convolute-bedded sandstone overlying a laminated, purple-red claystone. Complete *Semionotus* sp. (Figure 11.2) occur densely packed at the top of the clay and in the base of the sandstone. The underlying claystone also has some partial to complete fish and coprolites. The fish-bearing unit represents a single sedimentation event which entombed the result of a mass kill.

This fish assemblage is of particular significance because all of the individuals are so similar to each other in details of morphology and clearly belong to a single species. All of the fish have the same type of dorsal ridge scales, the same type of granular ornamentation around the nape region, and the same proportions. Several distinct size classes of fish are present, however, and these probably represent different year-classes. This assemblage shows the kind of individual variation we can expect in a single species of *Semionotus* and it stands in dramatic distinction to the huge amount of apparently intra-specific variation seen in the species flocks of semionotids in the Towaco Formation of the Newark basin (Stop 6.2). This example shows that these fish had about the same amount of variation within a population of one species that one might expect from a modern lacustrine teleost population.

5) Large-scale channel-delta sequence.

6) Steeply-dipping and faulted lower McCoy Brook Formation. Most faults appear to downdrop section to the west.

7) Faulted basalt breccia. This breccia contains basalt clasts of varying vesicularity and some red mudstone matrix, suggesting that the fault zone was open at the surface. Debris flow fabrics are apparently absent. These breccias appear as a cryptic tectonized combination of talus slope breccias of the type seen at Wasson Bluff (Stop 11.3) and what we call "rubblized" basalt (a fault zone product, see below). In any case, this type of deposit probably indicates that this fault zone was active during sedimentation.

8) Old Wife Point. This peninsula consists of fault slivers of North Mountain Basalt, dropped down to the west. Rocks on either side of thin, black, gouge zones consist of rounded clasts of basalt in a matrix of smaller basalt clasts and a waxy-looking basalt "flour" made up of a hydrobiotite-

vermiculite paste (Stevens, 1987). There are no exotic clasts and no red mudstone matrix. This is a type of cataclasite we term "rubblized" basalt (pseudo-breccia of Stevens, 1987) and it is typical of the fault zones cutting basalt on the north shore of the Minas Basin. The "rubblized" basalt tends to pass laterally into rotated columns or clearly less transported and milled basalt. We infer (see Stop 11.3) that this type of cataclasite is a product of fault movement under very low confining pressures, at near-surface conditions. The thicker gouge zone itself would be the fault, cutting the previously formed cataclasite under higher confining pressures at greater burial depth.

Stevens (1987) interprets the zone of subhorizontal columns as an intrusive basalt dike. Passage of the columns laterally into a cataclastic rubblized basalt and fault gouge, total lack of chilled margins, extreme variability in column orientation, and extensive slickenside and gouge development on all sides of all columns argues that the present attitude of the basalt columns is a consequence of fault-related rotation and does not represent a dike. Indeed the rotation sense of the columns is completely compatible with down-to-the-NW movement on the very visible faults bounding the point of the Old Wife.

To the east is a spectacular view of the Triassic-Jurassic boundary (frontispiece) and contact between the North Mountain Basalt and the Blomidon Formation. The gray and white band at the top of the Blomidon contains charred organic material and presumably corresponds to the gray palyniferous layers at Cape Blomidon (Stop 10.3), Central Clarence, Partridge Island, and Cape Split (Olsen, 1981). Based on the palynology at the latter four localities, the Triassic-Jurassic boundary should fall within this gray zone. Like the rest of the Blomidon, this interval appears cyclical.

9) Sand-patch cycles in the Blomidon Formation. Cycles very similar to those seen at Cape Blomidon (Stop 10.3) occur through the Blomidon here. Coarse sandstone, however, is common at the base of the sand patch cycles. These cycles are somewhat thicker (about 1.5 m) than those at Stop 10.3, which average 1.1 m.

10) Set of two sequences of fish- and conchostracan-bearing mudstone cycles. The upper sequence contains a distinctive red, gray, and yellow finely-laminated claystone and siltstone which may be correlative with the unit at 2570-2636 m at Stop 10.3. This unit is massively disrupted with the same sort of fissures and deformation as at Cape Blomidon. A bed of laminated red and gray claystone in the lower mudstone sequence is lithologically very similar to its homotaxial counterpart at 2905-3032 m at Stop 10.3. We tentatively conclude, pending very fine-scale measuring of the whole Blomidon section at this locality, that these are the same two mudstone cycles associated with the massive deformation exposed along the Blomidon shore.

11) The last outcrops of Blomidon Formation at Red Head show a beautiful example of dense domino-style faulting within beds. The low-angle faults with listric soles occur in beds roughly 25 m below the lower fish- and clam shrimp-bearing red mudstone sequence (Figure 11.3). Similar faulting occurs within the latter bed along the Blomidon shore (2905-3032 m at Stop 10.3). Rotation of blocks is extreme and it is obvious that there must be several levels of detachments within this section (Figure 11.4).

12) Fault with upper Wolfville Formation.

13) Eolian dunes in the Wolfville Formation. Hubert and Mertz (1980, 1984) have described the remarkable cliff exposures of large-scale eolian dunes at Red Head (Figure 11.4). According to Hubert and Mertz (1984), at these outcrops, "the uppermost Wolfville Formation consists of 32.5 m of eolian sandstone interrupted by a 3-m interval of fluvial sandstone". The average thickness of eolian cross bed sets is 1.6 m, with a maximum of 3 m, and the paleowinds blew to the southwest (254°) (Hubert and Mertz, 1984). As at Carrs Brook (Stop 11.1) ventifacts are common on the upper surfaces of the fluvial sandstones where they are in contact with eolian sandstones.

	Turn around and leave park. Return to NS 2.
121.8	Turn left (west) onto NS 2 at park exit towards Parrsboro and Amherst.
123.6	Outcrop of McCoy Brook Formation in stream cut on right.
124.7	View of Moose Island on the left.
126.3	Blue Sac Road.

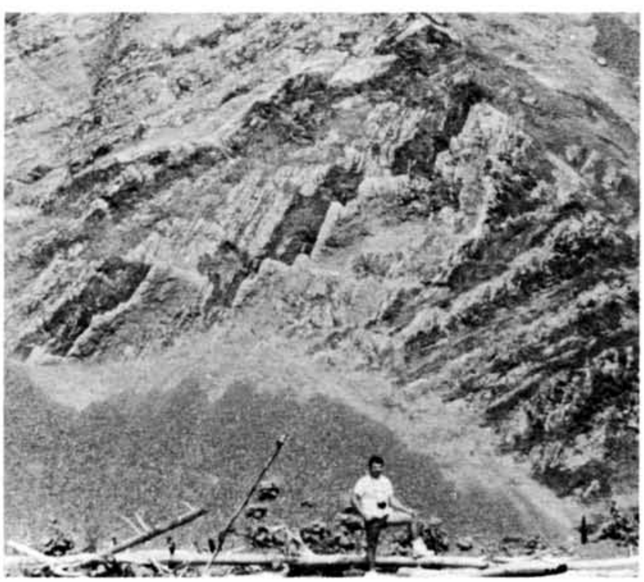

Figure 11.3: Domino-style faulting within the lower Blomidon Formation near Red Head, Stop 11.2. Roy Schlische for scale. Photo by P.E. Olsen.

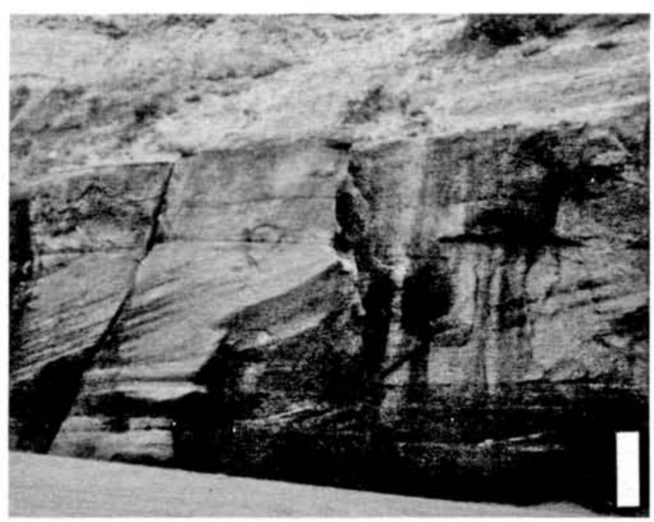

Figure 11.4: Eolian sandstones at Red Head, Stop 11.2. Scale is 2 m. Photo by P.E. Olsen.

126.4 Outcrops of Carboniferous lacustrine sediments.
136.5 Enter Parrsboro, Nova Scotia
137.6 Turn left at Parrsboro Square.
137.8 Turn left on road toward Glooscap Park and Greenhill (Two Island Road.)
140.9 Glooscap Park.
143.4 Look for small dirt road off to the right. Leave bus and walk down dirt road to the beach. We will be walking to the right (west) about 2.4 km. We will be picked up by the bus at the other end of the traverse.

STOP 11.3: WASSON BLUFF

Highlights: Synsedimentary deformation; Early Jurassic vertebrate remains.

Caution*: Some moderately-strenuous climbing over boulders on the beach; be especially careful of slippery seaweed-covered rocks.*

Structural Geology and Stratigraphy

(by R.W. Schlische and P.E. Olsen)

In the Parrsboro, NS, area the left-lateral Cobequid-Chedabucto fault, a subparallel splay of the Minas fault zone, has a relay geometry. The map pattern of faulting reveals a strike-slip extensional duplex (terminology after Woodcock and Fisher, 1986) (Figure 11.1). Rocks of the Newark Supergroup accumulated within basins bounded by a complex series of NE-striking normal faults and E-striking left-lateral faults. Structural complexity is introduced by block rotations adjacent to strike-slip faults and caving and slumping in this transtensional setting.

At Wasson Bluff spectacular exposures along the Minas Basin reveal the interplay between tectonics and sedimentation. Triassic formations vary markedly in thickness; the basal Wolfville Formation is completely absent in the Wasson Bluff exposures and only a veneer of conglomeratic Blomidon Formation is present. The Early Jurassic McCoy Brook Formation fills fault-bounded wedge and trough- shaped basins developed on the faulted upper surface of the North Mountain Basalt (Figure 11.5). Paleo-fault talus slope deposits and slide blocks are common in these sub-basins. McCoy Brook Formation debris flows consist exclusively of North Mountain Basalt clasts, testifying to the localized uplift of the lava flows (Tanner and Hubert, 1988). Left-lateral strike-slip and normal faults cut formations of all ages, and hydroplastic slickensides probably formed in incompletely lithified sediments. Neptunian dikes are common in the North Mountain Basalt and reveal important kinematic information. We shall examine all of these features on our trek along Wasson Bluff. The following discussion is tied to the sketches of the Wasson Bluff outcrops, beginning from the eastern end of the outcrop. Letters refer to specific localities on Figure 11.6.

At the immediate eastern end of the exposure and just to the west of the small stream, the unconformity between Newark Supergroup strata and Carboniferous basement is locally exposed in the modern talus slope (point **A** in Figure 11.6). The Blomidon Formation is dipping towards the beach (*i.e.*, southward) and consists of gray, red and purple conglomerate and sandstone with some hopper cast-bearing gray claystones. Also present is the step-faulted contact between the North Mountain Basalt and the Blomidon Formation (**B**). Hexagonal cooling joints are well developed immediately above the contact (**B**).

The bulk of the North Mountain Basalt from here westward to the eastern sub-basin is mostly "rubblized" basalt (see Stop 11.2). We hypothesize that this extensive zone of "rubblized" basalt marks a wide, predominantly left-lateral fault zone. This same fault zone apparently places McCoy Brook Formation against Carboniferous rocks to the east of these outcrops. Splays of this fault zone trending at a higher angle to the cliff face are present (**C**). The degree of rubblization increased towards these splay faults, and many are marked by narrow, chlorite-fiber slickensides. Again, we hypothesize that the "rubblized" basalt formed as a result of faulting under near-surface but not exposed conditions; the mineralized faults probably formed at greater depth as a result of burial.

Inbetween some zones of "rubblized" basalt are what we interpret as rotated basalt columns, much like those seen at Five Islands (Stop 11.2). Again, Stevens (1987) interprets these as portions of a dike. Again, chill margins are absent, and rotation of the columns is variable, but the sense of rotation is appropriate for down on the south motion of the bounding faults.

A fault-bounded block of paleo-fault talus slope deposit marks the eastern end of the first sub-basin (**D**). This sub-

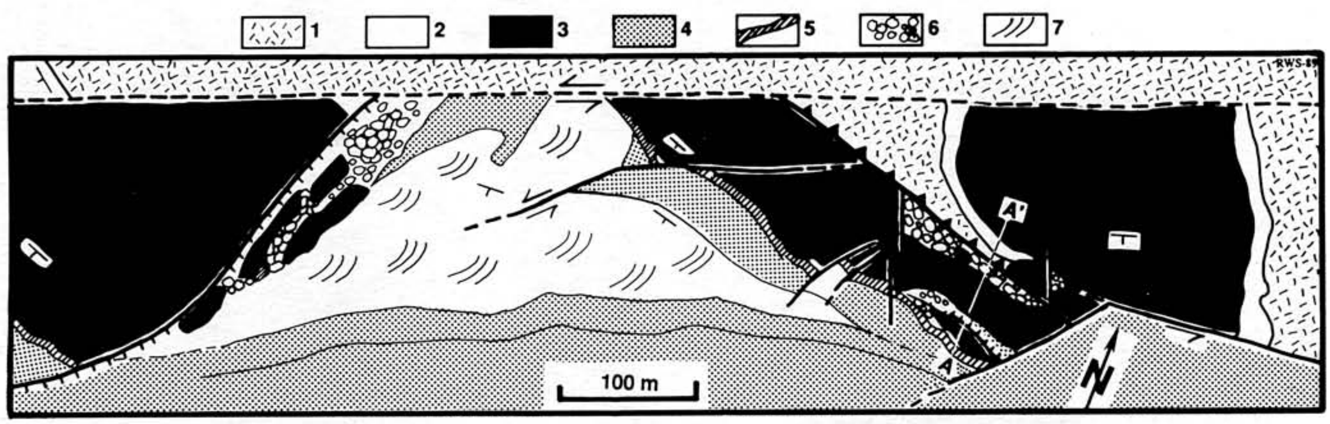

Figure 11.5: Geologic map of Wasson Bluff, Stop 11.3, showing sub-basin developed within the faulted upper surface of the North Mountain Basalt. Key to lithology: 1, Carboniferous basement; 2, Blomidon Formation; 3, North Mountain Basalt; 4, fluvio-lacustrine McCoy Brook Formation; 5, "fish bed"; 6, fault talus-slope deposits of the McCoy Brook Formation; and 7, eolian McCoy Brook Formation. The first seven drawings of Figure 11.6, from east to west, provide a natural cross section of this map. Section A-A' shown in Figure 11.7.

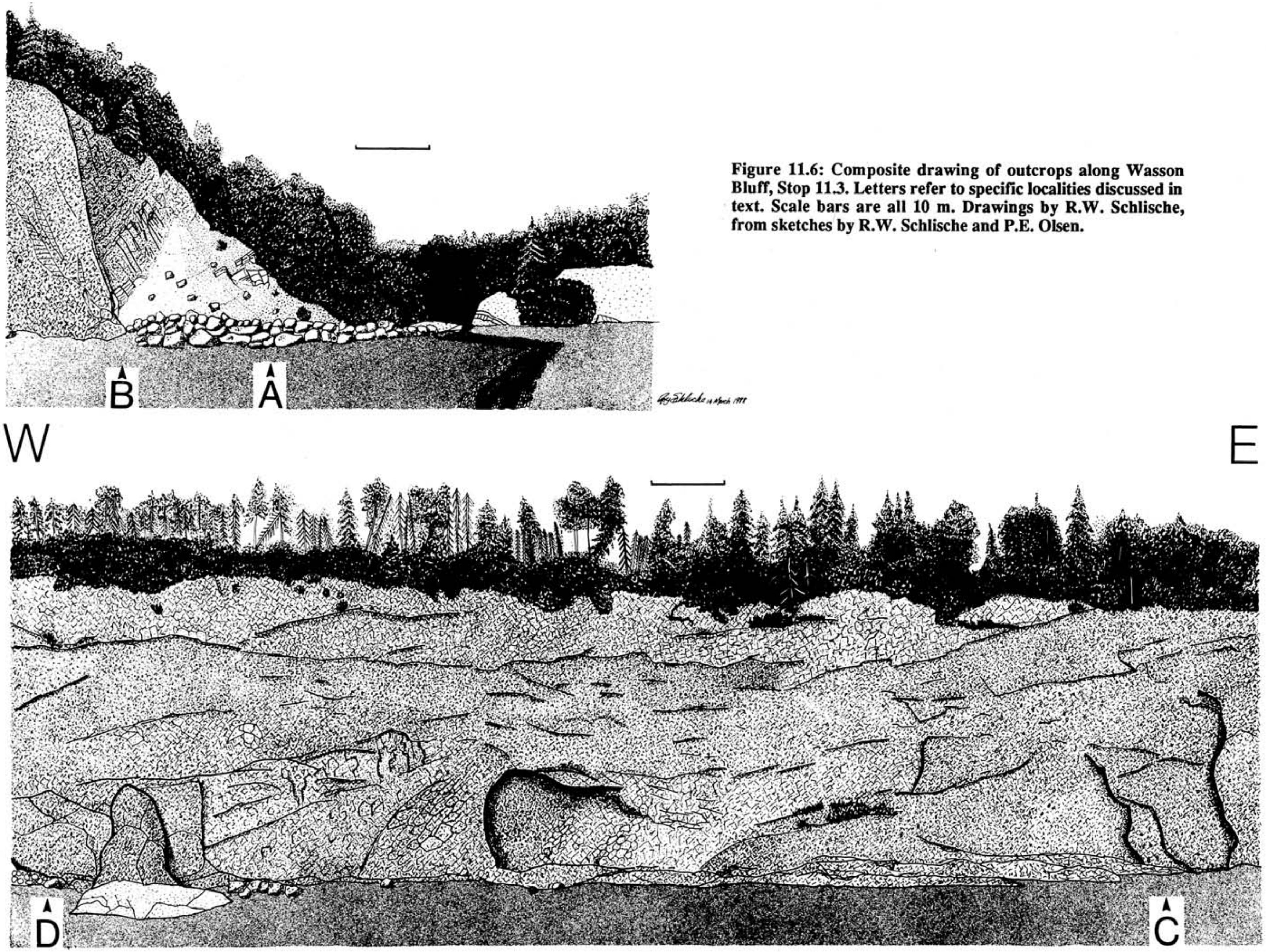

Figure 11.6: Composite drawing of outcrops along Wasson Bluff, Stop 11.3. Letters refer to specific localities discussed in text. Scale bars are all 10 m. Drawings by R.W. Schlische, from sketches by R.W. Schlische and P.E. Olsen.

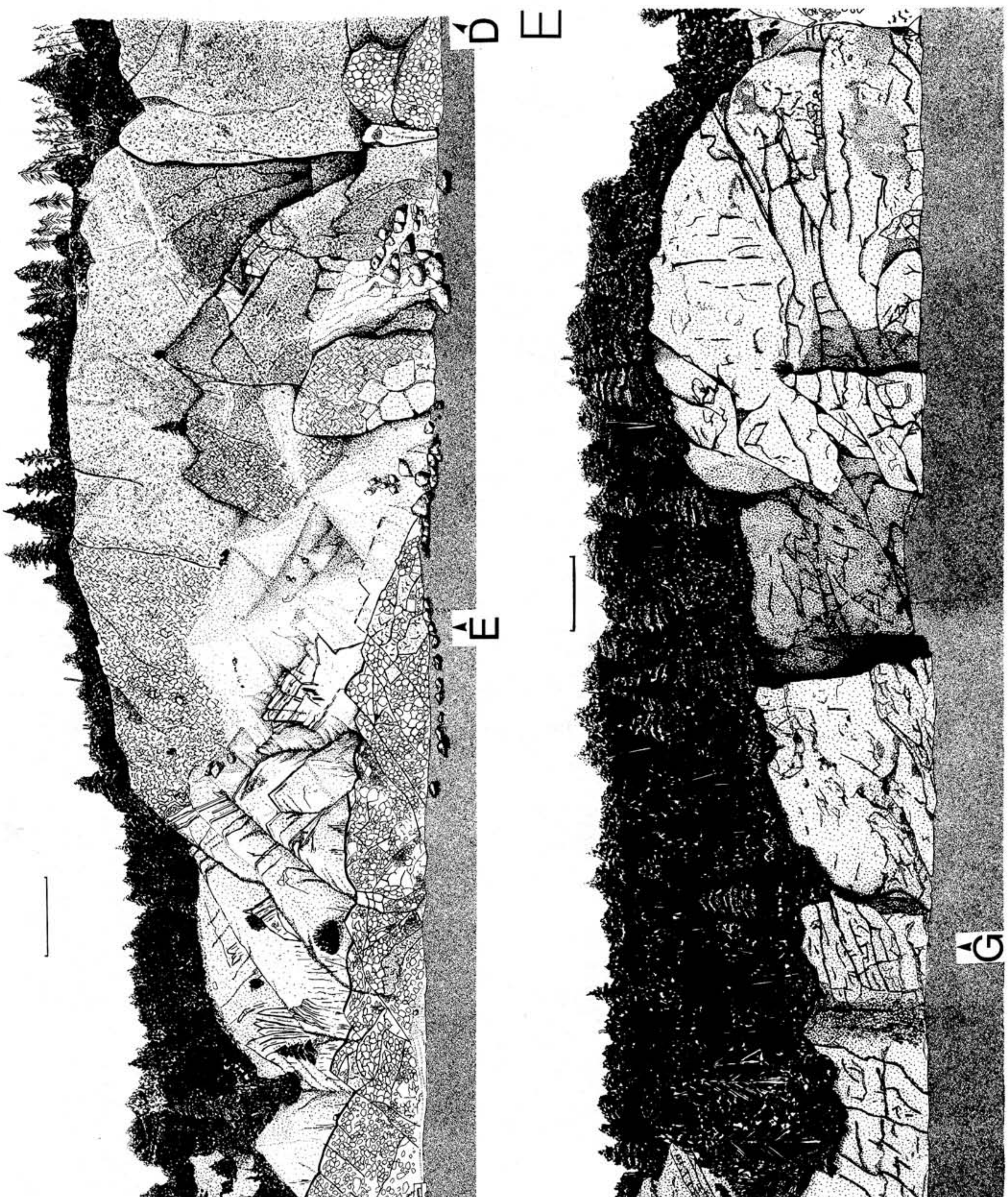
W
E
F
E
D
H
G

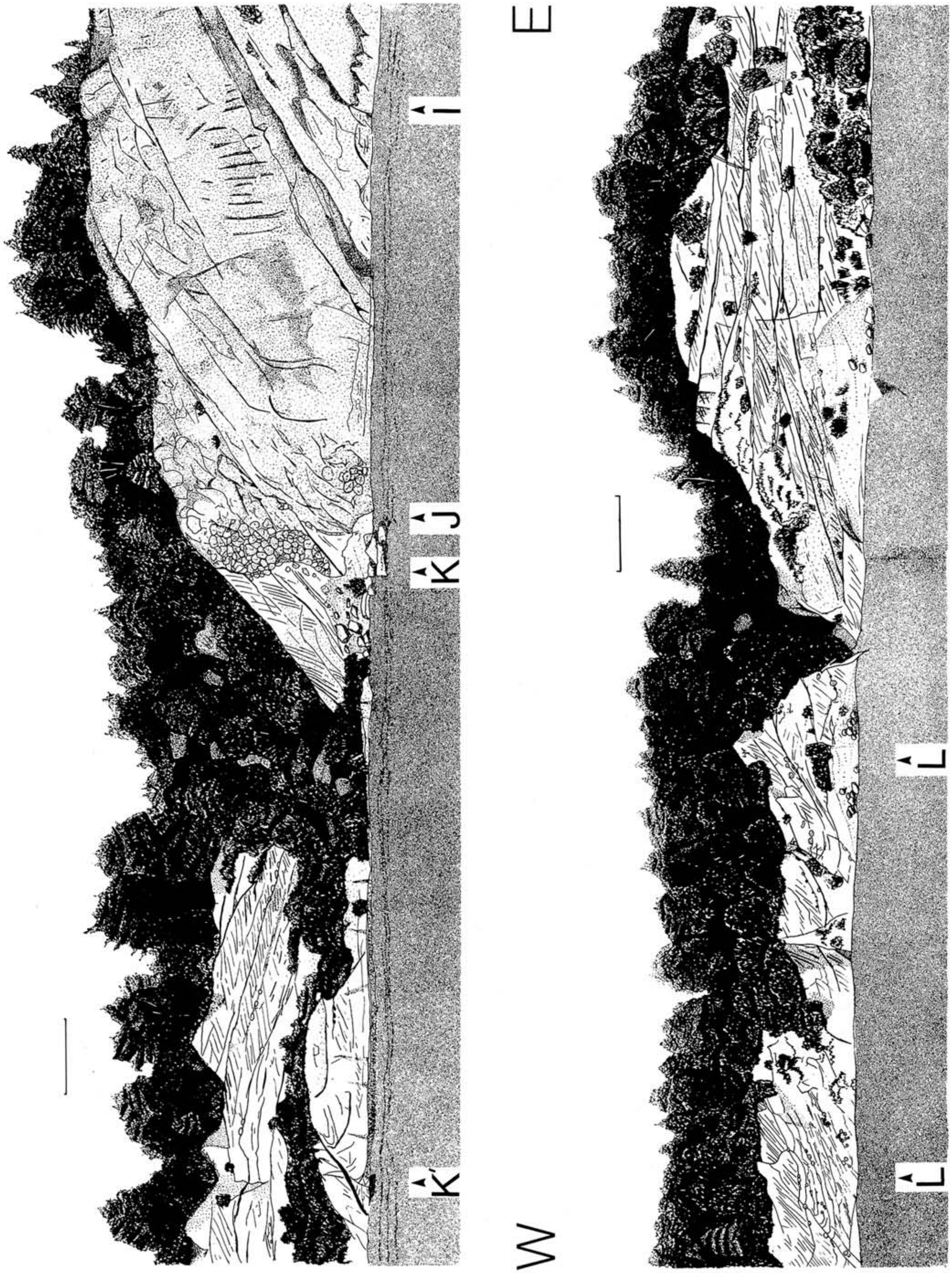
E
i
J
K'
K'
W
L
L'

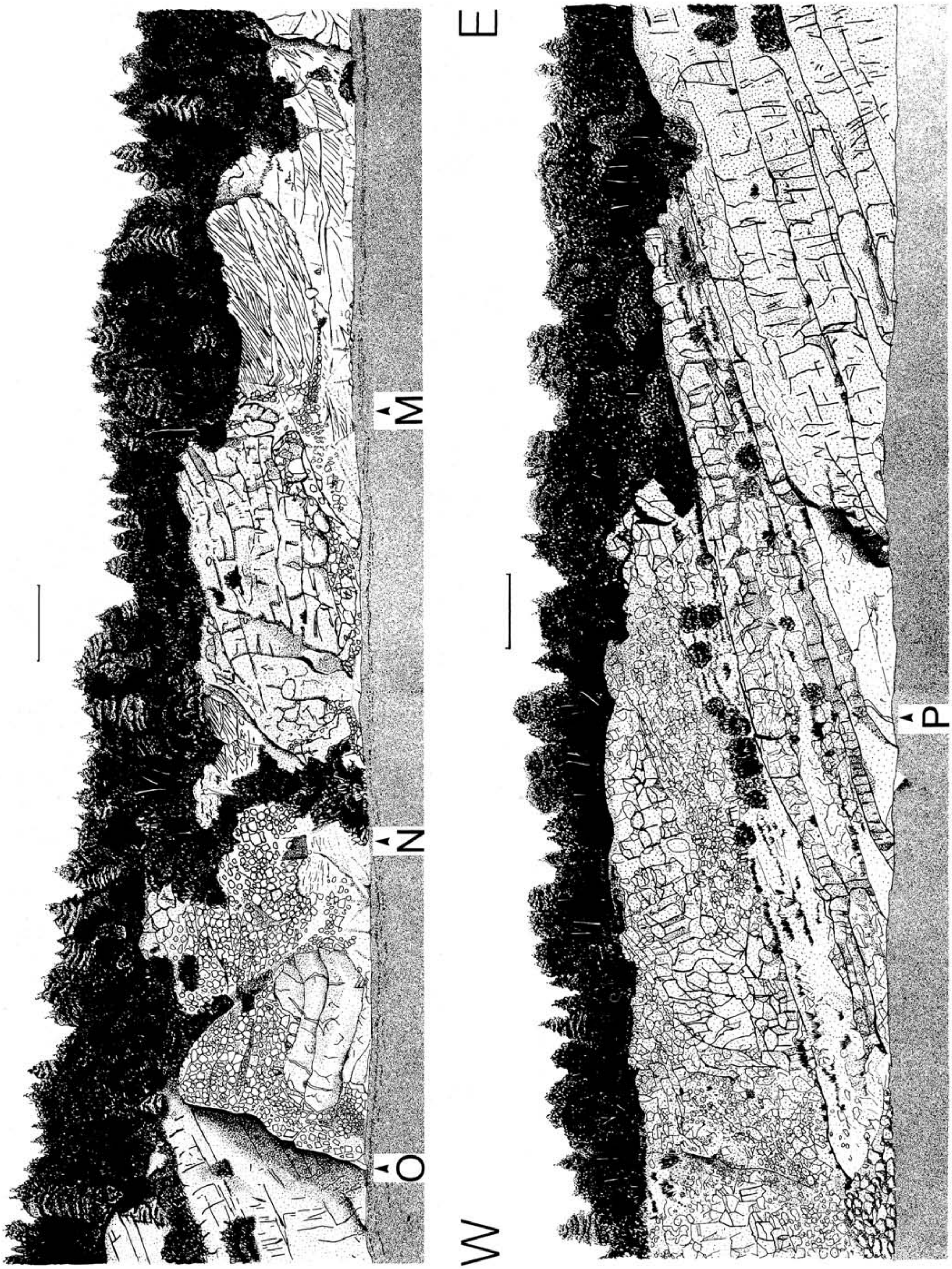
E
M
N
O
W
P

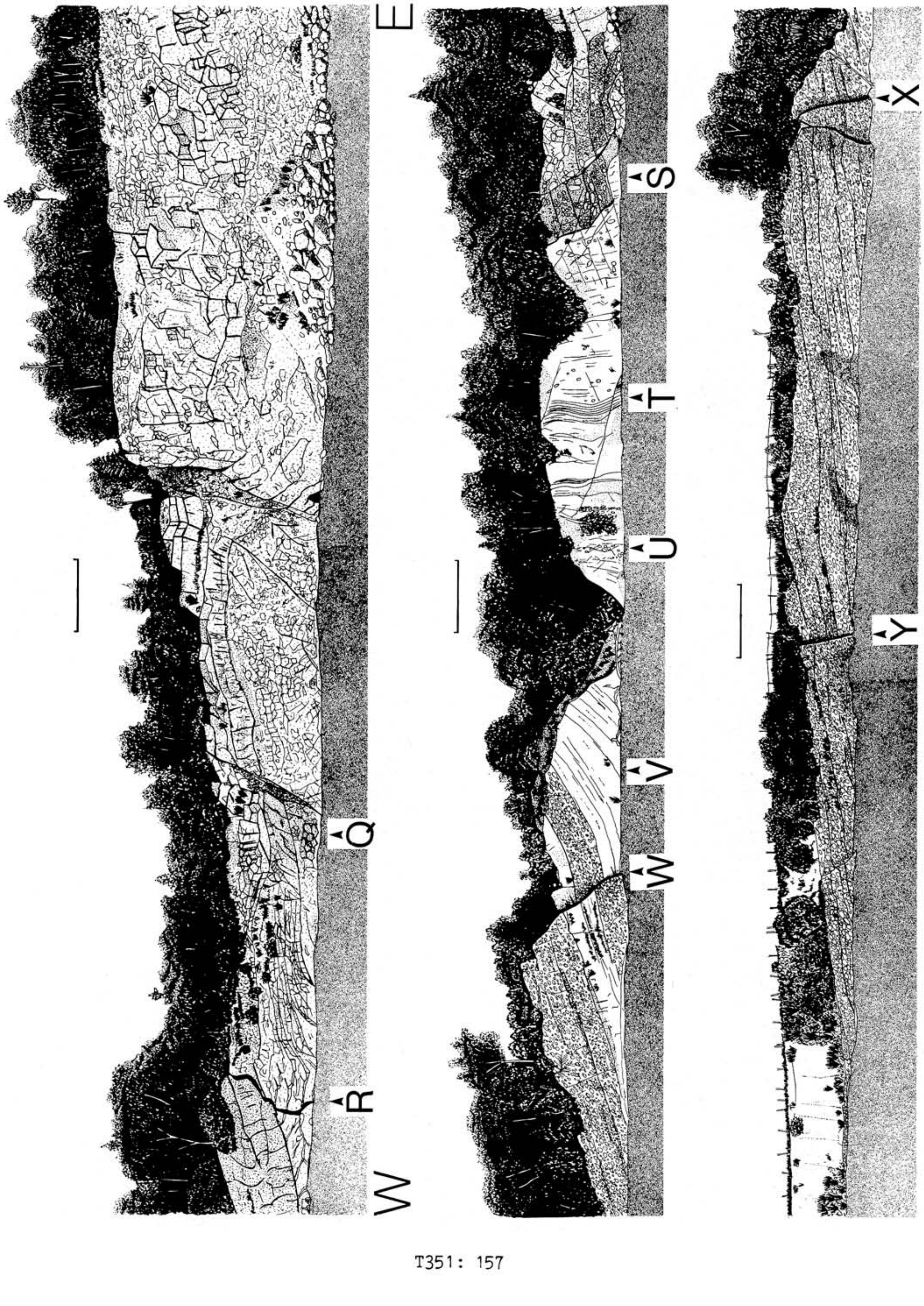
W
E
Q
R
S
T
U
V
W
X
Y

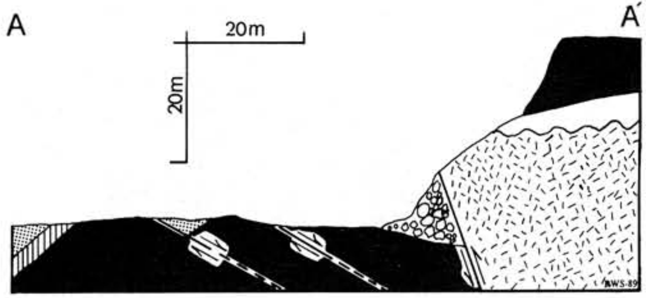

Figure 11.7: Cross-section A-A' (see Figure 11.5 for location) illustrating domino-style faulting and micro-basin development. If the "fish bed" is rotated to paleohorizontal, the reverse fault becomes a normal fault.

basin is easily recognized by the distinctive deposits consisting of angular clast-supported basalt breccia in a matrix of sandstone or mudstone. Large blocks of basalt are common (**E**). Sediment-filled voids among the basalt clasts show stratification which has yielded consistent facing directions throughout the outcrop, indicating deposition of the matrix after the accumulation of the basalt clasts. The matrix yields abundant reptile bones (see below).

These deposits at Wasson Bluff are invariably associated with faults and hence are interpreted to be fault talus slope accumulations. A high-angle reverse fault separated the talus slope deposits from the vertical Carboniferous basement rocks to the immediate northwest, which are unconformably overlain by the Blomidon Formation, in turn overlain by North Mountain Basalt (Figure 11.5). This is an extension of the same contact surface seen at **B**. South of the talus slope deposits are a series of north-dipping normal fault-bound "dominoes" of North Mountain Basalt (Figures 11.5 and 11.7). Basins developed in these fault blocks are filled with McCoy Brook Formation, which consists of brown, at least partially eolian, sandstone. The southernmost outcrop of basalt adjacent to the "dominoes" is overlain by a stratigraphically-distinct unit known informally as the "fish bed", consisting of green, purple, pink, and white fish-bearing lacustrine mudstone, limestone, and basalt gravel. We will see this unit elsewhere at Wasson Bluff (**J**, in beach at **I**, between **N** and **O**, and **S**). The fish bed is not present within the exposed dominoes to the north and therefore the sediments within these blocks should predate the fish bed (Figure 11.7). Note that if the "fish bed" is rotated to horizontal, the reverse fault adjacent to the talus slope deposits becomes a normal fault, and the normal faults associated with the "dominoes" are antithetic to it (Figure 11.7). Hence, the talus-slope deposits probably accumulated on the downthrown side of a normal fault. At the western end of this sub-basin, the talus slope deposits are faulted against North Mountain Basalt (**F**). This north-striking fault (Figure 11.5) is probably a transfer fault because it terminates against the "reverse" fault, and dies out to the south in the zone of "dominoes".

The top of one flow, another thin flow, and a third upper flow of the North Mountain Basalt are visible in the next stretch of outcrops. Here, the basalt is mostly massive and disturbed only by small faults. The green, red, and gray flows are each separated by vesicular horizons. This particular stretch of outcrop also contains numerous Neptunian dikes (**G**), which consist of mudstone, siltstone, and sandstone veins ranging in width from 0.5 to 25 cm. Narrow dikes are often silicified. Some of the dikes contain clasts of North Mountain Basalt as much as 5 cm in diameter. Therefore, in contrast to clastic dikes, these Neptunian dikes formed by the active extension of the North Mountain Basalt and were filled with sediment from above. The dikes often follow pre-existing fractures, such as cooling columns in the basalt, or are sinuous. A survey of the attitudes of the dikes in this region shows that those oriented NE-SW predominate; notably, these dikes are perpendicular to the regional extension direction inferred from the trend of the Shelburne dike.

The basalt flows in the region marked by **H** dip to the southwest. The uppermost gray basalt flow is overlain by the "fish bed", which can be excavated in the beach. The "fish bed" and other strata of the McCoy Brook Formation strike directly into the North Mountain Basalt in the cliff face, along which an east-west striking fault runs. The fault has offset the North Mountain Basalt—fish bed contact by approximately 25 m (Figure 11.5). At **I** this fault is exposed and juxtaposes the gray, vesicular uppermost basalt (on the south) against the next lower gray, vesicular basalt horizon (on the north). The fault zone is marked by a mineralized, slickensided plane with subhorizontal slickenlines. The basalt on either side of this plane is clearly "rubblized", indicating the fault origin of the "rubblized" basalt. The "rubblized" basalt is also extensively mineralized with the orange zeolite mineral chabazite, a common occurrence at Wasson Bluff. Other minor subhorizontal slickensided surfaces are present along the cliff face. The upper surface of the basalt contains numerous neptunian dikes, the offset of which along the east-west fault shows the motion to be almost pure strike-slip, agreeing with the slickenline directions.

The eastern end of the western sub-basin is marked by the onlap of the fish bed onto the upper surface of the North Mountain Basalt (**J**). Stratigraphically-higher strata appear to onlap boulders of North Mountain Basalt, which in turn rest against a high-angle wall of massive vesicular basalt (**K**). The western edge of the basalt wall is truncated by onlapping fluvial sandstone. Thin layers of basalt rubble are interbedded in the sandstone adjacent to the basalt. It is possible that the surface of the basalt was terraced by the lake which deposited the "fish bed", producing the evident paleorelief. The upper portions of the lacustrine sequence consist of red mudstone and sandstone beds, with the latter containing well-preserved reptile remains, some of which are articulated (see below).

The bulk of the basin fill of this sub-basin consists of a NW- to SW-dipping wedge of largely eolian dune sandstone of the McCoy Brook Formation (Figure 11.5). According to Hubert and Mertz (1984), at least 48 m of dune sand are present in this basin which yield paleo-wind directions towards 241°. Toward the western end of the sub-basin, basalt clasts within the dune sands become more abundant and larger (**L**); at the locality marked by **M** (Figure 11.6), eolian dune sands abut against a large slide block or domino of relatively intact basalt, producing an 8-m-high paleocliff with adjacent talus cones (Hubert and Mertz, 1984). According to Hubert and Mertz (1984) successive first order surfaces in the eolian sandstone are veneered with basalt boulders (some larger than 1 m) which rolled down-slope and were buried by advancing barchan dunes and barchoid ridges. As the northwestern normal fault boundary of the sub-basin (**O**) is approached, eolian dune sands interfinger with paleotalus slope deposits and another slide block of tectonically-disrupted basalt. These relationships indicate that the faulting responsible for sub-basin formation and sedimentation were coeval.

A prosauropod dinosaur skeleton recovered from the excavation at **N** was extensively faulted, its bones ductilely stretched. Polished and rounded 1 to 3-cm-diameter exotic metamorphic and igneous clasts found within the ribs of this dinosaur and presumed to be gastroliths were not faulted. We infer that faulting took place under low confining pressures in the relatively incompetent, probably partially unlithified sandstones. None of these intra-dinosaur faults are mineralized.

The southeast corner of the basalt block between **N** and **O** is notched and filled with the fish bed, containing its characteristic fauna, apparently in gross unconformable contact. We interpret this notch as a cavity produced by (wave?) plucking of a basalt boulder followed by onlap of the fish bed. The fish bed is truncated to the immediate southeast by a healed fault, the south side of which is orange sandstone and basalt breccia typical of the sub-basin at **O**. Again this series of contacts shows that faulting, erosion of the uplifted blocks, and sedimentation were contemporaneous.

The normal fault (as revealed by slickensides) at the northwestern edge of the western sub-basin (**O**) is typical of faults at Wasson Bluff. It consists of an upward-widening fault zone of (basalt) breccia in a matrix of sandstone and mudstone. The degree of brecciation and volume of sedimentary matrix increase toward the fault. This fault breccia is welded to the hanging wall and partially to the footwall, and is cut by a narrower zone of red fine-grained material, which is probably gouge, but resembles the infill of Neptunian dikes. This red material is then cut by narrow, mineralized, slickensided surfaces. We hypothesize that the matrix-rich breccia formed in a wide fault zone which was open at the surface, with the red gouge and mineralized slickensides having formed at greater depths as a result of burial. It therefore appears likely that fault zones narrow with depth (within the brittle field), with cataclasis becoming more confined, and with eventual mineralization.

Westward of the sub-basin are extensive exposures of North Mountain Basalt. Several flow units are present and dip to the southwest. At the contact between two flows, a wrinkle or flexure in the lower flow is filled with basalt from the upper flow (**P**). The wrinkle exhibits a left-lateral offset, but the cooling rims in the infilling upper basalt suggest that the offset occurred before the extrusion of the upper basalt. This is evidence of faulting during extrusion of the North Mountain Basalt.

Hexagonal cooling joints are well developed in some of the flow units. Many of these joints have served to localize the Neptunian dikes. In one example (**Q**), we see how the cooling joints oriented normal to the regional extension direction formed the widest Neptunian dikes.

At (**R**) is a sinuous 20- to 30-cm-wide vesicular basalt dike with clearly chilled margins. Its relationship to the surrounding units is completely obscure and it may represent no more than a injection of the last fluid material from the interior of a cooling flow into its already chilled upper surface.

A sedimentary matrix-rich, basalt-clast fault breccia crops out at **S**. The high-angle fault strikes WNW, and displays subhorizontal slickenlines. Immediately to the west of this fault, strata within the McCoy Brook Formation, including thinly-bedded gray lacustrine units, have been upturned to vertical (**T**). The fault zone between the vertical McCoy Brook Formation and the basalt contains phacoids of purple basalt gravel. A less-disturbed, similar-appearing gravel is present in the adjacent mud flat directly along strike and is apparently the fish bed. Moving westward, these strata gradually decrease in dip, becoming shallowly dipping where fluvial sandstones are interbedded with debris flows. Although direct evidence is lacking, we interpret this region of upturned strata to be a pressure ridge, a zone of compression that may have formed along a restraining bend in one of the master left-lateral strike-slip faults.

This region (**U**) is also marked by the presence of curved, clay-lined, fibrous slickenlines, which in part resemble the hydroplastic slickensides of Laville and Petit (1984). We agree with Laville and Petit (1984) that these surfaces were probably produced by faulting in incompletely-lithified sediments, as indicated by the presence of unsheared quartz grains.

The remainder of the outcrop consists of debris flows of the McCoy Brook Formation, and interbedded and overlying red sediments. The clasts of the matrix-supported flows consist exclusively of North Mountain Basalt. These have been further described by Tanner and Hubert (1988). Several WNW-striking, left-lateral(?) faults cut these debris flows. The interbeds of red clastics are riddled with abundant root mottles.

A view to the west and southwest shows a reverse fault throwing North Mountain Basalt over McCoy Brook Formation. Another fault to the south separates North Mountain Basalt from a tectonic mélange of Carboniferous rocks, which include boulders of garnet-bearing mylonite. This mélange probably represents a major splay of the Minas fault zone, reactivated by Mesozoic faulting. At least locally, it forms the southern margin of the Five Islands graben. The relationship between this Paleozoic inlier and Fundy Group rocks lying offshore and to the south along the hook of Cape Blomidon is unknown.

Paleontology (by P.E. Olsen)

Vertebrate fossils are surprisingly common in the McCoy Brook Formation fill of the synsedimentary graben at Wasson Bluff (Table 11.2; Olsen *et al.*, 1987). Although almost all of the units produce some bones, five specific facies produce abundant material and each has its own dominant taxa. These are: 1) limestones and siltstones of the "fish bed"; 2) talus slope breccias; 3) lake margin sandstones; 4) first-order surfaces between dune sandstones; and 5) playa sandstones.

The "fish bed" consists of green-gray and purple limestone and siltstone with usually sparse dissociated fish and reptile bones and common ostracodes. Where the fish bed intersects basalt scarps, such as between **N** and **O** and at **J**, it consists of basalt gravel and coarse mudstone, filling voids between basalt boulders, and in these areas it contains abundant disarticulated fish and dinosaur bones. Large *Semionotus* are by far the most common fish, followed by teeth of the hybodont shark *Hybodus* sp., and scales and skull bones of an undetermined redfieldiid palaeonisciform (Figures 11.8 and 11.9). Bones and teeth of a small ornithischian dinosaur, rare protosuchid crocodile scutes, and a several possible theropod dinosaur teeth have also been found.

Talus slope breccias, especially at **E**, have produced the largest number of bones. These breccias are essentially open framework clast-supported breccias in which the red and orange sandstone matrix filled in after the clasts found their resting place. Much like the talus slopes forming today on this beach, these McCoy Brook talus slopes contained many large empty spaces in which small animals could live. In order of abundance, the taxa found so far are a new genus of crocodile allied to *Protosuchus*, from the US southwest and *Hemiprotosuchus* (Bonaparte, 1971) from Argentina, the trithelodont mammal-like reptile *Pachygenelus* sp., a

Table 11.2: Faunal list for McCoy Brook Formation: B) Blue Sac; F) Five Islands; M) McKay Head; W) Wasson Bluff.

- Arthropoda
  - Crustacea
    - Ostracoda
      - *Darwinula* sp. (W)
- Pisces
  - Elasmobranchii
    - Hybodontidae
      - *Hybodus* sp. (W)
- Actinopterygii
  - ?Refieldiidae
    - undetermined skull bones and scales (W)
  - Semionotidae
    - *Semionotus* sp. (W, F)
- Reptilia
  - Synapsida
    - Trithelodontidae
      - *Pachygenelus* sp. (W)
  - Lepidosauromorpha
    - Sphenodontidae
      - *Glevosaurus* sp. (W)
      - undetermined genus (W)
  - Archosauria
    - Protosuchidae
      - new genus (W, B)
      - †*Batrachopus* spp. (M, F, B)
    - Sphenosuchidae
      - new genus (W)
      - †*Otozoum moodii* (B, M)
    - Prosauropoda
      - cf. *Ammosaurus* sp. (W)
    - Theropoda
      - cf. *Syntarsus* sp. (W)
      - †*Grallator* (*Grallator*) spp. (M, F, B)
      - †*Grallator* (*Anchisauripus*) spp. (W, M, F, B)
      - †*Grallator* (*Eubrontes*) sp. (F)
    - "Fabrosauridae"
      - cf. *Scutellosaurus* sp. (W)
    - two new genera (W)
      - †*Anomoepus* spp. (B, M)

sphenodontid similar to *Glevosaurus* sp. from the fissure fillings of Great Britain, a small crocodilomorph "sphenosuchid" similar to *Terrestrisuchus* (Crush, 1984) also from fissure fills, a small ornithischian dinosaur resembling *Fabrosaurus* ("*Lesothosaurus*") from southern Africa, and a small theropod dinosaur. Most material is dissociated, but some articulated material is present. Unfortunately, most bones and skeletons are truncated at one end or another by small faults, and much material appears chewed. Bone-bearing coprolites occasionally occur, suggesting that at least some of the remains may have been dragged into the talus piles by a predator or scavenger.

Lake margin and fluvial sandstones at **K** and **K'** produce the best-preserved material at Wasson Bluff. Because of poor exposure, with the exception of some unidirectional current ripples, and some dune-scale cross-bedding, few sedimentary structures have been observed in these units. Their association with laterally-persistent red mudstones are the main reason for thinking that these units are marginal to a lake. Scutes and teeth of a protosuchid crocodile are the most common bones followed by jaws and maxillae of the sphenodontid ?*Glevosaurus* sp., including two nearly complete skulls (Figure 11.10) and a partial skeleton. Parts of skulls of *Pachygenelus* sp. and rare scraps of prosauropod dinosaurs are also present.

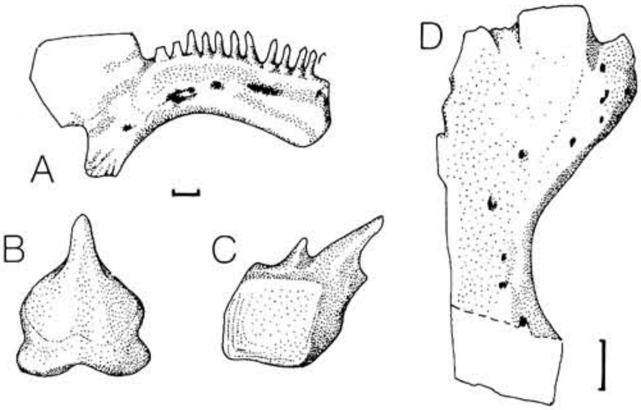

Figure 11.8: Scraps of the fish *Semionotus* sp. from "fish bed", location J, Figure 11.6, Stop 11.3: A) right lower jaw; B) single dorsal ridge scale; C) single flank scale; D) left frontal. Scale is 1 mm.

Intervals of basalt debris on the first order surfaces between eolian dune sets have produced a disarticulated prosauropod skeleton (cf. *Ammosaurus*) and mandibles of ?*Glevosaurus* sp. (**L**). A partially articulated prosauropod with gastroliths (again cf. *Ammosaurus*) has been recovered from the top of a mixed eolian—talus slope deposit as well (at **N**). All of the larger bones have been deformed by faulting as noted above.

Finally, laterally persistent beds of apparently ripple cross-laminated, water-laid, reworked eolian sandstone are found in the tidal flat at the top of the eolian sandstone wedge in the main half-graben. These sandstones contain

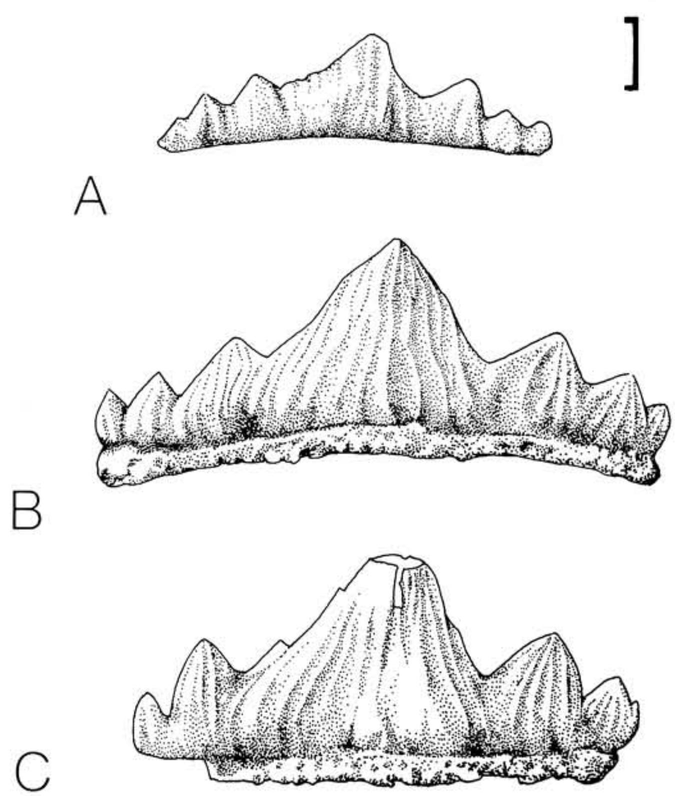

Figure 11.9: Three teeth of the hybodont shark *Hybodus* sp. Scale is 1 mm.

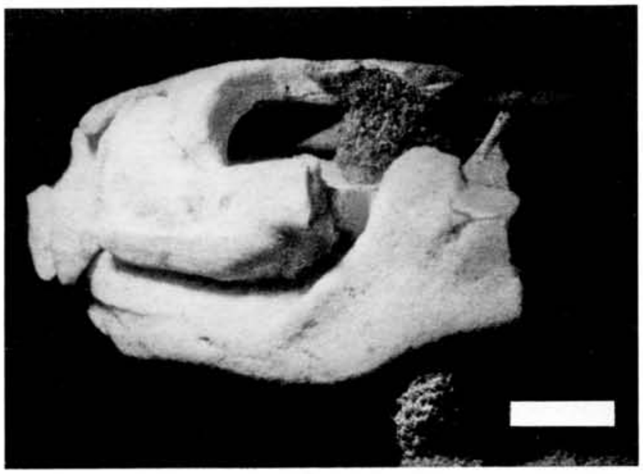

Figure 11.10: Skull of sphenodontid cf. *Glevosaurus* sp. from K', Figure 11.6, Stop 11.3. Scale is 4 mm. Photo by P.E. Olsen.

poorly preserved but abundant *Grallator* (*Anchisauripus*) cf. *sillimani* and *Batrachopus* sp. tracks.

A compilation of latest Triassic assemblages from other portions of the Newark Supergroup and other parts of the world (Olsen and Sues, 1986; Olsen *et al.*, 1987) shows that all of the families present in the Early Jurassic McCoy Brook assemblages were already present during the latest Triassic (Figure I.13). However, despite the fact that the Jurassic Nova Scotian assemblages come from a variety of facies, from fully aquatic to fully terrestrial, and the fossils are very common, the dominant late Triassic families of reptiles and amphibians are absent. This is also true of intra- and post-extrusive deposits from the rest of the Newark Supergroup. Thus, the McCoy Brook assemblages represent survivors of the massive Triassic-Jurassic extinction event, in which 43% of all terrestrial vertebrate families went extinct.

The McCoy Brook assemblages occur directly on top of the North Mountain Basalt, which based on geochemistry is probably the temporal equivalent of the Orange Mountain Basalt, and therefore the assemblage is plausibly correlated with the Midland Formation of the Culpeper basin, the Feltville Formation of the Newark basin and the Shuttle Meadow Formation of the Hartford basin. Based on the geochemical similarity of the North Mountain and Orange Mountain-Talcott basalt (Puffer *et al.*, 1988) and the cyclostratigraphy of the upper Blomidon and lower Scots Bay Formation, the McCoy Brook assemblages would be roughly 100,000 to 200,000 years younger than the Triassic-Jurassic boundary (based on data available at the time of this writing; Olsen *et al.*, 1987). The extinctions would have had to occur prior to this time. Thus, the McCoy Brook assemblages serve to shorten the amount of time over which the extinctions could have taken place by roughly 10 million years (Olsen *et al.*, 1988).

As noted by Olsen *et al.* (1987) everything we know of the terrestrial extinctions seems compatible with the timing of the massive invertebrate extinctions at the Triassic-Jurassic boundary and this is consistent with a global catastrophic event. The Manicouagan impact structure of Quebec is broadly correlative with the extinction event and following the impact theory of mass extinctions is plausibly implicated in the cause.

143.4 (Bus will turn around and meet passengers 1.5 miles back down the road toward Parrsboro.)
145.0 Passengers board bus.
149.0 Turn right at town square in Parrsboro. Go east on NS 2.
149.7 Stop for evening.

END OF TRIP

Acknowledgments

The editors wish to thank all the contributors for their fine additions to this guidebook. A hearty thank you also goes out to the reviewers of this manuscript: Ronald Litwin, Robert Weems, and David Gottfried for reviewing parts of the Geological Overview; and Alfred Froelich, Nicholas McDonald, and Joseph Smoot for the strength of mind and body to review the entire manuscript; we're sure you had as much fun finding our mistakes as we had in correcting them all. We thank Donald Baird, David Brown, Sarah Fowell, Alfred Froelich, Tucker Hentz, Mike Hozic, John Hubert, Patricia Renwick, ShayMaria Silvestri, Daniel Textoris, Al Traverse, Mickey Van Fossen, Walter Wheeler, and Lynn Zeigler for use of their unpublished data and their insights. We thank Patricia Gensel for use of the photographs in Figure 1.3 and the paleobotanical data for Stop 1.1. We are especially appreciative of all quarry managers and land owners who have granted permission to IGC for use of their quarries or property as field stops for this trip, and we thank Edward Belt for access to the Hitchcock collection in the Pratt Museum at Amherst College. PEO humbly thanks his parents and Cynthia Banach for not not loosing patience with him. RWS wishes to thank his family and friends for their understanding of my long absence during the preparation of this guidebook and Marge Levy for moral support. PJWG especially thanks Susan Roberts and Robin Balinsky for help in preparing parts of the road log. Funding for the research presented in this guidebook was gratefully received from the donors of the American Chemical Society administered by the Petroleum Research Fund (ACS-19878G2 to PEO), the National Science Foundation (grants BSR-87-17707 to PEO; EAR-87-21142 and EAR-86-18161 to D. Kent and PEO; EAR-87-21103 to G. Karner, M. Steckler, and PEO), the Nuclear Regulatory Commission (contract NRC-04-85-111-02 to L. Seeber and PEO), the National Geographic Society (grant 3008-84 to PJWG), Texaco Inc. (to PJWG), the U.S. National Committee for the International Geological Correlation Program to Project 219 (to PJWG), the Emory University Research Committee (to PJWG), and the COGEOMAP Program between the United States Geological Survey and the North Carolina State Geological Survey (agreement 14-08-0001-A0433 to P. Gallagher and W. Hoffman). Finally, we wish to thank the International Geological Congress, and especially Juergen Rheinhardt, for giving us the opportunity and financial support to show off these exciting basins to the world. This guidebook is Lamont-Doherty Geological Observatory Contribution 4446.

REFERENCES

Abdel-Monem, A.A., and Kulp, J.L., 1968, Paleogeography and the source of sediments of the Triassic basin, New Jersey, by K-Ar dating: *Geological Society of America Bulletin*, v. 79, p. 1231-1242.

Allmendinger, R.W., Nelson, K.D., Potter, C.J., Barazangi, M., Brown, L.D., and Oliver, J.E., 1987, Deep seismic reflection characteristics of the continental crust: *Geology*, v. 15, p. 304-310.

Ando, C.J., *et al.*, 1984, Crustal profile of a mountain belt: COCORP deep seismic reflection profiling in New England Appalachians and implications for architecture of convergent mountain chains: *American Association of Petroleum Geologists Bulletin*, v. 68, p. 819-837.

Ando, C.J., Cook, F.A., Oliver, J.E., Brown, L.D., and Kaufman, S., 1983, Crustal geometry of the Appalachian orogen from seismic reflection studies: *Geological Society of America Memoir 158*, p. 83-101.

Arguden, A.T., and Rodolfo, K.S., 1986, Sedimentary facies and tectonic implications of lower Mesozoic alluvial-fan conglomerates of the Newark basin, northeastern United States: *Sedimentary Geology*, v. 51, p. 97- 118.

Ash, S.R., 1980, Upper Triassic floral zones of North America, *in* Dilcher, D.L., and Taylor, T.N., eds., *Biostratigraphy of Fossil Plants*: Stroudsburg, PA, Dowden, Hutchinson, and Ross, p. 153-170.

Bain, G.L., and Brown, C.E., 1980, Evaluation of the Durham Triassic basin of North Carolina and techniques used to characterize its waste-storage potential: *U.S. Geological Survey Open-File Report 80-1295*, 133 p.

Bain, G.L., and Harvey, B.W., eds., 1977, *Field Guide to the Geology of the Durham Triassic Basin*: Raleigh, NC, Carolina Geological Society, 83 p.

Bain, G.W., 1932, The northern area of the Connecticut Valley Triassic: *American Journal of Science (5th Series)*, v. 23, p. 57-77.

Baird, D., 1957, Triassic reptile footprint faunules from Milford, New Jersey: *Museum of Comparative Zoology (Harvard University) Bulletin*, v. 117, p. 449-520.

Baird, D., 1986a, Middle Triassic herptofauna in Nova Scotia (Abstract): *Friends of the Newark Newletter*, no. 5, p. 10.

Baird, D., 1986b, Some Upper Triassic reptiles, footprints, and an amphibian from New Jersey: *The Mosasaur*, v. 3, p. 125-153.

Baird, D., and Olsen, P.E., 1983, Late Triassic herpetofauna from the Wolfville Fm. of the Minas Basin (Fundy Basin) Nova Scotia, Can.: *Geological Society of America Abstracts with Programs*, v. 15, p. 122.

Baird, D., and Take, W., 1959, Triassic reptiles from Nova Scotia. (Abstract): *Geological Society of America Bulletin*, v. 70, p. 1565-1566.

Barnett, J.A.M., Mortimer, J., Rippon, J.H., Walsh, J.J., and Watterson, J., 1987, Displacement geometry in the volume containing a single normal fault: *American Association of Petroleum Geologists Bulletin*, v. 71, p. 925-937.

Bell, H., Books, K.G., Daniels, D.L., Hoff, W.E., Jr., and Popenoe, P., 1979, Diabase dikes in the Haile-Brewer area, South Carolina, and their magmatic properties. *U.S. Geological Survey Professional Paper 1123*, p. C1-C17.

Berger, A.L., 1977, Support for the astronomical theory of climate change: *Nature*, v. 269, p. 44-45.

Berger, A.L., 1984, Accuracy and frequency stability of the Earth's orbital elements during the Quaternary, *in* Berger, A., Imbrie, J., Hays, J., Kukla, G., and Saltzman, B., eds., *Milankovitch and Climate, Part 1*: Dordrecht, Holland, D. Reidel Publishing Co., p. 3-40.

Berggren, W.A., Kent, D.V., Flynn, J.J., and Van Couvering, J.A., 1985, Cenozoic geochronology: *Geological Society of America Bulletin*, v. 96, p. 1407-1418.

Berner, R.A., 1981, A new geochemical classification of sedimentary environments: *Journal of Sedimentary Petrology*, v. 51, p. 359-365.

Berner, R.A., Baldwin, T., and Holdren, G.R., Jr., 1979, Authigenic iron sulfides as paleosalinity indicators: *Journal of Sedimentary Petrology*, v. 49, p. 1345-1350.

Berner, R.A., and Raiswell, R., 1983, Burial of organic carbon and pyrite sulfur in sediments over Phanerozoic time: a new theory: *Geochimica et Cosmochimica Acta*, v. 47, p. 855-862.

Birney, C.C., 1985, Sedimentology and petrology of the Scots Bay Formation, (Lower Jurassic), Nova Scotia, Canada: M.Sc. Thesis, University of Massachusetts, Amherst, 325 p.

Bluck, B.J., 1982, Texture of gravel bars in braided streams, *in* Hay, J.D., Bathurst, J.C., and Thorne, C.R., eds., *Gravel-Bed Rivers*: New York, John Wiley & Sons, p. 339-355.

Bock, W., 1952, Triassic reptilian tracks and trends of locomotive evolution: *Journal of Paleontology*, v. 26, p. 395-433.

Bonaparte, J.F., 1971, Los tetrapodos del sector superior de la Formatión Los Colorados, La Rioja, Argentina: *Opera Lilloana*, v. 22, p. 1-183.

Bond, K.R., and Phillips, J.D., 1988, Aeromagnetic imagery with geologic correlations for some early Mesozoic basins of the eastern United States, *in* Froelich, A.J., and Robinson, G.R., Jr., eds., *Studies of the Early Mesozoic Basins of the Eastern United States: U.S. Geological Survey Bulletin 1776*, p. 253-264.

Boyer, B.W., 1981, Tertiary lacustrine sediments from Sentinel Butte, North Dakota and the sedimentary record of ectogenic meromixis: *Journal of Sedimentary Petrology*, v. 51, p. 429-440.

Bradley, D.C., 1982, Subsidence in late Paleozoic basins in the northern Appalachians: *Tectonics*, v. 1, p. 107-123.

Bradley, W.H., 1929, Varves and climate of the Green River epoch: *U.S. Geological Survey Professional Paper 158E*, p. 86-110.

Bradley, W.H., 1963, Paleolimnology, *in* Frey, D., ed., *Limnology in North America*: Madison, WI, University of Wisconsin Press, p. 621-648.

Bradley, W.H., and Eugster, H., 1969, Geochemistry and paleolimnology of the trona deposits and associated authigenic minerals of the Green River Formation: *U.S. Geological Survey Professional Paper 496B*, 71 p.

Broecker, W.S., Thurber, D.L., Goddard, J., Ku, T., Matthews, R.K., and Mesolella, K.J., 1968, Milankovitch hypothesis supported by precise dating of coral reefs and deep sea sediments: *Science*, v. 159, p. 1-4.

Brown, A., *et al.*, 1952, Coal resources of Virginia: *U.S. Geological Survey Circular 171*, 57 p.

Brown, L.D., *et al.*, 1983, Adirondack-Appalachian crustal structure: the COCORP northeast traverse: *Geological Society of America Bulletin*, v. 94, p. 1173-1184.

Brown, P.M., *et al.*, 1985, Geologic map of North Carolina: *North Carolina Department of Natural Resources and Community Development, Geological Survey Section*, 1:500,000.

Bryan, P., and Gordon, R.G., 1986, Rotation of the Colorado Plateau: an analysis of paleomagnetic data: *Tectonics*, v. 5, p. 661-667.

Burton, W.C., and Ratcliffe, N.M., 1985, Compressional structures associated with right-oblique normal faulting of Triassic-Jurassic strata of the Newark basin near Flemington, New Jersey: *Geological Society of America Abstracts with Programs*, v. 17, p. 9.

Cameron, B., 1986, Jurassic fossils from the Scots Bay Formation: *Nova Scotia Department of Mines and Energy*, *Information Series 12*, p. 167-169.

Campbell, M.R., and Kimball, K.W., 1923, The Deep River coal field of North Carolina: *North Carolina Geological and Economic Survey Bulletin 33*, 95 p.

Cant, D.J., and Walker, R.G., 1976, Development of a braided fluvial facies model for the Devonian Battery Point Sandstone, Quebec: *Canadian Journal of Earth Sciences*, v. 13, p. 102-119.

Cant, D.J., and Walker, R.G., 1978, Fluvial processes and facies sequences in the sandy braided South Saskatchewan River, Canada: *Sedimentology*, v. 25, p. 625-648.

Carozzi, A.V., 1964, Complex öoids from Triassic lake deposit, Virginia: *American Journal of Science*, v. 262, p. 231-241.

Carroll, R.L., Belt, E.S., Dineley, D.L., Baird, D., McGregor, D.C., 1972, Excursion A59: Vertebrate Paleontology of Eastern Canada: *XXIV International Geological Congress, Montreal, Guidebook*, p. 1-113.

Chang, C.C., 1968, A gravity study of the Triassic valley in southern Connecticut: M.A. Thesis, Wesleyan University, Middletown, CT, 108 p.

Channell, J.E.T., Lowrie, W., Pialli, P., Venturi, F., 1984, Jurassic magnetostratigraphy from Umbrian (Italian) land section: *Earth and Planetary Science Letters*, v. 68, p. 309-325.

Chapman, R.W., 1965, Stratigraphy and petrology of the Hampden basalt in central Connecticut: *Connecticut Geological and Natural History Survey Report of Investigations 3*, 38 p.

Cisne, J.L., Gildner, F., and Rabe, B.D.,1984, Epeiric sedimentation and sea level: synthetic ecostratigraphy: *Lethaia*, v. 17, p. 267-288.

Clifford, W., 1887, The Richmond coal field, Virginia: *Manchester Geological Society Transactions*, v. 19, p. 326-358.

Colbert, E.H., 1960, A new Triassic procolophonid from Pennsylvania: *American Museum Novitates*, no. 2022, p. 1-19.

Cook, F.A., Brown, L.D., Kaufman, S., Oliver, J.E., and Petersen, T.A., 1981, COCORP seismic profiling of the Appalachian orogen beneath the coastal plain of Georgia: *Geological Society of America Bulletin*, v. 92, p. 738-748.

Cook, F.A., and Oliver, J.E., 1981, The early Paleozoic continental edge in the Appalachian orogen: *American Journal of Science*, v. 281, p. 993-1008.

Coombs, W.P., Jr., 1980, Swimming ability of carnivorous dinosaurs: *Science*, v. 207, p. 1198-1200.

Cope, J.C.W., Getty, T.A., Howarth, M.K., Morton, N., and Torrens, H.S., 1980, *A Correlation of Jurassic Rocks in the British Isles. Part One: Introduction and Lower Jurassic: Geological Society of London Special Report No. 14*, 73 p.

Cornet, B., 1977a, The palynostratigraphy and age of the Newark Supergroup: Ph. D. thesis, University of Pennsylvania, State College, PA, 505 p.

Cornet, B., 1977b, Preliminary investigation of two Late Triassic conifers from York County, Pennsylvania, *in* Romans, R.C., ed., *Geobotany*: New York, Plenum Publishing Corporation, p. 165-172.

Cornet, B., 1986, The leaf venation and reproductive structures of a Late Triassic angiosperm, *Sanmiguelia lewisii*: *Evolutionary Theory*, v. 7, p. 231-309.

Cornet, B., in press, Late Triassic angiosperm-like pollen from the Richmond basin of Virginia, U.S.A.: *Palaeontographica B*.

Cornet, B., and Olsen, P.E., 1985, A summary of the biostratigraphy of the Newark Supergroup of eastern North America, with comments on early Mesozoic provinciality, *in* Weber, R., ed., *III Congresso Latinoamericano de Paleontologia Mexico, Simposio Sobre Floras del Triasico Tardio, su Fitografia y Paleoecologia, Memoria*, p. 67-81.

Cornet, B., and Traverse, A., 1975, Palynological contributions to the chronology and stratigraphy of the Hartford basin in Connecticut and Massachusetts: *Geoscience and Man*, v. 11, p. 1-33.

Cornet, B., Traverse, A., and McDonald, N.G., 1973, Fossil spores, pollen, fishes from Connecticut indicate Early Jurassic age for part of the Newark Group: *Science*, v. 182, p. 1243-1247.

Cornet, B., and Ziegler, D., 1985, Structural styles and tectonic implications of the Richmond-Taylorsville Rift System, eastern Virginia (Abstract): *American Association of Petroleum Geologists Bulletin*, v. 69, p. 1434-1435.

Cossey, S.P.J., and Frank, H.J., 1983, Uranium mineralization and use of resistance log character in deltaic point bars: Franklin Mine, Karnes County, Texas: *American Association of Petroleum Geologists Bulletin*, v. 67, p. 131-151.

Costain, J.K. and Glover, L., 1983, Seismicity in the eastern United States and the role of crustal reflectivity. *U.S. Geological Survey Open File Report 83-843*, p. 207-220.

Courtillot, V., Vandamme, D., Besse, J., and Jaeger, J.J., 1988, Deccan volcanism at the Cretaceous-Tertiary boundary: *Global catastrophes in Earth history: an interdisciplinary conference on impacts, volcanism, and mass mortality*, Lunar and Planetary Institute and The National Academy of Sciences, p. 31-32.

Crespi, J.M., 1988, Using balanced cross sections to understand early Mesozoic extensional faulting, *in* Froelich, A.J., and Robinson, G.R., Jr., eds., *Studies of the Early Mesozoic Basins of the Eastern United States: U.S. Geological Survey Bulletin 1776*, p. 220-229.

Crosby, D.G., Jr., 1962, Wolfville map area, Nova Scotia: *Geological Survey of Canada Memoir 325*, 67 p.

Crush, P.J., 1984, A Late Upper Triassic Sphenosuchid Crocodilian from Wales: *Paleontology*, v. 27, p.131-157.

Dana, J.D., 1878, On "indurated bitumen in cavities in the trap of the Connecticut Valley." From the Report on the geology of Connecticut, by Dr. J.G. Percival: *American Journal of Science, 3rd series*, v. 16, p. 130-132.

Darton, N.H., 1890, The relations of the traps of the Newark System in the New Jersey region: *U.S. Geological Survey Bulletin 67*, 82 p.

Davis, D., Suppe, J., and Dahlen, F.A., 1983, Mechanics of fold-and-thrust belts and accretionary wedges: *Journal of Geophysical Research*, v. 88, p. 1153-1172.

Deane, J., 1861, *Ichnographs from the Sandstone of the Connecticut River*: Boston, Little, Brown, 61 p.

de Boer, J.Z., and Clifford, A.E., 1988, Mesozoic tectogenesis: development and deformation of 'Newark' rift zones in the Appalachians (with special emphasis on the Hartford basin, Connecticut), *in* Manspeizer, W., ed., *Triassic-Jurassic Rifting, Continental Breakup and the Origin of the Atlantic Ocean and Passive Margins*: New York, Elsevier, p. 275-306.

de Boer, J.Z., McHone, J.G., Puffer, J.H., Ragland, P.C., and Whittington, D., 1988, Mesozoic and Cenozoic magmatism, *in* Sheridan, R.E., and Grow, J.A., eds., *The Geology of North America, Volume I-2, The Atlantic Continental Margin, U.S.*: Geological Society of America, p. 217-241.

de Boer, J.Z., and Snider, F.G., 1979, Magnetic and chemical variations of Mesozoic diabase dikes from eastern North America: evidence for a hotspot in the Carolinas; part 1: *Geological Society of America Bulletin*, v. 90, p. 185-198.

Delevoryas, T., and Hope, R.C, 1971, A new Triassic cycad and its phyletic implications: *Postilla*, no. 150, p. 1-21.

Delevoryas, T., and Hope, R.C., 1973, Fertile coniferophyte remains from the Late Triassic Deep River basin, North Carolina: *American Journal of Botany*, v. 60, p. 810-818.

Delevoryas, T., and Hope, R.C., 1975, *Voltzia andrewsii*, n. sp., an Upper Triassic seed cone from North Carolina, U.S.A.: *Review of Palaeobotany and Palynology*, v. 20, p. 67-74.

Delevoryas, T., and Hope, R.C., 1981, More evidence for conifer diversity in the Upper Triassic of North Carolina: *American Journal of Botany*, v. 68, p. 1003-1007.

Demicco, R.V., and Gierlowski-Kordesch, E., 1986, Facies sequences of a semi-arid closed basin: the Lower Jurassic East Berlin Formation of the Hartford basin, New England, U.S.A.: *Sedimentology*, v. 33, p. 107-118.

Deninger, R.W., Dallmeyer, R.D., and Neathery, T.L., 1975, Chemical variations and K-Ar ages of diabase dikes in east-central Alabama: *Geological Society of America Abstracts with Programs*, v. 7, p. 482.

Dietz, R.S., 1986, Triassic-Jurassic extinction event, Newark basalts, and impact-generated Bahama nexxus: *Abstracts and Program of the 49th Annual Meeting of the Meteoritical Society*: Houston, Lunar and Planetary Institute, p. 1-10.

D'Invilliers, E.V., 1883, The geology of the South Mountain belt of Berks County: *Pennsylvania Geological Survey (2nd), Report DDD*, 441 p.

Donohoe, H.V., Jr., and Wallace, P.I., 1982, *Geological Map of the Cobequid Highlands, Colchester, Cumberland, and Pictou Counties, Nova Scotia*: Nova Scotia Department of Mines and Energy, 1:50,000.

Eaton, G.P., and Rosenfeld, J.L., 1960, Gravimetric and structural investigations in central Connecticut: *International Geological Congress, 21st Session, Copenhagen, Part II*, p. 168-178.

Ediger, V.S., 1986, Paleopalynological biostratigraphy, organic matter deposition, and basin analysis of the Triassic-Jurassic(?) Richmond rift basin, VA: Ph.D. thesis, The Pennsylvania State University, 547 p.

Ediger, V.S., Cornet, B., Goodwin, B.K., Ziegler, D.G., and Traverse, A., in preparation, Revised stratigraphic classification of the Richmond, Virginia rift basin, Triassic-(?)Jurassic deposits, and a summary of the geology of the area: for *Geological Society of America Bulletin*.

Emerson, B.K., 1891, On the Triassic of Massachusetts: *Geological Society of America Bulletin*, v. 2, p. 451-456.

Emiliani, C., 1966, Paleotemperature analysis of Caribbean cores P6304-8 and P6304-9 and a general temperature curve for the past 425,000 years: *Journal of Geology*, v. 74, p. 109-126.

Emmons, E., 1856, *Geological report of the Midland Counties of North Carolina:* New York, G.P. Putnam and Company, 352 p.

Emmons, E., 1857, *American Geology, Pt. VI.:* Albany, NY, Spraugue and Co., 152 p.

Eyerman, J., 1886, Footprints on the Triassic sandstone (Jura-Trias) of New Jersey: *American Journal of Science, 3rd Series*, v. 31, p. 72.

Faill, R.T., 1973, Tectonic development of the Triassic Newark-Gettysburg basin in Pennsylvania: *Geological Society of America Bulletin*, v. 84, p. 725-740.

Faill, R.T., 1988, Mesozoic tectonics of the Newark basin, as viewed from the Delaware River, *in* Husch, J.M., and Hozik, M.J., eds., *Geology of the Central Newark Basin: Fifth Meeting of the Geological Association of New Jersey*, Rider College, Lawrenceville, NJ, p. 19-41.

Faust, G.T., 1975, A review and interpretation of the geologic setting of the Watchung basalt flows, New Jersey: *U.S. Geological Survey Professional Paper 864-A*, p. A1-A42.

Faust, G.T., 1977, Joint systems in the Watchung basalt flows, New Jersey: *U.S. Geological Survey Professional Paper 864B*, p. B1-B42.

Fedosh, M.S., and Smoot, J.P., 1988, A cored stratigraphic section through the northern Newark basin, New Jersey, *in* Froelich, A.J., and Robinson, G.R., Jr., eds., *Studies of the Early Mesozoic Basins of the Eastern United States: U.S. Geological Survey Bulletin 1776*, p. 19-24.

Fluhr, T.W., 1941, The geology of the Lincoln Tunnel: *Rocks and Minerals*, v. 16, p. 115-119, 155-160, 195-198, 235-239.

Fontaine, W.M., 1883, Contributions to the knowledge of the older Mesozoic flora of Virginia: *U.S. Geological Survey Monograph 6*, 144 p.

Frey, R.W., Pemberton, S.G., Fagerstrom, J.A., 1984, Morphological, ethological, and environmental significance of the ichnogenera *Scoyenia* and *Ancorichnus*: *Journal of Paleontology*, v. 58, p. 511-528.

Froelich, A.J., and Gottfried, D., 1985, Early Jurassic diabase sheets of the eastern United States—a preliminary overview, *in* Robinson, G.R., Jr., and Froelich, A.J., eds., *Proceedings of the Second U.S. Geological Survey Workshop on the Early Mesozoic Basins of the Eastern United States: U.S. Geological Survey Circular 946*, p. 79-86.

Froelich, A.J. and Gottfried, D., 1988, An overview of Early Mesozoic intrusive rocks in the Culpeper basin, Virginia and Maryland, *in* Froelich, A.J., and Robinson, G.R., Jr., eds., *Studies of the Early Mesozoic Basins of the Eastern United States: U.S. Geological Survey Bulletin 1776*, p. 151-165.

Froelich, A.J., Leavy, B.D., and Lindholm, R.C., 1982, Geologic traverse across the Culpeper basin (Triassic-Jurassic) of northern Virginia, *in* Lyttle, P.T., ed., *Central Appalachian Geology*: *Geological Society of America Field Trip Guidebook*, p. 55-81.

Froelich, A.J., and Olsen, P.E., 1984, Newark Supergroup, a revision of the Newark Group in eastern North America: *U.S. Geological Survey Bulletin 1537A*, p. A55-A58.

Galton, P.M., 1976, Prosauropod dinosaurs (Reptilia: Saurischia) of North America: *Postilla*, no. 169, 98 p.

Gensel, P., 1986, Plant fossils of the Upper Triassic Deep River basin, *in* Gore, P.J.W., ed., Depositional framework of a Triassic rift basin: the Durham and Sanford sub-basins of the Deep River basin, North Carolina, *in* Textoris, D.A., ed., *Society of Economic Paleontologists and Mineralogists Field Guidebook, Third Annual Mid-year Meeting*, Raleigh, NC, p. 82-86.

Gibbs, A.D., 1984, Structural evolution of extensional basin margins: *Journal of the Geological Society of London*, v. 141, p. 609-620.

Gile, L.H., Peterson, F.F., and Grossman, R.B., 1966, Morphological and genetic sequences in carbonate accumulation in desert soils: *Soil Science*, v. 101, p. 347-360.

Glaeser, J.D., 1963, Lithostratigraphic nomenclature of the Triassic Newark-Gettysburg basin: *Proceedings of the Pennsylvania Academy of Sciences*, v. 37, p. 179-188.

Golebiowski, R., and Braunstein, R.E., 1988, A Triassic-Jurassic boundary section in the northern Calcareous Alps (Austria), *in* IGCP Project 199: Rare Events in Geology, Abstracts of Lectures, Excursion Guide: *Berichte der geologischen Bundesandstalt*, v. 15, p. 39-46.

Goodwin, B.K., 1970, Geology of the Hylas and Midlothian Quadrangles, Virginia: *Virginia Division of Mineral Resources Report of Investigations 23*, 51 p.

Goodwin, B.K., and Farrell, K.M., 1979, Geology and coal resources of the Richmond Triassic basin: *Virginia Division of Mineral Resources*, 115 p.

Goodwin, B.K., Ramsey, K.W., and Wilkes, G.P., 1986, *Guidebook to the Geology of the Richmond, Farmville, Briery Creek, and Roanoke Creek Basins, Virginia: Virginia Geological Field Conference, 18th Annual Meeting*, 75 p.

Goodwin, B.K., Weems, R.E., Wilkes, G.P., Froelich, A.J., and Smoot, J.P., 1985, Field Trip 4: The Geology of the Richmond and Taylorsville basins, east-central Virginia: *American Association of Petroleum Geologists, Eastern Section Meeting Guidebook*, 60 p.

Gordon, R.G., Cox, A., and O'Hare, S., 1984, Paleomagnetic Euler poles and the apparent polar wander and absolute motion of North America since the Carboniferous: *Tectonics*, v. 3, p. 499-537.

Gore, P.J.W., 1983, Sedimentology and invertebrate paleontology of Triassic and Jurassic lacustrine deposits, Culpeper basin, northern Virginia: Ph. D. thesis, The George Washington University, Washington, D.C., 356 p.

Gore, P.J.W., 1985, Triassic floodplain lake in the Chatham

Group (Newark Supergroup) of the Durham sub-basin of the Deep River basin, North Carolina: comparison to the Culpeper basin, Virginia: *Geological Society of America Abstracts with Programs*, v. 17, p. 94.

Gore, P.J.W., 1986a, Depositional framework of a Triassic rift basin: the Durham and Sanford sub-basins of the Deep River basin, North Carolina, *in* Textoris, D.A., ed., *Society of Economic Paleontologists and Mineralogists Field Guidebook, Third Annual Mid-year Meeting*, Raleigh, NC, p. 53-115.

Gore, P.J.W., 1986b, Late Triassic lacustrine deposits in the Deep River basin (Newark Supergroup), North Carolina, USA: *Abstracts Volume, Sediments Down-Under, 12th International Sedimentological Congress*, Canberra, Australia, p. 122-123.

Gore, P.J.W., 1986c, Facies relationships of fluvial and lacustrine deposits, Durham sub-basin, Deep River basin, North Carolina: *Society of Economic Paleontologists and Mineralogists Annual Midyear Meeting*, v. 3, p. 45.

Gore, P.J.W., 1988a, Late Triassic and Early Jurassic lacustrine sedimentation in the Culpeper basin, Virginia, *in* Manspeizer, W., ed., *Triassic-Jurassic Rifting, Continental Breakup and the Origin of the Atlantic Ocean and Passive Margins*, New York, Elsevier, p. 369-400.

Gore, P.J.W., 1988b, Paleoecology and sedimentology of a Late Triassic lake, Culpeper basin, Virginia: *Palaeogeography, Palaeoclimatology, Palaeoecology*, v. 62, p. 593-608.

Gore, P.J.W., 1988c, Lacustrine sequences in an Early Mesozoic rift basin: Culpeper basin, Virginia, USA, *in* Fleet, A.J., Kelts, K., and Talbot, M.R., eds., *Lacustrine Petroleum Source Rocks: Geological Society of London Special Publication 40*, p. 247-278.

Gore, P.J.W., in press, Toward a model for open- and closed-basin deposition in ancient lacustrine sequences: the Newark Supergroup (Triassic-Jurassic), eastern North America: *Palaeogeography, Palaeoclimatology, Palaeoecology*.

Gottfried, D., Annell, C.S., Beyerly, G.R., 1983, Geochemistry and tectonic significance of subsurface basalts from Charleston, South Carolina: Clubhouse Crossroads test holes #2 and #3: *U.S. Geological Survey Professional Paper 1313-A*, p. A1-A19.

Gray, N.H., 1982, Mesozoic volcanism in north-central Connecticut, *in* Joesten, R., and Quarrier, S.S., eds., *Guidebook for Field trips in Connecticut and South-Central Massachusetts: New England Intercollegiate Geological Conference, 74th Annual Meeting*, p. 173-193.

Grew, E.S., 1965, Impsonite from Rocky Hill, Connecticut: Unpublished Report, Connecticut Geological and Natural History Survey, Hartford, Connecticut, 18 p.

Hallam, A., 1981, The end-Triassic bivalve extinction event: *Palaeogeography, Palaeoclimatology, Palaeoecology*, v. 35, p. 1-44.

Hallam, A., 1988, The end-Triassic mass extinction event (Abstract): *Global Catastrophes in Earth history: An Interdisciplinary Conference on Impacts, Volcanism, and Mass Mortality*, Lunar and Planetary Institute and The National Academy of Sciences, p. 66-67.

Hamilton, W., 1981, Plate-tectonic mechanism of Laramide deformation: *Contributions in Geology [University of Wyoming]*, v. 19, p. 87-92.

Handy, W.A., 1976, Depositional history and diagenesis of lacustrine and fluvial sedimentary rocks of the Turners Falls and Mount Toby transition, north central Massachusetts: M.S. thesis, University of Massachusetts, Amherst, MA, 115 p.

Hansen, H.J., 1988, Buried rift basin underlying coastal plain sediments, central Delmarva Peninsula, Maryland: *Geology*, v. 16, p. 779-782.

Harland, W.B., Cox, A.V., Llellyn, P.G., Pinkton, C.A.G., Smith, A.G., Walters, A., 1982, *A Geologic Time Scale:* Cambridge, Cambridge University Press, 131 p.

Hatcher, R.D.,1972, Developmental model for the southern Appalachians: *Geological Society of America Bulletin*, v. 83, p. 1735-2760.

Hawkes, H.E., Wedow, H., and Balsley, J.R., 1953, Geological investigation of the Boyertown magnetite deposits in Pennsylvania: *U.S. Geological Survey Bulletin 995-D*, p. 135-149.

Haycock, E., 1900, Records of post-Triassic changes in Kings County, N.S.: *Proceedings and Transactions, Nova Scotian Institute of Science*, v. 10, p. 287-302.

Hays, J.D., Imbrie, J., and Shackleton, N.J., 1976, Variations in the Earth's orbits: pacemaker of the Ice Ages: *Science*, v. 194, p. 1121-1132.

Hellinger, S.J., and Sclater, J.G., 1983, Some comments on two-layer extensional models for the evolution of sedimentary basins: *Journal of Geophysical Research*, v. 88, p. 8251-8269.

Henika, W.S., 1981, Geology of the Spring Garden Quadrangle, Virginia: *Virginia Division of Mineral Resources Open-file Map and Report*.

Heltzer, M., 1987, The coal demon of Deep River: *The State - Down home in North Carolina*, v. 55, p. 14-17.

Hentz, T.F., 1981, Sedimentology and structure of Culpeper Group lake beds (Lower Jurassic) at Thoroughfare Gap, Virginia: M.S. Thesis, University of Kansas, Lawrence, KS, 166 p.

Hentz, T.F., 1985, Early Jurassic sedimentation in a rift-valley lake: Culpeper basin, northern Virginia: *Geological Society of America Bulletin*, v. 96, p. 92-107.

Heward, A.P., 1978, Alluvial fan sequence and megasequence models, with examples from Westphalian D-Stephanian B coalfields, northern Spain, *in* Miall, A.D., ed., *Fluvial Sedimentology: Canadian Society of Petroleum Geologists Memoir 5*, p. 669-702.

Hitchcock, E., 1818, Remarks on the geology and mineralogy of a section of Massachusetts on the Connecticut River, with a part of New Hampshire and Vermont: *American Journal of Science, 1st Series*, v. 1, p. 105-116.

Hitchcock, E., 1837, Fossil footsteps in sandstone and graywacke: *American Journal of Science, 1st Series*, v. 32, p. 174-176.

Hitchcock, E., 1858, *Ichnology of New England: A Report on the Sandstone of the Connecticut Valley, especially its Fossil Footmarks*: Boston, Wm. White, 220 p.

Hitchcock, E., 1865, *Supplement to the Ichnology of New England*: Boston, Commonwealth of Massachusetts, 96 p.

Hoffman, C.W., and Gallagher, P.E., 1988, Geologic map of the Southeast and Southwest Durham 7.5 minute quadrangles, North Carolina: *Geological Society of America Abstracts with Programs*, v. 20, p. 270.

Hoffman, C.W., and Gallagher, P.E., in preparation, Geology of the Southeast and Southwest Durham 7.5 minute quadrangles, North Carolina, USA: North Carolina Geological Survey Report.

Hope, R.C. and Patterson, O.F., III, 1970, *Pekinopteris auriculata*: A new plant from the North Carolina Triassic: *Journal of Paleontology*, v. 44, p. 1137-1139.

Hotz, P.E., 1953, Form of diabase sheets in southeastern Pennsylvania: *American Journal of Science*, v. 250, p. 375-388.

Hozik, M.J., 1985, Evidence for dominance of normal dip-slip motion on segment of Flemington fault in Newark Basin of New Jersey (Abstract): *American Association of Petroleum Geologists Bulletin*, v. 69, p. 1438.

Hubert, J.F., and Forlenza, M.F., 1988, Sedimentology of braided-river deposits in Upper Triassic Wolfville redbeds, southern shore of Cobequid Bay, Nova Scotia, Canada, *in* Manspeizer, W., ed., *Triassic-Jurassic Rifting, Continental Breakup and the Origin of the Atlantic Ocean and Passive Margins*: New York, Elsevier, p. 231-247.

Hubert, J.F., and Hyde, M.G., 1982, Sheet flow deposits of graded beds and mudstones on an alluvial sandflat-playa system:

Upper Triassic Blomidon redbeds, St. Mary's Bay, Nova Scotia: *Sedimentology*, v.29, p. 457-474.
Hubert, J.F., and Mertz, K.A.,1980, Eolian dune field of Late Triassic age, Fundy Basin, Nova Scotia: *Geology*, v. 8, p. 516-519.
Hubert, J.F., and Mertz, K.A., 1984, Eolian sandstones in Upper Triassic-Lower Jurassic red beds of the Fundy Basin, Nova Scotia: *Journal of Sedimentary Petrology*, v. 54, p. 798-810.
Hubert, J.F., and Reed, A.A., 1978, Red-bed diagenesis in the East Berlin Formation, Newark Group, Connecticut Valley: *Journal of Sedimentary Petrology*, v. 48, p. 175-184.
Hubert, J.F., Reed, A.A., and Carey, P.J., 1976, Paleogeography of the East Berlin Formation, Newark Group, Connecticut Valley: *American Journal of Science*, v. 276, p. 1183-1207.
Hubert, J.F., Reed, A.A., Dowdall, W.L., Gilchrist, J.M., 1978, Guide to the red beds of Central Connecticut: 1978 Field Trip, Eastern Section, Society of Economic Paleontologists and Mineralogists, *University of Massachusetts, Amherst, Department of Geology and Geography, Contribution No. 32*, 129 p.
Husch, J.M., *et al.*, 1988, A review of the petrology and geochemistry of Mesozoic diabase from the central Newark basin: new petrogenetic insights, *in* Husch, J.M., and Hozik, M.J., eds., *Geology of the Newark Rift Basin: 5th Annual Meeting of the New Jersey Geological Association*, Rider College, Lawrenceville, NJ, p. 149-194.
Hutchinson, D.R., and Klitgord, K.D., 1988a, Deep structure of rift basins from the continental margin around New England, *in* Froelich, A.J., and Robinson, G.R., Jr., eds., *Studies of the Early Mesozoic Basins of the Eastern United States: U.S. Geological Survey Bulletin 1776*, p. 211-219.
Hutchinson, D.R., and Klitgord, K.D.,1988b, Evolution of rift basins on the continental margin off southern New England, *in* Manspeizer, W., ed., *Triassic-Jurassic Rifting, Continental Breakup and the Origin of the Atlantic Ocean and Passive Margins*: Elsevier, New York, p. 81-98.
Hutchinson, D.R., Klitgord, K.D., and Detrick, R.S., 1986, Rift basins of the Long Island Platform: *Geological Society of America Bulletin*, v. 97, p. 688-702.
Irving, E., and Irving, G.A., 1982, Apparent polar wander paths Carboniferous through Cenozoic and the assembly of Gondwana: *Geophysical Surveys*, v. 5, p. 141-188.
Jenkins, F.A., 1970, The Chanares (Argentina) Triassic reptile fauna VII: the postcranial skeleton of the traversodontid *Massetognathus pascuali* (Therapsida, Cynodontia): *Breviora*, v. 352, p. 1-28.
Jung, W.W., 1968, *Hirmerella [sic] muensteri* (Schenk) Jung nov. comb., eine bedeutsame Konifere des Mesozoikums: *Palaeontographica B*, v. 122, p. 55-93.
Justus, P.S., 1967, Sequence of development of microscopic textures in diabase dikes of the Deep River Triassic basin, North Carolina: *Geological Society of America Abstracts with Programs, Annual Meeting*, p. 113.
Keppie, J.D. (compiler), 1979, *Geological Map of Nova Scotia*: Halifax, Nova Scotia Department of Mines and Energy, 1:500,000.
Keppie, J.D., 1982, The Minas geofracture, *in* St. Julien, P., and Beland, J., eds., *Major Structural Zones and Faults of the Northern Appalachians: Geological Association of Canada Special Paper 24*, p. 1-34.
King, P.B., 1971, Systematic pattern of Triassic dikes in the Appalachian region, second report: *U.S. Geological Survey Professional Paper 750D*, p. D84-D88.
Kirstein, D.S., 1970, Virginia Solite Plant and Quarry, *in* Thayer, P.A., Kirstein, D.S., and Ingram, R.L., eds., *Stratigraphy, sedimentology and economic geology of Dan River basin, North Carolina: Carolina Geological Society, Field Trip Guidebook*, p. 34-43.
Klein, G. deV., 1960, Stratigraphy, sedimentary petrology and structure of Triassic sedimentary rocks, Maritime Provinces, Canada: Ph. D. Thesis, Yale University, New Haven, CT, 262 p.
Klein, G. deV., 1962, Triassic sedimentation, Maritime provinces, Canada: *Geological Society of America Bulletin*, v. 73, p. 1127-1146.
Klein, G. deV., 1963, Regional implications of Triassic paleocurrents, Maritime Provinces, Canada: *Journal of Geology*, v. 71, p. 801-808.
Klein, G. deV., 1968, Sedimentology of Triassic rocks in the lower Connecticut Valley, *in* Orville, P.M., ed., *Guidebook for field trips in Connecticut: New England Intercollegiate Geological Conference, 60th Meeting, Connecticut Geological and Natural History Survey Guidebook 2*, p. 1-19.
Klitgord, K.D., and Shouten, H., 1986, Plate kinematics of the central Atlantic, *in* Vogt, P.R., and Tucholke, B.E., eds., *The Geology of North America, v. M, The Western North Atlantic Region*: Geological Society of America, p. 351-378.
Klitgord, K.D., Hutchinson, D.R., and Schouten, H., 1988, U.S. Atlantic continental margin; structural and tectonic framework, *in* Sheridan, R.E., and Grow, J.A., eds., *The Geology of North America, v. I-2, The Atlantic Continental Margin, U.S.*: Geological Society of America, p. 19-56.
Kominz, M.A., and Bond, G.C., 1988, A new technique for determining time in cyclic sediments-application to the Newark Supergroup: *Geological Society of America Abstracts with Programs*, v. 20, p. A327.
Koob, J.D., 1961, Triassic pollen and spore flora of the Cumnock Formation (Newark Series) of North Carolina: M.S. Thesis, University of Massachusetts, Amherst, MA, 47 p.
Langbein, W.B., 1961, Salinity and hydrology of closed lakes. *U.S. Geological Survey Professional Paper 412*, 20p.
Kotra, R.K., Gottfried, R.M., Spiker, E.C., Romankiw, L.A., and Hatcher, P.G., 1988, Chemical composition and thermal maturity of kerogen and phytoclasts of the Newark Supergroup in the Hartford basin, *in* Froelich, A.J., and Robinson, G.P., Jr., eds., *Studies of the Early Mesozoic Basins of the Eastern United States: U.S. Geological Survey Bulletin 1776*, p. 68-79.
Krohn, M.D., Evans, J., and Robinson, G.R., Jr., 1988, Mineral-bound ammonium in black shales of the Triassic Cumnock Formation, Deep River basin, North Carolina: *U.S. Geological Survey Bulletin 1776*, p. 86-98.
Krynine, P.D., 1950, Petrology, stratigraphy, and the origin of the Triassic sedimentary rocks of Connecticut: *Connecticut Geological and Natural History Bulletin 73*, 247 p.
Kümmel, H.B., 1897, The Newark System, report of progress: *New Jersey Geological Survey Annual Report for 1896*, p. 25-88.
Lambiase, J., and Rodgers, M.R., 1988, A model for tectonic control of lacustrine stratigraphic sequences in continental rift basins: *Lacustrine Exploration: Case Studies and Modern Analogues, American Association of Petroleum Geologists Research Conference*, Snowbird, Utah, September 7-9, 1988.
Langbein, W.B., 1961, Salinity and hydrology of closed lakes: *U.S. Geological Survey Professional Paper 412*, 20p.
Laville, E., and J.-P. Petit, 1984, Role of synsedimentary strike-slip faults in the formation of Moroccan Triassic basins: *Geology*, v. 12, p. 424-427.
Lea, I., 1851, [Remarks on *Clepsysaurus pennsylvanicus*]: *Proceedings of the Academy of Natural Sciences of Philadelphia*, v. 5, p. 205.
Leavy, B.D., Froelich, A.J., and Abram, E.C., 1983, *Bedrock Map and Geotechnical Properties of Rocks of the Culpeper Basin and Vicinity, Virginia and Maryland*: U.S. Geological Survey Map I-1313-C, 1:125,000.
Lee, K.Y., 1979, Triassic-Jurassic geology of the northern part of the Culpeper basin, Virginia and Maryland: *U.S. Geological*

Survey Open-File Report 79-1557, 29 p.
Lee, K.Y., 1980, Triassic-Jurassic geology of the southern part of the Culpeper basin and the Barboursville basin, Virginia: *U.S. Geological Survey Open-File Report 80-468*, 19 p.
Lee, K.Y., 1982, Thermal metamorphism of Triassic and Jurassic sedimentary rocks in the Culpeper basin, Virginia: *Geological Society of America Abstracts with Programs*, v. 14, p. 34.
Lee, K.Y., and Froelich, A.J., in press, Triassic-Jurassic stratigraphy of the Culpeper and Barboursville basins, Virginia and Maryland: *U.S. Geological Survey Professional Paper 1472*.
Lee, K.Y., and Froelich, A.J., 1985, Geochemical data for Triassic sedimentary and thermally metamorphosed rocks of the northern Culpeper basin, Virginia. *U.S. Geological Survey Open-File Report 85-217*, 20 p.
Lee, K.Y., Leavy, B.D., and Gottfried, D., 1984, Geochemical data for Jurassic diabase and basalt of the northern Culpeper basin, Virginia: *U.S. Geological Survey Open-File Report 84-771*, 19 p.
Lehman, E.P., 1959, The bedrock geology of the Middletown quadrangle: *State of Connecticut, Geological and Natural History Survey Quadrangle Report 8*.
LeTourneau, P.M., 1985a, Alluvial fan development in the Lower Jurassic Portland Formation, central Connecticut-implications for tectonics and climate, *in* Robinson, G.R., Jr., and Froelich, A.J., eds., *Proceedings of the Second U.S. Geological Survey Workshop on the Early Mesozoic Basins of the Eastern United States: U.S. Geological Survey Circular 946*, p. 17-26.
LeTourneau, P. M., 1985b, The sedimentology and stratigraphy of the Lower Jurassic Portland Formation, central Connecticut: M.A. Thesis, Wesleyan University, Middletown, CT, 247 p.
LeTourneau, P.M., and McDonald, N.G., 1985, The sedimentology, stratigraphy, and paleontology of the Lower Jurassic Portland Formation, Hartford basin, central Connecticut, in Tracy, R.J., ed., *Guidebook for Field Trips in Connecticut and Adjacent Areas of New York and Rhode Island: New England Intercollegiate Geological Conference, 77th Annual Meeting*, p. 353-391.
LeTourneau, P.M., and Smoot, J.P., 1985, Comparison of ancient and modern lake margin deposits from the lower Jurassic Portland Formation, Connecticut, and Walker Lake, Nevada: *Geological Society of America Abstracts with Programs*, v. 17, p. 31.
Liew, M.Y.C., 1976, Structure, geochemistry, and stratigraphy of Triassic rocks, north shore of Minas Basin, Nova Scotia: M.Sc. Thesis, Acadia University, Wolfville, N.S., 181 p.
Lindholm, R.C., 1979, Geologic history and stratigraphy of the Triassic-Jurassic Culpeper basin, Virginia: summary: *Geological Society of America Bulletin*, v. 90, p. 995-997.
Lindholm, R.C., Hazlett, J.M., and Fagin, S.W., 1979, Petrology of Triassic-Jurassic conglomerates in the Culpeper basin, Virginia: *Journal of Sedimentary Petrology*, v. 49, p. 1245-1262.
Long, P.E., and Wood, B.J., 1986, Structures, textures, and cooling histories of Columbia River basalt flows: *Geological Society of America Bulletin*, v. 97, p. 1144-1155.
Lorenz, J.C., 1988, *Triassic-Jurassic Rift-Basin Sedimentology—History and Methods*: New York, Van Nostrand Reinhold Company, 315 p.
Lucas, M., Hull, J., and Manspeizer, W., 1988, A foreland-type fold and related structures in the Newark rift basin, *in* Manspeizer, W., ed., *Triassic-Jurassic Rifting, Continental Breakup, and the Origin of the Atlantic Ocean and Passive Margins*: New York, Elsevier, p. 307-332.
Ludlam, S.D., 1969, Fayetteville Green Lake, New York; III. The laminated sediments: *Limnology and Oceanography*, v. 14, p. 848-857.
Lull, R.S., 1915, Triassic life of the Connecticut Valley: *Connecticut Geological and Natural History Survey Bulletin 24*, 285 p.
Lull, R.S., 1953, Triassic life of the Connecticut Valley [revised]: *Connecticut Geological and Natural History Survey Bulletin 81*, 336 p.
Lyell, C., 1847, On the structure and probable age of the coal field of the James River, near Richmond, Virginia: *Quarterly Journal of the Geological Society of London*, v. 3, p. 261-280.
Lyttle, P.T., and Epstein, J.B., 1987, *Geologic map of the Newark 1°x2° Quadrangle, New Jersey, Pennsylvania, and New York*: U.S. Geological Survey, Miscellaneous Investigations Series Map I-1715, 1:250,000.
Mangan, M.T., Wright, T.L., Swanson, D.A., and Byerly, G.R., 1986, Regional correlation of Grande Ronde Basalt Group, Washington, Oregon and Idaho: *Geological Society of America Bulletin*, v. 97, p. 1300-1318.
Manspeizer, W., 1980, Rift tectonics inferred from volcanic and clastic structures, *in* Manspeizer, W., ed., *Field Studies of New Jersey Geology and Guide to Field Trips: 52nd Annual Meeting of the New York State Geological Association*, Rutgers University, Newark, NJ, p. 314-350.
Manspeizer, W., 1982, Triassic-Liassic basins and climate of the Atlantic passive margins: *Geologische Rundschau*, v. 71, p. 895-917.
Manspeizer, W., 1987, Detachment faulting and evolution of the Atlantic passive margins: *Northeastern Geology*, v. 9, p. 223-231.
Manspeizer, W., 1988, Triassic-Jurassic rifting and opening of the Atlantic: an overview, *in* Manspeizer, W., ed., *Triassic-Jurassic Rifting, Continental Breakup and the Origin of the Atlantic Ocean and Passive Margins*: New York, Elsevier, p. 41-79.
Manspeizer, W., and Cousminer, H.L., 1988, Late Triassic-Early Jurassic synrift basins of the U.S. Atlantic margin, *in* Sheridan, R.E., and Grow, J.A., eds., *The Geology of North America, v. I-2, The Atlantic continental margin: U.S.*: Geological Society of America, , p. 197-216.
Manspeizer, W., and Gates, A.E., 1988, Alleghanian transpression and Triassic gravitational tectonics: precursors to the formation of asymmetric conjugate Atlantic margins: *Geological Society of America Abstracts with Programs*, v. 20, p. A218.
Manspeizer, W., and Olsen, P.E., 1981, Rift basins of the passive margin: tectonics, organic-rich lacustrine sediments, basin analyses, *in* Hobbs, G. W., III, ed., *Field Guide to the Geology of the Paleozoic, Mesozoic, and Tertiary Rocks of New Jersey and the Central Hudson Valley*: New York, Petroleum Exploration Society of New York, p. 25-105.
Mawer, C.K., and White, J.C., 1987, Sense of displacement on the Cobequid-Chedabucto fault system, Nova Scotia, Canada: *Canadian Journal of Earth Science*, v. 24, p. 217-223.
May, P.R., 1971, Pattern of Triassic-Jurassic diabase dikes around the North Atlantic in the context of predrift position of the continents: *Geological Society of America Bulletin*, v. 82, p. 1285-1292.
May S.R., and Butler, R.F., 1986, North American Jurassic apparent polar wander: Implications for plate motion, paleogeography, and Cordilleran tectonics: *Journal of Geophysical Research*, v. 91, p. 11,519 - 11,544.
May, S.R., Butler, R.F., Shafiqullah, M., and Damon, P.E., 1986, Paleomagnetism of Jurassic rocks in the Patagonia Mountains, southeastern Arizona: Implications for the North American 170 Ma reference pole: *Journal of Geophysical Research*, v.91, p. 11,545 - 11,555.
Mayr, E., 1984, Evolution of fish species flocks: a commentary, *in* Echelle, A., and Kornfield, I., eds., *Evolution of Fish Species Flocks*: Orono, ME, University of Maine Press, p. 3-11.
McBride, J.H., and Nelson, K.D., 1988, Integration of COCORP deep reflection and magnetic anomaly analysis in the southeastern United States: implications for origin of the

Brunswick and East Coast magnetic anomalies: *Geological Society of America Bulletin*, v. 100, p. 436-445.

McClay, K.R., and Ellis, P.G.,1987, Geometries of extensional fault systems developed in model experiments: *Geology*, v. 15, p. 341-344.

McCune, A. R., 1982, Early Jurassic Semionotidae (Pisces) from the Newark Supergroup: systematics and evolution of a fossil species flock: Ph.D. Thesis, Yale University, New Haven, CT, 371 p.

McCune, A.R., 1986, A revision of *Semionotus* (Pisces: Semionotidae) from the Triassic and Jurassic of Europe: *Paleontology*, v. 29, part 2, p. 213-233.

McCune, A.R., 1987a, Toward the phylogeny of a fossil species flock: semionotid fishes from a lake deposit in the Early Jurassic Towaco Formation, Newark basin: *Bulletin of the Yale Peabody Museum of Natural History*, no. 43, 108 p.

McCune, A.R., 1987b, Lakes as laboratories of evolution: endemic fishes and environmental cyclicity: *Palaios*, v. 2, p. 446-454.

McCune, A.R., Thomson, K.S., and Olsen, P.E., 1984, Semionotid fishes from the Mesozoic great lakes of North America, *in* Echelle, A., and Kornfield, I., eds., *Evolution of Fish Species Flocks*: Orono, ME, University of Maine Press, p. 27-44.

McDonald, N.G., 1975, Fossil fishes from the Newark Group of the Connecticut Valley: M.A. Thesis, Wesleyan University, Middletown, CT, 230 p.

McDonald, N.G., 1982, Paleontology of the Mesozoic rocks of the Connecticut Valley, *in* Joesten, R., and Quarrier, S.S., eds., *Guidebook for Field Trips in Connecticut and South-Central Massachusetts: New England Intercollegiate Geological Conference, 74th Annual Meeting*, p. 143-172.

McDonald, N.G., 1983, History of paleoicthyology in the Newark Supergroup basins, eastern North America: *Geological Society of America Abstracts with Programs*, v. 15, p. 121.

McDonald, N.G., and LeTourneau, P.M., 1988, Paleoenvironmental reconstruction of a fluvial-deltaic-lacustrine sequence, Lower Jurassic Portland Formation, Suffield, Connecticut, *in* Froelich, A.J., and Robinson, G.R., Jr., eds., *Studies of the Early Mesozoic Basins of the Eastern United States: U.S. Geological Survey Bulletin 1776*, p. 24-30.

McDonald, N.G., and LeTourneau, P.M., 1989, Taphonomic phosphate loss in Early Jurassic lacustrine fishes, East Berlin Formation, Hartford Basin, New England, U.S.A. (Abstract): *28th International Geological Congress*, Washington, D.C.

McHone, J.G., 1988, Tectonic and paleostress patterns of Mesozoic intrusions in eastern North America, *in* Manspeizer, W., ed., *Triassic-Jurassic Rifting, Continental Breakup and the Origin of the Atlantic Ocean and Passive Margins*: New York, Elsevier, p. 607-620.

McHone, J.G., and Butler, J.R., 1984, Mesozoic igneous provinces of New England and the opening of the North Atlantic Ocean: *Geological Society of America Bulletin*, v. 95, p. 757-765.

McIntosh, W.C., Hargraves, R.B., and West, C.L., 1985, Paleomagnetism and oxide mineralogy of Upper Triassic to Lower Jurassic red beds and basalts in the Newark basin: *Geological Society of America Bulletin*, v. 96, p. 463-480.

McLaren, D.J., 1988, [Meeting report of] rare events in geology: *EOS*, v. 69, p. 24-25.

McLaughlin, D.B., 1943, The Revere well and Triassic stratigraphy: *Proceedings of the Pennsylvania Academy of Science*, v. 17, p. 104-110.

McLaughlin, D.B., 1944, Triassic stratigraphy in the Point Pleasant district, Pennsylvania: *Proceedings of the Pennsylvania Academy of Science*, v. 18, p. 62-69.

McLaughlin, D.B., 1945, Type sections of the Stockton and Lockatong formations: *Proceedings of the Pennsylvania Academy of Science*, v. 19, p. 102-113.

McLaughlin, D.B., 1946, Continuity of strata in the Newark Series: *Michigan Academy of Science Papers*, v. 32, p. 295-303.

Meyertons, C.T., 1959, The geology of the Danville Triassic basin of Virginia: Ph. D. Dissertation, Virginia Polytechnic Institute, Blacksburg, VA, 188 p.

Meyertons, C.T., 1963, Triassic formations of the Danville basin: *Virginia Division of Mineral Resources, Report of Investigations No. 6*, 65 p.

Mickus, K.L., Aiken, C.L.V., Peeples, W.J., and Ziegler, D.G., 1988, A gravity and magnetic study of the Triassic Richmond basin, Virginia, *in* Manspeizer, W., ed., *Triassic-Jurassic Rifting, Continental Breakup and the Origin of the Atlantic Ocean and Passive Margins*: New York, Elsevier, p. 401-421.

Mihm, K.A., 1986, Geochemistry, petrography, and petrogenesis of the Belmont diabase sheet, northern Culpeper basin, Virginia, M.S. Thesis, University of Maryland, 202 p.

Nelson, R.H., 1964, Coal in basalt at Rocky Hill, Connecticut: *Rocks and Minerals*, v. 39, p. 461, 481.

Nelson, K.D., Arnow, J.A., McBride, J.H., Willemin, J.H., Huang, J., Zheng, L., Oliver, J.E., Brown, L.D., and Kaufman, S., 1985, New COCORP profiling in the southeastern United States. Part I: Late Paleozoic suture and Mesozoic rift basin: *Geology*, v. 13, p. 714-718.

Nilsen, T.H., 1982, Alluvial fan deposits, *in* Scholle, P.A., and Spearing, D., eds., *Sandstone Depositional Environments: American Association of Petroleum Geologists Memoir 31*, p. 49-86.

North American Commission on Stratigraphic Nomenclature, 1983, North American stratigraphic code: *American Association of Petroleum Geologists Bulletin*, v. 67, p. 841-875.

Ogg, J.G., Steiner, M.B., Oloriz, F., Tabera, J.M., 1984, Jurassic magnetostratigraphy; 1. Kimmerigian-Tithonian of Sierra Gorda, Carcabuey, southern Spain: *Earth and Planetary Science Letters*, v. 71, p. 147-162.

Olsen, P.E., 1977, Stop 11 [Paleontology of] Triangle Brick Quarry, *in* Bain, G.L., and Harvey, B.W., eds., *Field Guide to the Geology of the Durham Triassic Basin*: Carolina Geological Society, Raleigh, NC, p. 59-61.

Olsen, P.E., 1978, On the use of the term Newark for Triassic and Early Jurassic rocks of eastern North America: *Newsletters on Stratigraphy*, v. 7, p. 90-95.

Olsen, P.E., 1980a, The latest Triassic and Early Jurassic formations of the Newark basin (eastern North America, Newark Supergroup): stratigraphy, structure, and correlation: *New Jersey Academy of Science Bulletin*, v. 25, p. 25-51.

Olsen, P.E., 1980b, Triassic and Jurassic formations of the Newark basin, *in* Manspeizer, W., ed., *Field Studies of New Jersey Geology and Guide to Field Trips: 52nd Annual Meeting of the New York State Geological Association*, Rutgers University, Newark, NJ, p. 2-39.

Olsen, P.E., 1980c, Fossil great lakes of the Newark Supergroup in New Jersey, *in* Manspeizer, W., ed., *Field Studies of New Jersey Geology and Guide to Field Trips: 52nd Annual Meeting of the New York State Geological Association*, Rutgers University, Newark, NJ, p. 352-398.

Olsen, P.E., 1980d, A comparison of the vertebrate assemblages from the Newark and Hartford basins (early Mesozoic, Newark Supergroup) of eastern North America, *in* Jacobs, L. L., ed., *Aspects of Vertebrate History*: Flagstaff, AZ, Museum of Northern Arizona Press, p. 35-53.

Olsen, P.E., 1981, Comment on "Eolian dune field of Late Triassic age, Fundy Basin, Nova Scotia": *Geology*, v. 9, p. 557-559.

Olsen, P.E., 1982, Lockatong Fm. detrital cycles (Late Triassic, Newark Basin, N.J. and Pa.), giant lakes, and ecosystem efficiency: *Geological Society of America Abstracts with*

Programs, v. 14, p. 70.
Olsen, P.E., 1983, On the non-correlation of Newark Supergroup by fossil fishes: *Geological Society of America Abstracts with Programs*, v. 15, p. 121.
Olsen, P.E., 1984a: Comparative paleolimnology of the Newark Supergroup: a study of ecosystem evolution: Ph.D. Thesis, Yale University, New Haven, CT, 726 p.
Olsen, P.E., 1984b, Periodicity of lake-level cycles in the Late Triassic Lockatong Formation of the Newark basin (Newark Supergroup, New Jersey and Pennsylvania), *in* Berger, A., Imbrie, J., Hays, J., Kukla, G., and Saltzman, B., eds., *Milankovitch and Climate, Part 1*: Dordrecht, Holland, D. Reidel Publishing Co., p. 129-146.
Olsen, P.E., 1985, Distribution of organic-rich lacustrine rocks in the early Mesozoic Newark Supergroup, *in* Robinson, G.R., Jr., and Froelich, A.J., eds., *Proceedings of the Second U.S. Geological Survey Workshop on the Early Mesozoic Basins of the Eastern United States: U.S. Geological Survey Circular 946*, p. 61-64.
Olsen, P.E., 1985, Significance of great lateral extent of thin units in the Newark Supergroup (Lower Mesozoic, eastern North America)(Abstract): *American Association of Petroleum Geologists Bulletin*, v. 69, p. 1444.
Olsen, P.E., 1986, A 40-million-year lake record of early Mesozoic orbital climatic forcing: *Science*, v. 234, p. 842-848.
Olsen, P.E., 1988a, Continuity of strata in the Newark and Hartford basins, *in* Froelich, A.J., and Robinson, G.R., Jr., eds., *Studies of the Early Mesozoic Basins of the Eastern United States: U.S. Geological Survey Bulletin 1776*, p. 6-18.
Olsen, P.E., 1988b, Paleontology and paleoecology of the Newark Supergroup (early Mesozoic, eastern North America), *in* Manspeizer, W., ed., *Triassic-Jurassic Rifting, Continental Breakup, and the Origin of the Atlantic Ocean and Passive Margins*: New York, Elsevier, p. 185-230.
Olsen, P.E., 1988c, Tectonic, climatic, and biological modulation of lake sediments in the Newark Supergroup: *Lacustrine exploration: case studies and modern analogues, American Association of Petroleum Geologists Research Conference*, Snowbird, Utah, September 7-9, 1988.
Olsen, P.E., in press, Stratigraphy, facies, depositional environments, and paleontology of the Newark Supergroup, *in* Manspeizer, W., ed., Post-Paleozoic Activity: *The Geology of North America, The Appalachians*, Geological Society of America.
Olsen, P.E., and Baird, D., 1982, Early Jurassic vertebrate assemblages from the McCoy Brook Fm. of the Fundy Group (Newark Supergroup, Nova Scotia, Can.): *Geological Society of America Abstracts with Programs*, v. 14, p. 70.
Olsen, P.E., and Baird, D., 1986, The ichnogenus *Atreipus* and its significance for Triassic biostratigraphy, *in* Padian, K., ed., *The Beginning of the Age of Dinosaurs: Faunal Change Across the Triassic-Jurassic Boundary*: Cambridge, England, Cambridge University Press, p. 61-87.
Olsen, P.E., and Cornet, B., 1988a, Evidence for Early Mesozoic mass extinctions in eastern North American rift deposits (Late Triassic-Early Jurassic, Newark Supergroup), *in* IGCP Project 199, Rare events in geology: *Berichte der geologischen Bundesanstalt*, v. 15, p. 20.
Olsen, P.E., and Cornet, B., 1988b, The Triassic-Jurassic boundary in eastern North America: *Global Catastrophes in Earth History: An Interdisciplinary Conference on Impacts, Volcanism, and Mass Mortality*: Lunar and Planetary Institute and The National Academy of Sciences, p. 135.
Olsen, P.E., Cornet, B., and McDonald, N.G., 1989, Cyclostratigraphy of the Chicopee fish bed and adjacent strata: implications for the palynostratigraphy of the Portland Formation (Early Jurassic, Newark Supergroup): *Geological Society of America Abstracts with Programs*, v. 21, p. 56.
Olsen, P.E., and Fedosh, M., 1988, Duration of the early Mesozoic extrusive igneous episode in eastern North America determined by use of Milankovitch-type lake cycles: *Geological Society of America Abstracts with Programs*, v. 20, p. 59.
Olsen, P.E., Fedosh, M., and Schlische, R.W., in prep., Duration of Early Jurassic igneous extrusive events in Eastern North America and new method of measuring stratigraphic gaps: for *Geology*.
Olsen, P.E., and Flynn, J.J., 1989, Field guide to the vertebrate paleontology of Late Triassic rocks in the southwestern Newark basin (Newark Supergroup, New Jersey and Pennsylvania): *The Mosasaur*, in press.
Olsen, P.E., and Galton, P. M., 1984, A review of the reptile and amphibian assemblages from the Stormberg of southern Africa, with special emphasis on the footprints and the age of the Stormberg: *Palaeontologia Africana*, v. 25, p. 87-110.
Olsen, P.E., McCune, A.R. and Thomson, K.S., 1982, Correlation of the early Mesozoic Newark Supergroup by vertebrates, principally fishes: *American Journal of Science*, v. 282, p. 1-44.
Olsen, P.E., and Padian, K., 1986, Earliest records of *Batrachopus* from the southwestern U.S., and a revision of some early Mesozoic crocodilomorph ichnogenera, *in* Padian, K., ed., *The Beginning of the Age of Dinosaurs: Faunal Change across the Triassic-Jurassic Boundary*: Cambridge, England, Cambridge University Press, p. 259-273.
Olsen, P.E., Remington, C.L., Cornet, B., and Thomson, K.S., 1978, Cyclic change in Late Triassic lacustrine communities: *Science*, v. 201, p. 729-733.
Olsen, P.E., and Schlische, R.W., 1988a, New quantitative stratigraphic models of rifts based on orbitally induced lake level cycles (E. Mesozoic, Eastern North America) (Abstract): *American Association of Petroleum Geologists Bulletin*, v. 72, p. 231-232.
Olsen, P.E., and Schlische, R.W., 1988b, Quantitative rift basin evolution: application of extensional basin filling model to early Mesozoic rifts, E. North America: *Geological Society of America Abstracts with Programs*, v. 20, p. 59.
Olsen, P.E., and Schlische, R.W., 1988c, Unraveling the rules of rift basins: *Geological Society of America Abstracts with Programs*, v. 20, p. A123.
Olsen, P.E., and Schlische, R.W., 1988d, Unraveling the rules of rifts: *Lamont [Yearbook]*, p. 26-31.
Olsen, P.E., Shubin, N.H., and Anders, M.H., 1987, New Early Jurassic tetrapod assemblages constrain Triassic-Jurassic extinction event: *Science*, v. 237, p. 1025-1029.
Olsen, P.E., Shubin, N.H. and Anders, M.H., 1988, Triassic-Jurassic extinctions [reply to comment by Padian]: *Science*, v. 241, p. 1359-1360.
Olsen, P.E. and Sues, H.-D. 1986, Correlation of continental Late Triassic and Early Jurassic sediments, and patterns of the Triassic-Jurassic tetrapod transition, *in* Padian, K., ed., *The Beginning of the Age of Dinosaurs: Faunal Change across the Triassic-Jurassic Boundary*: Cambridge, England, Cambridge University Press, p. 321-351.
Olsen, P.E., Van Houten, F.B., *et al.*, 1988, Field guide to the Late Triassic portion of the Newark basin section in the Delaware Valley, New Jersey, *in* Husch, J., and Hozik, M., eds., *Geology of the Central Newark Basin: 5th Annual Meeting of the New Jersey Geological Association*, Rider College, Lawrenceville, NJ, p. 233-289.
Ostrom, J.H., 1972, Were some dinosaurs gregarious? *Palaeogeography, Palaeoclimatology, and Palaeoecology*, v. 11, p. 287-301.
Ostrom, J.H., and Quarrier, S.S., 1968, The Rocky Hill dinosaurs, *in* Orville, P.M., ed., *Guidebook for Field Trips in Connecticut: New England Intercollegiate Geological Conference, 60th Meeting, Connecticut Geological and Natural History Survey*

Guidebook 2, p. 1-12.
Palmer, J.P., 1971, Stratigraphy and geochemistry of the Scots Bay Formation, Nova Scotia: M.Sc. Thesis, Acadia University, Wolfville, N.S., 367 p.
Pannell, N.K., 1985, Dinosaur footprints at Oak Hill, Virginia: M.S. Thesis, George Washington University, Washington, D.C., 30 p.
Papezik, V.S., and Barr, S.M., 1981, The Shelburne dike, an Early Mesozoic diabase dike in Nova Scotia: mineralogy, chemistry, and regional significance: *Canadian Journal of Earth Sciences*, v. 18, p. 1341-1355.
Parker, J. M., III, 1977, Geology and mineral resources of Wake County: *North Carolina Department of Natural Resources, Geological Survey Section Bulletin 86*, 122 p.
Parker, R.A., Houghton, H.F., and McDowell, R.C., 1988, Stratigraphic framework and distribution of early Mesozoic rocks of the northern Newark basin, New Jersey and New York, *in* Froelich, A.J., and Robinson, G.R., Jr., eds., *Studies of the Early Mesozoic Basins of the Eastern United States: U.S. Geological Survey Bulletin 1776*, p. 31-39.
Parnell, J., 1983, Skeletal halites from the Jurassic of Massachusetts, and their significance: *Sedimentology*, v. 30, p. 711-715.
Patterson, O.C., 1969, The depositional environment and paleoecology of the Pekin Formation of the Sanford Triassic Basin, North Carolina: M.S. Thesis, North Carolina State University.
Pegram, W.J., 1986, The isotope, trace element, and major element geochemistry of the Mesozoic Appalachian tholeiite province: Ph.D. thesis, Massachusetts Institute of Technology.
Phillips, J.D., 1983, Paleomagnetic investigations of the Clubhouse Crossroads basalt, South Carolina: *U.S. Geological Survey Professional Paper 1313-C*, 18 p.
Philpotts, A.R., and Martello, A., 1986, Diabase feeder dikes for the Mesozoic basalts in southern New England: *American Journal of Science*, v. 286, p. 105-126.
Picard, M.D., and High, L.R., Jr., 1963, Rythmic alternations in the Triassic Chugwater and Brunswick Formations, Wyoming and New Jersey: *Contributions to Geology [University of Wyoming]*, v. 2, p. 87-99.
Picard, M.D. and High, L. R., Jr., 1981, Physical stratigraphy of ancient lacustrine deposits, *in* Etheridge, F.G., and Flores, R.M., eds., *Recent and Ancient Non-marine Depositional Environments: Models for Exploration: Society of Economic Paleontologists and Mineralogists Special Publication No. 31*, p. 233-259.
Pipiringos, G.N., and O'Sullivan, R.B., 1978, Principal unconformities in Triassic and Jurassic rocks, western interior United States—a preliminary survey: *U.S. Geological Survey Professional Paper 1035-A*, 29 p.
Plint, A.G., and van de Poll, H.W., 1984, Structural and sedimentary history of the Quaco Head area, southern New Brunswick: *Canadian Journal of Earth Science*: v. 21, p. 753-761.
Pollard, D.D., 1973, Derivation and evaluation of a mechanical model for sheet intrusions: *Tectonophysics*, v. 19, p. 233-269.
Powers, S.,1916, The Acadian Triassic: *Journal of Geology*, v. 24, p. 1-26, 105-122, 254-268.
Pratt, L.M., and Burruss, R.C., 1988, Evidence for petroleum generation and migration in the Hartford and Newark basins, *in* Froelich, A.J., and Robinson, G.R., Jr., eds., *Studies of the Early Mesozoic Basins of the Eastern United States: U.S. Geological Survey Bulletin 1776*, p. 74-79.
Pratt, L.M., Shaw, C.A., and Burruss, R.C., 1988, Thermal histories of the Hartford and Newark basins inferred from maturation indices of organic matter, *in* Froelich, A.J., and Robinson, G.R., Jr., eds., *Studies of the Early Mesozoic Basins of the Eastern United States: U.S. Geological Survey Bulletin 1776*, p. 58-63.
Price, J.W., Sr., 1956, A new locality for Upper Triassic vertebrate fossils in Lancaster County, Pennsylvania: *Proceedings of the Pennsylvania Academy of Sciences*, v. 30, p. 167-169.
Puffer, J.H., 1987, The Palisades sill and Watchung basalt flows, northern New Jersey: *Geological Society of America Centennial Field Guide, v. 5—Northeastern Section*, p. 91-96.
Puffer, J.H. and Lechler, P., 1980, Geochemical cross sections through the Watchung basalt of New Jersey, part 2: *Geological Society of America Bulletin*, v. 91, p. 156-191.
Puffer, J.H., Hurtubise, D.O., Geiger, F.J., and Lechler, P., 1981, Chemical composition and stratigraphic correlation of the Mesozoic basalt units of the Newark basin, New Jersey, and the Hartford basin, Connecticut, part 2: *Geological Society of America Bulletin*, v. 92, p. 515-553.
Ragland, P.C., Brunfelt, A.O., and Weigand, P.W., 1971, Rare-earth abundances in Mesozoic dolerite dikes from eastern North America, *in* Brunfelt, A.O., and Steinnes, E., eds., *Activation Analysis in Geochemistry and Cosmochemistry*: Oslo, Norway, Universitetsforlaget, p. 227-235.
Ragland, P.C., Hatcher, R.D., Jr., and Whittington, D., 1983, Juxtaposed Mesozoic diabase dike sets from the Carolinas: a preliminary assessment: *Geology*, v. 11, p. 394-399.
Ragland, P.C., and Whittington, D., 1983a, "Primitive" Mesozoic diabase dikes of eastern North America: primary or derived? *Geological Society of America, Abstracts with Programs*, v. 15, p. 92.
Ragland, P.C., and Whittington, D., 1983b, Early Mesozoic diabase dikes of eastern North America: magma types. *Geological Society of America Abstracts with Programs*, v. 15, p. 666.
Ratcliffe, N.M., 1980, Brittle faults (Ramapo fault) and phyllonitic ductile shear zones in the basement rocks of the Ramapo seismic zones, New York and New Jersey, and their relationship to current seismicity, *in* Manspeizer, W., ed., *Field Studies of New Jersey Geology and Guide to Field Trips: 52nd Annual Meeting of the New York State Geological Association*, Rutgers University, Newark, NJ, p. 278-307.
Ratcliffe, N.M., 1988, Reinterpretation of the relationship of the western extension of the Palisades sill to the lava flows at Ladentown, New York, based on new core data, *in* Froelich, A.J., and Robinson, G.R., Jr., eds., *Studies of the Early Mesozoic Basins of the Eastern United States: U.S. Geological Survey Bulletin 1776*, p. 113-135.
Ratcliffe, N.M., Burton, W.C., D'Angelo, R.M., and Costain, J.K., 1986, Low-angle extension faulting, reactivated mylonites, and seismic reflection geometry of the Newark basin margin in eastern Pennsylvania: *Geology*, v. 14, p. 766-770.
Ratcliffe, N.M., and Burton, W.C., 1985, Fault reactivation models for origin of the Newark basin and studies related to eastern U.S. seismicity, *in* Robinson, G.R., Jr., and Froelich, A.J., eds., *Proceedings of the Second U.S. Geological Survey Workshop on the Early Mesozoic Basins of the Eastern United States: U.S. Geological Survey Circular 946*, p. 36-45.
Ratcliffe, N.M., and Burton, W.C., 1988, Structural analysis of the Furlong fault and the relationship of mineralization to faulting and diabase intrusion, Newark basin, Pennsylvania, *in* Froelich, A.J., and Robinson, G.R., Jr., eds., *Studies of the Early Mesozoic Basins of the Eastern United States: U.S. Geological Survey Bulletin 1776*, p. 176-193.
Raup, D.M., and Sepkoski, J.J., 1982, Mass extinctions in the marine fossil record: *Science*, v. 215, p. 1501-1503.
Reeves, C.C., 1976, *Caliche: Origin, Classification, Morphology, and Uses*: Lubbock, TX, Estacado Books, 233 p.
Reinemund, J.A., 1955, Geology of the Deep River coal field, North Carolina: *U.S. Geological Survey Professional Paper 246*, 159 p.

Ressetar, R., and Taylor, G.K., 1988, Late Triassic depositional history of the Richmond and Taylorsville basins, eastern Virginia, *in* Manspeizer, W., ed., *Triassic-Jurassic Rifting, Continental Breakup and the Origin of the Atlantic Ocean and Passive Margins*: New York, Elsevier, p. 423-443.

Richardson, J.C., 1969, Former lake level fluctuations and their recognition: *International Association of Theoretical and Applied Limnology*, v. 17, p. 78-93.

Ridky, R.W., and O'Connor, J.V., 1979, The Culpeper basin of the Triassic lowlands of northern Virginia, *in* Exline, J. D., ed., *Guidebook for field trips in Virginia: National Association of Geology Teachers, Eastern Section*, p. 49-59.

Robbins, E.I., 1982, "Fossil Lake Danville": the paleoecology of a Late Triassic ecosystem on the North Carolina-Virginia border: Ph.D. Thesis, The Pennsylvania State University, State College, PA, 400 p.

Robbins, E.I., and Textoris, D.A., 1986, Fossil fuel potential of the Deep River basin, North Carolina, *in* Gore, P.J.W., ed., Depositional framework of a Triassic rift basin: the Durham and Sanford sub-basins of the Deep River basin, North Carolina, *in* Textoris, D.A., ed., *Society of Economic Paleontologists and Mineralogists Field Guidebook, Third Annual Mid-year Meeting*, p. 75-79.

Robbins, E.I., and Traverse, A., 1980, Degraded palynomorphs from the Dan River (North Carolina)—Danville (Virginia) basin, *in* Price, V., Jr., *et al.*, eds., *Geological Investigations of Piedmont and Triassic rocks, central North Carolina and Virginia: Carolina Geological Society Field Trip Guidebook*, section B, no. 10, 11 p.

Robbins, E.I., Wilkes, G.P., and Textoris, D.A., 1988, Coal deposits of the Newark rift system, *in* Manspeizer, W., ed., *Triassic-Jurassic Rifting, Continental Breakup and the Origin of the Atlantic Ocean and Passive Margins*: New York, Elsevier, p. 649-682.

Roberts, S.C., 1986, The Otterdale Sandstone, Richmond Triassic basin, Virginia: Senior Thesis, College of William and Mary, Williamsburg, VA, 35 p.

Rodgers, J.,1985, *Bedrock Geological Map of Connecticut*: Connecticut Geological and Natural History Survey, 1:125,000.

Robinson, G.R., Jr., 1988, Base- and precious-metal mineralization associated with igneous and thermally altered rocks in the Newark, Gettysburg, and Culpeper early Mesozoic basins of New Jersey, Pennsylvania, and Virginia, *in* Manspeizer, W., ed., *Triassic-Jurassic Rifting, Continental Breakup and the Origin of the Atlantic Ocean and Passive Margins*: New York, Elsevier, p. 621-648.

Romer, A.S., and Lewis, A.D., 1973, The Chanares (Argentina) Triassic reptile fauna VI: a chiniquodontid cynodont with an incipient squamosal-dentary jaw articulation: *Breviora*, v. 344, p. 1-18.

Root, S., 1988, Structure and hydrocarbon potential of the Gettysburg basin, Pennsylvania and Maryland, *in* Manspeizer, W., ed., *Triassic-Jurassic Rifting, Continental Breakup and the Origin of the Atlantic Ocean and Passive Margins*: New York, Elsevier, p. 353-367.

Rosendahl, B.R., 1987, Architecture of continental rifts with special reference to East Africa: *Annual Review of Earth and Planetary Science*, v. 15, p. 445-503.

Russell, I.C., 1879, On the physical history of the Triassic Formation in New Jersey and the Connecticut Valley: *New York Academy of Sciences Annals*, v. 1, p. 220-254.

Ryan, J.D., and Willard, B., 1947, Triassic footprints from Bucks County, Pennsylvania: *Proceedings of the Pennsylvania Academy of Sciences*, v. 21, p. 91-93.

Sanders, J.E., 1962, Strike-slip displacement on faults in Triassic rocks in New Jersey: *Science*, v. 136, p. 40-42.

Sanders, J.E., 1963, Late Triassic tectonic history of northeastern United States: *American Journal of Science*, v. 261, p. 501-524.

Schaeffer, B., and McDonald, N.G., 1978, Redfieldiid fishes from the Triassic-Liassic Newark Supergroup of eastern North America: *American Museum of Natural History Bulletin*, v. 159, p. 129-174.

Schlische, R.W., 1985, Faults of the northern Newark basin, New Jersey: Senior Thesis, Rutgers University, Newark, NJ, 50 p.

Schlische, R.W., and Olsen, P.E., 1987, Comparison of growth structures in dip-slip vs. strike-slip dominated rifts: eastern North America: *Geological Society of America Abstracts with Programs*, v. 19, p. 833.

Schlische, R.W., and Olsen, P.E., 1988a, A model for the structural evolution of the Newark basin: *Geological Society of America Abstracts with Programs*, v. 20, p. 68.

Schlische, R.W., and Olsen, P.E., 1988b, Structural evolution of the Newark basin, *in* Husch, J.M., and Hozik, M.J., eds., *Geology of the Central Newark Basin: 5th Annual Meeting of the New Jersey Geological Association*, Rider College, Lawrenceville, NJ, p. 43-65.

Schlische, R.W., and Olsen, P.E., in review, Quantitative filling models for continental extensional basins with applications to the early Mesozoic rifts of eastern North America: for *Journal of Geology*.

Seidemann, D.E., Masterson, W.D., Dowling, M.P., and Turekian, K.K., 1984, K-Ar dates and $^{40}Ar/^{39}Ar$ age spectra for Mesozoic basalt flows of the Hartford basin, Connecticut, and the Newark basin, New Jersey: *Geological Society of America Bulletin*, v. 95, p. 594-598.

Sepkoski, J.J., 1986, Phanerozoic overview of mass extinction, *in* Raup, D.M., and Jablonski, D., eds., *Patterns and Processes in the History of Life: Dahlen Konferenzen 1986*: Berlin, Springer-Verlag, p. 277-295.

Shaler, N.S., and Woodworth, J.B., 1899, Geology of the Richmond basin, Virginia: *U.S. Geological Survey Annual Report*, no. 19, pt. 2, p. 385-515.

Shannon, C.E., and Weaver, W., 1949, *The Mathematical Theory of Communication*: Urbana, IL, University of Illinois Press, 117 p.

Shelton, J.W., 1984, Listric normal faults: an illustrated summary: *American Association of Petroleum Geologists Bulletin, v. 68, p. 801-815.*

Sheridan, R.E., Olsson, R.K., Grow, J.A., and Miller, J., 1988, Vibroseis and gravity study of proposed Taconic suture under the New Jersey coastal plain: implications for continental growth: *Geological Society of America Abstracts with Programs*, v. 20, p. A184.

Silliman, B., Sr., 1816, [Personal Communications], *in* Cleaveland, P., *An Elementary Treatise on Mineralogy and Geology, etc.*: Boston, Cummings and Hilliard, p. 363.

Silvestri, SM., and Olsen, P.E., 1989, Ichnostratigraphy of the Jacksonwald syncline: the last 7 million years of the Triassic: *Geological Society of America Bulletin*, v. 21, p. 66.

Sims, S.J., 1968, The Grace Mine magnetite deposit, Berks County, Pennsylvania, *in* Ridge, J.D., ed., *Ore Deposits of the United States, 1933-1967, Volume 1*: American Institute of Mining and Metallurgical Engineers, p. 108-124.

Smith, R.C., II, Rose, A.W., and Lanning, R.M., 1975, Geology and geochemistry of Triassic diabase in Pennsylvania: *Geological Society of America Bulletin*, v. 86, p. 943-955.

Smith, T.E., and Noltimier, H.C., 1979, Paleomagnetism of the Newark trend igneous rocks of the north central Appalachians and the opening of the central Atlantic Ocean: *American Journal of Science*, v. 279, p. 778-807.

Smith, W.A., 1987, Paleomagnetic results from a crosscutting system of northwest and north-south trending diabase dikes in the North Carolina Piedmont: *Tectonophysics*, v. 136, p. 137-150.

Smith, D.G., and Smith, N.D., 1980, Sedimentation in anastamosed river systems: examples from alluvial valleys near

Banff, Alberta: *Journal of Sedimentary Petrology*, v. 50, p. 157-164.

Smoot, J.P., 1985, The closed-basin hypothesis and its use in facies analysis of the Newark Supergroup, *in* Robinson, G.R., Jr., and Froelich, A.J., eds., *Proceedings of the Second U.S. Geological Survey Workshop on the Early Mesozoic Basins of the Eastern United States: U.S. Geological Survey Circular 946*, p. 4-10.

Smoot, J.P., 1989, Fluvial and lacustrine facies of the early Mesozoic Culpeper basin, Virginia and Maryland: IGC Field Trip T213: Washington, D.C., American Geophysical Union, in press.

Smoot, J.P., in press, Section 5: Stratigraphic section of the Balls Bluff Siltstone at the Culpeper Crushed Stone Quarry, Stevensburg, Virginia, *in* Lee, K.Y. and Froelich, A.J., eds., Triassic-Jurassic stratigraphy of the Culpeper and Barboursville basins, Virginia and Maryland: *U.S. Geological Survey Professional Paper 1427*.

Smoot, J.P., and Katz, S.B., 1982, Comparison of modern playa mudflat fabrics to cycles in the Triassic Lockatong Formation of New Jersey: *Geological Society of America Abstracts with Programs*, v. 14, p. 83.

Smoot, J.P., and LeTourneau, P.M., 1989, Wave-formed shoreline deposits on alluvial fans: examples from modern Pyramid and Walker Lakes, Nevada, and the early Mesozoic Newark Supergroup, eastern USA (Abstract): *28th International Geological Congress*.

Smoot, J.P., and Olsen, P.E., 1985, Massive mudstones in basin analysis and paleoclimatic interpretation of the Newark Supergroup, *in* Robinson, G.R., Jr., and Froelich, A.J., eds., *Proceedings of the Second U.S. Geological Survey Workshop on the Early Mesozoic Basins of the Eastern United States: U.S. Geological Survey Circular 946*, p. 29-33.

Smoot, J.P., and Olsen, P.E., 1988, Massive mudstones in basin analysis and paleoclimatic interpretation of the Newark Supergroup, *in* Manspeizer, W., ed., *Triassic-Jurassic Rifting, Continental Breakup and the Origin of the Atlantic Ocean and Passive Margins*: New York, Elsevier, p. 249-274.

Smoot, J.P., and Robinson, G.R., Jr., 1988, Base- and precious-metal occurrences in the Culpeper basin, northern Virginia, *in* Froelich, A.J., and Robinson, G.R., Jr., eds., *Studies of the Early Mesozoic Basins of the Eastern United States: U.S. Geological Survey Bulletin 1776*, p. 403-423.

Sobhan, A.N., 1985, Petrology and depositional history of Triassic red beds, Bull Run Formation, eastern Culpeper basin, Virginia: M.S. Thesis, George Washington University, 225 p.

Spencer, A.C., 1908, Magnetite deposits of the Cornwall type in Pennsylvania: *U.S. Geological Survey Bulletin 359*, 102 p.

Spencer, R.J., 1986, *Geology of the Northeast Durham 7 1/2 Minute Quadrangle*: Unpublished Report for the U.S. Geological Society-North Carolina Geological Survey COGEOMAP Program, 1:24,000 scale map with text.

Stagg, J.W., 1984, Petrology of the basal conglomerate of the Triassic Pekin Formation, Sanford sub-basin, North Carolina: M.S. Thesis, University of North Carolina, Chapel Hill, NC, 71 p.

Steiner, M.B., 1986, Rotation of the Colorado Plateau: *Tectonics*, v. 5, p. 649-660.

Stevens, G.R., 1987, Jurassic basalts of northern Bay of Fundy region, Nova Scotia: *Geological Society of America Centennial Field Guide, v. 5—Northeastern Section*, p. 415-420.

Stevens, R.L., and Hubert, J.F., 1980, Alluvial fans, braided rivers, and lakes in a fault bounded semiarid valley: Sugarloaf Arkose (Late Triassic-Early Jurassic), Newark Supergroup, Deerfield basin, Massachusetts: *Northeastern Geology*, v. 2, p. 100-117.

Stewart, D.J., 1983, Possible suspended-load channel deposits from the Wealden Group (Lower Cretaceous) of southern England, *in* Collinson, J.D., and Lewin, J., eds., *Modern and Ancient Fluvial Systems: International Association of Sedimentologists Special Publication No. 6*, p. 369-384.

Stringer, P., and Lajtai, E.Z., 1979, Cleavage in Triassic rocks of southern New Brunswick, Canada: *Canadian Journal of Earth Science*, v. 16, p. 2165-2180.

Suchecki, R.K., Hubert, J.F., and Birney-de Wet, C.C., 1988, Isotopic imprint of climate and hydrogeochemistry on terrestrial strata of the Triassic-Jurassic Hartford and Fundy rift basins: *Journal of Sedimentary Petrology*, v. 58, p. 801-811.

Sues, H.D., Olsen, P.E., and Shubin, N.H., 1987, A diapsid assemblage from the Lower Jurassic of Nova Scotia, Canada, *in* Currie, P.M., and Koster, E.H., ed., *4th Symposium on Mesozoic Terrestrial Ecosystems, Drumheller; Short Papers: Occasional Papers of the Tyrell Museum of Paleontology*, v. 3, p. 205-207.

Suppe, J., 1985, *Principles of Structural Geology*: Englewood Cliffs, NJ, Prentice-Hall, 535 p.

Sutter, J.F., 1985, Progress on geochronology of Mesozoic diabases and basalts: *U.S. Geological Survey Circular 946*, p. 110-114.

Sutter, J.F., 1988, Innovative approaches to dating igneous events in the early Mesozoic basins of the eastern United States, *in* Froelich, A.J., and Robinson, G.R., Jr., eds., *Studies of the Early Mesozoic Basins of the Eastern United States: U.S. Geological Survey Bulletin 1776*, p. 194-200.

Sutter, J.F., and Smith, T.E., 1979, $^{40}Ar/^{39}Ar$ ages of diabase intrusions from Newark trend basins in Connecticut and Maryland: initiation of central Atlantic rifting: *American Journal of Science*, v. 279, p. 808-831.

Swanson, F.J., 1988, Proximal ecological effects of the 1980 eruptions of Mount St. Helens: *Global Catastrophes in Earth History: An Interdisciplinary Conference on Impacts, Volcanism, and Mass Mortality*: Lunar and Planetary Institute and The National Academy of Sciences, p. 188-189.

Swanson, M.T., 1982, Preliminary model for early transform history in central Atlantic rifting: *Geology*, v. 10, p. 317-320.

Swanson, M.T., 1986, Preexisting fault control for Mesozoic basin formation in eastern North America: *Geology*, v. 14, p. 419-422.

Tanner, L.H., and Hubert, J.F., 1988, Debris-flow and talus-slope conglomerates in the Lower Jurassic McCoy Brook Formation, Fundy Basin, Nova Scotia: *Geological Society of America Abstracts with Programs*, v. 20, p. 74.

Taylor, G.K., and Ressetar, R., 1985, Depositional and structural histories of Richmond and Taylorsville Triassic rift basins (Abstract): *American Association of Petroleum Geologists Bulletin*, v. 69, p. 1449.

Taylor, R.C., 1835, Memoir of a section passing through the bituminous coal field near Richmond, in Virginia: *Geological Society of Pennsylvania Transactions*, v. 1, p. 275-294.

Textoris, D.A., 1985, Resources and depositional environment of coal in the Triassic Deep River basin, North Carolina: *Final Report to U. S. Geological Survey, Grant number 14-08-0001-G-970*, 14 p.

Textoris, D.A., and Holden, C. J., 1986, Paleoclimatic change within a stratigraphic section, *in* Gore, P.J.W., ed., Depositional framework of a Triassic rift basin: the Durham and Sanford sub-basins of the Deep River basin, North Carolina, *in* Textoris, D.A., ed., *Society of Economic Paleontologists and Mineralogists Field Guidebook, Third Annual Mid-year Meeting*, p. 101-102.

Textoris, D.A., Stagg, J.W., and Wheeler, W.H., 1986, The "Millstone Grit", *in* Gore, P.J.W., ed., Depositional framework of a Triassic rift basin: the Durham and Sanford sub-basins of the Deep River basin, North Carolina, *in* Textoris, D.A., ed., *Society of Economic Paleontologists and Mineralogists Field Guidebook, Third Annual Mid-year Meeting*, p. 92-97.

Thayer, P.A., 1967, Geology of the Dan River and Davie County Triassic basins, North Carolina: Ph. D. Thesis, University of North Carolina, Chapel Hill, 178 p.

Thayer, P.A., 1970, Stratigraphy and geology of Dan River Triassic basin, North Carolina: *Southeastern Geology*, v. 12, p. 1-31.

Thayer, P.A., Kirstein, D.S., and Ingram, R.L., 1970, *Stratigraphy, Sedimentology, and Economic Geology of Dan River Basin, North Carolina: Carolina Geological Society Field Trip Guidebook*, Raleigh, NC, 44 p.

Thayer, P.A., Robbins, E.I., and Ziegler, D.G., 1982, Hydrocarbon potential of the Dan River-Danville Triassic basin, North Carolina and Virginia: *Geological Society of America Abstracts with Programs*, v. 14, p. 89.

Thomas, W.A., 1988, Early Mesozoic faults of the northern Gulf Coastal Plain in the context of opening of the Atlantic Ocean, *in* Manspeizer, W., ed., *Triassic-Jurassic Rifting, Continental Breakup and the Origin of the Atlantic Ocean and Passive Margins*: New York, Elsevier, p. 463-476.

Thompson, G.M., 1968, A magnetic study of fault-diabase dike relationships in the Cedar Creek Community, South Carolina: B.S. thesis, University of South Carolina, Columbia, SC, 27 p.

Thorpe, M.R., 1929, A new Triassic fossil field: *American Journal of Sciences*, v. 18, p. 277-306.

Tollo, R.P., 1988, Petrographic and major element characteristics of Mesozoic basalts, Culpeper basin, Virginia, *in* Froelich, A.J., and Robinson, G.R., Jr., eds., *Studies of the Early Mesozoic Basins of the Eastern United States: U.S. Geological Survey Bulletin 1776*, p. 105-113.

Tollo, R.P., Froelich, A.J., and Gottfried, D., 1989, Jurassic igneous rocks of the Culpeper basin, Virginia, Guidebook: *International Geological Congress Field Trip T201*, Washington, D.C., American Geophysical Union.

Tollo, R.P., Gottfried, D., and Froelich, A.J., 1988, Field guide to the igneous rocks of the southern Culpeper basins, Virginia, *in* Froelich, A.J., and Robinson, G.R., Jr., eds., *Studies of the Early Mesozoic Basins of the Eastern United States: U.S. Geological Survey Bulletin 1776*, p. 391-403

Tomkeieff, S.I., 1940, The basalt lavas of Giant's Causeway, District of Northern Ireland: *Bulletin of Volcanology, Series 2*, v. 6, p. 89-143.

Traverse, A., 1986, Palynology of the Deep River basin, North Carolina, *in* Gore, P.J.W., ed., Depositional framework of a Triassic rift basin: the Durham and Sanford sub-basins of the Deep River basin, North Carolina, *in* Textoris, D.A., ed., *Society of Economic Paleontologists and Mineralogists Field Guidebook, Third Annual Mid-year Meeting*, p. 66-71.

Traverse, A., 1987, Pollen and spores date origin of rift basins from Texas to Nova Scotia as early Late Triassic: *Science*, v. 236, p. 1469-1472.

Turner-Peterson, C., 1980, Sedimentology and uranium mineralization in the Triassic-Jurassic Newark Basin, Pennsylvania and New Jersey, *in* Turner-Peterson, C., ed., *Uranium in Sedimentary Rocks, Application of the Facies Concept to Exploration: Society of Economic Paleontologists and Mineralogists, Rocky Mountain Section, Short Course Notes*, p. 149-175.

Unger, J.D., 1988, A simple technique for analysis and migration of seismic reflection profiles from the Mesozoic basins of eastern North America, *in* Froelich, A.J., and Robinson, G.R., Jr., eds., *Studies of the Early Mesozoic Basins of the Eastern United States: U.S. Geological Survey Bulletin 1776*, p. 229-235.

Van Fossen, M.C., and Kent, D.V., 1989, Paleomagnetic data from the White Mountain magma series in New Hampshire support high latitude model of Jurassic apparent polar wander for North America [Abstract]: *EOS*, in press.

Van Houten, F.B., 1962, Cyclic sedimentation and the origin of analcime-rich Upper Triassic Lockatong Formation, west-central New Jersey and adjacent Pennyslvania: *American Journal of Science*, v. 260, p. 561-576.

Van Houten, F.B., 1964, Cyclic lacustrine sedimentation, Upper Triassic Lockatong Formation, central New Jersey and adjacent Pennsylvania: *Kansas Geological Survey Bulletin*, v. 169, p. 497-531.

Van Houten, F.B., 1969, Late Triassic Newark Group, north central New Jersey, and adjacent Pennsylvania and New York, *in* Subitzky, S.S., ed., *Geology of Selected Areas in New Jersey and Eastern Pennsylvania*: New Brunswick, Rutgers University Press, p. 314-347.

Van Houten, F.B., 1977, Triassic-Liassic deposits of Morocco and eastern North America: comparison: *American Association of Petroleum Geologists Bulletin*, v. 61, p. 79-99.

Van Houten, F.B., 1980, Late Triassic part of the Newark Supergroup, Delaware River section, west-central New Jersey, *in* Manspeizer, W., ed., *Field Studies of New Jersey Geology and Guide to Field Trips: 52nd Annual Meeting New York State Geological Association*, Rutgers University, Newark, NJ, p. 264-276.

Van Houten, F.B., 1987, Late Triassic cyclic sedimentation: Upper Lockatong and lower Passaic formations (Newark Supergroup), Delaware Valley, west-central New Jersey: *Geological Society of America Centennial Field Guide, v. 5—Northeastern Section*, p. 81-86.

Venkatakrishnan, R., and Lutz, R., 1988, A kinematic model for the evolution of Richmond Triassic basin, Virginia, *in* Manspeizer, W., ed., *Triassic-Jurassic Rifting, Continental Breakup and the Origin of the Atlantic Ocean and Passive Margins*: New York, Elsevier, p. 445-462.

Walker, K.R., 1969, The Palisades sill, New Jersey: a reinvestigation: *Geological Society of America Special Paper 111*, 178 p.

Ward, L.F., 1900, The older Mesozoic, *in* Status of the Mesozoic floras of the United States: *U.S. Geological Survey 20th Annual Report*, pt. 2, p. 213-748.

Webb, J.A., 1981, The radiometric time scale for the Triassic: *Journal of the Geological Society of Australia*, v. 28, p. 107.

Weems, R.E., 1980, An unusual newly discovered archosaur from the upper Triassic of Virginia, U.S.A.: *Transactions of the American Philosophical Society*, v. 70, p. 1-53.

Weems, R.E., 1987, A Late Triassic footprint fauna from the Culpeper basin, northern Virginia (USA): *Transactions of the American Philosophical Society*, v. 77, part 1, 79 p.

Weems, R.E., 1988, Structural vs. stratigraphic parsimony: an example from the Triassic Danville basin of Virginia/North Carolina (Abstract): *Virginia Journal of Science*, in press.

Weigand, P.W., and Ragland, P.C., 1970, Geochemistry of Mesozoic dolerite dikes from eastern North America: *Contributions to Mineralogy and Petrology*, v. 29, p. 195-214.

Wenk, W.J., 1984a, Seismic refraction model of fault offset along basalt horizons in the Hartford rift basin, Connecticut and Massachusetts: *Northeastern Geology*, v. 6, p. 168-173.

Wenk, W.J., 1984b, Seismic refraction model of depth of basement in the Hartford rift basin, Connecticut and Massachusetts: *Northeastern Geology*, v. 6, p. 196-202.

Wenk, W.J., 1984c, Gravity models of the upper crust beneath the Hartford rift basin, Connecticut and Massachusetts: *Northeastern Geology*, v. 6, p. 203-206.

Wetzel, R.G.,1983, *Limnology*: New York, Saunders, 767 p.

Wheeler, G., 1939, Triassic fault-line deflections and associated warping: *Journal of Geology*, v. 47, p. 337-370.

Wheeler, W.H., and Textoris, D. A., 1978, Triassic limestone and chert of playa origin in North Carolina: *Journal of Sedimentary Petrology*, v. 48, p. 765-776.

Wilkes, G.P., 1986, The Farmville basin and Briery Creek basin, *in* Goodwin, B.K., Ramsey, K.W., and Wilkes, G.P., eds., *Guidebook to the Geology of the Richmond, Farmville, Briery Creek and Roanoke Creek Basins, Virginia: Virginia Geological Field Conference, 18th Annual Meeting*, p. 26-34.

Wilkes, G.P., 1987, Geology of the Briery Creek Triassic basin, Virginia: *Virginia Minerals*, v. 33, p. 21-26.

Willard, B., et al., 1959, Geology and mineral resources of Bucks County, Pennsylvania: *Pennsylvania Geological Survey Bulletin C9*, 243 p.

Williams, H., and Hatcher, R.D., 1982, Suspect terranes and accretionary history of the Appalachian orogen: *Geology*, v. 10, p. 530-536.

Wise, D.U., 1988, Mesozoic stress history of the upper Connecticut Valley at Turners Falls, Massachusetts, *in* Bothner, W.A., ed., *Guidebook for Field Trips in Southwestern New Hampshire, Southeastern Vermont, and Northcentral Massachusetts: New England Intercollegiate Geological Conference, 80th Annual Meeting*, Keene, NH, p. 351-372.

Wise, D.U., and Robinson, P., 1982, Tectonics of the Mesozoic Connecticut Valley graben: *Geological Society of America Abstracts with Programs*, v. 14, p. 96.

Withjack, M.O., and Gallagher, J.J., 1983, The rifted basins of eastern India: *SEAPEX Proceedings*, v. 6, p. 41-57.

Witte, W.K., and Kent, D.V., 1987, Multicomponent magnetization of some Upper Triassic red beds from the Newark basin: *EOS*, v. 68, p. 295.

Witte, W.K., and Kent, D.V., 1988, Paleomagnetism of the Hettangian Newark basin extrusive zone: *EOS*, v. 69, p. 342.

Witte, W.K., and Kent, D.V., 1989, A middle Carnian to early Norian (~225 Ma) paleopole from sediments of the Newark basin: *Geological Society of America Bulletin*, v. 101, in press.

Witte, W.K., Kent, D.V., and Olsen, P.E., 1989, Pre- and post-folding magnetizations of the Late Triassic Passaic Formation sediments in southeast Pennsylvania: *Geological Society of America Abstracts with Programs*, v. 21, p. 76-77.

Woodcock, N.H., and Fischer, M., 1986, Strike-slip duplexes: *Journal of Structural Geology*: v. 8, p. 725-735.

Wu, F., Van der Voo, R., 1987, Paleomagnetism of Late Triassic alkaline plutons in southern Maine (abstr.), *EOS*, v. 68, p. 295.

Young, R.S. and Edmundson, R.S., 1954, Oolitic limestone in the Triassic of Virginia: *Journal of Sedimentary Petrology*, v. 24, p. 275-279.

Zen, E-an, ed., 1983, *Bedrock Geologic Map of Massachusetts*: U.S. Geological Survey, 1:250,000.

Ziegler, D.G., 1983, Hydrocarbon potential of the Newark rift system: eastern North America: *Northeastern Geology*, v. 5, p. 200-208.